Fire Induced Collapse of Tall Buildings

Graeme Flint

A Thesis presented for the degree of
Doctor of Philosophy

BRE Centre for Fire Safety Engineering
Institute for Infrastructure and Environment
University of Edinburgh
Scotland, UK
December 2005

Declaration

The work in this thesis is based on research carried out at the BRE Centre for Fire Safety Engineering, University of Edinburgh, Scotland under the supervision of Dr Asif Usmani, Professor José Torero and Dr Susan Lamont. No part of this thesis has been submitted elsewhere for any other degree or qualification and it is all my own work unless referenced to the contrary in the text.

Fire Induced Collapse of Tall Buildings

Graeme Flint

Submitted for the degree of Doctor of Philosophy
December 2005

Abstract

The last decade has seen some rapid advances in knowledge and theory with regard to the effects of fire on structures. In 1990 a major fire broke out in the Broadgate Phase 8 building while it was under construction. Even without most of its passive protection in place the building maintained stability. This event led to a series of tests at the BRE Cardington facilities. An 8 storey composite steel frame building was designed and constructed according to the relevant codes and practices. Analysis of the Cardington tests led to the discovery that such buildings were inherently more robust than previously thought. Design codes (and the approving authorities that regulate them) are now allowing performance based designs using complex thermo-structural analysis for buildings under severe fire conditions.

Methods of testing structural elements (both physical and analytical) have until now been based on relatively short spans, often 4-5m. The results of these tests have been used to validate the use of long span floor systems which may reach up to 18m. It is not yet entirely clear if such methods are appropriate.

With the collapse of the World Trade Center towers in September 2001 interest was understandably piqued as to the exact mechanisms involved. The WTC towers sustained substantial damage over several floors due to aircraft impacts but remained stable. Fires were ignited over several floors of each tower and as these fires progressed collapse was initiated.

This research project was designed to investigate possible mechanisms that fires could initiate that might lead to collapse of a tall building of similar design to the WTC Towers. It was not designed to be a forensic study and no initial damage was applied to the structure. The effects of fire on long span, truss based floor systems was investigated both locally and globally using finite element models.

The local mechanisms are investigated using a single truss. This highlights both the response of the floor system but also some possible interaction between the floor system and columns. The columns provide support to the floor for vertical loading but the floor also provides lateral support to the column. It is important to understand the effect that a fire might have on the interaction between these elements when considering the global building response so that collapse may be avoided. Several different heating regimes are investigated that can be related to different severities of fire and inclusion of different levels of fire protection.

Several possible global collapse mechanisms have been discovered using a 2D frame model that do not require connection failure or initial damage. A parametric study was undertaken using the 2D model to investigate the effects of different fire severities over multiple floors. The effect of adding additional redistribution mechanisms (i.e. hat truss) was also investigated.

The results of the 2D models were compared to results from 3D, half floor, multi-storey models. Similar responses may be seen in the 3D models as well as significant amounts of redistribution throughout the structure. There are several indications that the collapse mechanisms seen in the 2D models can occur in the 3D models.

Publications

Journal Papers

G.R. Flint, A.S. Usmani, S. Lamont, J.L. Torero, B. Lane, "Effect of fire on composite long span truss floor systems", Journal of Constructional Steel Research, Accepted 16th August 2005 (In Press)

G.R. Flint, A.S. Usmani, S. Lamont, J.L. Torero, B. Lane, "Structural response of tall buildings to multiple floor fires : Part 1 - General response", ASCE Journal Struct. Eng., Submitted August 2005

G.R. Flint, A.S. Usmani, S. Lamont, J.L. Torero, B. Lane, "Structural response of tall buildings to multiple floor fires : Part 2 - Parametric study", ASCE Journal Struct. Eng., Submitted August 2005

S. Lamont, B. Lane, G.R. Flint, A.S. Usmani, "Behaviour of structures in fire and real design - a case study", Journal of Fire Protection Engineering, Accepted April 2005

Conference Papers

S. Lamont, B. Lane, A.I. Jowsey, G. Flint, A.S. Usmani, J.L. Torero, *Innovative Structural Engineering for Tall Buildings in Fire*, JCSWS and IABSE Workshop on Robustness of Structures, November 2005

A.S. Usmani, G.R. Flint, A.I. Jowsey, S. Lamont, B. Lane, J.L. Torero, "Modelling of the Collapse of Large Multi-Storey Steel Framed Structures in Fire", The 4th

International Conference on Advances in Steel Structures, 2, 991-998, 13-15 June, 2005

B. Lane, S. Lamont, A.S. Usmani, J.L. Torero, G.R. Flint, A.I. Jowsey, "Robust Design of Tall Buildings in Fire - The Use of Analysis for Structural Fire Engineering Solutions", Interflam 2004, July 2004

G.R. Flint, A.S. Usmani, “Investigation into the Impact of Fire on the Twin Towers”, The 3rd International Structures in Fire Workshop, SiF2004, May 2004

Acknowledgments

Many people have assisted me in during the course of this research and I would like to extend my thanks to several in particular. My supervisors at Edinburgh University, Dr Asif Usmani and Professor José Torero have been of tremendous help continually throughout this project. I also very much appreciate the invaluable help, support and eternal patience of my industrial supervisor, Dr Susan Lamont.

Others who have provided me with a great deal of help and support include Dr Barbara Lane, Dr Antonis Giannopoulos and Mr Allan Jowsey for which I am grateful.

This work could not have been conducted without the support and encouragement of my family for which I am extremely grateful. I would also like to thank my friends, wherever they may lurk, for their support.

Funding for this project was provided jointly by the EPSRC and ArupFIRE and I would like to thank them for this opportunity.

Contents

List of Figures

Note : A3 diagrams of all model meshes used in this thesis may be found at the back of this volume

List of Tables

Chapter 1

Introduction

1.1 Background to the project

Although structural elements have been investigated in fire conditions for over a century, still little is known about the true response of a large, redundant structure to real building fires. Due to the complex nature of the problem, research has mostly been limited to single element testing and simplified analytical techniques. The results of these tests, which were designed at the start of the 20th century, have been used to create design codes that require prescribed levels of insulation to be applied to structural elements as fire protection. This system was designed to limit the temperature that structural elements might reach in a fire. Little consideration is given to the actual effects of heating in a real building.

A major fire in the Broadgate building in 1990, and the following Cardington tests, indicated that composite steel structures without fireproofing would not necessarily collapse under fire loading. Thus researchers and engineers working in the field have moved away from the more prescriptive design methods. Instead, more modern performance based design methods are being used. Tall buildings in particular require a highly engineered design for all possible load cases if they are to be cost-effective and safe.

Such performance based design methods are already used for ambient gravity, wind

and earthquake loading. These methods allow the level of safety in a building to be calculated in terms of risk probabilities. Thus the continued use of prescriptive codes for fire design introduces a grey area in the safety of a building. If such codes are followed then the building can currently be considered "safe" by default. However the true level of safety is unknown because the building response to fire loading is also unknown.

The advent of high powered computers and detailed computer models has meant that the problem can now be investigated in an efficient manner. Initial work was done by several research groups to understand the response of the Cardington frame to the applied fires. The validation of the computer modelling techniques to this known case has allowed researchers to move on to investigate other types of building design.

With the collapse of the World Trade Center towers in 2001, attention was again focussed on the lack of detailed knowledge about the effects of fires on buildings. The towers withstood the impact of the aircraft without immediate collapse hence the triggering mechanism may have been caused by the fires. This PhD project is based on trying to understand how a multi-storey fire might affect a tall building of a similar design to the WTC towers.

1.2 Aims of this research

This research is designed to advance understanding about the effect of fires on large structures which incorporate modern construction techniques.

The aims of the PhD project are as follows :

- Investigate the local effect of fire on long span, composite truss floor systems.
- Investigate global effects of fire on such floor systems when in place in a tall building.

- Identify possible collapse mechanisms in tall buildings undergoing multiple floor fires.

A structure similar in nature to the World Trade Center towers was investigated. Computer models of various portions of the structure were created using the ABAQUS Finite Element Modelling package and analysed under fire conditions.

1.3 Outline of thesis chapters

Chapter 2

Review of Tall Building Design

In this chapter a brief discussion of the current methods of tall building design for various loading regimes, including fire, will be presented . The aim of this discussion is to highlight the differences that currently exist between structural design for ambient loading and for fire conditions. The modes and consequences of structural failure will also be discussed in terms of disproportionate and progressive collapse.

The findings of recent research into composite steel structures in fire is presented and the current level of research into long span floor systems in fire is also discussed.

Chapter 3

Local effects of heating on long span trusses

This chapter reports on an investigation of the effects of heating on a long span truss floor system. The ABAQUS finite element package is used to model the structure including fully non-linear behaviour and thermal expansion effects. Different boundary conditions and heating regimes are investigated to understand the response of the truss members to fire. The effects of heating on the lateral restraint available from the slender floor systems to a column have also been studied. The results and analysis indicate that composite truss flooring systems may not fail

suddenly. Individual member buckling seems to be a much more gradual occurrence linked to material failure and expansion based geometry change rather than sudden "failure".

Chapter 4

Structural response of tall buildings to multiple floor fires : Part 1 - General response

This chapter reports on an investigation of the global effects of Fire on long span truss floor systems in a tall building environment. The effects of fire spread over multiple floors of a building are the focus of this research, especially where this may lead to progressive collapse.

This study analyses results from an investigation of a 2 dimensional model of a multi-storey office building. The model is representative of the type of construction used in the World Trade Center 1&2 towers including a hat truss system. The local and global response of the model is described over the course of a 3 floor fire reaching a peak compartment temperature of 800^oC .

Chapter 5

Structural response of tall buildings to multiple floor fires : Part 2 - Parametric study

This chapter presents the results of a further investigation of the structure presented in Chapter 4 [78]. It is designed to indicate the differences in response of a tall building utilizing long span, truss based floors when subjected to a variety of fire regimes. Changes to material properties and structural layout are also included.

Chapter 6

3D Single Floor Response

This chapter describes the methods used to create a single floor model of a building similar to the WTC towers. Validation is presented between various models used in moving the analysis from a Full Resolution Single Truss to a Half Resolution Half Symmetry model. A general description of the response of a single floor Half Symmetry model is also presented.

Chapter 7

Effect of Fire on 3D Multi-storey models

This chapter describes the construction and response of large, 3D, multi-storey models. A short description of the importance of the correct boundary conditions leads into the main discussion of results. Several different versions of the model were run using a variety of fire regimes. The effects of a hat truss were also investigated. Due to the extremely complex nature of these models convergence difficulties were frequently encountered . Explicit versions of the models were investigated to determine efficiency and accuracy.

The aim of this chapter is to investigate large, 3D, multi-storey models under similar circumstances to those investigated in Chapter 5. This will indicate whether or not the failure mechanisms described in Chapter 4 for a simple 2D model are realistic responses in large buildings of this nature.

Chapter 8

Conclusions and Further work

Chapter 2

Review of Tall Building Design

In this chapter a brief discussion of the current methods of tall building design for various loading regimes, including fire, will be presented . The aim of this discussion is to highlight the differences that currently exist between structural design for ambient loading and for fire conditions. The modes and consequences of structural failure will also be discussed in terms of disproportionate and progressive collapse.

The findings of recent research into composite steel structures in fire is presented and the current level of research into long span floor systems in fire is also discussed.

2.1 Current Structural Fire Research

2.1.1 Cardington Tests

For the past century the design of structures for fire loading has been dominated by prescriptive codes. The basis of these codes has been the standard fire resistance test that is used around the world to test single elements in response to a prescribed heating regime. It is now well understood, both in the research and consulting communities, that the standard test does not give a good indication of the actual response of a real structure in a real fire. Lamont [1] provides a critical review

of the current state of testing and design for structures in fire. Ove Arup has also published a report [2] describing current codes and practices world wide and providing a framework for future research needs in the area of structural fire safety in the United States of America.

The main impetus for change in the way buildings are designed for fire conditions was the result of several events in the 1990s. The first was the fire in the Broadgate [3] building while it was under construction. Although very little of the fire protection prescribed by the design codes had been applied the severe fire conditions did not cause global collapse of the structure. Another major fire soon after (Churchill Plaza [4]) reinforced the observations that composite steel framed buildings were more robust in fire than previously thought. Specifically no failure was seen even when members had far exceeded the temperature where failure would have been deemed to occur in a standard fire test. On the basis of these events an extensive research project was conducted at the BRE large building test facility at Cardington [4] to investigate the response of such buildings to major compartment fires. An 8 storey building was designed according to normal practices for office buildings and constructed in one of the large volume facilities at Cardington. The detailed results of this testing and the theoretical and numerical modelling work [1, 5–7] that followed may be found elsewhere. A brief summary of the findings follows :

- Composite steel framed buildings exhibit inherently stable behaviour under fire due to the highly redundant nature of the structural form
- This behaviour is characterized by several thermo-mechanical phenomena, which interact. This complex interaction is highly dependent upon the structural layout and the thermal regime of the fire compartment considered
- Interconnectivity between structural elements leads to levels of restraint that is hard to quantify and this leads to a complex distribution of forces within a structure. Single element testing will not adequately capture this .

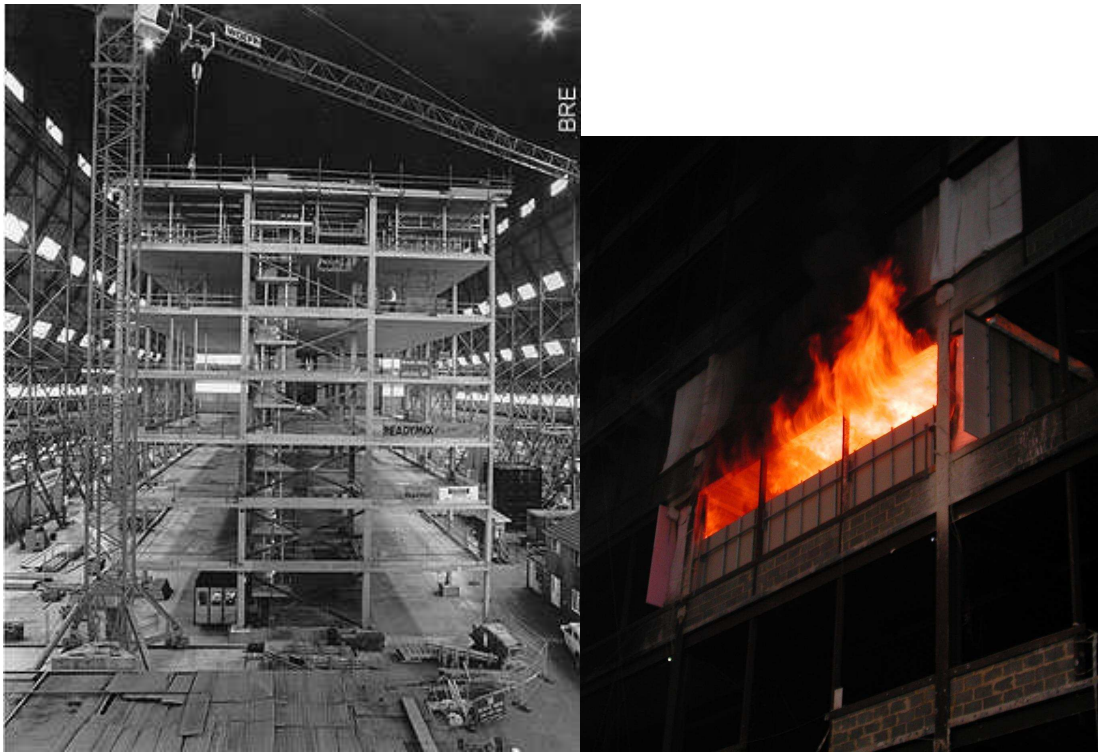

(a) (b)

Figure 2.1: Cardington Frame Tests [11, 12]

As well as a greater understanding of the effect of fire on structures the Cardington experiments have allowed performance based design guidance to be produced. Relatively simple techniques [8–10] have been produced that allow designers to include the enhanced strength available to structures in fire.

As "Performance Based Design" becomes more popular and accepted for fire design, more complex methods become available for designing buildings to withstand fire loading [13]. Treating a fire as another load case on a structure only really becomes possible using performance based techniques. This has worked well for other loading conditions such as earthquakes [14]. There are currently few (barely into double figures) buildings that have been designed to take advantage of this trend but the number is growing [15].

For all the advances the Cardington tests have allowed in the field of Fire Safety

Engineering the results of this series of tests do not tell the whole story. The configuration of the majority of the Cardington tests were all contained within relatively small compartments leaving questions as to the effect of larger fires on structures. Most of the investigations undertaken using the Cardington results have been in the area of modelling the experiments [6, 7, 16, 17]. This research has then been used to investigate single element response testing different types of boundary condition and temperature regime [18–20]. Research into connection response has also been conducted [21, 22].

Concentration on updating our knowledge on the local effects of fire on structures is important but it does not necessarily allow the full picture to be seen. The fires in the World Trade Center towers, for instance, had the potential to include the entirety of a floor, and due to the nature of the ignition event, took place over multiple floors. While the events of September 11th 2001 were unforeseen they were not totally improbable and other extreme events are possible that may affect tall buildings in a similar way, such as those surrounding the large scale fire in the Torre Windsor building in Madrid in February 2005 [23]. Thus the effects of fire upon the whole building structure, especially a high rise building, are in need of investigation.

2.2 Tall Building Design

As with all buildings the primary purpose for a tall building is to transfer load from the supported floors down to the foundations. Various different methods can be used to achieve this, primarily utilizing a combination of steel and concrete. For more detailed information on this subject a design guide such as that written by Taranath [24] should be consulted. A short summary of the kinds of construction techniques available for tall buildings will be presented here, along with how such buildings are protected against fire relative to how they are designed for all other loads.

2.2.1 Ambient Design for Live Loading

The design of tall buildings differs from that of low-rise structures in that the loading regimes that the structure has to support become much more complex. Not only do the higher gravity loads need to be transferred to the foundations but increased loading caused by wind must be taken into account. As buildings increase in height so the building surface area increases. This combined with increasing wind speed at greater altitude leads to wind load requiring special consideration. Depending on geographical location, other extreme loading conditions must also be considered, such as earthquakes. For tall, flexible buildings such loading can cause serious problems. As is indicated in Taranath [24] tall buildings may be considered to be a vertical cantilever under wind loading. This means the structure will have to withstand substantial lateral shear forces combined with bending and overturning moments.

Linked to the ability to survive such loading are the consequences of failure. If a low-rise building collapses then the effects tend to be extremely localized and therefore more acceptable. If a 100 storey building collapses then the already substantial loss could be greatly multiplied if the collapsing building intersects with other structures. The main concern of official regulators is life safety of building occupants but property protection and financial factors are also of concern to clients and insurers. The economic and environmental impact of a tall building collapse can be substantial. For instance the fires in, and the collapse of, the World Trade Center towers (WTC 1&2) produced large volumes of smoke and concrete dust that affected many New York residents. The collapse of the towers also destroyed the place of work and business of many thousands of people. As well as the destruction of the towers themselves the collapse impinged upon, and caused at least partial collapse of, WTC buildings 3 through 6. The total collapse of WTC 7 was caused entirely due to fire initiation by debris alone. No major structural damage was created in WTC 7 through the collapse of the WTC 1&2 towers. The eventual total economic cost of the collapse of all these buildings will also have to include such long term and wide spread factors as legal fees and increased insurance premiums.

Thus tall buildings are designed to ensure the safety and welfare of the occupants and local population over the design life of the building.

Design for Gravity Loads. The simplest load case that designers have to consider is the normal gravity loading on the structure. The weight of most materials that could be used in the structure or that are to be stored within the building are well documented [25] and can usually be easily determined. Gravity induced live loading is defined in the Eurocode [25], for example, depending on classifications linked to the building use (e.g. residential, office, shopping, etc). These values have been derived after many years of building surveys with regards to contents.

Gravity loads under ambient conditions can be dealt with using the normal design equations available in the various design codes dealing with construction in different materials [26–31]. For design of tall buildings the most common materials used for the main structural framing are steel and concrete. The behaviour of these materials under simple, static loading are well understood hence it should then be a relatively simple matter to take the loading from any part of the structure down to the foundations by manipulation of material strengths and section sizes.

In certain cases dynamic forces need to be taken into account. Such dynamic loading can be due to internal loading requirements, such as for dance floors or heavy, oscillating machinery, or due to external requirements, such as wind or earthquake loading (which will be discussed later).

The structural elements of tall buildings may be split into several different classes.

- Foundations - Support all loading from structure above.
- Core - Often toward the middle of the structure. Contains structural elements designed to withstand gravity and wind induced lateral shear.
- Floors - Transfer gravity loads to columns. Also help distribute lateral forces throughout the building using membrane action. Provide lateral support for columns.

- Outer Columns/Frame - Usually resisting a combination of gravity loads and forces caused by wind induced bending moments.
- Internal Framing - Can be provided to assist any of the above in withstanding loads. Also often provided to distribute loads properly throughout the structure. In large office developments this class of element will be kept to a minimum in order to maximize the commercial lettable space on each floor.

A combination of these elements is used in the design of a tall building.

A common design for tall buildings is to combine a strong core with heavy outer columns, effectively creating a tube structure, e.g. the World Trade Center towers [32]. This combination, using a minimum of internal framing between the core and the outer columns, requires long span floors to be installed.

With the advancement of computer aided techniques designs have become more ambitious. One example is the Bank of China Tower in Hong Kong (Figure 2.2) which relies on a large, cross braced space frame structure to withstand gravity loading as well as wind forces. The internal structure on this building has also been minimized with the use of long span floor systems. Such structures have to use Performance Based criteria in all aspects of their design as prescriptive code objectives are too restrictive.

Design for Wind Loads. The design of structures for wind have a similar end goal to that of gravity loading.

- The structure is to remain standing under the worst loading that is likely to occur in the lifetime of the building
- Deflections (static and dynamic) are to be limited so as not to damage brittle fittings and/or cause discomfort to the building occupants

The exact methods used to define the wind load a building is to be designed for change depending on which design code is to be followed in different countries. However the fundamental principles are always the same, as follows:

Figure 2.2: Bank of China, Hong Kong [33]

1. Determine basic design wind speeds
2. Determine extra factors caused by gusting
3. Determine factors to be included for local terrain characteristics
4. Convert into an equivalent static loading case of pressure across all faces of building
5. Local design of cladding
6. Global design of structure

The first 3 items usually involve reference to a combination of empirical data tables and probabilistic methods to determine the severity of the wind event to be designed for. The 4th item is a simplification of the problem from a complex dynamic problem to a static problem that can use design calculations that are similar to

those for gravity load design. The main difference is that the loading is perpendicular to the gravity load and may increase or decrease loads to be resisted by different structural elements. The last 2 steps are the final design stages for the various elements in the structure.

Resistance to wind loading can be included in several ways. The most easily recognizable method is to include simple cross bracing to the existing structural frames. Such methods are easy and cost effective to add to low rise buildings. For tall building design the complexity of the building requires the bracing systems to be included at an early stage. Horizontal bracing systems, outrigger trusses and belt trusses can all add to the lateral stiffness of the structure and are designed to spread wind loads evenly throughout the structural frame. Other methods may also be used. For structural tube and space frame based buildings the lack of internal framing means that the wind loading must be resisted by other means. In the World Trade Center, for instance, the perimeter columns of the building were designed to take a combination of wind and gravity loading with the emphasis firmly on wind load. The building acted as a cantilever under wind loading and the resulting bending moments were resisted by axial forces in the outer columns. Analysis of the strength of the outer columns indicates that gravity design loads would only account for about 20% of the column capacity and the rest is allocated to wind load resistance. The majority of the gravity loading was to be taken by the core structure.

Due to increases in height and surface area tall buildings require a more advanced approach to wind resistance. As well as being subjected to large wind loads tall buildings will also have a significant impact on the air flow in the surrounding area and this must also be taken into account. Excessive downdrafts, for instance, can make transit of nearby pavements and roads dangerous or uncomfortable. In addition any other buildings in the vicinity will need to be able to withstand the altered wind forces. This variability in loading and effect on surrounding buildings makes designing to a prescriptive code difficult and inefficient.

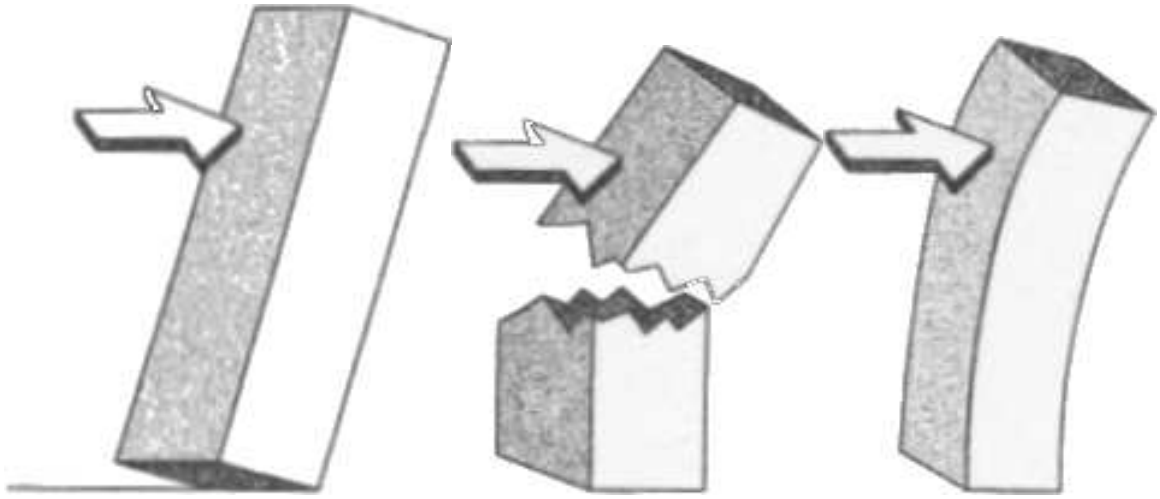

(a) Overturning (b) Structural Failure (c) Excessive Deflections

Figure 2.3: Wind Effects to be Resisted [24]

In recent years performance based systems have become more available as wind tunnel testing has become more prevalent and designers attempt to create ever more efficient structures. For example, Eurocode 1 Part 1.4 [34], which deals with wind loading, includes a provision that allows calculations to be supplemented by appropriate wind tunnel testing. Different types of model can be tested to get data for overturning, shear and bending forces, the pressures affecting each of the building faces and the effect the building will have on other structures nearby as the incident wind flow is deflected.

However even with the advanced nature of the wind design systems in place around the world it is apparent that more research needs to be done. Over the course of the NIST investigation into the events at the World Trade Center in September 2001 a comparison of different US wind codes was conducted [35]. Two separate, independent tests were also conducted, by commercial testing laboratories, on the WTC towers to determine, retrospectively, the design wind loads that would be applied if the towers were to be designed today. A difference in wind loads of up to 40% was seen between the two studies. Two of the 30 recommendations NIST produced from their investigation of the WTC collapse focus on reviewing

the current wind design codes to allow more consistent results.

The biggest advantage wind loading has over fire loading, in terms of application in codes, is the relative ease with which the load case can be derived. Many years of recording wind speeds and investigation into fluid dynamics has led to a robust system to determine design wind speeds. Such data recording is easier, and cheaper to obtain, as wind is a significantly less destructive environment than fire. What is currently absent from fire design is a reliable, generalized method for producing realistic worst case fire scenarios for whole buildings.

Design for Earthquake Loads. Earthquake loading is similar to wind loading in that it requires the designer to take into account the likely lateral loading that may occur to the building and allow it to be transferred to the foundations. The main difference in this case is that it is the foundations that are moving and imparting loading through the internal structure of the building rather than being an external load applied to the outside of the structure. As earthquakes occur less frequently than other load cases the design of a tall building will not necessarily be dictated by this load case. Such lateral load cases will generally be resisted by suitable application of systems of shear walls and bracing. Structural joint design is also very important in allowing the whole building to resist earthquake forces.

As with wind loading it is not economical, or necessary, to design a building for every conceivable load case. Performance based regulations on the level of earthquake to be withstood are now common. The frequency and intensity of earthquakes in a particular area can be predicted using the various data produced by organizations such as the Geological Survey groups of the UK [36] and the US [37]. Local building codes will then stipulate the way in which such data can be turned into loads to apply to the structure.

The general shape of the building can have a significant effect on its vulnerability. Designing a building with a regular, simple and evenly distributed structure makes it easier to predict the response of the building and reduces the possibility that unforeseen local weaknesses could occur and instigate progressive collapse. Eurocode

8 takes into account the regularity and simplicity of a building design by allowing for different levels of simplification of analysis and strength reduction factors. Taranath [24] also indicates that symmetrical plan layouts are recommended for buildings in seismically active zones. Asymmetry can lead to significant torsional movement and stress concentrations that are difficult to predict.

Consideration should be given to the layout of the building foundations as well as the structure above ground. A well designed foundation will transmit ground forces into the building in an even manner again avoiding stress concentrations and disproportionate overload on individual members. Effects of ground vibration on the soil around the foundation should also be considered to avoid foundation settlement caused by such phenomena as soil liquefaction, rupture and slope stability, etc.

Earthquakes require the entire structure of a building to work together in resisting the forces created by ground actions. As such, the structure must be robust enough in all its joints and connections to allow the structural members to dissipate the earthquake energy. Ductile behaviour in the joints is the preferred response as it allows energy to be dissipated while still allowing time for users of the building to become aware of the structural damage and vacate the building.

In a similar manner to wind loading, earthquakes can easily be measured remotely and recording equipment has been installed in many locations around the globe. While prediction of an individual earthquake has yet to be introduced reliably the results of such events have been recorded throughout the world. This has led to reliable, relatively simple methods to produce worst case loading for a given structure in a given location. Once reliable statistical data is available on the effects of a load case it can be analyzed to produce a method for worst case loading that can be used in design.

Acceptance Criteria The standard Eurocode design methods for gravity, wind and earthquake loading define Ultimate and Serviceability Limit States. These are load and deflection criteria that must be satisfied. Safety factors are included in

the design equations for loads and materials that allow for statistical variation. For gravity loading the Ultimate Limit State (ULS) is that no structural elements will fail under the prescribed loading. The Serviceability Limit State (SLS) is based on deflections and states that under normal use the deflections in the building will not exceed certain levels that may lead to damage of brittle finishes or discomfort in the users of the building.

Wind loading limit states are directly analogous to the gravity states with the Ultimate state relating to failure of structural elements. The Serviceability limit state again relates to deflections and the comfort of building occupants. If the building is not comfortable to occupy due to excessive movement then it is not fit for purpose.

Earthquake loading is also subject to several levels of requirements, analogous to the Ultimate and Serviceability limit states for wind loading. According to Eurocode 8 [14] a certain level of earthquake must be withstood by the building with no damage, the damage limitation state. This is analogous to the Serviceability Limit State from gravity load design. After a more powerful earthquake a building must remain standing but a certain amount of structural damage is allowed as long as local and global collapse are avoided, the Ultimate Limit State. For the ULS the objective is life safety and therefore the building and its foundations must remain stable enough such that lives will not be put at risk. Sliding and overturning stability must be maintained and local and global collapse mechanisms avoided. The SLS is more concerned with property protection and continuation of use. Life safety is implicitly included in the no damage criteria. Unlike other load cases the ability of earthquakes to knock loose facades and sections of building envelope is dealt with explicitly. Again for life safety reasons, to avoid portions of non-structural materials falling to the ground, provision must be made to attach these items with earthquake-proof fittings.

As long as it can be shown that the structure can satisfy these design criteria then it will be deemed fit for purpose and acceptable. By comparison, prescriptive design for fire does not have these performance criteria. As long as the structural

members have the appropriate thickness of fire protection applied then the full structural response of the building is not required by design codes.

2.2.2 Current Structural Design for Fire

Although the use of fire engineering techniques is becoming more popular in the design of buildings the most common design method involves following the appropriate prescriptive code. Life safety is the main goal of these codes, both of the building occupants, local residents and of firefighters who may have to conduct operations in the building. The UK building regulations for stability are deemed to be satisfied for fire if a building can be seen to survive for a "reasonable period" of time under fire conditions [38, 39]. Fire spread criteria are also part of the regulations. The fire resistance period for a compartment should be long enough to allow evacuation of the building occupants and to allow the Fire Brigade to conduct operations (firefighting and/or search and rescue) safely within the building. The design codes therefore use time based rating systems for evacuation and structural stability. The prescriptive codes currently in use require the application of passive (e.g. inert insulation) and/or active (e.g. sprinklers) fire protection systems to attain these rating times. The basis for designing structural members to meet these conditions is provided through the various standard tests that are in use throughout the world [40–42], which are all fundamentally the same. Individual structural members and small assemblies are tested in a furnace which applies a standard heating regime, based on the furnace gases following a temperature-time curve (the "standard fire"). Various criteria are monitored and when at least one is met the test is terminated. Criteria include insulation (based on temperatures of the unexposed face of a wall or floor), flame passage (simulating breach of compartmentation) and deflections. The time elapsed before any of the criteria are reached is the designated fire resistance period of the tested assembly measured at 30, 60, 90 and 120 minutes only.

However, the times indicated by compliance with such codes are not based on real

time nor do they relate directly to each other, i.e. escape times do not correlate directly with times for structural resistance. The structural fire resistance times are based on a period of exposure to the standard fire. Hence the fundamental differences between realistic "natural fires" and the standard fire mean that the structural fire resistance times, as designated by the codes, bear no relation to the real time that a building might survive a fire.

Escape times are designed to allow full evacuation of each threatened compartment before untenable conditions are reached, through ingress of smoke and heat or by structural failure. Ideally the time to untenable conditions is infinite. Lamont [1] and Arup [2] have produced critical reviews of the current design codes and as such this work will not be repeated here.

The effects of fire on a structure are not considered using the same limit state method used for other load types. For ambient design the response of the structure to the loads is an integral part of the limit state system. For fire design it is the temperature reached, rather than the structural response, that is the design criteria. This then limits the worst case situations purely to the possible fires that may occur in a compartment when in reality a worst case will be a combination of fire severity and structural response. For tall buildings the thickness of fire protection on structural elements is simply increased to achieve longer fire resistance periods. Additionally design codes often allow passive fire protection to be reduced if active suppression systems are present. Sprinklers are not 100% reliable and can be disabled hence, for a true worst case scenario, should always be disregarded. As the design then satisfies the code requirements the implication is that the building is "safe". In reality the safety of the building cannot be quantified properly as the structural response is not known.

The limited size of most fire resistance test furnaces means that the long span floors commonly installed in modern high rise buildings cannot be tested in full. Thus, the rating of the system will be based on results from short/partial spans, commonly 4-5m long sections, but are then applied to beams of all lengths. Thus a gap in knowledge exists as to the full response of long span floors under fire

conditions. This is true for standardized testing as well as realistic "Natural Fire" situations.

The materials used in the design of tall buildings (i.e. steel frame or concrete frame) may in part be chosen in relation to how easy it is to attain the required fire resistance rating according to the codes as well as other measures of efficiency and cost effectiveness. Concrete has historically been perceived as generally superior under fire conditions. The low thermal conductivity of the material limits the rate at which thermal degradation affects a concrete structure (especially the steel reinforcement). A reinforced concrete structure can therefore be inherently fire resistant.

Concrete is a complex material, however, and the exact response of it to fire has yet to be fully explained. The basic structure of the material is a combination of coarse and fine aggregate suspended in a cementicious gel matrix. Different types of concrete mix can lead to different strengths but this also leads to different proportions of materials, water content and air voids. All of these elements react differently under heating which leads to the complex nature of the material response. As well as loss of strength and stiffness, heating can induce "spalling" in concrete.

Spalling is believed to be made up from a combination of responses [43,44]. Thermo-mechanical effects include restrained thermal expansion and differential thermal expansion, both between the aggregate and the cement gel and due to thermal gradients induced in the member. The other main component in the production of spalling comes from increased pore pressure due to expansion of included fluids (i.e. water and air). Stresses created by these actions can cause portions of the exposed faces of a concrete member to detach, sometimes explosively. This loss of material has two main effects in structural reinforced concrete members. The first is that it reduces the sectional area of concrete in the member. The second is that it reduces the amount of protective cover provided to the reinforcement bars. If this cover is lost then the rebar will be more severely affected by a fire and the bond between the steel and the concrete can be lost. All of these factors will reduce the capacity of a concrete member.

Under current guidelines the provision of fire protection is the responsibility of the Architect rather than the Structural Engineer. This reinforces the view that the provision of structural fire protection is something done elsewhere in the design process rather than being integrated with the rest of the structural design. The findings and analysis of the Cardington experiments [1, 6, 7] have led to the call, from researchers and consultants alike, that fire design should be incorporated in the full structural design process in a similar way to wind and earthquake design. As it stands, design to current prescriptive codes results in an assumption that as long as the code is followed then the building will be completely safe. With wind, gravity and earthquake loading the design loads are based on a statistical analysis that allows us to define just how safe the building actually is. In addition, as these load cases are integrated into the structural design of the building, it is possible to predict the response of the structure under such load cases. For fire design there is no such procedure and hence the level of safety is unquantified and the response of the building is largely unknown.

Design codes for wind and earthquake loads already require the designer to include structural elements designed to withstand the specific forces of the load case. Similarly it would be useful in a full performance based design code for fire loads to have provision for additional structure to provide alternate load paths. In the case of the WTC towers the presence of hat trusses in the top 3 floors of the building increased their capacity to withstand fire, even though they were not designed to cope with such loading. In other tall buildings belt, hat and outrigger trusses could provide additional redistribution options to transfer forces from members affected by fire back to the core, or other unaffected locations. The design of such structural members would be made more efficient if fire were to be included in the initial structural design.

Including comprehensive fire design as part of the initial structural design will increase the knowledge of the structural response and therefore the quantifiable level of safety inherent in a design. As modern building design becomes more efficient, to reduce steel tonnage, the natural reserves of strength (due to over

engineering) are being gradually reduced. This makes it vital for the design of safe buildings that all possible load cases are considered in a quantifiable manner.

2.2.3 Structural Failure

Internal dead and live loading of a structure can usually be quantified and can therefore be designed for easily, with the structure being kept well within the realms of elastic behaviour. Wind and earthquake loading require a more involved approach to determine a suitable worst case loading but, again, various statistical methods are available to reduce the uncertainty in the maximum likely load case. However, due to the unpredictability of nature (human and otherwise) it is always possible that an event outside the range considered will occur, overloading all, or part, of the structure and causing damage.

Under Performance Based Design systems the risk associated with a particular event is a combination of the probability of occurrence coupled with the level of consequence. As buildings get taller so the consequences of a structural failure increase. Safety factors are used throughout the modern design process as a buffer against probabilities being exceeded. Safety factors in materials guard against the material being weaker than specified, factors in wind design are designed to guard against the possibility of the wind being stronger than predicted or even that the building (including its contents) will be lighter than expected. It is this built in reserve of strength that buildings are using under fire conditions. Modern fire design codes consider each component as a separate entity. It is the robustness included for other factors (such as wind and earthquake) that allows the building to act as a whole frame. However, as such factors are not specifically designed for fire conditions it is the author's opinion that they should not be relied upon in this way. As such systems are designed for other purposes there is no explicit knowledge of their response to fire conditions. The inclusion of fire design in the main structural design stage would ensure that such systems are capable of withstanding all load cases.

Figure 2.4: Ronan Point Collapse

As well as guarding against total collapse, modern buildings must have elements intended to mitigate disproportionate and progressive collapse within the structure. Progressive collapse can be defined as the propagation of failure mechanisms through a structure after some initiating event. In the 1960s a gas explosion in a corner flat in the Ronan Point [45] tower block caused the progressive collapse of the entire corner of the building. The explosion blew out the precast, modular walls of the flat which allowed the structure above to collapse down onto the floor below which caused a chain reaction down the side of the building. UK building codes now require specific provision to be given to prevent such progressive failure while US codes are only now beginning to consider this problem explicitly. Disproportionate collapse is defined as the failure of a disproportionate amount of structure due to a much smaller initial event.

When discussing the collapse of structures, either total or partial, then a useful

measure is the vulnerability of the structure [46]. Vulnerability and Robustness are reciprocal measures of the same thing, i.e. the ability of a building to withstand damage. A building can be said to be Robust if it can survive an event it was not designed for without collapse taking place. A Robust structure will have multiple redundancies in important structural members and will have the capacity to redistribute load to other parts of the structure in the event of a local failure. A Vulnerable structure is one that has few alternate load paths and allows a small local failure to propagate through the structure and cause partial or total collapse.

It is often hard to define the vulnerability of a structure, especially in a complex high rise building. The number of individual members involved makes it hard to judge where weak points may exist. The current method for determining vulnerability is to predict some possible extreme events (i.e. extreme wind events, major traffic accidents or terrorist bombs), remove affected members and then evaluate the remaining structure. This allows for a partial indication of the robustness of a structure in certain discrete areas. As the vulnerability is assessed as a direct result of individual events it would be impossible to cycle through all the possible damage events and therefore categorize the entire structure. Argawal *et al* [47] have studied this problem in detail and have produced a hierarchical system that allows an entire structure to be assessed in terms of connectivity. It evaluates the level of connectivity between all members in a structure and assigns a robustness value. Weak points within the structure, i.e. those locations in which there are few connections between sub-structures, can then be identified and appropriate actions taken. This system decouples the consequence from the extreme event and instead highlights areas that could make the structure vulnerable to progressive or disproportionate collapse. Due to being removed from the initiating event this system could be utilized for fire engineering as well as other low probability, extreme events.

In discussions of collapse it is rarely solely a question of the strength of the individual members. As it is the entire frame of the building that is resisting any loading it is therefore important for the members to be connected in such a way

that the frame stays effective. For ambient gravity design it is conservative to consider structural elements individually. For other load cases this simplification may not be appropriate. For example, the effectiveness and robustness of joints is an important part of the earthquake resistance of a building. Thus joint forces need to be identified and sufficient capacity allowed for to resist all load cases, including fire.

Collapse in a structure (be it partial, progressive, disproportionate or total) can be caused by any of the possible load cases. Currently such effects are only properly investigated for loading at ambient conditions, when effects due to fire loading can create similar results.

2.3 Long Span Steel Floor Systems in Fire

The investigation of single steel elements and steel frames under fire conditions is well advanced at this point using both numerical and analytical techniques [7, 19, 48, 49]. At this point most of the emphasis has been on investigating normal UB and UC sections. While these are the most frequently used structural elements in normal low-rise office type buildings, there are many different types of steel members and floor systems used. Taller and more unusual buildings often use more efficient structural layouts. In order to keep a tall building cost effective architects and designers try to be as efficient as possible by using long span lightweight flooring systems. Such flooring systems utilize strength increases available in composite construction as well as long open web beam systems. In the UK use of cellular beam sections is common as they allow services to be integrated into the structural zone of the floor. This allows the floor system to be designed with a smaller total depth. Trusses can also be used to create such long span floors, e.g. the World Trade Center towers [32, 50]. It is still not well understood what effect a major fire will have on this slender system. Currently the main design guidance available for structures in fire is based upon conventional UB and UC sections and it is not known if this is applicable to such long span flooring systems. As mentioned

previously, in Section 2.2.2, the length of beam used in testing is often considerably different to that used in practice. For long span floor beams it is common for only a 4-5m length to be tested while the commonly installed lengths range from 12m to 18m. Just as the effects of boundary conditions [51] have been seen to drastically alter the response of steel elements in response to fire so other scaling factors (such as truss height and length) could also create issues that such small scale testing might not pick up [52].

With the collapse of the World Trade Center in 2001 interest naturally arose as to the processes involved in the collapse. As the towers remained standing after the initial impact it was clear that the subsequent fires combined with impact damage to create the failure mechanism. While the towers had been extensively designed for wind and gravity loading the fire design was based on prescriptive inclusion of fireproofing.

The WTC towers were designed in the late 1960s and used what was then an innovative long span flooring system to provide large, open floors for offices. The flooring system was based on long span trusses which were then insulated by spray on, mineral fibre based fire protection [50, 53, 54]. The system was not fire tested during the life of the buildings.

With the apparent lack of information of the effect of fire on assemblies that do not involve "normal" construction methods a significant gap exists in the knowledge base. The ultimate goal of research into structures, under any type of loading, is to gain an understanding of how structures and materials react. The findings of such research may eventually be incorporated into design codes and allow better, safer and more efficient buildings to be designed. In particular, the NIST investigation [55] into the response of the towers to gravity, wind and fire loading as well as their response to the aircraft impacts is likely to guide design code development for many years to come.

One of the earliest responses published about the effects of fire on the WTC trusses came from Quintiere *et al* [56]. This paper focussed on the disparity reported in the thicknesses of fire protection between the two WTC towers as the primary reason for

the difference in times to collapse. A logical collapse mechanism was then proposed which involves the expansion of the truss and buckling of the truss diagonals leading to rupture of the truss-column connections. Failure of the connections allows the floor to drop onto the floor below initiating progressive collapse. Composite action between the truss and the concrete floor slab does not appear to have been taken into account in the formulation of the theory. While the restrained nature of the truss diagonals has been mentioned it does not appear to have been taken into account in the buckling analysis. Only material degradation is mentioned as a factor in the buckling of the truss diagonals and as such the "failure" temperature is based on this. Another correlation that is presented by Quintiere et al is based upon the prescriptive criteria of standard testing. This again links the complete failure of the WTC towers to the time taken for the steel members to attain a certain temperature. In each case the time taken to attain the "failure" temperatures is comparable to the time between the impact of the aircraft into the towers and the final collapse.

While this analysis was based upon assumptions and data that was valid at the time of writing, various data have now been published that make this particular scenario unlikely. Analysis of the video evidence compiled of the event indicates that temperatures within the building were significantly lower than the 900^oC assumed here [57]. Another problem with this theory is that it equates the failure of a single truss element to the failure of the building as a whole. Extra time is allowed for the fire to penetrate the non-fire rated ceiling tiles found in the building, however extra time is not allowed for the collapse mechanism to propagate through the fire floors. As the Cardington tests have shown, composite steel framed buildings exhibit complex redistribution of load under fire conditions that this simplified analysis cannot capture. The timeline of events presented is a logical progression from impact to collapse. However, it is the view of the author and others [58] that the simplified analysis does not provide a suitable explanation to allow for the final conclusion and that the correlation between the analytical times to failure and the timeline of the real events are likely to be coincidental. Furthermore this analysis

only predicts a "failure" criteria rather than providing a view on the actual response of the truss to fire conditions.

A detailed study of the effect of fires on long span composite floor trusses has been done by Choi [59] at Sheffield University. The main body of the work done by Choi deals with the aim of modifying a long span truss based floor system to meet the performance criteria of the standard fire test. 2D Trusses are investigated with varying loading, level of restraint and level of fire protection. The heating regimes were all based on standard test [40] fire curves and much of the discussion of results is in terms of failure temperatures related to this heating. Sheffield University's own finite element modelling program (Vulcan) was used throughout.

A significant amount of detail was given about the fire regimes and material models used in the project.

Two major local failure mechanisms were identified in this work :

1. Buckling of truss diagonals near the supports
2. Yield of the bottom truss chord at mid-span

The first mechanism appeared to have caused problems for the modelling software and was investigated by removal of the affected truss diagonals after buckling loads had been reached. As the first mechanism could produce a sudden failure it was deemed reasonable that the truss diagonal section sizes be increased until the limiting factor was the bottom chord of the truss. This would create a more ductile response that is preferred in cases of structural failure (as opposed to sudden, brittle failure) and is somewhat easier to model.

A 3D section of floor was also investigated with regard to limiting the maximum displacement in the floor. Symmetry was used to reduce the model to 1/4 of a rectangular panel. Support at the corner was theoretically provided by a column but in the model only vertical restraint was provided at this point. The edges of the concrete were assumed to be free in rotation and translation based on an interpretation of the Cardington tests [60]. This is conservative in the later stages

of the analysis as the model will be unable to support tensile membrane action over the boundaries. It may also introduce errors near the start of the analysis as it will not allow restrained thermal expansion to occur in the concrete.

The primary aim of the 3D modelling appears to have been an attempt to induce a compression ring near the boundaries of the concrete. This was done by increasing the stiffness of the supporting edge beams.

Part of the work done by Choi was a 2D recreation of the long span WTC floor trusses [61]. A model was tested using the VULCAN FE software that Sheffield University has been developing. Symmetry was used so only one half of the truss is in the model. Several cases were investigated.

- Loading of 3.9kN/m^{2}and 4.8kN/m^2
- Prescriptive 2 hour fire protection and no protection on the truss
- With a supporting column and simply supported

Eurocode material properties were used for the steel and concrete. The compartment temperature development followed the ISO834 [41] fire curve and the member temperatures were inferred using a heat transfer program.

For the protected cases little effect was seen on the trusses and over the 60 minutes of the test midspan deflection was limited to about L/100. For the unprotected cases the analyses stop at the point where a critical element buckles. Midspan deflections are about L/20. The point of failure was between 10 and 20 minutes into the analysis depending on support conditions. The difference in loading cases was seen not to produce significantly different effects, in line with previous work [7, 16].

This work helps our understanding of the local effects of heating on a truss. If a truss can be kept cool enough it will survive and react well. Buckling is seen in at least one of the truss diagonals unless the diagonal section is increased to counter this effect. Several of the restrained models show push-out of the support and catenary action toward the end of the analysis. While models were run to

determine the response of a truss after buckling of the diagonals they involved alteration of the structure and restarting of the analysis. This was not done for the WTC model, however a progression is described from the buckling of the first diagonal to the full development of catenary action. Global effects described in the work are limited to comments on the stability of connections.

Another major piece of work done on this subject was done by Usmani et al [62] at Edinburgh University. This work took a 2D representation of the WTC 18m span trusses through 12 storeys and focussed on the global response of the structure to various types of fires. The model used for this investigation may be seen in Figure 2.5. The findings of this paper were most interesting on a global scale. A possible collapse mechanism was identified that quickly led to progressive collapse of the rest of the model. As well as providing a mechanism for moving the floor loads to the columns the floors were also providing lateral restraint to the columns. As the floors expanded and displaced due to thermal expansion and bowing this lateral restraint is lost. Added to this is the pseudo static effect of the lateral displacement of the column, creating extra P-δ moments in the column, and the dynamic effect of the actual movement of the column. As the column section buckles the floors above also come down. Thus a collapse mechanism that does not require rupture of connections appears.

Usmani [63] then followed up by examining in detail the response of the floors over the course of a multiple floor fire. The data from the previous paper [62] was analysed and a further progressive collapse mechanism was identified. Simple disconnection of the fire floors would not be enough to buckle the columns until either a large number of floors had disconnected (10 or more at ambient) or the temperature of the column was raised sufficiently to degrade material properties. The tensions caused by the movement of the fire floors would lead to large compressions being generated in the unaffected floors above and below the fire floors. Lateral failure of these ambient floors would again lead to sudden, high compressions being generated in the next floors up and down the building. Beyond a certain point such a mechanism would be self-sustaining and progressive collapse would occur.

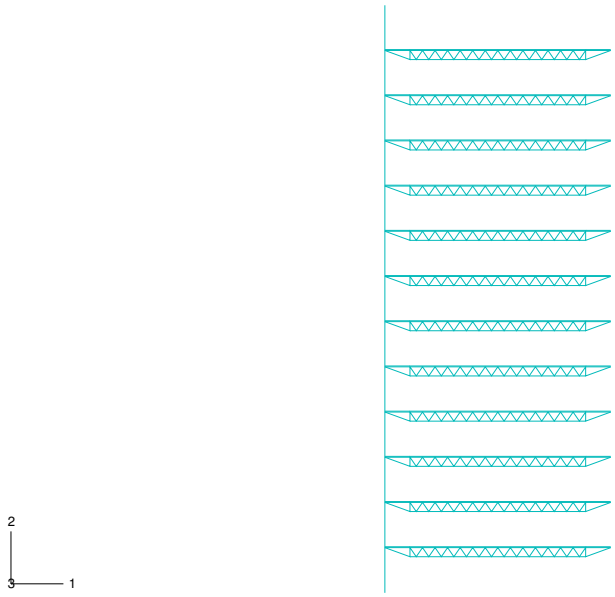

Figure 2.5: Model Used by Usmani *et al.* [62]

Thus the previous work in the subject indicates various mechanisms that need to be looked for in any analysis of long span floor systems. Local and global mechanisms must be identified and the response of the structure should be tracked for the duration of the fire or to final collapse.

2.3.1 NIST Investigation

To date the largest effort to understand the effects of fire on truss based floor systems has come from the National Institute of Standards and Technology (NIST) in the US. This group was given the responsibility of conducting the forensic investigation into the effects of the impact and fire damage on the WTC towers. A large amount of testing was also done both physically and using computational models to try and recreate the events of the 11th of September 2001. This work was done contemporaneously with the research conducted for this PhD.

The stated goals of the NIST investigation [32] were :

- To investigate the building construction, the materials used, and the technical conditions that contributed to the outcome of the WTC disaster.
- To serve as the basis for:
  - Improvements in the way buildings are designed, constructed, maintained and used;
  - Improved tools and guidance for industry and safety officials;
  - Recommended revisions to current codes, standards, practices; and
  - Improved public safety.

The full report was split into 8 sections (Projects 1-8) based on the different areas to be investigated. These areas are :

1. Original design and as built condition of the towers [32]
2. The baseline performance and response to the aircraft impact [35]
3. Analysis of steel material strengths [64]
4. Active fire protection systems [65]
5. Likely progression of fires [57]
6. Structural response and collapse sequence [52]
7. Escape and egress of occupants [66]
8. Response of emergency services [67]

A significant amount of work was done to verify the factors listed above, however only Project 6 [52] has much relevance to the results of this PhD program. Project 1 [32] was also extremely useful for verifying the layouts of the structural models used. Project 6 of the NIST report (along with the corresponding appendices [68, 69]) contains details of the analyses, both physical and computational, conducted to

examine the response of the WTC tower structures to fire. In summary, several different models were investigated focussing on smaller subsystems of the buildings and then the data gained from these models was amalgamated into a hybrid global model. The global model represented the buildings from several floors below the impact zone (a model was constructed for each tower) to the top of the roof. The data to construct the WTC towers models used by NIST is presented in Project 1 of the NIST report [32]. Much of this data had been previously released by other agencies [50, 53, 54].

Physical Testing. Physical testing of the WTC floor truss systems was undertaken as part of Project 6. As the floor system was highly innovative when it was designed there was no official rating available for it under fire conditions. Both the Architect and the Engineer of record made recommendations that fire tests should be performed on the floors but there is no record of these ever having taken place. NIST therefore recreated several portions of the floor system using original fabrication specifications in order to test them. The two main portions of the floor were the long span (18m) and the short span (10m). NIST chose the shorter span system to recreate due to ease of fit into existing facilities. Several other sections of floor were also created at half scale (length of 17 feet (5m) rather than 35feet (10m), similarly half depth of truss but same section sizes) in order to gain additional information about the ability of the floor system to retain the integrity, insulation and load bearing capacity functions measured during the standard fire resistance test [42]. The tests conducted on the full scale floor systems indicate that the original design, had it been tested, would have been deemed adequate according to the standard test with 0.75" thick fire protection on the trusses (50% thicker than the amount originally specified and half of the upgraded thickness). However it was also found that the half scale tests produced significantly better results than the full scale structure. This leads to the conclusion that had the full 18m span floor system been tested then it would have performed less adequately in the standard test than the 10m span version. Therefore care needs to be taken when applying

scaling factors to the results of standard testing of such long span floor systems. The tests were also discontinued when "imminent failure" of the system seemed likely based on deflections. Collapse of the floor systems was therefore not seen. Some interesting data can be taken from the fire resistance tests about the spalling of concrete and the heat transfer through the thermal insulation but as the fire was a standard curve then the results of these tests may be quite different from a real compartment fire. The NIST study of the fire tests includes recommendations as to factors in the tests that require further investigation, such as the effect of restraint conditions on test results and the effects of test scale.

Research [70] has already shown that the response of structures under fire conditions is intimately linked to the level of restraint available to the structural elements. The primary response in a fire is expansion of the structural elements. This is only converted into forces where restraint is available. Thus the response of a structure to fire will always be dependant on the location and the severity of the fire. This also makes it very difficult to evaluate structural members individually as the true level of restraint is hard to evaluate and may change depending on the fire regime.

Connection Models. Initial computer models included high resolution tests on the truss "knuckles" that were used to allow composite action between the truss and the concrete slab. These knuckles (Figure 2.6) were formed by the diagonal bars where they projected above the truss top chord, into the concrete, and were used in the long span floor areas where shear studs would be used today. These models replicated physical tests done on the knuckle system in 1967 and indicate failure criteria for the composite connection at temperatures ranging from ambient up to 900°C.

High resolution models of the various connections used in the WTC towers between the trusses and other elements were also investigated. Material degradation due to high temperatures was included and the connection was subjected to various types of load. Shear failure and tensile failure were identified, as was a failure of the holding bolts which, coupled with large displacements in the truss, would allow

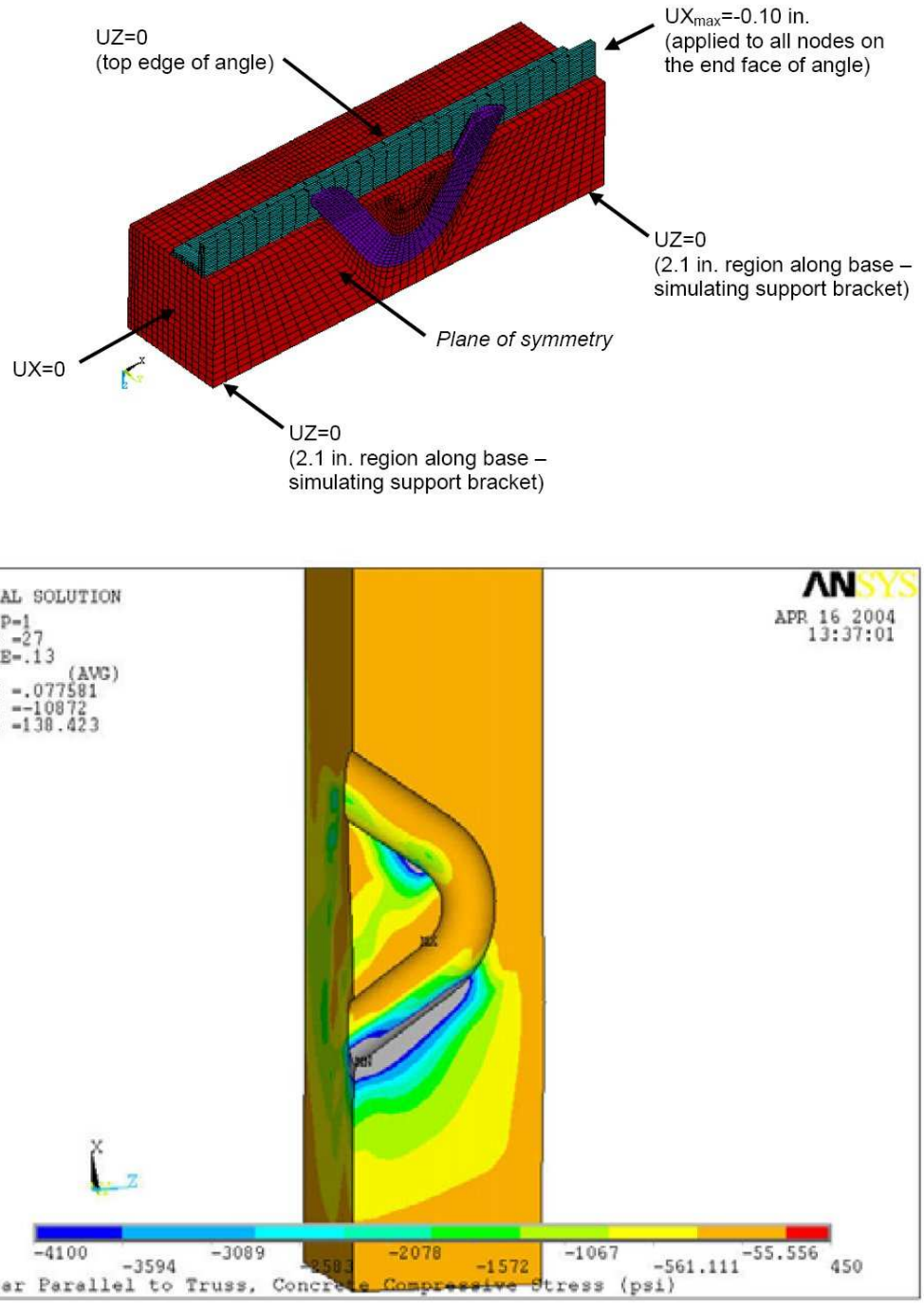

Figure 2.6: NIST Knuckle Model [68]

the truss end to "walk off" the connection seat. The forces necessary to initiate these failures were identified for temperatures ranging from ambient to 1000°C. As each truss was made up from various separate sections welded together it was possible that the connections holding the trusses together could fail. However it was found that the connecting welds were stronger than the connected sections and this mechanism was not pursued.

Single Truss Models. The initial structural model produced was of the long span trusses which made up the outer floor area of the building. This model was created with the aim of designating "failure" mechanisms that could be applied to later models. A further aim was to use this model as a basis of comparison to simplified truss models that could be used in later, larger scale models. In order to maintain numerical efficiency in the computer model only one of the twinned, main trusses was modelled along with its associated portion of slab. The model used can be seen in Figure 2.8.

The boundaries on the long sides pass between the two sub-trusses that make up the main truss (this means only one truss was modelled) and at the midspan point of the concrete. Connection into the core structure was modelled at one end while the other end was connected into half of a standard, exterior column section. The other half of the column was assumed to be on the other side of the boundary. The structure also included a horizontal "strap anchor" that led from partway down the truss to an intermediate column and provided some connectivity between the main floor structure and the columns not directly connected to trusses. A boundary was again assumed to pass through the intermediate column and hence only half was included. Multiple "break" elements were included to represent the strengths of the various connections that had been investigated, including the connections to the core and column as well as the composite knuckles. Forces in excess of that needed to fail the connections would trigger the break elements and disconnect the appropriate nodes. Full symmetry does not appear to have been applied to the long edges of the slab. Rotational restraint was included but lateral restraint appears

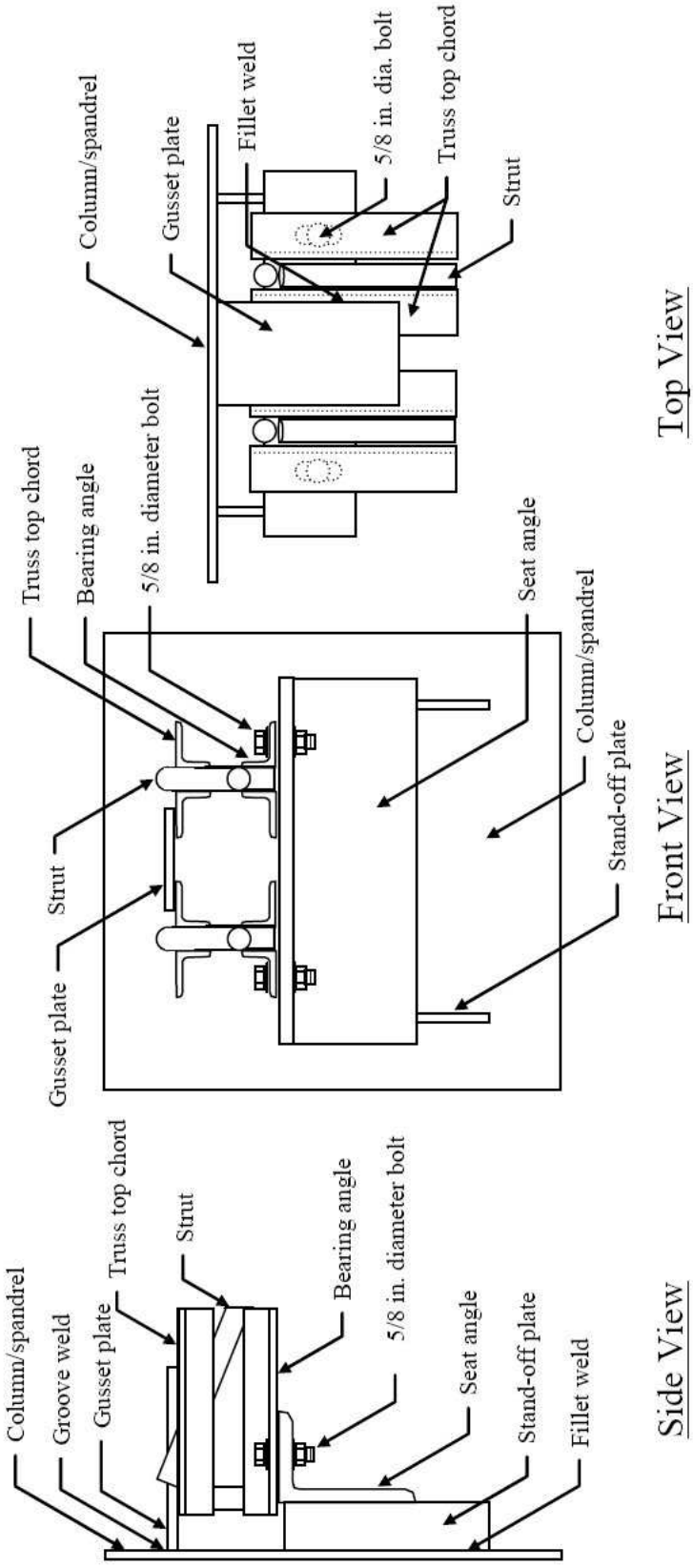

Figure 2.7: NIST Connection Detailing [68]

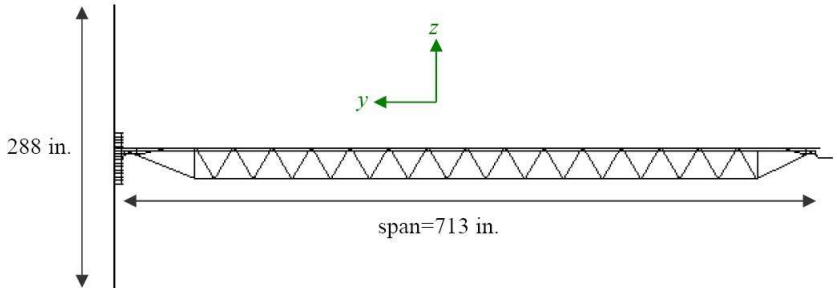

(a) Side Elevation

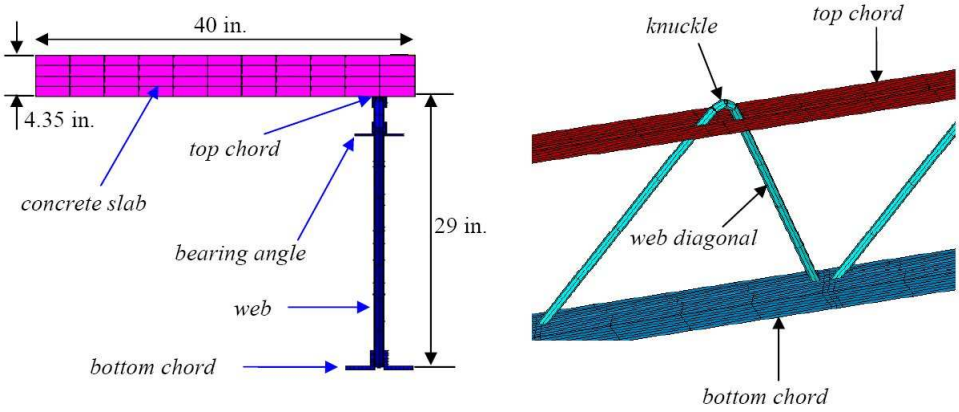

(b) Cross-section

(c) Top and bottom chords and web diagonals

Figure 2.8: NIST Single Truss Model [68]

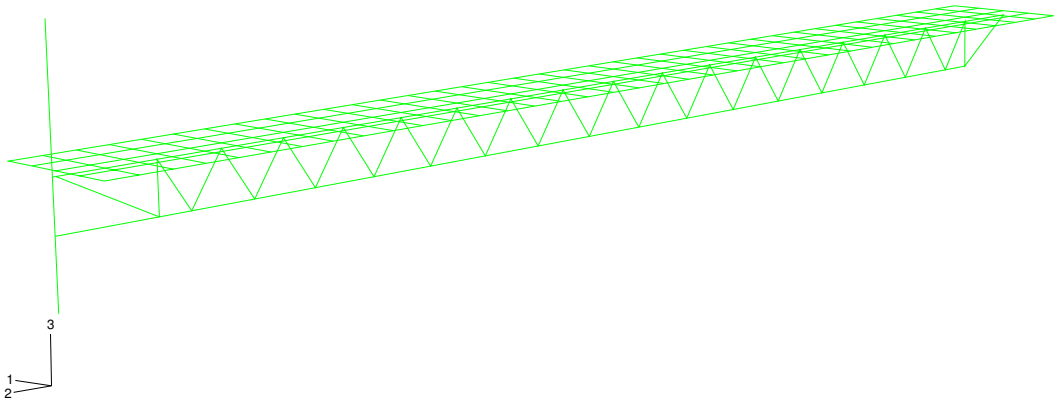

Figure 2.9: 3D Single Truss model (Chapter 3) [71]

to be absent. As the model does not include a large width of slab this should not be a major issue due to the small expansions expected in this direction. A lack of restraint to thermal expansion in the short direction of the slab may alter the response of the floor slab. Lateral restraint was supplied to the top chord of the truss.

The model used by NIST in Figure 2.8 can be compared to the model used for this research project in Figure 2.9. The major difference is that the model used for this PhD includes the main double truss as a single entity and includes the full width of associated concrete. Boundary conditions for this model are therefore different. For more detail of this model please see Chapter 3 or the published paper [71].

The visco-elastic dampers that had been installed on the bottom chord of the trusses were ignored in all NIST models as any movement caused by the fire loading would occur too slowly to activate the dampers.

The fire regime applied to the NIST model consisted of assumed time-temperature

curves applied to the various structural members. Steel temperature increased linearly from 20°C to 700°C over 1800s then up to 900°C at 2400s. The concrete slab had a linear gradient through depth with top surface going from 20°C to 300°C (at 1800s) then on to 500°C (At 2400s) and the bottom surface going from 20°C to 700°C then to 900°C. This represents a relatively small difference between the average slab temperature and the steel temperature.

The steel was modelled accurately and explicitly included the effects of creep at high temperatures. The concrete slab was included with realistic material properties but did not include any reinforcement. Also the concrete slab in this model was represented by several layers of solid elements rather than the shell elements which were used in later analyses.

The results that are presented for this model in Appendix C [68] of Project 6 include force plots from selected members as well as truss midspan and column deflections. The analysis clearly shows yielding and buckling in several of the truss diagonals and several of the knuckles fail. Due to the inclusion of failure modes for the various connections the entire truss was deemed to have failed when it walked off the exterior truss seat at a steel temperature of 730°C. There appears to have been no validation by NIST between the physical standard testing and the ANSYS models. Mention was also made of equating convergence failure of the model with collapse. It is not clear if the model was being run under the Explicit or Implicit version of ANSYS, although the creep strain in the steel is described as being calculated using an implicit time integration method. Using Implicit, or Quasi-static, formulations convergence failure can be caused by relatively insignificant local instabilities in the model as well as global scale failures and collapse.

A further simplified truss model was produced for inclusion in larger scale models. The twin trusses were merged into a single truss with element sections of equivalent areas of steel. A single beam element was used to form each sub-member. While this would normally restrict the possibility of the truss members to buckle, a break element was included to allow for this situation. The break element was set up such that it would have the full member properties before the trigger load and the

properties of the buckled section afterward. A full validation of this method was not supplied and possible errors created by this two state process have not been qualified or quantified. The knuckle connection failure mechanism was neglected for the simple truss analysis and this was justified by the similarities found when comparing the results from the two truss models. Reinforcement was again absent from the concrete as it was modelled using shell elements with a simple bilinear material model with the same strength in tension as compression. The data used in all the material models were temperature dependent.

The results of the simplified truss model were not supplied in detail. A simple comparison of the two models, showing truss midspan and column deflections was provided. The comparison of such deflections does not necessarily indicate that the same processes are happening in both models. Force plots taken from truss members and the floor membrane force may have served as a better basis for comparison. A comparison of the forces within the structure would give a better indication that the same response is occurring.

Isolated Floor Models. The simplified truss model was then translated into a series of single floor models. Individual models were produced for floors 93 to 99 (inclusive) for WTC1 and floors 79 to 83 (inclusive) for WTC2. As an example the mesh for an undamaged, standard floor may be seen in Figure 2.10. These individual models were run using a selection of damage and fire regimes as detailed in Project 2 [35] and 5 [57] of the NIST report. Again the purpose of these models was to identify failure modes for the various structural elements and to evaluate the temperature at which failure would occur.

In order to maintain numerical efficiency several sets of structural members were removed to reduce the number of degrees of freedom required. These include :

1. Deck Support Angles
2. Bridging trusses outside two-way zones
3. Spandrel studs connecting spandrel beam and the slab edge

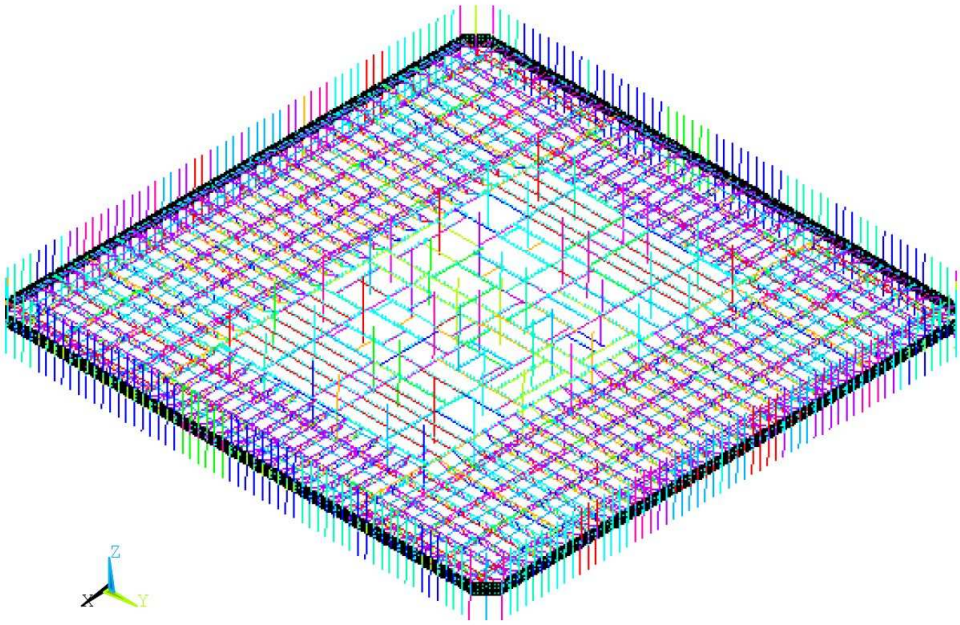

Figure 2.10: NIST Single Floor Model (Undamaged) [68]

4. Strap anchors

NIST ran an initial model and it was deemed that these elements could be removed without affecting the overall performance of the structure. See Figure 2.11 for details of the modified model and Figure 2.12 for the original location of the removed elements. During the construction of the towers a series of deck support angles was installed between the main trusses to support the slab decking while the concrete was being poured. These small members were disregarded in the floor model. The removal of these members is not likely to have much of an effect on the final response of the structure. Their small section size means that they would heat up quickly and that expansion forces would be limited. It is likely that the response from these members would be dictated by the response of the composite decking.

The bridging trusses ran transverse to the main trusses and helped distribute the slab loads back to the main trusses as well as providing lateral stability to the main truss bottom chord. These elements were removed from the areas where the main trusses have direct connection into the core. As the bridging trusses consisted

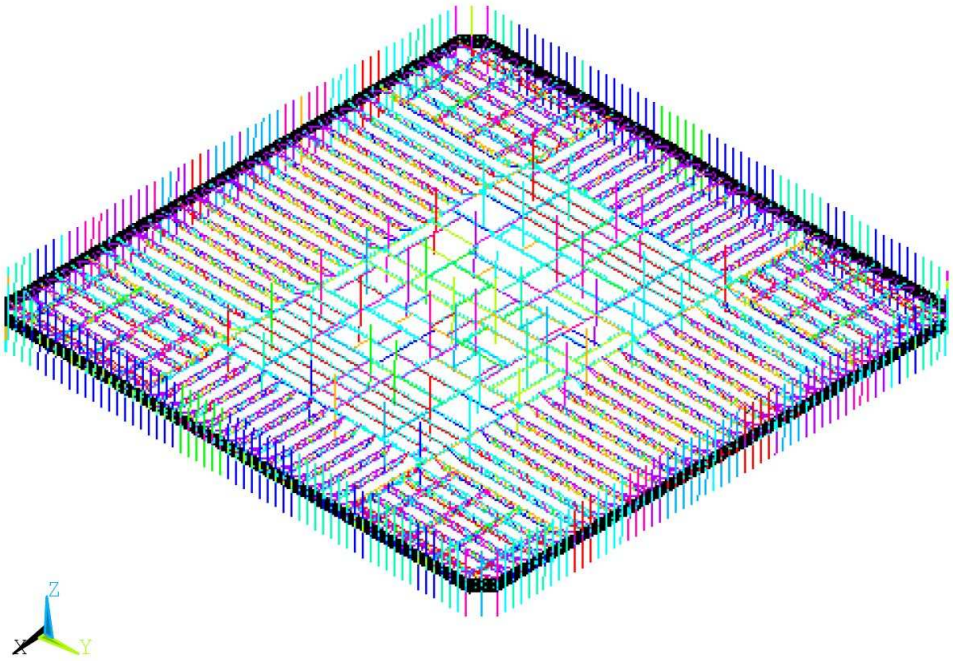

Figure 2.11: NIST Modified Single Floor Model (Undamaged) [68]

only of a single truss (rather than the doubled main trusses) NIST deemed that at elevated temperatures these members would buckle quickly and therefore not have significant impact. Some verification is reported in Project 6 that the bridging trusses did not have much of an impact. It is not clear if this was also verified using the damaged floor models as the transverse bridging trusses would have helped distribute load as well as providing some stability to the main trusses. While small compared to the main truss lines the bridging trusses were still substantial structural elements in their own right providing stability to the main trusses and supporting the floor slab. It is the belief of this author that more verification is needed before these elements can be disregarded.

The spandrel studs provided some stability to the spandrel beams by linking them to the floor slab. The failure of this linkage was not expected to alter the overall response of the structure and hence the link itself was neglected. In addition the material properties of the spandrel beams were altered to keep the yield strength below the elastic buckling strength. This may have introduced inaccuracies in the restraint available to the intermediate columns, although the slender nature of the

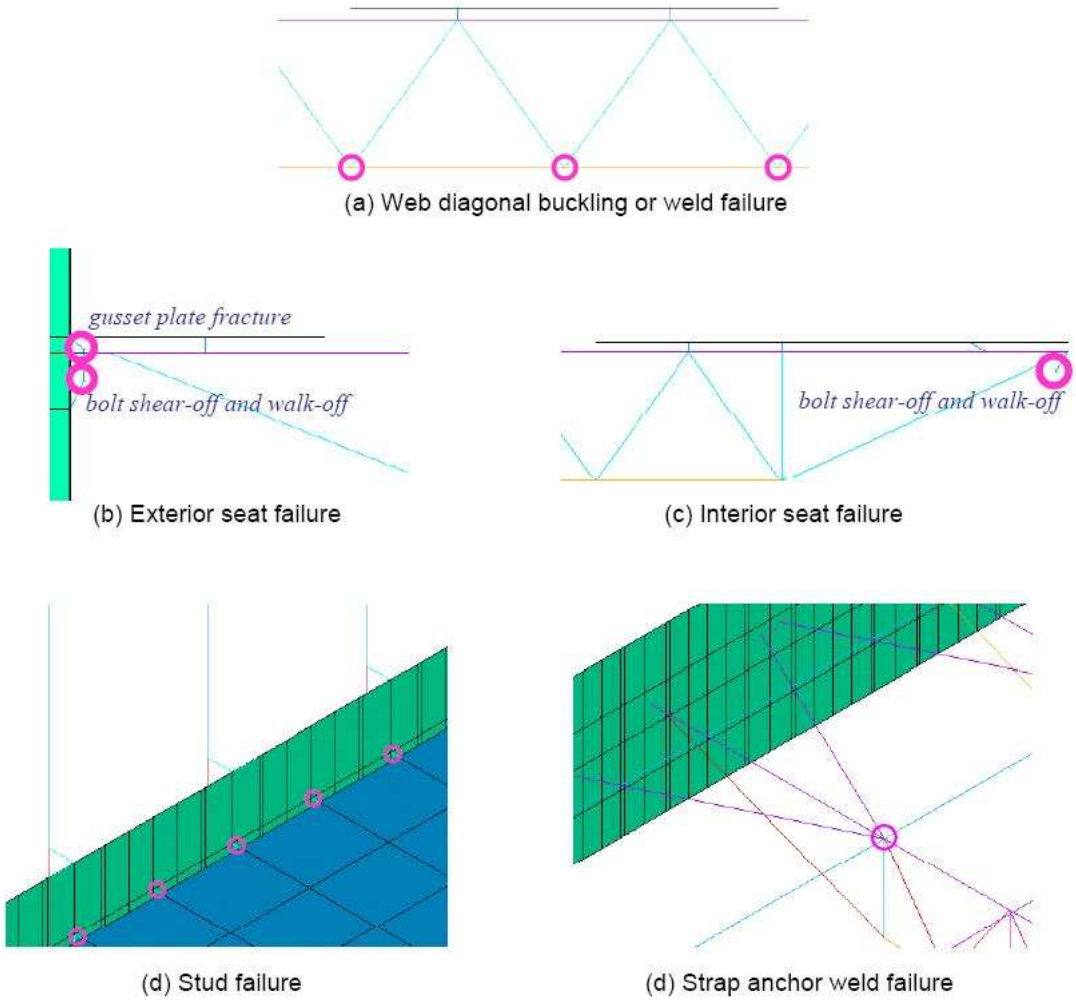

Figure 2.12: NIST Removed Elements [68]

spandrel beams means that they would buckle under relatively low load and not be able to provide much bending resistance after that point. As the altered material model was a simple bilinear model the tensile and compressive strengths are the same. This again leads to the question of whether the intermediate columns would receive the correct amount of restraint from the rest of the floor structure.

The strap anchors are the elements reported in the description of the single truss model providing stability and connectivity to the intermediate columns. The removal of these elements was justified on the grounds that the connection between the straps and the trusses, and the shear studs connecting the straps and the floor slab, were creating convergence issues. While the removal of these elements will help with convergence it also seems likely that this will isolate the intermediate columns even further. This change will also increase the forces in the connection between the main trusses and the outer columns as floor membrane forces have no other path to the intermediate columns. This may give a false indication of connection forces and thus the failure mechanisms in the floor.

As before, break elements were introduced to represent the buckling of truss diagonals as all the truss sub-elements were represented by single beam elements and knuckle failure was ignored. The visco-elastic damper on the bottom chord was also disregarded.

The boundary conditions were applied to the top and bottom of all columns. Vertical restraint was provided at column bases or at the top if the column was severed at any point below (including models of floors below). The core columns were free in horizontal translation but fixed in rotation. The outer columns were fixed in the direction perpendicular to the wall face (i.e. fixed from outward movement) but free in the transverse direction.

The results presented show clearly that the columns connected to trusses take significantly more loading than the intermediate columns. This isolation may be enough to cause errors in the distribution in forces and in the identification of the correct forces in the connections, leading to incorrect failure mechanisms.

It is indicated that the forces and displacements were taken from these individual floor models and used as a basis for lateral floor membrane forces applied to columns in other multi-floor models. Due to the individual nature of the floor models this is not a good assumption. The restraint provided to the expanding trusses from the columns will change depending on the distance from a rigid support to the floor in question. In a single floor fire a single floor model will provide the correct restraint. In a multiple floor fire the length of column acting as a spring restraint changes and the restraint from a single floor length of column no longer adequately captures the response. The level of restraint to the floor from the columns will affect the connection forces and outward displacement of the columns as well as the vertical deflections in the floor. Project 6 Appendix D [69] briefly notes this inaccuracy but it is not obvious in the text of the main report.

The results of the single floor models were used as a first approximation input into the global models which are discussed below.

Multi-floor Column Model. A further model was considered before the final work on the global model was conducted. This model involved the analysis of a detailed 9 storey length of 9 adjacent columns and their accompanying spandrel beams. Splices between columns and spandrel beams were included. This model was designed to show failure mechanisms involving the columns when subjected to loss of restraint from failed floors and from extra gravity loading. Splice failure was considered as well as buckling failure of the columns but as beam elements were used local buckling of column plates were not captured. The model was validated against a reference structural model from elsewhere in the NIST study. Results from this series of analyses indicate that the spandrel and column splice connections were sturdy enough to survive (at least partially) large forces. These forces resulted from the relative movement of the columns to which the spandrels were attached. Column instability was to be expected when multiple floors no longer provided restraint but instead pulled the column in.

Global Model. The final global models of each tower were an amalgamation of the results of previous models along with further separate models of the outer wall and the core. As the global models involved a large number of floors, steps were taken to reduce the number of degrees of freedom. First, and most importantly, the detailed floor systems, including trusses and connections, were removed and replaced by an equivalent membrane. The removal of the composite system of steel and concrete means that the effects of thermal expansion would not create realistic results. Therefore thermal expansion was ignored in the floor membrane, although temperature dependent elastic properties were included. The key failure modes that had been identified in the previous analyses were then applied as time dependent loads and disconnections representing the sagging floor and failed connections respectively. Push out of the columns, due to thermal expansion, before sagging of the floor systems relieves such lateral movement, does not appear to have been considered.

The fire-induced damage was applied separately to the thermal effects on materials. For each 10 minute period of the global analyses two separate steps were undertaken. The first would include the fire-induced damage through disconnections of some trusses from columns and application of forces to a selection of truss-column connections. The thermal degradation on the materials would then be included by the running of a second step in which the temperature was varied. These two steps were assumed to accurately represent the response of the structure over the same 10 minutes of the analysis. As both of these action on the structure vary with time it does not seem to be valid to treat them separately. Such a method will not allow the structure to perform in a realistic manner.

As the previous models had mostly included models with a single floor it was necessary to modify the fire-induced damage to follow more accurately the results of a multiple floor simulation. A further exterior wall model was investigated for each tower which included 17 storeys, over the general impact zone, and the entire length of the tower face. A trial and error set of analyses were conducted on these models in order to find a distribution of floor connection forces that would create

column displacements matching those seen in the media footage of the WTC tower collapses.

The methods and assumptions used to gain output from these global models seems much more focussed on matching results to those taken from media footage than investigating the mechanisms involved. It is assumed that if the computer model can create a similar displaced shape to that seen on the day that the correct mechanics will have been captured. This is a poor assumption, especially when major components of the structure, i.e. the floors, are not being explicitly included in the model. Additionally the assumption that the effects of thermal expansion and bowing can be applied as a set of point loads on the column separately to the effects of thermal degradation will not produce realistic results.

A key finding of the NIST report was that had the towers not been hit by aircraft, and had the structure and fireproofing not been damaged then they were likely to have remained standing under fire conditions. This case was never studied using their global model system. This conclusion appears to be mainly founded on the assumption that if the fireproofing is present then the structural steel will never reach significant temperatures over the course of a fire. If a fire burns for long enough then any level of fireproofing can be overcome as it merely increases the time the structure takes to heat up. This again leaves the issue that the response of the structure in fire is not known.

NIST Conclusions. The conclusions of the NIST investigation of the events of 11th September 2001 are split into 30 recommendations spread over 8 areas of interest defined by the report. NIST cannot make these points into code requirements but has recommended that the code writing groups take an interest and include them.

Eleven of the recommendations (grouped into 3 of the areas of interest) are structural and cover a mixture of wind, fire and progressive collapse criteria. The rest of the recommendations are directed at egress, active protections systems, procedures and practices and education. A brief description of the appropriate recommenda-

tions, with some comments, are as follows :

Group 1 of the recommendations is based on increasing the structural integrity that design codes require in a building. Consideration of progressive collapse is the focus of recommendation 1, which should move US design codes into line with other international codes (such as the UK).

Recommendations 2 and 3 focus on wind loading. The finding of Project 2 that two independent groups evaluated wind loads with differences of up to 40% was an obvious concern. Recommendation 2 calls for increased repeatability of wind tunnel tests and more consistent methods for estimating wind loading from such tests. Recommendation 3 calls for stricter limits on sway in tall buildings. The research required for this group of recommendations will be advantageous to the industry as it will allow a more consistent wind design method to be followed.

The second group of recommendations is designed to enhance the fire resistance of structures. Currently there are few differences between classification methods used for relatively low rise buildings (with around 10 floors) and tall buildings. Recommendations 4, 5 and 6 call for review and improvement of the technical basis for design and testing of structural systems and fire protection. These points are designed to aid the move from prescriptive to performance based design. The aim is to introduce into design more detailed knowledge about the risks and response of buildings to fires. While these recommendations in general provide items of interest to a performance based system there is a partial fall-back to prescriptive design in the recommendation for limitation of compartment areas. Commercial problems may also be engendered through an implied call for an increase in the use of fire resistant glazing, particularly in facades.

A detailed evaluation of the standard testing system is also recommended by NIST, as it may allow the large volume of data currently in existence to be used to predict the true response of structural systems to fire. This work should not block research into newer and better test methods however as it may not be possible for the standard test data to be used in such a way. As well as the structural testing there is a call for the testing methods of fire protection to be reviewed, especially

for Spray-applied Fire Resistive Material (SFRM) type protection (this was the primary type of fire protection applied to the WTC tower trusses). This will allow greater knowledge of the response of such materials to loading and events of all types.

The final recommendation (number 7) in this group calls for the inclusion of a "structural frame" approach to fireproofing. It calls for design codes to demand that structural members connected to, and supporting, columns be protected to the same "fire resistance rating" as the columns themselves. This appears to move back from the general call for performance based design as it implies a prescriptive, blanket increase of fire protection on certain members. More focussed, performance based objectives may have served better in this case.

The final group of structural recommendations (Recommendations 8 to 11) are focussed on providing performance based objectives for designing new buildings and providing retrofits for existing buildings. This includes research into new materials for both structural members and fire resistive materials. The recommended objective is to allow a structure to survive to burn-out in an uncontrolled, natural fire without partial or global collapse. Standard methodology for identifying critical structural locations and suitable fire scenarios have yet to be introduced. Suitable tools will also need to be evaluated for structures under fire conditions.

These design tools should also be supported with the most accurate data possible regarding material properties under elevated temperatures. A performance based framework for such methods is essential as it would allow safe, efficient and controlled access to new materials and technologies as they are deemed suitable and become available for use in construction. Another aspect that needs to be addressed with regard to the recommended move toward performance based design is education. The engineers and designers using the new tools and methods will need to be properly educated in their use and, possibly more importantly, their limitations. As performance based design allows for highly efficient designs, with little unassigned reserve capacity, a competent user is required to ensure that the correct methods are being followed. Similarly the regulatory bodies enforcing the design

codes need to understand fully and comprehensively how they may be applied.

Already in the UK fire engineering consultancies are being asked about their compliance with the NIST recommendations. This indicates that these recommendations will have an impact on the worldwide development of building codes. It is important that any advances or changes to current design methods, based on the NIST recommendations, are considered properly and implemented intelligently.

2.4 Conclusions

The current methods for designing structures for various load cases have been described. In particular the difference between the current methods for designing for ambient load cases and designing for fire should be noted. As computational tools become more powerful, design for fire should be included in the structural design in the same way as other extreme events, such as wind and earthquake loading.

The current state of the art in structural fire safety research has identified important phenomena that the current building design and regulation system do not take into account. The work done on the Cardington frame, in particular, has highlighted the limitations of the current standard testing regimes. Such testing is done on "normal" structural elements, such as 4-5m UB and UC sections, and is then applied to the design of modern, long span floor systems. It is not yet clear if this is valid and indications are that the span of a section (or floor system) will have a significant effect on the global response of a structure.

Recent work highlighting the response of long span, truss based floor systems has been described. This work can be compared to earlier work conducted on other types of structural system highlighting the differences and how this might alter the design of such structures. Particularly the work conducted by NIST contemporaneously with this program of research has been evaluated. The detailed sub-structure models produced by NIST have the potential to provide interesting results on the

effect of fire (and structural damage) on such structures. The final, global models, however, are structured in such a way that analysis of the general effect of fire on a building is impossible. Some work on the subject has focussed on the local response of the truss and then theorized how this might propagate throughout the rest of the structure while a small amount has been done on more global effects.

The 30 recommendations for design presented in the NIST report on the collapse of the WTC towers include 11 focussing on structural issues. NIST supports a move to more performance based design systems but until such systems are fully realised a blanket increase in fire protection is recommended for certain members. Until now slabs and beams could be protected at a lower rating than the columns they connect to. NIST recommends that a "structural frame" approach be followed and that any structural member connecting into a column is rated at the same level as the column. This will give a short term gain in fires as it will delay the heating of the critical structural elements but it will not stop thermal effects completely. Thus research into the effects of heating on a structure are absolutely critical to allow the proper design of buildings for fire.

Chapter 3

Local effects of heating on long span trusses

This chapter reports on an investigation of the effects of heating on a long span truss floor system. The ABAQUS finite element package is used to model the structure including fully non-linear behaviour and thermal expansion effects. Different boundary conditions and heating regimes are investigated to understand the response of the truss members to fire. The effects of heating on the lateral restraint available from the slender floor systems to a column have also been studied. The results and analysis indicate that composite truss flooring systems may not fail as suddenly. Individual member buckling seems to be a much more gradual occurrence linked to material failure and expansion based geometry change rather than sudden "failure".

3.1 Introduction

Much research has been and is currently being done to try and recreate accurately the effects of fire on structures, including the effects of redistribution within the structure and the associated changes in load carrying mechanisms [1, 7, 13]. This work has mostly focussed upon the most common and simplest structural forms

currently used. As such most of the research to date tends to involve Universal Beam (UB) and Universal Column (UC) sections in standard grid formations of 6-9m spans.

In the aftermath of the events of 11th September 2001 it has become more apparent that other structural forms need to be investigated under fire conditions. Modern tall office buildings, especially, are using structural designs that are distinctly different from the more common forms of 9m spans of UBs on a standard column grid. Such buildings often incorporate long span, slender floor systems to maximize the lettable area without columns interfering with the space. Typical systems include cellular steel beams or trusses composite with the floor slab

This chapter reports on an investigation of the local effects of heating on a long span truss floor system. Different boundary conditions and heating regimes are investigated to understand the response of the truss members to fire. The effects of heating on the lateral restraint available from the slender floor systems to a column have also been studied.

The ABAQUS finite element package is used to model the structure including fully non-linear behaviour and thermal expansion effects.

3.2 Model Description

The results in this chapter are based on 2 different structural models created and analysed using the ABAQUS Finite Element Analysis software. The first is a 3D model of a single 18.5m long truss acting compositely with 2m width of concrete slab above. A pinned connection into a column is used as support at one end of the truss, the other end is free to rotate but restrained from translation (assumed to be connected to a rigid core structure). The second structural model is a 2D representation of a substantial portion of a long span composite truss frame building. It shows a slice through the full width of the building under investigation and includes several floors. The truss systems used in the 2D model are equivalent to the truss in the 3D model.

Member	Truss Top	Truss Bottom	Truss Diagonal
Size	95x38mm	130x38mm	40mm Dia.

Table 3.1: Truss Member Section Sizes

3.2.1 Structural Details

3.2.1.1 Material Models

In both of the models non-linear material properties have been used for steel and concrete using material models native to ABAQUS. For more details on the material models used in this research project please refer to Appendix A. For ambient steel a standard elastic-plastic relationship has been used with steel strength as $300N/mm^2$. Eurocode [72] properties have been used for steel at high temperature. The concrete is assumed to follow a "Damaged Plasticity" type model which is included in ABAQUS [73]. The concrete has been modelled as $30N/mm^2$ lightweight concrete. Standard Eurocode [74] properties have also been used for this material.

3.2.1.2 3D Single Truss Model

The 3D Single Truss model is intended to represent the basic assembly used to support long span floors in multi-storey high rise buildings similar to the World Trade Center towers. The long span, lightweight truss system allows a large area of floor to be supported with few internal columns. Figure 3.1 shows the model mesh used while Figure 3.2 shows the dimensioned general arrangement. All connections have been assumed to be indestructible.

Table 3.1 indicates the member sizes used in the truss :

All truss members have been represented using 3D linear beam elements. A slight imperfection has been applied to the truss diagonals as a sin curve with a maximum out of plane displacement of 1mm at the centre of the 900mm long member.

In the 3D model used in this investigation the slab is modelled as a 100mm thick slab of lightweight C30 concrete. Reinforcement has been included as a welded

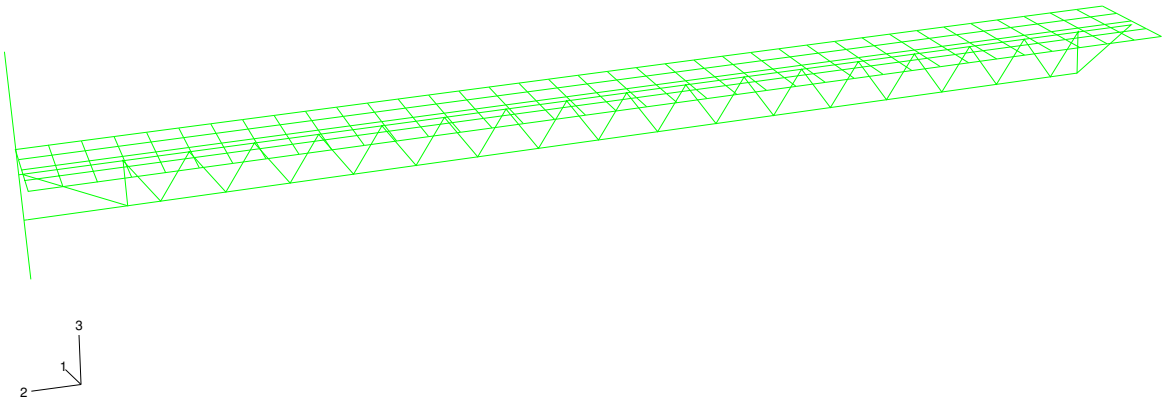

Figure 3.1: 3D Model Mesh

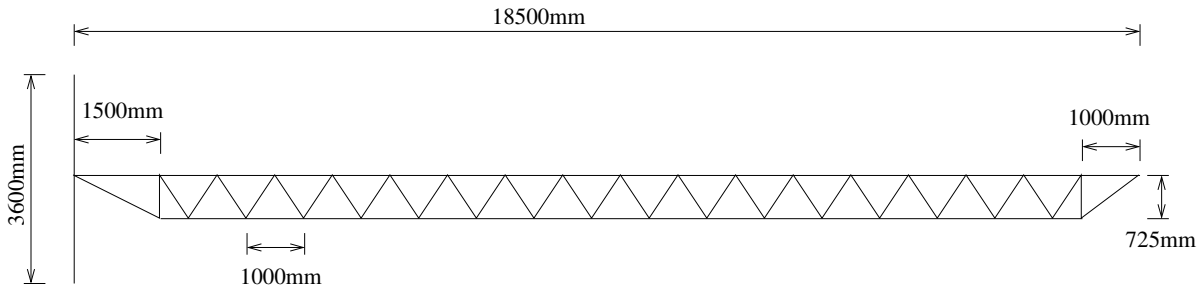

Figure 3.2: 3D Model General Arrangement

wire fabric mesh of 6mm bars at 100mm spacing in both directions. A layer of this mesh exists in both the top and the bottom of the slab. Typically these slabs would be cast on a profiled metal deck but the effect of this has been deemed negligible [7, 16]. Any significant heating of the underside of the slab would quickly cause the deck to debond from the concrete due to differential thermal expansion. Any deck has therefore been ignored. The slab is connected to the truss to allow composite action to take place.

The column is a 700x350mm box section with the long sides (parallel to Axis 1) made up of 6mm thick plate while the short sides (parallel to Axis 2) are 12mm thick. The conversion from the original column size to this new section can be seen in Figure 3.3. This change was made to represent the high density of columns around the perimeter of the building that would support the gravity loading while not altering the out of plane stiffness of the column line.

Boundary conditions in all the models were designed to represent a realistic link into the structure around them. The concrete slab was fully fixed in translation and rotation at the connection into the core representing the continuation of the slab into the rest of the building. The slab was subjected to symmetry boundary conditions along the long sides and left free at the column end to represent the edge of the building. No direct connection was made between the concrete slab and the outer column as all interaction is assumed to occur through the composite connection to the truss top chord. The upper chord of the truss is pinned into the column and into the core. The lower end of the column has been fixed in all translations and rotations while the upper end is fixed in all rotations and in horizontal translation. It can, however, move vertically. Additional loading has been applied to the top of the column to represent a number of floors above. Horizontal restraint has also been provided to the main trusses at the points where transverse trusses in a real structure could have been connected.

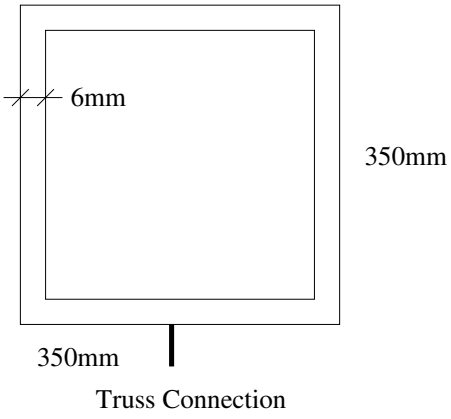

(a) Original Column Section

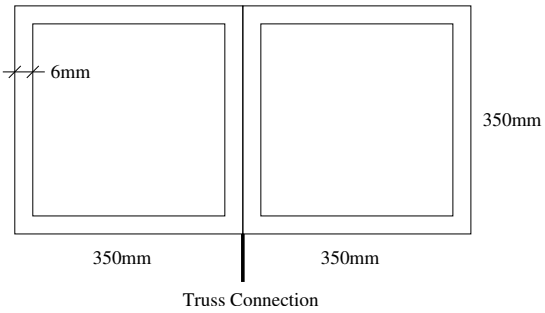

(b) Two Columns Side by Side

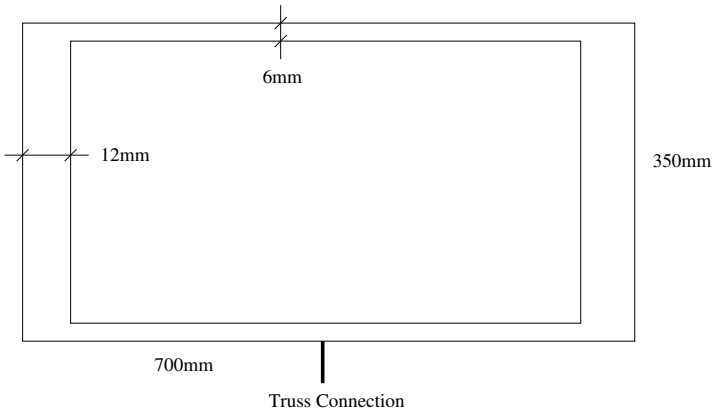

(c) Column Section Used in Model

Figure 3.3: Column Section

3.2.1.3 2D Multi-floor Model

The 2D model was included in this study in order to investigate the response of the truss when it is placed within a full structure, albeit a slice of it. It is included in this chapter to investigate how the local response changes between models. The model used in this part of the investigation comprises 12 storeys over the full width of the building. Figure 3.4 shows the model used for this part of the analysis. This model was based on the same data as for the 3D model described earlier. The 2D model includes the core area of the building, which was constructed using rolled steel beam sections spanning between columns. The beams used in the core of this model are all 406x178x54UB sections. The core columns have all been assumed to be built up sections with 400x50mm flange plates and 300x30mm web plates. These sections were chosen based on the assumed building loads. A load ratio check was made to ensure that the core members would not be too stiff. The members were evaluated by comparing the moment caused by the fire limit state loading (0.8 x Live + 1.0 x Dead) to the ambient capacity of the section [39]. A value of around 0.6 is generally considered to be acceptable. The slab in the core is 125mm thick and contains the same level of reinforcement as the outer slab, that is 2 layers of 6mm wire mesh at 100mm spacing in both directions, one each top and bottom. The bottom of the columns have been fully fixed in rotation and translation. Additional loading has also been applied to the top of the columns. As in the 3D model this is in order to represent appropriately loaded floors above the level of the main floors included in the model. The tops of the columns have been fixed in rotation and horizontal translation but are allowed to translate vertically.

Note : The 2D model is, in practice, modelling a structure that is infinitely long and that has major core framing every 2m. This creates a core that is significantly stiffer than it would be in a 3D model of the whole structure. However it allows a truss system on multiple floors to be modelled relatively easily.

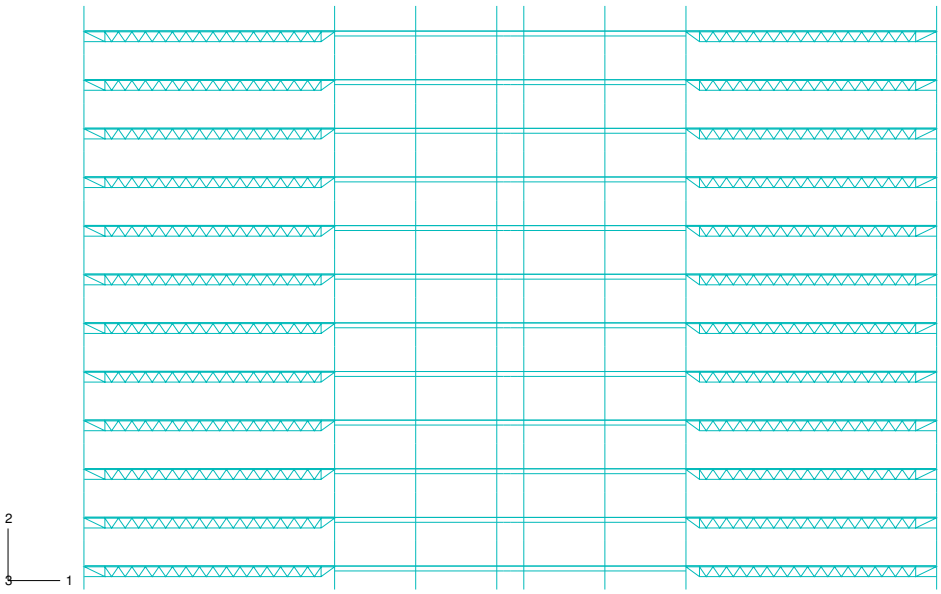

Figure 3.4: 2D Model Mesh

3.2.2 Fire Input

The compartment temperatures are based upon a generalized exponential curve given by :

$$T(t) = T_o + (T_{max} - T_o)(1 - e^{(-at)}) \tag{3.1}$$

where T_{max} and T_o are the maximum and ambient compartment temperatures respectively. t represents the time over which the model is analysed. a is an arbitrary 'rate of heating' parameter. 4 different fires were investigated with compartment temperature profiles shown in Figure 3.5. The 500^{o}C, 600^{o}C and 800^{o}C fires all had $a = 0.005$. This creates a compartment fire with a rapid temperature increase coupled with a period of stable temperature. The 800^{o}C Slow Fire profile is based on a= 0.001 which produces a longer heating curve with no steady state period. Example temperature time distributions, under the 800^{o}C fire, for unprotected truss and protected column elements as well as the 100mm thick floor slab may be seen below in Figure 6.6. Due to the nature of A.1 any alteration to either the a

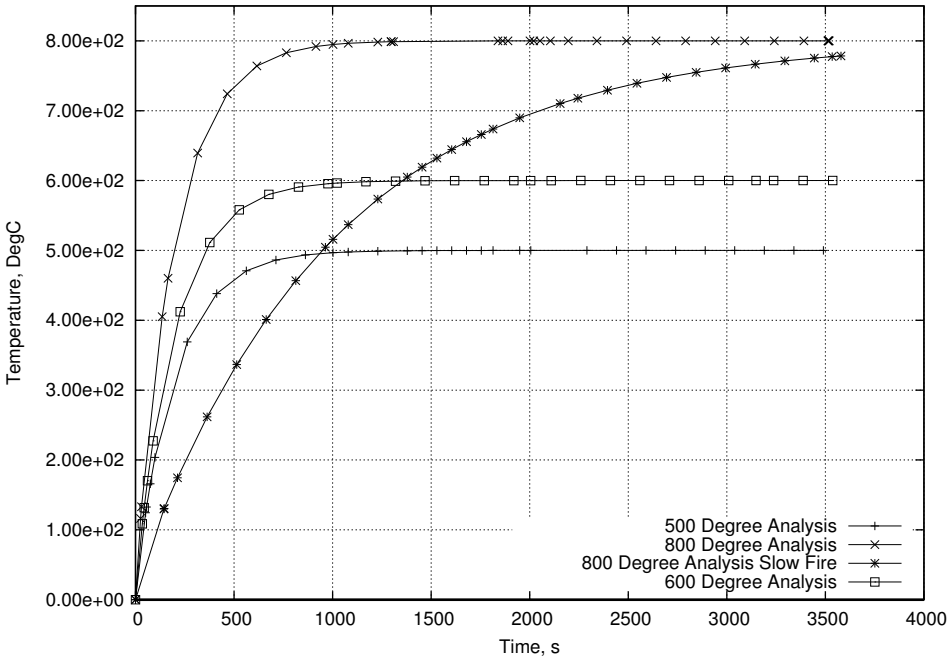

Figure 3.5: Steel Temperature-Time Plot Comparison

value or the maximum temperature has implications on the rate of heating.

The truss is assumed to have no protection and is therefore assumed to equal the compartment temperature. The column is assumed to be protected with a fire rated material and therefore undergoes more limited heating (see Figure 6.6 for details). In addition the external columns are also in contact with the outside atmosphere which would result in a lower temperature.

In all the models the temperature distribution in the concrete slab is described by applying individual time-temperature curves to 5 different points through the depth of the slab. The points used are the top and bottom surfaces, the quarter points and the mid depth of the slab. The time temperature distributions used in this study were taken from a 1D heat transfer analysis [75].

In the case of the 3D model the above fire regime was applied as if the fire existed on the floor below that being modelled. The slab was assumed to be a compartment boundary hence only steel below the slab would be affected by the fire. The slab temperature distributions were created as if it was heated from beneath only.

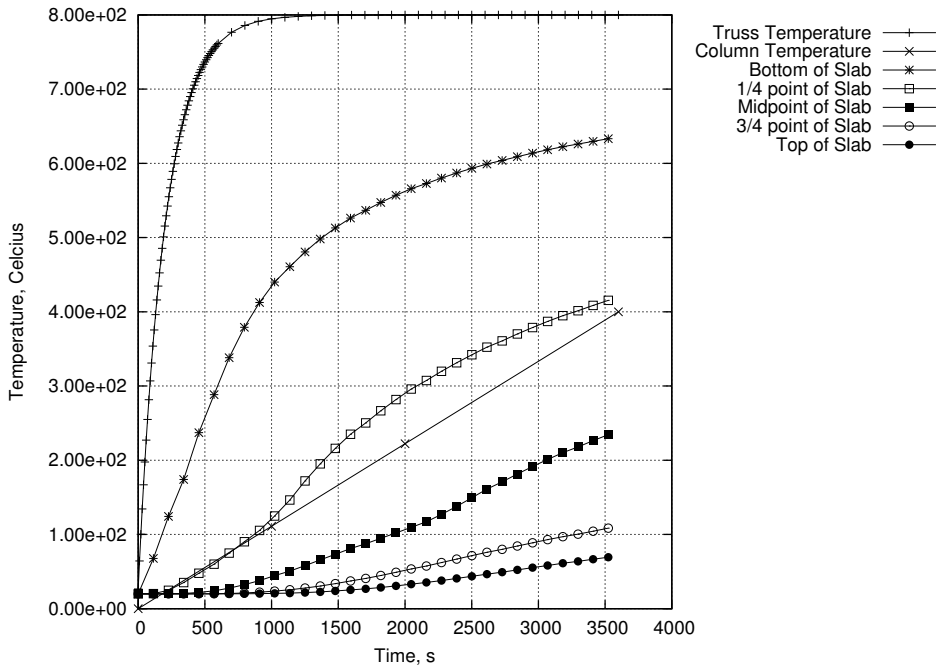

Figure 3.6: Temperature-Time Distributions for 800^{o}C Analysis

In the 2D model the fire regime was applied to 3 floors at the midheight of the model. The structural members affected are the outer columns, the trusses and the areas of concrete slab supported by trusses. The core members were kept entirely at ambient conditions on the assumption that integrity of vertical compartmentation was maintained.

It has been assumed that the top side of the slab on each fire floor was likely to be extremely well insulated by floor coverings and suspended floor systems. This will therefore stop most radiation from a fire above reaching the floor slab itself. Little heating will be induced by convection either, due to the fact that hot gases will naturally rise to the top of the compartment. Therefore, the heating of the floor slab in the 2D model has been assumed to take place from beneath only, even when there are fire compartments above the slab.

3.3 Discussion of Results

In all the models described in this report a two step analysis system was used, unless stated otherwise. The first step is a loading step included to allow the structure to be correctly loaded before any heating. The second step is a temperature loading step in which the various structural members are subjected to the fire regime(Figure 6.6). The main comparisons were made between a case where the steel retains much of its strength and a case where the steel has very little strength. The former case was realized with a regime using 500^{o}C as a maximum compartment temperature. This would induce a moderate amount of thermal expansion (of around 0.7%) while the steel retains around 80% of its ambient strength and 60% of its stiffness. The latter case used a maximum compartment temperature of 800^{o}C. This creates a larger level of thermal expansion (around 1%) and produces significant material degradation with the steel retaining only around 10% of its ambient strength and stiffness.

In addition to these primary fire regimes two others will be reported. The first involves a 600^{o}C maximum compartment temperature and is a case placed midway between the extremes to verify the results. The second is a slow rising version of the 800^{o}C fire. In this way the effect of a large change in the rate of heating can be investigated.

In general the graphs in this chapter show time related data. Data plotted against compartment or steel temperature would give misleading results after 1000s as the temperature becomes constant at that point. Comparisons between the 500^{o}C and the 800^{o}C analyses will often be made in terms of temperature to create a point of reference.

A distinction is made between catenary and membrane action. Catenary action is used to describe trusses when material degradation and large displacements allow them to act as a draped tensile member in a similar manner to normal UB sections under such conditions. Membrane action is used to describe the response of the floor slab. Although the models described in this chapter are not far removed

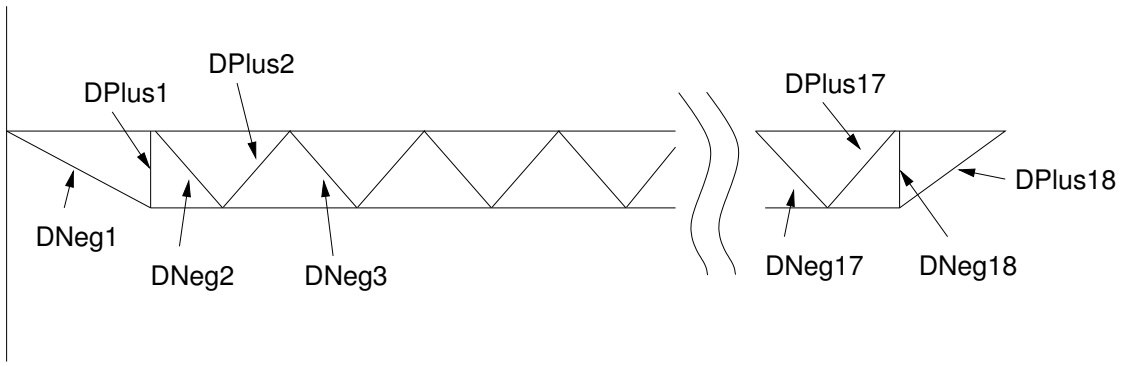

Figure 3.7: Diagonal Labelling System

from a 2D analysis they do include the slab as shell elements and hence membrane action is a more appropriate description. Catenary/membrane action is used to describe the response of the floor system as a whole as the composite nature of the construction makes use of the combined strength of the slab and truss.

3.3.1 3D Single Truss Model

3.3.1.1 Local Response of Truss

This part of the report deals with the responses of the single truss model to the two different fire regimes described previously. The response of the 500°C analysis will be presented first. The force responses of the various truss members may be found in Figure 3.8. The plots for the truss diagonals have been split into D+ (DPlus) and D- (DNeg) groups. These relate to the direction of their slope as seen in the diagram in Figure 4.6. The diagonals in each group have been numbered sequentially from left to right.

As can be seen in the force plots in Figures 3.8 and 3.9 and in the deflection plot in Figure 3.10 the truss reacts suddenly to the initial sharp heating gradient of the fire curve and then stabilizes as the truss steel temperature levels out. Because it is highly restrained by the concrete slab the top chord (Figure 3.8.a) expands against the restraint and begins to yield at about 120°C. The axial force in the other truss members also peak at this point and then drop off sharply. However this does not

seem to be linked to the same kind of sudden unrecoverable buckling failure that is seen in the top chord. As can be seen in the force plots for the diagonals (Figure 3.9.a and b) and the bottom chord (Figure 3.8.b), after the initial peak and trough the members start to come under increasing load again. This indicates that these truss members have not buckled hence the system does not immediately move into catenary action. This last item is backed up by the fact that the top truss chord never goes into tension. If tensile membrane action were to occur in the slab then the elongation of the slab would overcome the compression in the top chord caused by expansion and the top chord members would go into tension. Hence the slab has taken over the compressive loading normally seen in the top chord and is therefore effectively the top chord of the truss.

The deflection plot in Figure 3.10 also indicates that sudden buckling failure does not occur. After an initial phase of rapid deflection the truss deflection rate drops dramatically. This is because the steel has reached its maximum temperature and is no longer expanding. All further deflection will be driven by the slab which is still heating up. As the steel only reaches 500^{o}C it still has 60% of its elastic modulus and 80% of its strength left and can therefore resist the slab movement. The linear increases in axial force within the truss diagonals and bottom chord support this.

The 800^{o}C analysis produces very similar trends to the analysis presented above. The results from the 800^{o}C analysis may be found in Figures 3.10, 3.11 & 3.12. The initial heating stage (i.e. the first 1000s) for the 800^{o}C analysis proceeds similarly to the 500^{o}C analysis. The initial peaks in both analyses occur at a truss temperature of about 300^{o}C and reach similar force levels. As the steel heating rate reduces the truss cannot sustain the same forces in the higher temperature analysis due to increased thermally induced material degradation. Extra deflection caused by the continued heating of the slab cannot be resisted by the truss and the truss diagonals begin to buckle at about 900s into the analysis (around 790^{o}C). The buckling starts at the most highly loaded diagonal (DPlus 2 from Figure 3.12) and spreads along the beam as time progresses. This first diagonal is the same as that predicted by Choi *et al* [61] however, after the initial buckling, sudden failure

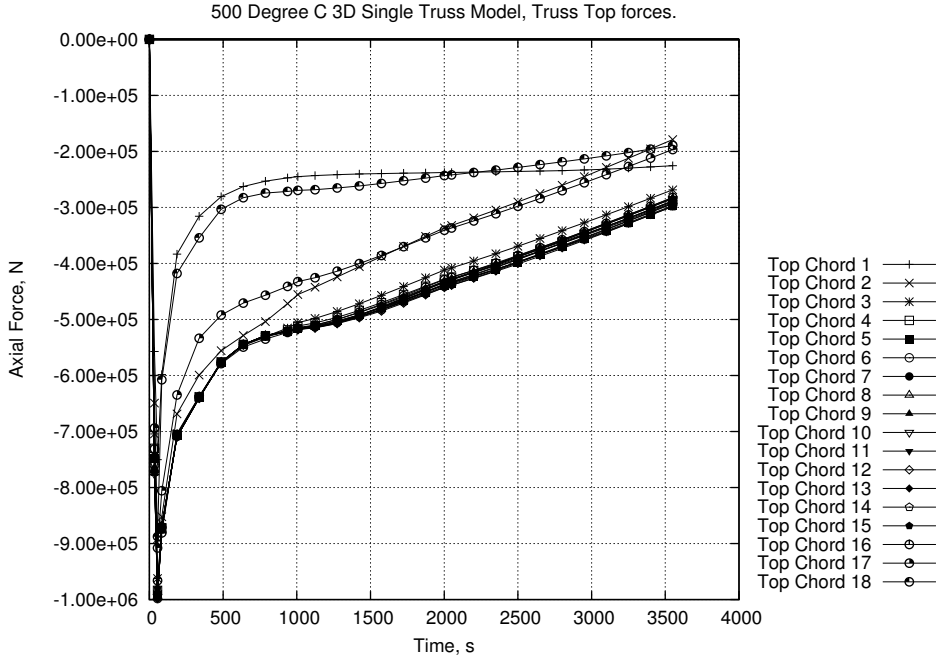

(a)

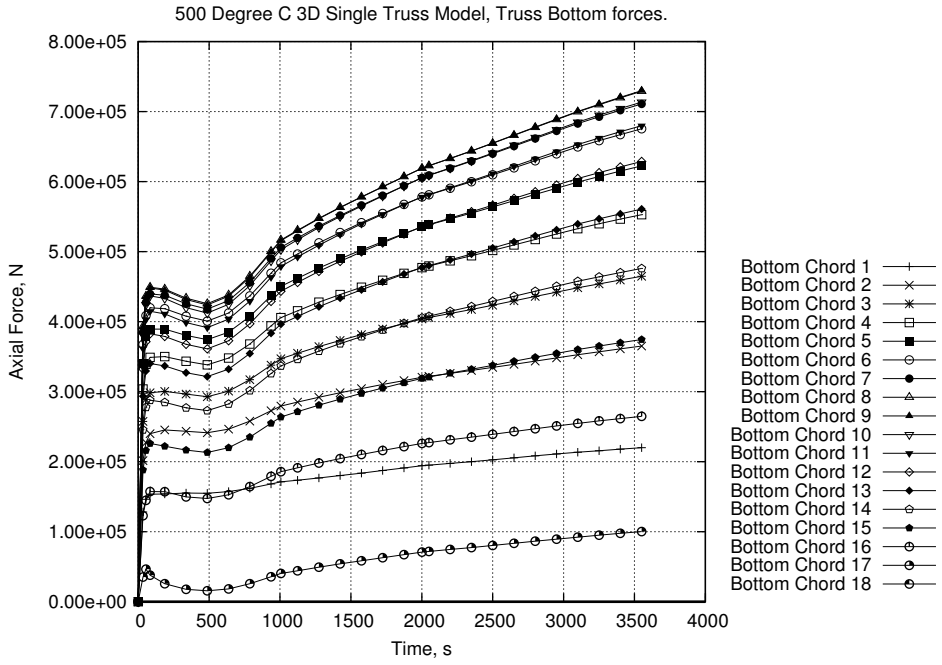

(b)

Figure 3.8: Truss Chord Axial forces, 500^{o}C Analysis

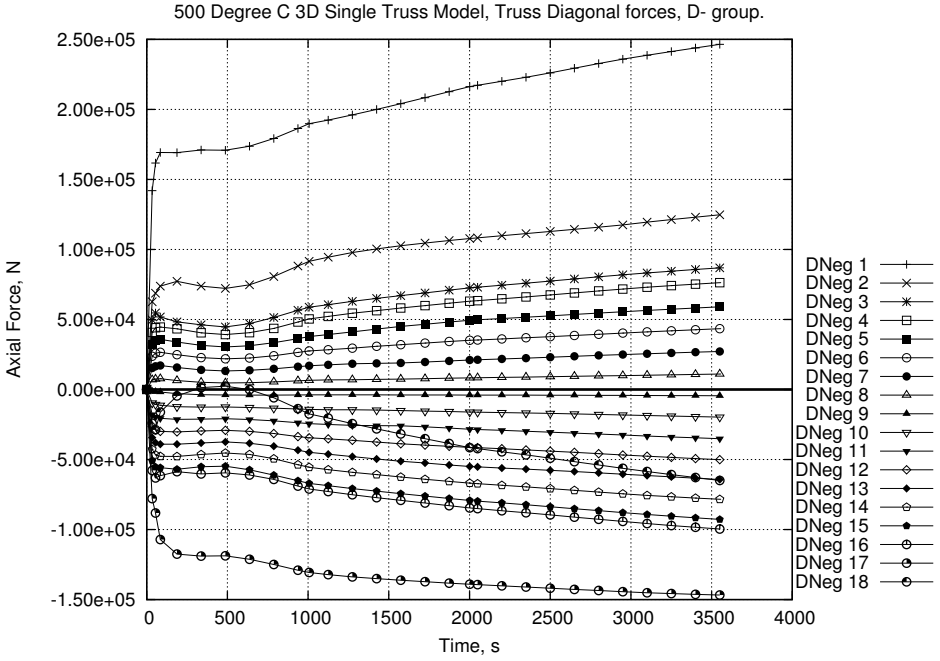

(a)

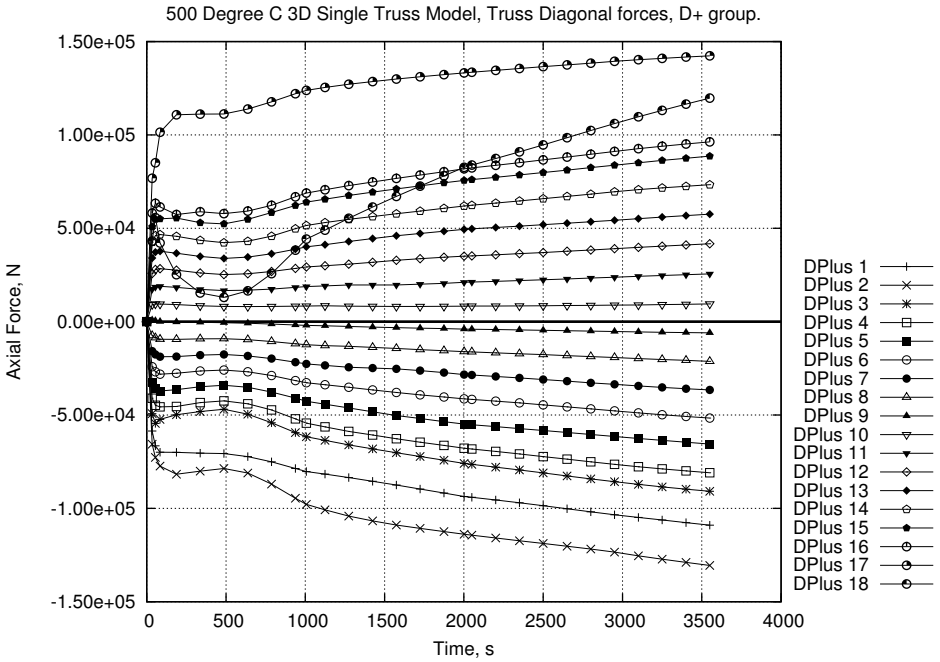

(b)

Figure 3.9: Truss Diagonal Axial forces, 500^{o}C Analysis

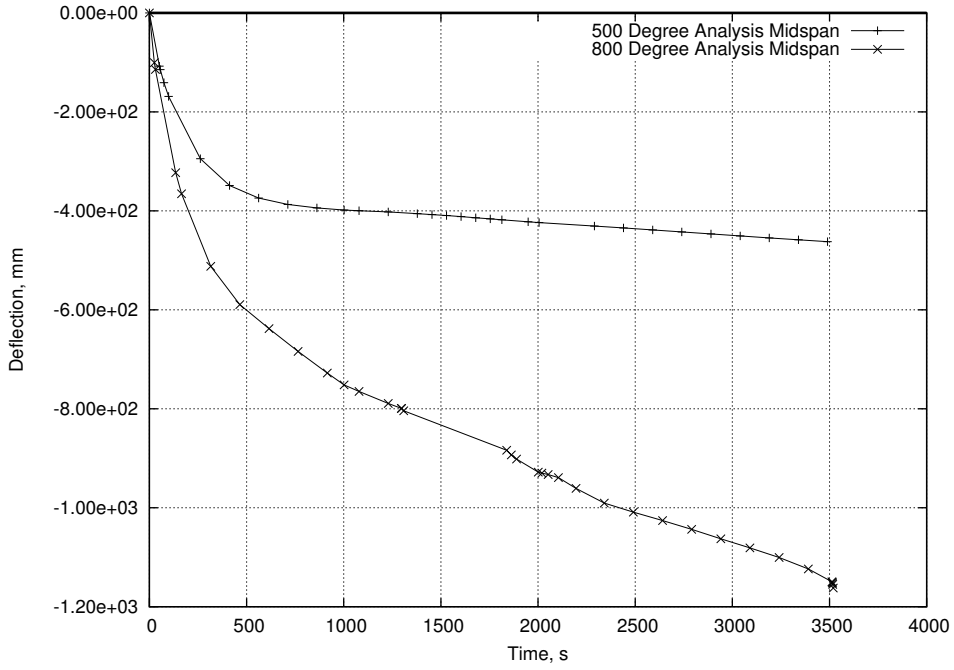

Figure 3.10: Midspan Deflection

of the truss as a whole does not occur as predicted by this paper.

As can be seen in the deflection plot (Figure 3.10) this failure of the truss does not drastically affect the midspan displacement rate for the 800°C analysis. This is because the floor system has already moved into catenary/tensile membrane action and therefore it is the slab which is determining the rate of displacement. By this point the truss is too weak to withstand the extra vertical movement caused by the expanding slab. Figure 3.13 shows the horizontal membrane force that the floor is applying to the column. At the point where the truss diagonals begin to buckle (around 1000s) the floor has already been in tension for about 750s. The reduction in tension (and increase in compression in the cooler analysis) in the connection to the column is because of the continued heating of the floor slab. This will induce extra horizontal expansion as well as vertical displacement at the midspan of the truss.

In the 800°C analysis catenary action is observed in the truss as the whole of the top chord goes into tension, as does the floor membrane force. The 500°C analysis does not show this behaviour. Indeed the forces observed to be transferred into

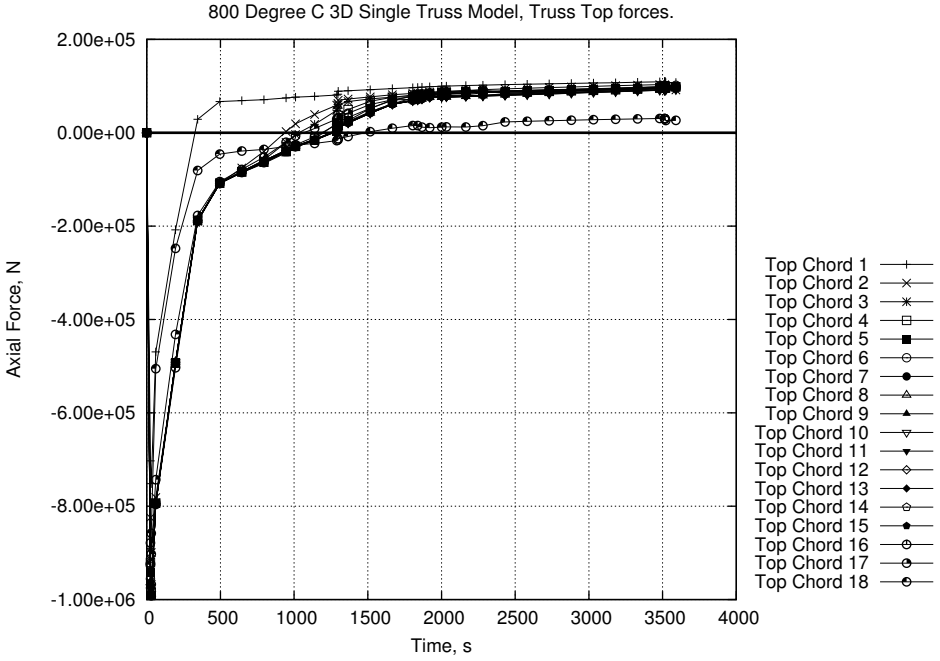

(a)

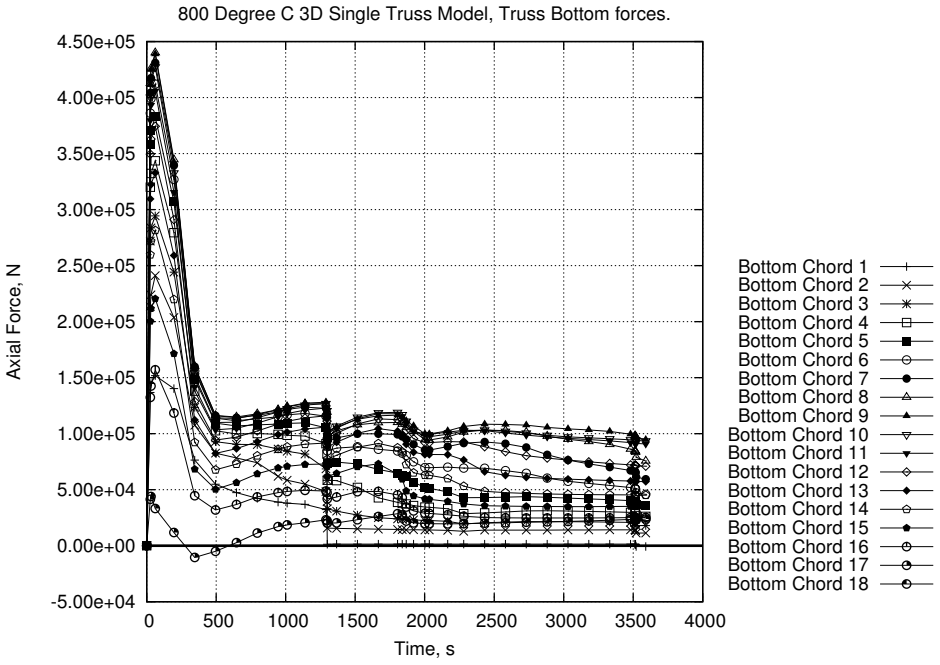

(b)

Figure 3.11: Truss Chord Axial forces, 800^{o}C Analysis

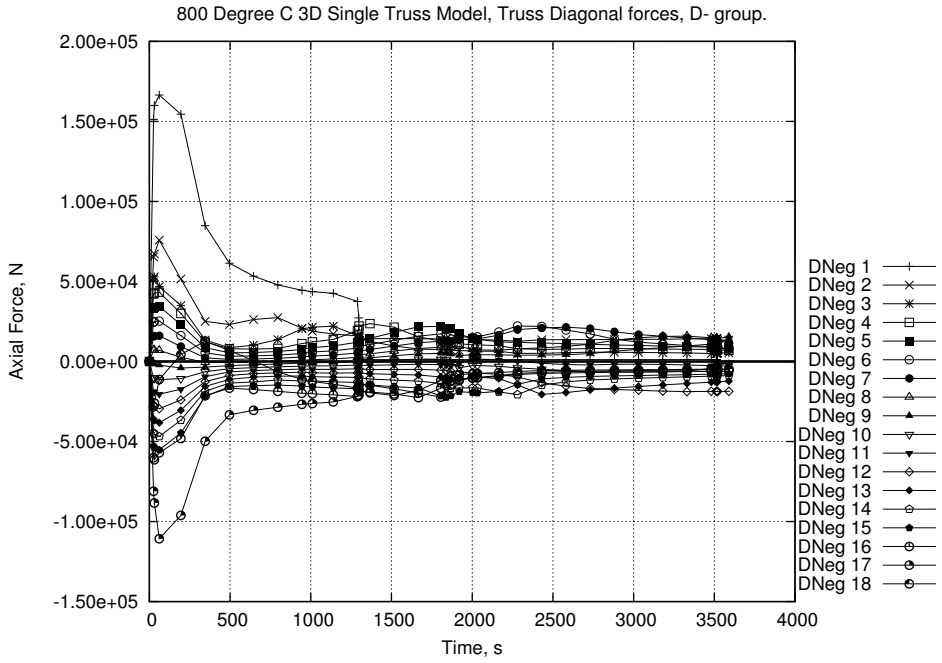

(a)

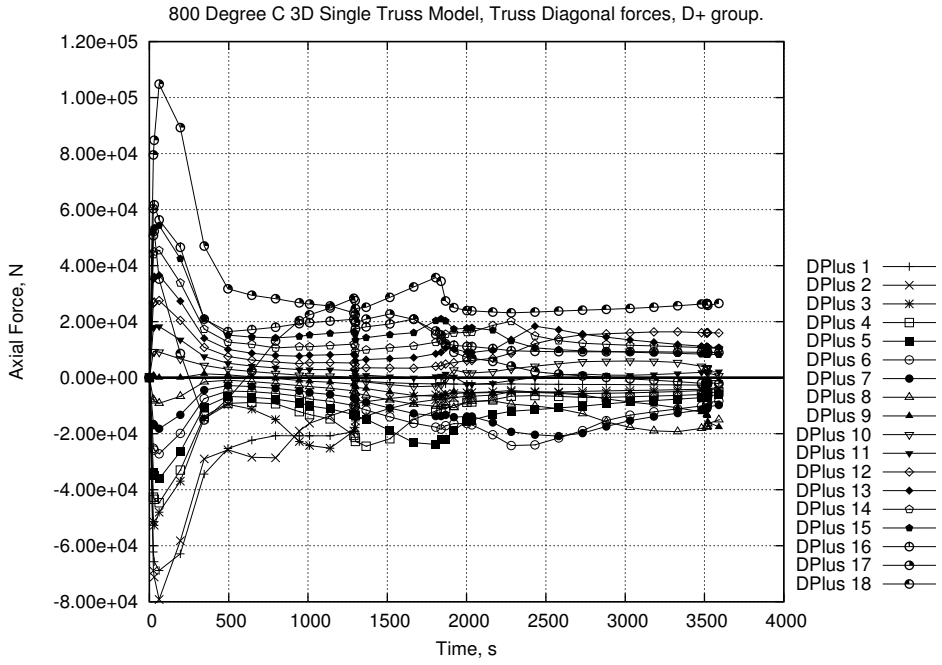

(b)

Figure 3.12: Truss Diagonal Axial forces, 800^{o}C Analysis

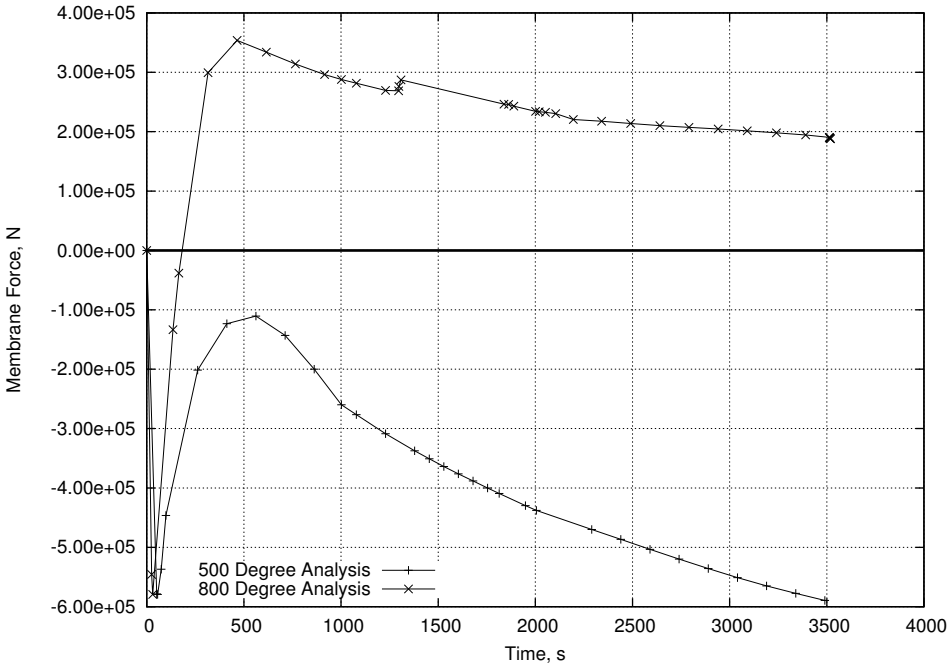

Figure 3.13: Floor Membrane Forces

the connection at the column (Figure 3.13) show that the truss system remains in compression for the cooler analysis while the high temperature analysis shows significant tension.

The phenomena described above indicate that the failure of a composite truss floor system is not due to sudden failure of the truss but rather acts in a similar way to a normal composite beam [7]. The system deflects smoothly downwards and will go into catenary action if the fire is hot enough. It is therefore reasonable to state that geometric and thermal effects could have a greater influence than the strength of the truss.

The final displaced shape of the 800°C model may be seen in Figure 3.14. The buckled diagonals are clearly shown at both ends of the truss in agreement with previous work [59].

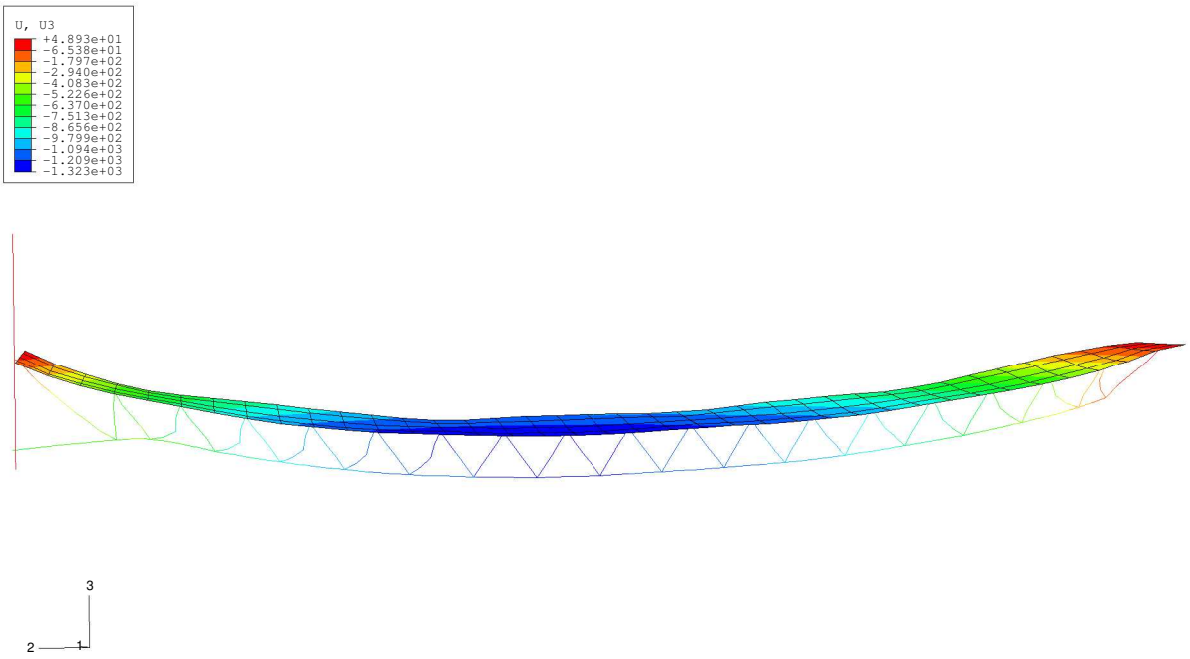

Figure 3.14: Final Displaced Shape, 800°C Analysis

3.3.1.2 Floor System Response

Classical buckling failure tends to show a particular response, especially when examining force-deflection plots. The force will reach a peak and then sudden failure of the system will occur, which is expressed as sudden, rapid deflection coupled with a sharp drop in load in the system. Examining the overall response of the floor based on the results shown in Figure 3.15 it would appear that this is exactly what is occurring.

However with classical buckling theory you would expect that the truss midspan deflection rate will suddenly accelerate as elastic forces are relieved through a change in geometry. This is not seen in the models. Plotting midspan deflection of the truss against steel temperature rather than time shows linear behaviour even after the membrane force of the floor is seen to peak and drop off. This indicates that the deflections as well as the forces seen in the analyses are directly linked to the expansion caused by increase in temperature, i.e. a geometry driven system rather

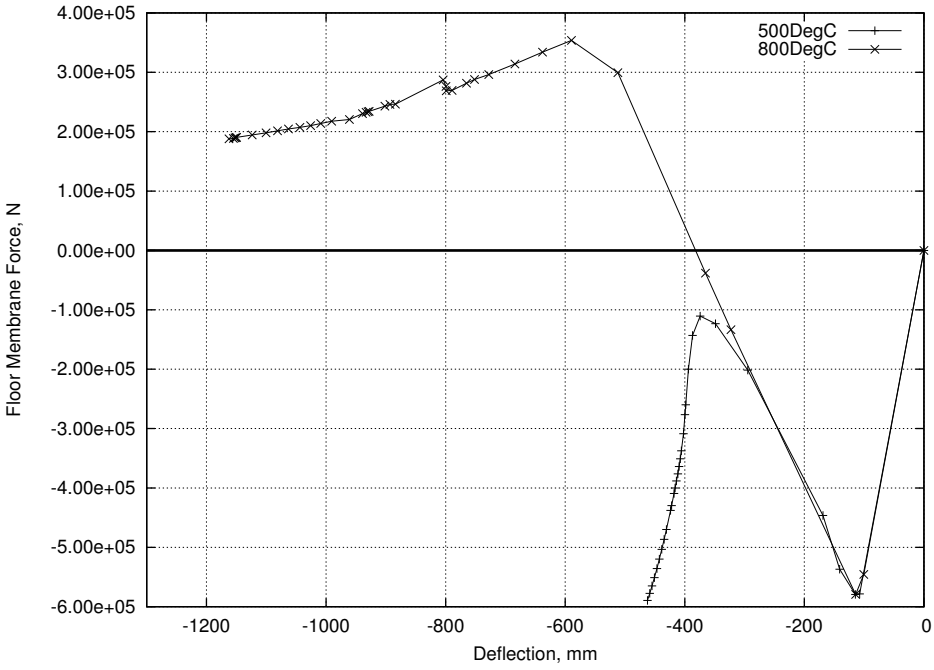

Figure 3.15: Truss Membrane Force vs Midspan Deflection

than a force driven system. This theory is advanced further in the Truss Restraint to Column section (3.3.1.3).

One of the more obvious failure mechanisms seen in structural members under fire conditions is "runaway" failure. This is when the midspan deflection rate increases greatly over a small increase in temperature. It indicates that the member can no longer support the applied load because of degradation of material strength. This kind of failure was not seen in either of the 3D single truss analyses conducted (see Figure 3.10). This is likely to be due to the rather high level of restraint at the boundaries of the model combined with the strong secondary load path provided by the concrete slab acting in tensile membrane action.

3.3.1.3 Truss Restraint to Column

Effect on Lateral Restraint due to Temperature In a multi-storey building loss of several floors worth of lateral restraint may lead to progressive collapse of the building above the fire floors as the column buckles over a greater length than was initially designed for. Geometrical changes caused by the heating of the floor

will lead to a reduction in the level of restraint to the column. However it is not initially clear at which point restraint will be lost completely.

The reason for conducting the small scale model tests described in this section is to allow us a greater understanding on the effects of heating on a composite truss floor system. This in turn has to be applied to the use of trusses in larger scale global models. As has been seen in several different investigations [1, 7, 13, 76, 77] composite floor systems reach a point where the mechanism used for load transfer changes from the normal bending/shear force to a catenary/tensile membrane action. For localized fires in one or two bays of a single floor of a structure this is not likely to have much of an impact as the inherent redundancy built into buildings redistributes the new forces. However when you get larger, multiple floor fires in large multi-storey buildings then the effects could lead to progressive collapse of the structure.

This section looks at the effects of fire on a composite floor truss system with respect to the ability of the truss to restrain the supporting column. As can be seen in the force plots in the above sections (Figures 3.8, 3.11 & 3.15) there are several responses that indicate buckling is occurring. Sharp force peaks and sudden load relaxation can be seen in both the response of the top chord and in the overall floor membrane force response, although these do occur at slightly different times.

In order to investigate the level of restraint that the truss might provide to the column the following procedure was followed. The 3D Single Truss model described above was allowed to run through the initial loading step as normal and then allowed to run into the second step. When the steel reached certain temperatures the heating was plateaued at that level and an extra force was applied horizontally to the truss-column connection. This loading took place in a 3rd step and was induced by moving the truss-column boundary inward. A summary of this procedure may be found in Figure 3.16. The column was moved at a constant rate. The truss invariably failed at some point in the 3rd step and the maximum membrane force withstood by the truss was deemed to be the level of restraint available to the column. At lower temperatures the truss in the general area of the column

Case	Plateau Time	Plateau Temp.	Failure Mech.
High Temp 1	20s	100^{o}C	Crumple
High Temp 2	55s	200^{o}C	Crumple
High Temp 3	90s	300^{o}C	Crumple
High Temp 4	130s	400^{o}C	Crumple
High Temp 5	190s	500^{o}C	Deflect
High Temp 6	275s	600^{o}C	Deflect
High Temp 7	400s	700^{o}C	Deflect
High Temp 8	1000s	800^{o}C	Deflect

Case	Plateau Time	Plateau Temp.	Failure Mech.
Low Temp 1	95s	200^{o}C	Crumple
Low Temp 2	175s	300^{o}C	Crumple
Low Temp 3	320s	400^{o}C	Crumple
Low Temp 4	1000s	500^{o}C	Deflect

Table 3.2: Column Restraint Models : Summary

connection crumpled suddenly while at higher temperatures the floor system as a whole fails and large extra midspan deflections occur.

Table 3.2 shows the different parameters used in each run. "Plateau Time" indicates the time the analysis took to reach the temperature indicated under the heading "Plateau Temperature". "Failure Mech." indicates the mechanism by which the truss failed as the column was moved inward. "Crumple" indicates that the truss and slab around the column connection failed, "Deflect" indicates that the movement of the column induced extra midspan deflection of the floor. This extra midspan deflection is possible as several more of the truss diagonals buckle, especially at the core end of the truss.

Two sets of runs were conducted. One used the 800^{o}C heating curve (High Temp) while the other used the 500^{o}C heating curve (Low Temp). This has implications as to the rate of heating as well as the maximum temperature reached. As can be seen in Figure 3.5 the 500^{o}C curve heats up the steel less quickly as well as attaining a lower maximum temperature. This difference in heating regime will also have some effect on the response of the concrete. As seen in Table 3.2 the higher temperature series of experimental models were subjected to the horizontal force at intervals of

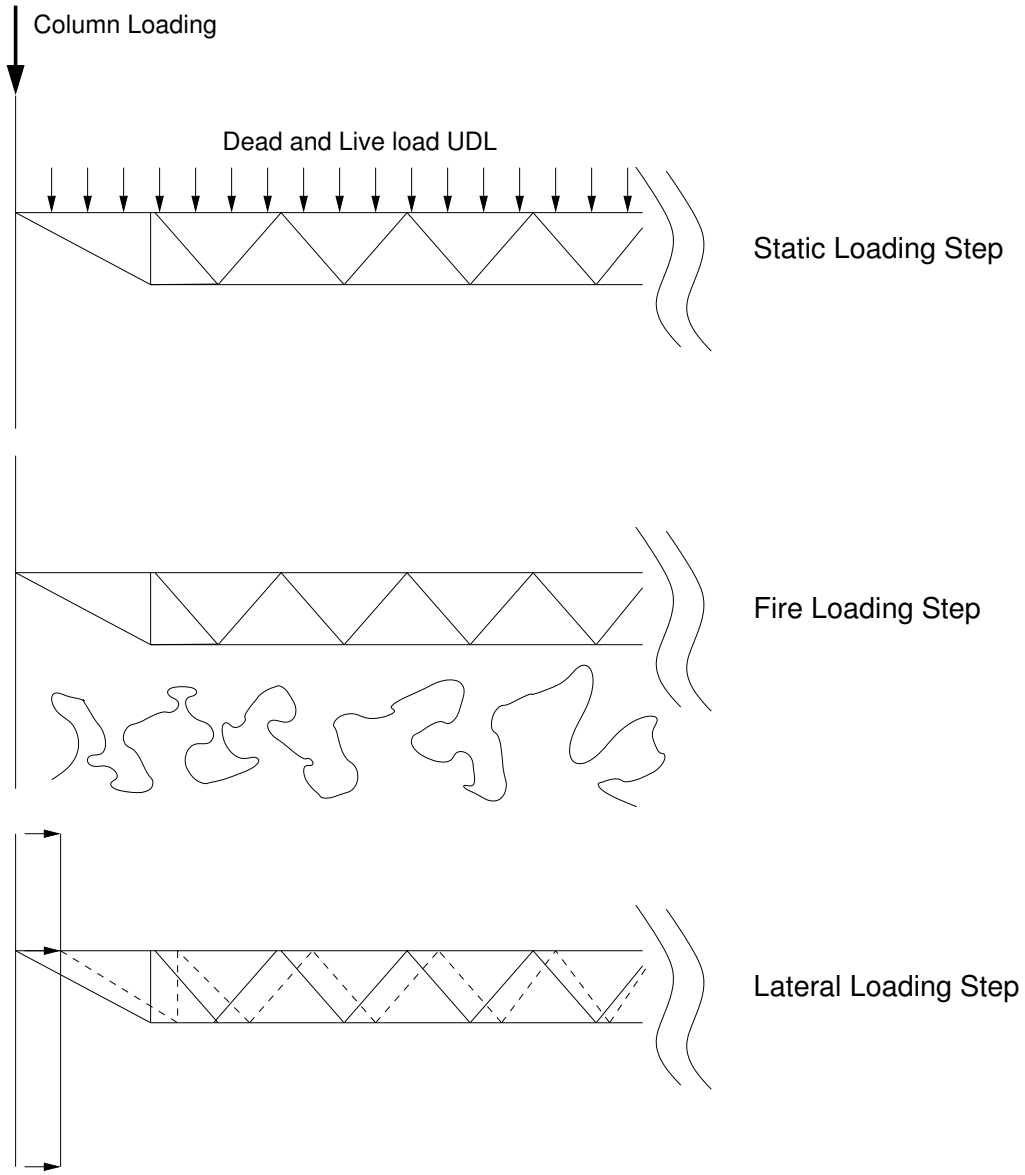

Figure 3.16: Lateral Restraint Test Procedure

100^{o}C from Ambient up to the maximum temperature in the model (800^{o}C). The lower temperature series was tested at 200, 300, 400 and 500^{o}C.

The analyses ranging from ambient to 800^{o}C will be discussed here first. Figure 3.15 shows the membrane force in the floor with respect to midspan vertical deflection over the second step for a full 3600s run. Comparing this to Figure 3.17 one can see that the general profile has been maintained. The spikes going down from the main profile are due to the extra lateral compressive load being applied in the 3rd step of each of the test cases. Figure 3.17 also shows that the responses shown by curves "High Temp 2" to "High Temp 5" (corresponding to temperatures between 200 and 500^{o}C) are very similar. The maximum level of restraint available to the column stays reasonably constant as the temperature increases across the range. After 500^{o}C material degradation has reached such a stage that runaway failure occurs rather than a sudden bucking failure. The force required to initiate failure is also significantly smaller than at lower temperatures. The "High Temp 1" analysis was plateaued at 100^{o}C and is before the heat induced peak membrane force in the floor. As can be seen in Figure 3.17 this analysis shows a restraint force similar to the analyses conducted after the "buckling" peak force. This indicates that this peak in the force is not a failure of the truss. What is especially interesting in this plot is that even after the flooring system has moved into catenary action due to temperature induced displacement (High Temp 6) it can still withstand a certain amount of compression before failing.

Figure 3.18 is a comparison plot between the results of the "Low Temp" series of tests and the corresponding "High Temp" tests. Even though the heating regimes are very different the results are almost identical. This indicates that it is the maximum unprotected steel temperature reached rather than the rate of heating that affects the restraint capacity of the floor system.

Effect of Different Boundary Conditions The model series testing column restraint described above also led to a further investigation of the effects of boundary conditions on the early response of the truss. Three boundary conditions were

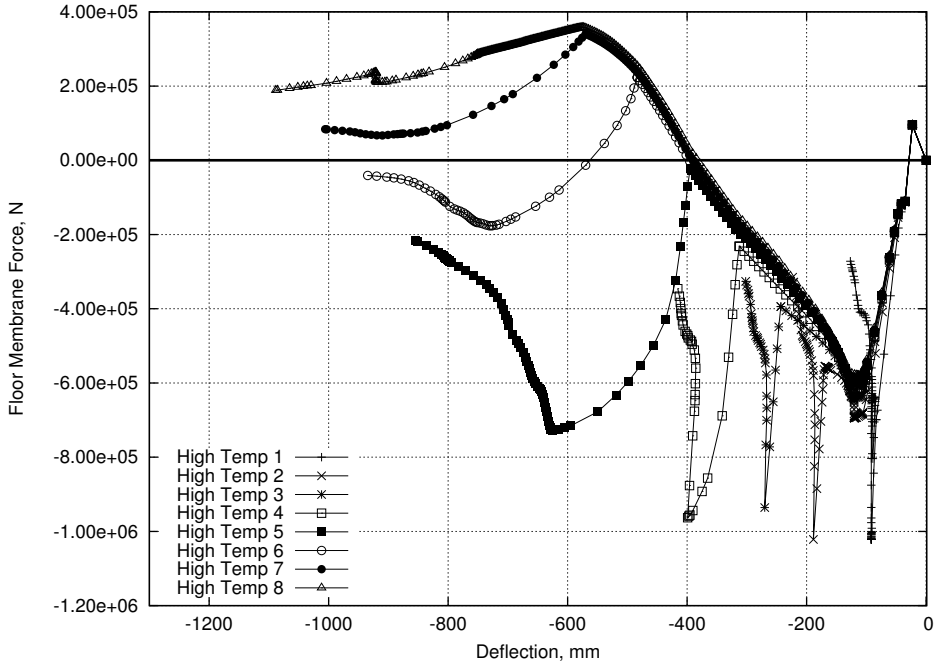

Figure 3.17: Midspan Deflection vs Floor Membrane Force, Test Cases

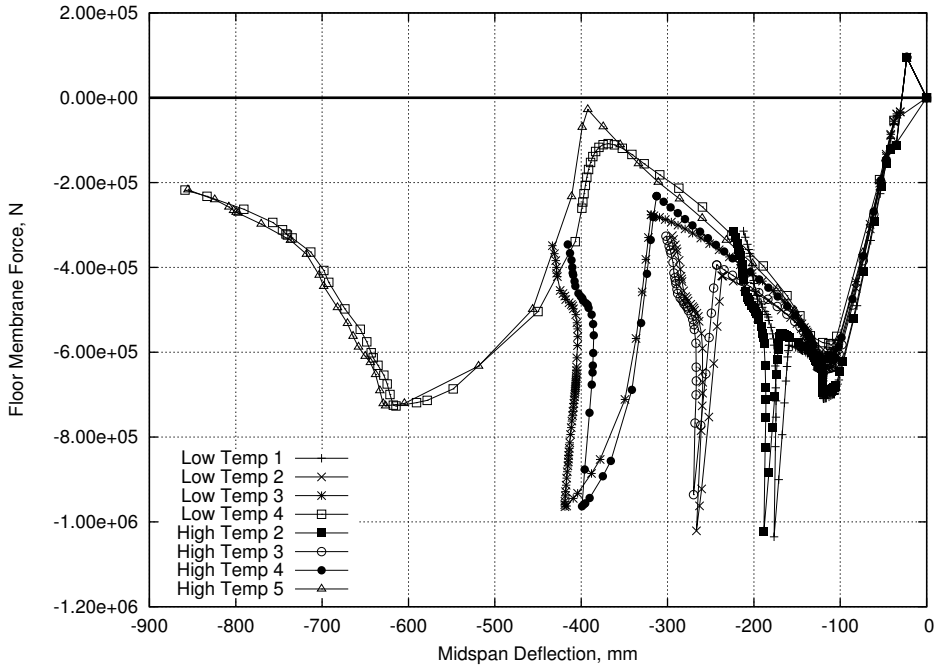

Figure 3.18: Comparison between test series

investigated using the 3D truss model over the first 1000s of the 800^{o}C fire regime. The first was exactly the same model as described in the Model Description section with a column forming the truss boundary (Base case). The other two models consisted of the ultimate bounds of the possible restraint created by the column. The first had the column end of the truss restrained in all 3 translations (Fixed case). The other bound had the truss free to move in the axial direction of the truss (Free case). In all cases the edge of the concrete slab at the column end of the truss was left unrestrained. Again all actions of the slab would be transmitted through its connection to the truss.

Again the graphs in Figure 3.19 look at the floor membrane forces and the deflections at truss midspan and column-truss connection. Comparing the Membrane forces it can be seen in Figure 3.19 that restraint does make a difference, which was to be expected. In the fully fixed case the membrane force reaches the maximum force that the top chord can handle and then the floor buckles. In the free case it develops no compression and in the Base case with the column it lies somewhere in between. The support end displacements show the complimentary action, with no movement in the Fixed case, some in the Base case and a maximum in the Free case.

3.3.2 Secondary Fire Regimes

The analyses conducted for this section were intended to expand on the bounds created by the main analyses. The compartment temperature-time profiles of these fire regimes may be found in Figure 3.5. The first to be discussed is the 600°C analysis. This was designed to check the responses discussed for the bounding cases against a fire regime between these bounds. At the maximum compartment temperature the steel will be retaining around 30% of its ambient stiffness and slightly less than 50% of its ambient strength. The local truss member forces may be seen in Figures 3.20 & 3.21. Comparison of these plots to their equivalents for the 800°C (Figures 3.11 & 3.12) and 500°C (Figures 3.8 & 3.9) analyses shows

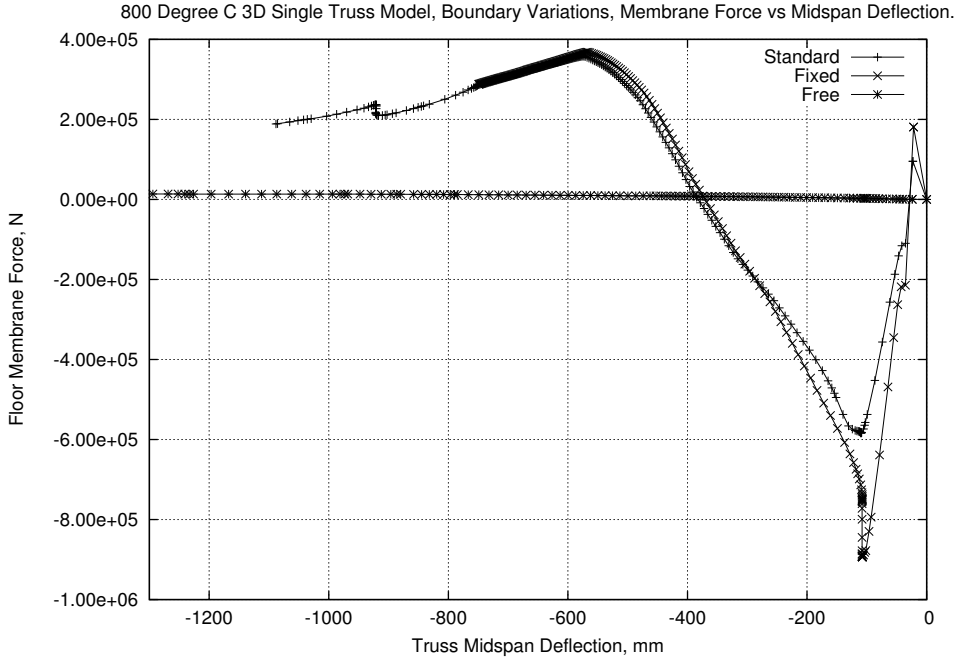

(a)

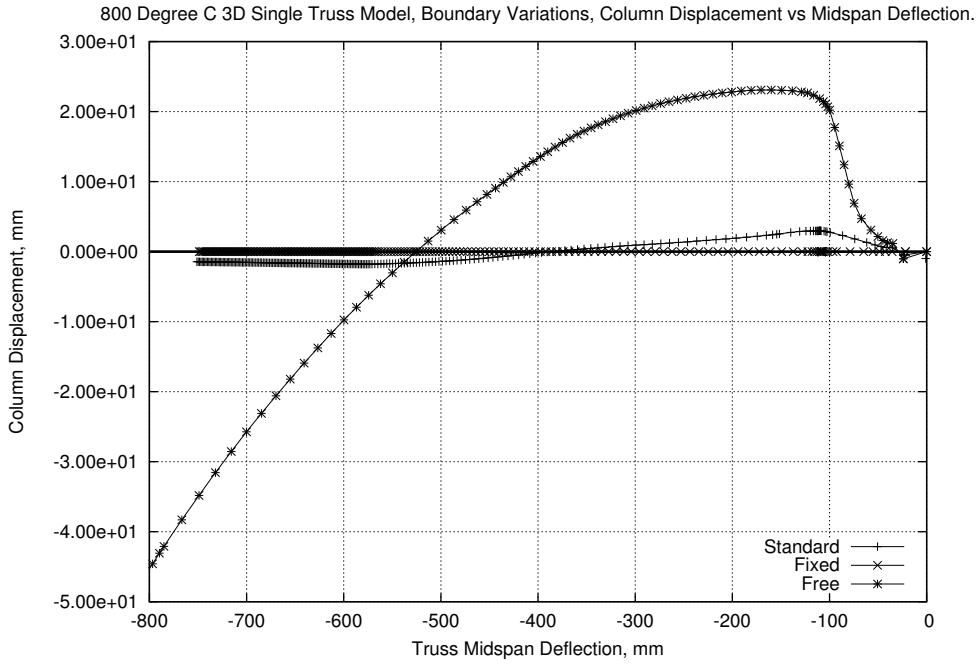

(b)

Figure 3.19: Deflection and Force Plotted against Midspan Deflection

that the 600°C analysis does indeed lie between the bounds. The top chord forces, shown in Figure 3.20.a, are reaching the point of transitioning to tensile action at the end of the analysis in a similar manner to that shown in the 800°C analysis at about 1500s. This response is not seen in the 500°C analysis at all. The response of the truss bottom chord and the diagonals in the 600°C analysis resembles the 500°C analysis quite closely. The response of these members also captures a clearer picture of the buckling in the diagonals. At around 3200s DPlus 2 (Figure 3.21.b) shows a sudden drop in axial force. This is mirrored by a sudden increase in the force in DPlus 3 as extra compressive load is transferred to it. This response is also apparent in the corresponding tensile diagonals DNeg 2 and DNeg 3 in Figure 3.21.a. The effect of this buckling can be seen all along the bottom truss chord (Figure 3.20.b) as a general lowering of tension after about 3200s. As this buckling occurs after the steel has stopped heating, it is caused by the truss attempting to resist the movement of the floor slab as it continues to expand. The timing of this buckling, as seen in the force responses, matches the visual indications in the displaced shape of the truss.

The second additional fire regime was a slow-growing version of the 800°C fire. It was designed to replicate a system where a small amount of fire protection was present and hence while the steel followed the slow curve the concrete used the same temperature-time profile as the original 800°C analysis. Figures 3.22 & 3.23 shows the axial force response of the truss members. In this case the top chord reacts slightly differently from the original 800°C analysis. By the end of the analysis the top chord hasn't transitioned into tensile action. Referring between the results for the other truss members in Figures 3.22 & 3.23 and those for the original 800°C analysis, in Figures 3.11 & 3.12, shows other differences. The responses in the Slow 800°C analysis are much smoother and show little evidence of buckling in the force response of the truss diagonals, although the truss top chord again yields and buckles early. Similarly, even at the end of the analysis, there are no visual cues indicating buckled truss diagonals. This is likely because the steel is always expanding, allowing it to accommodate more easily the movement of the floor slab.

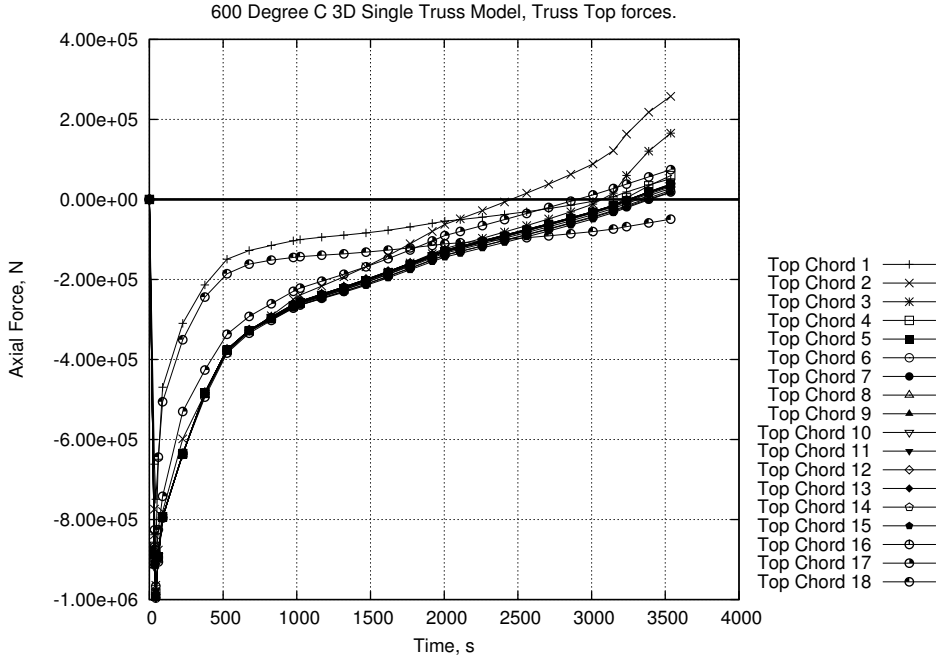

(a)

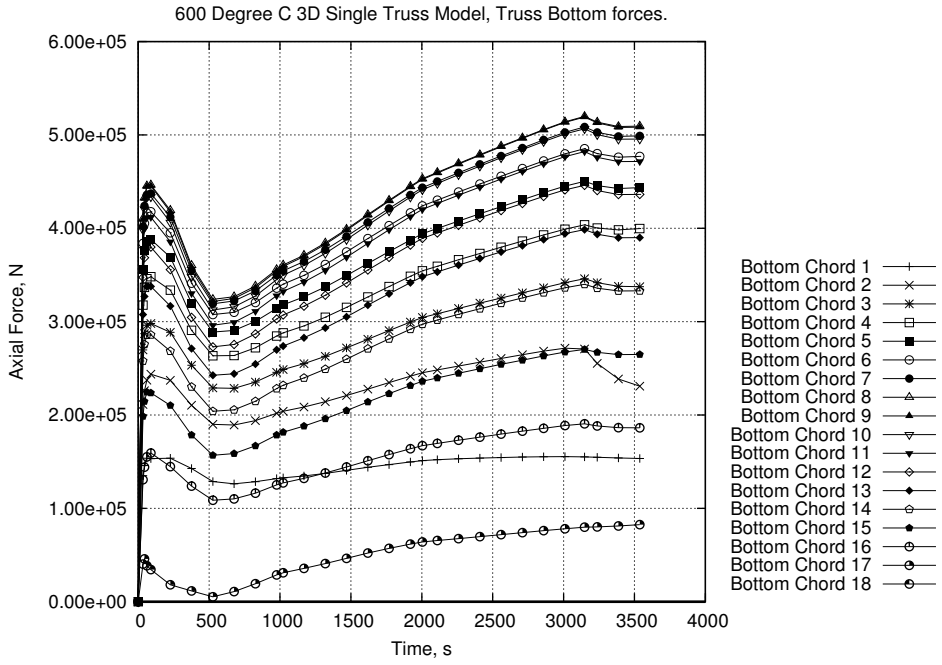

(b)

Figure 3.20: Truss Chord Axial forces, 600°C Analysis

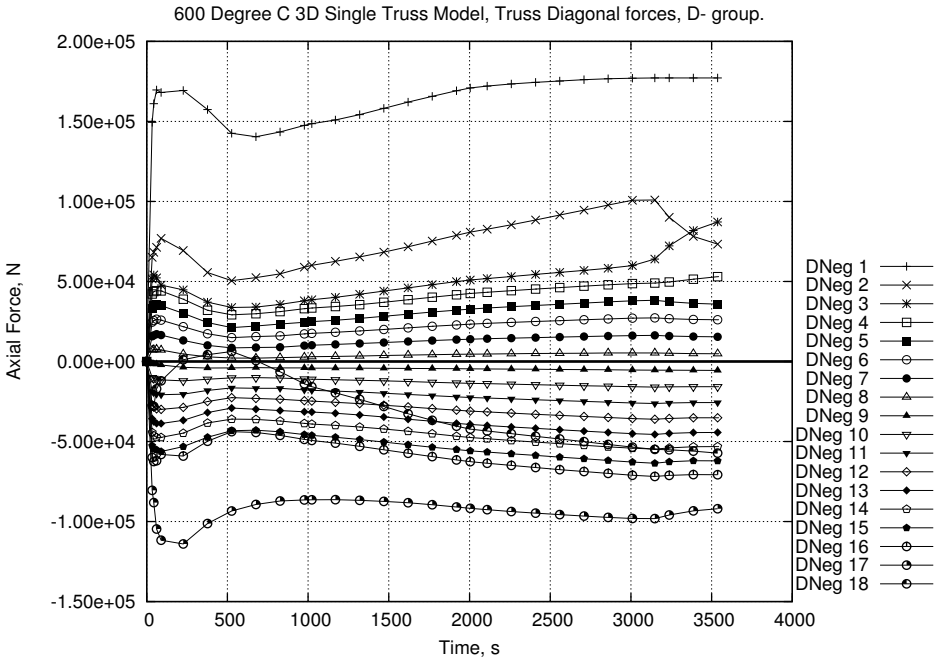

(a)

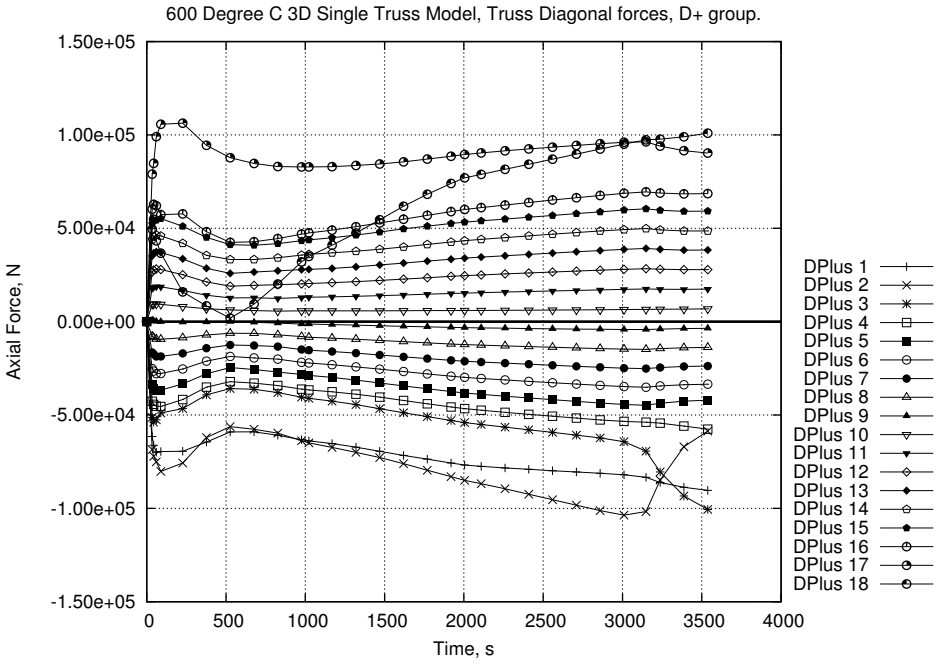

(b)

Figure 3.21: Truss Diagonal Axial forces, 600°C Analysis

There is no point where the steel is not expanding and having to resist the extra movement of the slab. The force response of the truss members reflects this by showing a smoother profile than that of the original 800^{o}C analysis.

Comparison of the more global responses of midspan deflection and connection forces, shown in Figure 3.25, again shows marked similarity between all the cases. The same trends are apparent in each, especially the 600^{o}C case where it sits midway between the two bounding cases. If the same responses are presented with respect to temperature, as shown in Figure 3.25, then there is an extremely close correlation. Even though the heating rates are different, the midspan deflection rates with respect to temperature (Figure 3.25.a) are virtually identical until the points when the various analyses reach their maximum temperature. While it appears that runaway is occurring in this plot this is not in fact the case. The fire regime used in the models reaches a plateau after 1000s. Therefore any change in response after this time will also be plateaued.

Examination of Figure 3.26, showing the midspan deflection against the floor membrane force, also indicates a similar response across all the cases.

The biggest differences between the cases occur as the models get within about 50^{o}C of the steel maximum temperature. This stage occurs around 400s before the end of heating so it is likely caused by the difference in heating rates in the steel as compared to those of the concrete. It is possible then that there is some critical difference in heating rate between the concrete and steel. If the difference is within a certain range then the results are similar regardless of actual rates used. Further work would need to be done to identify this phenomenon in more detail.

3.3.3 2D Multi-floor Model

As this study is concerned with the response of only the truss assembly rather than the structure as a whole the data presented here will be based on the response of a single floor in the 2D structure. Global responses will not be studied in depth. In this case the 8th floor of the structure will be investigated. The 8th floor has

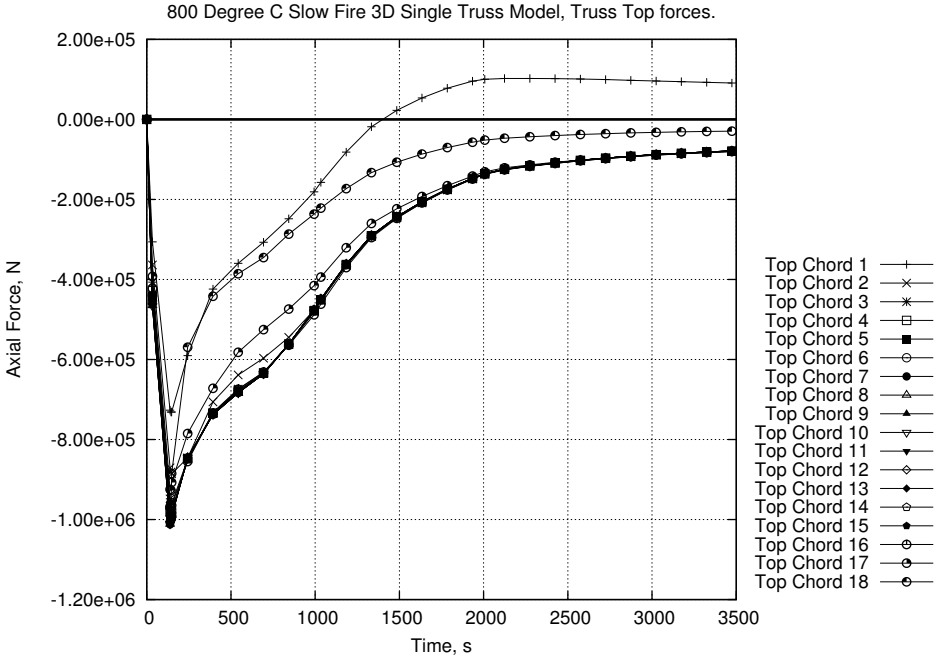

(a)

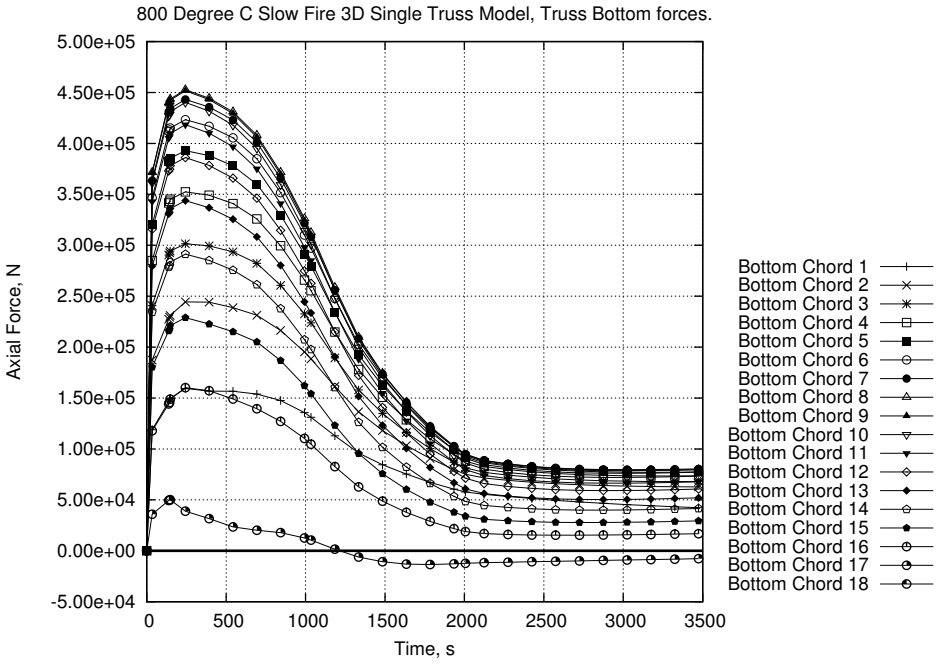

(b)

Figure 3.22: Truss Chord Axial forces, Slow 800^{o}C Analysis

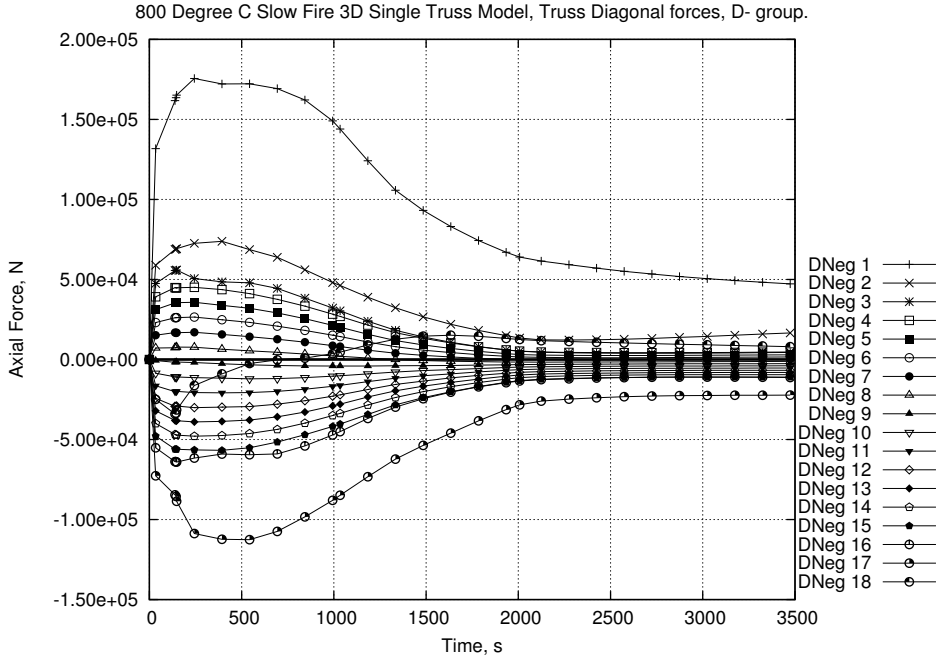

(a)

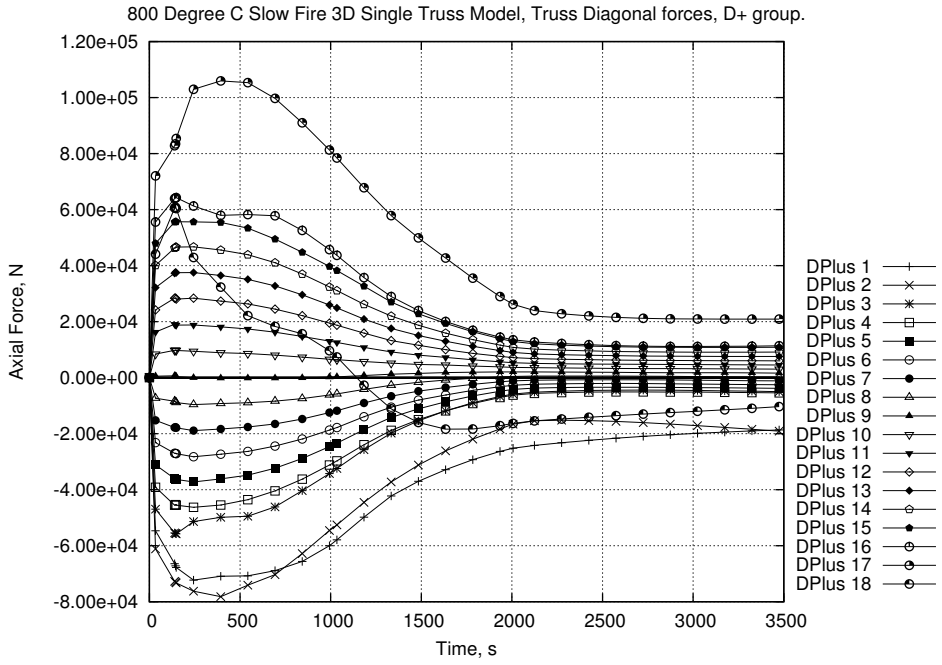

(b)

Figure 3.23: Truss Diagonal Axial forces, Slow 800^{o}C Analysis

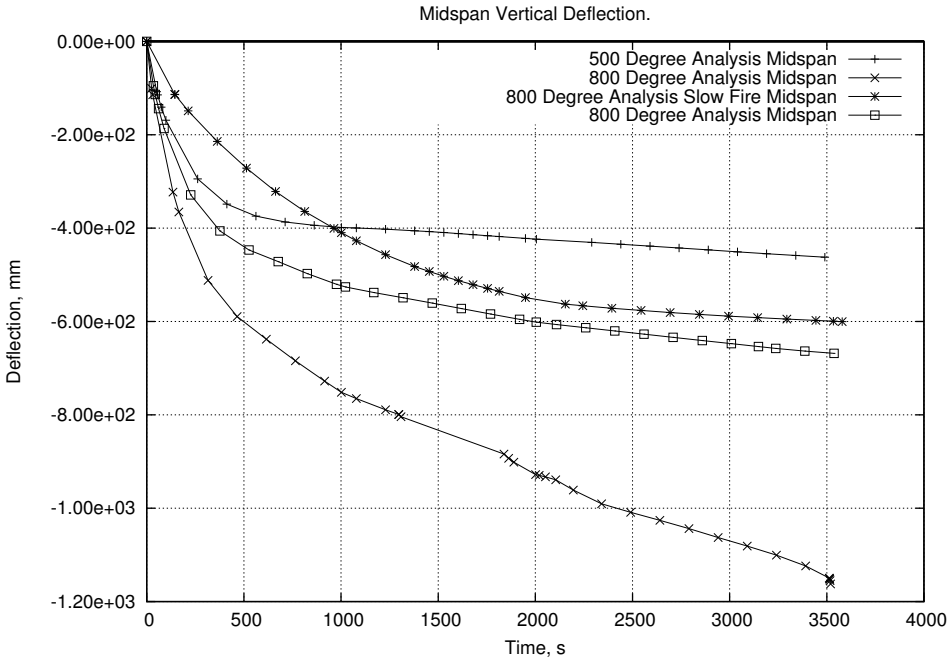

(a)

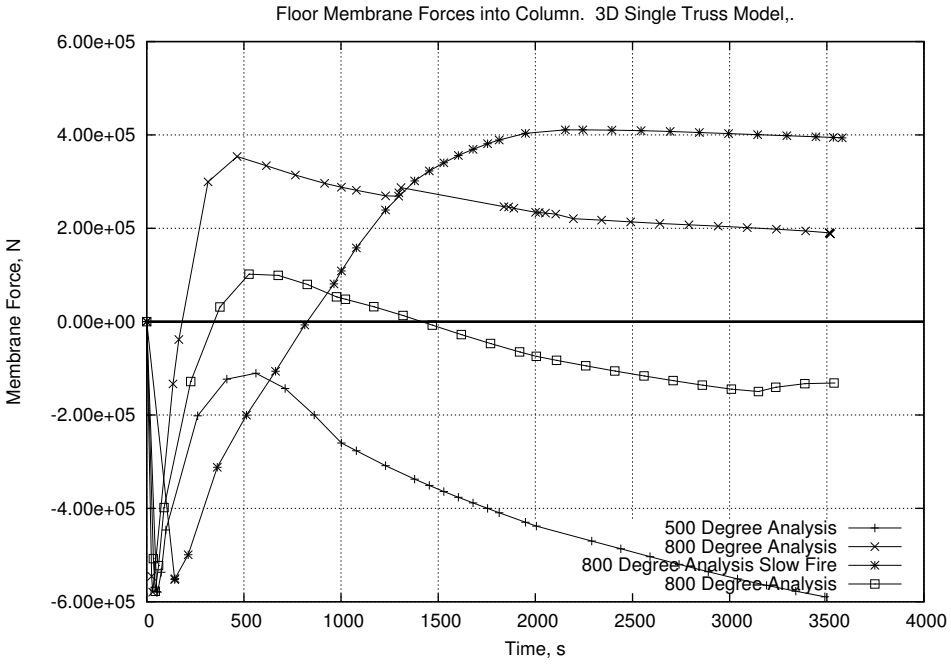

(b)

Figure 3.24: Floor System Response Comparison with respect to Time

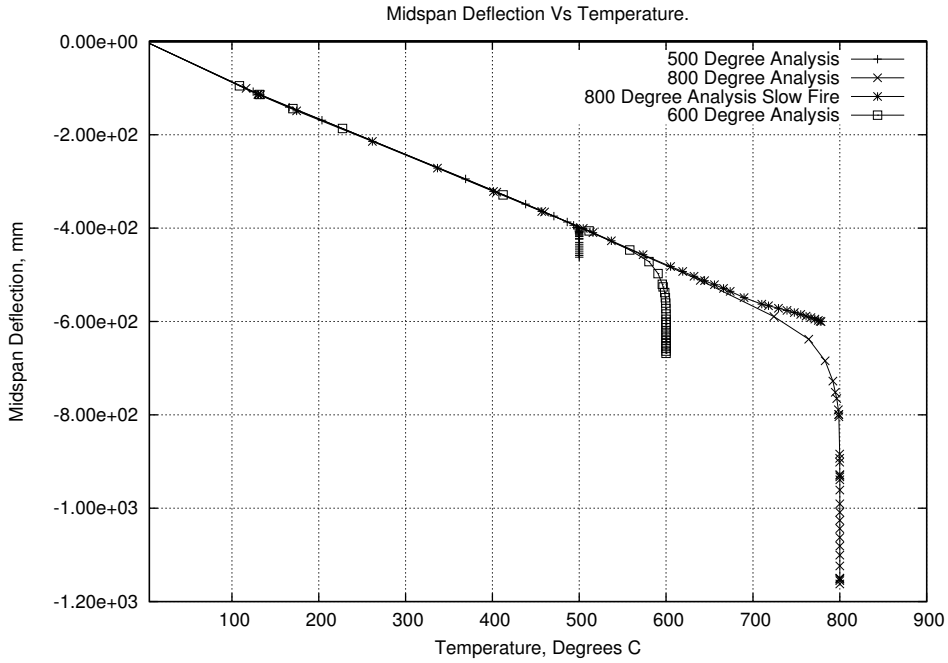

(a)

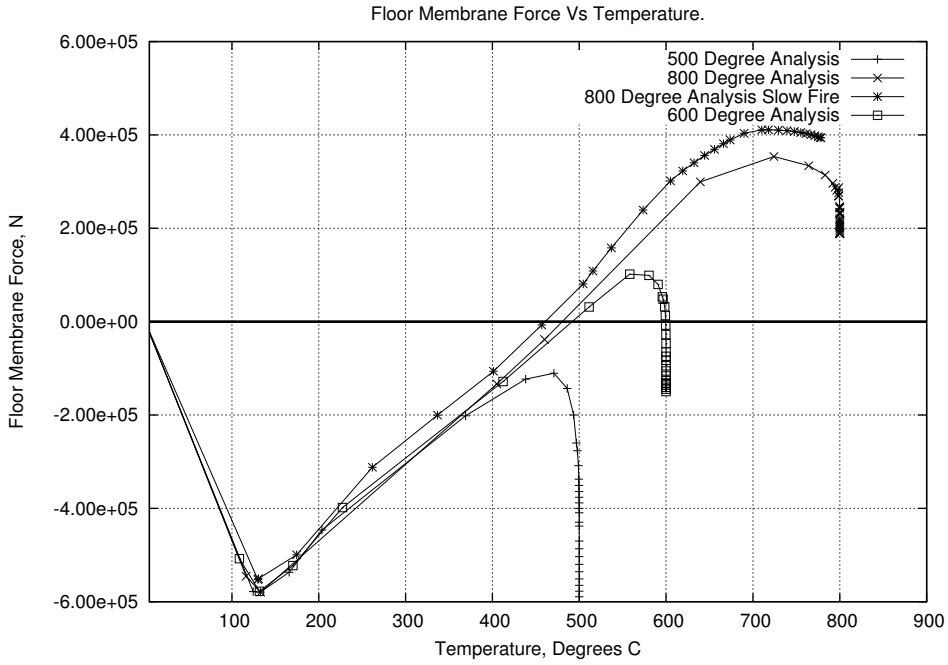

(b)

Figure 3.25: Floor System Response Comparison with respect to Temperature

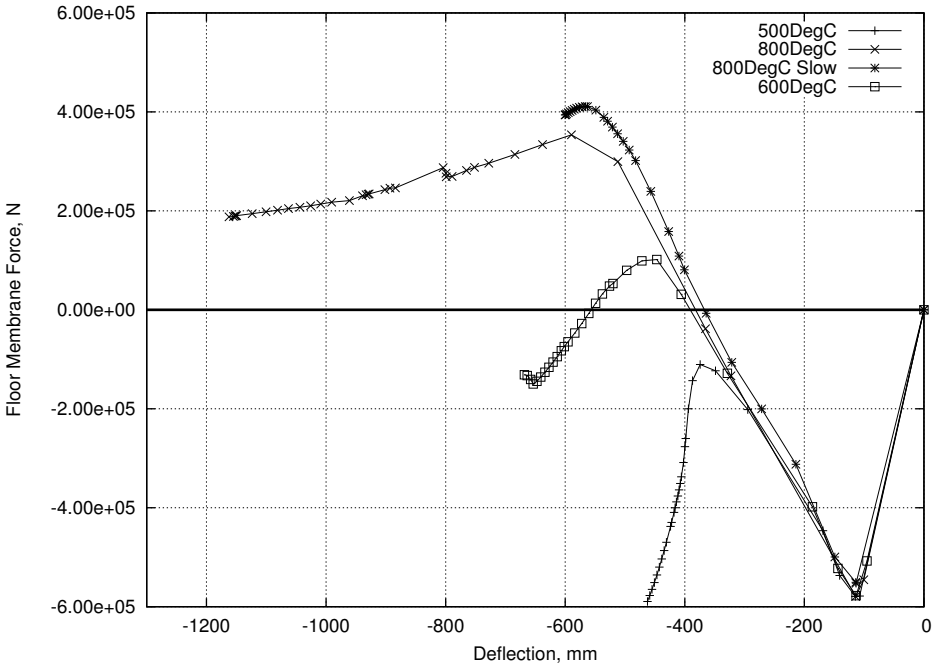

Figure 3.26: Truss Membrane Force vs Midspan Deflection, All Cases

been chosen as it is the top floor of the building to be affected by fire and as such is the closest match in the 2D model to the structure investigated in the 3D model. It should be noted that in this analysis the building failed at the outer columns. Enough data is available, however, to investigate the response of the truss system before the global failure occurs.

Comparing Figures 3.27, 3.28 & 3.29 to their counterparts in the 3D analysis section (Figures 3.11, 3.12 & 3.10 respectively) the similarities are clear. The response of the truss top chord in the 2D analysis is virtually identical to the 3D analysis further reinforcing the theory that this member reaches yield. The difference in global restraint does not affect the top chord because the local level of restraint to each sub-member of the chord remains the same. The main difference between the 2D and 3D analyses is that the responses of the bottom chord and the diagonals appear to react more slowly in the 2D case. The peaks are in a similar range between the analyses but the drop off is much slower. This again would indicate that it is not a sudden buckling failure but rather a gradual redistribution and shedding of forces as material degradation takes effect and the truss deflects. This

slower response is likely to stem from the lower level of restraint applied at the column end of the truss. In the 3D analyses the rigid restraints (column boundary conditions) are extremely close to the end of the truss. In the 2D analysis the large number of floors between the effective column restraints and the fire floor truss ends allows the column to flex more thereby reducing the restraint applied directly to the end of the displacing trusses.

The deflection plot for the 2D analysis shown in Figure 3.29 also shows a somewhat different trend when compared to the 3D models. The initial deflection rate matches closely. At about 250s the deflection rate in the 2D analysis increases slightly. This is the point in the 2D analysis when the column begins to be pulled back inward by the deflecting floors. The deflection rate then becomes more moderate at about 400s as the rate of heating in the steel reduces. Runaway failure is then obvious as the building collapses.

Further analysis of results shows that this extra deflection is caused by the failure of the column rather than further failure of the truss. The column is pulled out of plane enough that moments induced by floor tensions and P-δ cause plastic hinges to occur in the column creating a mechanism. This then becomes a global phenomenon and is described in more detail in Chapter 4.

3.3.4 Analysis Of Floor Response

In the top of the truss the compression is initially held by the combination of the concrete slab and the top chord of the truss. As the steel top chord heats up, the compression in it increases as it expands against the restraint of the concrete. The force due to expansion is much bigger than the force induced by the ambient loading. When the top chord reaches yield, the compression due to the ambient loading has to be moved into the concrete slab. As the top chord buckles it can't take back that compression due to the loading. In addition the expansion of the steel will induce tension in the concrete slab which will help stabilize it against the load that is transferred to it from the top chord. Again, as the top chord yields and

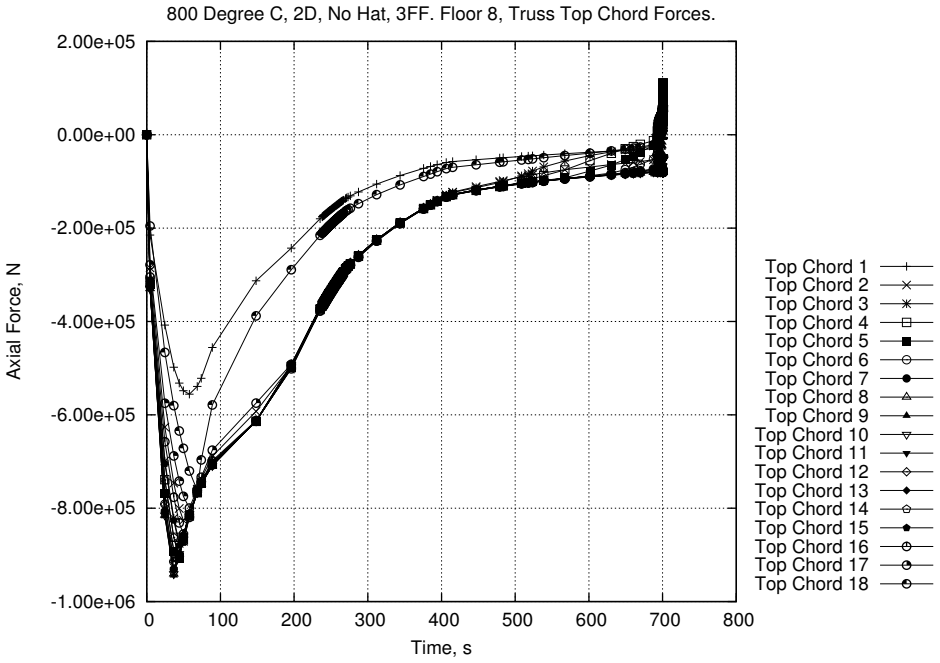

(a)

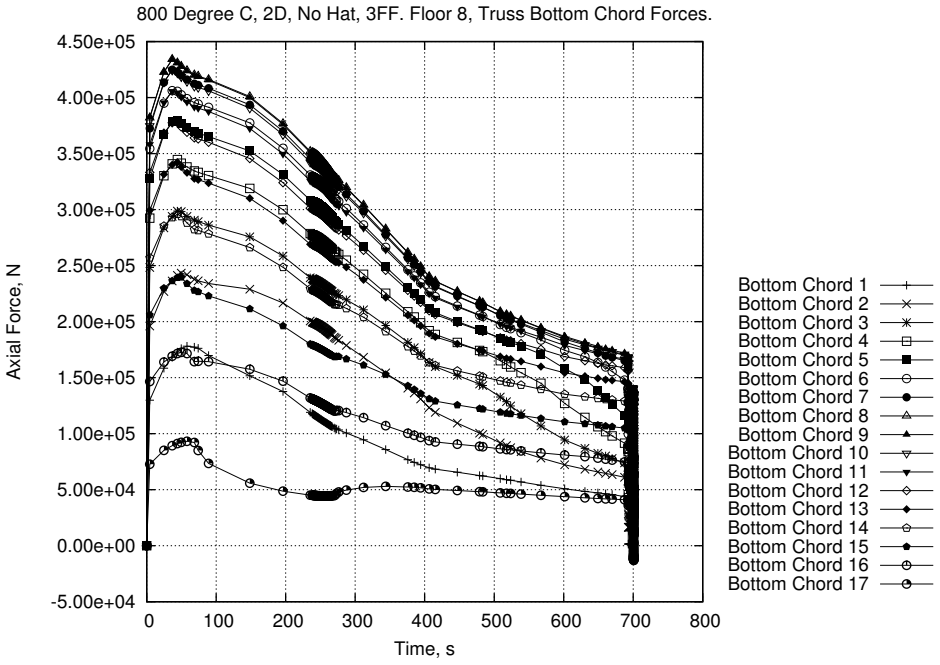

(b)

Figure 3.27: Truss Chord Axial Forces, 2D analysis

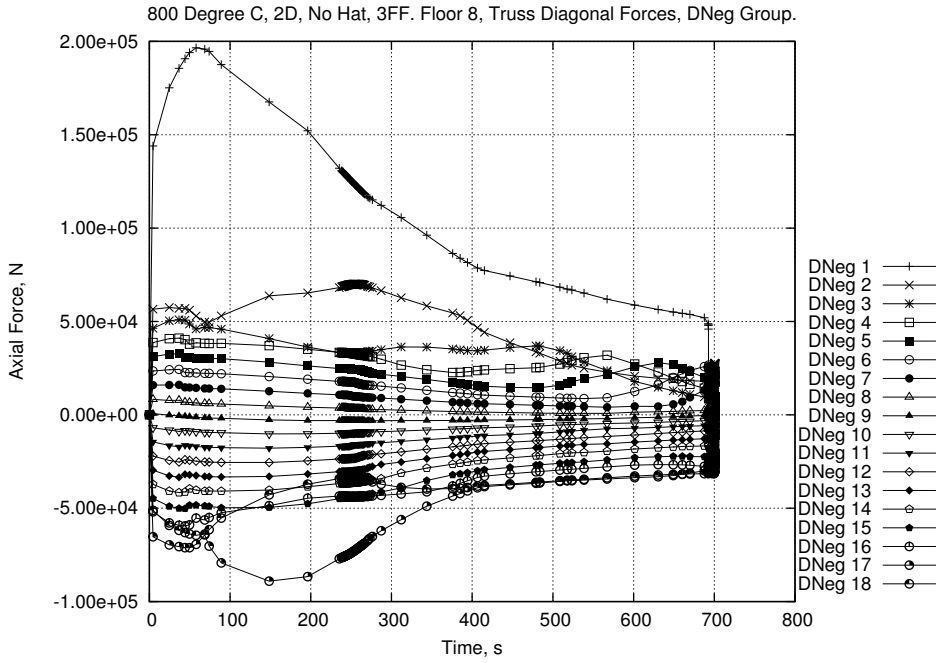

(a)

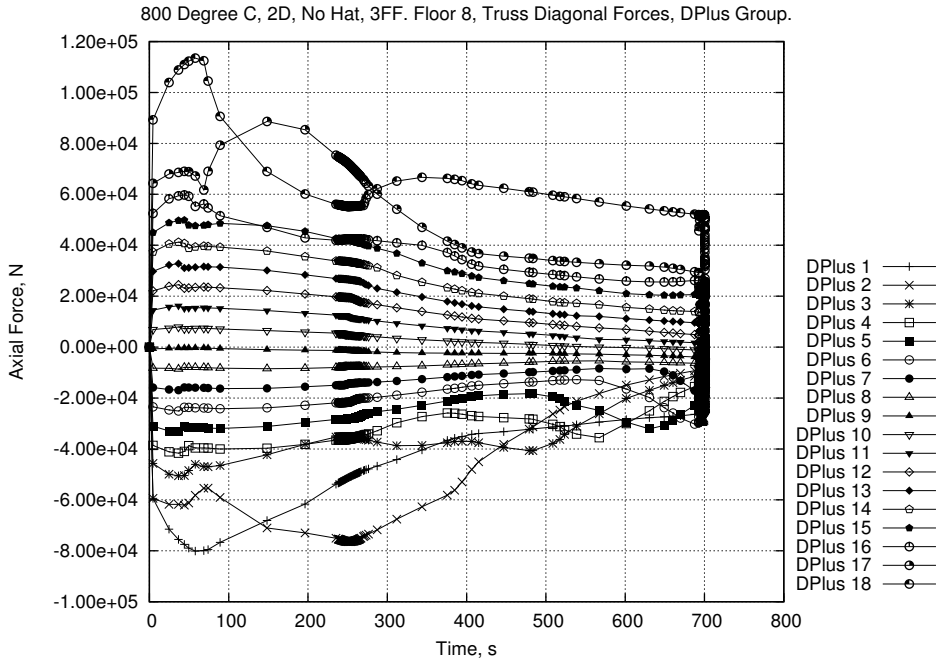

(b)

Figure 3.28: Truss Diagonal Axial Forces, 2D analysis

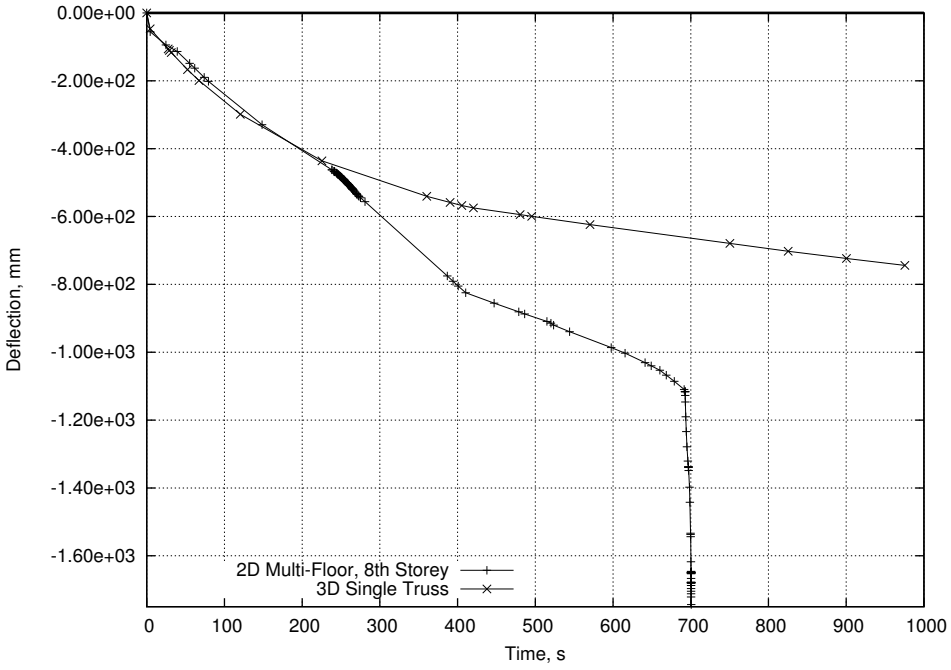

Figure 3.29: Midspan Deflection, 2D Model

buckles this stabilizing force drops. All this leads to the truss effectively losing the compressive strength of the top chord which will reduce its I value. This may be enough to induce a suitably large midpoint deflection in the truss so that it can no longer sustain the high compression forces created by its expansion and so the force in the floor system reduces. This, again, will assist the move into catenary action as the steel material properties degrade and the floor loads are held up solely by the floor slab.

The above would seem to indicate that the top chord of the truss is intimately linked to the "buckling" of the floor system. In the various analyses conducted for this chapter the top chord fails at a different point in time to the "buckling" of the floor system as a whole. Depending on the restraint available at the column end and the heating regime, the top chord may fail either before or after the peak membrane force in the floor system.

3.4 Conclusions

The results and analysis provided above indicate that composite truss flooring systems do not fail suddenly. Individual member buckling seems to be a much more gradual occurrence linked to material failure and thermal expansion based geometry change rather than sudden "failure" at the start of the analysis. This explanation is based on the indications that the truss members do not permanently lose their strength. After the initial force peaks in all the members the force drops off but then begins to increase again before stabilizing to a certain extent. In the deflection plots there is no indication of classical buckling response. The deflection rate is reasonably high and steady for the first stages of the analysis and reduces when the steel temperature begins to level off. Other indications also appear to point toward thermally induced geometrical change being the primary instigator of all the other responses.

As well as this stabilization of forces it has been shown that the floor system retains a significant amount of membrane strength even after severe heating and deflections have occurred. This leads to the conclusion that a significant amount of restraint may still be available to a column connected to this kind of floor system.

A further investigation of secondary heating regimes indicates similarities in response over the range investigated. The differences are in line with the different temperatures reached by the steel and therefore the level of thermal expansion and material degradation sustained. The use of the general exponential compartment fire curve allows for a range of regular fires to be investigated and easily compared. In particular it highlights the difference in a situation where the steel is heated over the duration of a fire and a situation where the steel reaches a maximum, stable temperature.

The differences in structural layout and applied fire regime preclude the models presented here from being directly compared to previous work [1, 59] on structures in fire. However, several of the general responses, such as deflection patterns and member buckling, show good agreement qualitatively.

Comparing the results of the trusses modelled in isolation to results gained from a larger model indicate that these individual truss models provide a useful view of the local internal forces and the generalized response of the floor system. However, assuming that all connections remain intact, failure of a building constructed using this type of flooring system does not appear to be linked to a sudden local failure in a particular truss but is rather linked to a global failure mechanism involving columns over multiple floors. This view ignores the fact that these floor systems may be too flexible (or insufficiently stiff), which leads them to destabilize the columns by applying large moments on them through membrane tension.

Chapter 4

Structural response of tall buildings to multiple floor fires :

Part 1 - General response

This chapter reports on an investigation of the global effects of Fire on long span truss floor systems in a tall building environment. The effects of fire spread over multiple floors of a building are the focus of this research, especially where this may lead to progressive collapse.

This study analyses results from an investigation of a 2 dimensional model of a multi-storey office building. The model is representative of the type of construction used in the World Trade Center 1&2 towers including a hat truss system. The local and global response of the model is described over the course of a 3 floor fire reaching a peak compartment temperature of 800^{o}C .

The results show that large displacements can occur in buildings with long span floors without collapse. However if columns fail then collapse is rapidly instigated. Additional structural members, such as hat trusses, that allow redistribution of loads from affected columns to other structural members have a significant beneficial impact on the robustness of the building.

4.1 Introduction

Detailed research has led to new understanding of composite steel frame buildings in fire [1, 7, 13]. This work has mainly focused upon the most common and simplest structural forms currently used, involving rolled steel sections in frames with composite floor decks. In the aftermath of the events of 11th September 2001 and the Torre Windsor fire in Madrid, it has become apparent that other structural forms need to be investigated under fire conditions. More specifically, unlike most research to date based on single floor fires, multiple floor fires and their role in initiating potential progressive collapse mechanisms need to be investigated in order to develop an understanding of such failures as witnessed on the 11th of September 2001 in New York. Modern office buildings often use plans that are distinctly different to the usual regular grid based plans on which most design calculations are based. Such buildings also often incorporate long span floor systems which maximize the letable area without columns interfering with the space.

This chapter presents the results of an investigation of the effects of multi-floor fires in tall buildings incorporating long span truss floor systems. A fire has been applied over several floors and indicates a failure mechanism involving failure of the columns. The effect of load redistribution by the addition of a hat truss system to the top of the building has also been investigated.

As the official NIST report on the collapse of the WTC towers does not include results from 2D models it is not possible to make a direct comparison between methods. Comparison of midspan deflections and column movements between the models reported here and a simplified single truss model reported in Section 4.2.4 in the NIST investigation [52] show that similar orders of magnitude are evident.

The commercial finite element modelling program ABAQUS is used to model the structure under investigation. The program can accurately predict the large displacements commonly seen in structures in fires as well as allowing for the degradation of the materials at high temperatures and the geometric effects of heating (thermal expansion and bowing).

4.2 Model Description

This study analyses results from an investigation of a 2 dimensional model of a multi-storey office building. The model is representative of the type of construction used in the World Trade Center 1&2 towers. Several different versions of the model were run with differences in boundary conditions, structural layout, fire regimes and material properties. Two of these models shall be presented here to describe the failure mechanisms encountered. Figures 4.1 & 4.2 show the layout used for the two models to be presented here. The two models use the same structural systems over the bottom 12 main storeys while one includes a "hat truss" system at the top of the building that allows for additional load redistribution between the columns. The model is a slice through the full 63m width of a building and consists of 12 storeys. It has been assumed that the floors being modelled do not represent the full height of the building hence extra loading has been applied to the top of the columns. This extra loading represents the weight of further floors above those being modelled and increases the load ratio of the outer columns to about 0.2. In the model which includes the hat truss structure at the top of the building (Figure 4.2) the loading has been applied at the interface between the 12 main floors and the extra floors which make up the hat truss system.

The main floors are split into outer areas supported by long span trusses and the inner, core area, supported by a beam and slab floor system. The slab has been modelled as composite with all beams and trusses but is not connected to the columns.

The trusses supporting the outer areas have been modelled using the section sizes shown in Table 4.1. The member sizes were based on data taken from various reports [32, 50, 53, 54] on the structure of the World Trade Center Towers as this was a successful design of a long span truss floor system.

The outer columns are 700x350mm box sections with the long sides (Perpendicular to Axis 1 in Figures 4.1 & 4.2) made up of 6mm thick plate while the short sides (Parallel to Axis 1 in Figures 4.1 & 4.2) are 12mm thick.

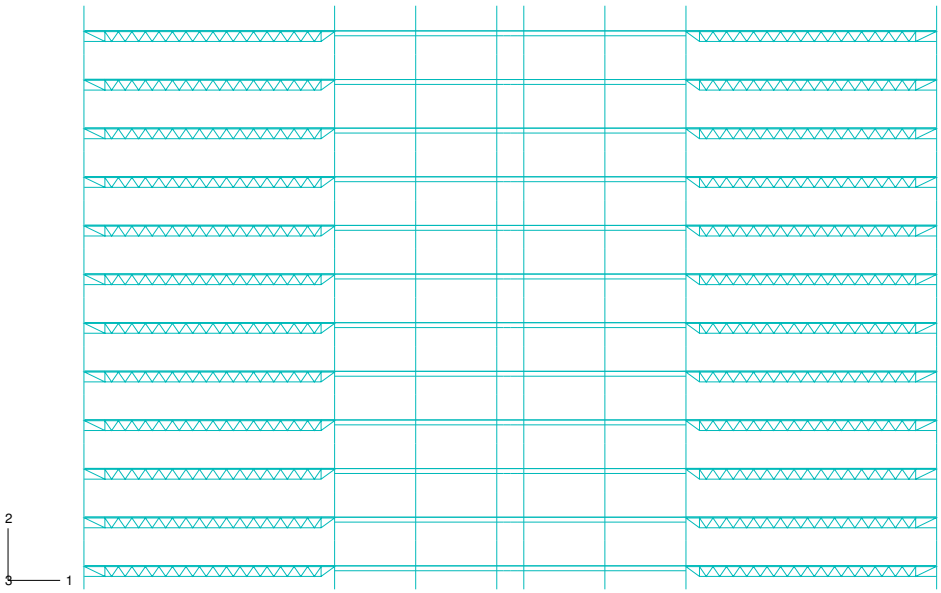

Figure 4.1: 2D Main Floors Model

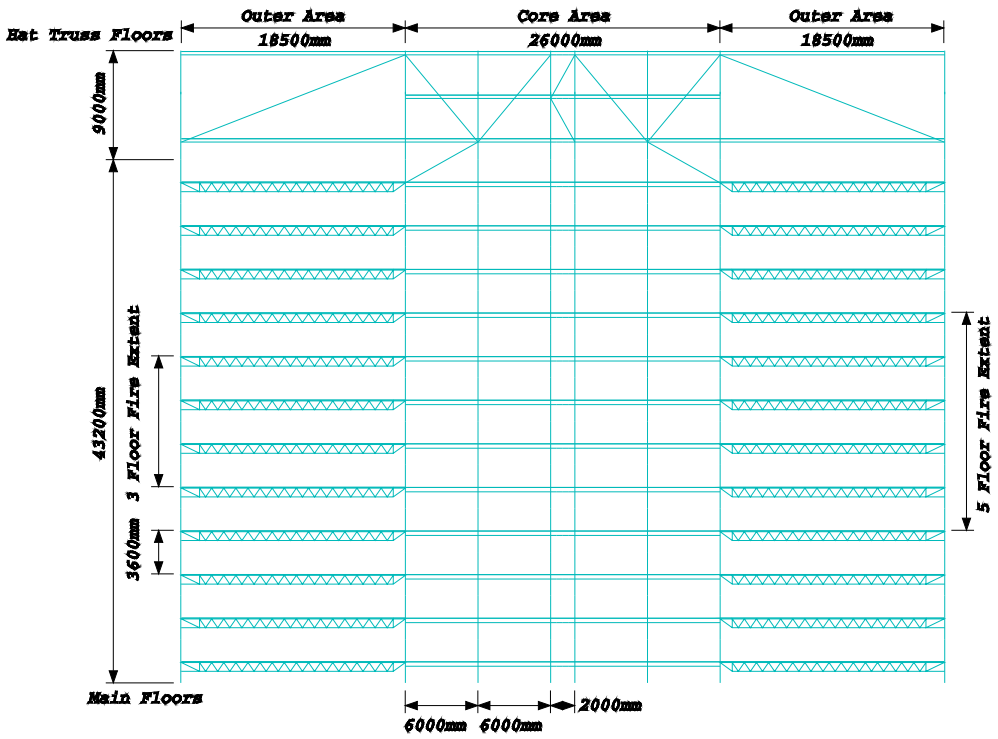

Figure 4.2: 2D Hat Truss Model

Member	Top Chord	Bottom Chord	Diagonal
Size	95x38mm	130x38mm	40mm Dia.

Table 4.1: Truss Member Sizes

The core members have been sized for the full 42x26m core of the real structure, despite the 2D nature of the model, in order to produce a reasonably stiff core structure. The core is assumed to be constructed using rolled steel beam sections spanning between columns. The beams used in the core of this model are all 406x178x54UB sections. The columns have all been assumed as built up sections with 400x50mm flange plates and 300x30mm web plates. The diagonal members that make up the hat truss have been included as 406x178x54UB sections in the appropriate model. These members were sized using an estimate of the floor loads.

The floor loading used throughout this model includes direct gravity loading for the steel structure and a distributed load of 3kN/m^{2}to account for the dead load of the floor slab and live loading on the floor. This value is similar to the value used by NIST in the official investigation of the World Trade Center collapse [52]. In the NIST models this value is justified as the design loading with a reduction factor of 0.25 applied to the Live Load. This loading might be considered light, compared with fire design loading in the UK (0.5 x Design Live Load [39]), but it has been shown in previous work [1, 7] that the applied loading only begins to become dominant when structural members are close to failure, i.e. the loading will affect the time to failure but not the response.

In each of the above models the concrete slab has been included as a layer of 2-noded linear beam elements above the tops of the trusses and beams. The slab over the trusses is 100mm thick while the slab in the core is 125mm thick. Reinforcement has been included in the slabs as a separate group of nodes and elements running through the midpoint of the slab that are tied to the slab nodes. This reinforcement has been modelled as a smeared layer of steel with the sectional area as that given by 2 layers of welded wire mesh combined (1 layer, of 6mm diameter bars running in both directions at 100mm pitch, each in the top and bottom of the slab).

All structural elements were modelled using linear beam elements and sufficiently large numbers of elements were used to allow for non-linear effects. Steel and concrete properties for elevated temperatures have been extracted from Eurocodes 2 and 3 [26, 27]. This data includes stress-strain curves and Young's Modulus at different temperatures. The concrete has been modelled using a "damaged plasticity" model included in ABAQUS [73].

In each of these models all connections between beams/trusses and columns are assumed pinned. This accurately models the kind of connection used between truss and column. Pinned connections were also used in the core. The base of all the columns have been fully fixed in rotation and translation. In the model including the hat truss the only boundary conditions applied are those at the base of the columns. This will allow sway mechanisms to be identified. In the model without the hat truss the tops of the columns are fixed in horizontal translation and all rotation but are allowed to translate vertically.

4.3 Fire Input

In this study the compartment temperatures are based upon a generalized exponential curve given by :

$$T(t) = T_o + (T_{max} - T_o)(1 - e^{(-at)}) \tag{4.1}$$

where T_{max} and T_o are the maximum and ambient compartment temperatures respectively. t represents the time over which the model is analysed. a is an arbitrary 'rate of heating' parameter and for the purposes of this chapter has been taken as 0.005. The applied temperature time distribution for the 100mm thick floor slab may be seen in Figure 4.3 which has been used for both of the models presented here.

The truss is assumed to have no protection and is therefore assumed to equal the compartment temperature. The outer columns are assumed to be protected with

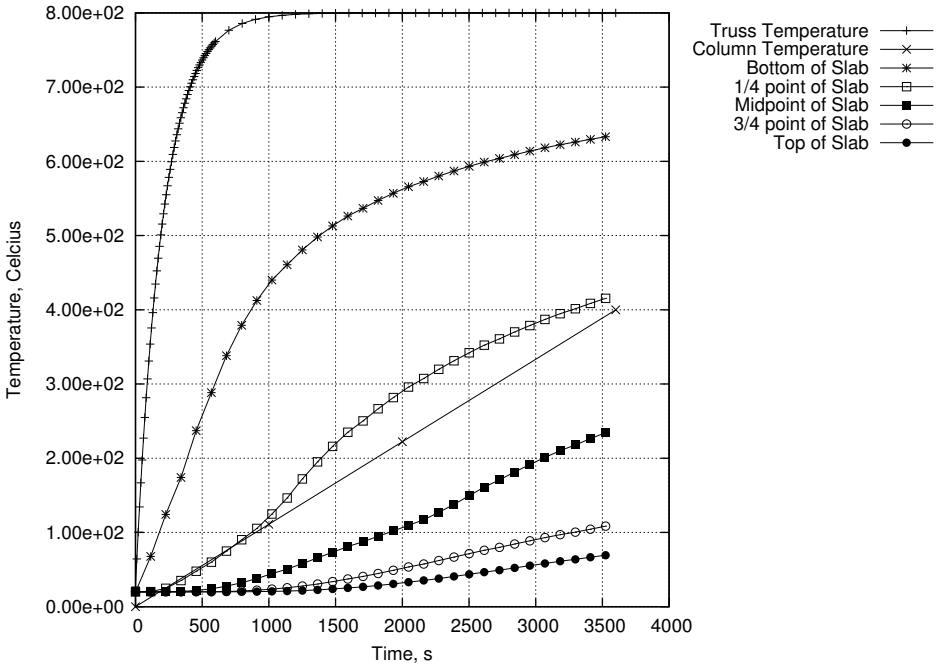

Figure 4.3: Temperature Time Distributions

a fire rated material and therefore will undergo more limited heating.

In both models the concrete slab has a realistic temperature distribution applied through its depth based on a heat transfer analysis from the fire [75]. This is done by applying individual time-temperature curves to 3 different points through the depth of the slab (top, bottom and midpoint). The slab was assumed to be heated from one side only even when it was between two floors that were on fire. This assumption is based on the amount of insulation that can normally be found on the upper side of an office building floor slab. Floor coverings, service gaps and suspended floor systems will all reduce the amount of radiation reaching the actual slab while convection will keep the hottest gasses away from the floor.

This fire regime was applied to the outer areas of several floors over the mid-height of the model. The number of floors under fire conditions is one of the parameters studied here. The structural members affected are the outer columns, the trusses and the associated areas of concrete slab. The core members were kept entirely at ambient conditions on the assumption that integrity was maintained by the core compartmentation.

Scenario	Max. Temp.	Hat Truss	No. of Fire Floors	Expan.*	Heated From
1	800°C	No	3 (5, 6 & 7)	Yes	Below Only
2	800°C	Yes	3 (5, 6 & 7)	Yes	Below Only

* Note : This column indicates whether the material properties used in the scenario included thermal expansion effects.

Table 4.2: Model Summary

4.4 Model Summaries

Table 5.1 shows the list of models presented in this chapter.

4.5 Results

4.5.1 General Response

For a detailed account of the responses of conventional structures under fire conditions please refer to previous work done in this area [1, 13, 76, 77]. In summary :

- In general, conventional composite steel frame structures have a much greater reserve of strength available under fire conditions than previously thought.
- Often, the effect of material degradation on the response of the structure is of secondary importance compared to the effect of restrained thermal expansion (including thermal bowing).
- Large deflections are also most often a result of restrained thermal expansion and bowing rather than the action of "load" on "structural members of reduced capacity" with consequent large mechanical strains.

In general the response of the structure investigated in this report matches well with the findings of these previous works. However because of the relative complexity of a truss system compared to a simple I-beam there are some important differences.

4.5.1.1 Truss Response

The following describes the general response of a truss system acting compositely with a concrete slab under the effects of fire. A more detailed discussion of these effects may be found in Flint *et al* [71].

In the cases investigated here the steel is assumed to be unprotected and hence heats up rapidly. As the concrete has a much lower thermal conductivity this leads to differential thermal expansion between the steel and the concrete. The top chord of the truss is highly restrained by the slab and hence as soon as it starts expanding it goes into compression, as may be seen in Figure 4.4.a, yields at around 100^{o}C and then unloads thereafter. The truss bottom chord and diagonals (Figures 4.4.b and 4.5 respectively) are much less restrained than the top chord and hence do not show the same sudden failure. As the bottom chord is the least restrained it allows the expansion of the steel to alter the truss geometry. With a suitably high temperature being applied to the steel the combination of expansion and material degradation will lead to buckling of the truss diagonals and then progressive failure of the truss. This, added to the general degradation of the steel strength as the temperature rises, leads to large deflections in the floor. With this change the truss will carry less and less of the load and the floor will move into tensile membrane action. Depending on the level of restraint, further expansion of the slab is converted into a combination of increased vertical deflection and lateral expansion.

Note : The plots for the truss diagonals have been split into D+ (DPlus) and D- (DNeg) groups. These relate to the direction of their slope as seen in the diagram in Figure 4.6. The diagonals in each group have been numbered sequentially from left to right.

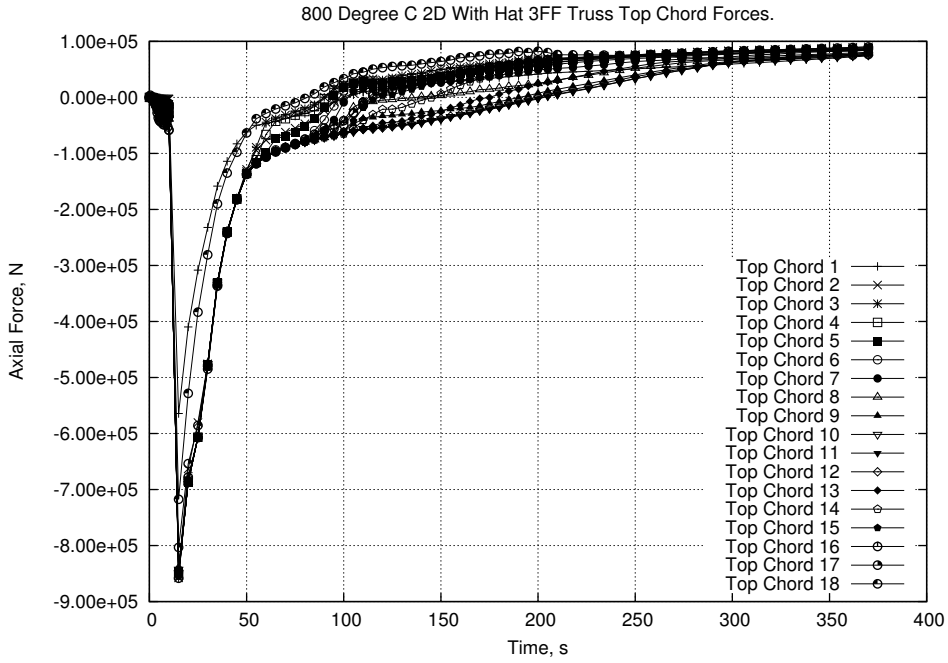

(a)

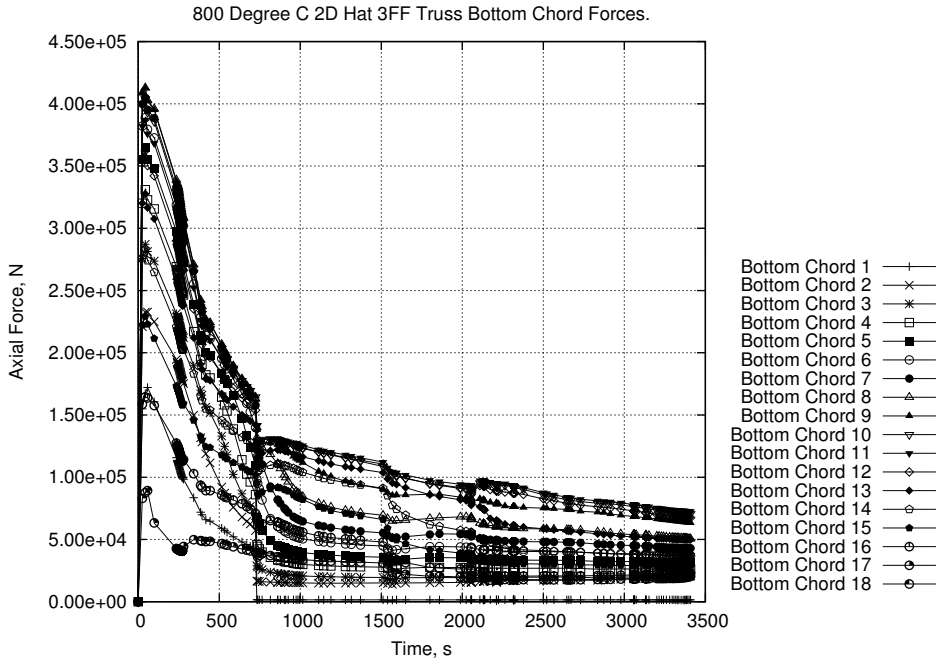

(b)

Figure 4.4: Truss Chord Axial Forces

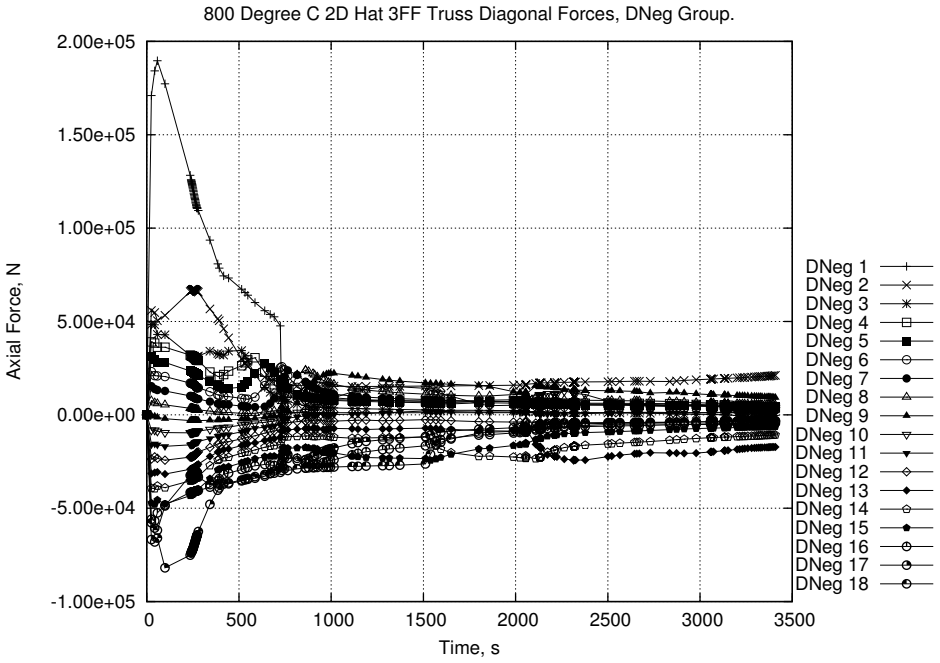

(a)

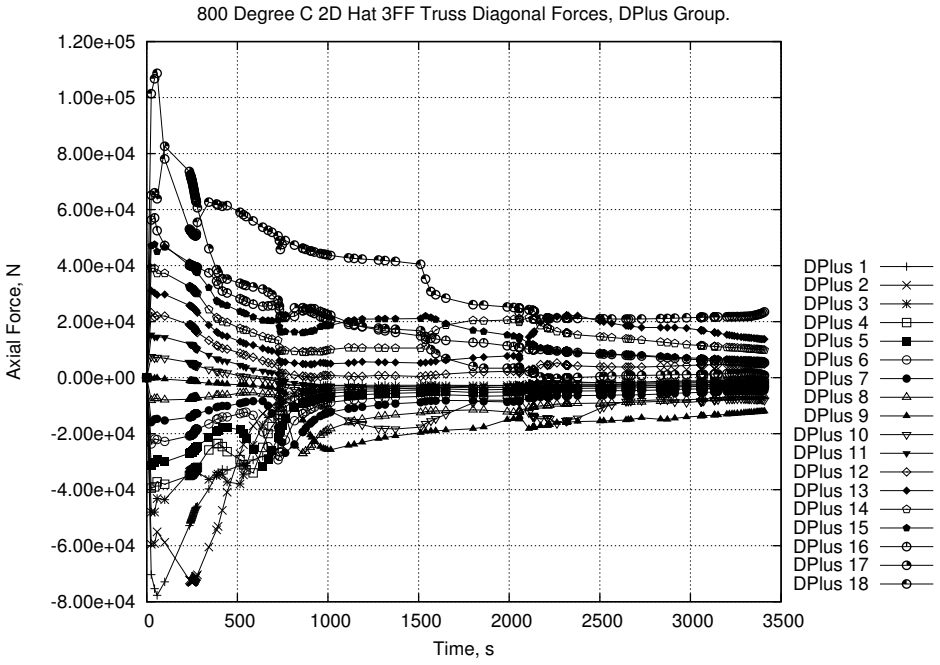

(b)

Figure 4.5: Truss Diagonal Axial Forces

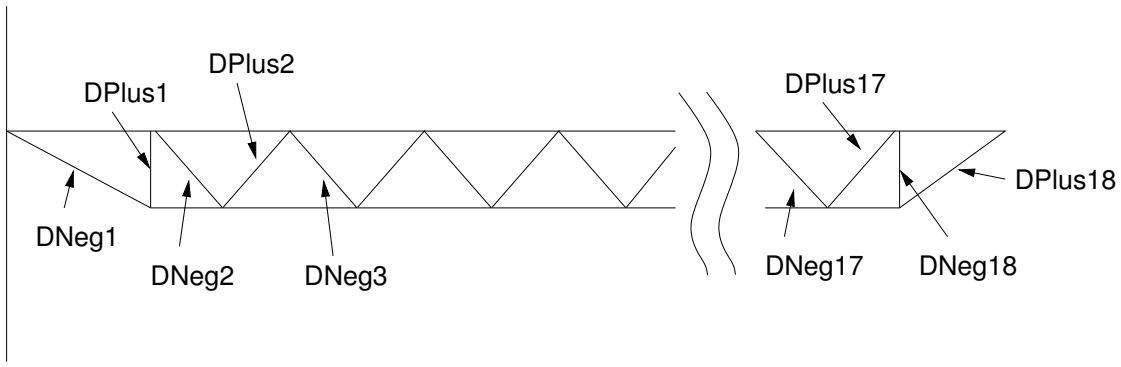

Figure 4.6: Diagonal Labeling System

4.5.1.2 Global Response

Scenario 1 - Without Hat Truss Below is a description of the observed global response of Scenario 1 (see Table 5.1 for details) that ended in collapse of the model after about 700s.

All the floors affected by fire (6, 7 & 8)start to expand. As the fire floors 6 and 8 are adjacent to cool floors (5 & 9), they go into high compression as they expand against the restraint provided by the column (see Figure 4.7). The cool floors (5 and 9) adjacent to the fire floors go into tension as the column is pushed out and pulls these floors along. These floors then act as pivots on the outer columns and the next floors up/down go into compression to a lesser degree. The middle fire floor does not undergo the same forces due to the actions of the column at that level. The expansion of the fire floors (6 and 8), at the interface of the heated and unheated floors, forces the outer columns to move into a curve. This curve means that tension is developed in the 7th floor connection as this floor is expanding at the same rate as the other fire floors while the column at that level is moving out further due to compatibility. This phase occurs as the steel heats up rapidly over the first 200-300 seconds. Figure 4.7.a shows the early stages of the fire while 4.7.b shows the full analysis to failure.

As the interface fire floors (6 & 8) begin to lose stiffness they retract and the outer columns also begin to return until the floors move into tensile membrane/catenary

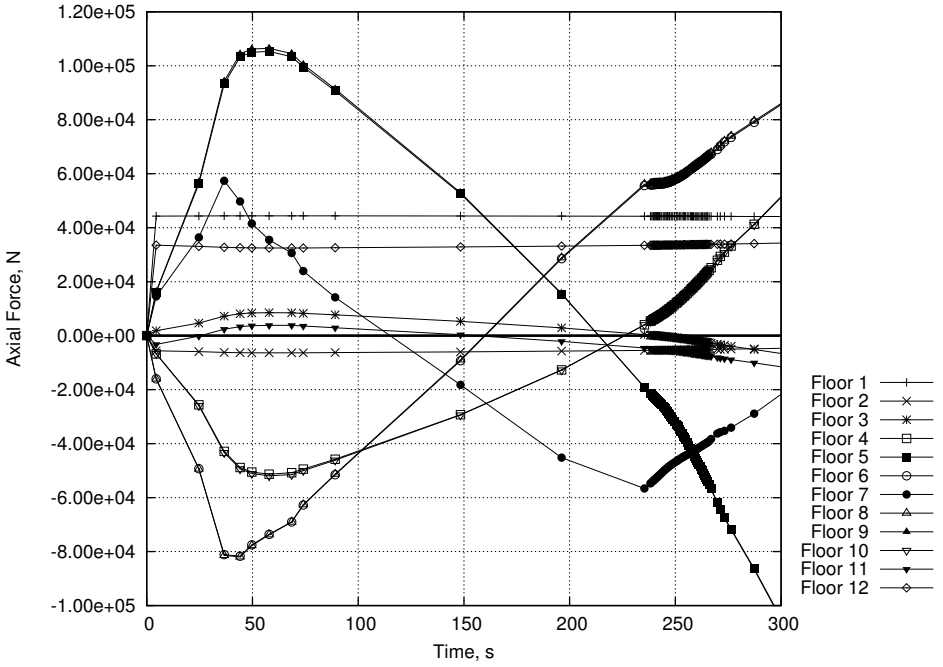

(a)

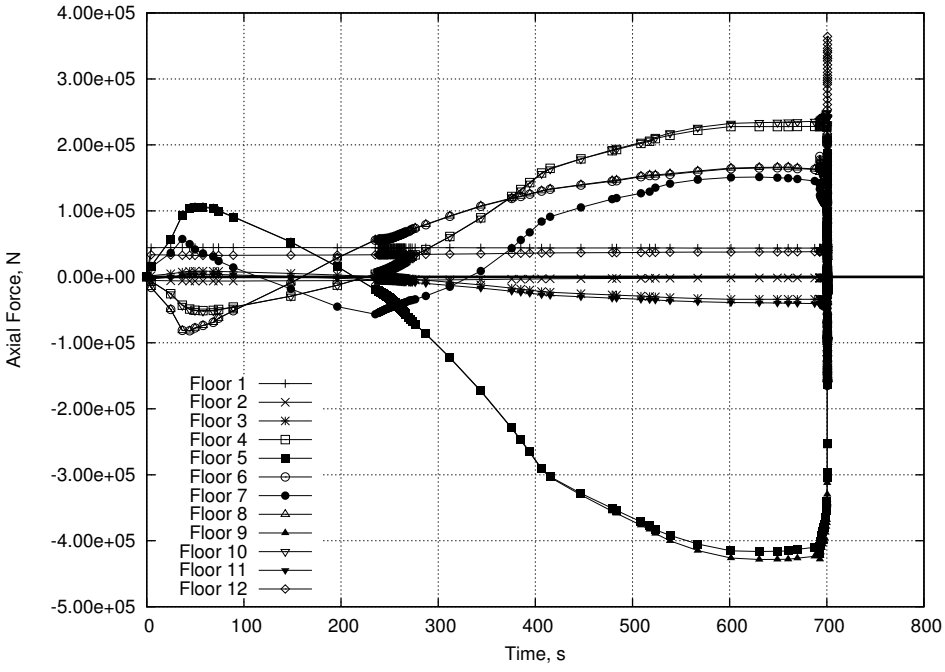

(b)

Figure 4.7: Scenario 1 : Floor Membrane Forces

action and actively pull the column inward. To counter this the cool adjacent floors (5 & 9) go into compression. The forces again pivot their way through the rest of the cool structure. As the interface fire floors lose stiffness they move into tension and middle fire floor moves into compression as the column moves back in. The middle fire floor (7) is subjected to compression for up to 330s before large deflections in the floor take it into tension.

Following the plot of horizontal displacement in one of the outer columns at the different floor levels in Figure 4.8.a shows the onset of failure at about 700s. Referencing this against the moments present within the column shown in Figure 4.8.b, indicates a clear plateauing toward the end. Figure 4.9 shows the failure envelopes of the column section under combined axial force and bending moments as derived from ABAQUS and from the Eurocode 3 equations. For the ABAQUS failure envelope a 1m length of the column was subjected to different axial forces, up to the maximum capacity of the section, and then moments were applied until failure ocurred. Plastic capacity has been reached and hence the failure of the outer columns is due to the attainment of a plastic mechanism with hinges at the connections of floors 5, 7 and 9. The Eurocode 3 equations appear to overpredict the plastic capacity of the section at relatively low axial loads. The final displaced shape of the structure may be seen in Figure 4.10.

In order to understand the processes involved in the movement of the outer column an analysis was conducted comparing the moments in the column taken directly from ABAQUS to those produced by theory. The outer column was simplified into a fixed ended beam as shown in Figure 4.11 with the fire affected floors (6, 7 & 8) being represented purely by a horizontal force. The effect of the cool interface floors, above and below the fire floors, was modelled by assuming a fixed end at that point. Simple bending theory was applied to create equations for the moment at points A, B and C as caused by forces H1, H2 and H3. These forces are the horizontal component of the forces in the truss-column connections as taken directly from ABAQUS. Additionally the P-δ moment at C was calculated using the applied load P and the horizontal deflection of point C again taken directly

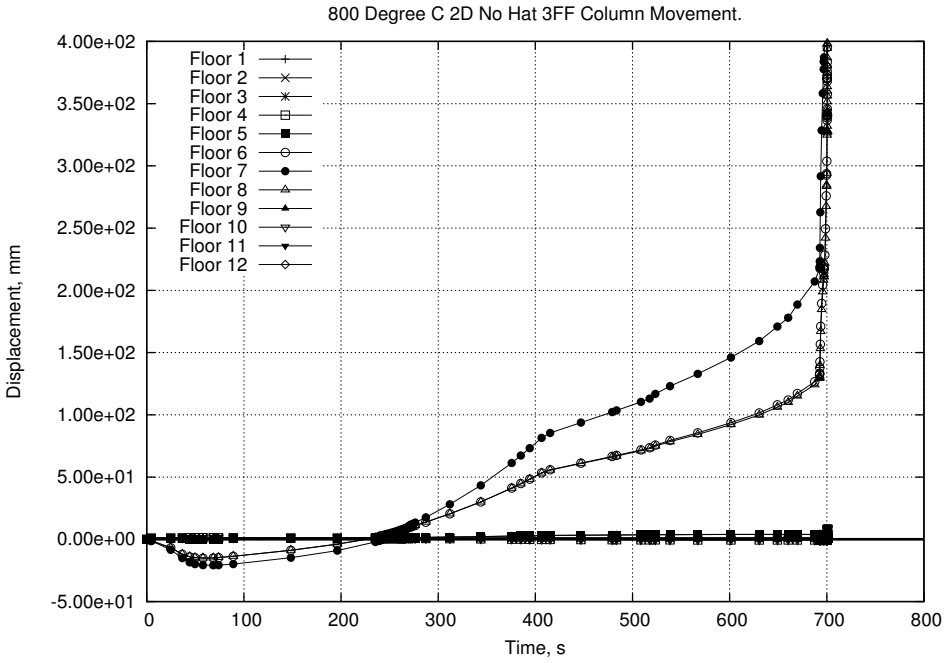

(a)

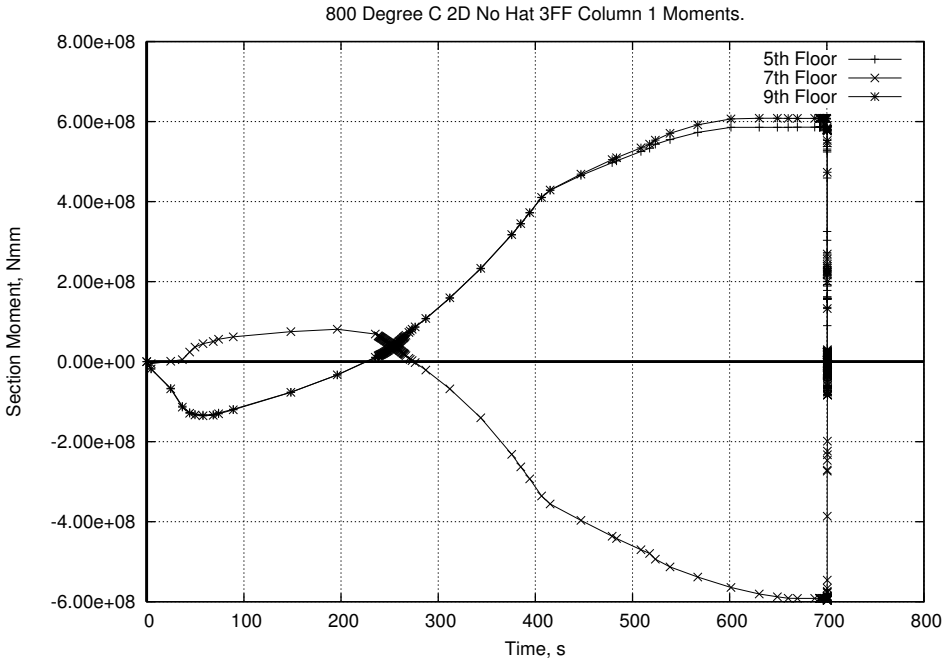

(b)

Figure 4.8: Scenario 1 - Horizontal Column Movement

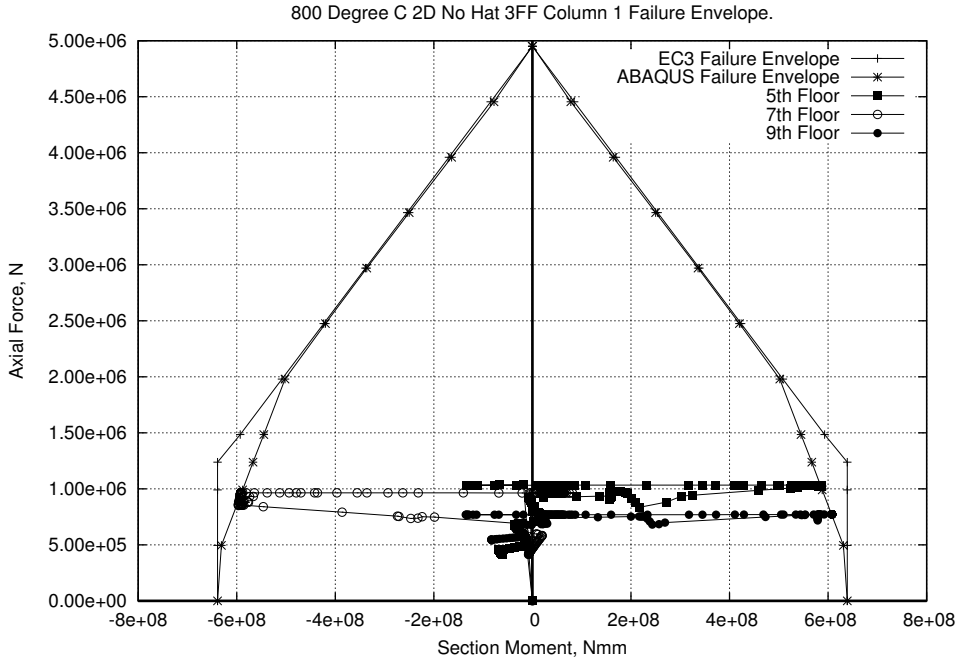

Figure 4.9: Column Failure Envelope

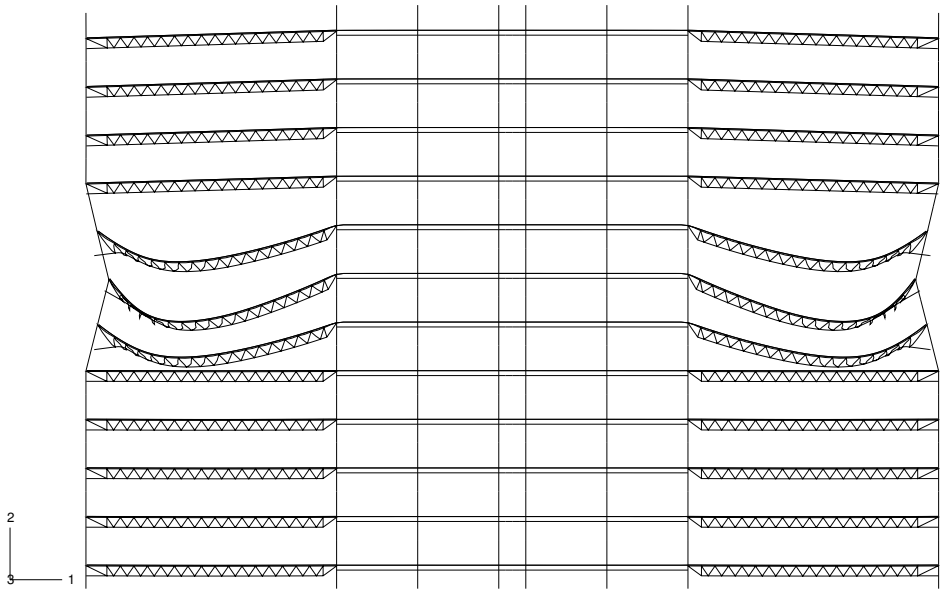

Figure 4.10: Scenario 1 Final Displaced Shape

from the ABAQUS analysis.

Figure 4.12 shows the comparison between the figures taken from the simplified theory and those taken directly from ABAQUS. The results match very closely. For *MA* and *MB* the moment can be seen to be somewhat higher for the theory but this can be explained by the choice of boundary conditions. The full ABAQUS model effectively has spring supports at floors 5 and 9 due to the continuation of the columns. The fully fixed supports assumed for the theory calculations naturally attract a higher moment. For *MC* it is clear that under the conditions present in this model it is the moment caused by the floor pull in forces that is dominant. The *P-δ* moment grows in significance over the course of the analysis but even near collapse is smaller than the midspan moment caused by the floor forces. However as collapse progresses the *P-δ* moment increases at a much higher rate. When these moments are combined then the theory closely matches the model. If a larger load was applied to the column or if the column section was stiffer (therefore deflecting less) then the P-delta component of the moment would be more or less, respectively. The effects of altering column section must be carefully balanced against the forces found in the floors. A reduction in column lateral displacement will help reduce *P-δ* moments but will also increase connection forces leading to possible failure.

The theory calculations did not take into account the vertical component of the floor forces but as the results match so closely it can be assumed that the effect of these vertical forces are negligible.

Failure of this structure is a result of the inability of the structure to redistribute loads away from affected areas. The lack of redistribution is clear from Figure 4.13.a. Not only do the floors in this scenario lose the ability to provide lateral restraint to the column but they actively pull the columns out of plane. With enough displacement in the columns the ability to hold up the floors above is lost and progressive collapse is initiated. Figure 4.13.b plots the vertical displacement at the top of each of the columns in the model and shows runaway in the outer columns. Note : the columns are numbered sequentially from left to right. Hence Columns 1 and 8 are the external columns while Columns 2 to 7 are core columns.

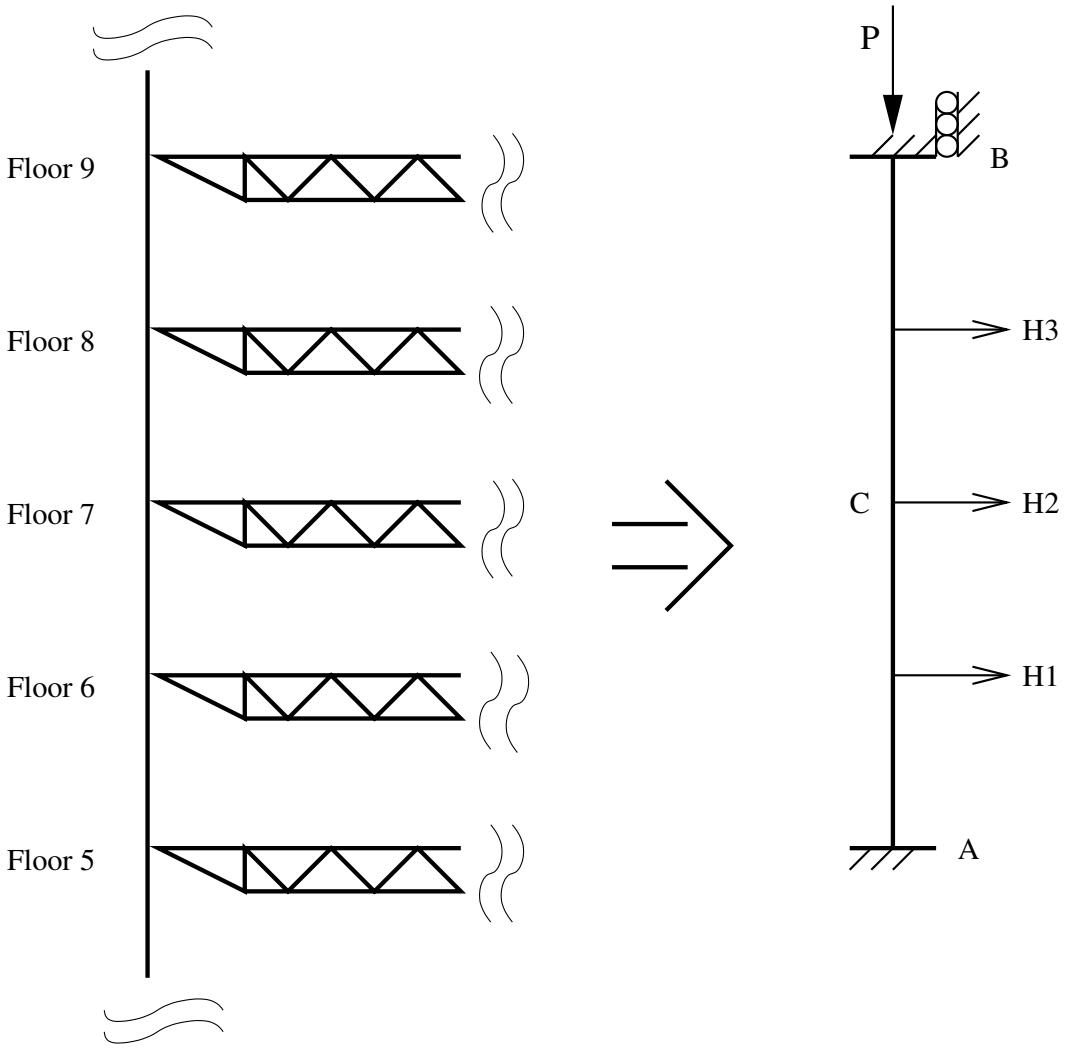

Figure 4.11: Column Theory Simplification

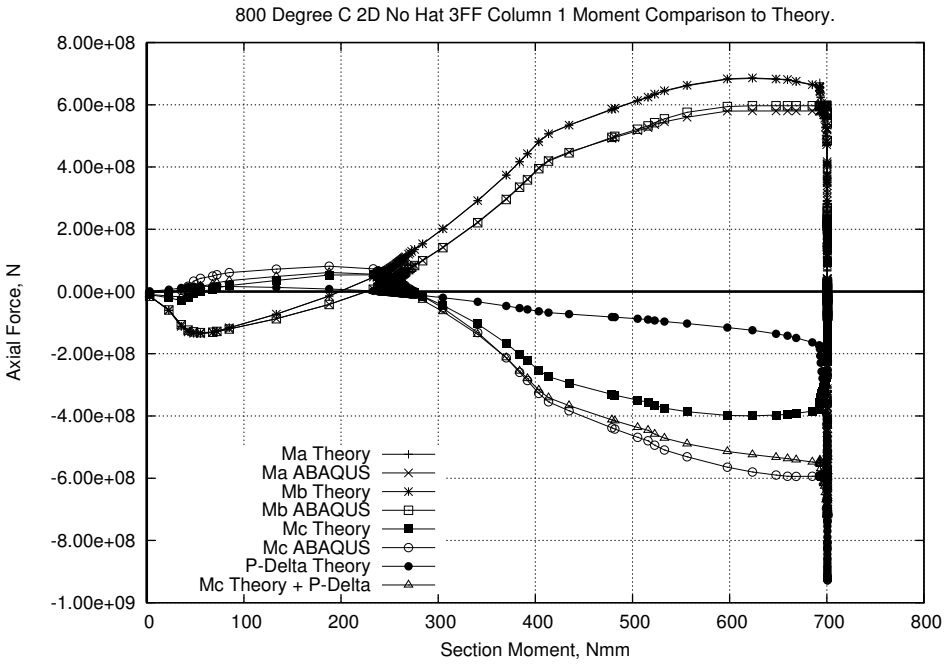

Figure 4.12: Column Moment Theory Comparison

Scenario 2 - With Hat Truss Scenario 2 effectively continues from where Scenario 1 ends as the initial responses are the same. Where the structure in Scenario 1 fails, the redistribution available from the hat truss allows Scenario 2 to continue for significantly longer before eventual failure. However the structure in this scenario also appears to collapse after around 3500s.

Clear redistribution can be seen in the reactions at the column base (Figure 4.14) for Scenario 2 unlike Scenario 1 (Figure 4.13.a) where no such action is seen. It is significant that in Scenario 1 the structure fails at the point where Scenario 2 shows significant load being transferred from the outer columns to the core. In Scenario 1 the outer columns over the fire floors are pulled in by the floors until they can no longer sustain the axial compression of the floors above. The hat truss allows the outer columns above the fire floors to move from compressive to tensile action when the columns can no longer sustain the compressive loads. This tensile force then allows the hat truss to move the load to the core columns.

Figure 4.15 shows the membrane forces in the floors, with Figure 4.15.a concentrating on the start of the analysis and Figure 4.15.b showing the full analysis to

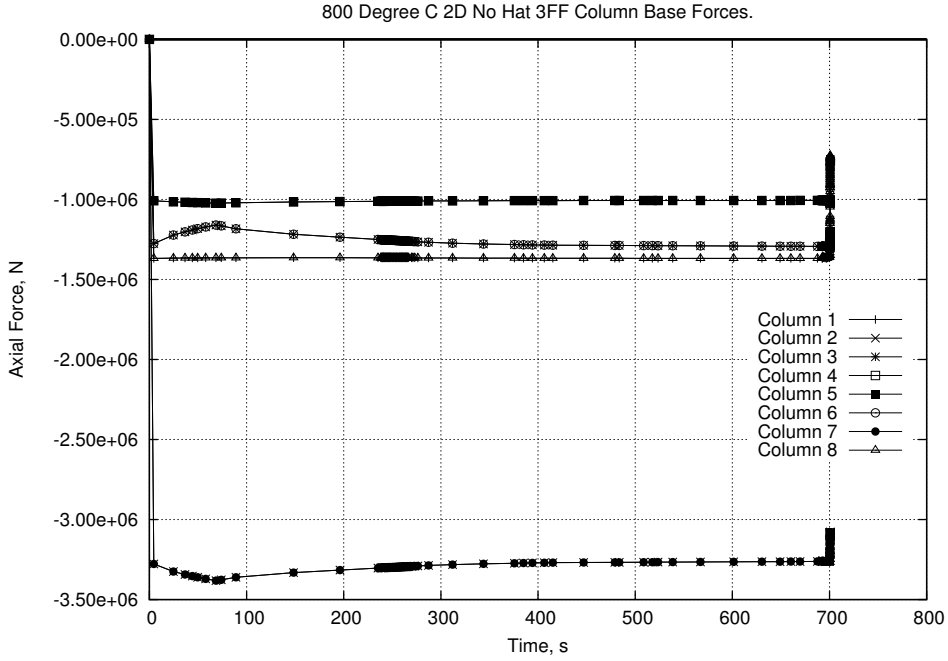

(a)

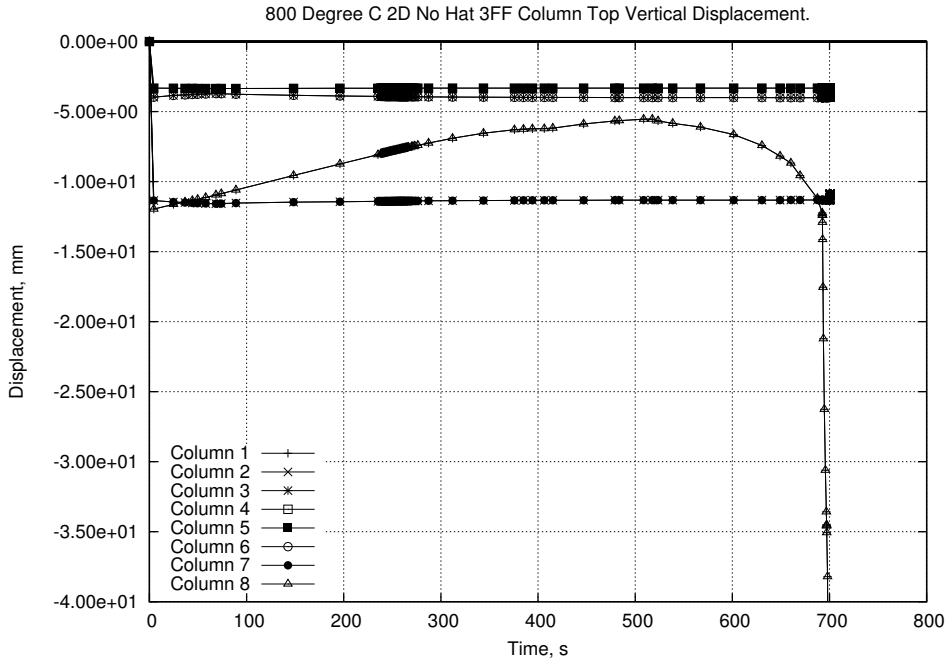

(b)

Figure 4.13: Scenario 1 Column Responses

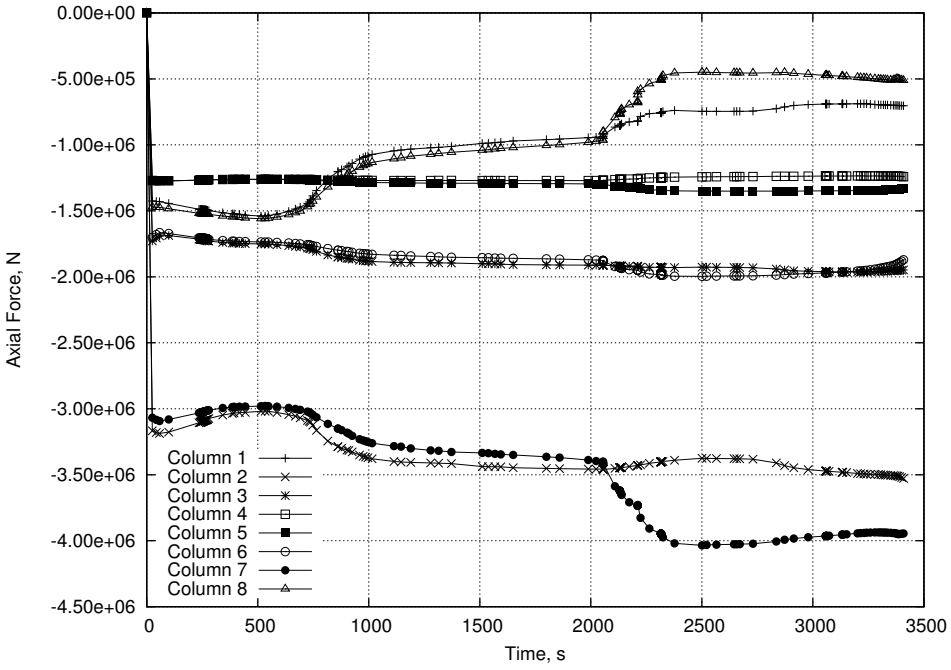

Figure 4.14: Scenario 2 : Column Support Forces

model failure at around 3400s. The early response is the same as that for Scenario 1 (Figure 4.7). As the fire floors move into full tensile membrane action the structure stabilizes itself using the secondary load path through the hat truss. The outer columns see large forces pulling them in due to the fire floors hanging from their connections. To counter this the cool interface floors (5 and 9) above and below the fire floors move into high compression. The lateral loading on the outer columns then pivots its way up and down the building with floors 4 and 10 moving into substantial tension and floors 3 and 11 seeing a slight increase in compression. The building in this case can support such loading but it does show the possibility that the cool interface floors could buckle under the high compression which would again initiate a progressive collapse mechanism similar to that described in the work by Usmani [63]. Introducing a stiffer column section would reduce deflections under the same loading hence increase tension in the connections between the fire affected floors and the column.

Examining the moments in the outer columns indicates that plastic hinges form at the connections between floors 5, 7 and 9. Figure 4.16.a shows the moments

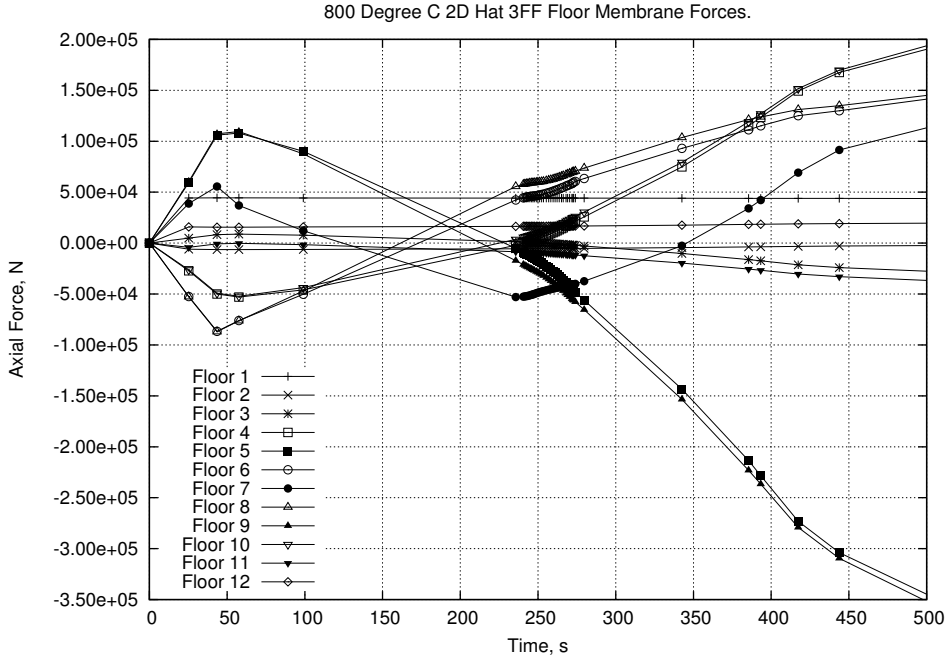

(a)

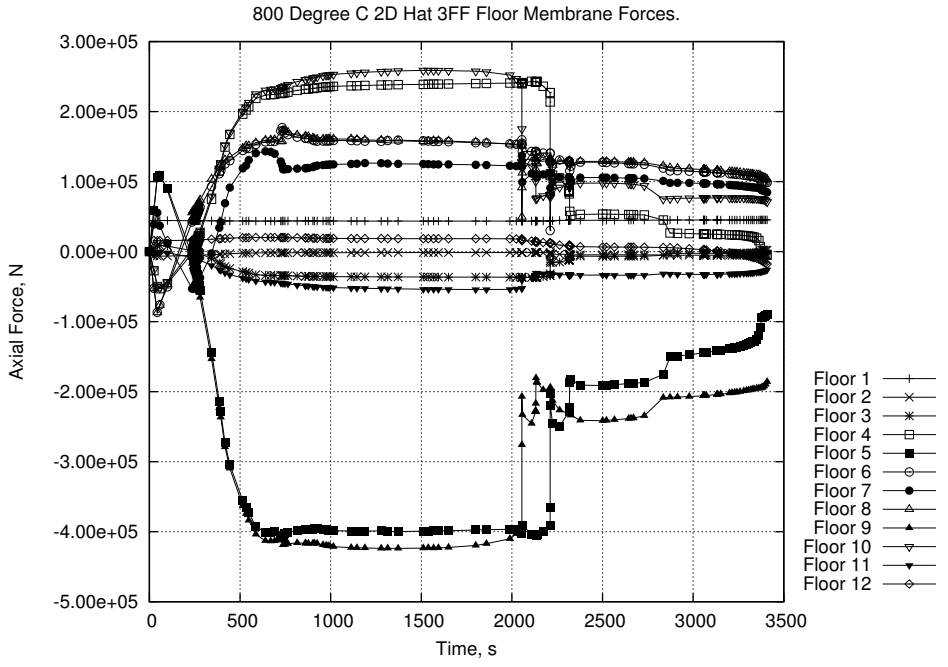

(b)

Figure 4.15: Scenario 2 : Floor Membrane Forces

at these locations in Column 8 with respect to time while Figure 4.16.b shows the plastic failure envelope for combined compression and bending. The envelopes shown are derived from an investigation of the section capacity using ABAQUS and from the Eurocode 3 equations for combined axial load and bending moment. Plastic hinge formation is again apparent at floors 5, 7 and 9. The hat truss is able to redistribute the axial load of the fire floors and above into the core leading to a reduction of axial force in the column. It is apparent that the columns follow the failure envelope as this redistribution occurs. The ability of the hat truss to redistribute load means that the mechanism that is formed in the columns is not able to collapse the structure until the hat truss is also overwhelmed.

Figure 4.17 shows the building at the end of the analysis. Plastic hinges are apparent in the outer columns at the cool interface floors (5 and 9) and at the connection to the middle fire floor (7). Indications that the hat truss is reaching the limit of its capacity can be seen in Figure 4.17 at the interface between the outer areas and the core. Distortions in the structure can be seen on both sides but are more obvious on the right hand side of the core. A final indication of failure is the vertical deflections that can be seen in Figure 4.18. The hat truss has reached the end of its capability and column 8 begins to collapse. This however shows an unsymmetric collapse mechanism with Column 1 being pulled up as Column 8 collapses.

4.6 Conclusions

This chapter analyses expected responses of a large building under fire conditions and reports on an interim stage in the investigation into the effects of fire on buildings with long span, truss based floor systems. The 2 dimensional nature of the models used in the investigation presented here means care should be taken in drawing definite conclusions from the results of this study. The results match well with other work in this area [71].

This investigation is not meant to be a fully inclusive forensic study of a particular building and as such includes several assumptions that affect its applicability to

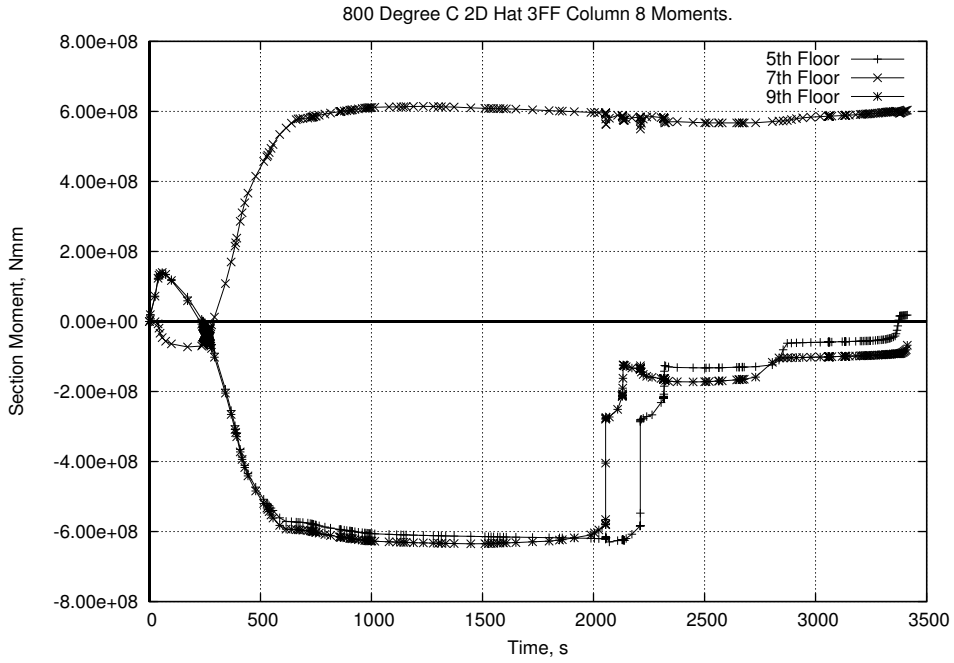

(a)

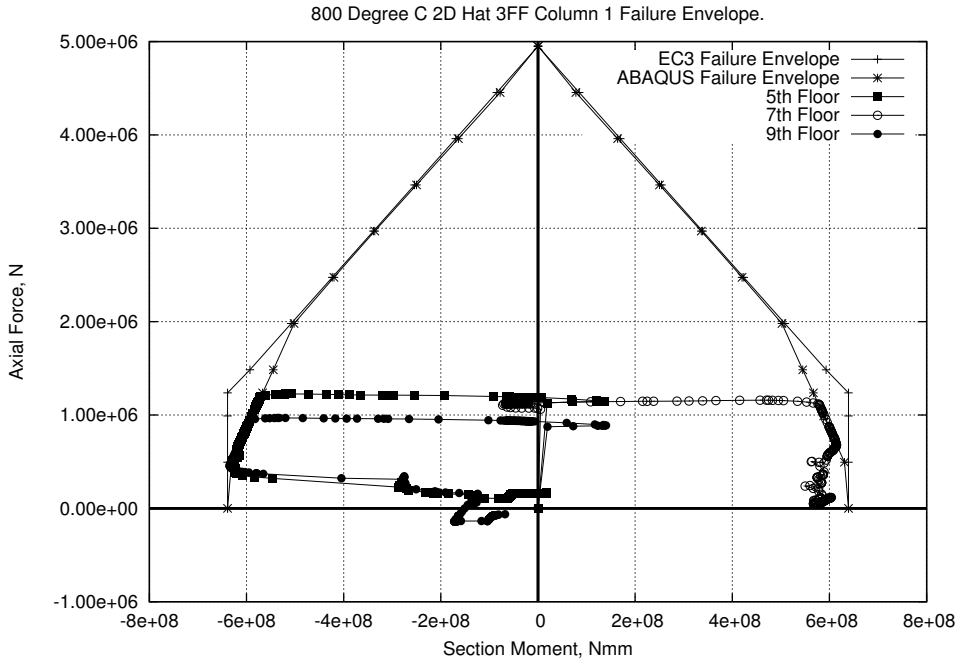

(b)

Figure 4.16: Scenario 2 : Column Moments

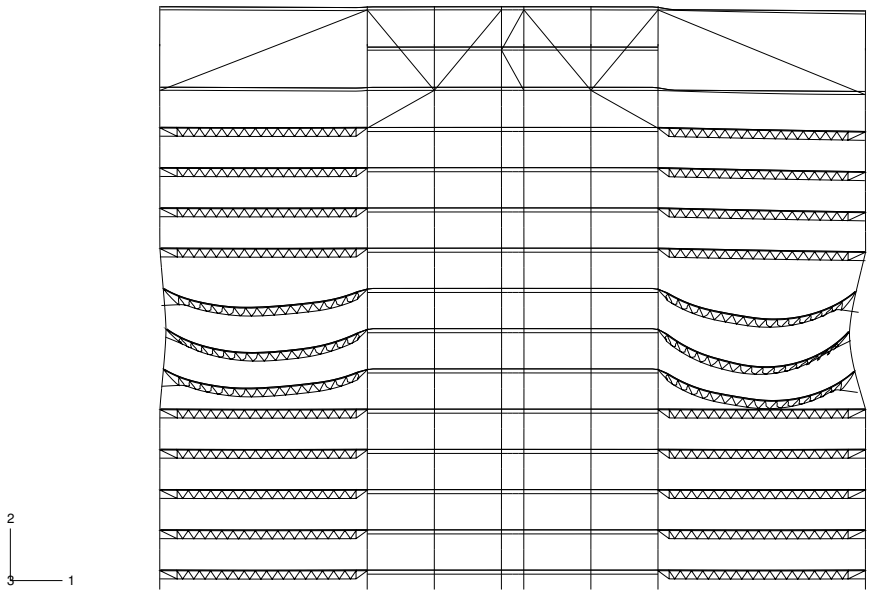

Figure 4.17: Scenario 2 : Structural Failure

real structures. First of all the models involved are all 2D. Secondly connections have been modelled such that failure may not occur. A simple comparison between the forces seen in the column-truss connection elements and the capacity of the connections as calculated by NIST [52] for the World Trade Center towers is possible. This shows that the maximum tension in the fire affected floors is under 200kN and therefore well within the expected total connection capacity of 260kN at around 800^{o}C. The total connection capacity includes the truss seat system as well as additional members connecting the trusses to nearby columns.

Other effects that would appear in a real building but have not been considered here include direct interaction between floors. At the high level of midspan deflection that appears in some of the models it is possible that spalling and partial floor failure may occur and directly increase the loading on lower floors. This again would lead to dynamic forces being applied that could cause failure of these floors. In particular this would be a problem in the cool interface floor below the fire floors.

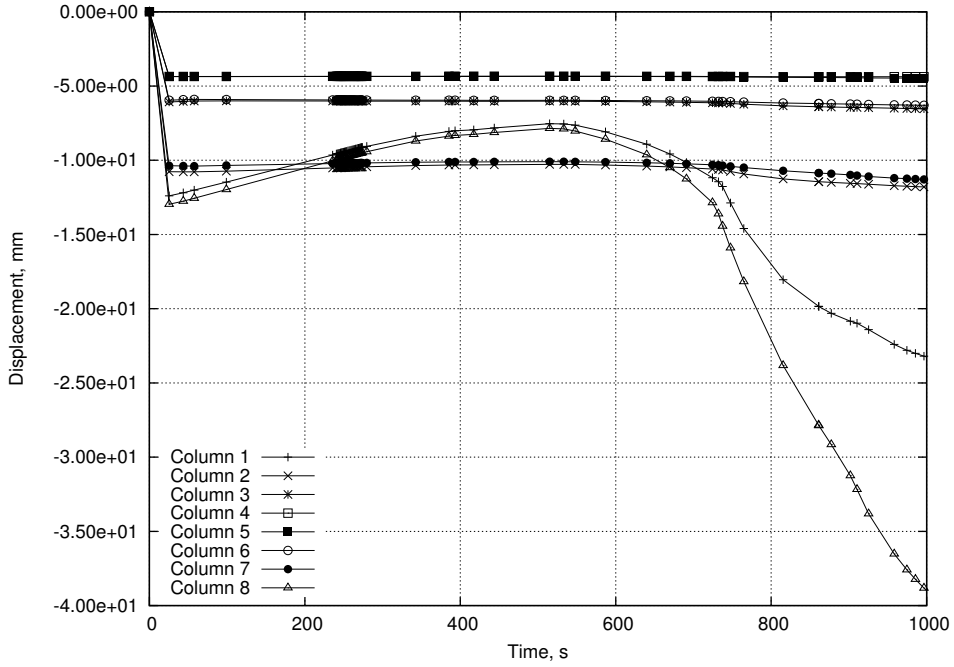

(a)

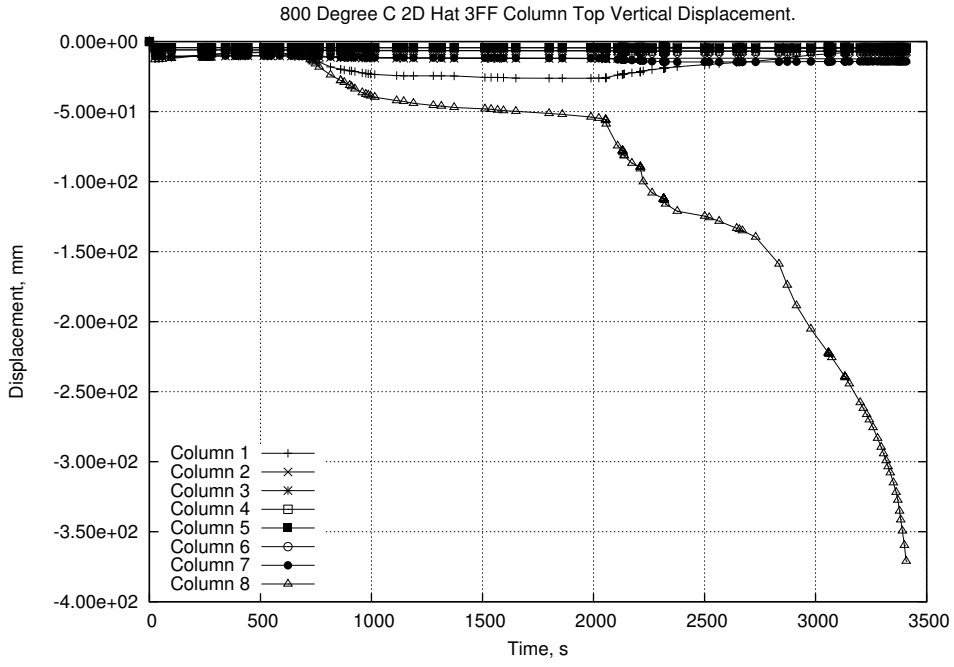

(b)

Figure 4.18: Scenario 2 : Column Top Vertical Displacement

Failure of this interface floor would increase the demand on the floor below, and so on.

Large displacements may be seen in the floor trusses under fire loading which can have a significant effect on the response of the columns. Global failure mechanisms are based around failure of the outer columns after they have been drawn inward by tensile membrane action in the trusses and form plastic hinges at floor-column interfaces. A heavier column section would limit the deflections and moments within the column but would lead to higher forces in the truss-column connections leading to the possibility of progressive collapse from connection failure or progressive failure of floors in compression [63].

If the possibility of redistribution exists then a new load path will be established and the building will stabilize. Collapse will then occur when all possible strength reserves have been exhausted. Such global mechanisms involve the full structure of the building and would not be found in a model of a smaller region of the building.

The next stage in this project is to move to a full 3D model of a similar number of floors to the models presented here. This will remove some of the limitations introduced by the 2D aspect of this study as well as allowing for a greater degree of realism in the fire regimes applied to the structure.

Chapter 5

Structural response of tall buildings to multiple floor fires :

Part 2 - Parametric study

This chapter presents the results of a further investigation of the structures presented in Chapter 4 [78]. It is designed to indicate the differences in response of a tall building utilizing long span, truss based floors when subjected to a variety of fire regimes. Changes to material properties and structural layout are also included.

The general responses and collapse mechanisms seen in earlier work (Chapters 3 & 4) are seen throughout the models presented here. Changes to the various factors in the structural model also provide distinct changes to the response.

5.1 Introduction

Chapter 4 presented a detailed study of the response of a large, multi-storey steel framed office building utilizing long span composite truss floor systems. The result of Chapter 4 was the identification of 2 possible collapse mechanisms for such structures with a 3rd being identified in this chapter. Further work was then conducted to define how changes in the conditions present in the structure would affect the instigation of such collapse mechanisms.

This chapter presents the results of an investigation of a set of parameters affecting

the response of the same building to multiple floor fires. These parameters include changes to boundary conditions, structural redundancy, fire regime and material properties. The parameters chosen have a direct impact on the collapse mechanisms found in Chapter 4. Some parameters, such as the inclusion of thermal expansion, have been extensively investigated for other structures [1, 7, 16] and it is important to show that these assumptions still apply. Research is still being conducted by others [52] that does not include the full effect of thermal expansion. Results presented later in this chapter indicate that care should be taken using such assumptions in computer modelling as the outcome can vary considerably. Models should include the correct physics for the situation being modelled. The main comparisons being made in this chapter, however, are to do with the fire regime involved and the extra robustness afforded the structure by the addition of a hat truss. The response of a structure is linked to the loading it is subjected to hence a range of fire regimes need to be investigated to create bounds for instigation of collapse.

The commercial finite element modelling program ABAQUS is used to model the structure under investigation. The program can accurately predict the large displacements commonly seen in structures in fires as well as allowing for the degradation of the materials at higher temperatures and the geometric effects of heating (thermal expansion and bowing).

The results of Chapters 3 & 4 are summarized here to allow comparison between the cases presented in Section 5.3.

- Compatibility within the structure due to thermal expansion is the main driving force for the full response of the structure.
- Trusses do not suddenly buckle early in the fire but rather deflect steadily and move into catenary action in a similar manner to Universal Beam sections.
- Buckling of individual truss web diagonals is seen as restrained thermal expansion and thermal degradation of the material properties take effect.

Scenario	Max. Temp.	Hat Truss	No. of Fire Floors	Expan.*	Heated From
1	800^{o}C	No	3 (5, 6 & 7)	Yes	Below Only
2	800^{o}C	No	3 (5, 6 & 7)	No	Below Only
3	500^{o}C	No	3 (5, 6 & 7)	Yes	Below Only
4	500^{o}C	No	5 (4, 5, 6, 7 & 8)	Yes	Below Only
5	800^{o}C	No	5 (4, 5, 6, 7 & 8)	Yes	Below Only
6	800^{o}C	Yes	3 (5, 6 & 7)	Yes	Below Only
7	500^{o}C	Yes	3 (5, 6 & 7)	Yes	Below Only
8	800^{o}C	Yes	3 (5, 6 & 7)	No	Below Only
9	800^{o}C	Yes	3 (5, 6 & 7)	Yes	Above and Below
10	500^{o}C	Yes	5 (4, 5, 6, 7 & 8)	Yes	Below Only
11	800^{o}C	Yes	5 (4, 5, 6, 7 & 8)	Yes	Below Only

* Note : This column indicates whether the material properties used in the scenario included thermal expansion effects.

Table 5.1: Model Summary

- Failure is related to the stability of the outer columns and the restraint available from the floors.

- Plastic hinge mechanisms appear in outer columns.

- Additional redistribution systems (hat truss) appear to increase building survivability substantially.

5.2 Model Summaries

Table 5.1 shows the list of models investigated for this chapter. Scenarios 1 and 5 are the analyses presented in Part 1. The geometry used in each of the models is as described in Section 2 of Part 1. The fire regimes are based on the equation presented in Section 3 of Part 1. The fire regime was one of the parameters examined in this study. A 500^{o}C peak compartment temperature fire was examined as well as the 800^{o}C peak presented in Part 1. Fires over 5 floors were investigated as well as fires over 3 floors.

5.3 Detailed Model Results

5.3.1 Scenario 1 - Base Case 1 : No Hat Truss, 800^{o}C Peak Temperature, 3 Floor Fire

This model is subjected to a peak temperature of 800^{o}C over floors 5, 6 & 7 with the concrete being heated from the underside only, on all appropriate floors. No hat truss is used in this scenario. The material models for steel and concrete include thermal expansion.

As presented in Part 1Chapter 4, membrane forces in the fire floors, as shown here in Figure 5.1, are sufficient to displace the outer columns significantly out of line. Compression forces in the early stages of heating push the columns out by around 25mm. As the floor system deforms, by sagging, the outer columns return to their original position before tensile action in the fire floors pulls them inward. When the columns are displaced sufficiently the combination of bending moments, from the floor lateral loading, and increasing P-δ action, from the increasing eccentric displacement in the columns, causes plastic hinges to form in the columns as discussed in Part 1. This allows mechanisms to form leading to the collapse of the outer floors. Figure 5.2.a shows the moments in the outer column with respect to time. This data is then overlaid on the failure envelope for the column under combined axial force and bending moments in Figure 5.2.b.

The deflection plots in Figure 5.3 show runaway vertical deflections in both the midspan of the truss and in the outer columns. The floor runaway can be seen to begin on the fire floors, which also spreads to the cool floors above as the columns begin to collapse. Figure 5.3.b also shows how the tops of the outer columns initially rise because of thermal expansion. At 250s into the analysis the middle fire floor deflection increases more than the other fire floors indicating that sagging is taking place and the column is being drawn back inward. This phenomenon is also indicated in Figure 5.3.b as the rate of displacement reduces from the initial linear rate to a curve. As the column continues to be drawn inward by the sagging

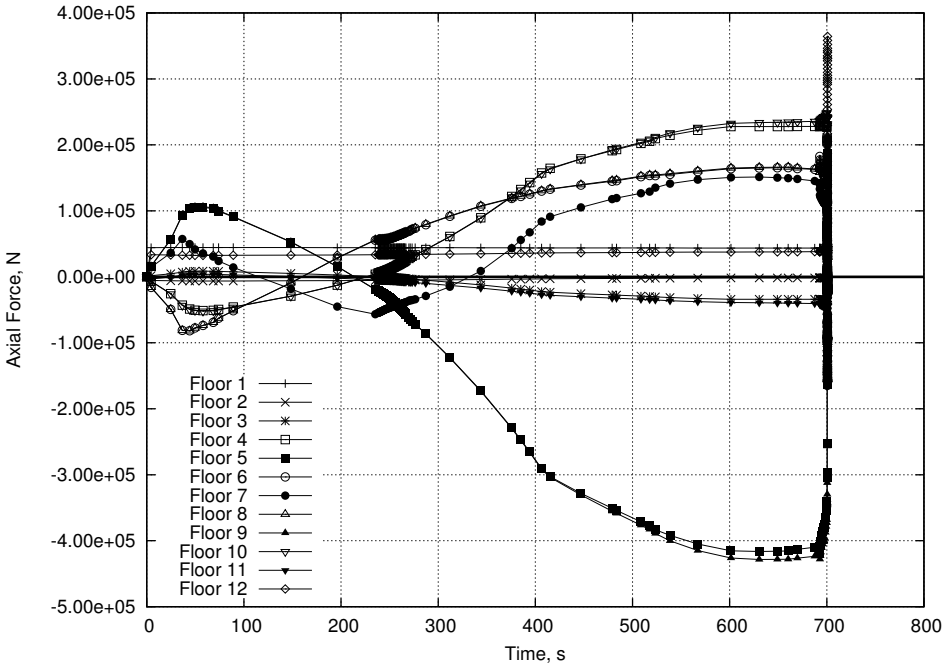

Figure 5.1: Scenario 1 : Floor Membrane Forces

of the trusses the top of the outer columns begin to drop back down. A numerical test of a single column confirmed that, without the horizontal displacement in the column caused by the movement of the floors, the column stays stable and simply expands upward due to thermal expansion. This indicates a direct relationship between the vertical movement in the top of the column, as shown in Figure 5.3.b, and the horizontal movement of the columns, as caused by the movement of the fire floors, rather than being induced by material failure at elevated temperatures. In this case the lack of bending moment and serious thermal degradation of material properties means that the column has sufficient axial capacity to expand freely. Runaway deflection of the tops of the columns is a direct indicator of collapse. The deflected shape at the point the analysis terminated may be seen in Figure 5.4.

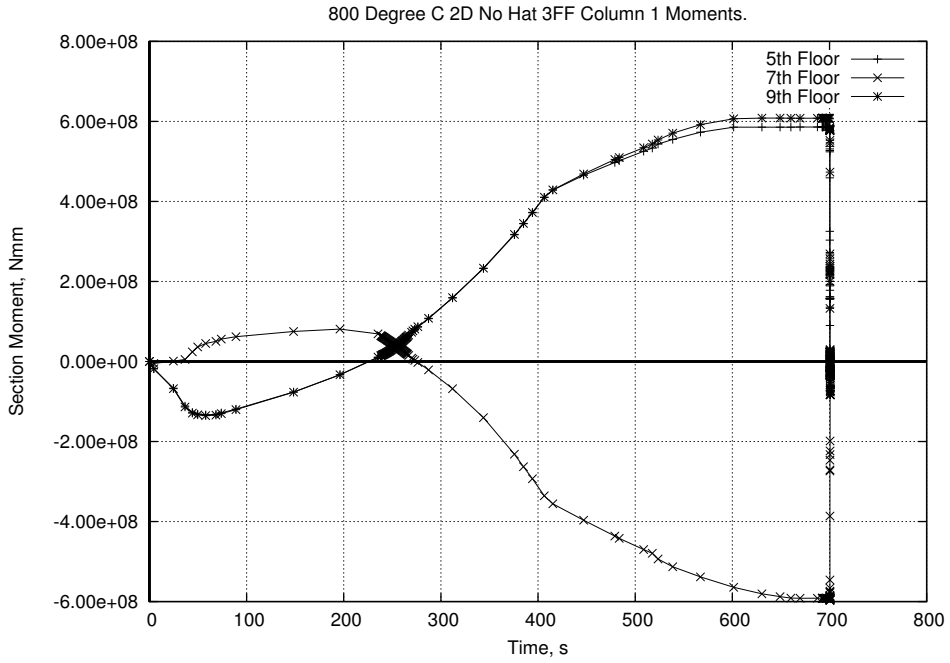

(a)

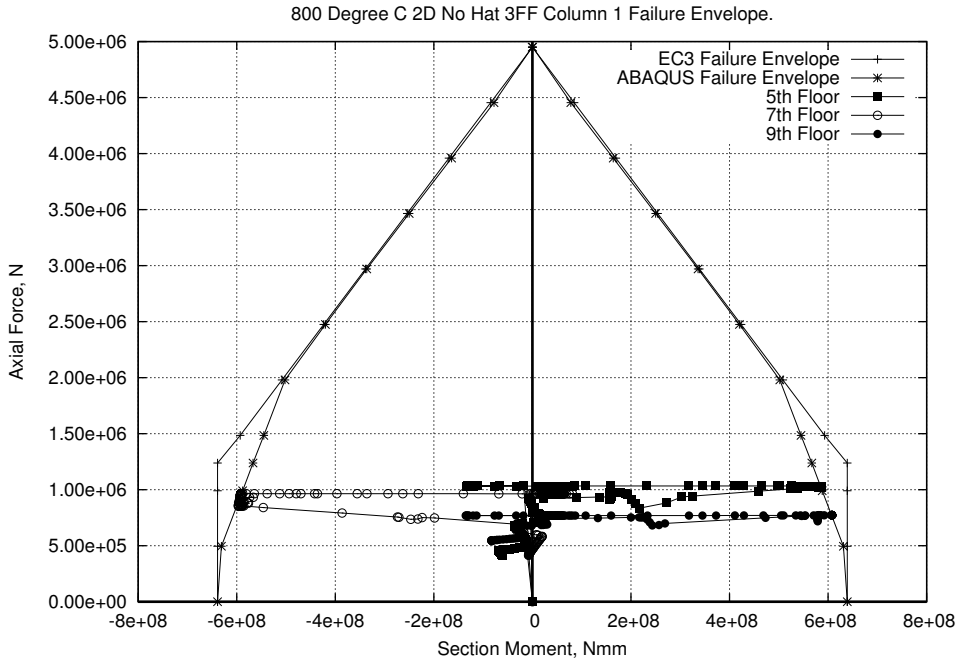

(b)

Figure 5.2: Scenario 1 : Column Moments

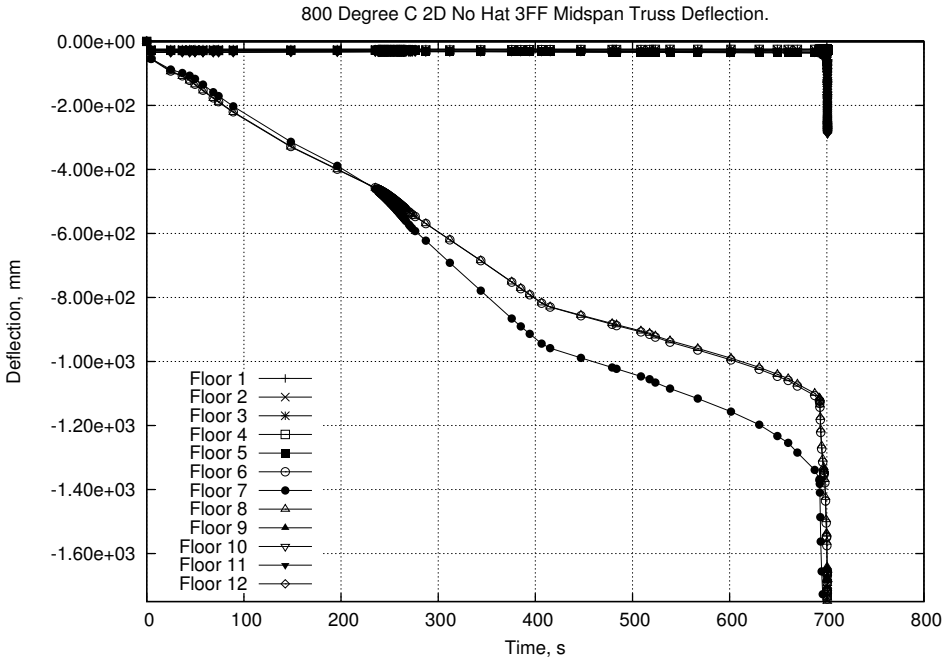

(a)

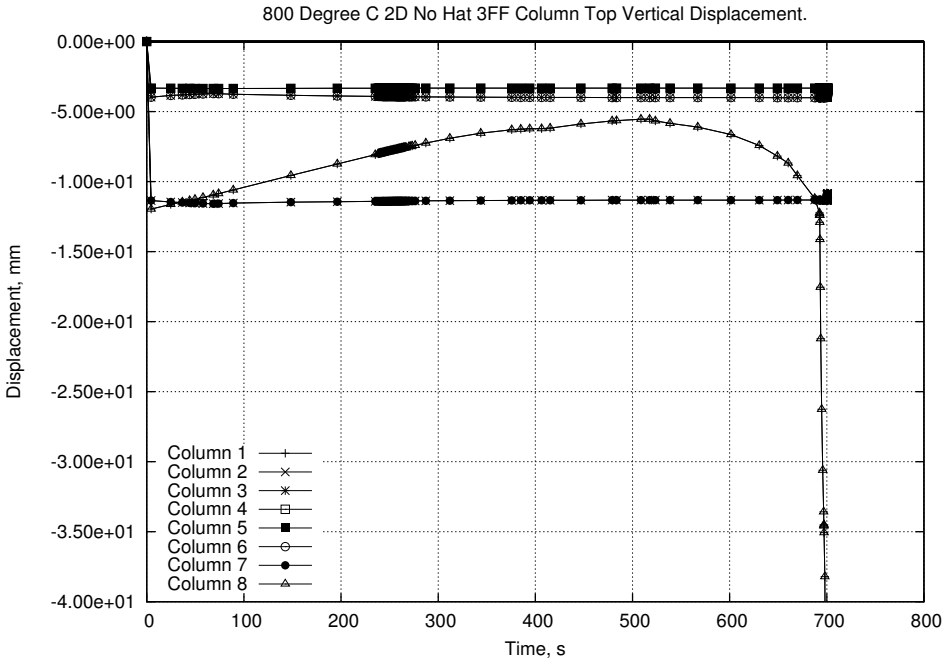

(b)

Figure 5.3: Scenario 1 : Deflections

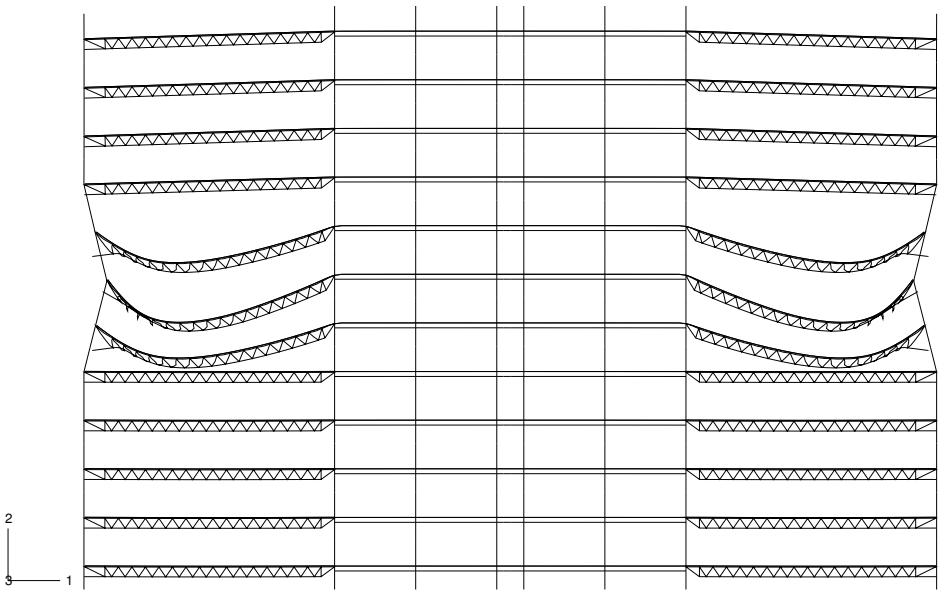

Figure 5.4: Scenario 1 : Failure

5.3.2 Scenario 2 - No Hat Truss, No Thermal Expansion, 800^{o}C Peak Temperature, 3 Floor Fire

This scenario is identical to Scenario 1 except that thermal expansion has been removed from all material properties.

This change greatly alters the initial response of the structure. With no additional thermal expansion induced compression in the truss members, the response becomes entirely dependent on the degradation of the material properties as the temperature increases. Figures 5.5 & 5.6 show a comparison between a selection of truss members under Scenarios 1 and 2. The most obvious difference is the response of the truss top chord. The lack of thermal expansion removes completely the sudden, rapid yielding of this member. The rapid yielding of this member in Scenario 1 does not immediately initiate failure of the truss but it will introduce extra loading into the floor slab that is absent in Scenario 2. The plots from Scenario 2 for the other truss members are broadly similar to Scenario 1 but do not

show some of the more extreme values.

The change in response by removing thermal expansion appears to make the structure slightly more stable, with final collapse occurring after about 1000s rather than 700s for Scenario 1. The comparison of deflections between Scenario 2 and Scenario 1 shown in Figure 5.7.a indicates that, without the effects of expansion, runaway occurs somewhat later. In terms of time Scenario 2 collapses around 300 seconds after Scenario 1 which appears to be significant. However, in terms of temperature of the compartment, and therefore the exposed steel, there is only about 20°C difference. As with previous research in this area [1, 7, 16] it can be seen in Figure 5.7.a that the large, early deflections in the midspan of the truss caused by restrained thermal expansion are not predicted by Scenario 2.

The collapse of the outer columns is shown clearly in Figure 5.7.b but the lack of thermal expansion leads to no initial upward movement in the column. While not necessarily significant in this scenario it is more of an issue when the hat truss is included.

Failure in this model is similar to Scenario 1 in that thermal degradation of the truss steel allows tensile membrane action to appear. This leads to significant inward displacements in the outer columns that leads to plastic mechanisms in the outer columns and then collapse. The complex interaction between the floors evident in the early stages of Scenario 1 (Figure 5.1) is not seen in the equivalent plot for Scenario 2 (Figure 5.8.a). A direct comparison between some of these results can be seen in Figure 5.8.b. After around 500s the material degradation caused by elevated temperatures begins to be the guiding factor in the truss response. This response can also be seen in Figure 5.7.a where the midspan truss deflections in both scenarios show similar results. This in turn means that the floors in both scenarios are in the same configuration and transfer the same forces into the columns. Hence the forces acting on the floors just before collapse are the same in each scenario as the gravity loading is the same.

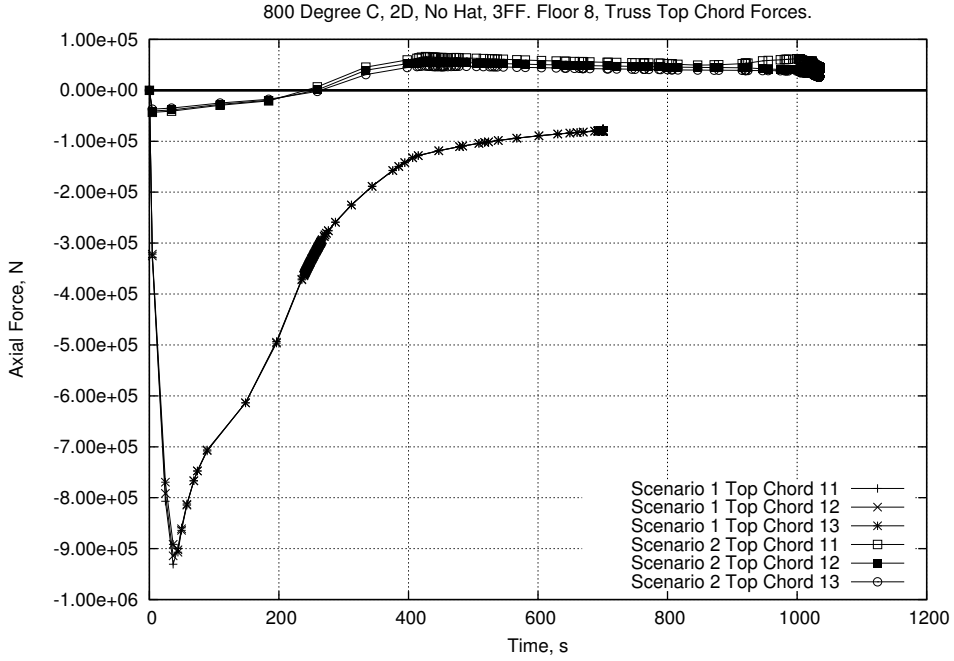

(a)

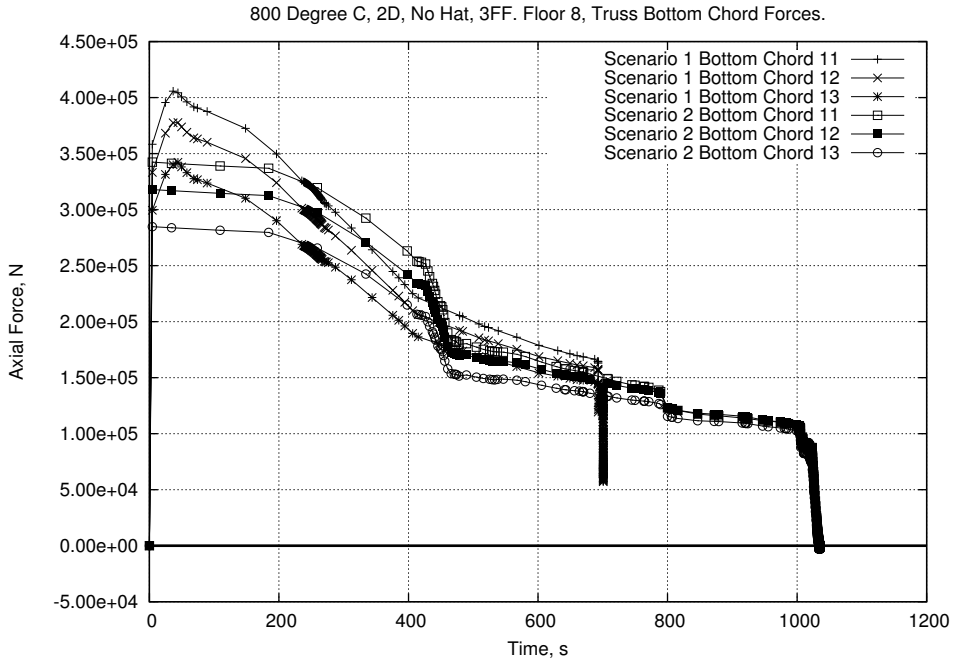

(b)

Figure 5.5: Scenarios 1 & 2 : Comparison of Truss Chord Forces

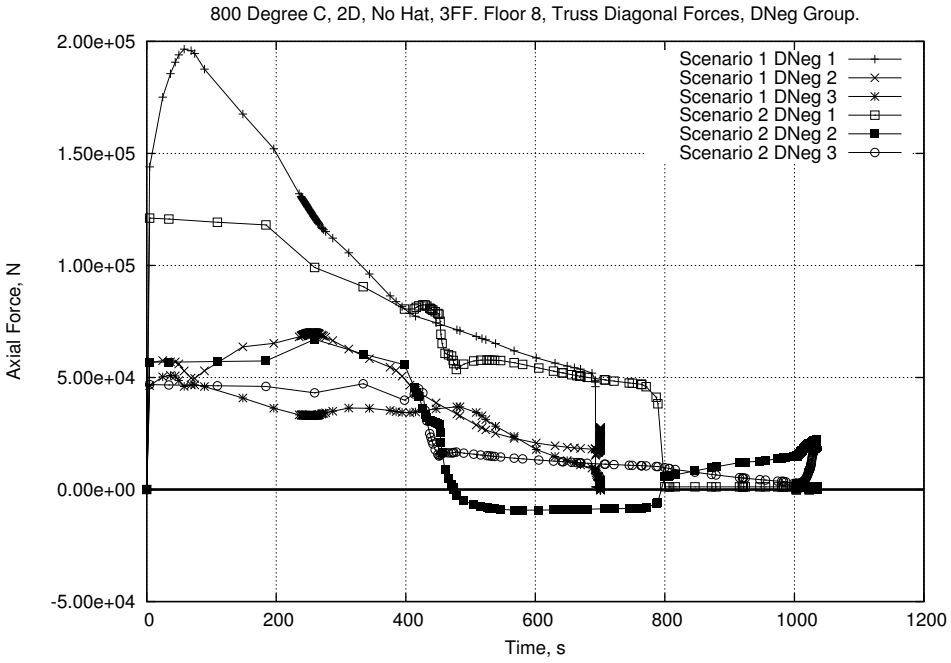

(a)

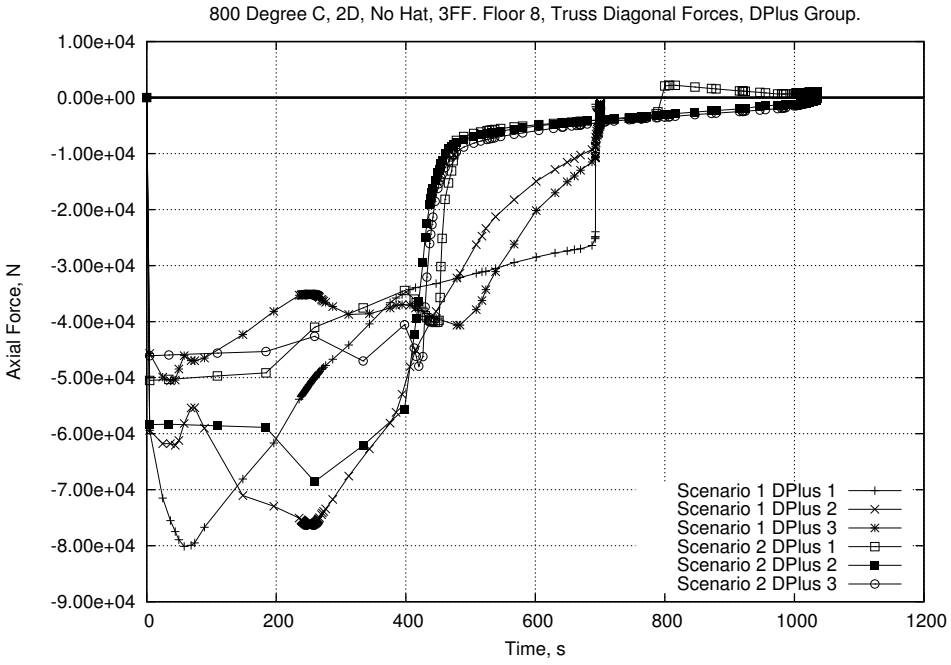

(b)

Figure 5.6: Scenarios 1 & 2 : Comparison of Truss Diagonal Forces

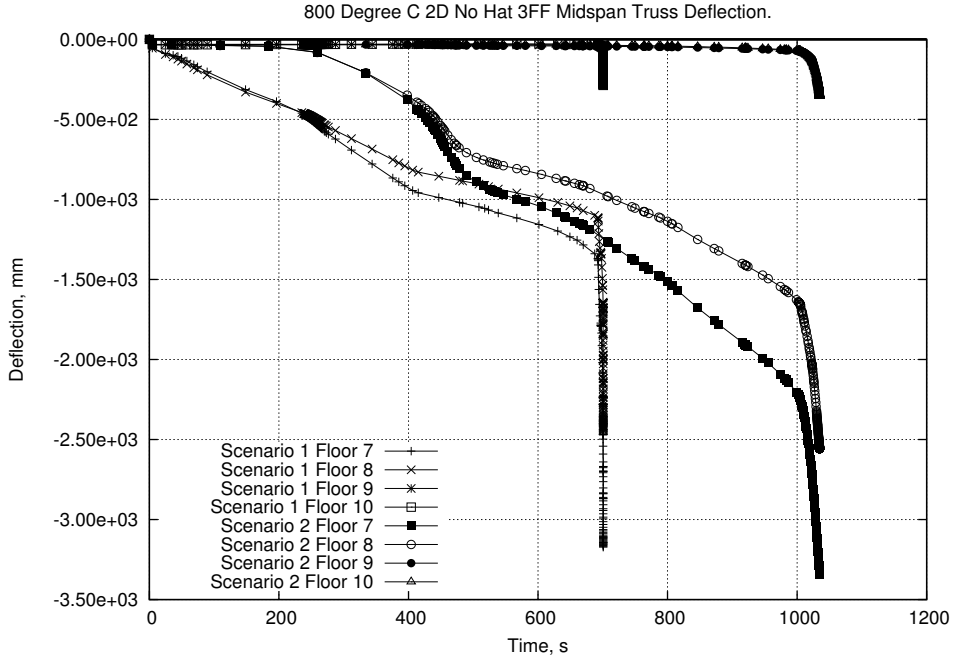

(a)

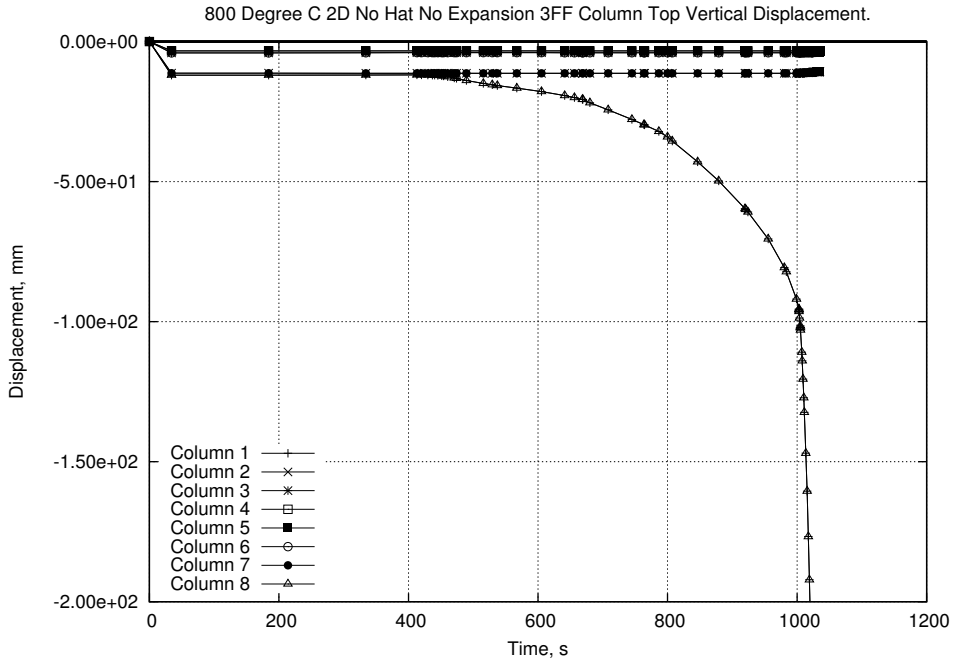

(b)

Figure 5.7: Scenario 2 : Deflections

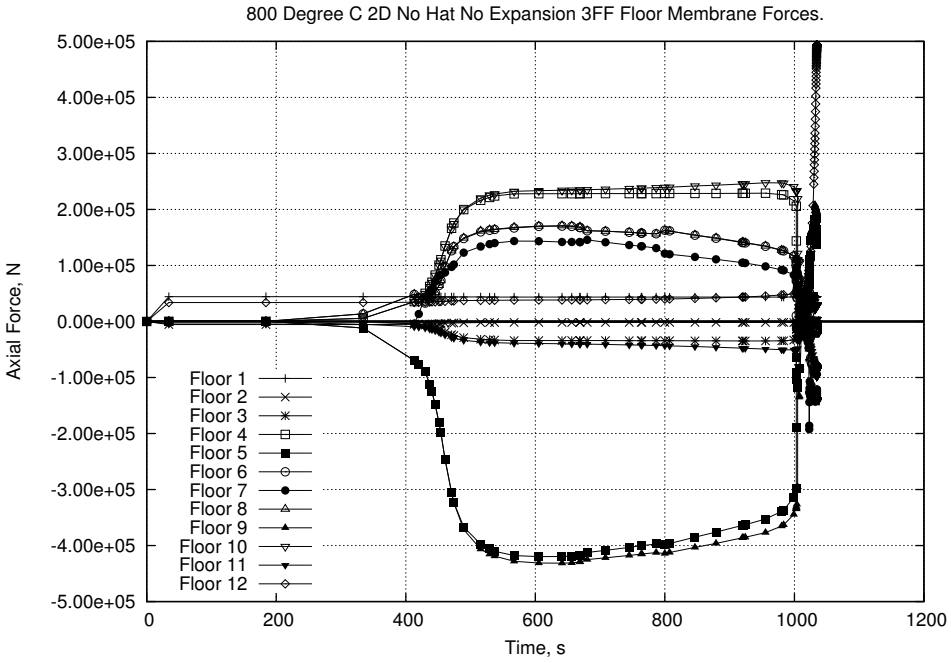

(a)

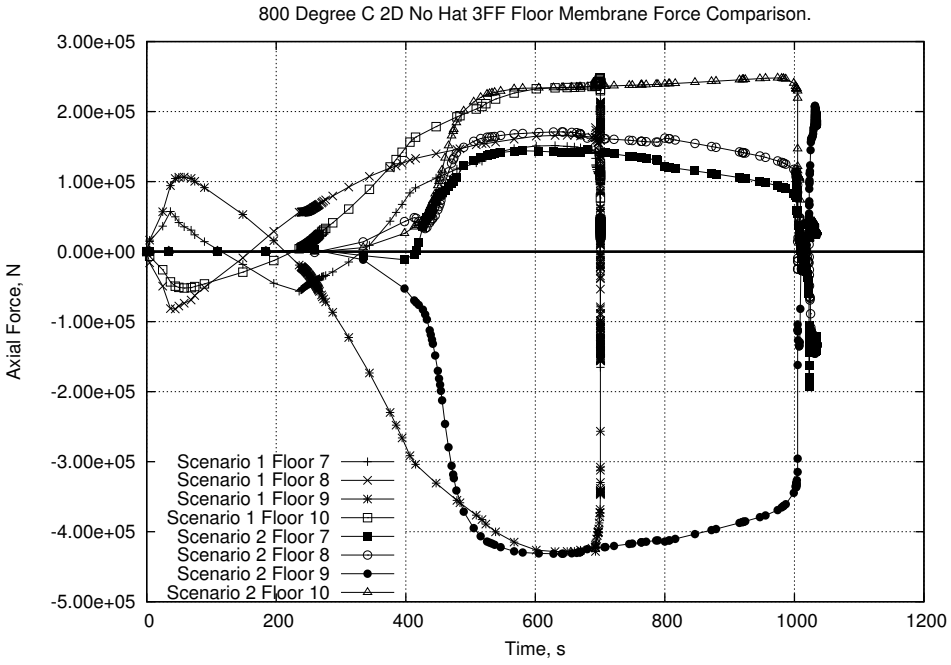

(b)

Figure 5.8: Scenario 2 : Floor Membrane Forces

5.3.3 Scenario 3 - No Hat Truss, 500^{o}C Peak Temperature, 3 Floor Fire

Scenario 3 was conducted as an initial test on the differences between a 500^{o}C peak temperature and an 800^{o}C. However, as very little response was seen this scenario was not investigated in depth.

5.3.4 Scenario 4 - No Hat Truss, 500^{o}C Peak Temperature, 5 Floor Fire

Scenario 4 was investigated to see if the structural model would show collapse if a relatively cool fire affected more floors than assumed in the base case. In this scenario a maximum compartment temperature of 500^{o}C affecting 5 floors over the midheight of the structure (5 to 9) was assumed.

This case remains stable (even without a hat truss) to the end of the analysis, as structural steel below 550^{o}C retains over 60% of its ambient strength and over 45% of its stiffness. In the initial stages of the analysis significant midspan deflections may be seen in the trusses (Figure 5.9.a) but when the steel reaches its maximum temperature this deflection stops and the trusses resist further movement. The linear rise in midspan deflection seen on all floors can be related to the expansion of the outer columns seen in Figure 5.9.b. The floors below the fire floors are not affected by this movement.

The initial expansion of the trusses pushes the outer columns out as can be seen in Figure 5.9.c. After the steel has stopped heating the continuing expansion of the concrete slab pushes the columns out further. The fire interface floors (5 & 9) stay in significant compression throughout the analysis as shown in Figure 5.10 while the three middle fire floors (6, 7 & 8) move between tension and compression. These floors move into tension initially as they are expanding at the same rate as the fire interface floors but due to compatibility with the columns in flexural curvature over the height of the fire floors these floors must displace more. This effect is also

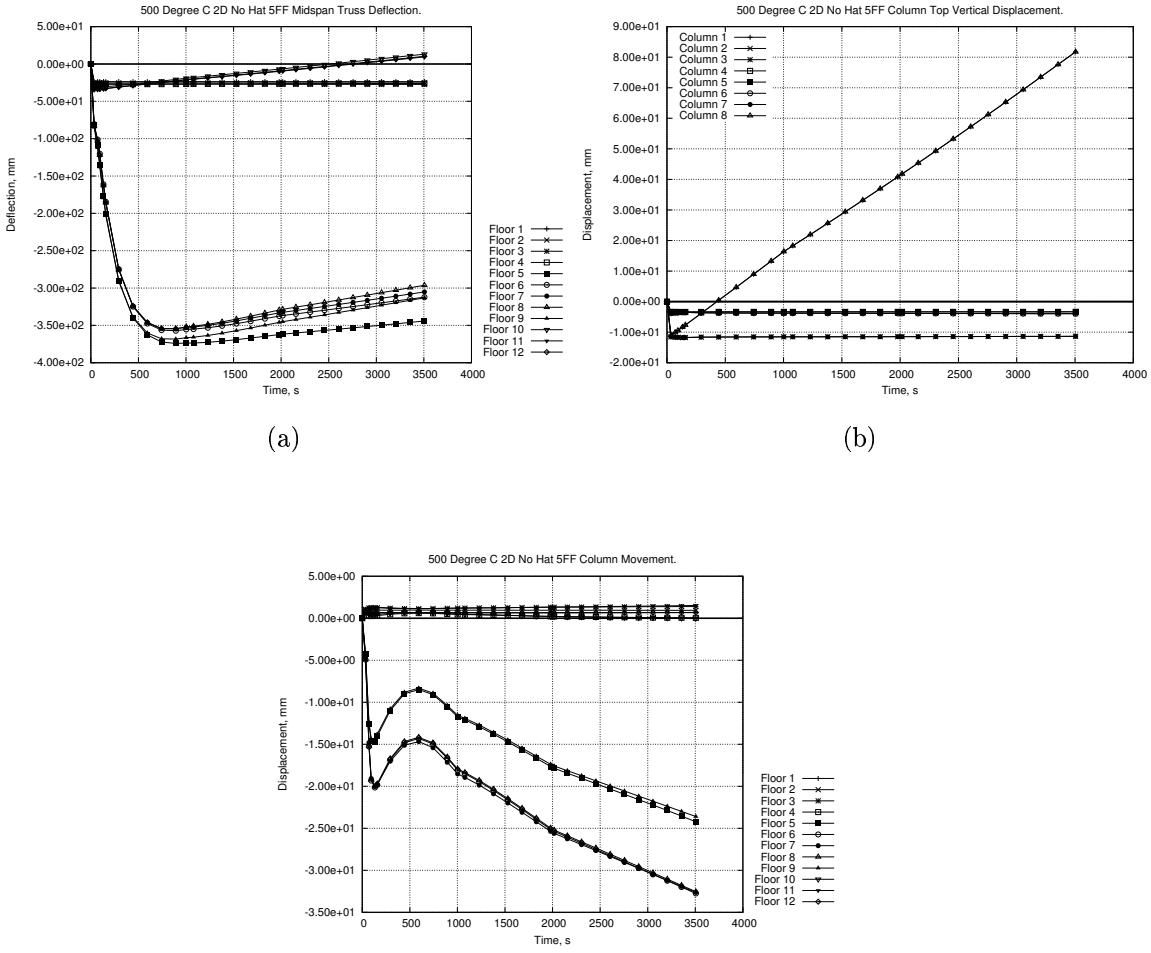

Figure 5.9: Scenario 4 : Deflections

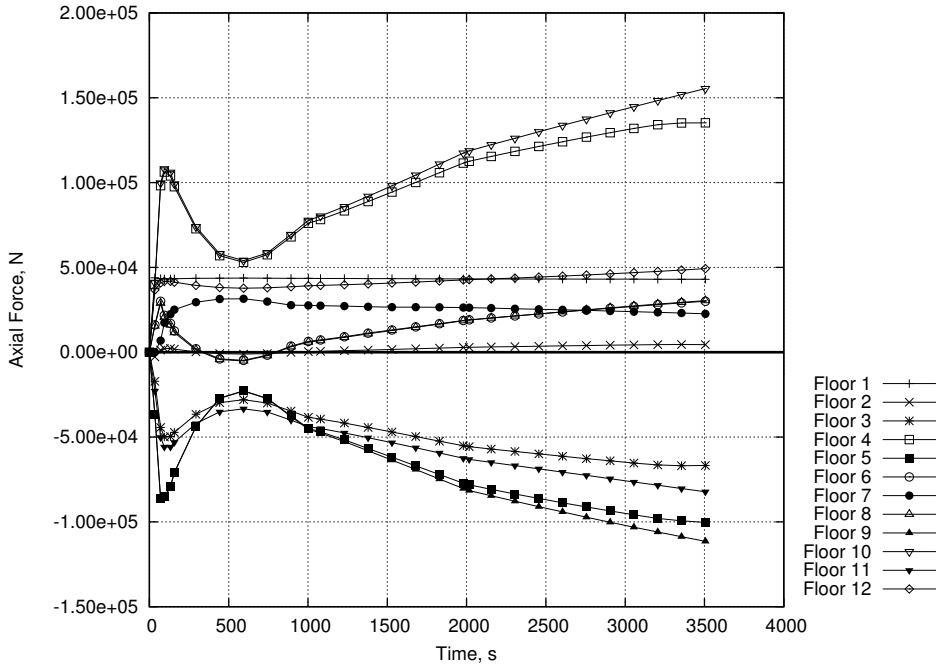

Figure 5.10: Scenario 4 : Floor Membrane Forces

described in Section 5.1.2 of Chapter 4. The relatively small displacements keep the outer columns well within their combined moment-axial load failure envelope (Figure 5.11). Figure 5.12 shows the model at the end of the analysis over a 3600 second fire.

While this model remained stable throughout the analysis time it does indicate a further possible failure mechanism. Sufficient outward displacement of the outer column may lead to large P-δ moments and further outward movement. This may lead to connection failure, particularly on the middle fire floors subject to the highest tension, but then progressing up and down the building, and thus loss of restraint from these floors leading to collapse. A simplified and exaggerated diagram of this mechanism may be found in Figure 5.13. As each of the fire floors undergoes the same expansion restraint effects from, and compatibility with, the column will create compressions in the interface fire floors and tensions in the intermediate fire floors, as described in Part 1. As further outward displacement occurs higher tensions will be found in the middle fire floor connection which could lead to failure. This loss of restraint will increase the forces in the connections in

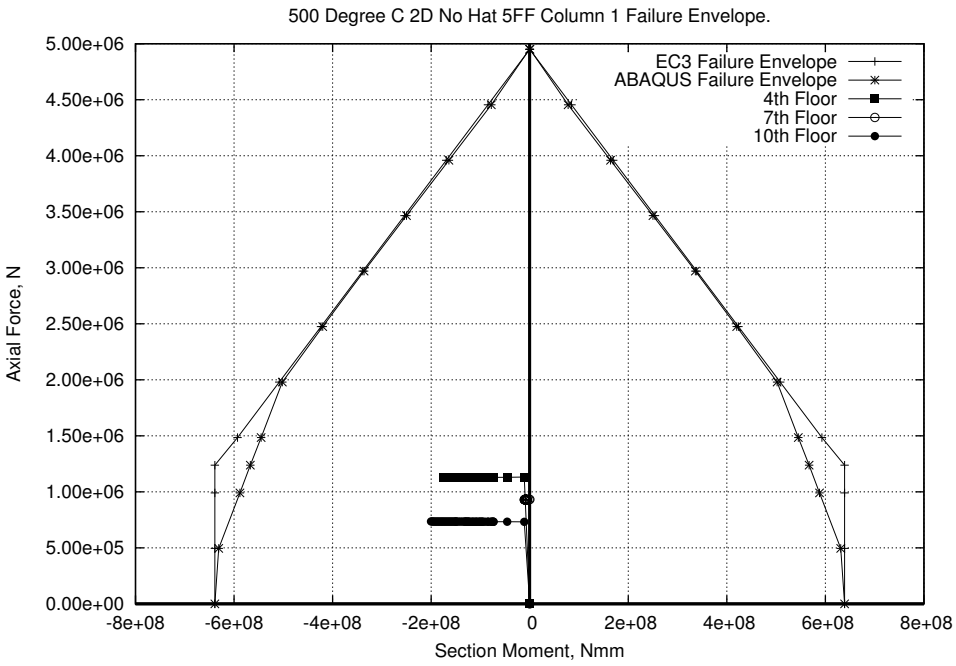

Figure 5.11: Scenario 4 : Column Capacity

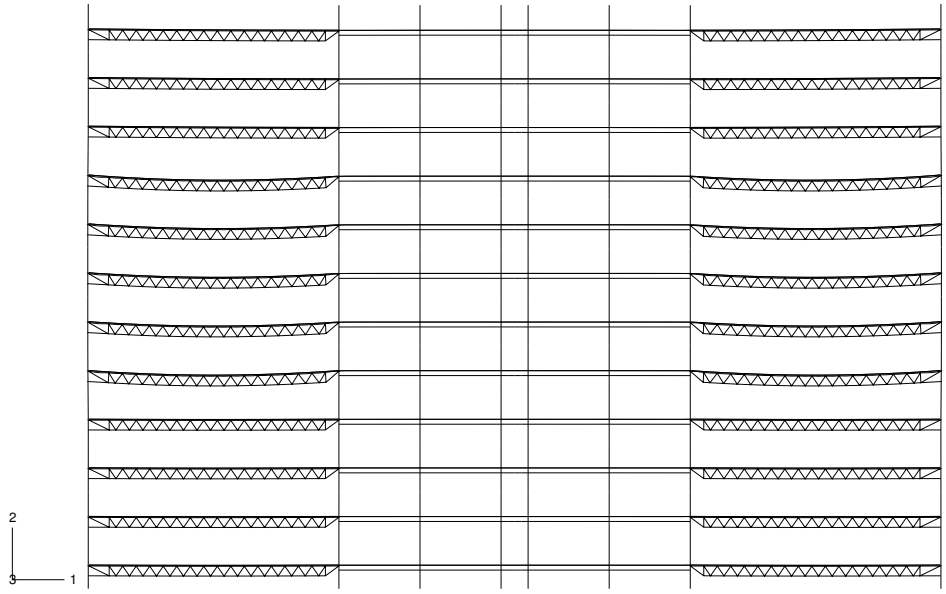

Figure 5.12: Scenario 4 : Final Displaced Shape

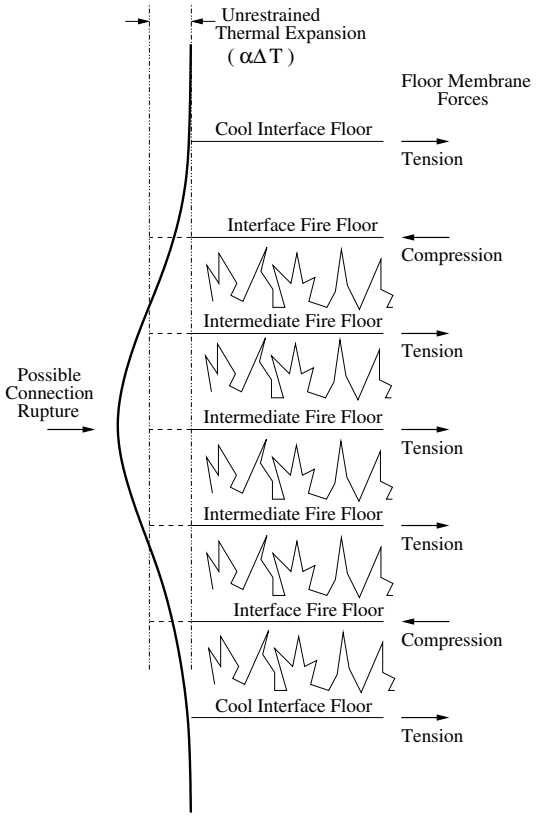

Figure 5.13: Tensile Connection Failure

the floors above and below which could lead to further, progressive failure.

5.3.5 Scenario 5 - No Hat Truss, 800^{o}C Peak Temperature, 5 Floor Fire

To further investigate the effects of a more widespread fire the regime from Scenario 1 was applied to 5 storeys. As could be expected this model fails in the same way as Scenario 1 but significantly faster. Scenario 1 survives for roughly 700s while Scenario 5 collapses after only 440s.

5.3.6 Scenario 6 - Base Case 2 : With Hat Truss, 800^{o}C Peak Temperature, 3 Floor Fire

The failure mechanisms encountered thus far all involved the outer columns forming plastic hinges and allowing collapse to initiate. To investigate this mechanism a hat truss was added at the top of the building. Apart from this addition to the structure Scenario 6 is the same as Scenario 1. The hat truss system allows the structure to transfer loads from the outer columns to the core. This makes a significant difference to the survivability of the building.

The local effects of heating on the trusses may be found in Chapter 4. On a more global scale however there are several interesting points to note. Figure 5.14 clearly shows significant amounts of load transfer between the outer columns and the core. In Scenario 1 as soon as the outer columns (1 and 8) fail, the floors above the fire collapse as their primary, and only, support is removed. In Scenario 6 the column at and above the fire floors act in tension and the hat truss transfers this loading to the core columns and stops the upper storeys from collapsing. As can be seen in Figure 5.15, after 1000s the column horizontal displacement and the truss midspan deflection rates reduce as the steel temperature levels out. At 2000s there is another step increase in displacement rates. At this point the hat truss structure comes under increased loading. The main diagonal in the hat truss between columns 7 and 8 (on the right hand side of the building) reaches yield at around 2500s and the integrity of the hat truss begins to fail after about 3400s. As soon as the hat truss becomes unstable, the structure reverts to the same collapse mechanism as seen in Scenario 1.

Convergence failure occurred at around 3400s in the analysis. Indications of run-away failure may be seen in all of the deflection plots in Figure 5.15 but especially in Figure 5.15.c showing the vertical displacement at the top of the columns.

The redistribution of the floor membrane forces may be seen in Figure 5.16.a. Again it is apparent that by the time the steel has reached maximum temperature the structure has adopted a secondary load path that allows the building to avoid

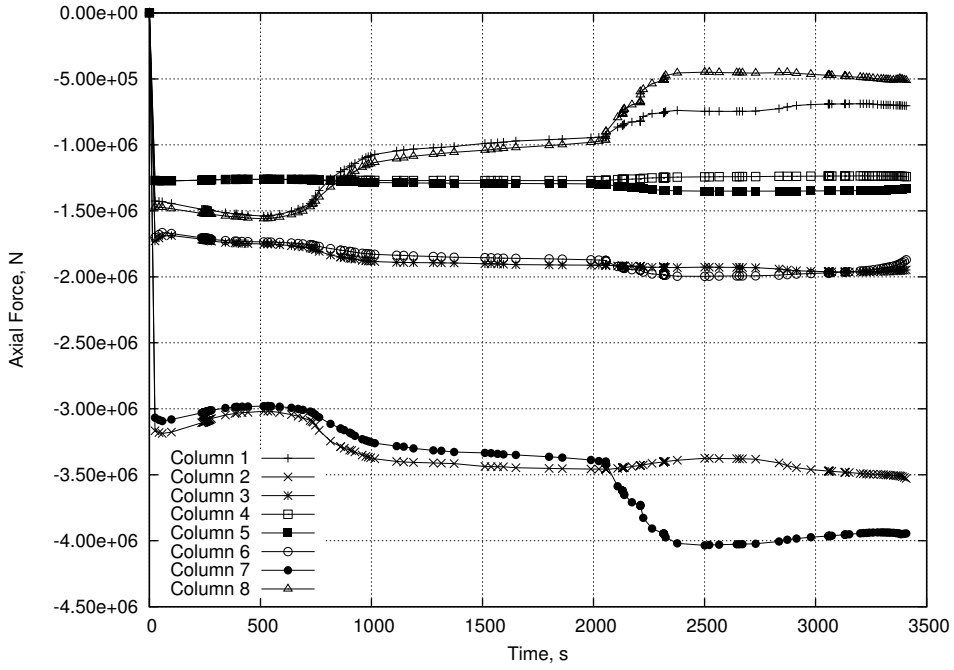

Figure 5.14: Scenario 6 : Column Base Forces

collapse. The cool interface floors above and below the fire floors move into high levels of compression to support the intervening fire floors as they move into tensile membrane action. The next floors above and below the cool interface floors move into a lesser amount of tension as the floor reaction forces are transmitted back up and down the column with the interface floors as the fulcrum.

Direct comparison to the results from Scenario 1 shown in Figure 5.16.b show a great deal of similarity between the results. The early response is not greatly affected by the presence of the hat truss.

5.3.7 Scenario 7 - With Hat Truss, 500^{o}C Peak Temperature, 3 Floor Fire

Scenario 7 was investigated to allow a direct comparison between the effects of high and low temperatures. A 3 floor fire is implemented over the midheight of the main floors (affecting floors 6, 7 & 8). Maximum compartment temperature is 500^{o}C.

As with Scenario 4 after the initial heating stage is over the structure resists further

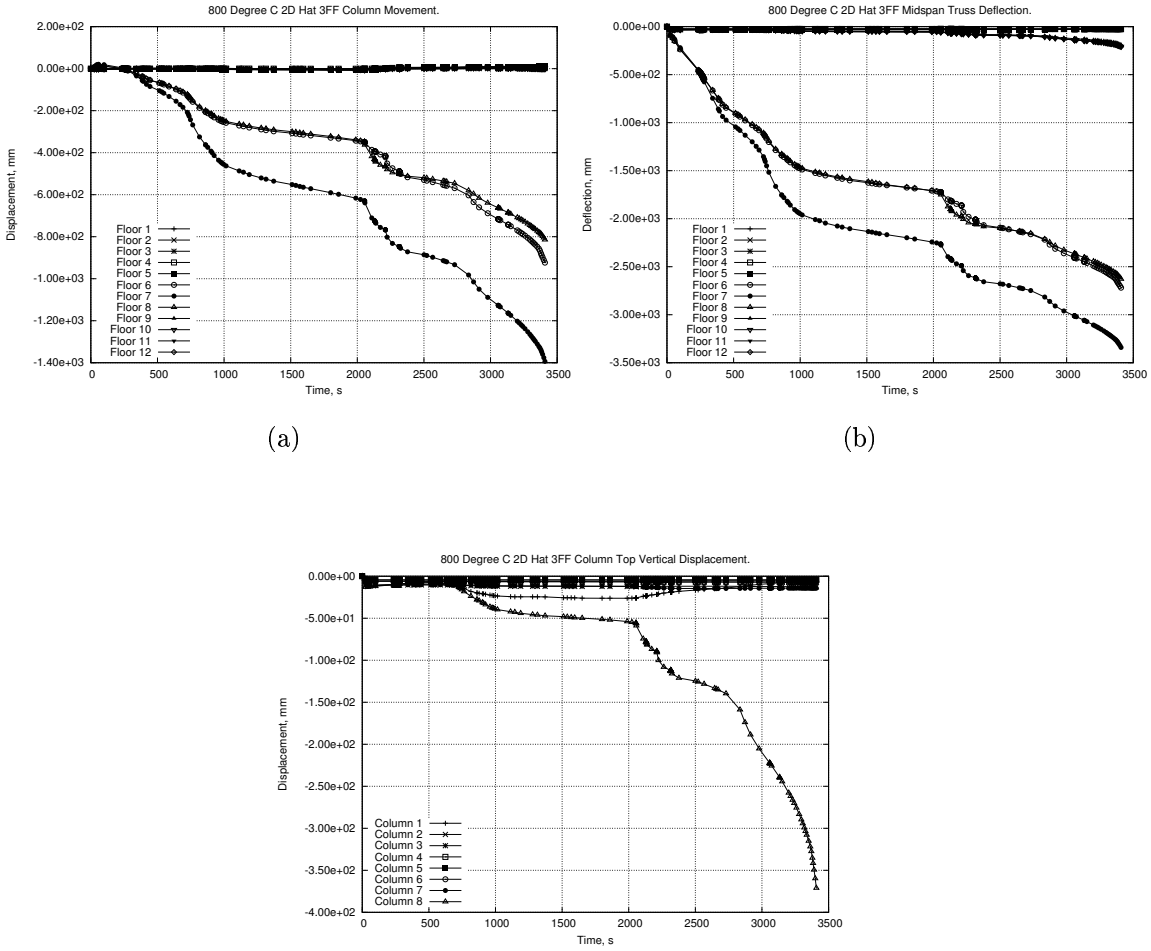

Figure 5.15: Scenario 6 : Member Displacement

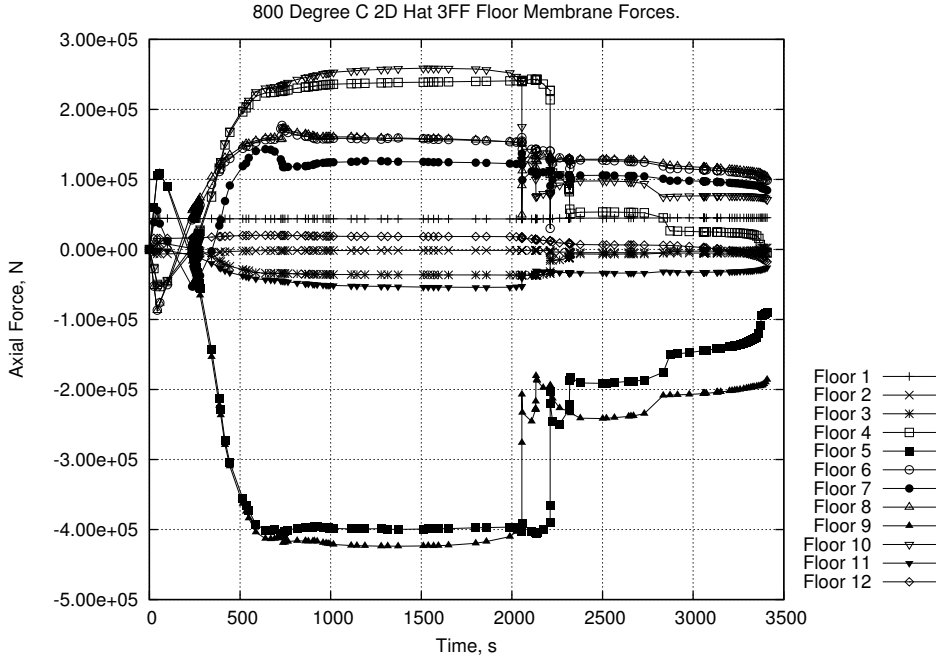

(a)

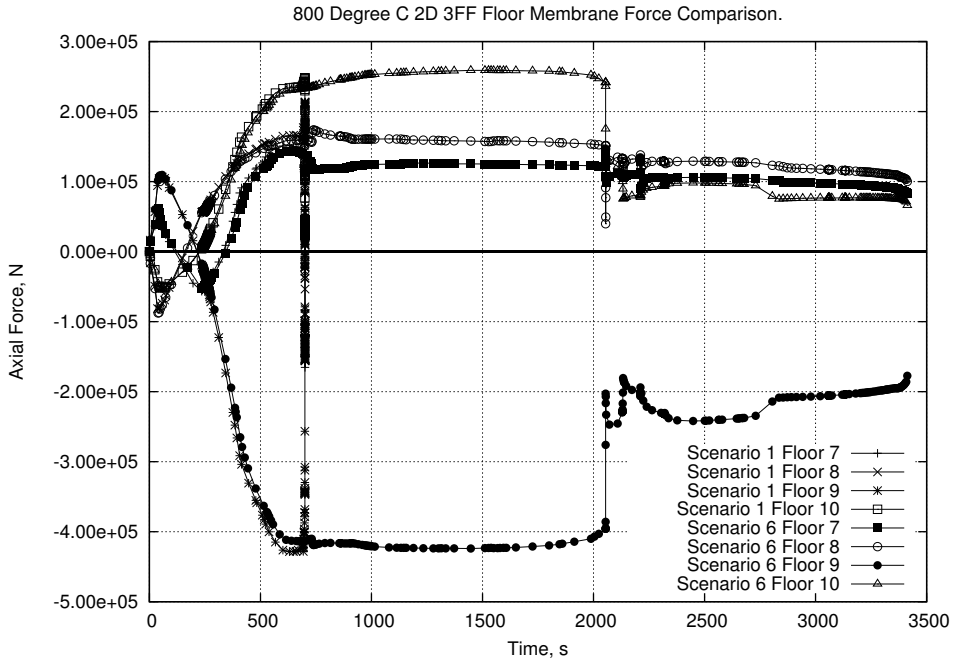

(b)

Figure 5.16: Scenario 6 : Floor Membrane Forces

movement. Expansion of the outer columns, restrained by the hat truss at the top, draws loading to these members from the core columns (Figure 5.17.a). The outer columns start at a low load ratio so the additional loading is well within column capacity. In addition there is less lateral displacement of the outer columns so no significant reduction of the axial capacity of these members is expected due to P-δ moments. An interesting phenomenon that appears in this scenario is that the entire building begins to sway soon after the start of the analysis as seen in Figure 5.17.b. This movement is linked to the expansion of the fire floors as the movement closely follows the heating regime. As soon as the steel stops heating the sideways movement stops. some recovery is also seen throughout the rest of the analysis. This movement accounts for the disparity in the column forces. This sway mechanism is likely to be caused by the way the expanding columns are interacting with the hat truss as it is the only asymmetric portion of the model.

5.3.8 Scenario 8 - No Thermal Expansion, With Hat Truss, 800^{o}C Peak Temperature, 3 Floor Fire

This scenario is similar to Scenario 2 as it is intended to investigate the effects of removing thermal expansion and whether the response will change due to the presence of the hat truss. The reactions of the structural members are also similar to Scenario 2 as the direct comparison in Figure 5.20.b indicates. This figure shows a similar correlation to the comparison between Scenarios 1 and 6 in Figure 5.16.b. The presence of the hat truss makes little difference until the point at which it is required to support the change in loading as the outer columns are deformed. The redistribution of load is again seen between columns in Figure 5.18.a while part b of this figure shows a direct comparison of the response of two columns between Scenario 8 and Scenario 6. This shows the close similarity that can arise in some of the responses between the model with thermal expansion and the model without.

Due to the lack of additional forces induced by expansion the response of Scenario 8 is dictated by the degradation of material properties caused by heating. However

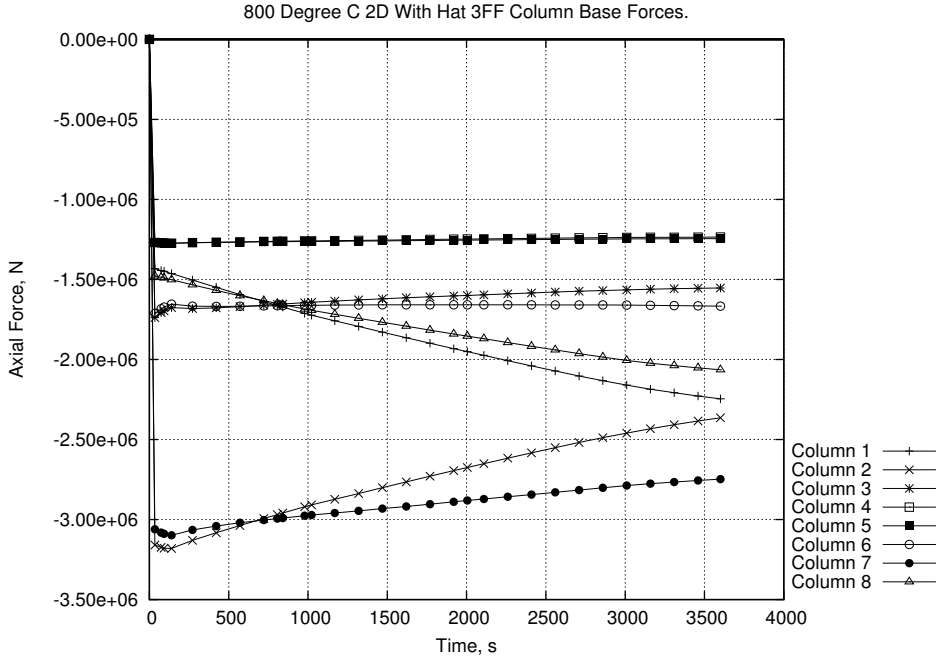

(a)

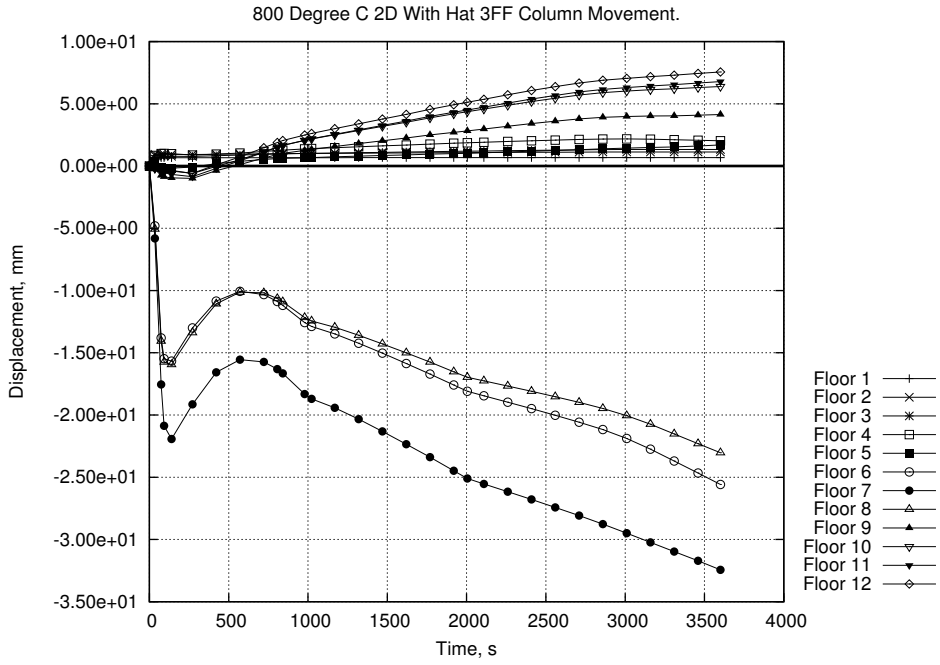

(b)

Figure 5.17: Scenario 7 : Column Reactions

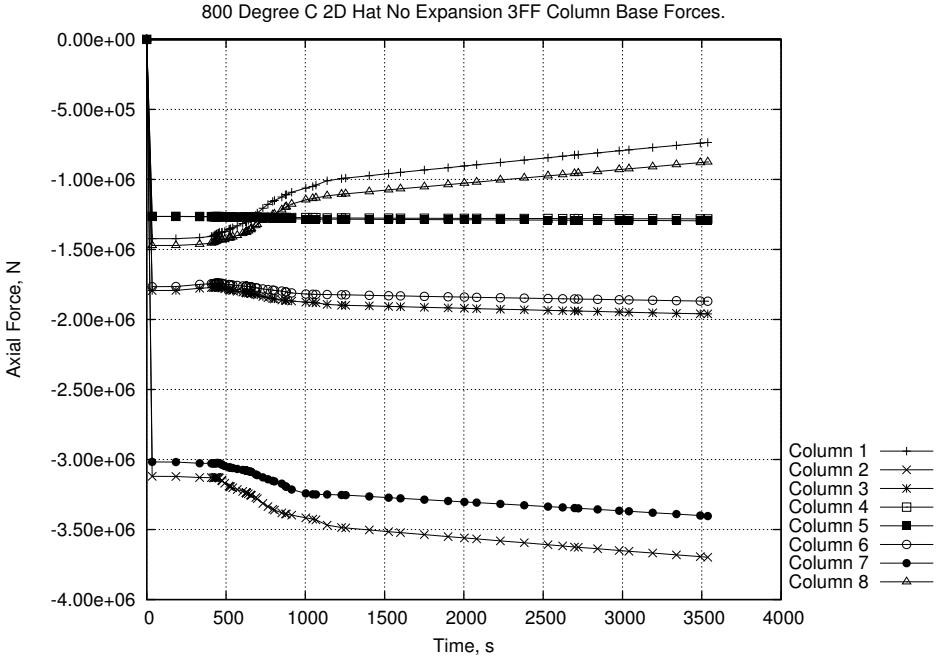

(a)

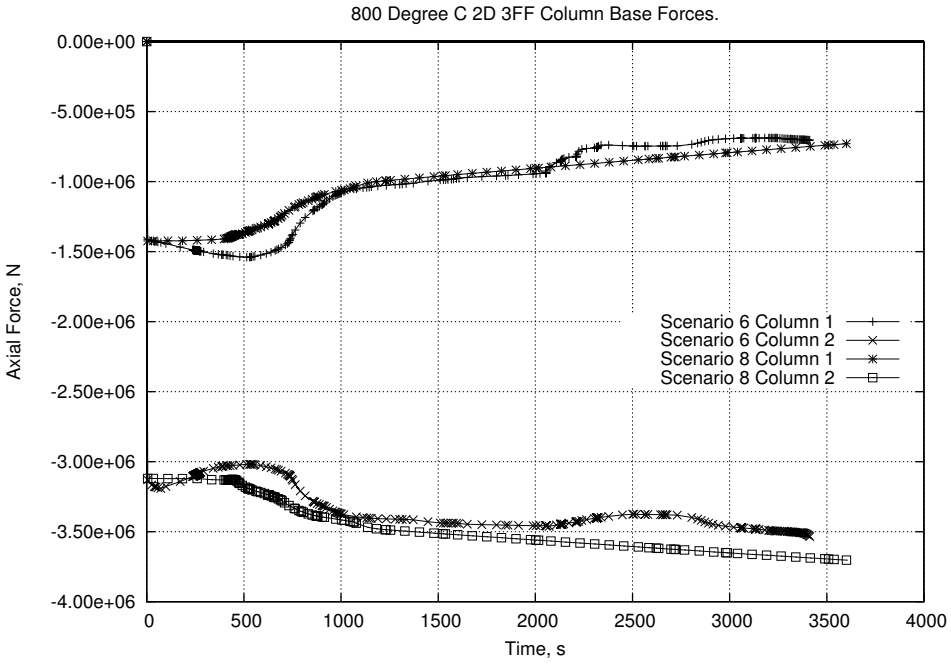

(b)

Figure 5.18: Scenario 8 : Column Base Forces

while the overall global response shows similarities to Scenario 6 in trends the actual results can be very different. Figure 5.19.a shows the very different floor deflections that arise in Scenarios 6 and 8 (scenarios with and without thermal expansion effects, respectively) while a comparison between the column vertical deflections in Figure 5.19.b and Figure 5.15.c show that Scenario 8 does not suffer the same kind of runaway failure that appears in Scenario 6. An examination of Figure 5.20.c will show the marked similarity in the final forces in the floors between the two scenarios. This reinforces the theory from Flint et al [71] that it is the thermally induced displacements in combination with the forces that determine the true structural response.

It is the authors' belief that response close to failure should not be modelled without including all available information about the structure and the materials being used. In Scenario 6 the structure was seen to fail toward the end of the analysis time and includes several complex redistribution events. Scenario 8 reaches the end of the analysis without producing an obvious failure response.

5.3.9 Scenario 9 - Slab Heated Above and Below, With Hat Truss, 800^{o}C Peak Temperature, 3 Floor Fire

Scenario 9 is another iteration of Scenario 6, now with heating assumed to affect both sides of the floors (top and bottom) bounding the fire compartments. This scenario was investigated to see if any major differences arose when using the assumption that the slab is heated from below only. Temperature distributions were again calculated using the 1D heat transfer program utilized throughout the course of this project [75].

The steel still heats up considerably more quickly than the concrete hence the early stages of the analysis are fundamentally the same as Scenario 6. The same responses can be seen in the steel truss sections and a direct comparison may be found in Figures 5.21 & 5.22. It is during the later stages of the analysis that the differences become more obvious. Figure 5.23 shows the membrane forces in

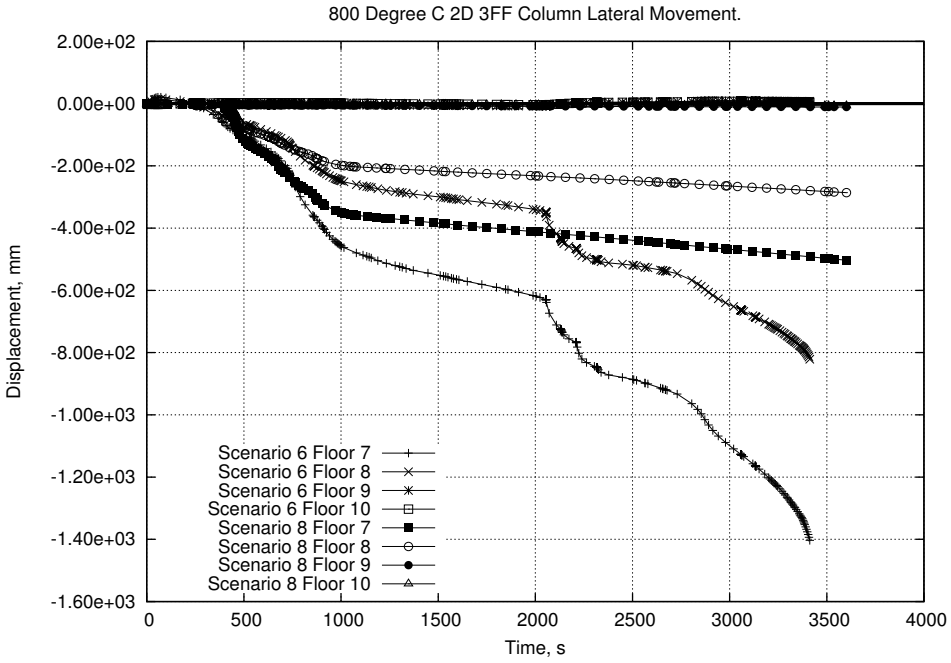

(a)

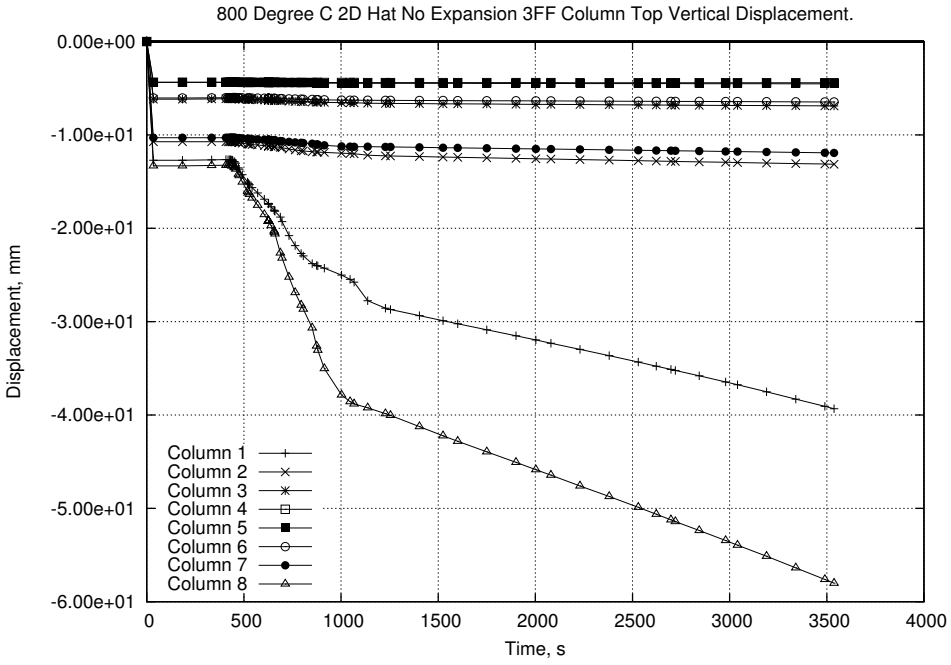

(b)

Figure 5.19: Scenario 8 : Column Displacement

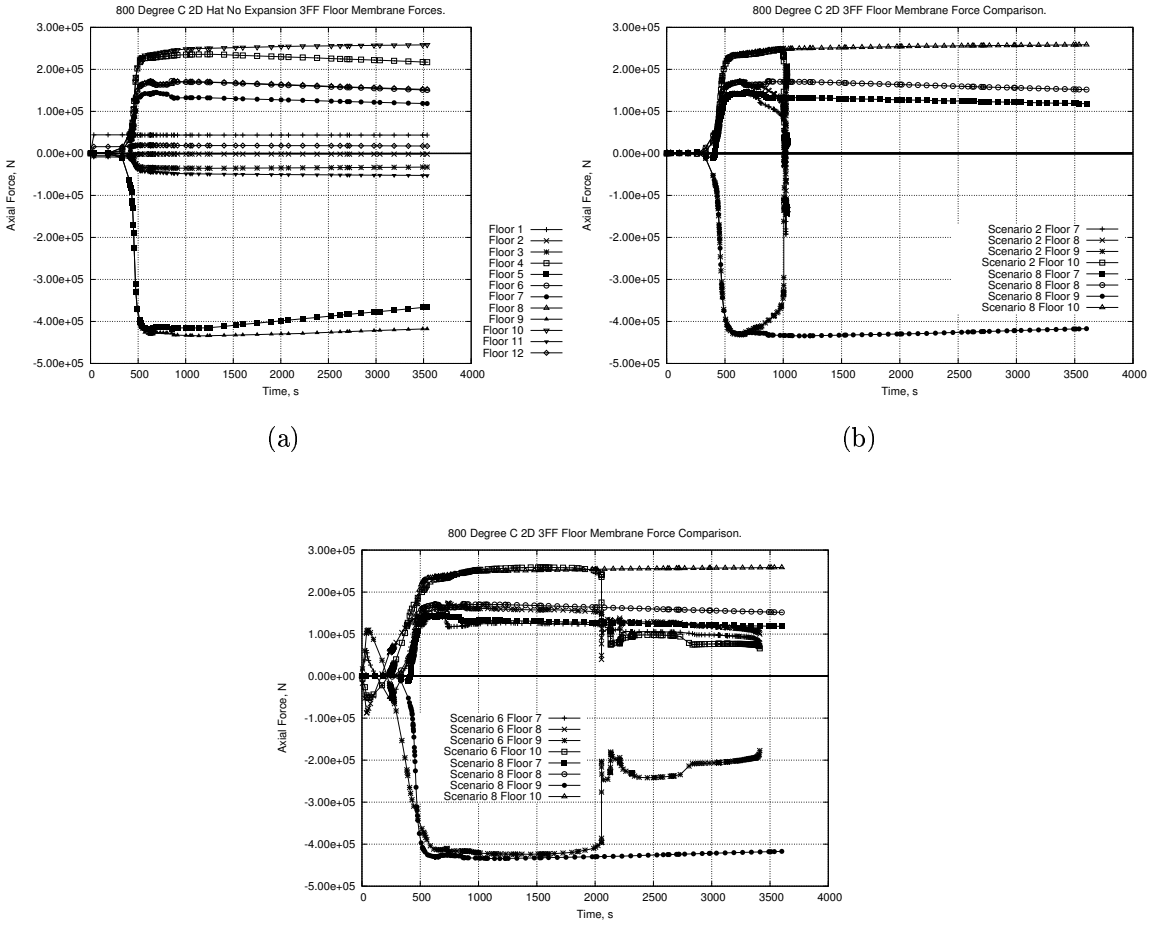

Figure 5.20: Scenario 8 : Floor Membrane Forces

the floors. It is substantially the same, however the effect of the additional floor heating may be seen in the higher forces in floors 3 and 4 . As the 5th floor now has additional compressive force applied it affects the 4th floor which in turn affects the 3rd floor (conversely under closer examination the tension developed in the 5th floor is slightly less). If the member displacements for Scenario 9 (Figure 5.24 for column displacement and Figure 5.25 for midspan truss deflection) are compared with those of Scenario 6 the differences are apparent, but not significant. Some extra outward movement of the column may be seen at the 5th floor while the expansion of the slab on floors 6 to 8 has the effect of reducing the inward movement of the column.

Scenario 9 follows the results of Scenario 6 very closely and therefore may be close to the same kind of failure seen in Scenario 9. However convergence problems in the later stages of this analysis do not allow a definite answer to be obtained.

5.3.10 Scenario 10 - With Hat Truss, 500^{o}C Peak Temperature, 5 Floor Fire

Scenario 10 uses the same geometry as Scenarios 6 to 9 and the same fire regime as Scenario 4. This model was primarily done as a test to see the effects of restraint of the hat truss on the expanding columns. As Scenario 4, which does not include the hat truss present in this model, remains stable throughout the analysis no redistribution is actually necessary. The global response of the building does change slightly due to the added restraint of the hat truss.

The greatest difference may be seen in the column base reactions. Figure 5.26 clearly shows some redistribution caused by the expansion of the outer columns. The additional compression caused by this expansion is clearly well within the capacity of the columns. In addition the upward movement of the upper floors transfers some of the load from the inner columns to the outer columns. The disparity between the column forces on either side can again be attributed to a sway mechanism forming. Figure 5.27 shows the horizontal movement of the column at different floor heights. As the column movement due to the movement of the trusses

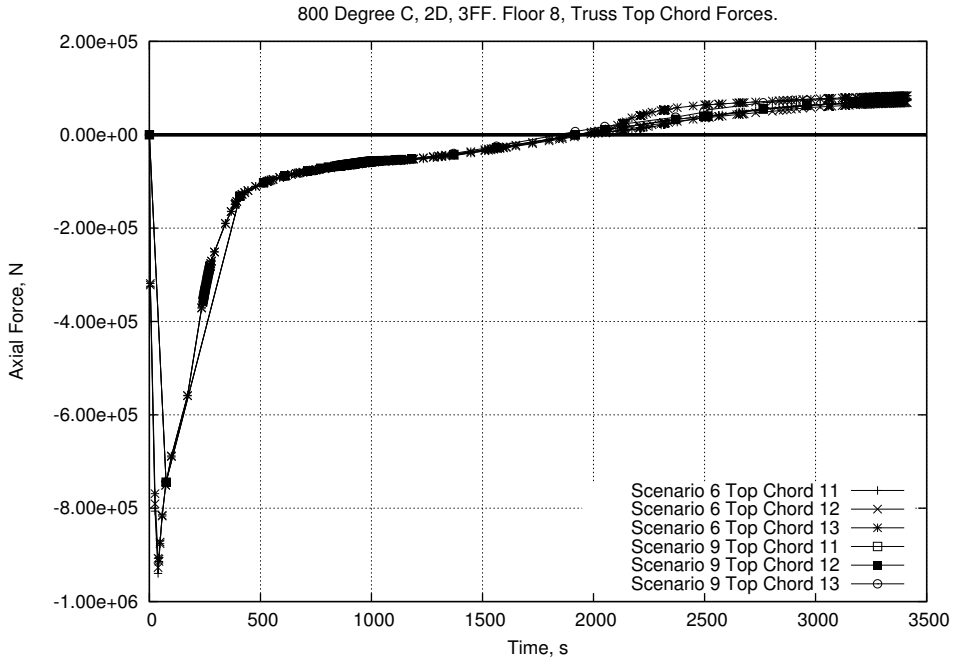

(a)

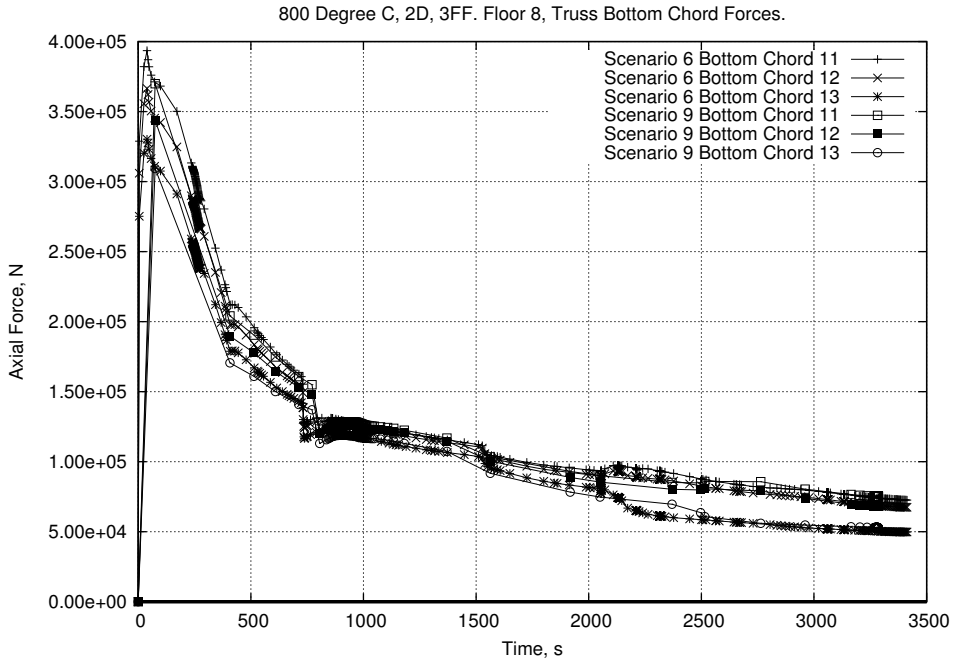

(b)

Figure 5.21: Scenario 9 : Truss Chord Force Comparison

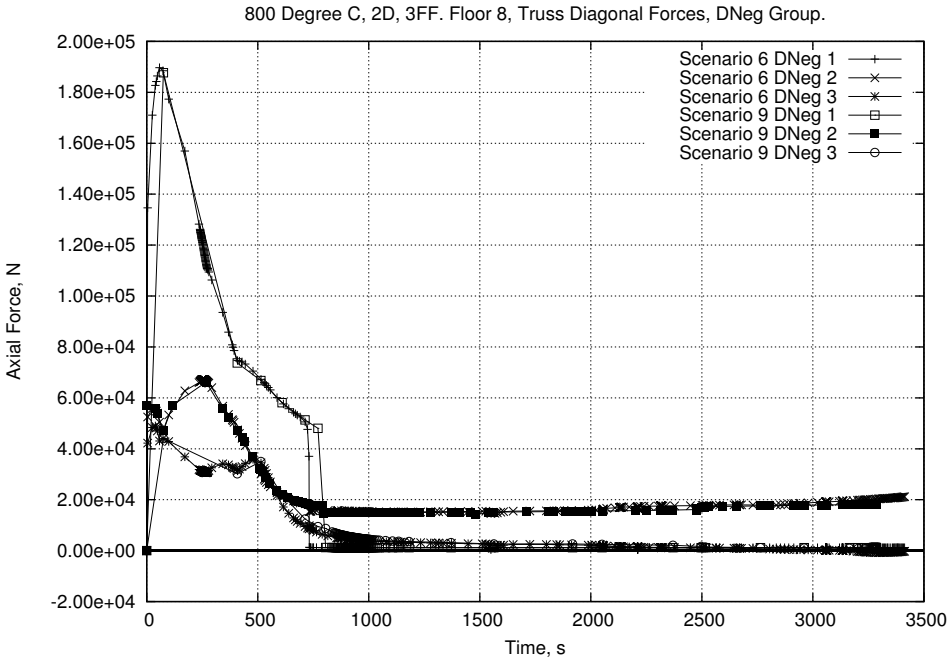

(a)

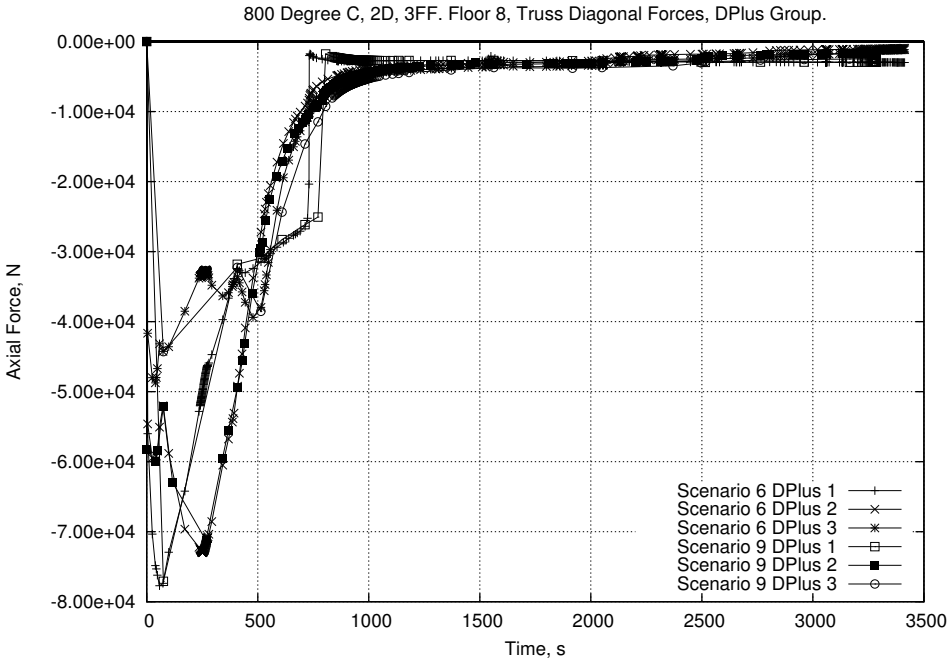

(b)

Figure 5.22: Scenario 9 : Truss Diagonal Force Comparison

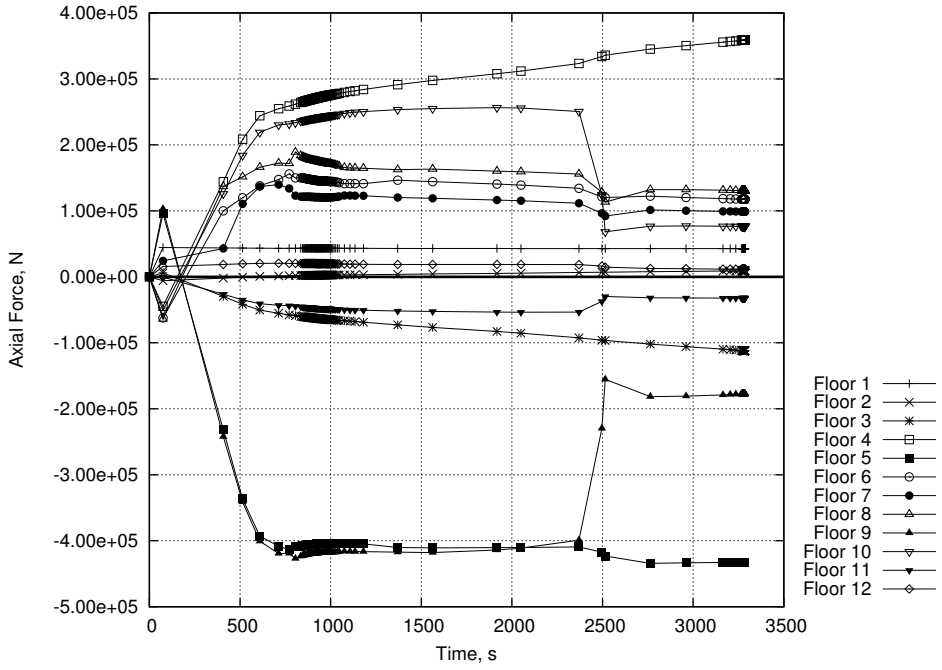

Figure 5.23: Scenario 9 : Floor Membrane Forces

is relatively small the large sway swamps this reaction. As with Scenario 7 the sway appears to be linked to the movement of the trusses and the building resists further movement as the steel stops expanding.

Other than this the response of Scenario 10 is virtually identical to that of Scenario 4.

5.3.11 Scenario 11- With Hat Truss, 800^{o}C Peak Temperature, 5 Floor Fire

This scenario again uses the geometry that includes the hat truss for direct comparison to Scenario 5. It also uses the same fire regime as Scenario 5. The response of the truss members in the fire floors is in line with the other scenarios presented here and in Chapter 4 as may be seen in Figures 5.28 & 5.29. The presence of the hat truss again adds a significant amount of extra stability that is not present in Scenario 5. Clear redistribution between columns is evident (Figure 5.32) at around 400s when Scenario 5 fails.

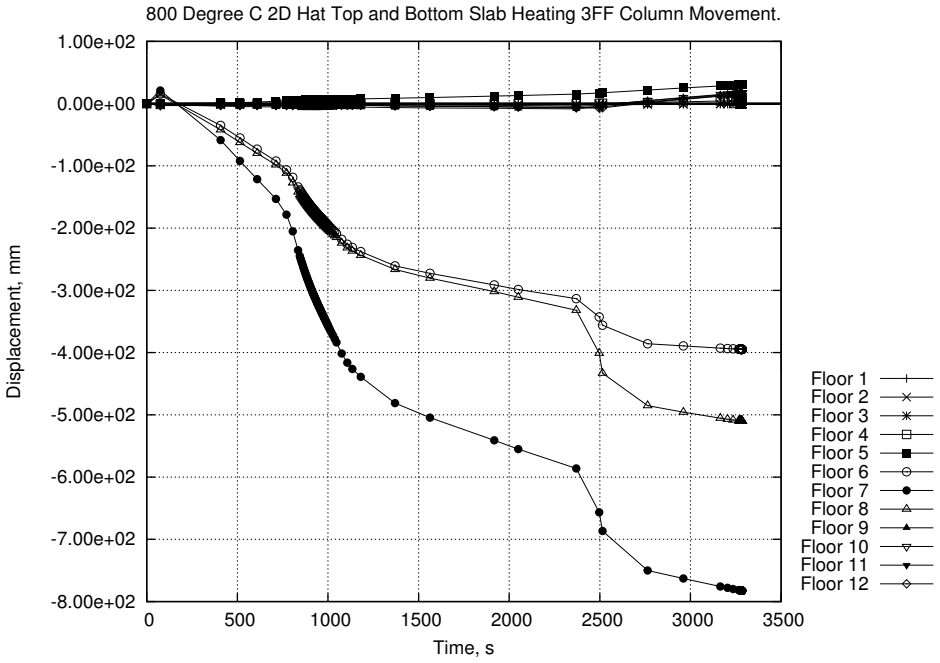

(a)

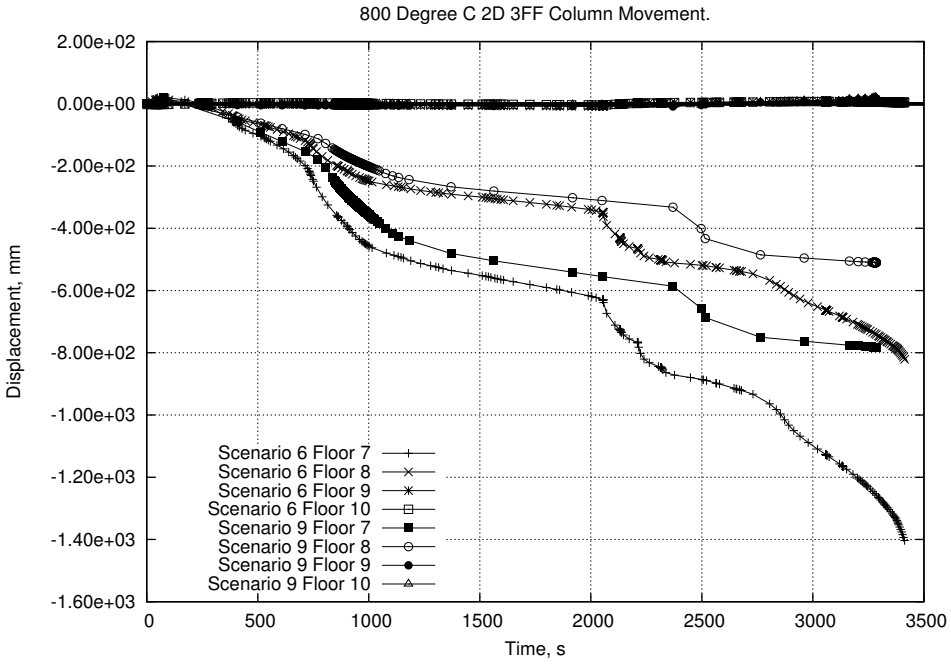

(b)

Figure 5.24: Scenario 9 : Column Lateral Displacement

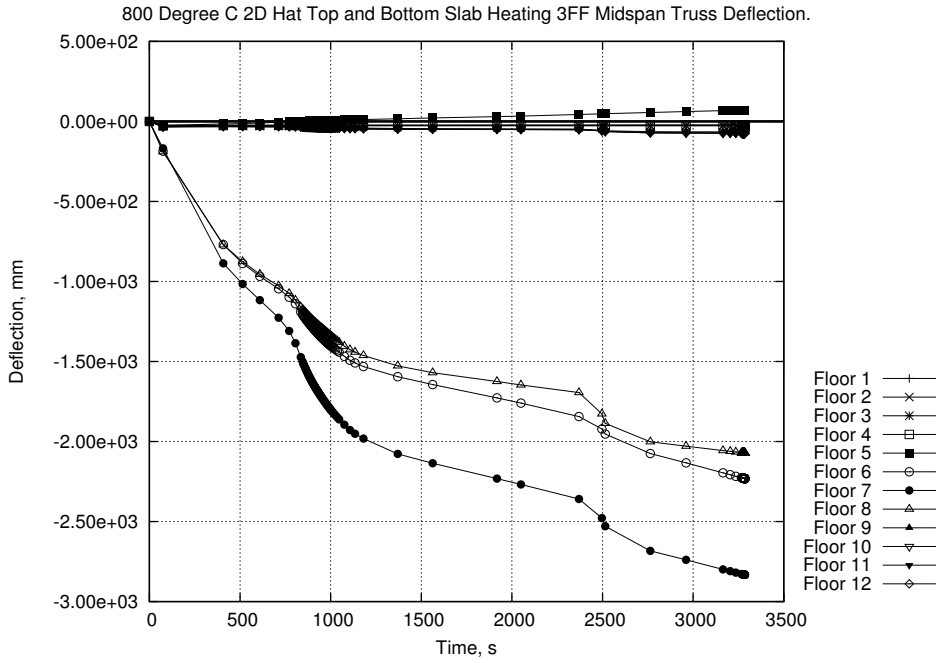

(a)

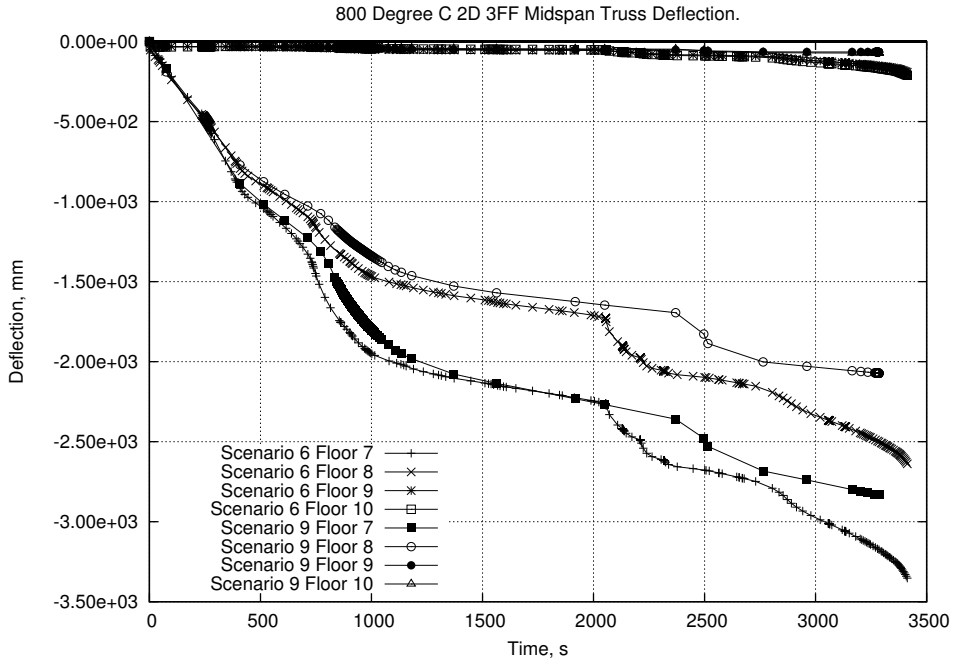

(b)

Figure 5.25: Scenario 9 : Midspan Vertical Displacement

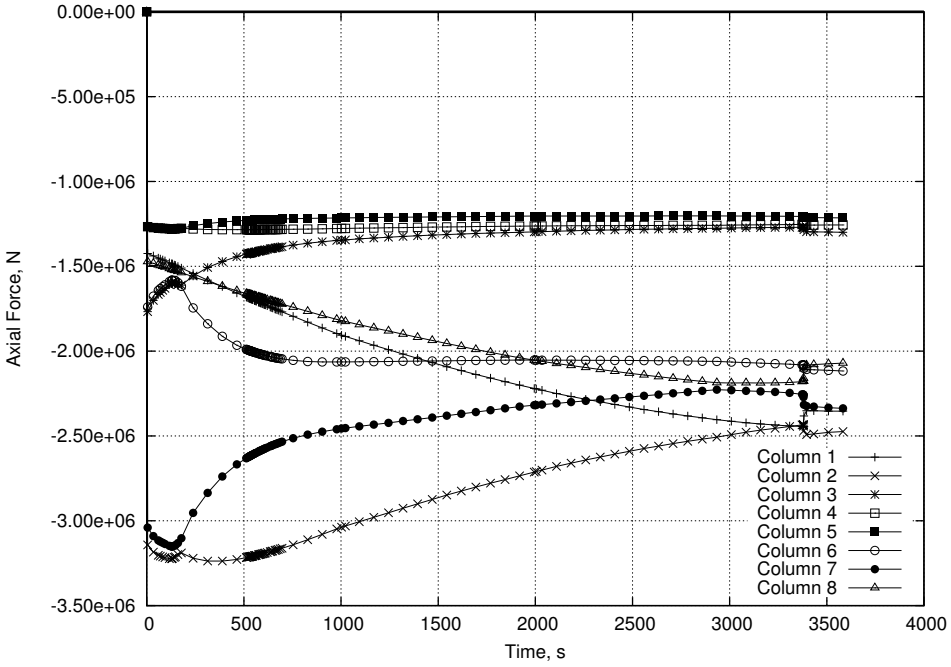

Figure 5.26: Scenario 10 : Column Base Forces

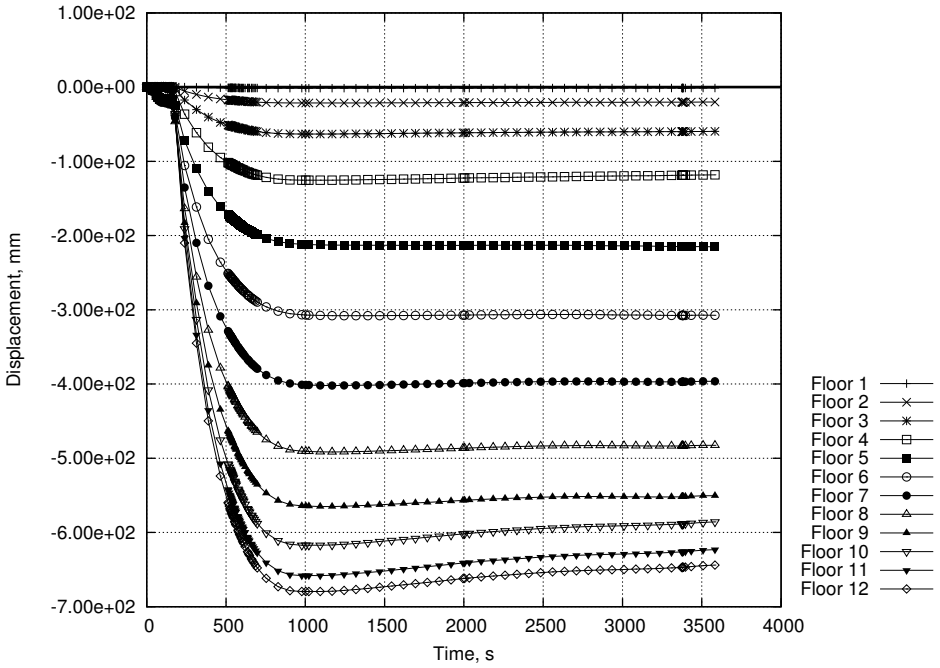

Figure 5.27: Scenario 10 : Sway Mechanism

Similarities can be seen between the responses shown in Figures 5.30 to 5.32 and their counterparts from Scenario 6 (Figures 5.14 to 5.16). The higher demand on the hat truss system in the 5 floor fire of Scenario 11 leads to much earlier failure.

5.4 Conclusions

This chapter analyses responses of a large building under various fire conditions and reports on an interim stage in the investigation into the effects of fire on buildings with long span, truss based floor systems. The 2 dimensional nature of the models used in the investigation presented here means care should be taken in drawing definite conclusions from the results of this study. The results match well with the results presented in previous chapters.

This investigation is not meant to be a fully inclusive forensic study of a particular building and as such includes several assumptions that affect its applicability to real structures. First of all the models involved are all 2D. Secondly, connections have been modelled such that failure may not occur. A simple comparison between the forces seen in the column-truss connection elements and the capacity of the connections as calculated by NIST [52] for the World Trade Center towers is possible. This shows that the maximum tension in the fire affected floors is under 200kN and therefore well within the expected total connection capacity of 260kN at around 800^{o}C. The total connection capacity includes the truss seat system as well as additional members connecting the trusses to nearby columns.

Other effects that would appear in a real building but have not been considered here include direct interaction between floors. At the high level of midspan deflection that appears in some of the models it is possible that spalling and partial floor failure may occur and directly increase the loading on lower floors. This again would lead to dynamic forces being applied that could cause failure of these floors. In particular this would be a problem in the cool interface floor below the fire floors. Failure of this interface floor would increase the demand on the floor below, and so on.

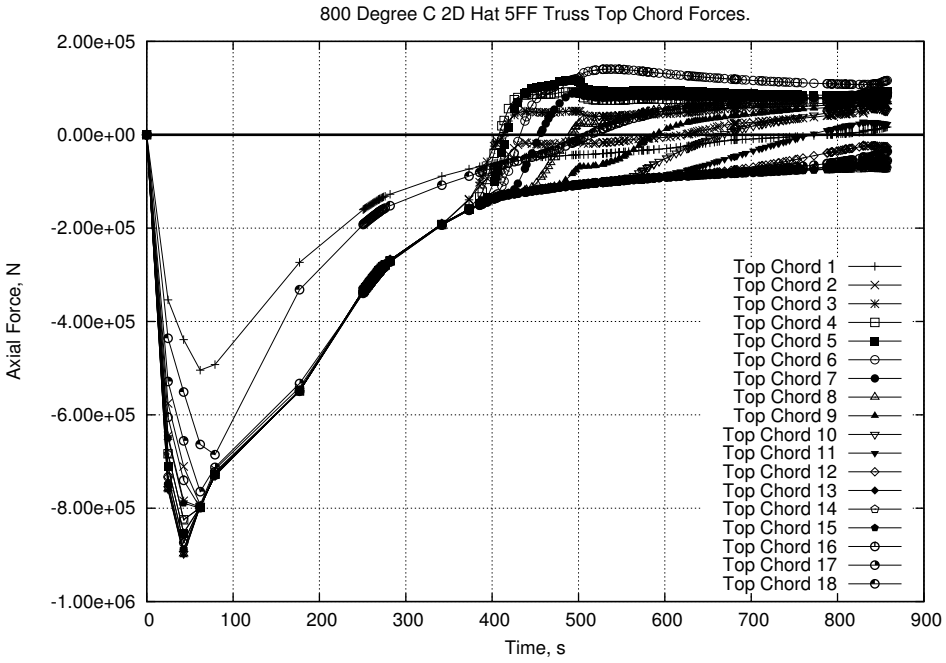

(a)

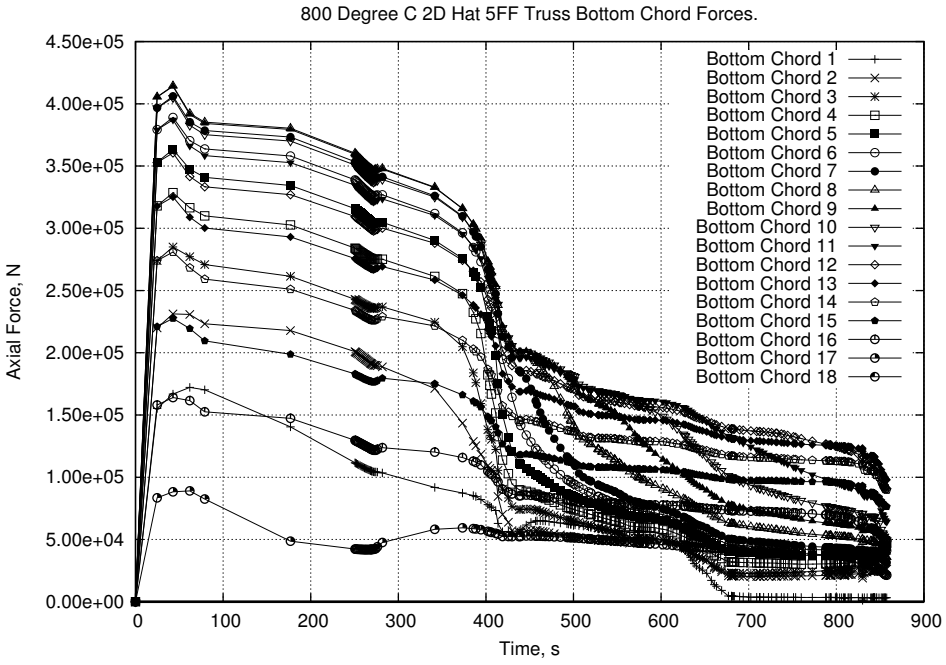

(b)

Figure 5.28: Scenario 11 : Truss Chord Axial Forces

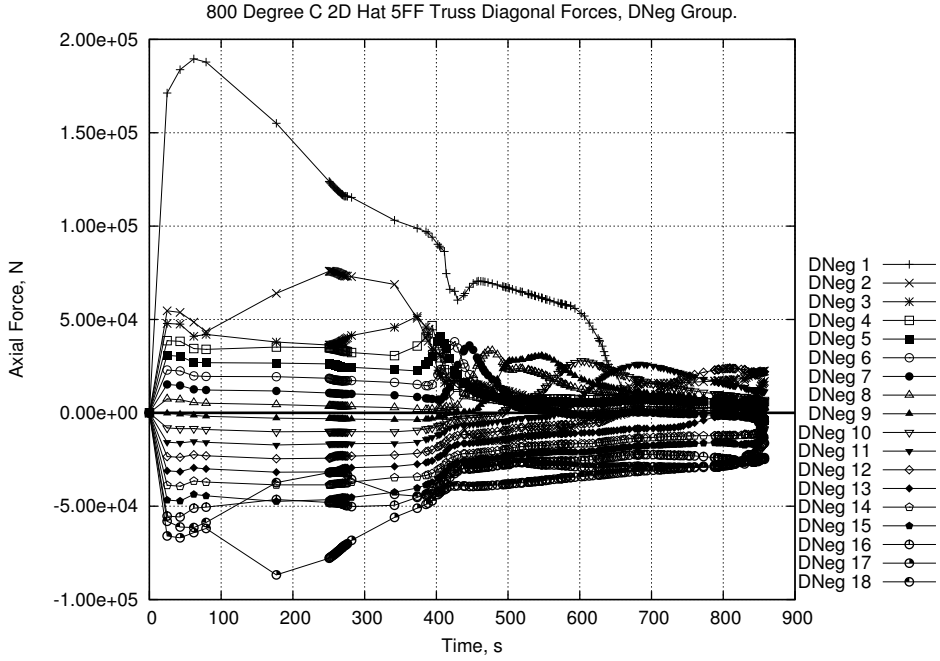

(a)

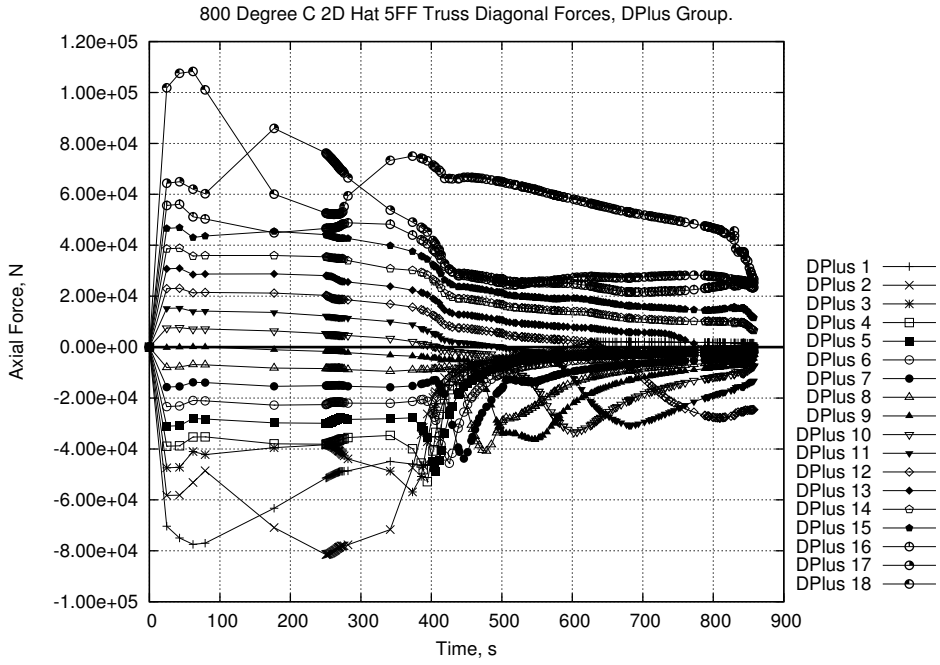

(b)

Figure 5.29: Scenario 11 : Truss Diagonal Axial Forces

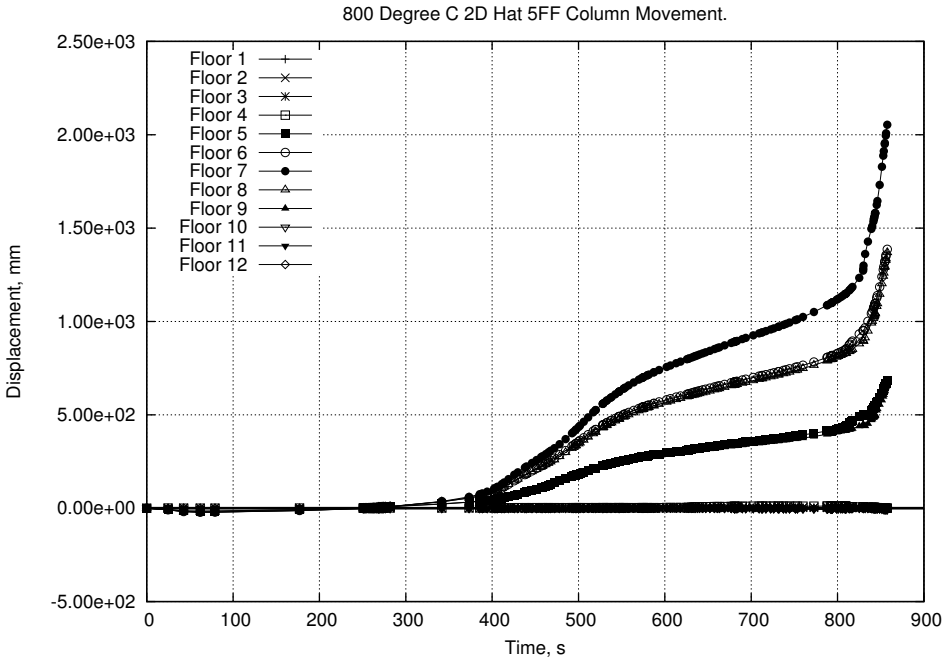

(a)

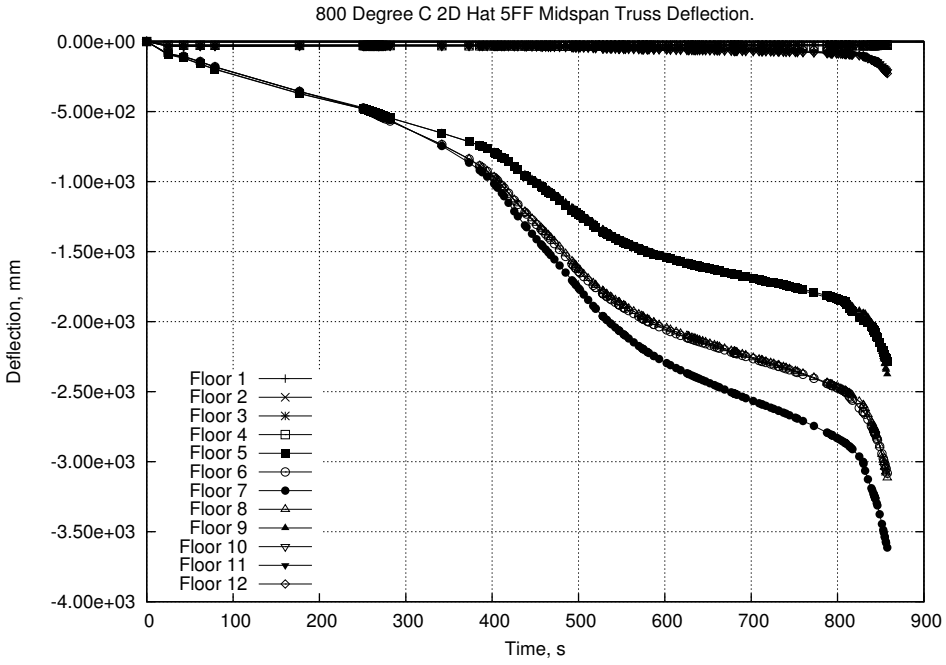

(b)

Figure 5.30: Scenario 11 : Member Displacement

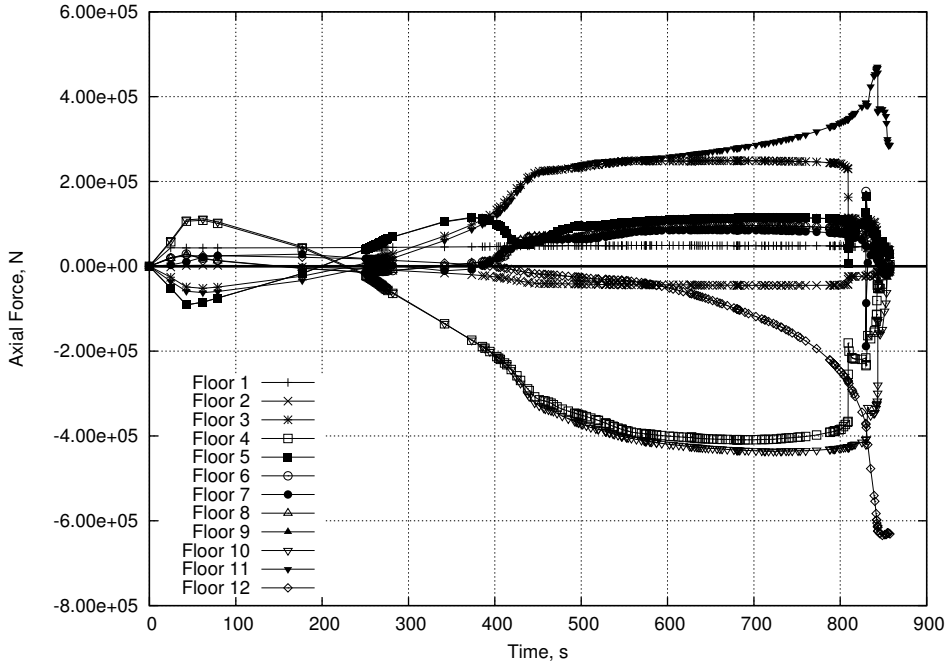

Figure 5.31: Scenario 11 : Floor Membrane Forces

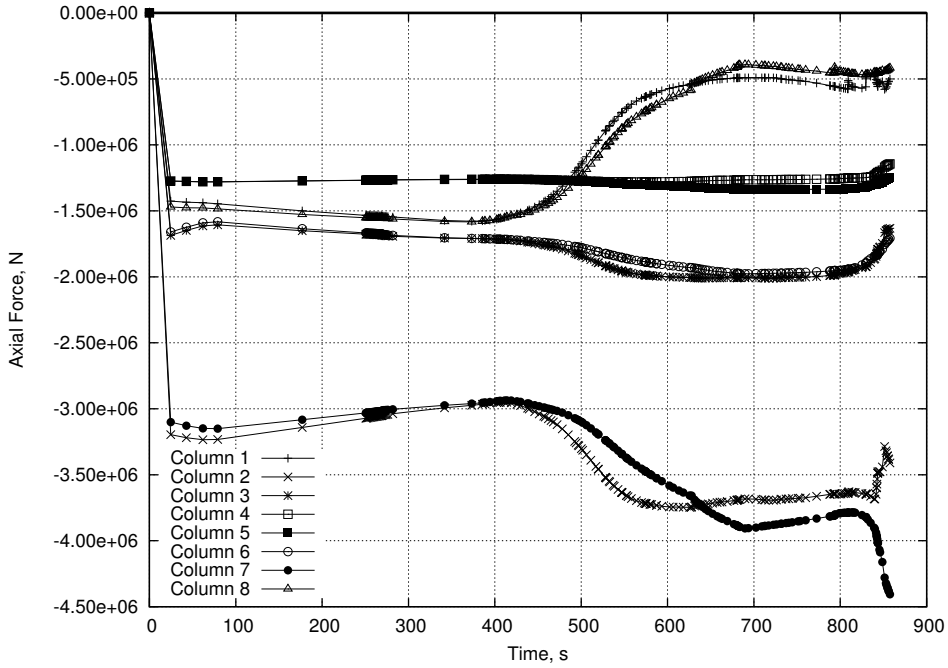

Figure 5.32: Scenario 11 : Column Base Reactions

The main conclusions that may be drawn from this study is that under moderate fire conditions (especially low temperature fires) large buildings can retain a great deal of stability, even if several floors are affected. If additional redistribution mechanisms (such as hat or belt trusses) are introduced then the fire resistance of the building can be enhanced considerably.

Initial failure mechanisms are based around failure of the columns after they have been drawn inward by tensile membrane action in the trusses. If the possibility of redistribution exists then a new load path will be established and the building will be less vulnerable to fire. Collapse will occur when all possible strength reserves have been exhausted. Such global mechanisms involve the full structure of the building and would not be found in a model of a smaller region of the building.

800^{o}C fire regimes produced significantly more movement in the structure compared to 500^{o}C fire regimes. The lower temperature scenarios produced models that resisted further movement after the steel stopped heating while at the higher temperature the steel was too weak to withstand extra slab deflection.

Moving from a fire over 3 floors to a fire over 5 floors increases the threat to the structure. As long as temperatures can be kept low then movement in the structure can be kept to a minimum allowing it to transfer loads in a similar manner to that for ambient conditions. In a severe fire over 5 floors then the horizontal forces applied to the column are increased. This leads to plastic hinges appearing more quickly in the column and hence a reduced time to collapse. In all cases the move from 3 floor fires to 5 floor fires increased the effect on the structure and, in the 800^{o}C scenarios, substantially reduced the time to collapse.

The heating regime on the floor slab, comparing heating from both sides to heating from below only, does not create a drastic difference in the final response of a structure under the assumed fire conditions. In the early stages of the fire the primary driving force is the thermal expansion of the steel truss and the relationship between that and the concrete slab. At such an early stage the slow rate of propagation of the heat through the concrete keeps it at a low temperature compared to the steel. In the later stages the extra movement caused by the slab expansion

is supported by the change in load bearing system of the floor into catenary action and, ultimately, by the hat truss redistributing the load from the failing outer columns into the core.

The inclusion of thermal expansion effects is important due to the complex interaction that occurs in multi-storey models. If such effects are not included then the deflections seen in the early stages of the analyses would not be seen. The comparison between models with and without thermal expansion also shows how different the reactions can be. Comparisons between Scenarios 1 and 2 show somewhat similar results throughout the analysis while comparison between Scenarios 6 and 8 show very different results. Some important redistribution effects are not picked up by Scenario 8 (not including thermal expansion). The conclusion that can be taken from this point then is that the simple, initial failure mechanism is not greatly affected by the removal of thermal expansion effects but when substantial redistribution is available then the later responses are not captured correctly.

The next stage in this project is to move to a full 3D model of a similar number of floors to the models presented here. This will remove some of the limitations introduced by the 2D aspect of this study as well as allowing for a greater degree of realism in the fire regimes applied to the structure.

Chapter 6

3D Single Storey Response

This chapter describes the method used to create a single storey model of a building similar to the WTC towers [32, 50, 54]. Validation is presented between various models used in moving the analysis from a Full Resolution Single Truss to a Half Resolution Half Symmetry model. A general description of the response of a single storey Half Symmetry model is also presented.

6.1 Model Description

6.1.1 Material Models

The models presented here utilize the ABAQUS Concrete Damaged Plasticity model. 30N/mm^2 lightweight concrete has been used for the floor slab and Eurocode 2 [74] properties for ambient and high temperatures have been followed. The structural steel uses a simple elastic-plastic model assuming a yield strength of 300N/mm^2. Eurocode 3 [72] has been used to determine the properties of the steel at elevated temperature. Please see Appendix A for more details on the material models used.

Resolution	Truss Top	Truss Bottom	Truss Diagonal
Full	95x38mm	130x38mm	40mm Dia.
Half	190x38mm	192x50mm	60mm Dia.

Table 6.1: Main Truss Member Section Sizes

Resolution	Truss Top	Truss Bottom	Truss Diagonal
Full	48x38mm	65x38mm	28mm Dia.
Half	48x38mm	65x38mm	36mm Dia.

Table 6.2: Transverse Truss Member Section Sizes

6.1.2 Half Resolution 3D Single Storey Model

The aim of this research is to investigate multi-storey mechanisms induced by fire. A high level of interaction was expected to occur between the various elements of the complex structure as heating was imposed. This would affect the run times and the ease with which the models converged hence it was necessary to make the large, 3D models as efficient as possible. To this end it was decided to create the single storey model in "half resolution". Rather than modelling the structure with columns every metre and main truss lines every 2m the distances were increased to 2m and 4m respectively. This increase in spacing results in an increase in section sizes to properly capture the response of the structure. This also means that each truss in the half resolution model supports twice the floor area of the full resolution model. As a further method of decreasing the number of degrees of freedom in the model the number of truss diagonals used was also changed. Hence the section areas of the truss diagonals in the half resolution model are not exactly twice that of the full resolution model.

The basic differences can be seen in Figure 6.1 and the section sizes for the various truss members are compared in Tables 6.1 & 6.2. The single truss models indicated in Figure 6.1 were also used as a basis of comparison for checking results of the single storey model. For more detailed results of these models see Chapter 3 for the full resolution model and Section 6.3 for details of the half resolution single storey model.

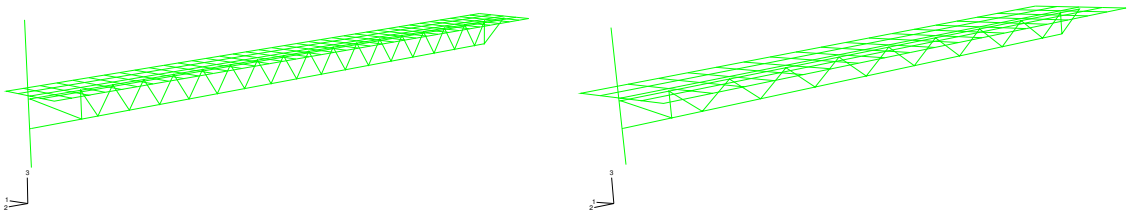

(a) Full Resolution (b) Half Resolution

Figure 6.1: Truss Resolution Comparison

The single storey model can be seen in Figure 6.2. The slab has been omitted for clarity.

As the investigation progressed it became apparent that the half resolution models were still too large to complete in a reasonable run time. This led to the construction of a half symmetry model of the half resolution floor using the general arrangement shown in Figure 6.3. The model mesh can be seen in Figure 6.4 where again the slab has been omitted for clarity. The primary failure mechanisms being investigated are those indicated in Chapter 4 and hence the symmetry model would still capture the mechanisms of most interest. Failure was deemed unlikely to be triggered in the short span areas.

The trusses were made up of 2 noded, linear beam elements using Timoshenko beam formulation (B31 [73]). Euler-Bernoulli beam elements were investigated (see Appendix A for details) but were found to converge less quickly hence were not used in the final models. The truss diagonals each had at least 4 elements to allow buckling responses to be captured. Similarly the top and bottom chords had at least 4 elements between points at which the diagonals connected. The diagonals and the chords used the same nodes at these points hence were rigidly connected. Although trusses are assumed to be pinned for analytical purposes, in reality these joints are welded hence a rigid connection is reasonable. As with the

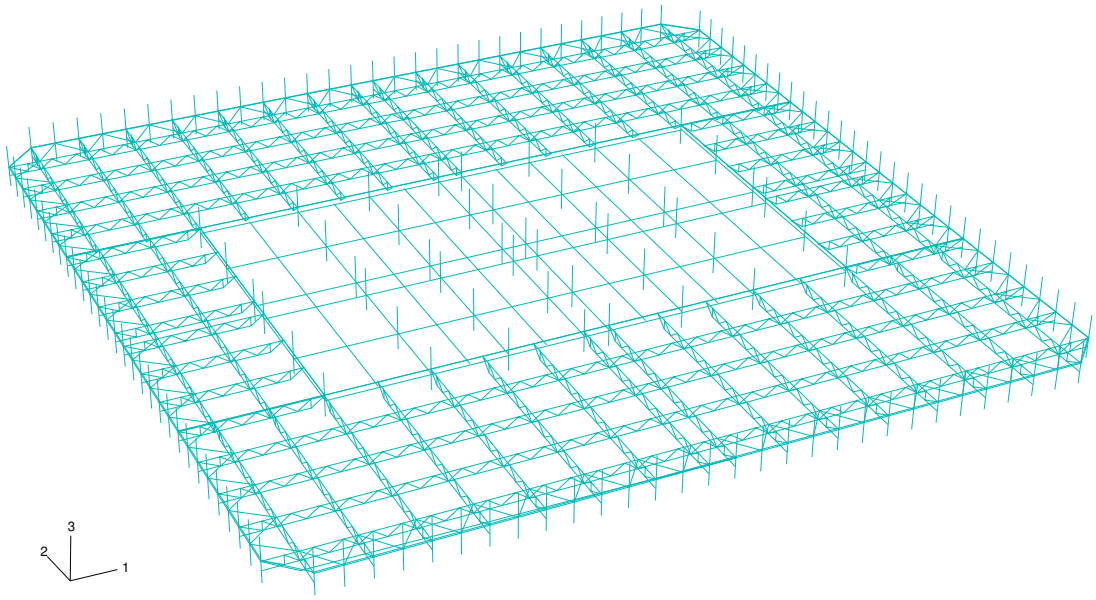

Figure 6.2: Single Storey Mesh

3D Single Truss model described in Chapter 3 a sin curve based imperfection was applied to the truss diagonals. In the half resolution model the maximum out of plane imperfection applied was 5mm at the centre of the diagonal over a length of around 1.2m. By comparison the full resolution model described in Chapter 3 had a 1mm imperfection applied over a length of around 900mm. Thus both of these imperfections are relatively small, in the range of 0.1-0.5%.

The concrete slab was modelled using 4 noded, general purpose shell elements with reduced integration (S4R [73]). The slab over the trusses was 100mm thick while the slab in the core was 125mm thick. Reference to the real structure of the WTC towers indicates that the slab was cast on profiled composite decking. Such decking was not included here in order to keep the complexity of the slab to a minimum. It has been shown in previous work that ignoring composite decking has a negligible effect on the response of a structure [1,16]. The same reinforcement was included in both the outer and core areas. This was welded wire fabric with 6mm diameter bars

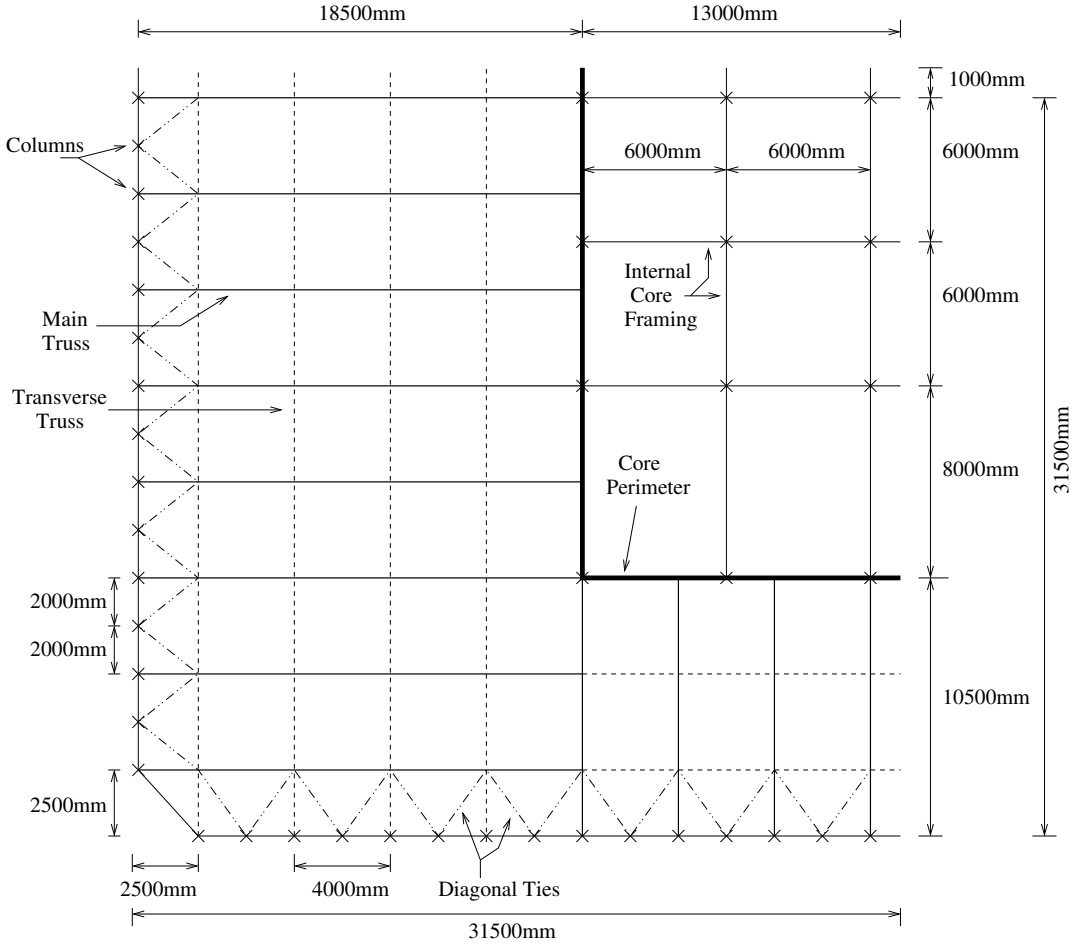

Figure 6.3: Symmetry Model General Arrangement

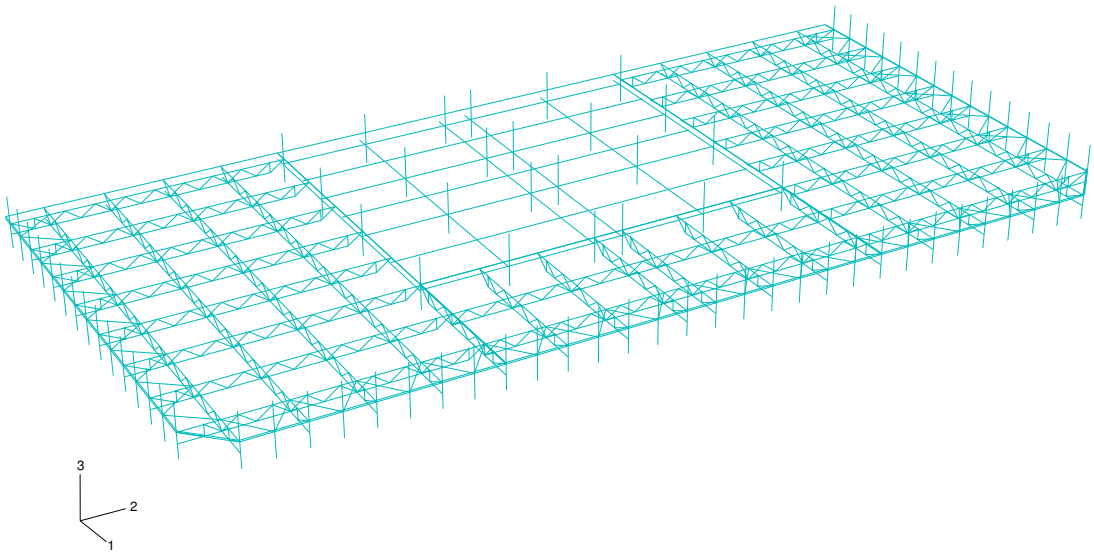

Figure 6.4: Symmetry Model Mesh

at 100mm pitch running in both directions. One layer was provided in both the top and bottom of the slabs and both the core and outer slabs used a cover depth of 30mm. The slab was rigidly attached to the top chord to simulate composite action. This connection was applied wherever slab nodes and truss top chord nodes coincided. In the case of the WTC tower floors the truss was only connected to the slab through the "knuckles" where the truss diagonals passed through the top chord rather than modern, more closely spaced stud type connections. Compared to this system the model has an increased resistance to buckling in the top chord due the the shorter effective length. However due to the changes in truss geometry in the move from full to half resolution the effective length of the top chord in the model is effectively being kept the same as in the WTC tower floor case. The high level of restraint supplied to the individual top chord sections also means that they will yield and buckle at a relatively low temperature as seen in Chapter 3.

The top and bottom chords of each truss had a small, rigid connector element

through which it was attached to the outer columns. This element allowed connection forces to be evaluated. All connections were assumed to remain intact over the course of the analysis. Data from the WTC towers indicates that a visco-elastic damper was part of the connection system for the bottom chord. Assuming the unit would be able to survive under fire conditions, any movement induced by the fire would be too slow to activate the damping unit. Therefore this connection was disregarded.

The change to half resolution involved reducing the number of columns in the model. In order to keep the correct vertical resistance and outward stiffness of the column lines the columns in the half resolution model were taken as being two of the true column sections placed next to each other. This was then simplified down into a single 700x350mm box section for each column with 6mm thick long sides and 12mm thick short sides. B31 elements were used for the columns. This alteration may be seen in Figure 6.5.

The columns spanned from 1800mm below the floor slab to 1800mm above. This is a half floor span above and below. As the models presented in this chapter are of a single storey only then this will mean that the columns will provide higher restraint to the floor system than would occur if the columns spanned a full storey height above and below the floor. This is not an ideal situation but it does allow a direct comparison to the single truss models which also have this column arrangement. Additionally having the floor constructed in this method allowed for greater efficiency in moving from a single storey to a multi-storey model. As the column boundaries in the multi-storey model would be remote from the fire affected floors the half length of column between the first and last floors and the boundaries would not affect the restraint to the fire floors.

The spandrel beam was also modelled using B31 elements. These elements connected directly into the column nodes and hence had rigid connections. The spandrels were 1320mm deep and 10mm thick. This is a very extreme section for a beam element to represent so a model was tested using shell elements (Section 6.2.4) for the spandrel beams which showed little difference in the behaviour of the

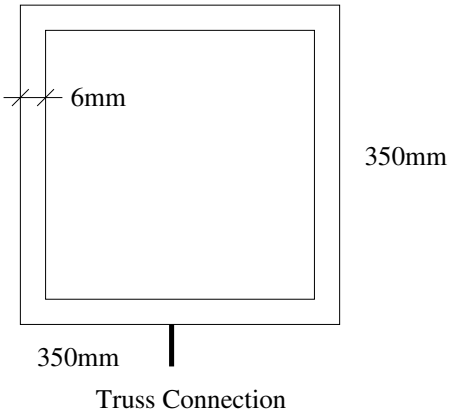

(a) Original Column Section

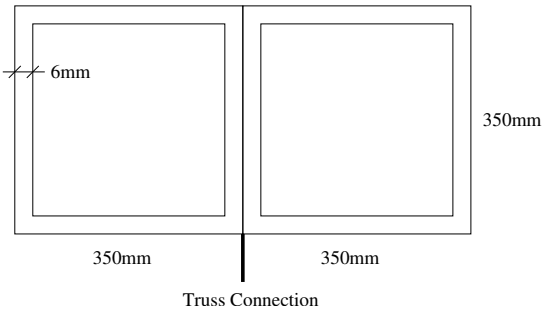

(b) Two Columns Side by Side

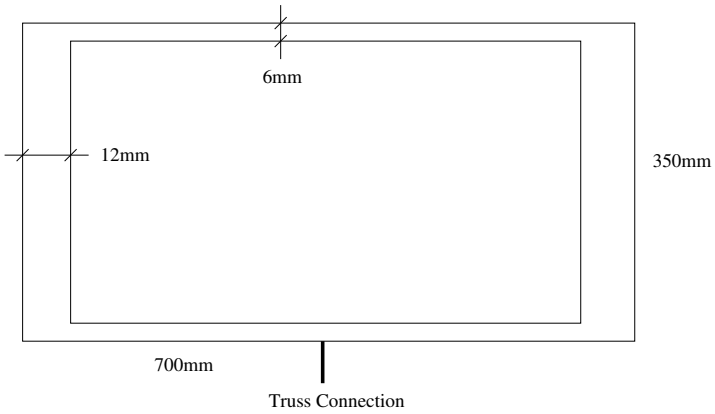

(c) Column Section Used in Model

Figure 6.5: Column Section

spandrels.

In the core the main beams were taken as those spanning in the "1" direction. These beams were not continuous and pinned to the columns. The main beams on the perimeter of the core were 533x210x82UBs while the internal beams were 406x178x54UBs. The transverse core beams (in the "2" direction) were continuous over their supports but were again pinned to the supporting columns and main beams. The perimeter transverse beam was taken as 305x127x42UB while the internal beams were 305x102x28UB sections. These sections were chosen after a simple analysis with assumed loading was conducted. A further load ratio check was also done in accordance with BS5950 [39] to check that the sections would not be too stiff. The recommended load ratio is 0.6 when the code prescribed loading under fire conditions is divided by the maximum capacity of the section at ambient. All the sections in the core were in the range of 0.52 to 0.6 for this load ratio.

In order to stabilize the intermediate columns, i.e. the columns not connected directly to main trusses, diagonal members were added between the first main-transverse truss connection and the intermediate columns. This link was modelled as a simple truss element (only capable of axial translation). In the WTC structure these elements were firmly embedded in the concrete slab hence buckling of these members was not likely and they would be well protected from fire.

6.1.3 Fire Input

The compartment temperatures were generated using the same method that was presented in Chapter 4. As before, the time-temperature profile in the compartment was based upon a generalized exponential curve given by :

$$T(t) = T_o + (T_{max} - T_o)(1 - e^{(-at)}) \tag{6.1}$$

where T_{max} and T_o are the maximum and ambient compartment temperatures respectively. t represents the time over which the model is analysed. a is an arbitrary 'rate of heating' parameter and for the purposes of this section has been taken as

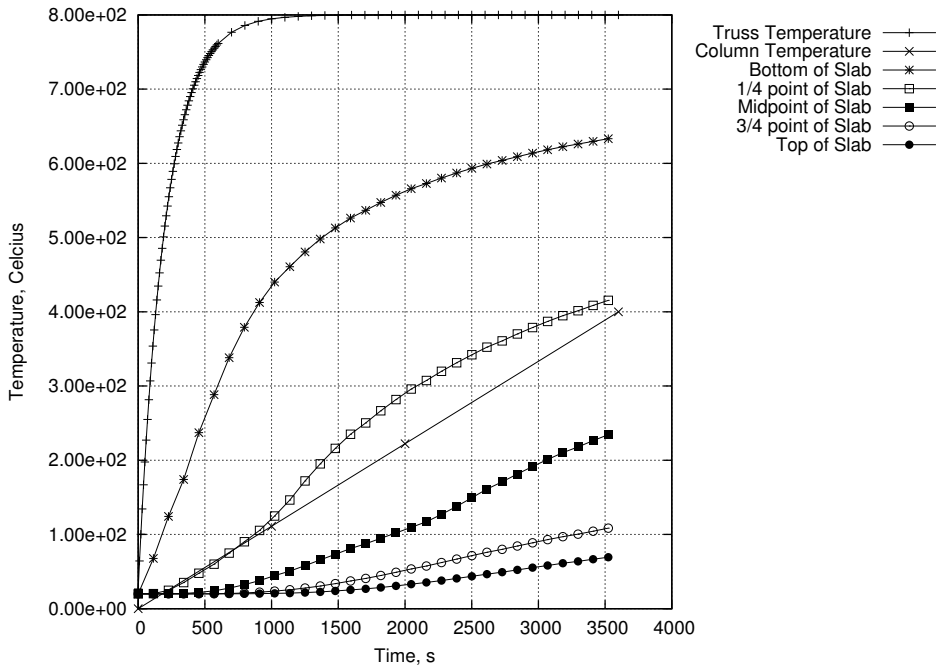

Figure 6.6: Temperature-Time Distributions for 800^{o}C Analysis

0.005. Again a compartment fire with a rapid temperature increase followed by a period of steady temperature is generated. This allows a direct comparison to be made with the models investigated previously. The models run for the comparisons presented later in this chapter all used the temperature time distributions shown in Figure 6.6. In all models where core structure is present it was assumed that the fire was limited to the outer truss supported areas only. The core was always assumed to be at ambient.

The trusses are assumed to have no protection and are therefore assumed to equal the compartment temperature. The column is assumed to be protected with a fire rated material and therefore undergoes more limited heating (see Figure 6.6 for details). In addition the external columns are also in contact with the outside atmosphere which would result in a lower temperature.

In all the models the temperature distribution in the concrete slab is described by applying individual time-temperature curves to 5 different points through the depth of the slab. The points used are the top and bottom surfaces, the quarter points and the mid depth of the slab. The time temperature distributions used in

Name	Structure	Resolution	Symmetry	Imperfection
3DSTFR	3D Single Truss	Full	NA	1mm
3DSTHR	3D Single Truss	Half	NA	5mm
Imperf5	3D Single Truss	Full	NA	5mm
3DSFHRSym2	3D Single Storey	Half	Half	5mm
FRQuarterFloor	3D Quarter Floor	Full	1/4	None

Table 6.3: Model Summary

this study were taken from a 1D heat transfer analysis [75].

The above fire regime was applied as if the fire existed on the floor below that being modelled. The slab was assumed to be a compartment boundary hence only steel below the slab would be affected by the fire. The slab temperature distributions were determined assuming it was heated from underneath only for the same reasons given in Chapter 4.

6.2 Results Validation

6.2.1 Single Truss Models : Full and Half Resolution

The first step in converting from a single truss model to a full floor model was to ensure that the global results coming from both systems would match adequately. This section presents a comparison of the two 3D single truss models shown in Figure 6.1. As the truss geometry itself is changed the local results will also change and hence the direct comparison of individual truss member forces becomes less important. The results to be focussed on are those indicated in Chapter 4 as important for determining the global response of a structure. These include :

- Membrane forces transferred from floor to column
- Column outward lateral movement
- Midspan floor deflection

Results for the floor response are presented in Figures 6.7 to 6.9. As the Half Resolution model was changed to take into account an increased floor area an increase in membrane force was expected. Figure 6.7.a shows that the Half Resolution model has around double the membrane force of the Full Resolution model. Figure 6.7.b indicates how the increased stiffness of the extra columns keeps the outward displacement of the columns at the same level. Midspan deflections, as shown in Figure 6.8, show good agreement between the two models.

Figure 6.9 shows some of this data in a slightly different form. Similar to the results in Chapter 3 a comparison of the "buckling" response was made. Part .a of this figure shows the raw data while part .b shows a comparison when the full resolution floor membrane force has been multiplied by a factor of 2 to match the increase of supported area of the half resolution model. The results in Figure 6.9.b match extremely well.

The results of the Half Resolution models presented here are truncated due to convergence difficulties. However, the results indicate that Half Resolution models will respond in a similar manner to a Full Resolution model.

6.2.2 3D Single Truss : Imperfections

Another alteration was made in the truss geometry in the move from full resolution to half resolution. The out of plane imperfection applied to the truss diagonal was increased from 1mm, over the diagonal length, to 5mm to aid convergence. In the full resolution model this is a change from around Length/880 to L/175. When applied to the half resolution models the change in length of the truss diagonals means that the 5mm imperfection is around L/250. The results presented in this section are of a comparison between two Full Resolution models, one with the initial 1mm imperfection and the second with a 5mm imperfection. The results were taken from the nodes indicated in Figure 6.10. In the graphs shown in Figures 6.11 and 6.12 the Base analysis (3DSTFR analysis) uses a 1mm imperfection while the Imperf5 results are taken from the model with a 5mm imperfection. There

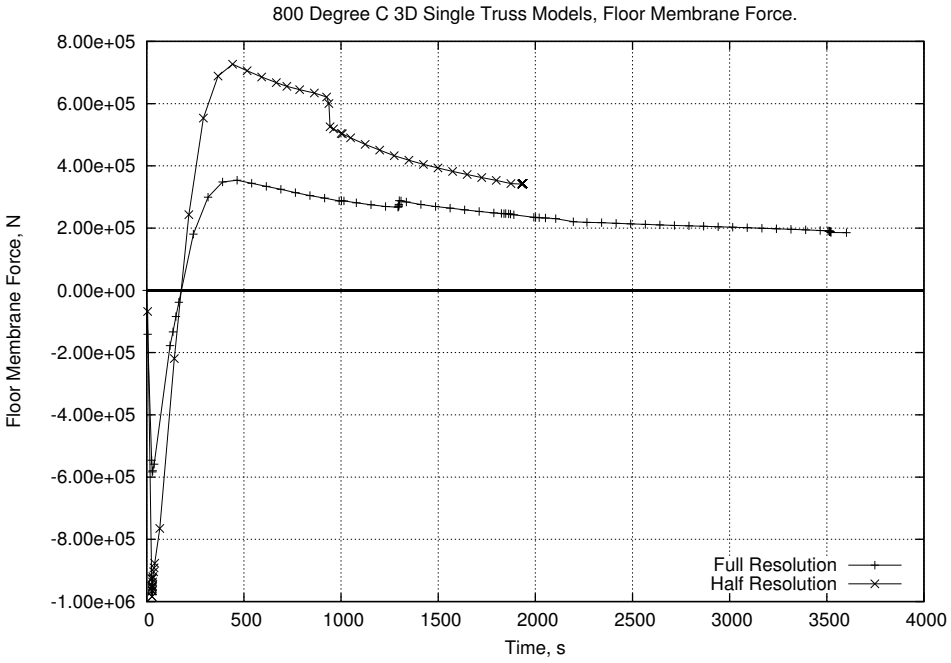

(a)

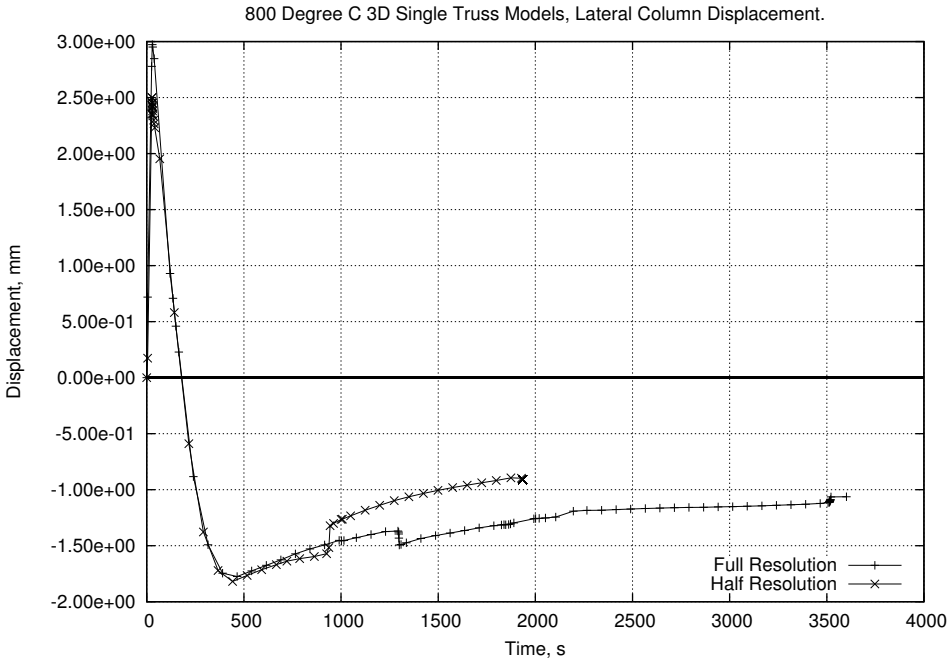

(b)

Figure 6.7: Resolution Comparison : Floor Membrane Forces and Displacements

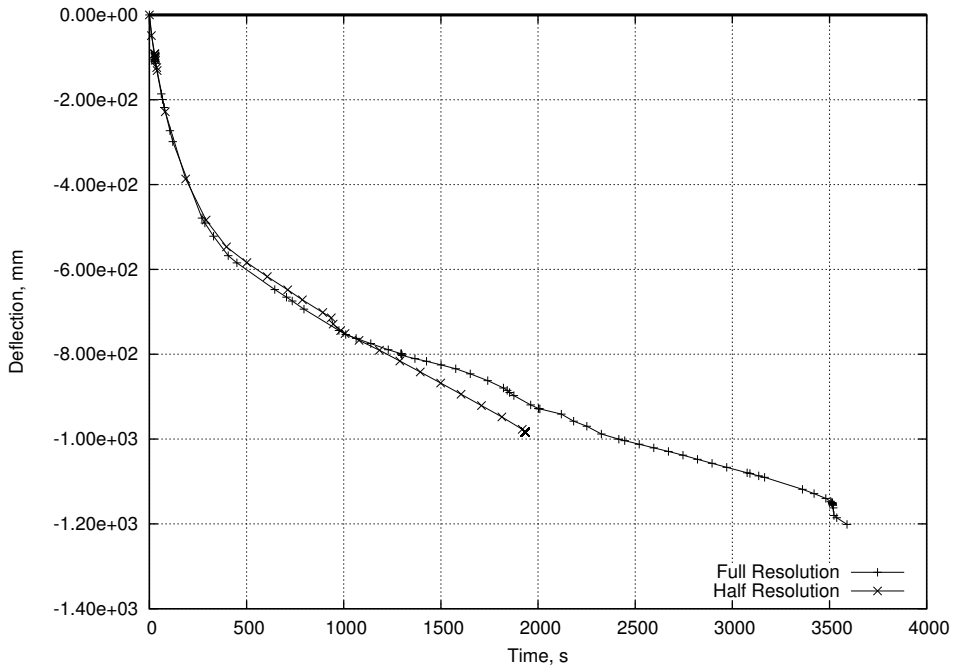

Figure 6.8: Resolution Comparison : Midspan Deflection

are small differences between the different models when the truss member forces are investigated, as shown in Figure 6.11. However as Figure 6.12 indicates these minor differences have very little effect on the overall response of the floor.

As the results match so well it can be assumed that an increase to a 5mm imperfection in the truss diagonals will not induce premature failure of the truss as compared to a 1mm imperfection. In addition the change from 1mm to 5mm meant that around 20% fewer iterations were needed for the analysis to complete.

6.2.3 3DSTFR to 3DSFHRSym2

The results presented here are designed to verify the results of a half resolution, half floor symmetry model (referred to hereafter as the symmetry model) against those already produced for a full resolution single truss (referred to in the remainder of this chapter as the single truss model). The inclusion of more of the floor plate means that the relative restraint levels will change somewhat between the single truss and the full floor model. This creates difficulties in comparing the results from

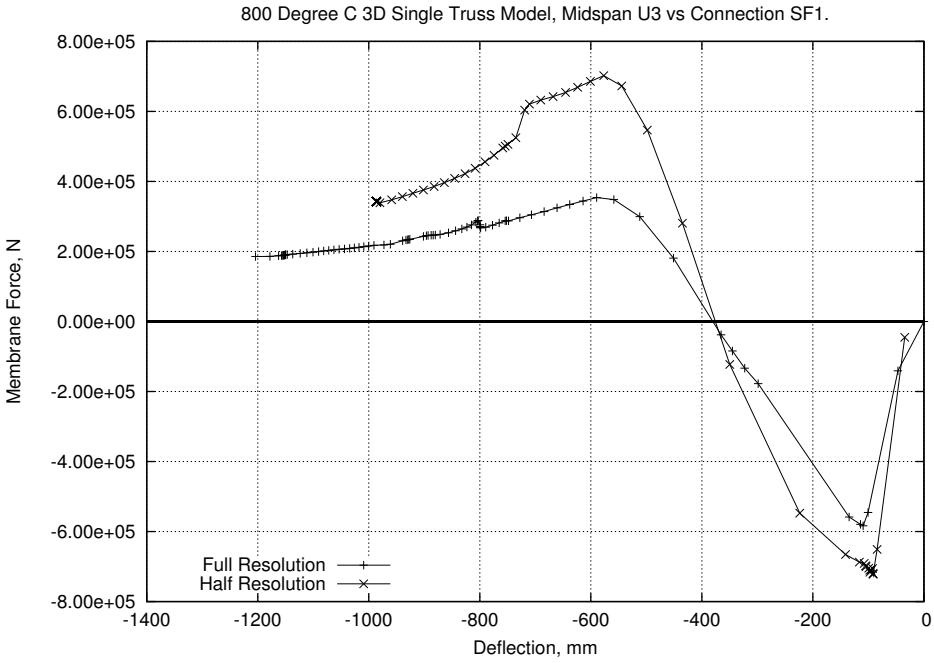

(a)

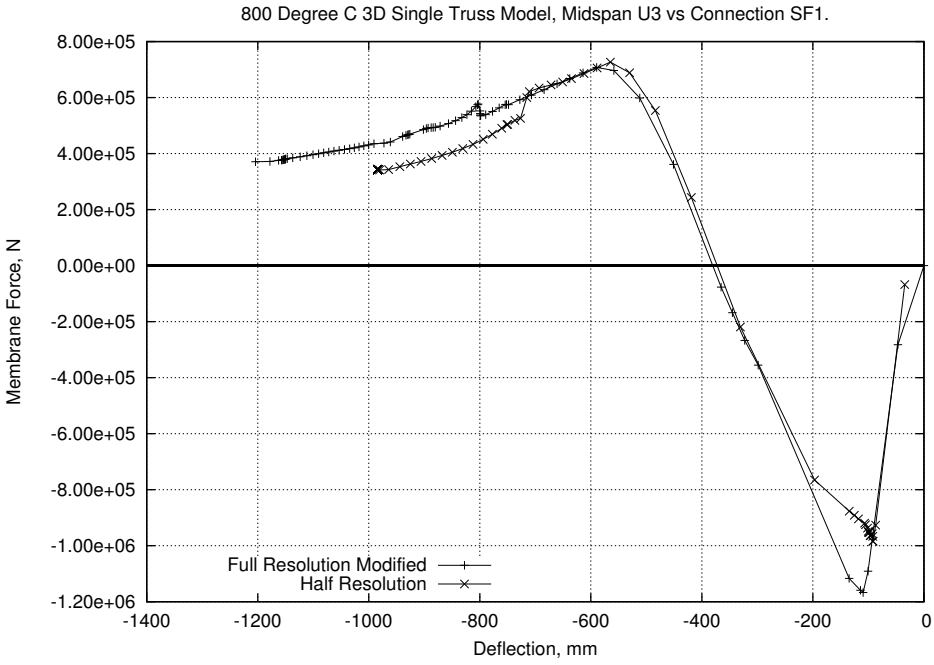

(b)

Figure 6.9: Resolution Comparison : Floor Response

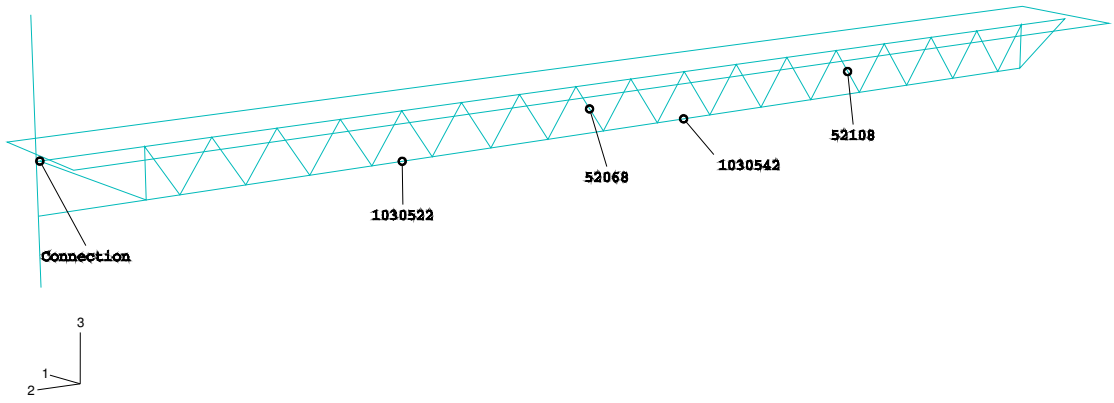

Figure 6.10: Imperfection Comparison : Node Location

the single truss model to an individual truss in the symmetry model due to the increased redundancy in the structure. As such the results from a selection of floor trusses will be included in the comparison graphs. The results for the symmetry model are taken from the trusses in Area 2 marked in Figure 6.13 while results marked as 3DST are from the full resolution single truss model (Figure 6.1.a and 3DSTFR in Table 6.3).

Figure 6.14.a shows a comparison of the truss connection forces between the long span trusses in the symmetry model and the single truss model. The responses are similar with the forces in the symmetry model being around double that of the single truss model. This is expected as the trusses in the symmetry model are supporting double the floor area of the single truss model. Figure 6.14.b shows the equivalent outward forces on the intermediate columns, as transmitted through the diagonal ties connecting them back into the trusses. For comparative purposes the connection forces from the single truss model and Truss 12 of the symmetry model

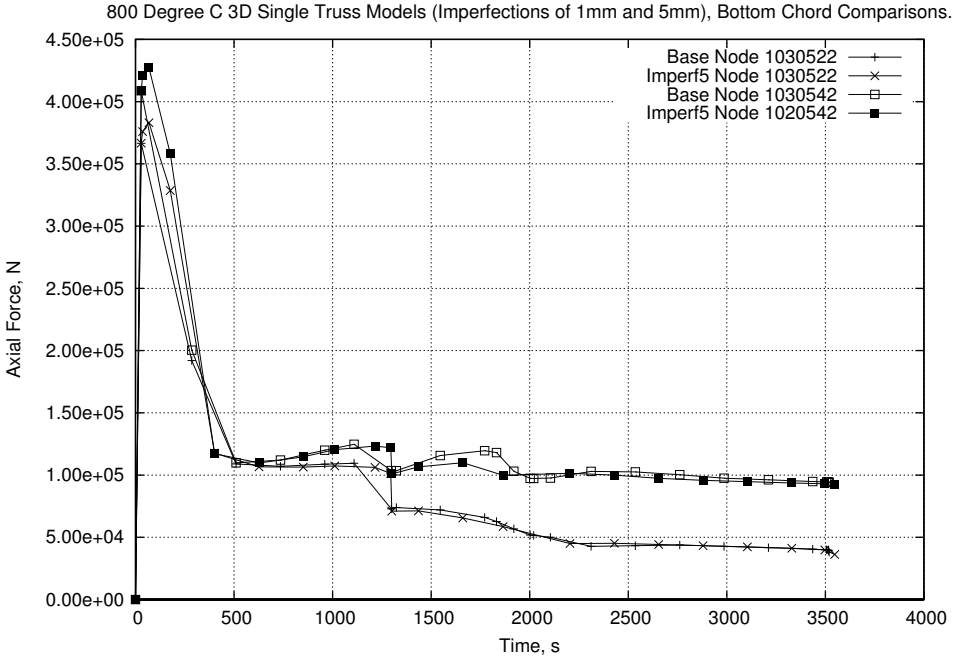

(a)

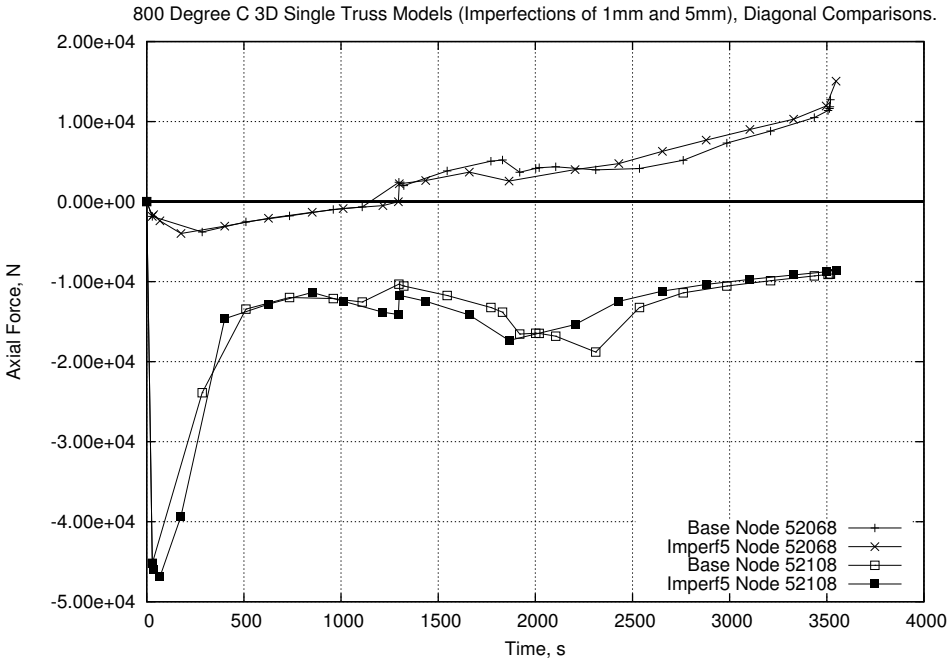

(b)

Figure 6.11: Imperfection Comparison : Truss Member Forces

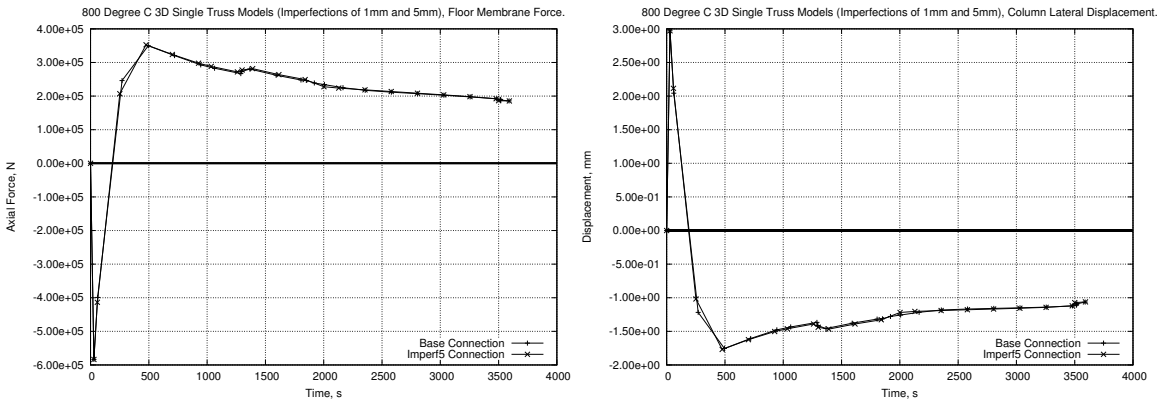

(a) (b)

Figure 6.12: Imperfection Comparison : Floor Membrane Results

have been included. The forces into the intermediate columns is of the same order as the forces in the main truss connections, although the response has a significant amount of lag involved. This lag indicates that there is a gradual redistribution of forces through the structure as the fire progresses. A more detailed investigation of this response may be found in Section 6.3.

Figure 6.15 presents comparisons between the two models for midspan deflection (graph a) and the lateral displacement of the column (graph b). The plots of midspan displacement show close similarity between the single truss and the symmetry model. The disparity in the results in the column lateral displacement plot can be explained by the change in overall stiffness caused by including more than a single truss. Figure 6.7.b shows a direct comparison between the half and full resolution versions of the single truss model and the results match well. Hence the move to the symmetry model allows increased outward movement. This is likely due to the difference in how the intermediate columns are connected into the rest of the structure. In the single truss model the presence of the intermediate columns are included as part of the model column (please refer to Chapter 3 for details) while in the symmetry model they are included as separate entities with their own connection to the trusses.

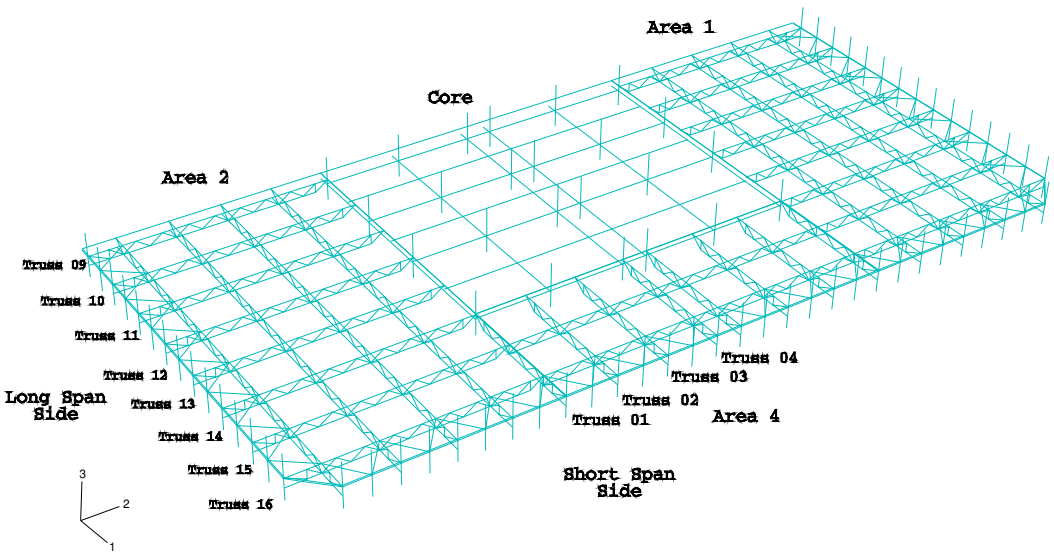

(a)

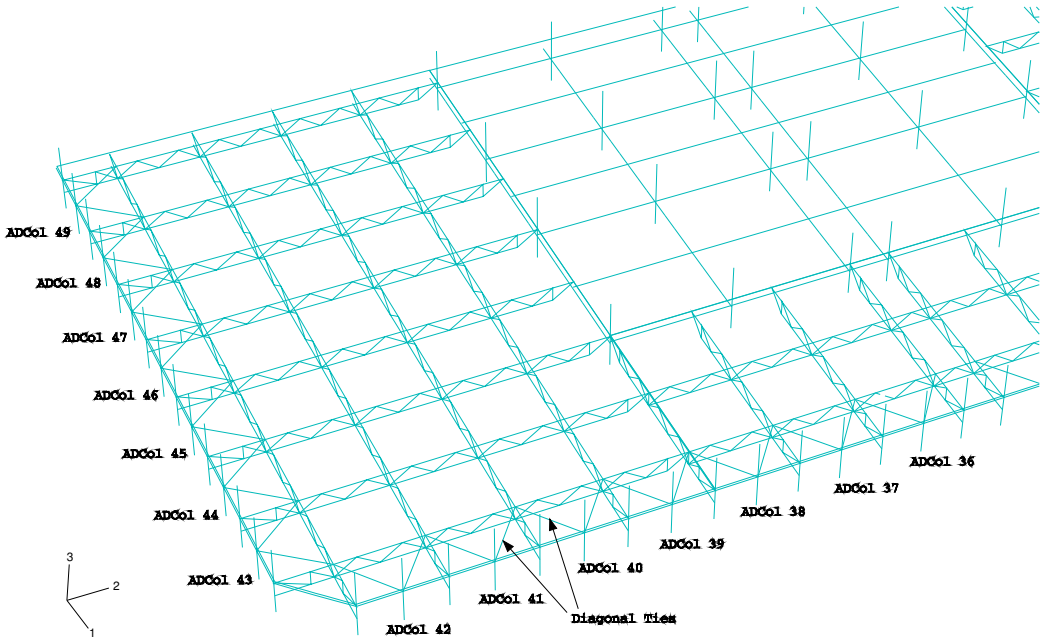

(b)

Figure 6.13: Floor Verification : Output Member Locations

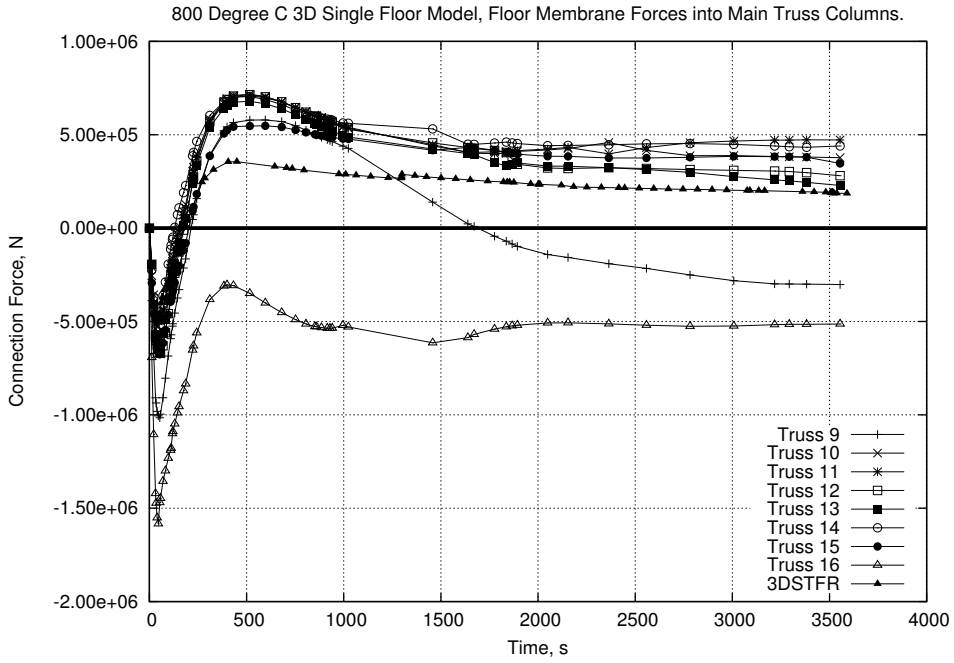

(a)

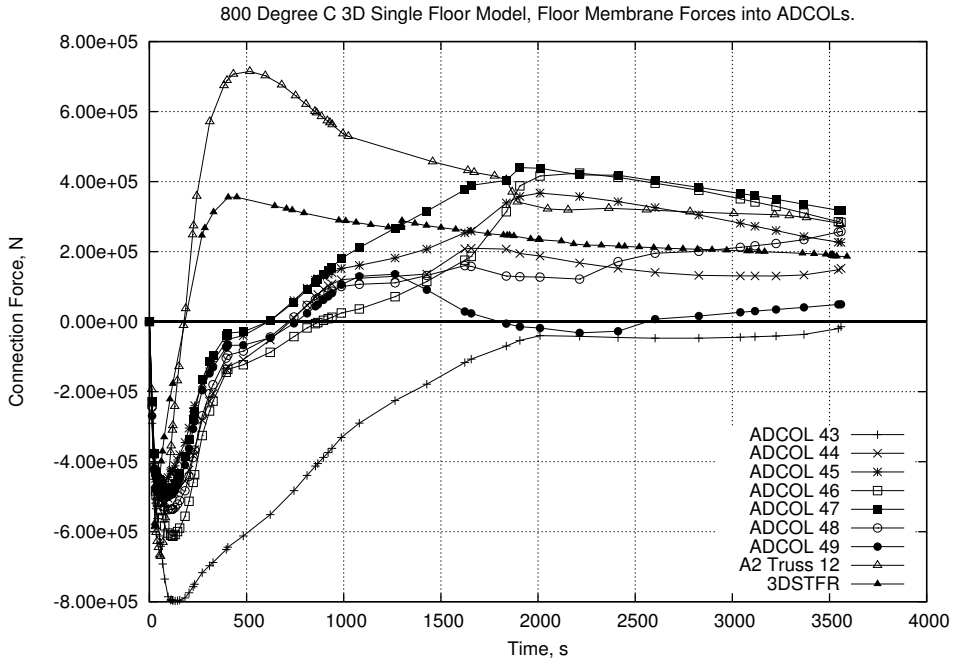

(b)

Figure 6.14: Floor Verification : Floor Membrane Forces

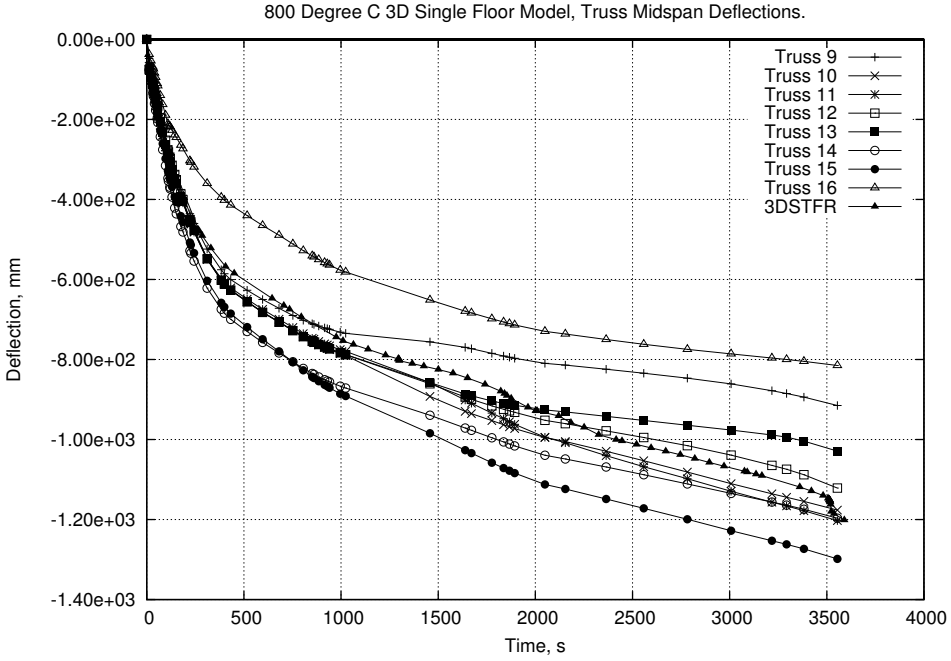

(a)

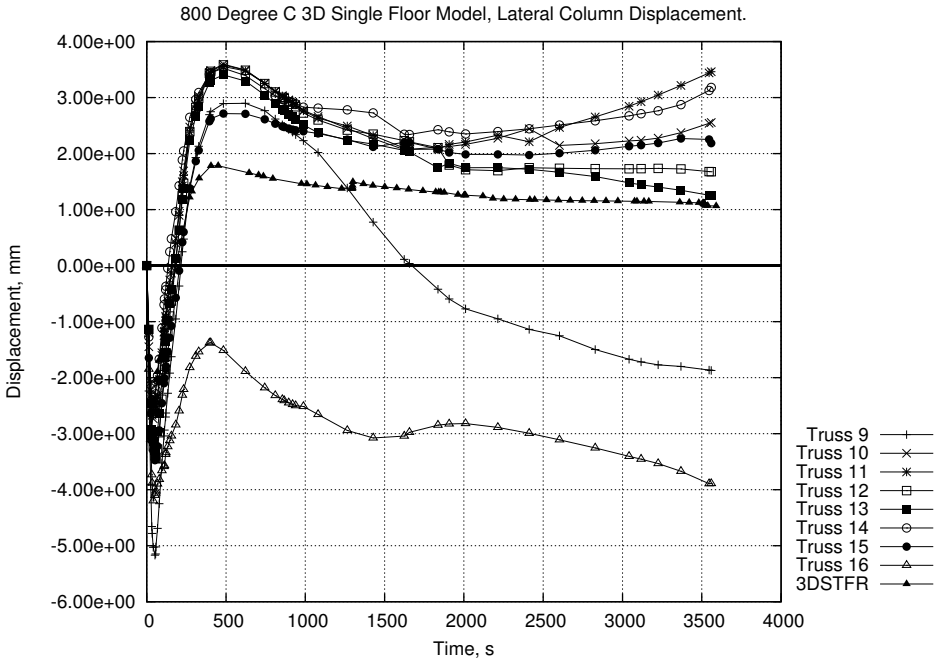

(b)

Figure 6.15: Floor Verification : Displacements

A different method of evaluating the response of the model is shown in Figure 6.16. This figure compares the force-displacement curves of the various trusses in the symmetry model to that of the single truss model. Figure 6.16.a shows the raw data while Figure 6.16.b shows the same data with the single truss forces being increased by a factor of 2. As with Figure 6.9.b when the resolution correction factor is applied to the single truss model, the final response is extremely similar to those of the symmetry model.

The data presented in this section again indicates that the global response of the floor system is not qualitatively altered by the change from full resolution to half resolution. Some exceptions should be noted. Trusses 9 & 16 produce somewhat different results. Truss 16 runs close to the short span side column line and the compatibility resulting from its location alters the truss response. The initial response of Truss 9 is very similar to the other trusses. As the steel heating becomes constant and the slab continues to heat the extra thermal expansion causes "ripples" to appear in the slab. Compatibility between the weak truss and the stronger slab causes lower deflections in the truss. This behaviour is explained in more detail in Section 6.3.

6.2.4 3DSFHR to FRQuarterFloor

During the course of this PhD the official investigation into the WTC towers collapse was also progressing. A further full resolution model was built by other members of the research team [79] in order to check and validate some of the modelling choices that had been made. This model would also provide a platform for direct comparison with the official NIST models. As this model would be highly detailed it was designed to include only a quarter of a floor to maintain numerical efficiency when moving to multiple floor models. This was relatively easy to implement as the WTC towers were biaxially symmetric. The mesh for this model may be seen in Figure 6.17 where the slab has been omitted for clarity. The quarter symmetry single storey model is substantially the same as the half resolution

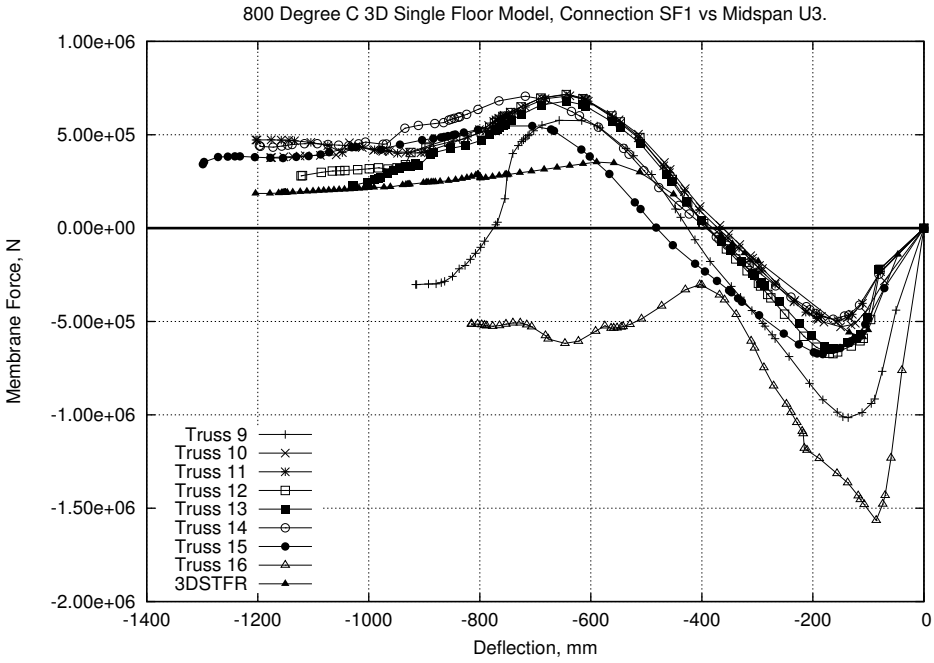

(a)

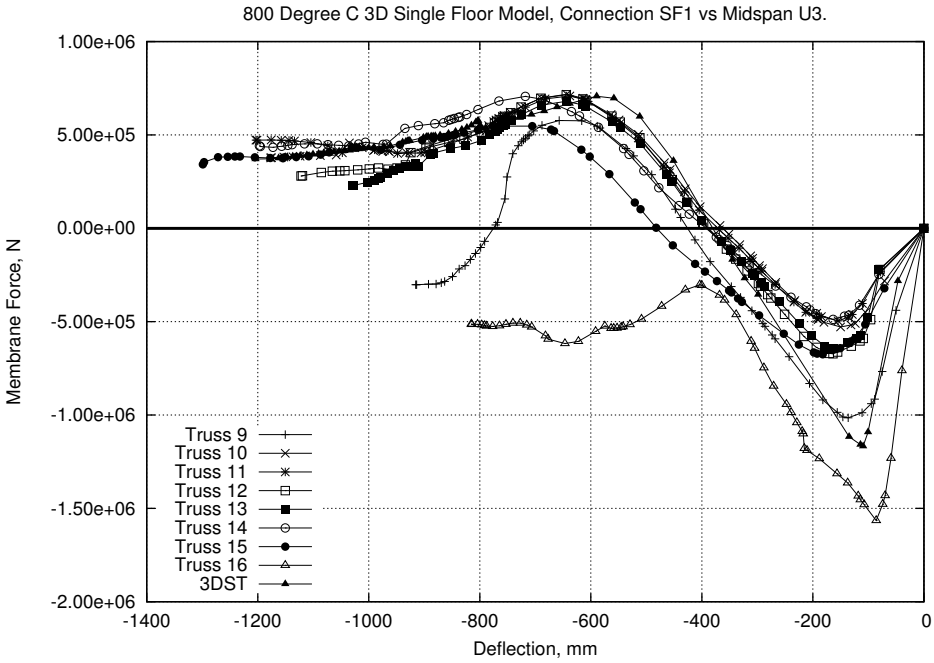

(b)

Figure 6.16: Floor Verification : Force - Displacement

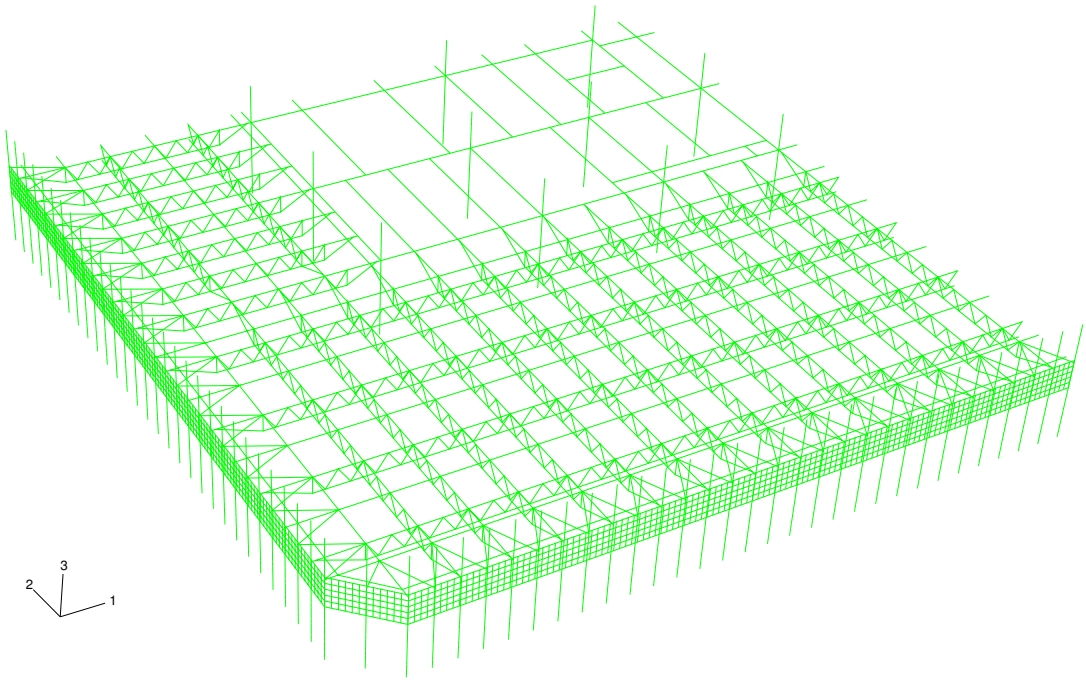

Figure 6.17: Quarter Floor Comparison : Model Mesh

models described previously although no imperfections were applied to the truss diagonals.

Except for the change in resolution the only other effective difference is that the lower columns in the quarter floor model are double the length of the half resolution symmetry model. Ideally the column lengths in both models would be the same length, thus providing the same level of restraint to the floor system. A difference in the method used to construct the two models has led to a difference in the column lengths. The drawbacks to the column length on the symmetry model are described in more detail in Section 6.1.2. The change in restraint between the symmetry model and the quarter floor model can be seen in some of the results although it does not change the general response types.

The final displacements of the quarter floor model may be seen in Figure 6.18. Similarities can be seen if a comparison is made between the half resolution symmetry model in Figure 6.22 (Section 6.3). Maximum displacements are over 1m and the

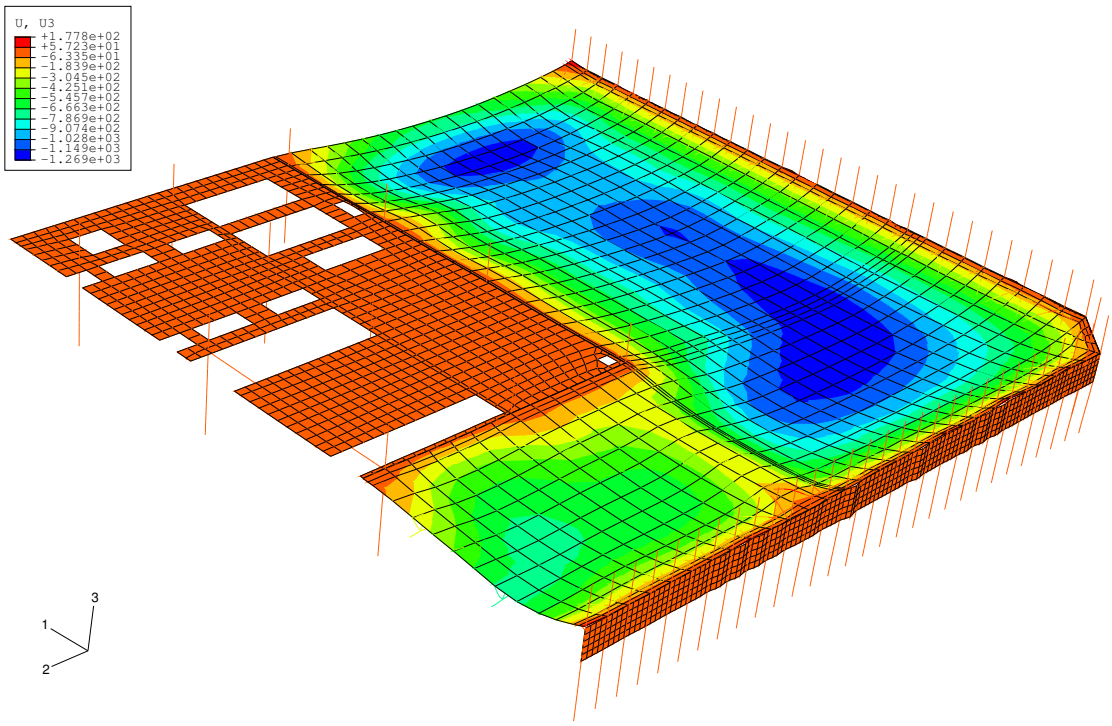

Figure 6.18: Quarter Floor Comparison : Displacement Contours

areas in the outer corners show somewhat higher displacements than elsewhere in the long span areas. Both models also capture reduced displacements on the truss in Area 4 that borders Area 2.

A closer examination of results based on the forces at the truss-column connections also shows good agreement. Figure 6.19 shows comparisons of the long span truss-column connection forces between a representative truss from the half resolution symmetry model (Area 2, Truss 12), the full resolution 3D single truss model and the quarter floor model. The quarter floor trusses are numbered sequentially from the truss nearest the symmetry boundary. The responses have been split over two graphs to aid clarity. The general response shape is very similar and when a resolution scaling factor of 2 is applied (see Figures 6.7 and 6.9 in Section 6.2.1) to the quarter floor model then the results are very close. The difference seen between the 3D single truss model and the quarter floor model can be attributed to the lower restraint conditions found in the quarter floor model. The lower restraint is

a consequence of the longer columns. In Figure 6.19.b the forces in the connection can be seen to change substantially the closer to the short span side column line the trusses are. This is expected as compatibility issues will have to be resolved within the structure.

The effects of the lower restraint can also be seen in the horizontal movement of the columns and the vertical deflection at the midspan of the long span trusses. The former may be seen in Figure 6.20.a while the latter is shown in Figure 6.20.b. Again the plots show a selection of trusses from the quarter floor model against Truss 12 of the symmetry model and the full resolution single truss model. Even though the differences in connection force are relatively small it leads to a large difference in the column movement. Assuming a theoretical beam under similar loading then it may be seen that displacements increase in relation to the change in length cubed so a small change in the column length can lead to large extra displacements. The change in restraint also creates around a 200mm difference in the midspan deflection. As the columns are less stiff it becomes easier for the floor system expansion to push the columns out rather than creating extra midspan deflection.

Neither of the models compared in this section would give completely accurate results in an analysis of a single storey fire. This is because the columns in both models do not extend far enough. However the comparison between the full resolution quarter floor model and the half resolution symmetry model indicates that the change in resolution does not dramatically change the global response of the structure. The major differences seen between the two models can be attributed to the change in restraint to the trusses caused by different column lengths. This reinforces the point that restraint to a structure must be properly represented if the correct response is to be modelled. Multiple floor fires can only be properly modelled by including multiple floors. In addition it should be ensured that there is a suitable amount of structure beyond the fire floors to allow the correct restraint conditions to be applied.

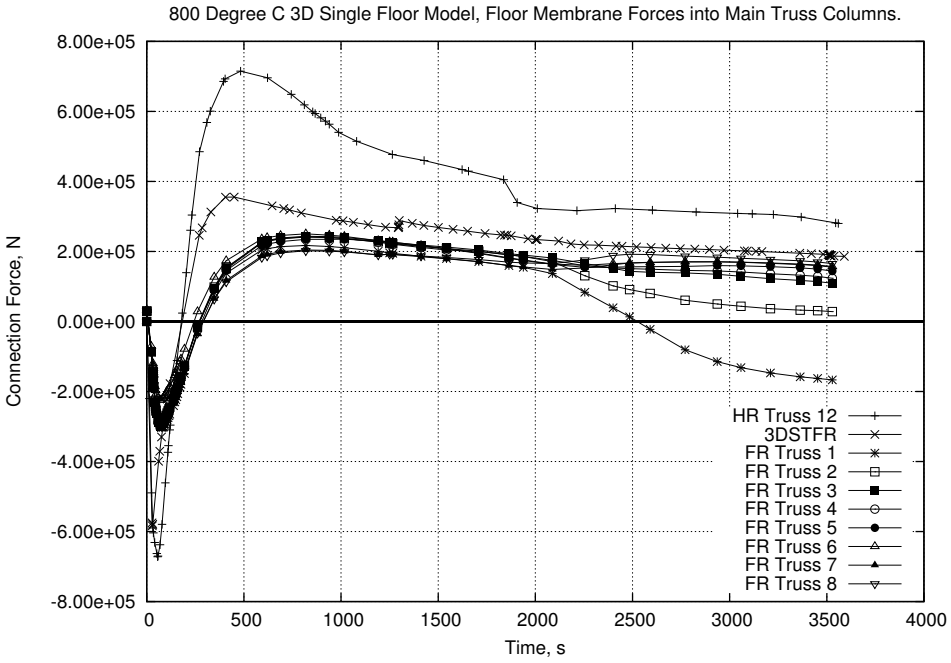

(a)

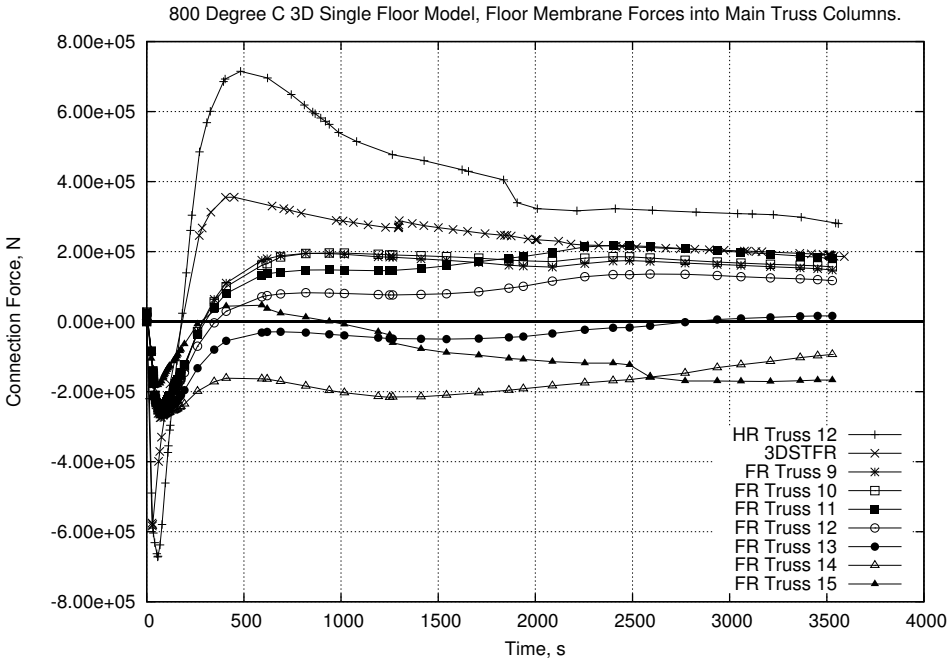

(b)

Figure 6.19: Quarter Floor Comparison : Floor Membrane Forces

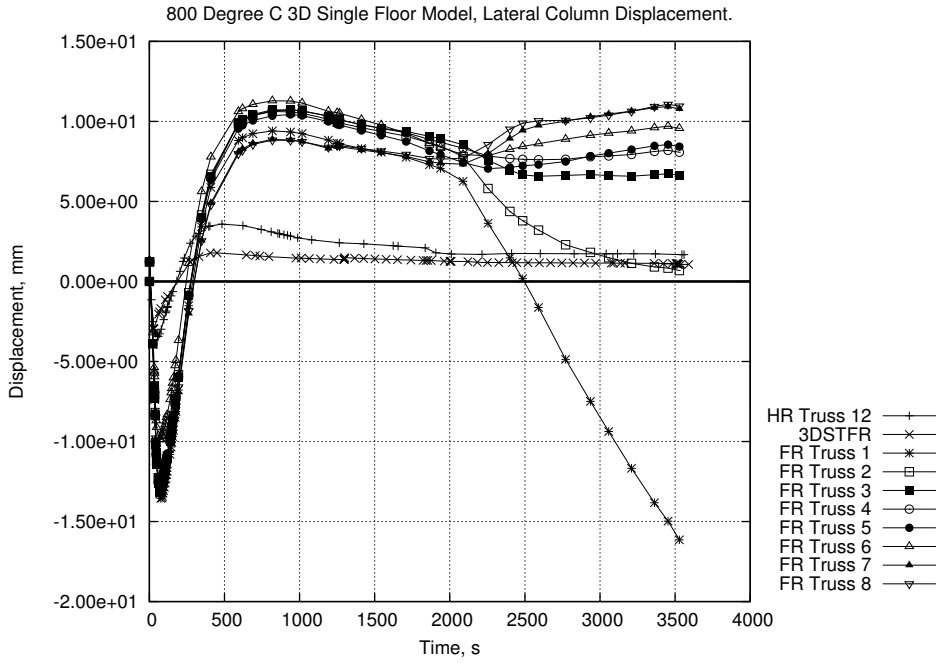

(a)

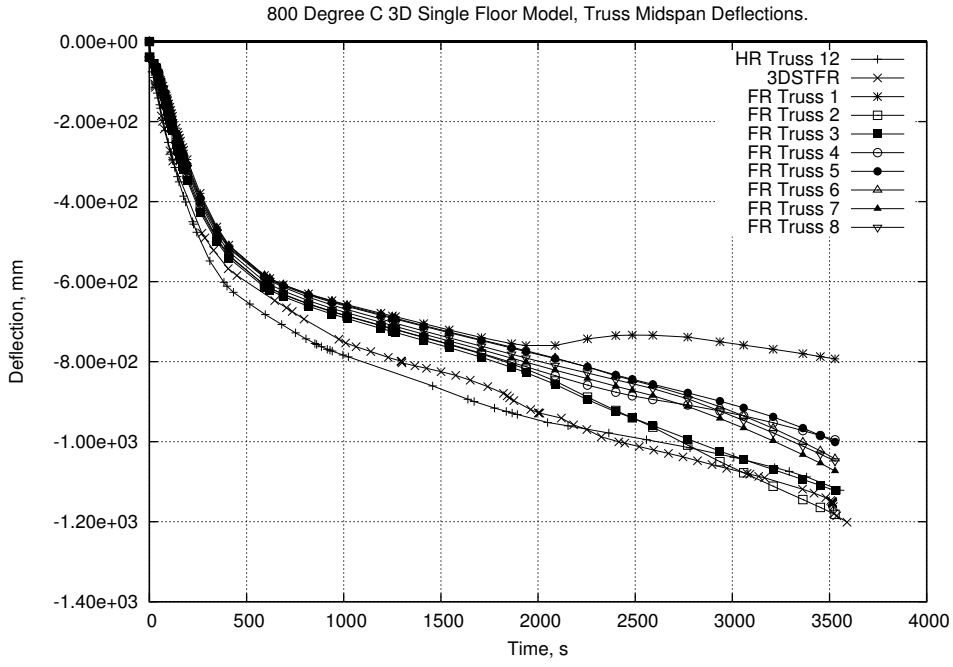

(b)

Figure 6.20: Quarter Floor Comparison : Displacements

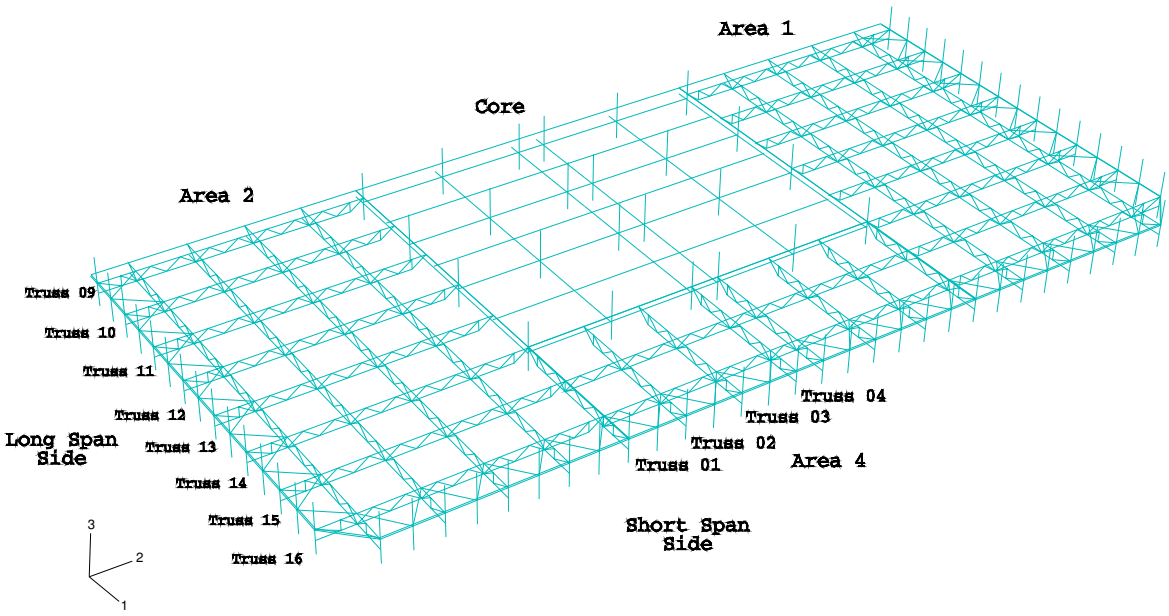

Figure 6.21: Single Storey : Model Areas

6.3 General Results from Single Storey Model

For analysis the half floor symmetry model can be split into 4 separate types of area. The core (Area 5), the long span and corner areas (Areas 1 & 2) and the short span area (Area 4). The results for trusses in the long span Area 2 and the short span Area 4 will be presented here. A diagram of these areas may be found in Figure 6.21 while Figure 6.22 shows the displaced shape of the single storey model. The displaced shape is taken at the point the steel reaches its maximum temperature (at 1000s) and the end of the analysis (at 3600s) in Figures 6.22.a and .b respectively.

Final deflections in the long span areas are large at around span/13 while the short span areas are at around span/20. This equates to around 1400m and 500mm deflections respectively. As the majority of this deflection is driven by thermal expansion, rather than mechanical strains, the model can sustain these large deflections until the end of the analysis. The outside corner of Areas 1 and 2 show

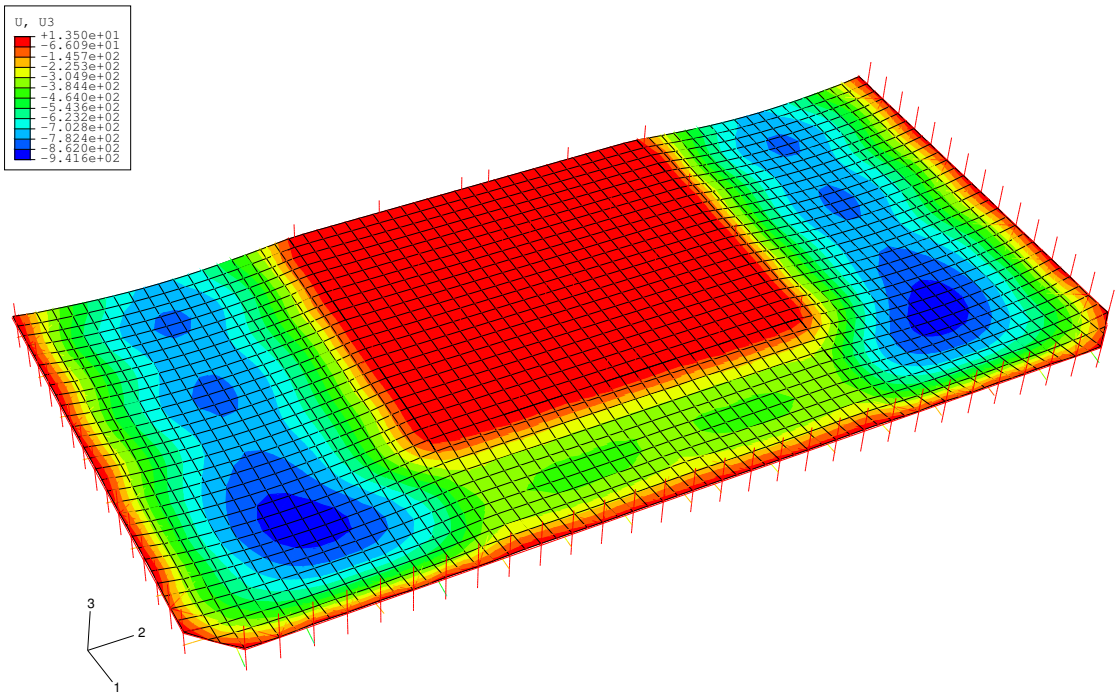

(a) At end of steel heating (1000s)

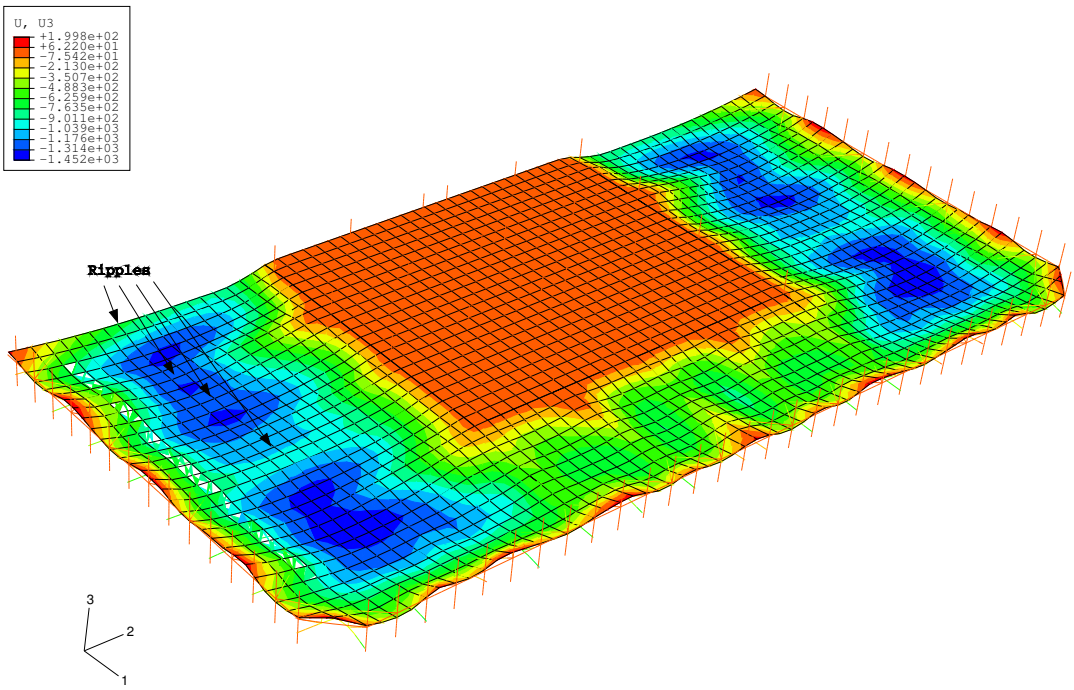

(b) At end of analysis (3600s)

Figure 6.22: Single Storey : Displaced Shape

increased deflection compared to the rest of these areas due to the increased restraint the slab in this area gains from having columns on 2 sides.

As mentioned in Section 6.2.1 a direct comparison cannot be made of the local truss forces between the full and half resolution single truss models. Similarly a comparison between the long and short span truss member forces would not yield useful results (particularly because the model is in half resolution). A more useful comparison is again to look at the results that reflect the global response of the building.

The short span expands less due to the fire. Thus the effects of both mean thermal expansion and bowing due to thermal gradient through the depth of the floor system are less for the short span area. This coupled with the stiffer nature of the short span means that the midspan deflection is lower, for Area 4 Trusses 01 to 04, as indicated in Figure 6.23.a. The creates higher outward movement of the columns connected to these trusses as shown in Figure 6.23.b. After the heating of the truss steel ends, at about 1000s, the further propagation of heat through the slab, and the consequent expansion, begins to push the columns outward again in the short span Area 4. The columns in the long span areas (A2 Truss 09 to 16) react somewhat differently. Initially they are also pushed out but are quickly pulled back inward. The majority of the columns in Area 2 remain pulled inside their original position for the duration of the analysis. The exceptions to this are Trusses 09 and 16 which are discussed in the next paragraph. As the long span Area 2 is much more slender than Area 4 the further expansion of the slab is converted preferentially into midspan deflection rather than significant outward movement of the column.

This response is also indicated in the midspan deflections seen in Figure 6.23.a. The response of Truss 16 is dictated by compatibility with the structure as it is closely connected to the columns on the short edge of the floor area, hence it does not display similar results to the rest of the trusses. Truss 09 acts in a different manner due to a high level of compatibility with the floor slab. As the steel reaches maximum temperature at 1000s it stops expanding. The concrete slab,

however, continues to heat up. The steel is no longer strong enough to resist easily the further deflections caused by the expansion of the slab (as indicated by the continued deflection in Figure 6.23.a) but it provides enough restraint to set up "ripples" in the floor. The final displaced shape shown in Figure 6.22.b clearly shows these ripples in the long span area directly adjacent to the core. The corner area also shows some indications of rippling above the trusses but these appear to be smothered somewhat by the higher deflections in this area. Hence the results of Truss 9 are dictated, to a certain extent, by the response of the floor slab. The early stages of deflection in this truss follow a similar path to the other trusses, as shown in Figure 6.23.a. After 1000s the rate of deflection is clearly less than the other trusses. Trusses 12 and 13 also show this effect but to a lesser degree.

The positioning of the ripples in the floor are likely to be linked to the connectivity of Trusses 9 and 12. As can be seen in Figure 6.21 these trusses are directly connected to major core framing. An unbroken line of structural elements follows the plane of each of these truss lines through the full width of the model. As the steel stops expanding the extra strength in these more highly restrained trusses will create the initial imperfections in the slab that will increase in size with further expansion.

As can be seen in Figure 6.23.b the columns attached to the main trusses in Area 2 are pushed back outward slightly after around 500s. This is caused by the increasing lateral expansion of the slab compared to the slowing of the midspan deflection. In all the trusses except 9 and 16 it is an effect that is beginning to be countered by the end of the analysis (i.e. inward column displacement rate begins to increase).

The ripple in the slab over Truss 9 means that more of the slab expansion is converted into outward movement rather than vertical deflection. The response of Truss 16 is again primarily dictated by its proximity to the short span side columns.

Hence the response of the floor trusses in the 3D half symmetry single storey model is dictated mainly by the applied fire. However, later in the analysis compatibility effects appear to be caused by the continuity provided by the slab and column connections.

The floor membrane force plots shown in Figure 6.24 complement the responses shown in Figure 6.23. The short span forces are somewhat higher than the normal long span values as indicated in Figure 6.24 (Trusses 9 and 16 in the long span area are again special cases due to their proximity to boundaries). Figure 6.24.a focuses on the start of the analysis while Figure 6.24.b shows the same data for the entire analysis time. The differences in stiffness between the floor areas leads to the short span floor moving back into compression even after large deflections have occurred.

The relative contribution of each column to the whole building response can also be determined by examining the column outward movement. Figure 6.25 shows the positions of the long span outer columns at different times through the analysis (negative displacements indicate outward movement). These plots include the intermediate columns that are not directly connected into main truss lines. The path follows the columns from the connection to A2 Truss 16 to the connection to A2 Truss 09. Figure 6.25.a shows the first 500s of the analysis while plot .b shows the whole analysis time. At the start of the analysis the ambient loading creates a slight difference in displacements although it can be seen that all of the columns are being utilized to support the floor. As the primary movement in the early stages of the analysis is being driven by the trusses expanding the biggest effect on the structure initially is on the columns directly connected to the trusses. In the first 50s the expansion of the floor creates a reasonably regular outward movement of the column line. As the trusses begin to pull the columns back in, the response becomes more irregular as the columns directly connected to trusses are affected more. The biggest movement can be seen to occur between 150 and 300s which can be linked to the large changes in force in the A2 trusses, from compression to tension, seen in Figure 6.24. This change in force arises as the long span floor moves into tensile membrane/catenary action due to large, thermally induced deflections.

After 300s there are no sudden large changes in the response but the displacement in the columns can be seen to gradually even out. This equalisation can also be seen in Figure 6.14.b in Section 6.2.3. As the analysis continues past about 2000s

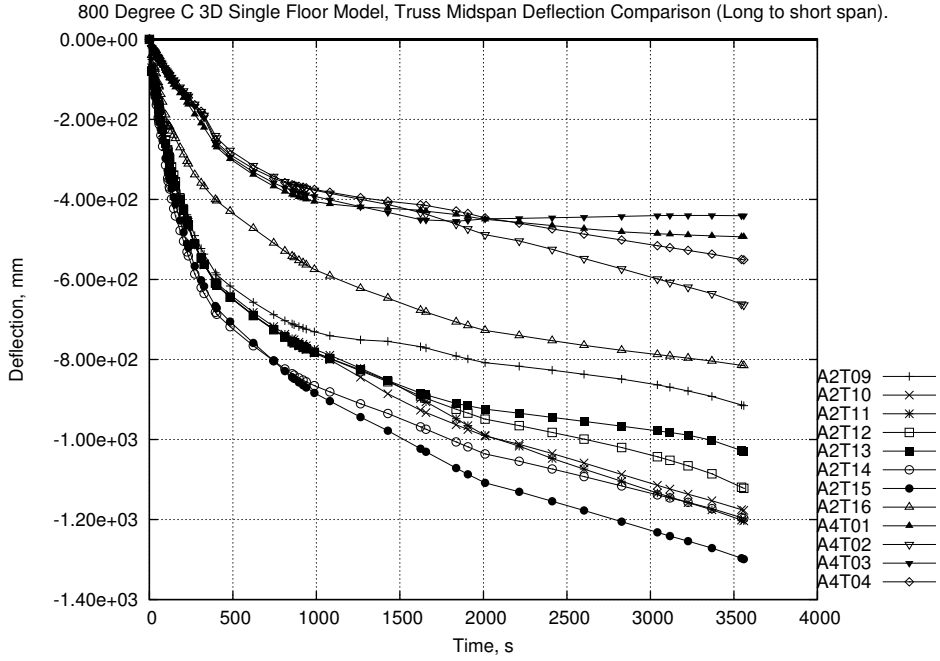

(a)

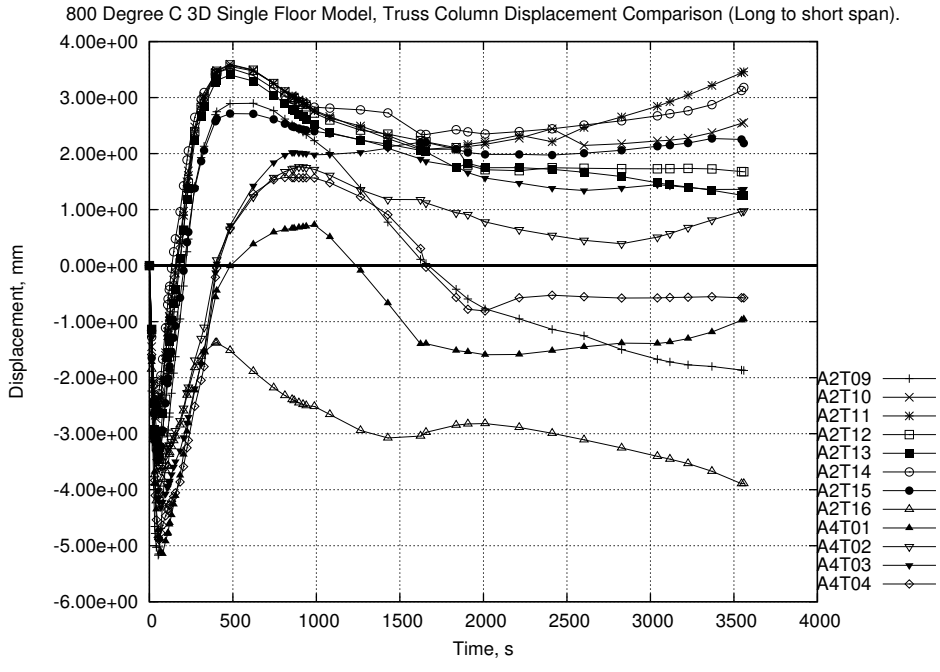

(b)

Figure 6.23: Single Storey : Displacement Comparisons

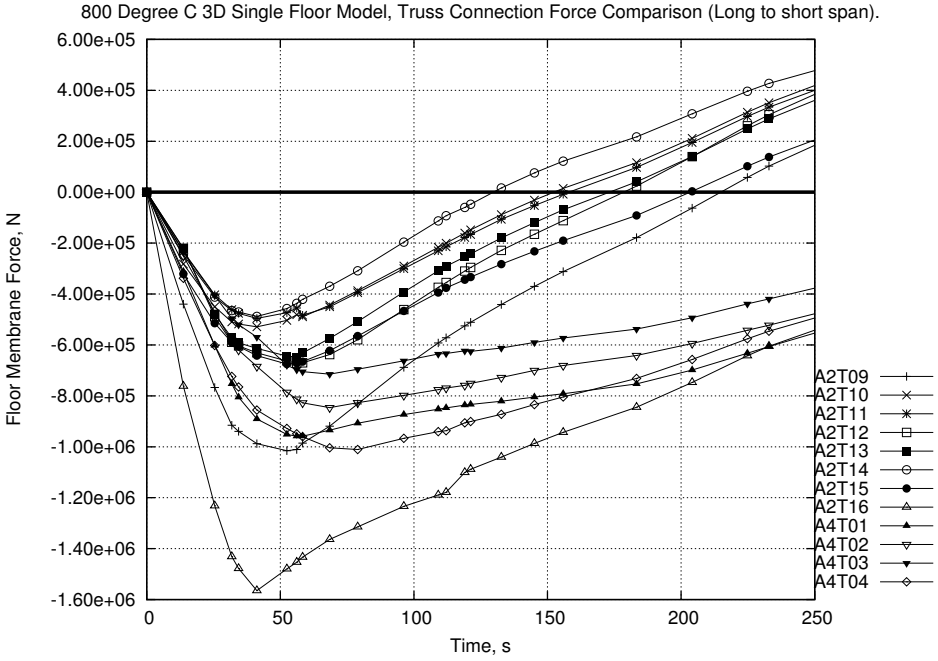

(a)

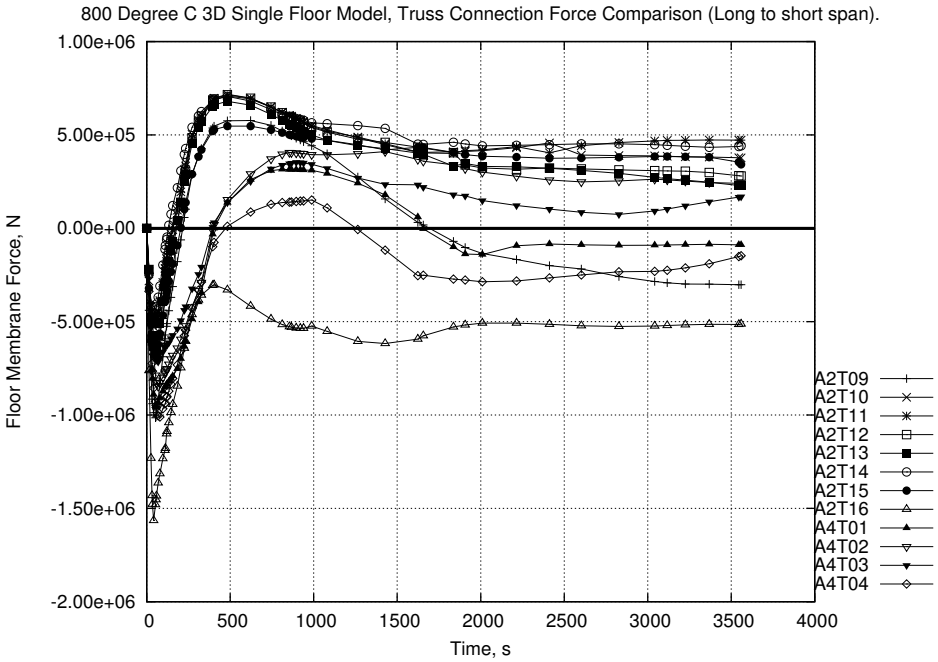

(b)

Figure 6.24: Single Storey : Floor Membrane Forces

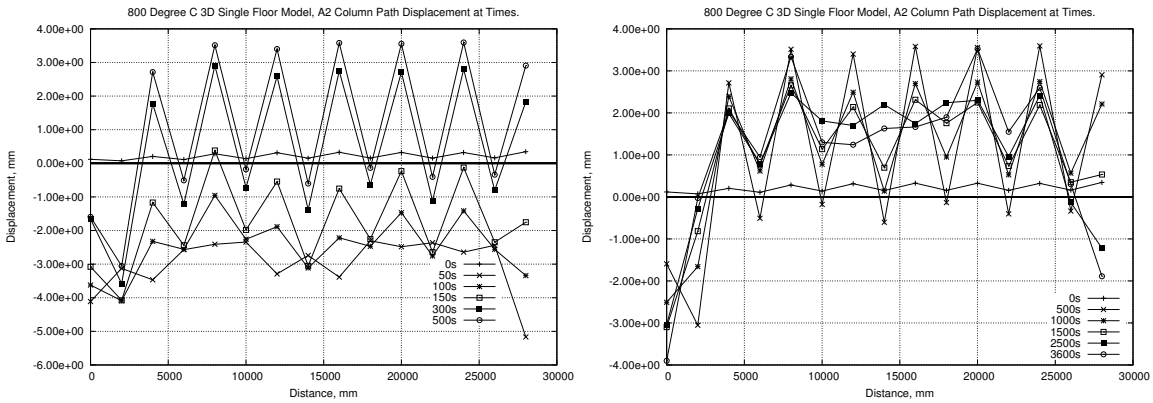

(a) (b)

Figure 6.25: Single Storey : A2 Column Path

the horizontal forces being applied to the intermediate columns begins to match those in the main columns. This equalization is caused by an increased amount of force being transferred through the connections to the intermediate columns as the trusses pull the main columns out of position.

The outward movement seen at all times on the left hand side of the plot (A2 Truss 16) is caused by the compatibility issues of Truss 16 being closely tied to the columns at the corner of the building. The more extreme movements seen on the right hand side of the plot can be attributed to the compatibility between the floor slab and A2 Truss 09 that has been discussed earlier in this section.

At the corners of the core there is a transition zone as the floor moves from the long span floor area, which is spanning in the 2 direction, and the short span area, which is spanning in the 1 direction. Compatibility effects can be seen here as the column line on the short span side of the model transitions from one area to the other. Figure 6.26 shows the movement of the column line on the short span side of the model. Plot a shows the first 500s while plot b shows results for the whole analysis time. Positive displacement represents outward movement.

As with the long span side columns the initial gravity loading induces a small amount of movement that is evident in all the columns (truss and intermediate).

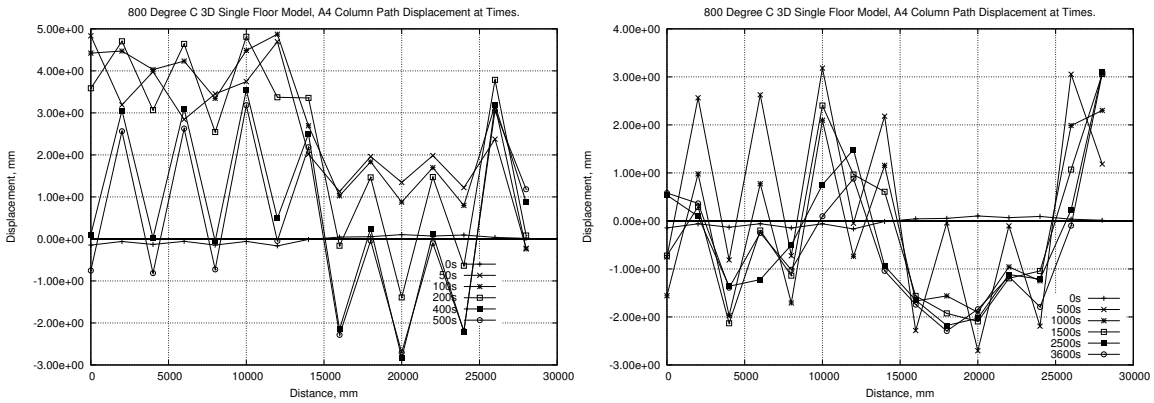

(a) (b)

Figure 6.26: Single Storey : A4 Column Path

Even at this stage there is a difference between the columns supporting the short span trusses and the columns supporting the Area 2 transverse trusses. Again there is a sudden and relatively large outward movement of the columns all along the column line but this time the two areas produce differences. As the analysis progresses the truss columns again exhibit a more rapid response with the intermediate columns lagging behind somewhat. Another phenomenon that arises is that the columns at the border between Area 2 and Area 4 begin to get pushed out again toward the end of the analysis. This reversal can clearly be seen in the displacement plots in Figure 6.23. The movement of Area 4 Truss 01 can be explained as this truss is directly on the border of two zones that are trying to go into tensile membrane action with the primary spanning direction at 90^o to each other.

Figure 6.26also shows that as the analysis reaches the end the column line again begins to equalize the displacements between the truss columns and the intermediate columns.

A brief investigation of the moments being induced in the columns indicate that none of the columns are near failure. Figure 6.27 shows 2 examples of columns from the model. The graphs show the moments at the top and bottom and at

the midspan. This is plotted against the axial force in the column and shown in relation to the failure envelope of the columns section in combined axial load and bending. Figure 6.27.a shows the results for the column connected to Truss 13 in Area 2 while Figure 6.27.b shows the results for the column connected to Truss 03 in Area 4. These results match well with similar results from the Full Resolution Single Truss model in Chapter 3.

6.4 Conclusions

This Chapter presents the results of various stages of verification and comparison for intermediate models between the 3D Full Resolution Single Truss model and the final Half Resolution 3D Half Symmetry Multi-storey models. The construction of the various models is also presented along with the fire regime the models have been subjected to.

The change in resolution is designed to lower the number of degrees of freedom in the multi-floor model while keeping the important aspects of the truss based floor system. Thus direct comparison of the forces in the truss members between models of different resolutions is not possible as they are different entities. The aim of this PhD is to investigate the global response of a structure, and hence such a comparison is not necessary. It is important, however, that the global response of the structure is not altered too much by the move from full to half resolution.

Comparison between Full and Half resolution Single Truss models indicates that the global response of the truss is similar in both cases.

Comparison between Full Resolution Single Truss and Half Resolution Half Symmetry Single Storey models indicates that the response of the trusses is similar between the two cases but compatibility can have a significant role depending on truss location.

A sine-based imperfection was added to the truss diagonals in order to aid convergence. A check was made to ensure that adding, and increasing, such a device

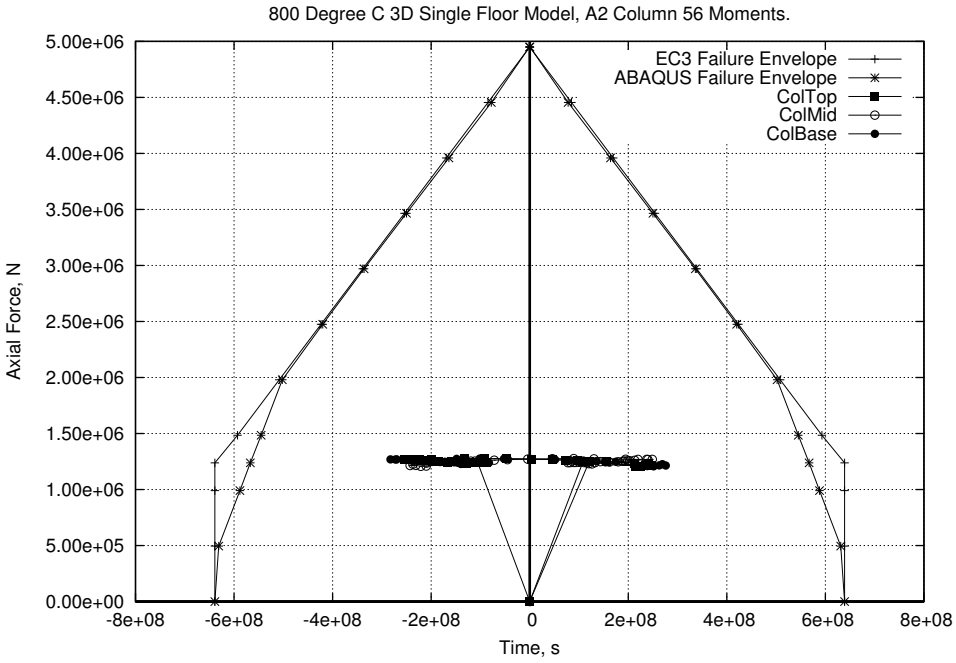

(a)

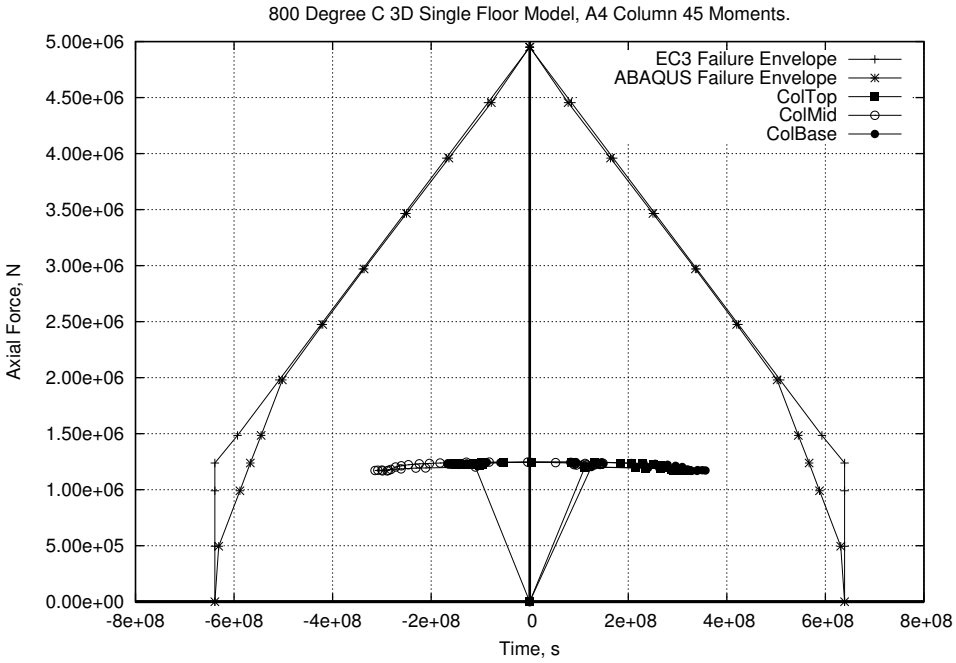

(b)

Figure 6.27: Single Storey : Column Moments

would not adversely affect the response of the structure. The differences between the model with and without the imperfection may be found in Appendix A. This indicates that the imperfection does not significantly change the response while increasing significantly the convergence rate of the model. The results presented in Section 6.2.2 indicates that this imperfection may be increased from 1 to 5mm with little further effect.

Further comparison to a very high resolution model of the WTC tower floors (created by other members of the research team [79]) again indicates that the change to half resolution will produce reasonable results. Investigation of the global response of both models shows good agreement and also highlights the effect that restraint has on a structure. The high resolution model included longer column lengths than the symmetry model and this has a discernible effect on the movement of the columns and the floor slab as well as affecting the connection forces.

Finally some general results from the Half Resolution Single Storey Symmetry model have been presented. The response on the global scale has been investigated using the same output that has been reported previously in this thesis for the 3D Single Truss and the 2D Multi-floor models (Chapters 3, 4 and 5 respectively). This allows an insight into how the model will react and can help with the move from a single storey to a multi-floor model.

The results of the single storey model also provide an insight into the difference in response between the long span areas and the short span areas. In general the heating of the long span areas leads to much larger deflections than the short span. However the higher stiffness of the short span areas leads to higher floor membrane compression from the floor to the columns and therefore higher outward column movement.

The results of the single storey model should only be taken as indicative. The restraint conditions at the truss supports (i.e. the connection of the trusses to the main columns) combined with the thermally induced movement of the floor system dictate the force and displacement response of the structure. As indicated in Chapter 4 the individual floor response can change considerably as more floors

are added to the model and more storeys become affected by fire.

An investigation of a single storey model can be useful for inclusion in the design of a building. If sufficient justification can be made for assuming that floor to floor compartmentation will not be breached then a single storey model is sufficient. It should be noted again that a single storey model to be used for design purposes should include full height columns above and below the floor under investigation in order to correctly capture the level of restraint in the structure. If tensile membrane/catenary action is seen in the floor then the ambient floors should be checked to make sure it can successfully withstand the additional forces that would be transferred to it. The structure beyond the boundaries of the model must always be able to withstand the forces seen in the model supports.

No collapse was seen in any of the models investigated for this chapter. As with the single truss model presented in Chapter 3 this is likely to be due to the relatively short length (and therefore high stiffness) of the columns.

The conclusion that the half resolution models provide a good representation of the full resolution structure allows the use of the half resolution geometry in the final, multi-storey 3D models. The results of these models will be presented in the next chapter.

Chapter 7

Effect of Fire on 3D Multi-storey models

This chapter describes the construction and response of large, 3D, multi-storey models. A short description of the importance of the correct boundary conditions leads into the main discussion of results. Several different versions of the model were run using a variety of fire regimes. The effects of a hat truss were also investigated. Due to the extremely complex nature of these models convergence difficulties were encountered frequently. Explicit versions of the models were investigated to overcome numerical convergence problems.

The aim of this chapter is to investigate large, 3D, multi-storey models under similar circumstances to those investigated in Chapter 5. This will indicate whether or not the failure mechanisms described in Chapters 4 and 5 are realistic responses in large buildings of this nature.

7.1 Model Details

7.1.1 Structural and Fire Models

The structural model used here is based on the half resolution, half floor symmetry model described in Chapter 6. As with the 2D work reported in Chapter 4 the main part of the model was made up of 12 storeys. In some cases 3 additional storeys were added to the top of the structure, containing the hat truss assembly. The main 12 storey model can be seen in Figure 7.1, along with a constituent floor, while the additional hat truss floors may be seen in Figure 7.2

For more details on the structure used in this model please refer to Chapter 6.

The structural model shown in Figure 7.1 was used for all of the scenarios except Scenario 8, which used a full resolution model. The structure in Scenario 8 used the most accurate structural data available to create a replica of a quarter of a floor in the WTC towers. Due to the size of the individual floors in this model it was run over 7 storeys only, using the Explicit version of ABAQUS.

The fires used in this chapter are based on those used in the 2D analyses described in Chapter 4. They have been applied in the manner described in Chapter 6. In most of the cases presented here the outer structure, including the outer columns and the spandrel beams, was not heated. It was found that inclusion of heating in these parts of the structure caused increased convergence problems. The previous models presented in this thesis heated the affected columns linearly to 400°C. At this temperature steel retains its full strength and 70% of its stiffness so it is unlikely that the change in material properties would alter the response of the structure until close to the end of the analysis.

The lack of thermal expansion in the outer columns is a more important issue. The small change in geometry that would occur in the models without a hat truss are unlikely to change the response greatly as the top of the model is free to expand upward. The extra restraint in the hat truss models will create differences and these are discussed under the appropriate model headings below.

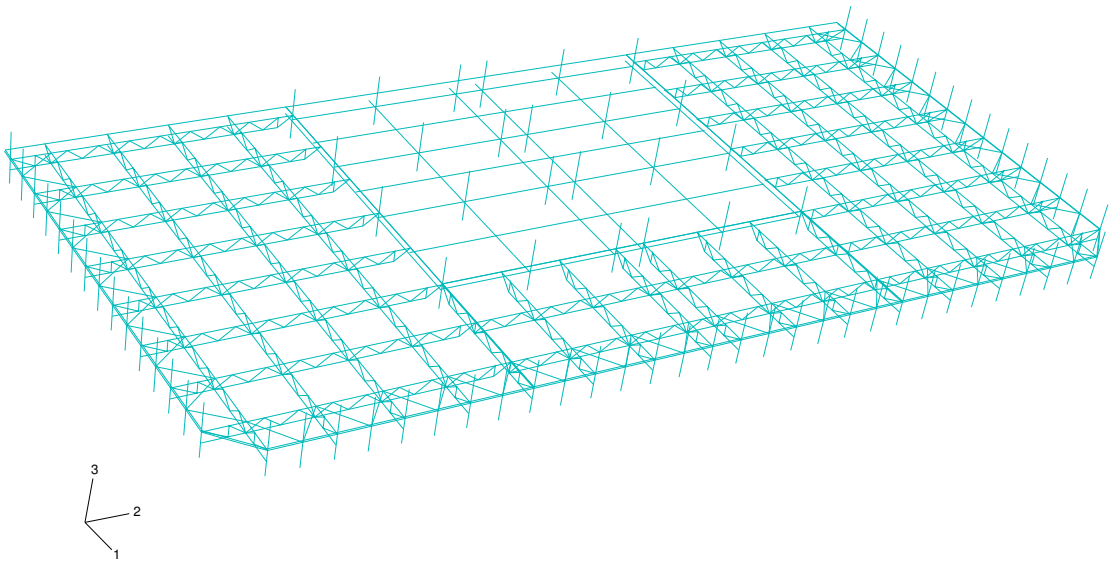

(a) Single Storey

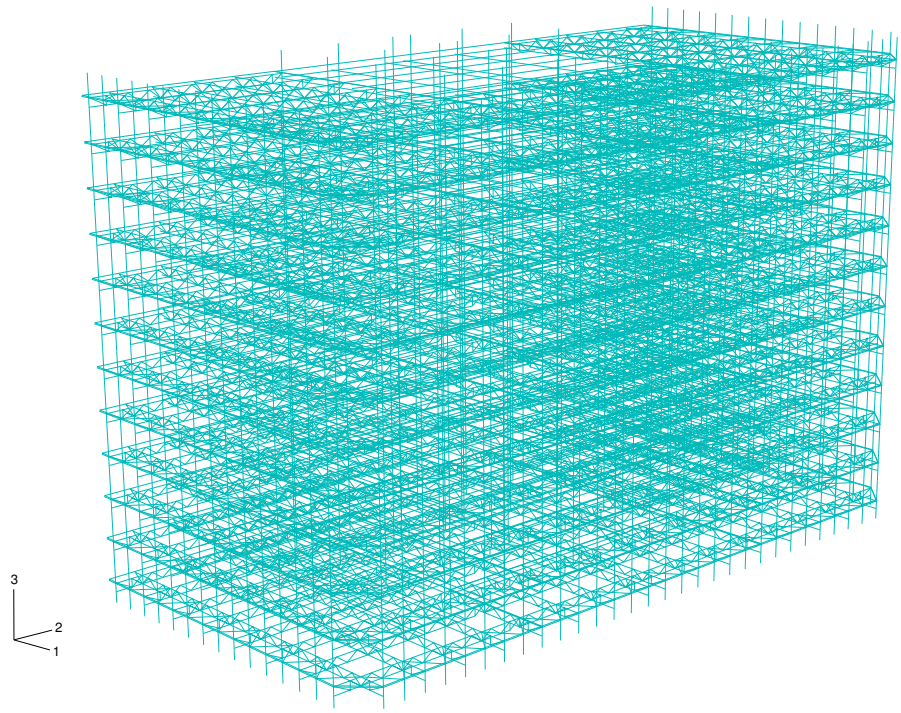

(b) Main Floors

Figure 7.1: 3D Multi-storey Model Mesh

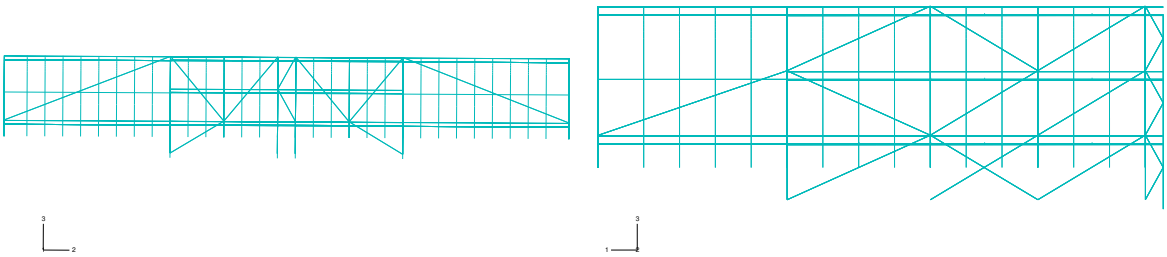

(a) Front Elevation

(b) Side Elevation

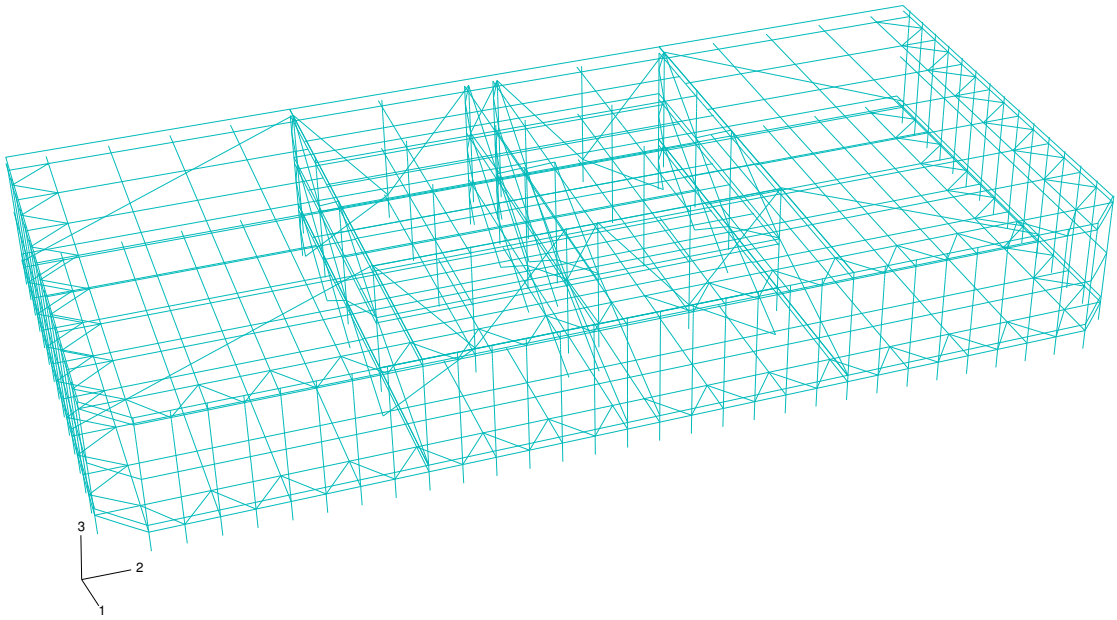

(c) Isometric

Figure 7.2: Hat Truss Floors

Scenario	Solver	Fire Floors	Peak Temp.	Column Heated†	Hat Truss
1 (Base)	Static	3(5,6&7)	800°C	No	No
2	Static	5(4,5,6,7&8)	800°C	No	No
3	Static	3(5,6&7)	500°C	No	No
4	Static	3(5,6&7)	800°C	No	Yes
5	Static	3(5,6&7)	800°C	Yes	Yes
6	Explicit	3(5,6&7)	800°C	No	No
7	Explicit	5(4,5,6,7&8)	800°C	No	No
8	Explicit	3(3,4&5)*	800°C	No	No

* Note : Scenario 8 uses a higher resolution structural model.
† Note : The same heating is included in the spandrel beams.

Table 7.1: Model Summary

7.1.2 Analyses Conducted

Table 7.1 includes a summary of the models conducted using the structure described in Section 7.1.1. These models include a variety of alternatives to the Base case. Explicit and Quasi-static versions of the model were run to allow evaluation of collapse mechanisms. Fires with a peak temperature of 800°C were evaluated over 3 and 5 floors. A fire with a peak temperature of 500°C was evaluated on 3 floors only. Finally the inclusion of the hat truss was evaluated.

With many of the cases, particularly the Quasi-static versions, collapse is not shown directly due to convergence difficulties. However there are strong indications of imminent collapse.

7.2 Results

In general the results from the analyses presented here will be taken from the locations pictured in Figure 7.3. In the output graphs to minimize the space taken up by the legends several abbreviations have been used as follows :

- 1Sty refers to the single storey 3D model from Chapter 6.
- Scenario has been abbreviated to Sc, e.g. Scenario 1 changes to Sc 1.

- Floor will often be abbreviated to Fl, e.g. Floor 8 to Fl8.
- The models have been split into separate areas, as described in Chapter 6 and shown in Figure 7.3. Areas 2 and 4 are of most interest and will be abbreviated to A2 and A4 respectively.
- Within the floor areas there are several trusses of interest. These trusses will be indicated by Tx where x refers to the truss number shown in Figure 7.3. Hence "A2T12" refers to Truss 12 in Area 2.
- Main columns are those directly supporting trusses and are referred to in relation to the truss being supported.
- The intermediate columns are those columns in between truss lines and are referred to as AdCol in the graphs of output.
- Quasi-static and Explicit models may be indicated by Sta and Exp, respectively

7.2.1 Remoteness of Boundary Conditions

A brief comparison between results from the single floor 3D model (1Sty) and Scenario 1 (Sc 1) again shows the importance of including the correct boundary conditions in a model. Figure 7.4 shows a direct comparison between the two models using floor membrane forces (plot .a) and column lateral displacement (plot .b). The response in Scenario 1 is taken from Area 2 on the 8th floor. In terms of fire regime applied this is the most comparable floor to the single storey model with a single fire compartment below the slab and ambient conditions above.

The structure of each floor is exactly the same, as is the fire regime (on a floor by floor comparison). The differences in response come about from the different length of column involved in each model. The single storey model has a half-floor worth of column extending above and below the floor (total length of 3.6m) before it encounters rigid boundary conditions. Scenario 1 has a total length of 14.4m

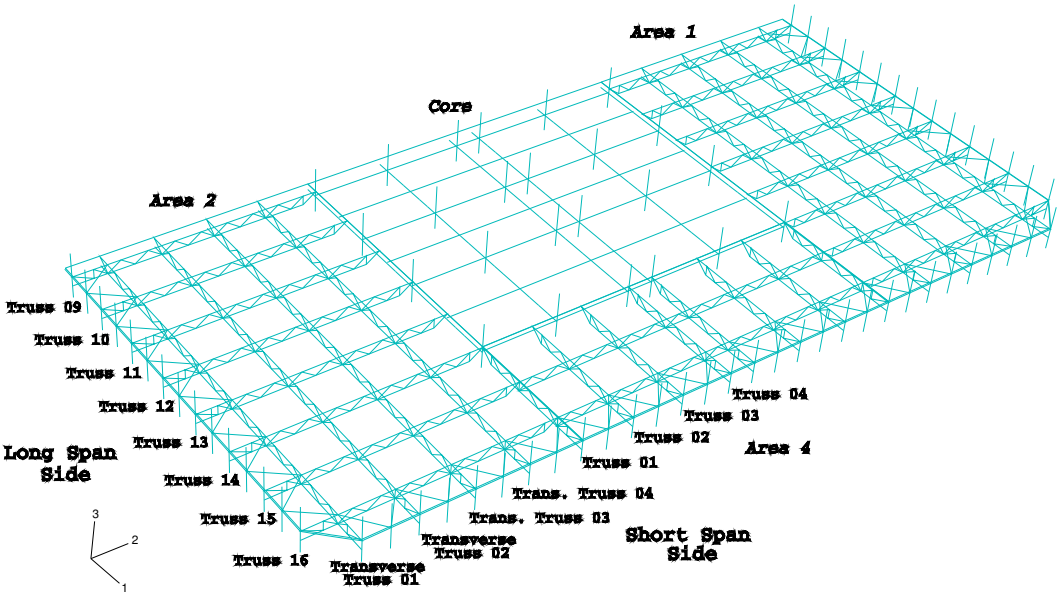

(a)

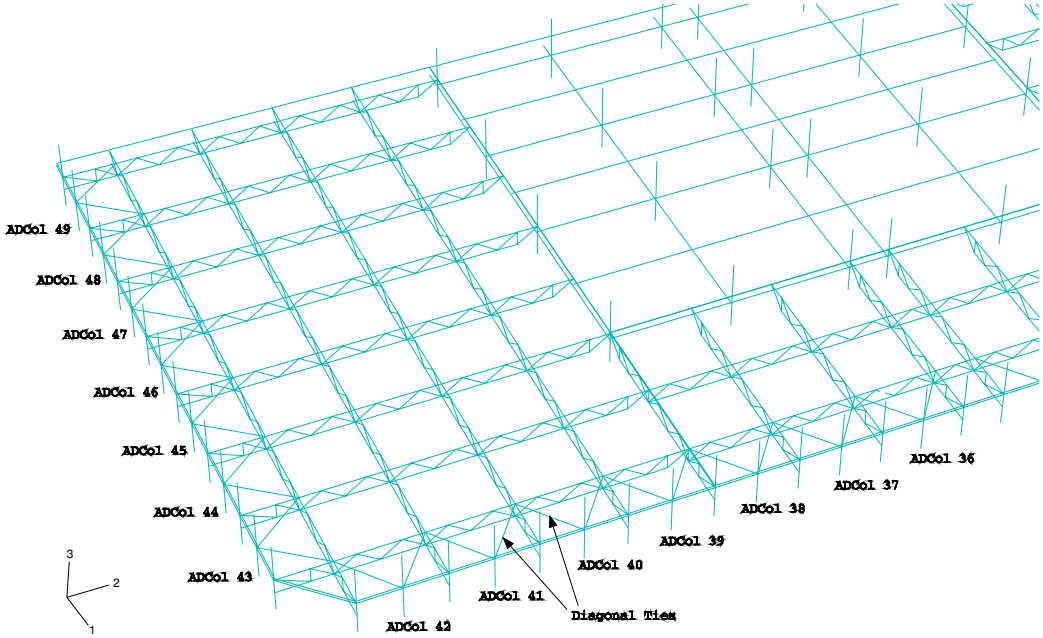

(b)

Figure 7.3: Output Member Location

between relatively rigid supports (i.e. cool interface floors) and 43.2m between rigid boundary conditions. The multiple floor nature of the fire in Scenario 1 means that even if the single floor model been conducted with a full floor height of column above and below the floor then the results would still differ considerably. The disparity in results seen in Figure 7.4 again indicates that single floor models should not be used to infer the response of a multiple floor system. The sensitivity of the thermal expansion induced response to column/building edge restraint is such that even a minor change in boundary conditions could cause large differences.

7.2.2 Global Response

7.2.2.1 Scenario 1 (Base Case) : Quasi-static, 3FF, No Hat, 800°C

Comparison to 2D results. To determine the validity of the response of the 3D multi-storey models it is useful to compare results between the 3D models presented here and the 2D models presented in Chapters 4 & 5. This comparison also assists in understanding the response of the 3D multi-floor models in general. As it is the global response that is of interest the primary variables to be considered will be those that indicated the failure mechanisms described in Chapter 4. These are : floor membrane forces, column lateral movement, column moments and vertical movement at the top of the columns. The midspan deflection of the trusses is also presented as a useful measure of similarity between global response of models, if not a direct indication of global failure.

It should be noted that in Chapter 6 a scaling factor was applied to the full resolution models before comparison was made to the half resolution models. The comparison between Scenario 1, here, and the 2D model also includes a resolution difference. The floor system in the 3D model attributes double the area to each of the trusses and will therefore apply twice the membrane forces seen in the full resolution 2D model. However this will be split between the columns that are directly connected to the trusses and the intermediate columns, which also have a connection to the floor system. The 2D model presented in Chapter 4 included a

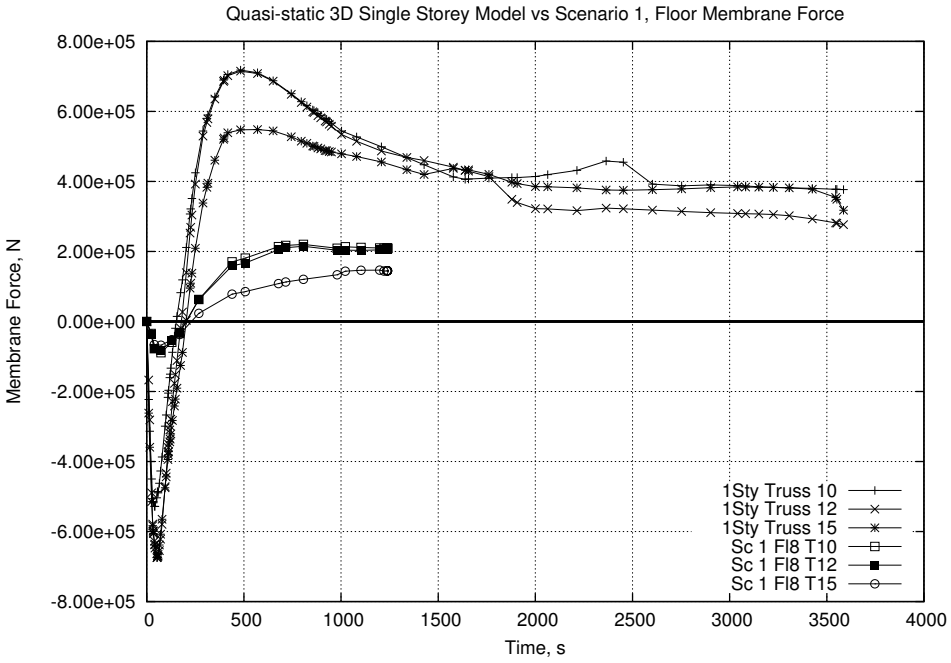

(a)

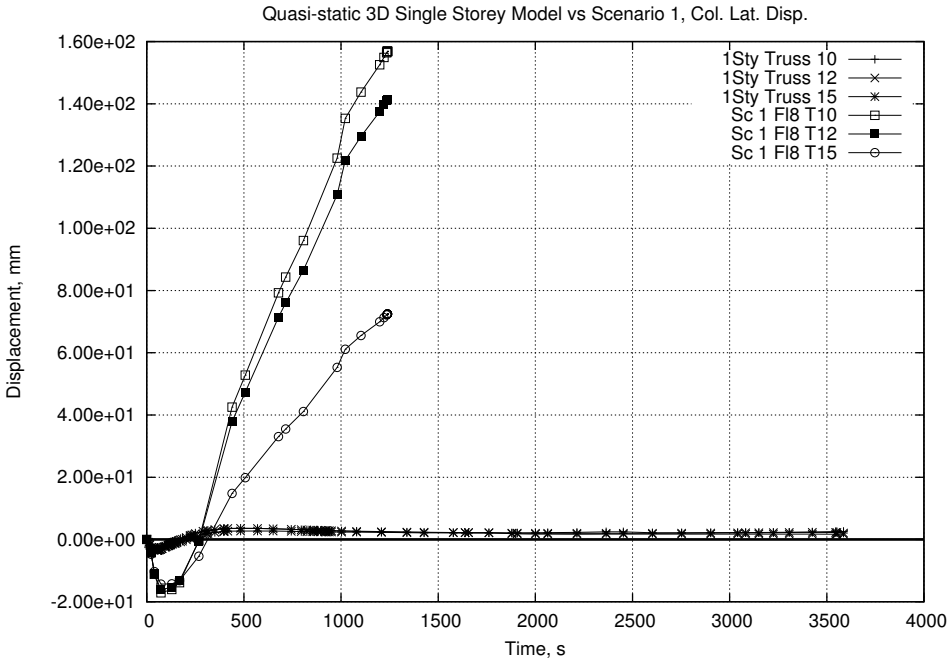

(b)

Figure 7.4: Local Response : Floor Membrane Response

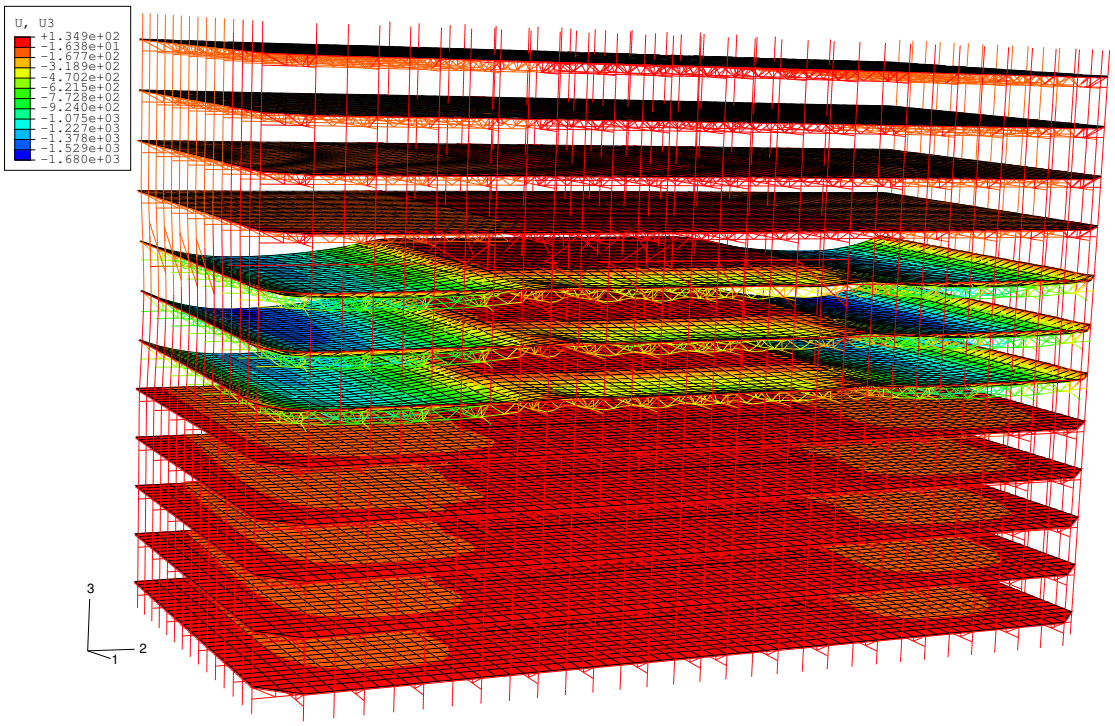

Figure 7.5: Scenario 1 : Displaced Shape

double-section column connected to the truss. The half resolution 3D model effectively has 2 double section columns attached to the main trusses. This means that the forces, as taken from the 2D analysis, may be compared directly to those found in the 3D model connections.

Figure 7.5 shows the final displaced shape of the model. Large midspan deflections can be seen in the fire floors. Relatively large inward movement of the columns is also present. The model failed to converge at around 1250s with no clear collapse mechanisms manifested. However, investigation and comparison of the results with the earlier 2D models indicates that failure could be imminent.

As the 3D models contain multiple truss lines, as opposed to the single truss line of the 2D model, then the results will not match exactly as load redistribution takes place. Figures 7.6 &7.7 show the membrane force from floors 6, 7 and 8 into the columns, as experienced by the truss connection. These are the floors affected by the fires. In these graphs positive force indicates tension and negative values

indicate compression. Figures 7.6.a and 7.7.a show excellent agreement between the generic 2D value and the spread of values for the 3D model. The early stages of the analysis, between 0 and about 300s show slightly more tensile behaviour in the 2D model. After about 400s until failure of the 2D model the results from the 2D analysis lie well within the spread of 3D results. For Figure 7.6.b the results for the 2D analysis show some significant differences to the 3D results. However the maximum tensile and compressive forces of the 2D model are matched well by the 3D model. In all of the 3D analyses Truss 16 has significantly different results. This is due to its proximity to the short span side columns. Compatibility between the short side of the Area 2 slab and the columns means that Truss 16 cannot relieve thermal expansion strains by deflecting and therefore experiences higher forces in the truss. In Figures 7.6.a and 7.7.a (for floors 6 and 8, the interface fire floors) this compatibility is shown as an increase in compressive forces. For Figure 7.6.b (floor 5, the middle fire floor) compatibility dictates high compression to begin with and then higher tensions toward the end of the analysis. As thermal degradation of the material increases the forces in the truss decrease. This response can also be seen in Truss 15 but to a much lesser extent. Figure 7.7.b shows a direct comparison between truss line 12 in Area 2, over multiple floors, and the results from the 2D analysis. Truss line 12 is the closest comparable truss line between the 2D and the 3D models. The results are again comparable with the 3D model showing all the same basic responses as the 2D model.

Figures 7.8 & 7.9 show the movement of the columns that is complimentary to the forces engendered in the truss connections. Again a direct comparison is made between the 3D and 2D results. Figures 7.8.a and 7.9.a show the movement in the fire interface floors (floors 6 and 8) while Figure 7.8.b shows the middle fire floor (floor 7). The column movement is taken at the truss connection to the column and hence does not include the intermediate columns. The movement of the intermediate columns will be examined later. As the 2D model did not include these intermediate columns then it is understandable that it will have greater inward deflection than the 3D model later in the analysis. The slight

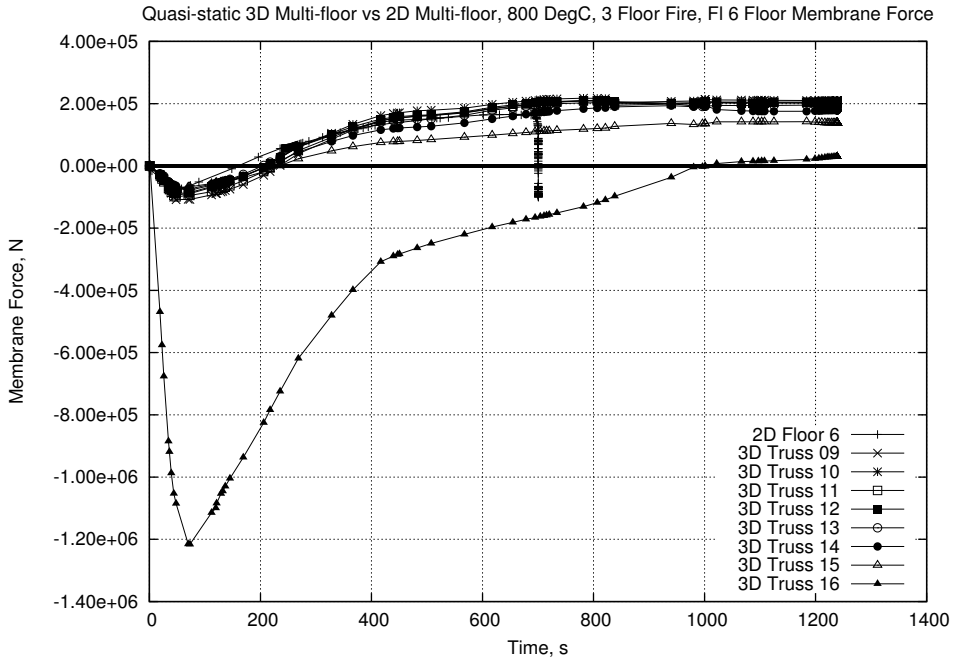

(a)

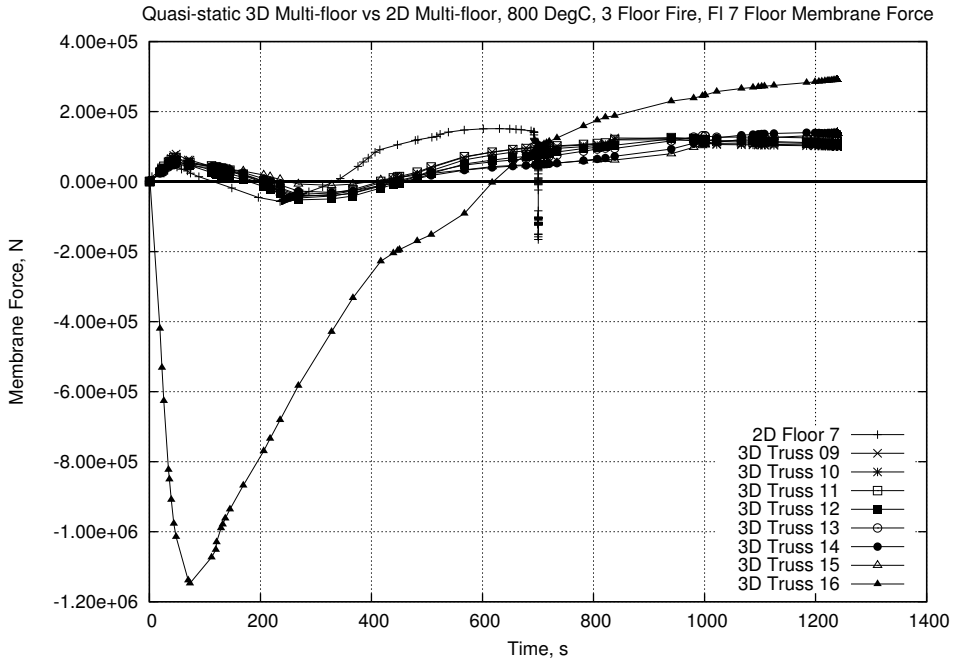

(b)

Figure 7.6: Scenario 1 : Long Span Side Floor Membrane Forces

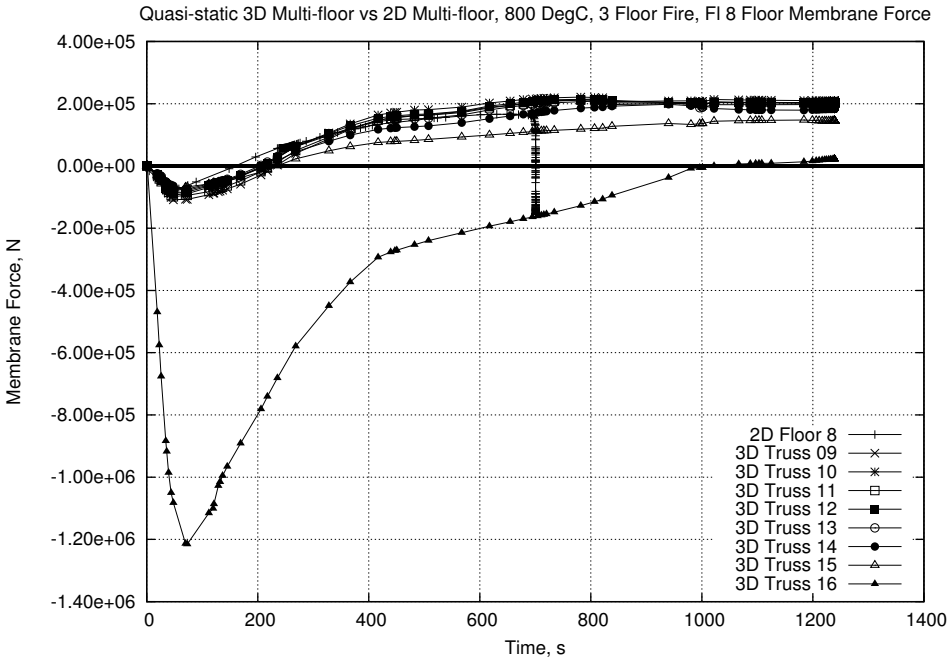

(a)

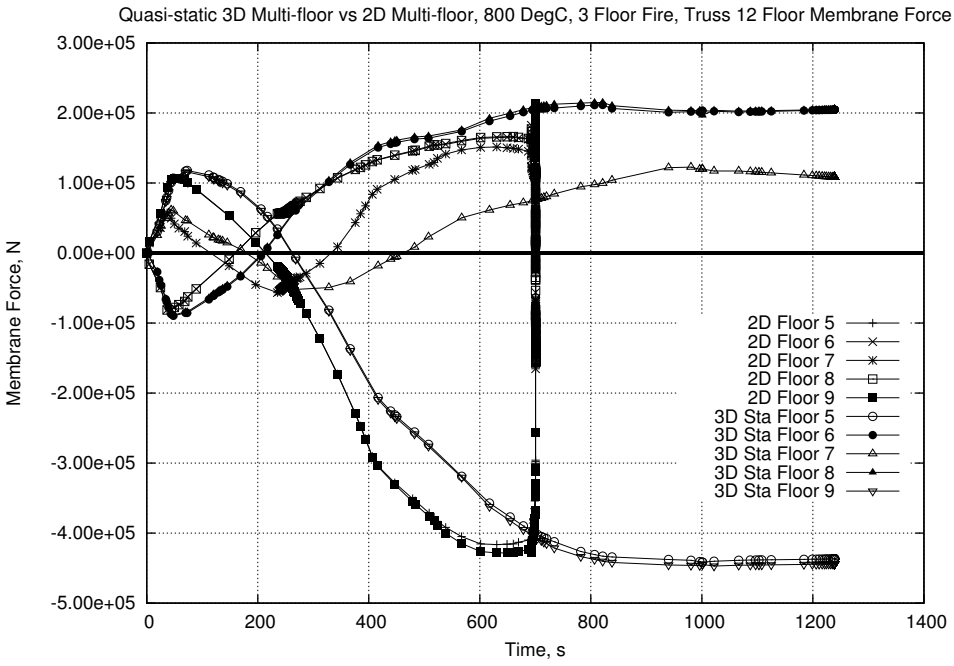

(b)

Figure 7.7: Scenario 1 : Long Span Side Floor Membrane Forces (Cont'd)

difference in outward movement between the 2D and 3D analyses is also a factor of the slight difference in floor membrane forces seen in Figures 7.6 & 7.7. This difference can be attributed to the change in force distributions in the floor system when moving to the 3D model.

All the major changes in deflection response seen in the 2D model are captured in the 3D version, including the slight step change in deflection rate at 400s. The greatest difference is that where the 3D model can redistribute load laterally between the columns the 2D model cannot. This is a more redundant model as the whole structure is involved in resisting the forces. Hence differential movement of the columns appears. The most movement is seen in the least restrained columns in the centre of the wall (attached to Trusses 9 and 10) while the more restrained column at the corner of the building (attached to Truss 16) exhibits the least movement. This gradation is clearly shown in Figure 7.10.a and can be directly, and favourably, compared to the results of the NIST report [69] in Figure 7.10.b. The NIST results show considerably greater displacements primarily due to the greater number of floors on fire but the general response is very similar. It should be stressed that the results from the NIST global models were the result of an extensive trial and error method using sub-models of the walls with applied forces to represent the floors. The results from this research project came about entirely from interaction within large and small models of the whole structure.

A generalised view of the column response may be seen in Figures 7.11.a and .b. In the early stages of the fire the lateral expansion of the floors pushes the column out. As the floors bow and sag in the later stages this draws the columns inward. This can be matched against the displaced shape of the column attached to Truss 12 in the 3D model in Figures 7.11.c and .d. For more details on this mechanism in the 2D models please refer to Section 4.5.1.2.

While it may not be a definite indication of collapse in a structure a comparison of midspan deflection can indicate how similar the responses of the 2D and 3D models are. As with the column lateral movement and the floor membrane forces there is a good agreement between the 2D and 3D models as can be seen in Figures 7.12

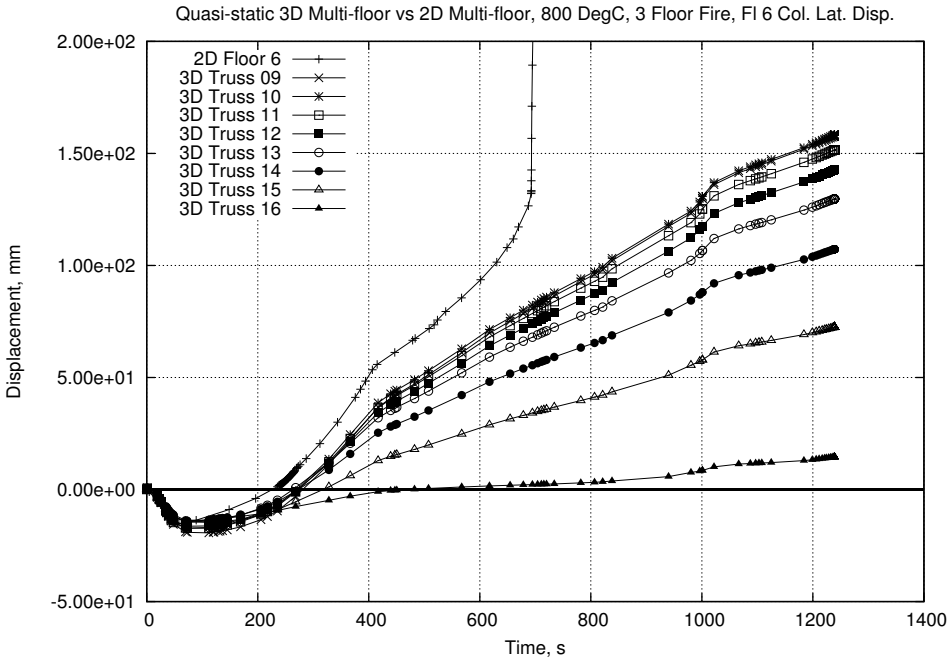

(a)

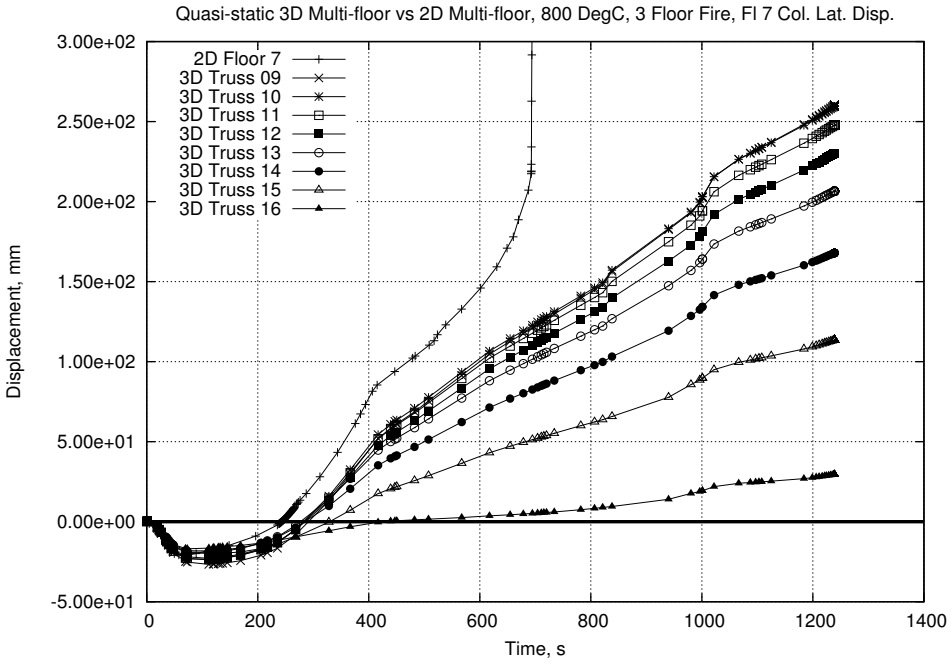

(b)

Figure 7.8: Scenario 1 : Column Lateral Displacement

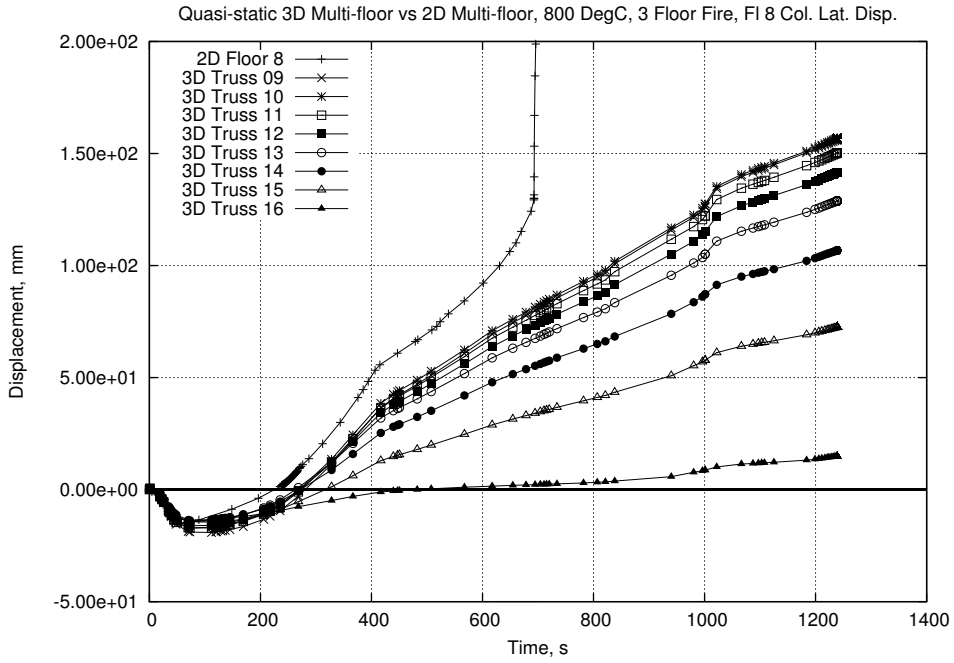

(a)

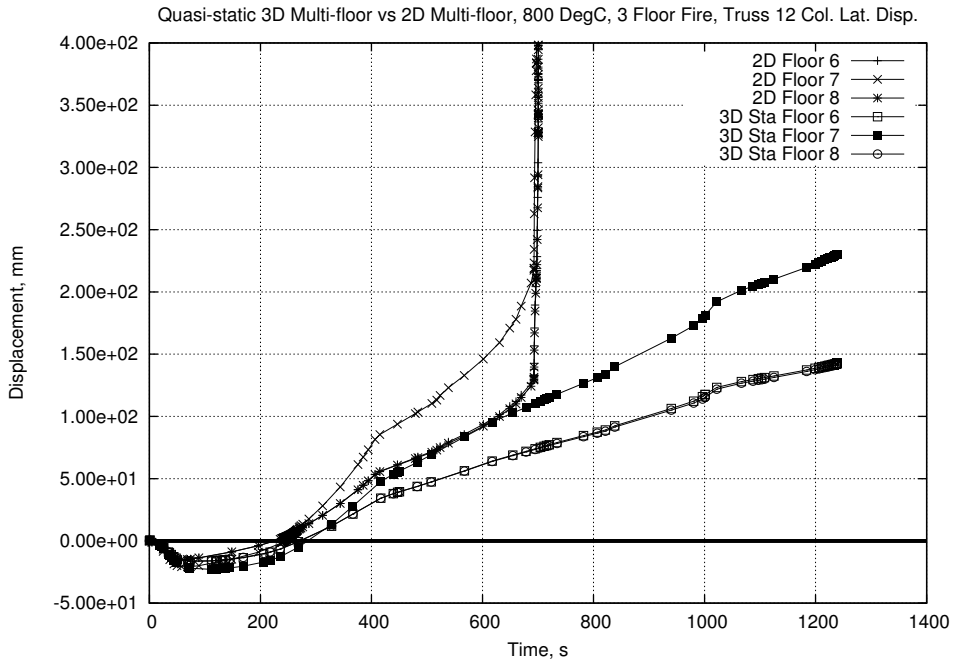

(b)

Figure 7.9: Scenario 1 : Column Lateral Displacement (Cont'd)

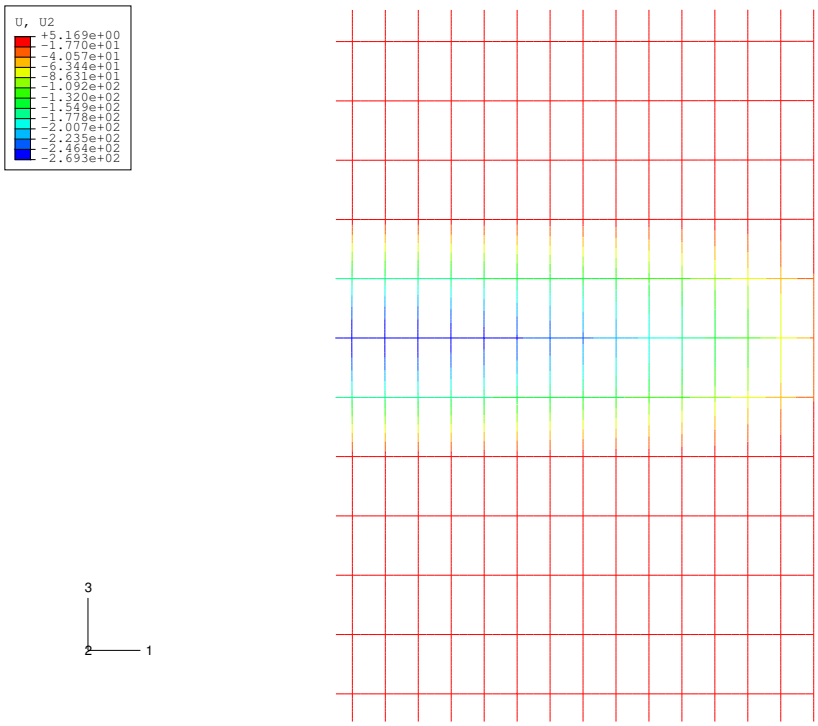

(a)

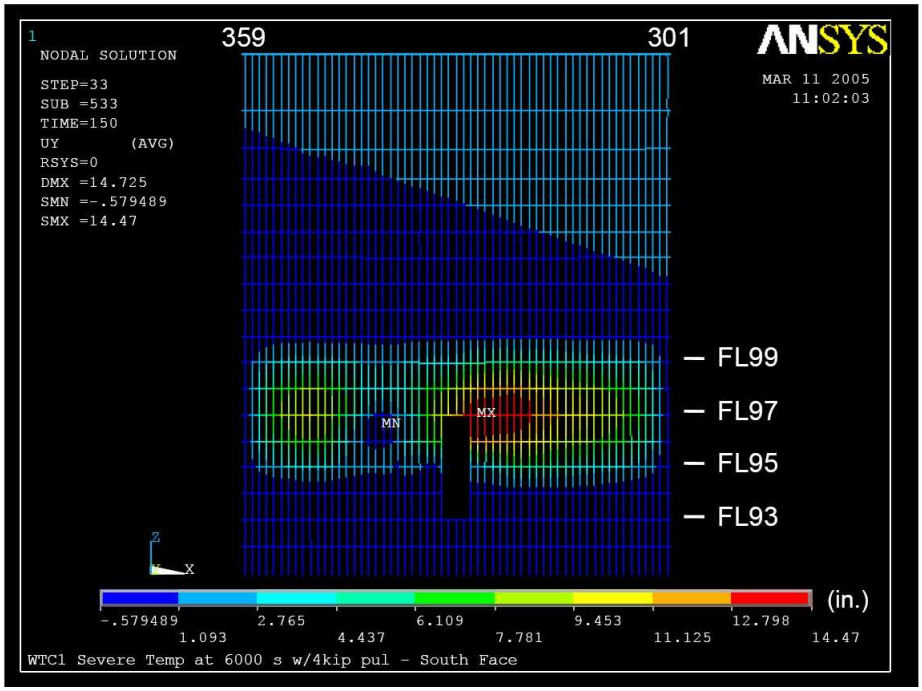

(b)

Figure 7.10: Scenario 1 : Column Displacement Contours

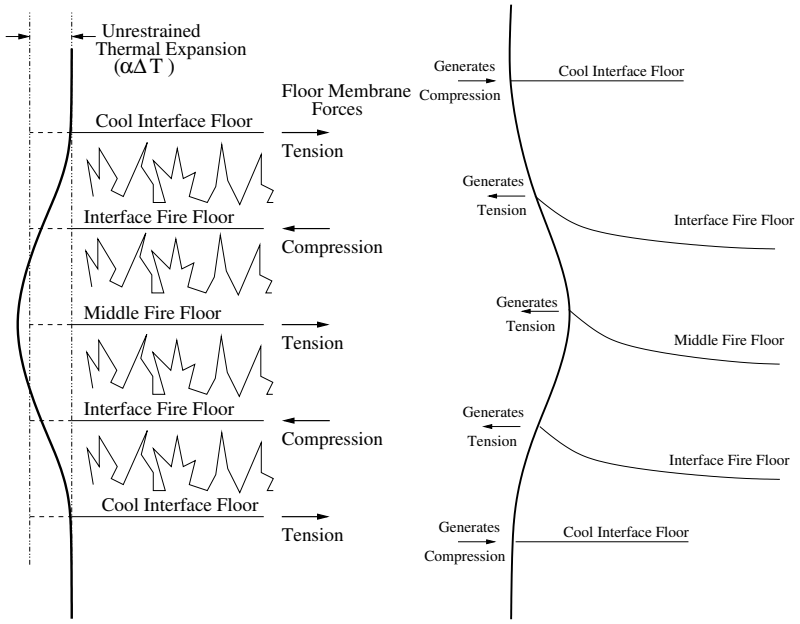

(a) (b)

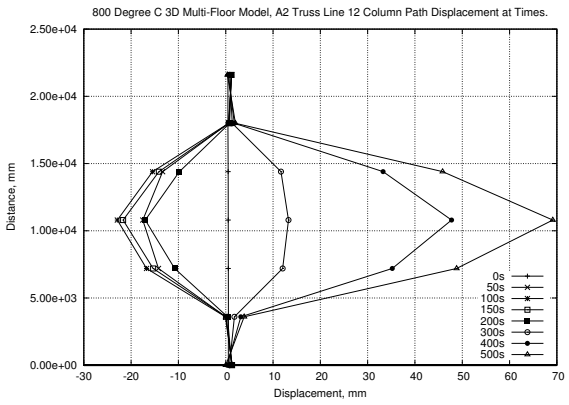

(c)

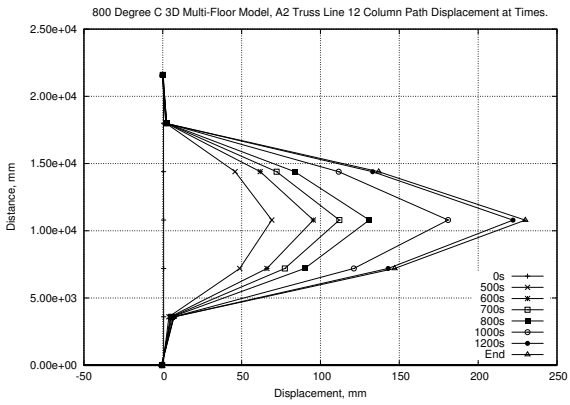

(d)

Figure 7.11: Scenario 1 : Truss Line 12 Column Displacement

& 7.13. The 3D results show all the same changes in profile, even if the results do not match exactly. As with the column movement the midspan deflection shows a gradual reduction when moving from the areas of lower restraint in the middle of the building, at Truss 9, to the more highly restrained corner of the building at Truss 16.

The main indications of failure in the 2D models were based on the moments and vertical displacements induced in the columns. The pull-in forces from the floor, coupled with additional $P - \delta$ moments from the movement of the column, yield the column in combined axial force and bending. Once a mechanism is formed runaway vertical deflection would result. The full explanation of the mechanisms taking place in the columns, including the yield criteria in combined axial load and bending, may be found in Chapter 4. The 2D model without the hat truss has no way to redistribute the effects on the column. The 3D model survives considerably longer before convergence failure of the analysis occurs. A comparison of column moments between the 2D and 3D models can be seen in Figures 7.14 & 7.15. The results were taken at the positions where plastic hinges initiated in the 2D model with 3 floors on fire, i.e. at the 5th, 7th and 9th floors. As with the other responses the moments in the columns increase in a gradual manner along the face of the building as the columns share the load. The first columns to reach yield are the least restrained central columns. Again collapse is not obvious in the model, however the graphs clearly show that by the time the analysis fails to converge the majority of the truss line columns have reached yield. Although not shown here the response of the intermediate columns progresses in a very similar manner to the main columns.

Figure 7.16 shows the vertical displacement at the top of a selection of the columns. Figure 7.16.a shows a direct comparison between the 2D columns and truss line 12 in Scenario 1. Figure 7.16.b shows the movement in the columns in Area 2, both on the long span and short span sides. Neither of these plots show irrefutable evidence of runaway in the columns of Scenario 1 in the same way seen in 2D Col 8. Plot .b does show some quite large displacements and an increasing displacement rate. It

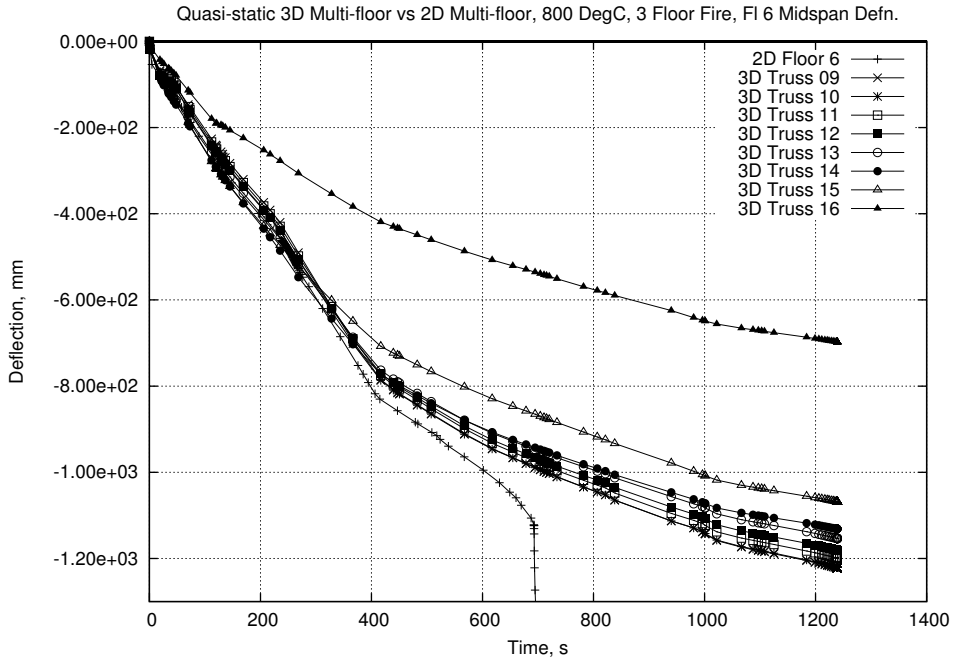

(a)

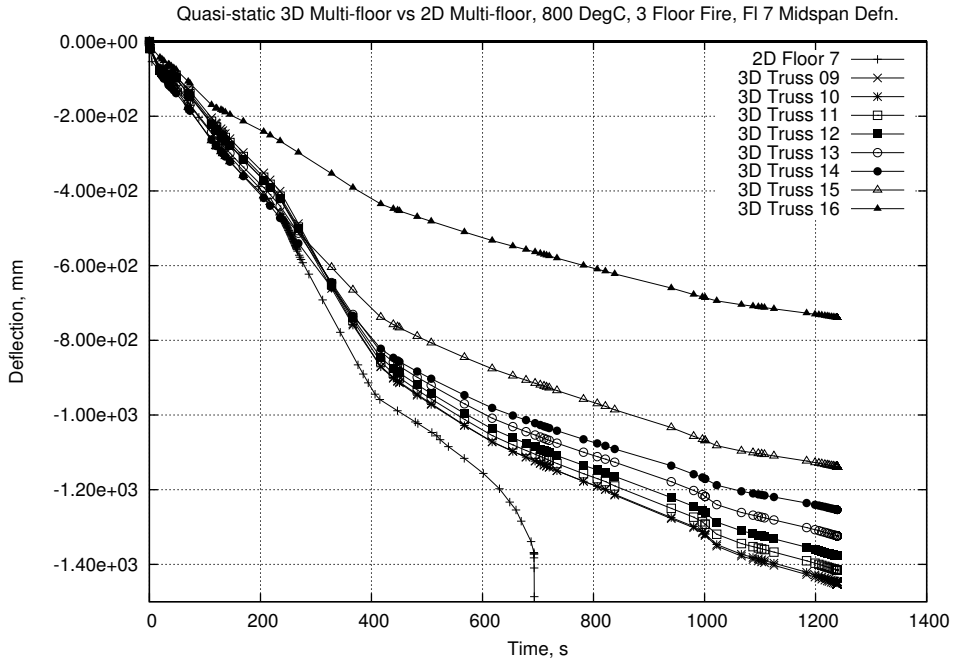

(b)

Figure 7.12: Scenario 1: Midspan Deflection

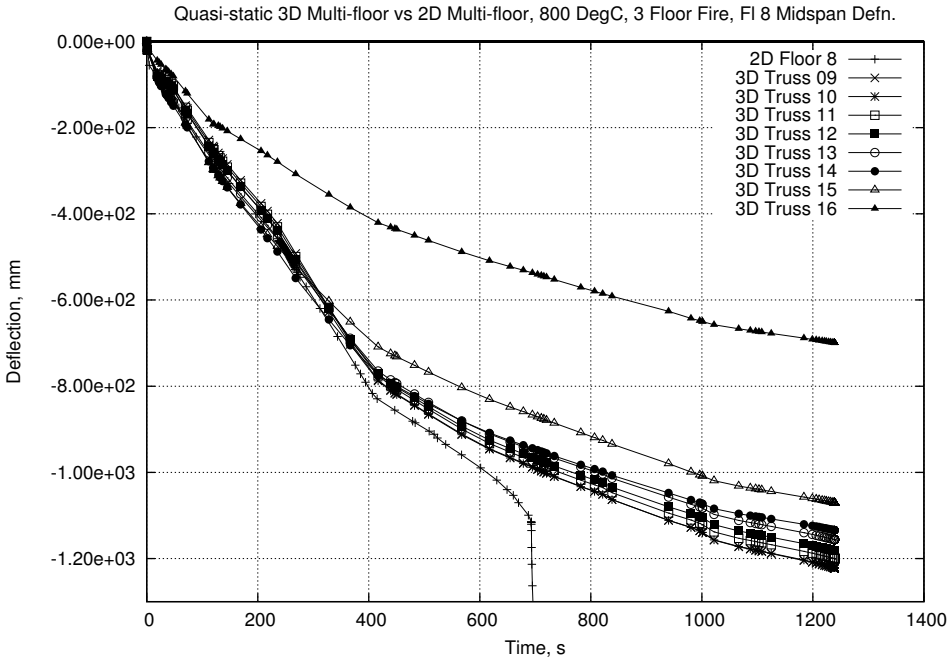

(a)

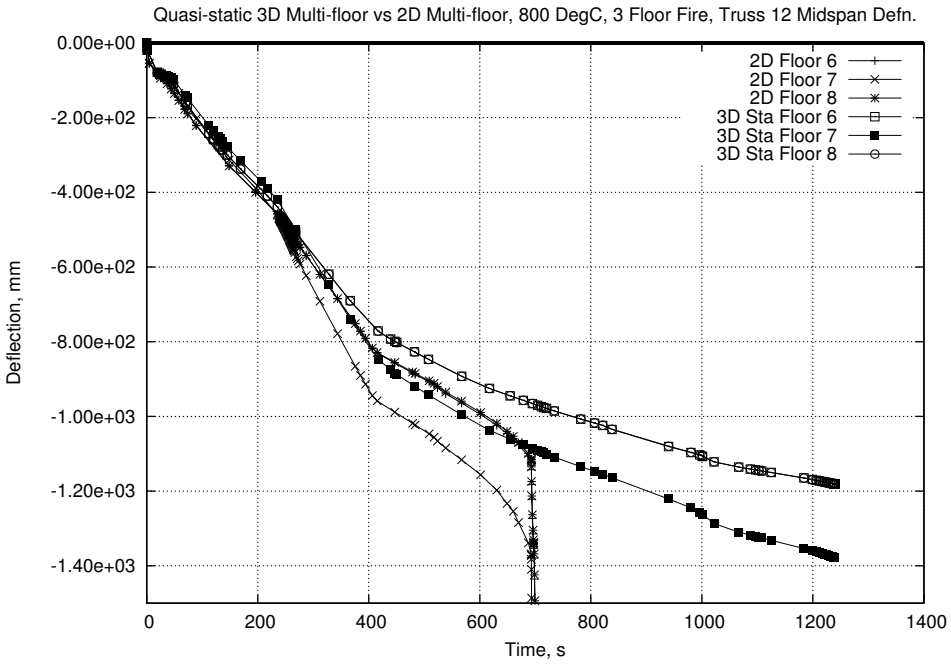

(b)

Figure 7.13: Scenario 1: Midspan Deflection (Cont'd)

is likely, however, that global collapse of the structure is imminent. The transition between the stable structure and global collapse in the 2D model was extremely sudden. In addition, if the effects of expansion in the column are removed from the 2D model then Scenario 1 has reached the same level of displacement in several of the outer columns. Hence the runaway in the outer columns of the 3D analysis could be the trigger that causes convergence failure of the model.

The high level of agreement between the results indicates that the failure mechanisms discovered in the 2D models are applicable to the 3D models. A major source of discrepancy between the results may stem from the lack of heating of the outer structure (i.e. the columns and the spandrel beams) in the 3D model. Another source of difference between the connection forces in the 2D and 3D models may be attributed to uneven distribution of forces between main truss columns and intermediate columns. The direct connection between trusses and main columns attract somewhat higher load than the less direct connection to intermediate columns.

Short Span Area Results. Comparison with the results of the 2D analyses only allows verification of the long span truss areas. The 3D model also allows evaluation and investigation of the short span trusses. The results from the short span side of the building are less extreme than those from the long span areas. This is primarily because of the lower levels of thermal expansion induced in the shorter spans.

The interface between Area 2 and Area 4 in the 3D model is well delineated by a discontinuity in the floor deflections. This phenomenon is clear in Figure 7.17 near the line of Area 4 Truss 1. This truss acts as a support to the "core" ends of Area 2 Trusses 15 and 16 and lies on the same grid line as the edge of the core. The cause of this peak in the slab is again likely to be induced by compatibility effects. At the point at which the analysis fails the slab is still relatively cool for most of its depth. The membrane action over the rest of Area 2 is relatively uniform which appears to be affecting the interface area even though it is not being rigidly supported by the core structure.

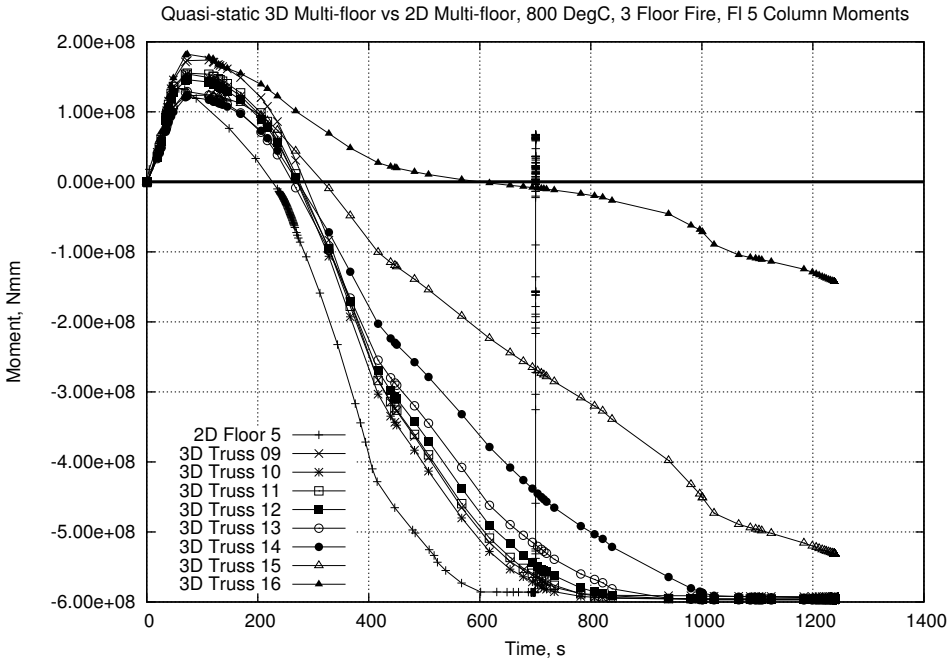

(a)

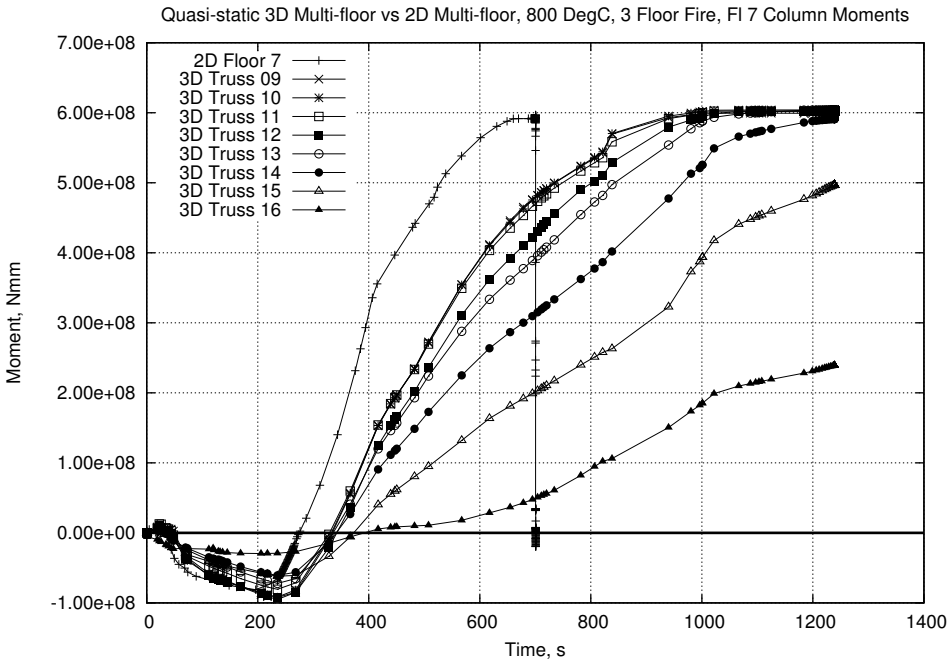

Figure 7.14: Scenario 1 : Long Span Side Column Moments

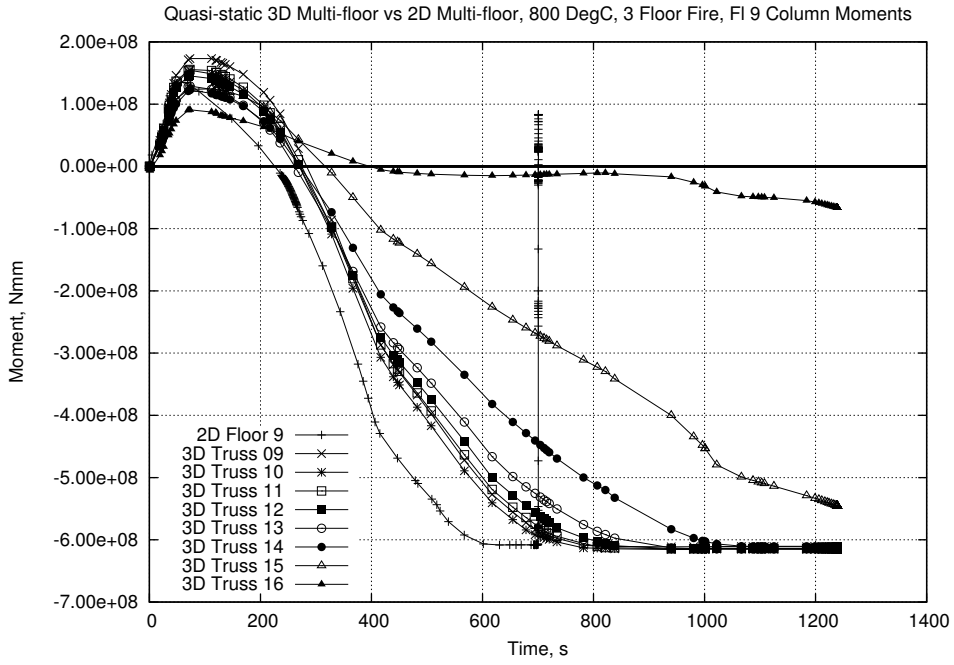

(a)

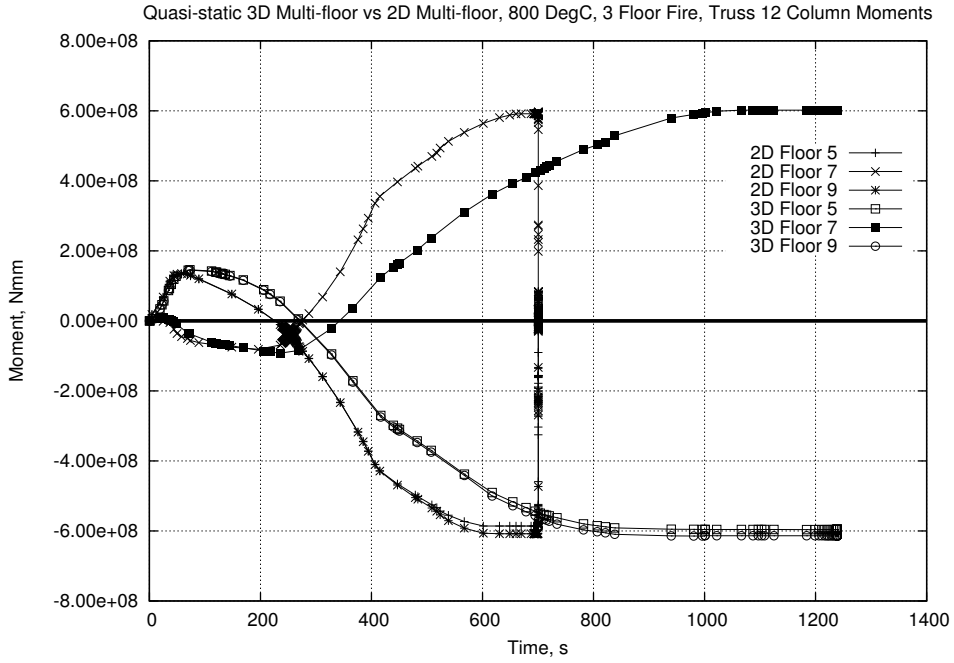

Figure 7.15: Scenario 1 : Long Span Side Column Moments (Cont'd)

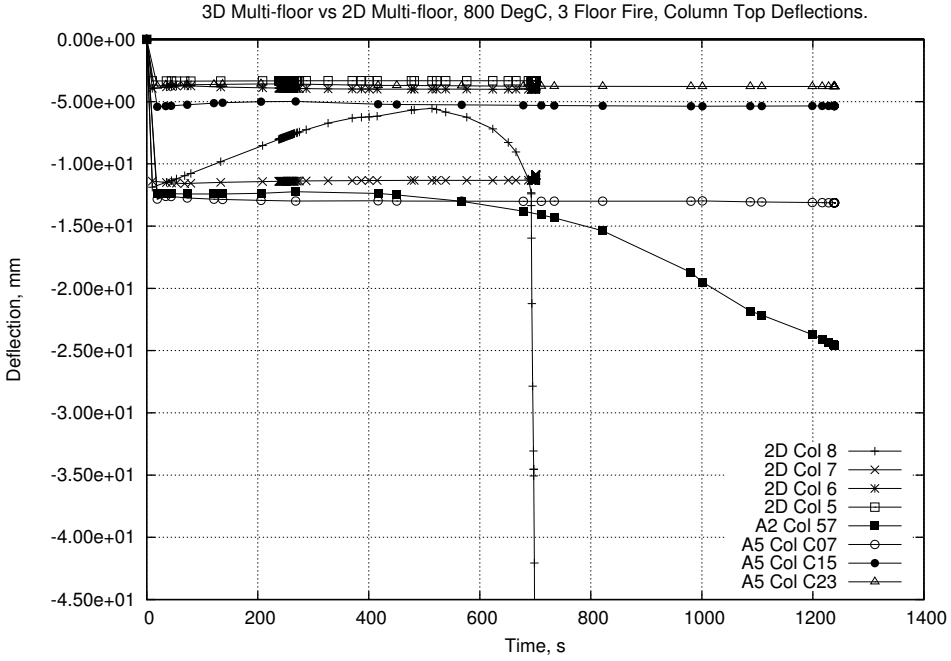

(a)

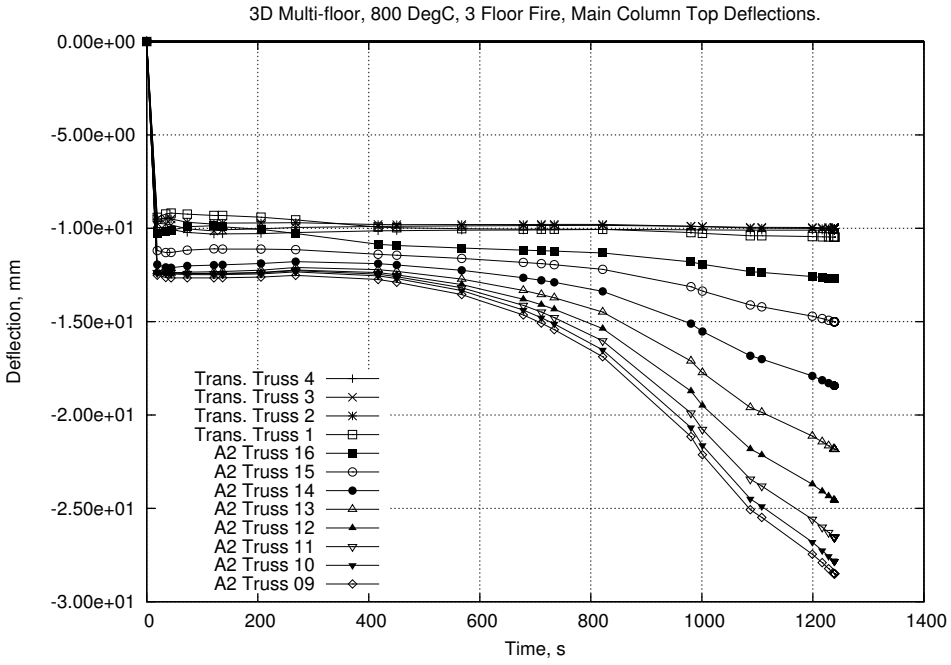

(b)

Figure 7.16: Scenario 1 : Area 2 Column Vertical Displacement

Away from the interface area the response of the short span trusses is similar to that of the long span trusses except the maximum deflections are about half that of the longer span. The extra stiffness, and lower deflection, of the short spans are readily indicated by Figure 7.18. These plots show the line of the column displacement at different times through the analysis for two of the fire floors (Figures 7.18.a and .b for floor 7 and Figures 7.18.c and .d for floor 6). The column lines start with Area 4 Truss 4 (See Figure 7.17) on the left hand side of the plot and run to the corner of Area 2 on the right hand side. Outward movement in Figure 7.18 is indicated by positive values. Intermediate columns are included in these plots. Fire floor 8 reacts in a very similar manner to Floor 6 and hence is not presented here. These plots make it apparent that the columns attached to the short span trusses (and the intermediate columns between) spend a substantial amount of the analysis outward of their original position. It is only toward the end of the successful analysis time that the column line is drawn inward in the centre of Area 4. The stiff interface between Areas 2 and 4 is again obvious. The columns at this point are kept outward of their initial position for the duration of the analysis. This reaction is in contrast to the response of the columns supporting the short end of Area 2. Away from the stiffer areas of the Area 4 interface and the corner of the building the columns are drawn inward relatively quickly.

Comparing Figure 7.18 with the corresponding column movement plots of the long span side (Figure 7.19) shows a significant difference. Due to the change in axis when moving from the short span side to the long span side, in Figure 7.19 outward movement is indicated by negative values. On the long span side the columns are being drawn inward by around 300s (the same is true of the columns supporting the short side of Area 2). The short span trusses of Area 4 take considerably longer to generate movement enough to draw their supporting columns inward.

One major similarity between the response on the long span side and the short span side is that the intermediate columns become more and more involved as the analysis continues. In both Figure 7.18 and Figure 7.19 the initial position of the columns lies around 0mm displacement, caused by their response to the ambient

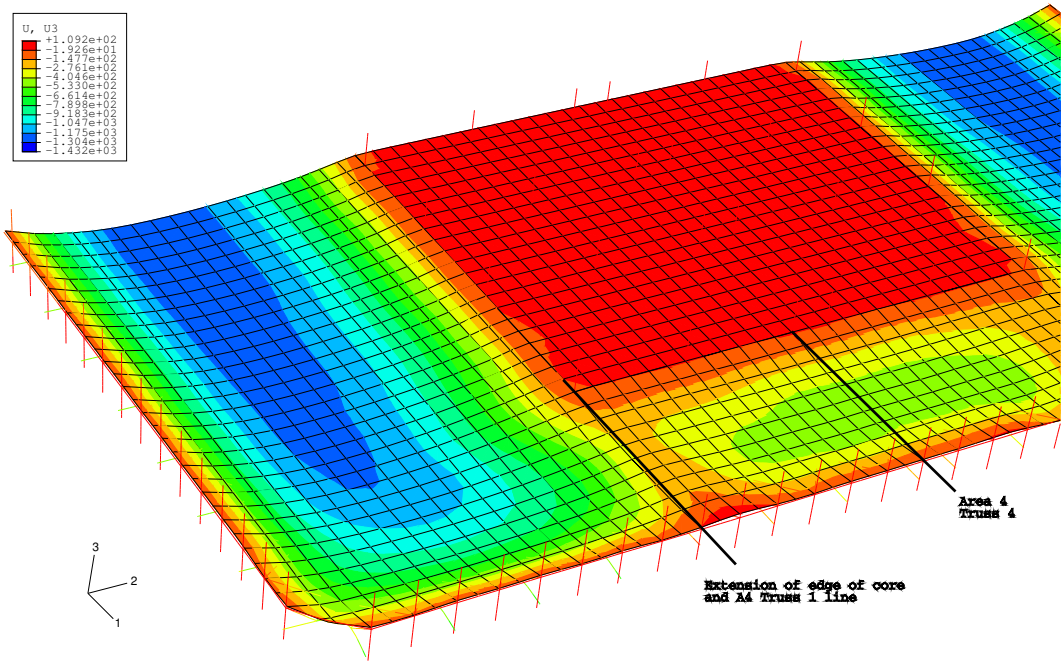

Figure 7.17: Scenario 1 : Floor 8 Displacements

loading. The expansion of the floor is reasonably equally resisted by all columns. However once the floors begin to pull the columns back inward it is clear that the columns directly connected to trusses are affected more quickly. This is most obvious in Figures 7.19.a and .c as the analysis progresses from about 200s. As the main columns begin to reach yield the intermediate columns become more involved in resisting the inward movement until the point of convergence failure (at around 1250s) when the column distribution is a reasonably smooth curve. At this point the columns from Area 2 Truss 9 to Truss 14 have reached yield (Figure 7.14). As mentioned previously the uneven distribution of forces between the main columns and the intermediate columns may explain some of the differences between the results reported for Scenario 1 and those taken from the 2D analysis.

7.2.2.2 Scenario 2 : Quasi-static, 5FF, no hat, 800°C

Part of the aim of this research was to produce possible bounds on collapse of the models. As Scenario 1 did not show obvious collapse a more onerous fire regime

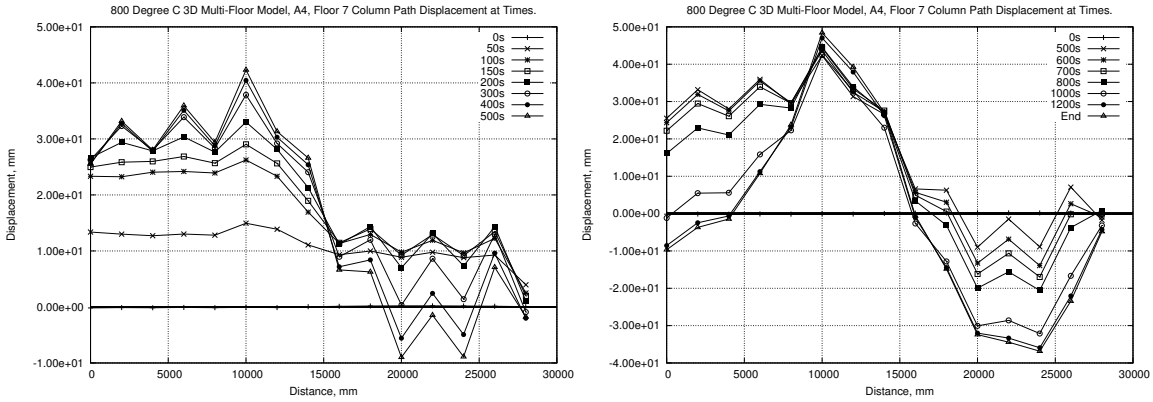

(a) (b)

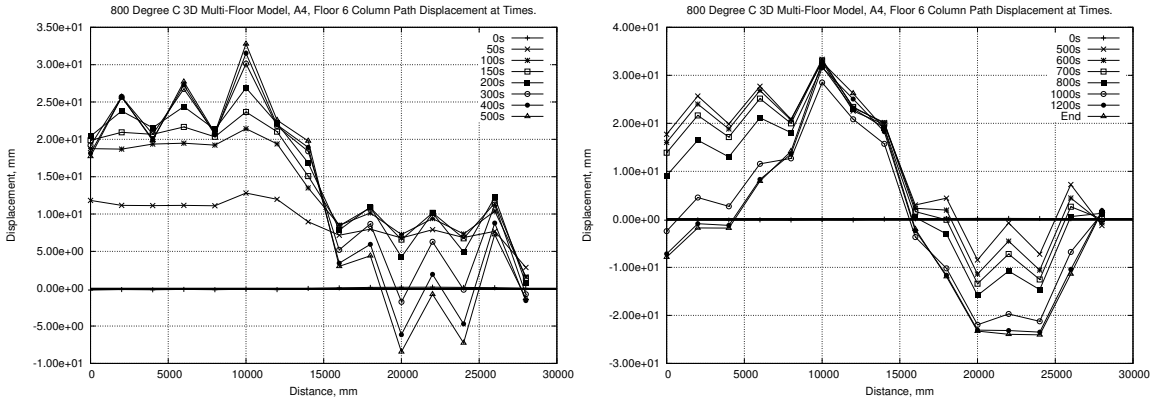

(c) (d)

Figure 7.18: Scenario 1 : Area 4 Column Paths

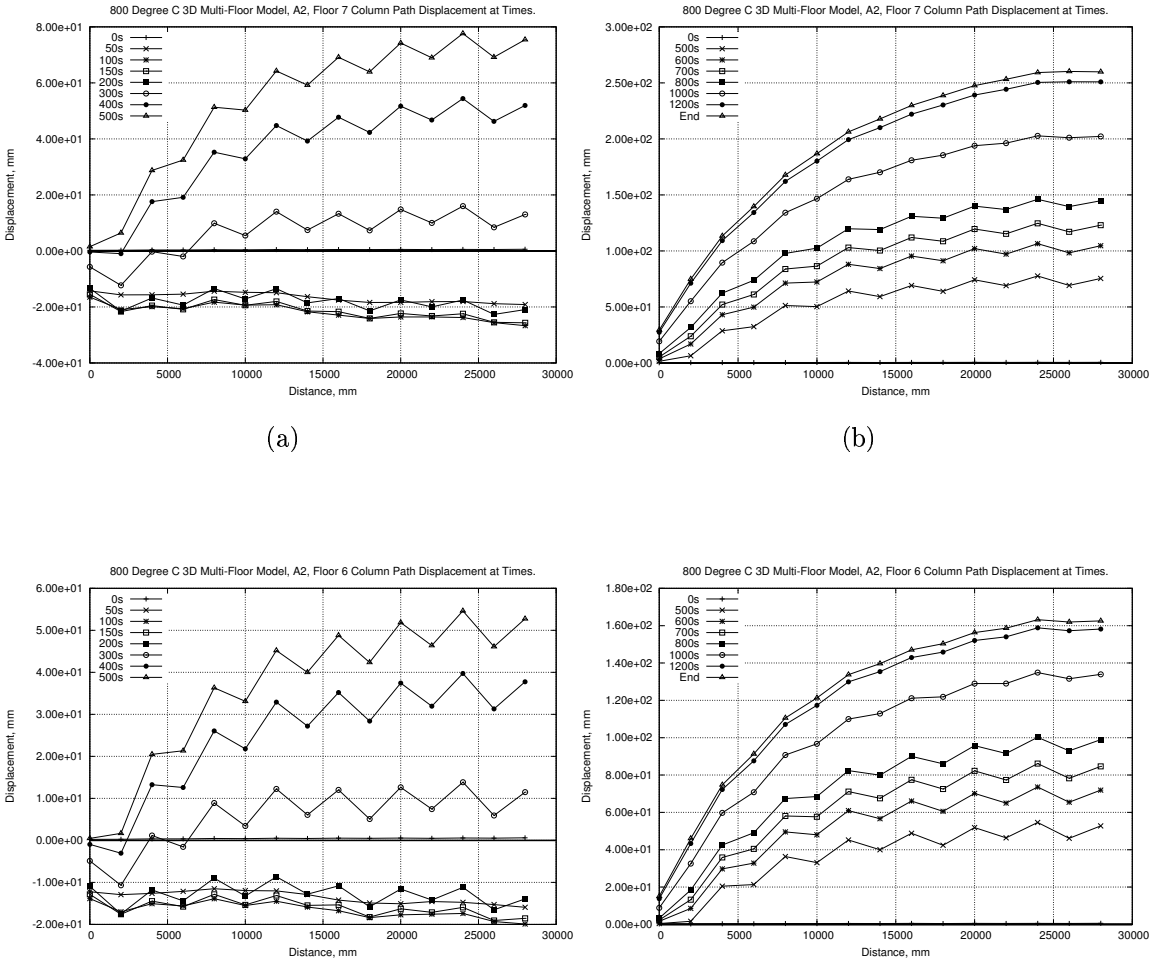

Figure 7.19: Scenario 1 : Area 2 Column Paths

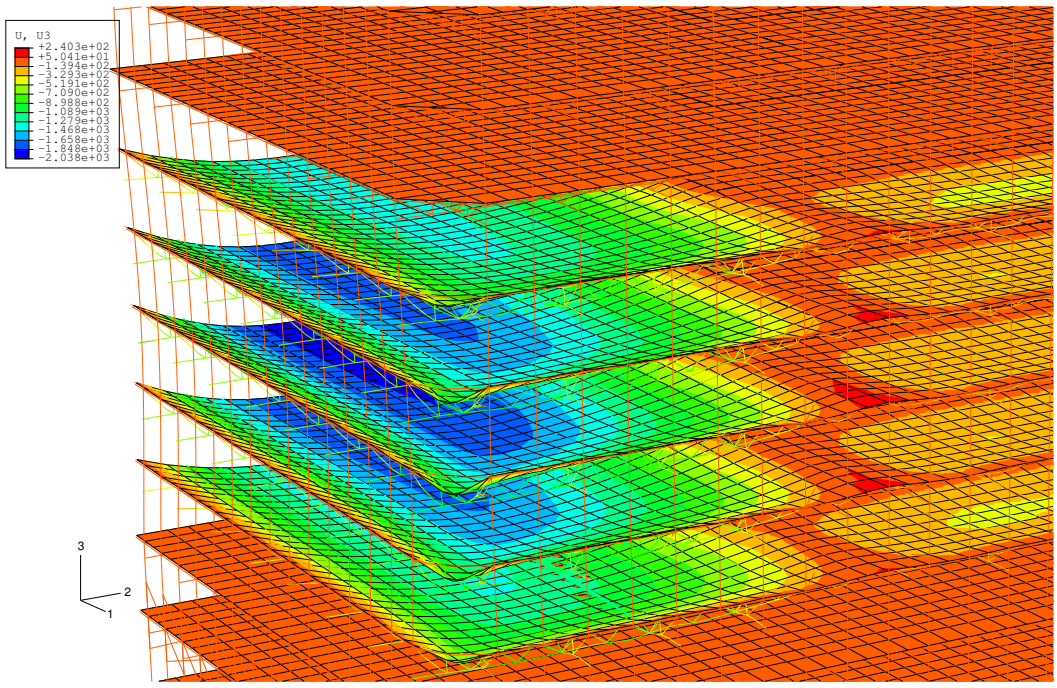

Figure 7.20: Scenario 2 : Final Displaced Shape

was applied to the structure. The fire zone was extended by one floor above and below the initial fire zone. As with Scenario 1 no clear collapse mechanisms were seen as the model failed to converge at around 750s. A brief calculation shows that the 3D multi-floor model with 5 floors on fire fails to converge at about 63% of the time that the 3 floor fire analysis takes before failing to converge. This is about the same proportion as is seen when comparing the times to collapse between the 2D models. This may be coincidence but it may also point toward the failure to converge as an indication of imminent collapse.

Figure 7.20 shows a close up of the final displaced shape in the main areas of interest. The general response is similar to the 3 floor fire version with large deflections (up to about 2m) occurring in the long span areas. The interface between the long and short span areas again shows a relatively stiff area and the short span areas show maximum deflections of around 500mm.

Examination of the connection forces again shows a good correlation between the 3D and 2D results. Figure 7.21 shows a comparison between the connection forces for all columns lines on floors 5 and 6, while Figure 7.22.a shows floor 7. These

graphs include a direct comparison to the equivalent 2D results. Results for floors 8 and 9 are not shown as they are broadly similar to the results for floors 6 and 5 respectively. Figure 7.22.b takes the results from truss line 10 through all the fire affected floors (5 to 9) and compares them to the 2D model. There is a good match between results for the first 250s before they begin to diverge. As with Scenario 1 the 2D model has significantly less ability to spread load throughout the structure and hence weakens much faster than the 3D model.

Comparison of the other factors examined in Scenario 1, such as midspan deflection and column lateral displacement show similarly close results. Figures 7.23 & 7.24 show the moments in the columns over the time of the analysis. Plot .a refers to the hinge location at the 4th floor, plot .b refers to the midpoint hinge location at floor 7 and plot c refers to the upper hinge at floor 10. Floors 4 and 10 are again the cool interface floors and are analogous to fixed supports if the system is converted into basic beam theory (please refer to Section 4.5.1.2 for more information on this conversion). The plots in Figures 7.23 & 7.24 show good agreement with the 2D results for the majority of the analysis time. Another telling indication of imminent collapse is that at the point the model fails to converge all 3 hinge points have reached yield. The hinges at floors 4 and 10 show that the majority of the columns have been at yield for a significant amount of time and yet the building remained stable. As soon as a significant number of columns start to reach yield at the mid-span (i.e. at floor 7) the analysis failed to converge. This is the same situation as can be seen in Figures 7.14 & 7.15 for Scenario 1. The "support" hinge points (plot .a in Figures 7.14, 7.15, 7.23 and 7.24) show yield for a significant time and the analysis fails when the column attached to Truss 14 reaches yield at the "mid-span" of the column. The direct comparison of Truss 10 over several floors to the 2D analysis results in Figure 7.24.b again shows the close correlation between responses.

Toward the end of the analysis large, unrecoverable displacements are seen at the top of the columns. Figure 7.25 shows these vertical deflections for the main columns in Area 2. No complete runaway is seen but a relatively high rate of

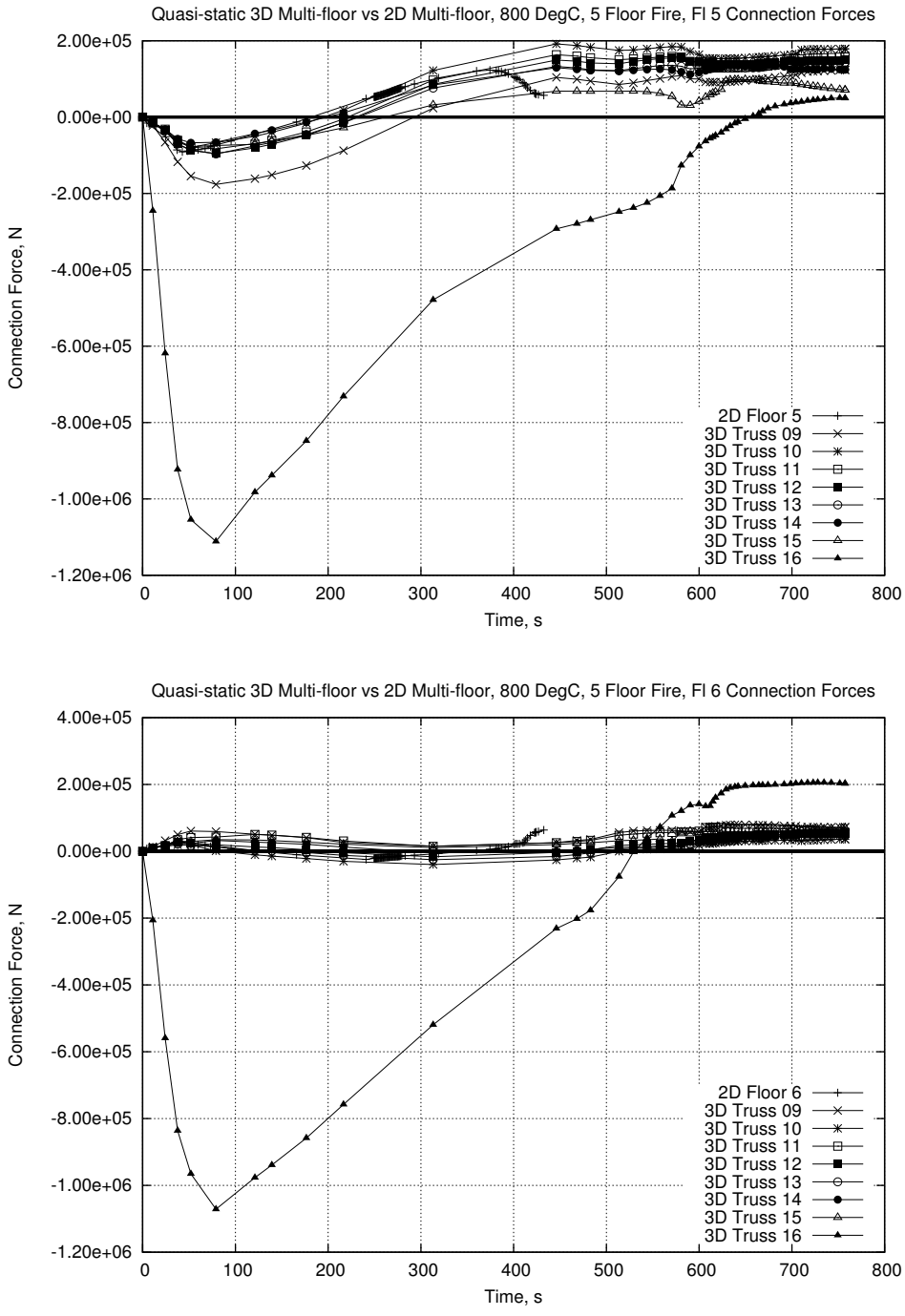

Figure 7.21: Scenario 2 : Floor Membrane Forces

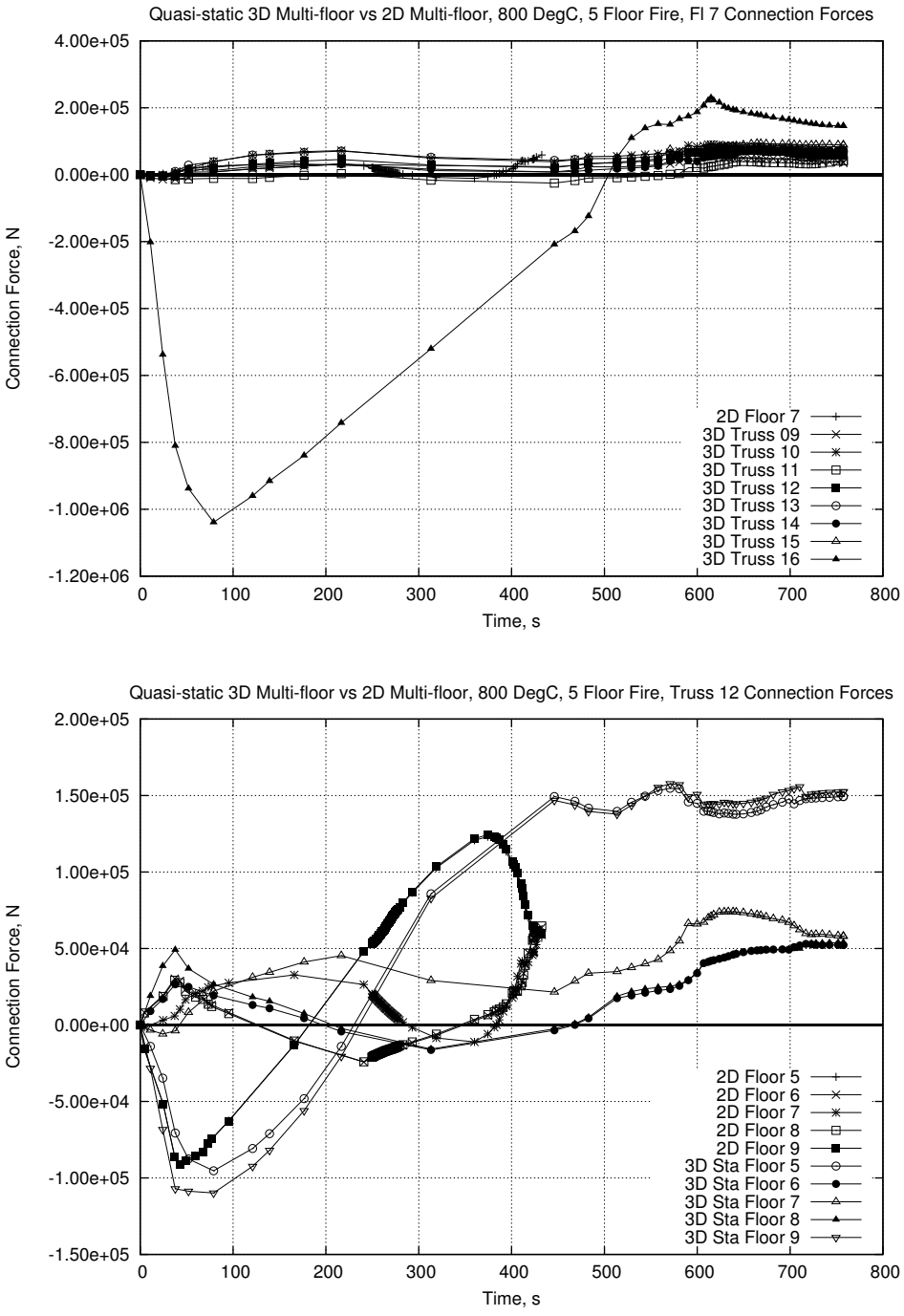

Figure 7.22: Scenario 2 : Floor Membrane Forces (Cont'd)

displacement is seen toward the point of convergence failure. Increasingly rapid vertical movement is also seen in the columns supporting the transverse trusses, which are found on the short span side of the building. This indicates that the stiff corner of the structure is also losing integrity

This further strengthens the theory that the convergence failure in these models indicates imminent failure of the model structure. These results also indicate a possible further refinement to the collapse theory from Chapter 4. The model appears to be stable until the column on truss line 14 yields. Truss 14 on each floor corresponds to the corner of the core. It is possible that as the core becomes more removed from supporting the outer structure, stability is lost. A simpler alternative is that the structure has a critical number of columns that need to yield before the system becomes unstable.

Scenario 2 is a much closer match to the model investigated in the official NIST report [52] on the WTC Towers due to the higher number of fire affected floors. Figure 7.26.a shows the final column displacement contours for the long span side of the building. Figure 7.26.b shows a result presented in the NIST report for the South wall of WTC1, which is also pictured in Figure 7.8. The NIST method of including thermal actions involved the use of "thermally induced damage". This effectively converted the effects of thermal expansions in the floor into equivalent static loading that was then applied to the global model. Figure 7.26.b shows the response of the NIST model when several of the connections between trusses and columns were disconnected and the remainder subjected to roughly 18kN (4kips) inward forces. NIST reported a maximum inward displacement of around 380mm (15") under this inward load, although the effect was apparently not enough to trigger collapse. According to the NIST report a uniform inward pull force of upward of 22kN (5kips) on the surviving truss-column connections would be needed to trigger instability. Comparison between the NIST model and Scenario 2 indicates that although the loading and fire scenarios applied to the two models were very different the final displaced shape at failure of the model (either through collapse or convergence failure) is similar. Furthermore the level of horizontal loading being

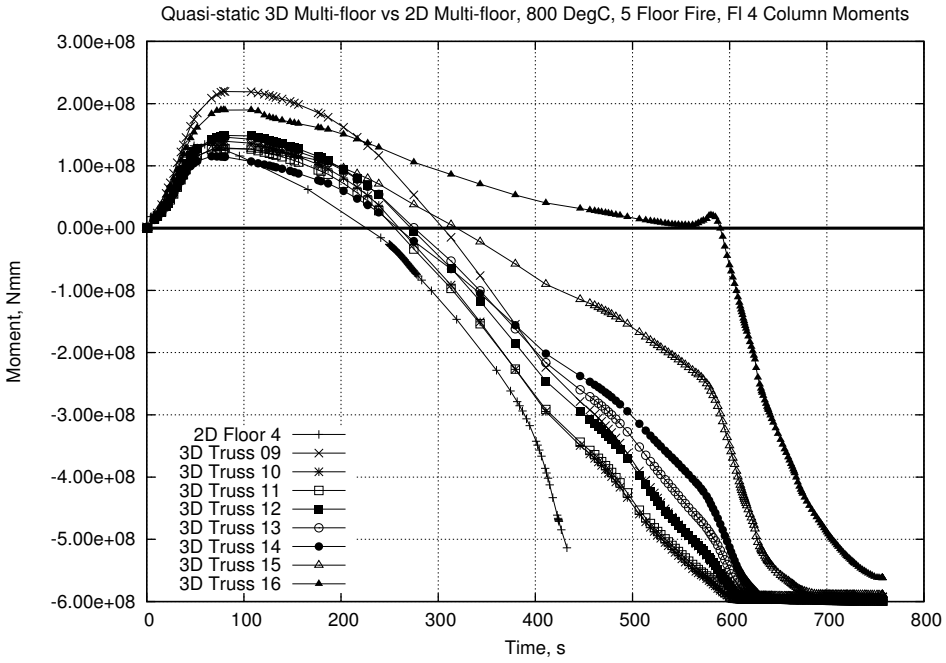

(a)

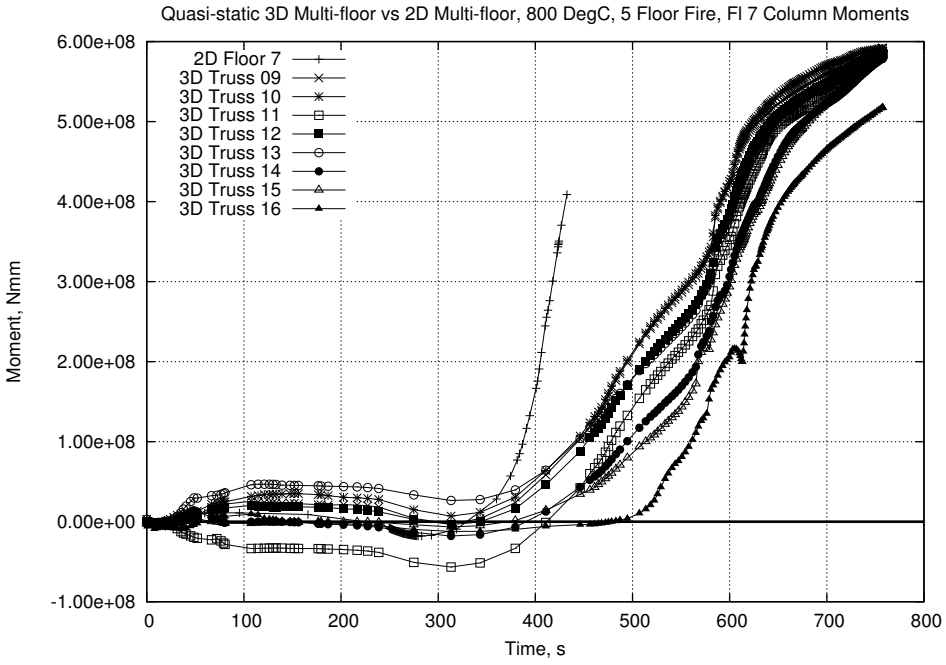

(b)

Figure 7.23: Scenario 2 : Column Moments

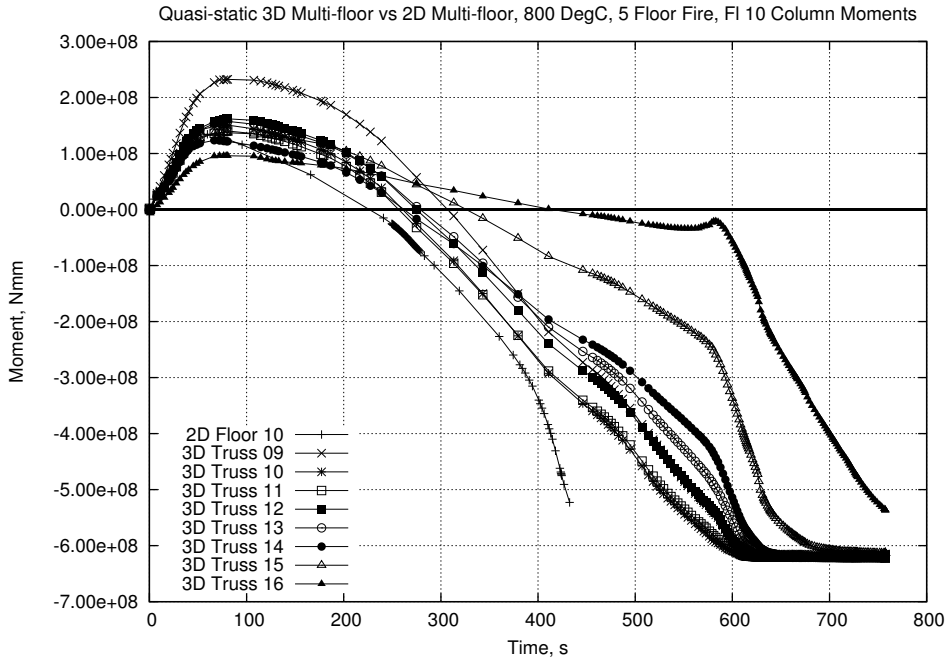

(a)

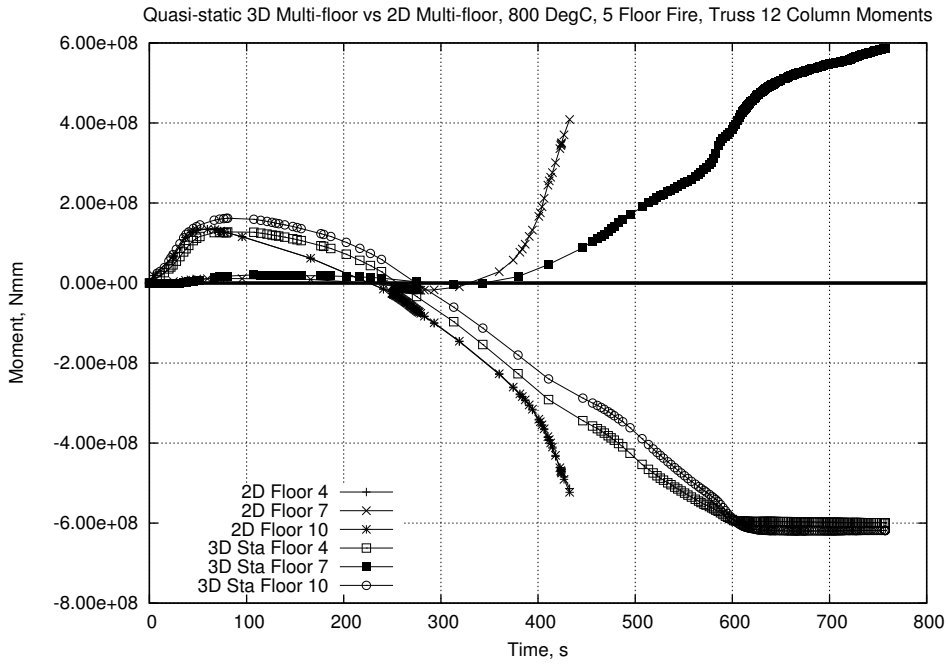

(b)

Figure 7.24: Scenario 2 : Column Moments (Cont'd)

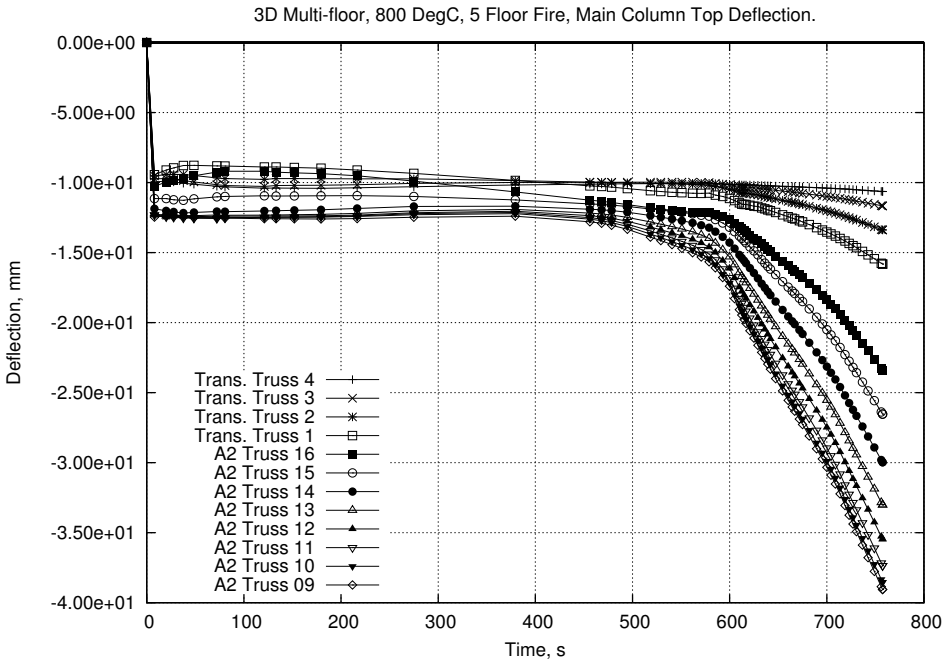

Figure 7.25: Scenario 2 : Column Vertical Deflections

applied to the columns by the thermal action on the floors in Scenario 2 is of the same order of magnitude to that being directly applied in the NIST model.

The main conclusions to be drawn from Scenario 2 are that :

1. The results from the model are valid as they match similar responses seen in other models.

2. The fire over 5 floors brings the model to a state of failure more quickly than the 3 floor fire scenario.

This second point can be highlighted by comparing the magnitude of deflections in the outer columns between Scenario 1 and Scenario 2 (Figure7.28). The 5 floor fire creates considerably more displacement in the corner columns on both walls. As both sides of the corner are being drawn inward significantly this will affect the durability of the global structure. In Scenario 1 the corner, and the short span side in general, are less affected.

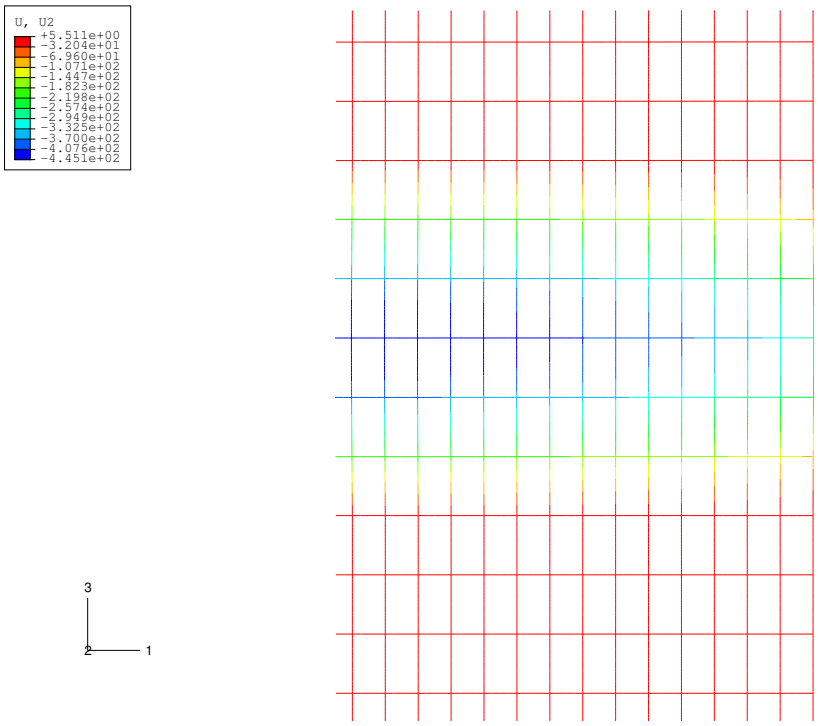

(a)

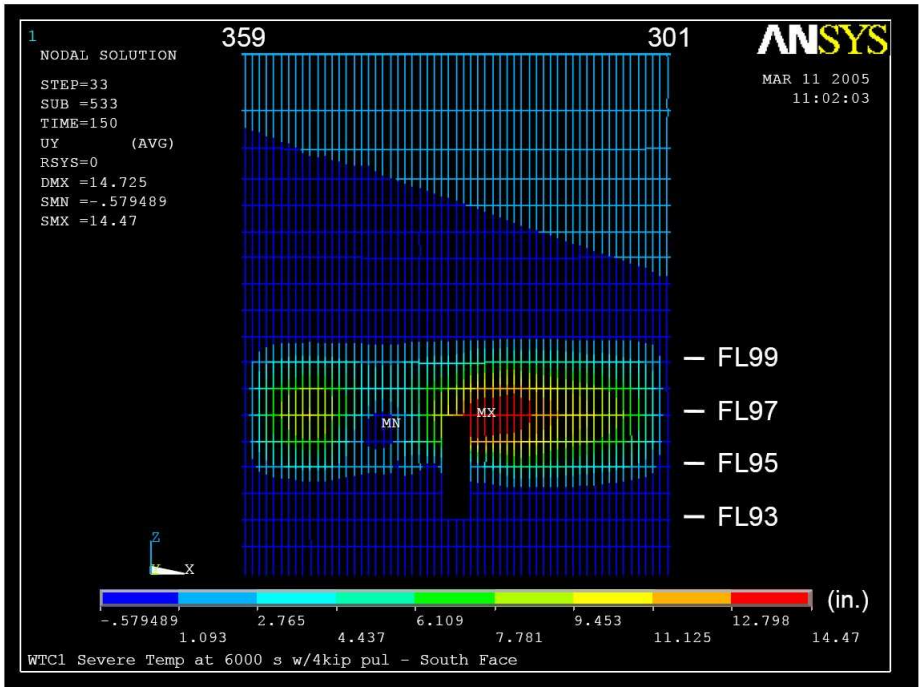

(b)

Figure 7.26: Scenario 2 : Long Span Side Column Displacement Contours

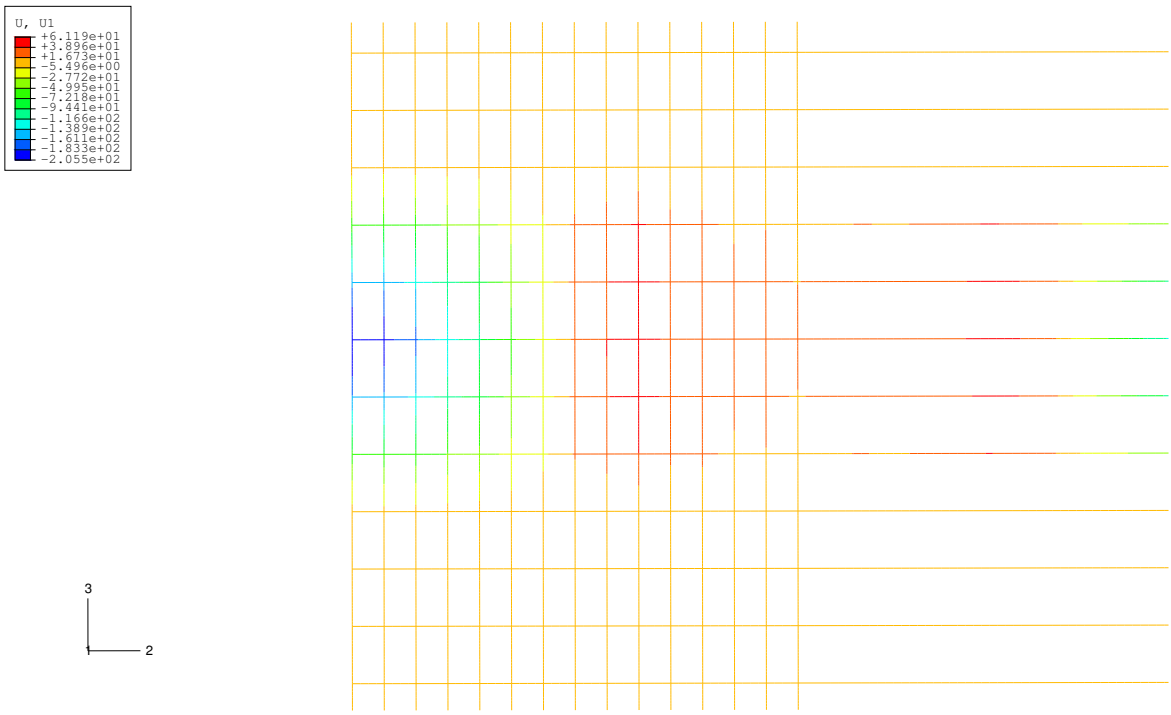

Figure 7.27: Scenario 2 : Short Span Side Column Displacement Contours

7.2.2.3 Scenario 3 : Quasi-static, 3FF, no hat, 500°C

This scenario was run to check the numerical stability of the structural model. Scenarios 1 and 2 failed to converge, rather than showing definite collapse. It was possible that the convergence difficulties were due to local, rather than global, instabilities in the model. Scenario 3 was again affected by a fire on 3 floors but this time the maximum temperature reached in the compartment was 500°C. In the 2D analyses this fire regime was observed to cause relatively little movement in the structure so it was expected that the 3D model would react in a similar manner. As the 2D model with this fire regime was not investigated in depth the results of Scenario 3 will be compared to Scenario 1 directly. Again truss line 12 will be used as a basis of comparison.

The deflections on the 8th floors (top interface fire floor) at the point of convergence failure can be seen in Figure 7.29. This floor shows the maximum deflections in the model and so the rest of the structure has been omitted for clarity. The deflections

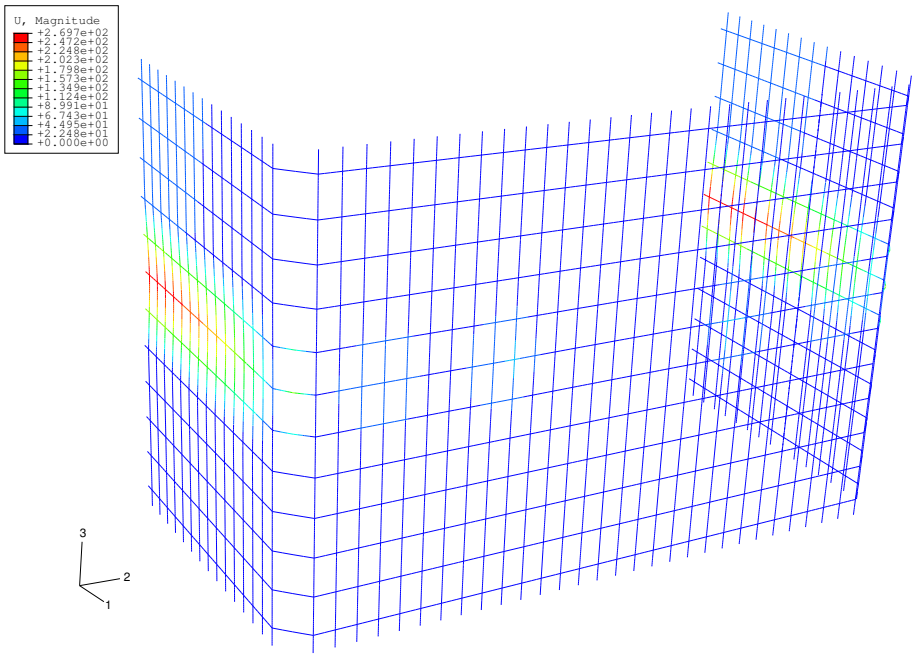

(a) Scenario 1 : 3 Floor Fire

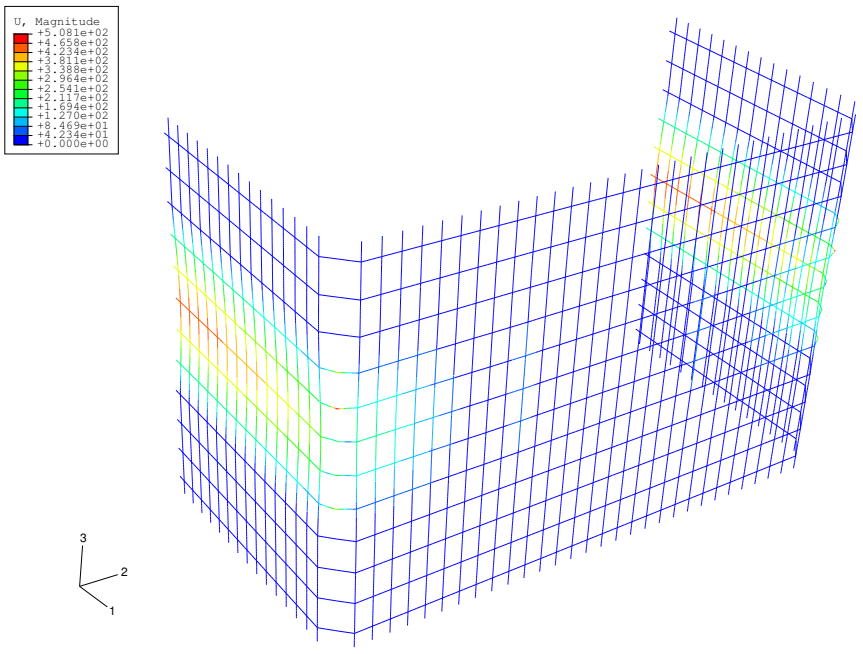

(b) Scenario 2 : 5 Floor Fire

Figure 7.28: Scenario 1 & 2 : Final Column Displacement

here are substantially less than in Scenario 1 (less than half), even at the same time. Figures 7.30 & 7.31 show the midspan deflections of the long span trusses in Scenario 3 and compares them to Truss 12 of Scenario 1. As Figure 7.31.b shows there is a slight difference in the manner of the deflections when compared across the three fire floors. In Scenario 1 it is the middle fire floor that has the highest deflections, while in Scenario 3 it has the lowest deflections. This is due to the compatibility effects of the column. In Scenario 3 the column is moved outward and remains outside its initial position, as shown in Figures 7.32 & 7.33. In Scenario 1 the column initially moves outward but returns through its initial position relatively quickly and is pulled inward by the tensile membrane action of the floors.

As indicated in Chapter 3 the lower temperature of the truss means that the steel retains much of its strength, as well as expanding less. This also leads to the truss being increasingly loaded as the analysis progresses as the steel heating rate reduces compared to the slab rate. The steel drives the initial expansion but as it reaches a steady temperature it has to resist the continued movement induced by the slab heating. An examination of the stresses in the steel members at the point of convergence failure shows yield level stresses being induced in the transverse trusses. It is then likely that the failure in convergence is caused by a local buckling problem in these members rather than a global collapse mechanism in the structure as a whole. The stability of the 2D models using the 500°C fire regime, and the results of the 3D single truss model are in line with this theory.

A brief examination of the column moments in Figure 7.34 indicates that they are well within the failure envelope.

To conclude, this scenario was introduced to investigate the effect of a cooler fire on the structure. Ideally it was designed to be a less onerous load case that the structure would easily resist. As the lower temperatures allow the steel to retain more strength for longer it appears that local instabilities in the model limit the convergence of this scenario.

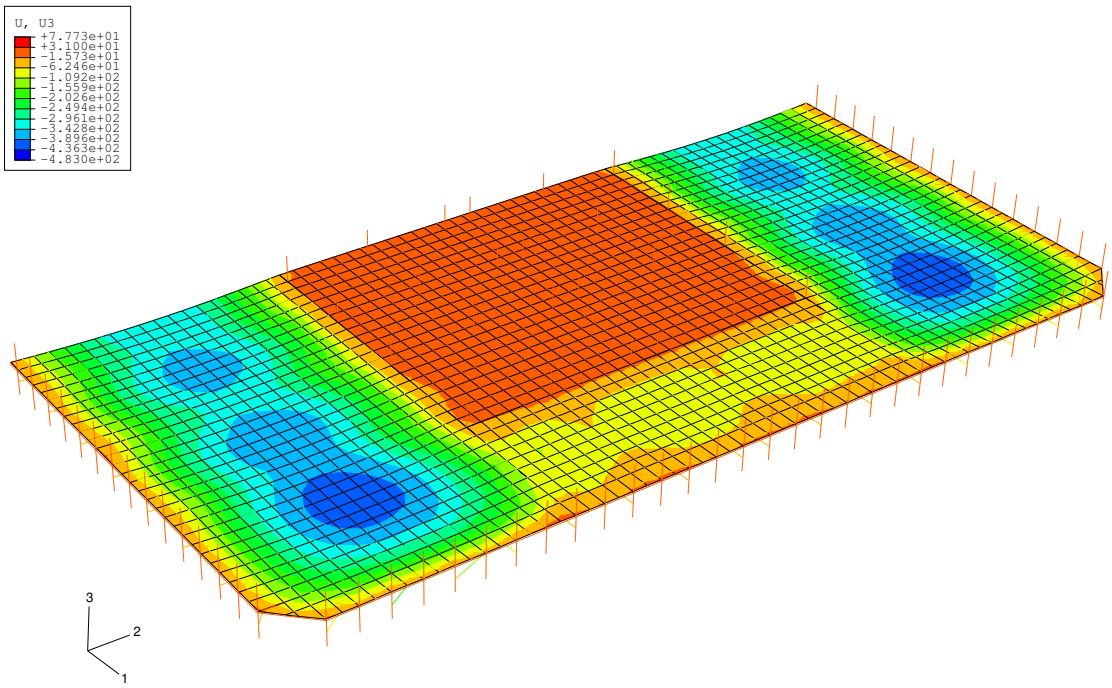

Figure 7.29: Scenario 3 : 8th Storey Deflections at Convergence Failure

7.2.2.4 Scenario 4 : Quasi-static, 3FF, hat truss, 800°C, outer structure not heated

The other important issue that the 2D analyses (Chapters 4 & 5) investigated was the effect of adding a hat truss to the structure. In the case of the WTC towers there was additional steelwork included in the top 3 storeys of the building to help support an antenna. Only WTC1 was actually fitted with an antenna but both buildings had the appropriate support structure. Under the fire conditions of September 11th 2001 these extra members acted as additional outrigger trusses and helped redistribute forces between the core and the outer columns. In the official NIST investigation into the the collapse of the WTC towers [52] they cite the hat truss as transferring load from the core to the outer columns as the core columns shortened in and around the affected floors. In the work done for Chapter 4 it was found that a 2D model with similar attributes to the WTC towers was capable of transferring significant loads from the outer columns to the core. This

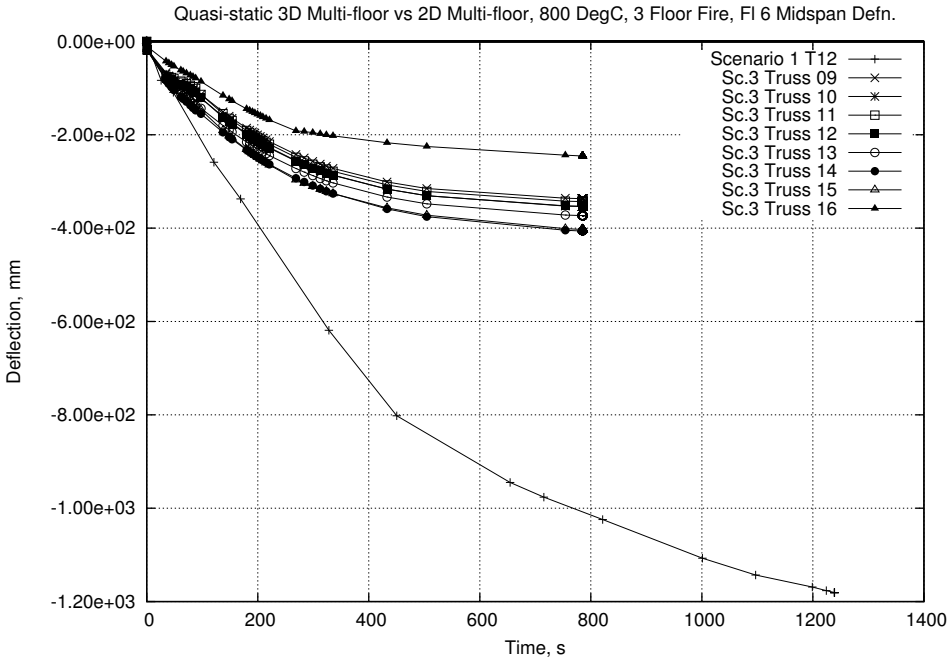

(a)

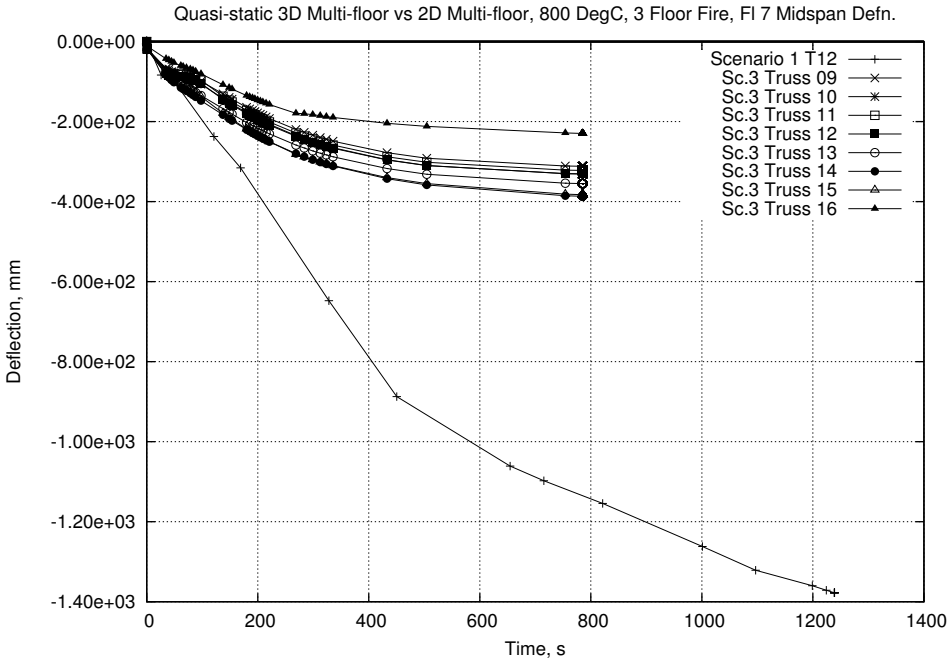

(b)

Figure 7.30: Scenario 3 : Area 2 Midspan Deflection

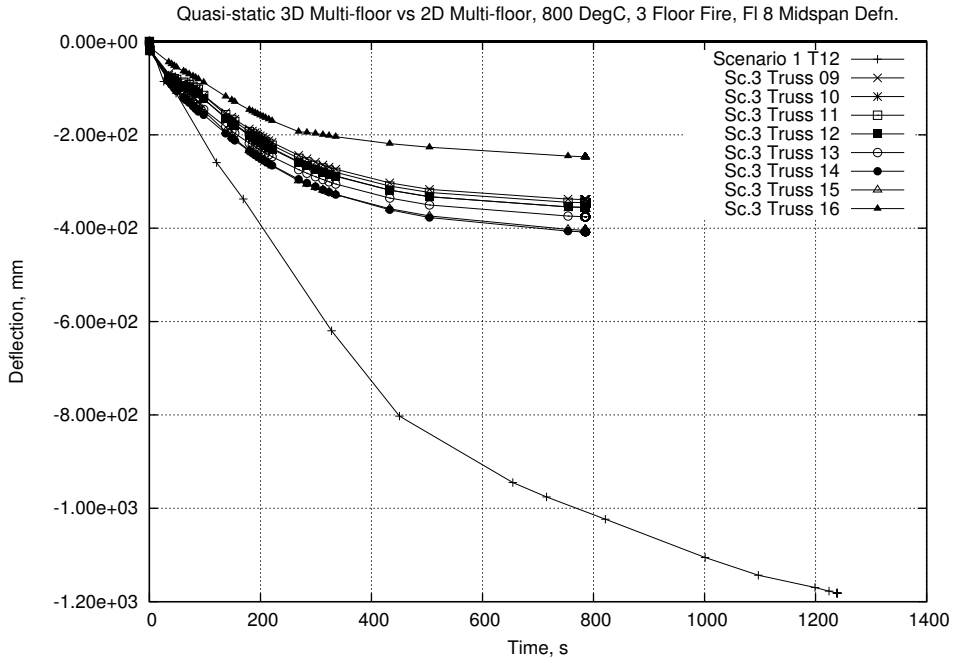

(a)

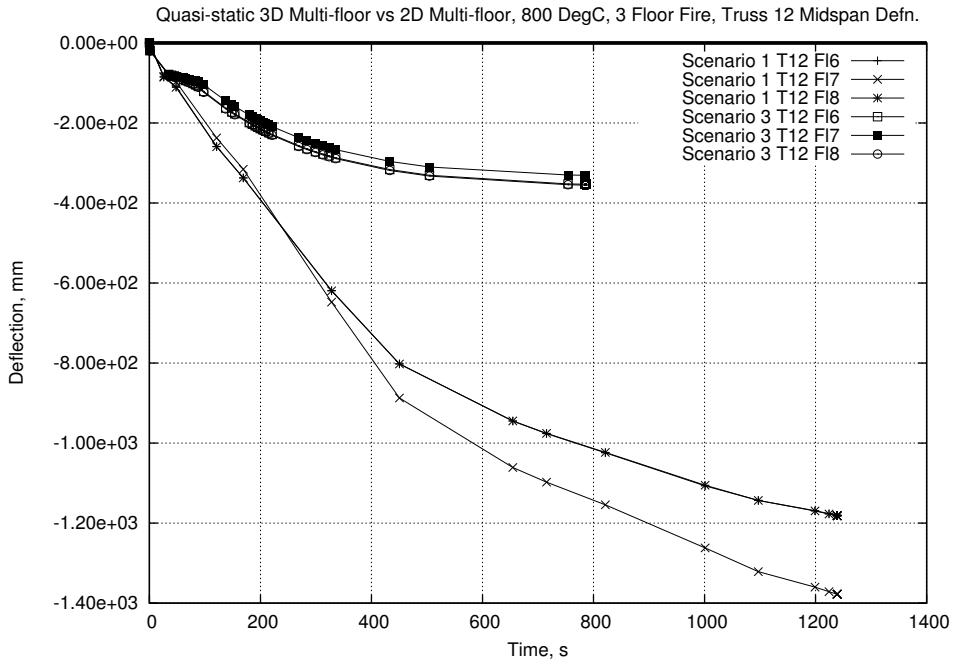

(b)

Figure 7.31: Scenario 3 : Area 2 Midspan Deflection (Cont'd)

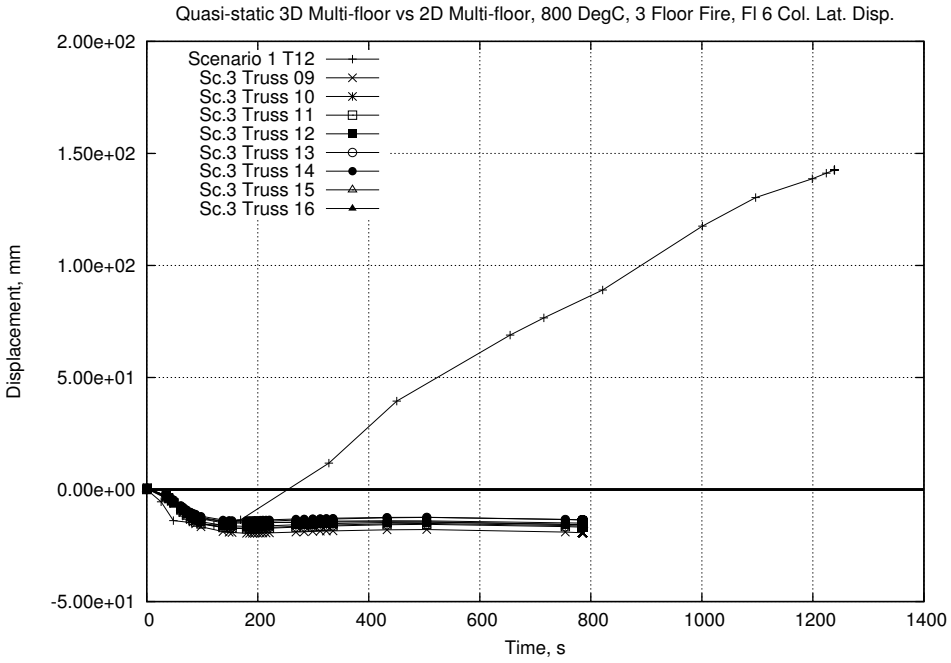

(a)

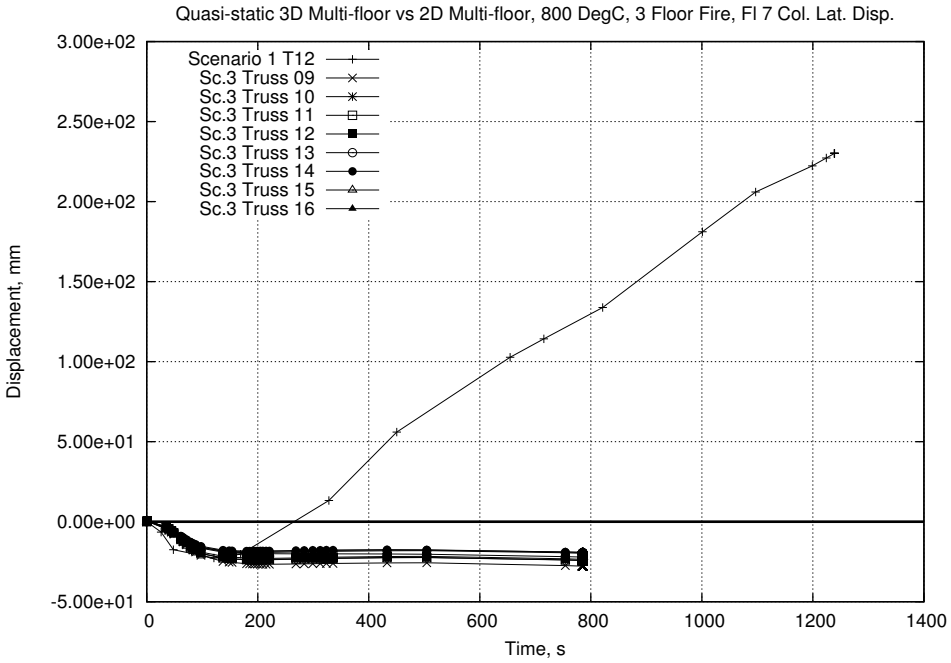

(b)

Figure 7.32: Scenario 3 : Column Lateral Displacement

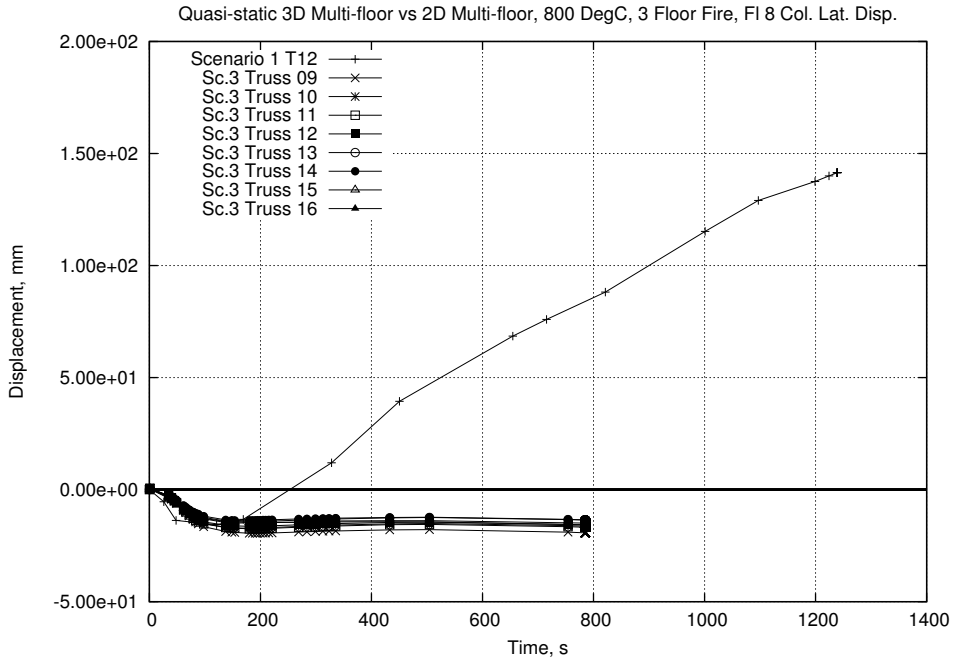

(a)

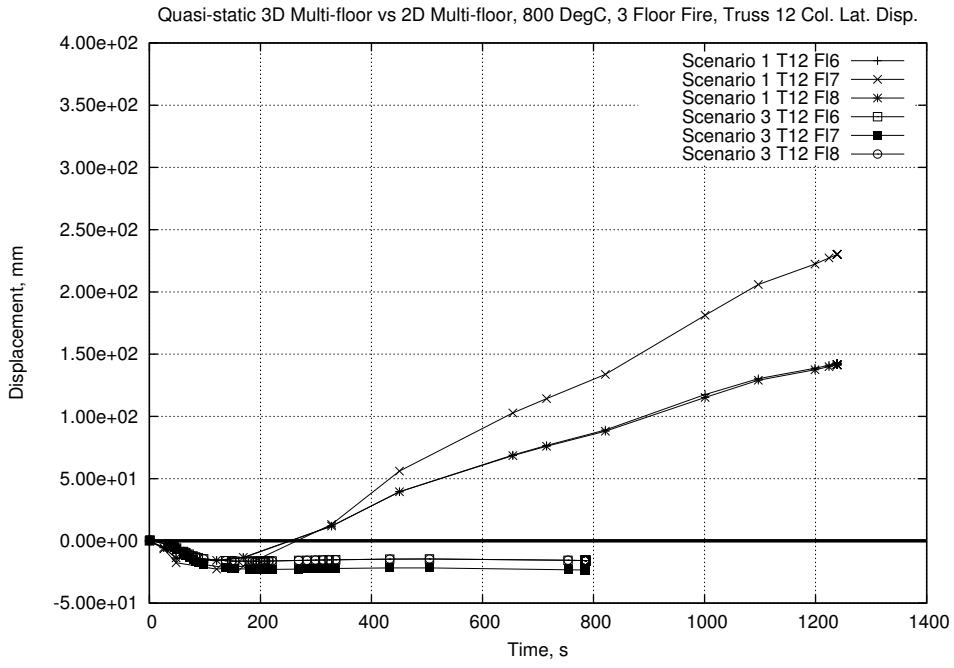

(b)

Figure 7.33: Scenario 3 : Column Lateral Displacement (Cont'd)

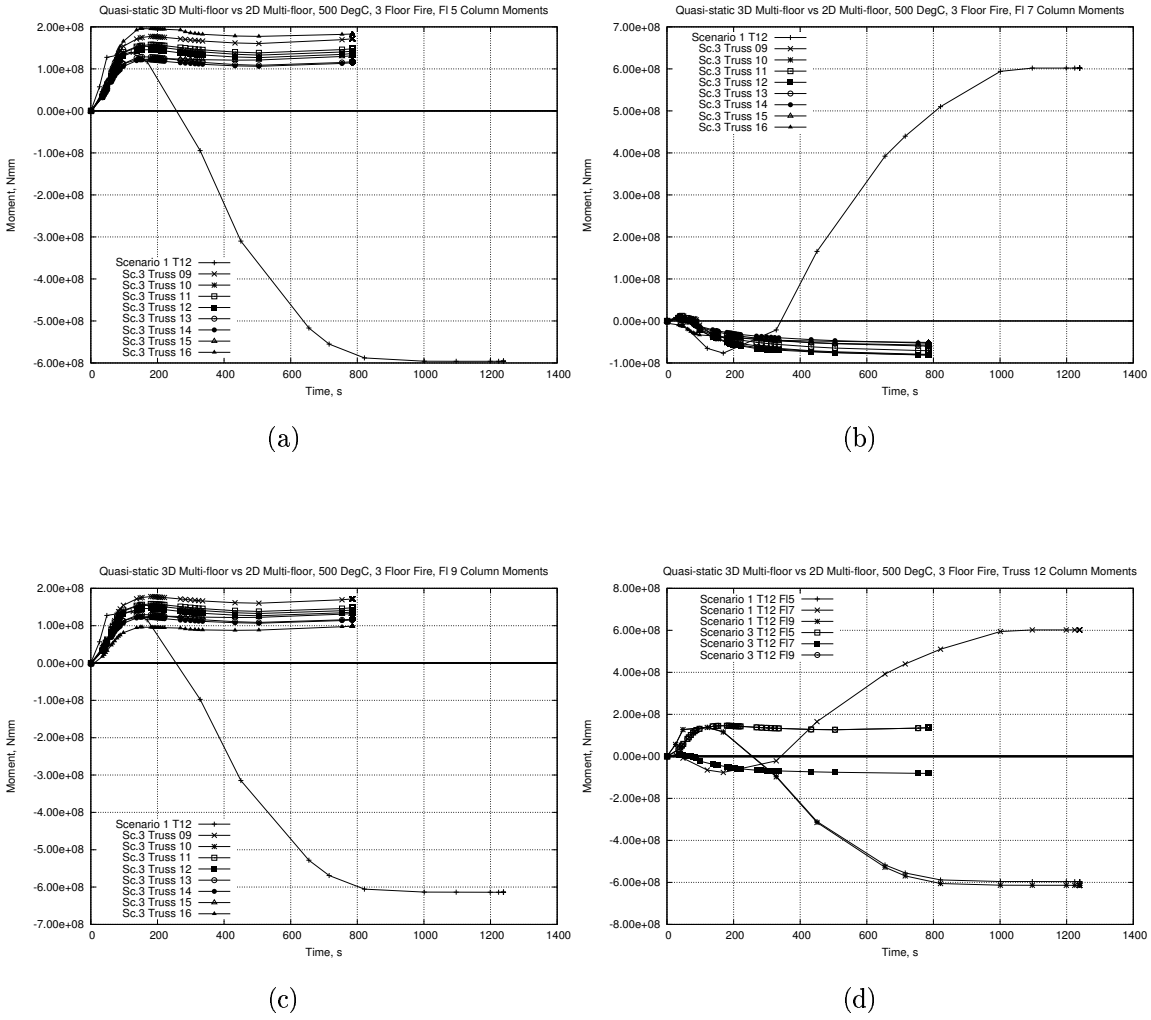

Figure 7.34: Scenario 3 : Column Moments

ability allowed the structure to survive considerably longer when compared to the model without the hat truss.

It was therefore of considerable interest to see if the 3D model would exhibit the same characteristics. Unfortunately convergence issues again became the deciding factor and none of the 3D models with the hat truss managed to run to completion or collapse. The clearest result of Scenario 4 is that the addition of the hat truss has a negligible effect on the global response of the structure. Figures 7.35 & 7.36 show the floor membrane forces in the connections. Results from Scenario 4 are compared to a 2D model with the same fire regime and a hat truss (Scenario 6 in Chapter 5) for Figures 7.35 and 7.36.a. Figure 7.36.b compares the results of Truss 12 on several floors between Scenario 4, Scenario 1 and the 2D hat truss model. The comparison in Figure 7.36.b reinforces the idea that the addition of the hat truss does not significantly alter the early response of a structure to a fire. The responses of Scenario 1 and Scenario 4 are extremely similar. The results from the 2D work presented in Chapter 4 indicate that it is only once a failure mechanism has been initiated that the hat truss will become fully engaged. The initial failure mechanism will then re-form once the hat truss is overcome. Unfortunately the 3D models did not reach far enough into the analysis time to allow a similar effect to be seen.

As with the comparisons for Scenario 1 (Section 7.2.2.1, Figures 7.6-7.15) the 3D results match well with the 2D results. The same trends are seen in all the analyses compared in Figures 7.35 & 7.36.

As collapse was not seen in either Scenario 1 or Scenario 4 it is difficult to determine the effect of the hat truss in the 3D models. A comparison of the forces seen in the column bases will give the best indication of the redistribution needs and capabilities. The locations of the output can be seen in Figure 7.37.Figure 7.38.a compares the column forces in a slice through Truss 12 in both Scenario 1 and Scenario 4. Again this is the most comparable section to the 2D models so Figure 7.38.b shows results for the 2D hat truss model and Scenario 4. The primary difference between the traces in Figure 7.38.a (comparing Scenario 1 and Scenario

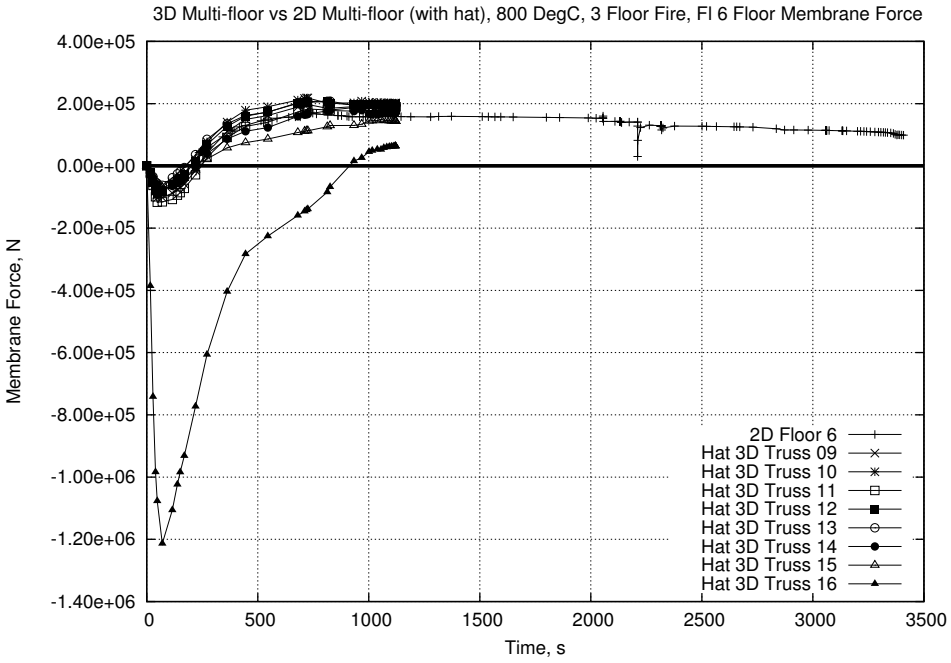

(a)

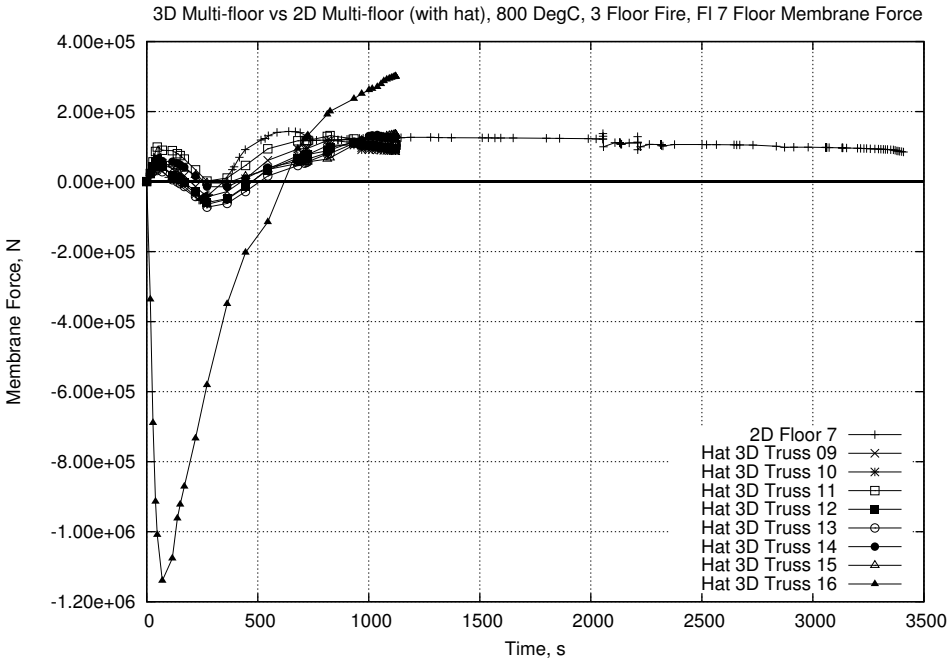

(b)

Figure 7.35: Scenario 4 : Floor Membrane Forces

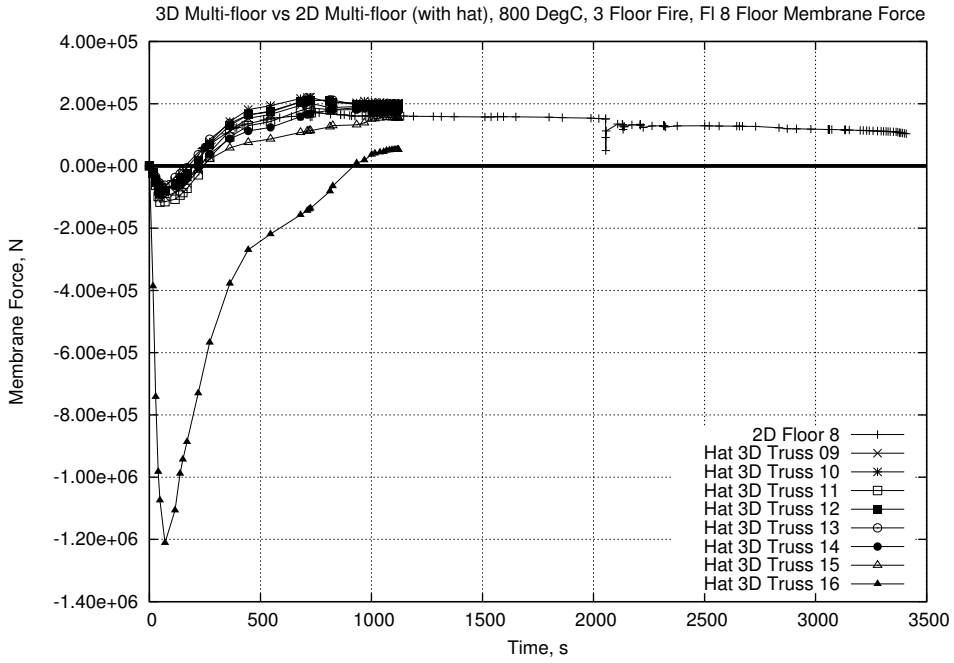

(a)

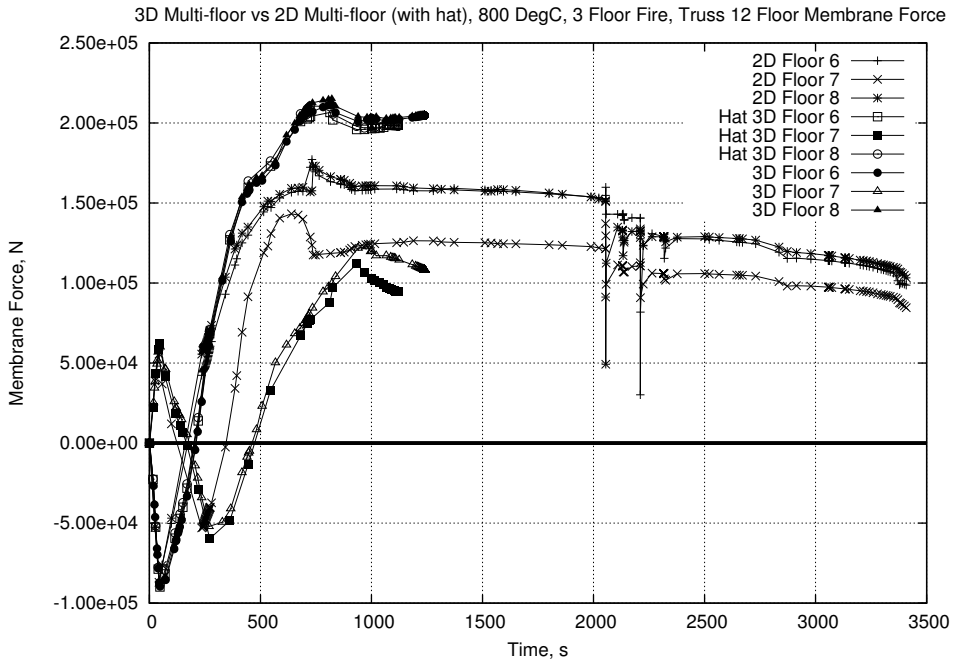

(b)

Figure 7.36: Scenario 4 : Floor Membrane Forces (Cont'd)

4) is that Scenario 4 has the extra weight of the hat truss floors. The presence of the hat truss will also help redistribute gravity loading in a slightly different manner to Scenario 1. Hence each column in Scenario 4 does not take a fixed amount of extra loading. When comparing the trends in Figure 7.38.a the similarities are clear. A close examination of the traces for A2 Col 57 and A5 Col C7 in Figure 7.38.a shows a slightly higher gradient for Scenario 4 just before convergence failure. Logically this should be the effect of the hat truss transferring the load between the outer columns and core more efficiently, although it may be due to an unforeseen mechanism.

The comparison between Scenario 4 and the 2D variant, in Figure 7.38.b, shows significantly less agreement than the other comparisons shown above. This is again primarily down to the change from the 2D to the 3D models. In the 2D model the loading was not corrected (i.e. increased) to take account of the relatively small strip of core being included. The core columns in the 3D analysis therefore exhibit significantly higher forces. The columns in the 3D analysis were sized relative to the load upon them and under ambient, gravity loading are at less than 50% capacity. Some of the trends remain the same, however, with the outer columns (A2 Col 57 and 2D Col 8) showing some redistribution back into the adjacent core columns.

Examination of a greater number of columns along the building faces also shows that the general response is extremely similar between Scenarios 1 and 4. Figure 7.39.a shows the response, in Scenario 4, of the columns in Area 2 that are attached to trusses. Figure 7.39.b shows the response of the intermediate columns (please refer to Figure 7.3 for details of column locations). For the first 700 seconds of the analysis there is little change in the column forces. As the columns in the centre of the long span side are drawn further inward then they begin to shed load. It is at this point in Figure 7.38.a that the core columns begin to take increasing load. Figure 7.39 also shows the columns toward the corner of the building begin to take increasing load. The columns toward the corner are being displaced significantly less and hence can take further loading. Figure 7.39.b indicates that the intermediate columns are reacting in a very similar manner to the main columns. There is

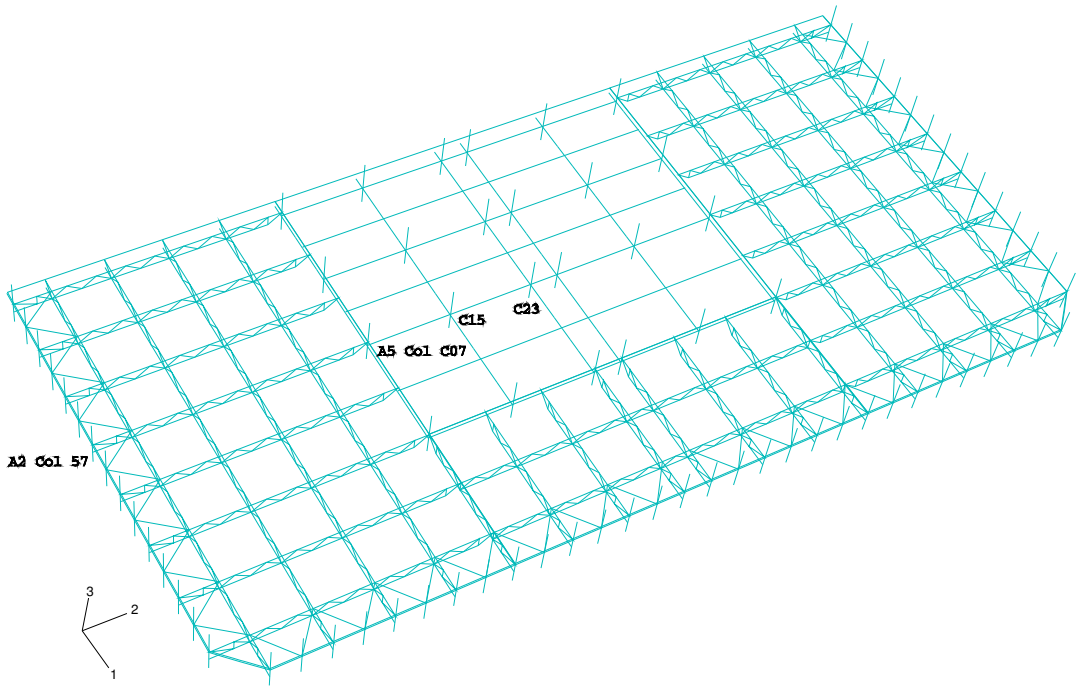

Figure 7.37: Scenario 4 : Column Base Output Locations

some difference in maximum loading as the spandrel beams do not evenly distribute the loading from the main columns to the intermediate columns. However the loads on the intermediate columns change in the same manner as the main columns. The responses for AdCols 49 to 45 show a staged redistribution of loading as each column in turn is pulled further inward and sheds load on the the adjacent columns. The relative clarity of the staged redistribution of the intermediate columns may be related to the lag which is seen between displacement of the main columns and that of the intermediate columns. Reference to Figure 7.19 shows this response for Scenario 1 which is a very close match, in this regard, to Scenario 4.

The redistribution of load in Scenario 4 (and indeed in a similar manner in Scenario 1) is being performed both by the spandrel beams through the outer structure and through the hat truss and floor structure to the core. Due to the convergence failure before clear mechanisms have formed in the outer columns it is not clear to what extent the hat truss would be able to continue this redistribution.

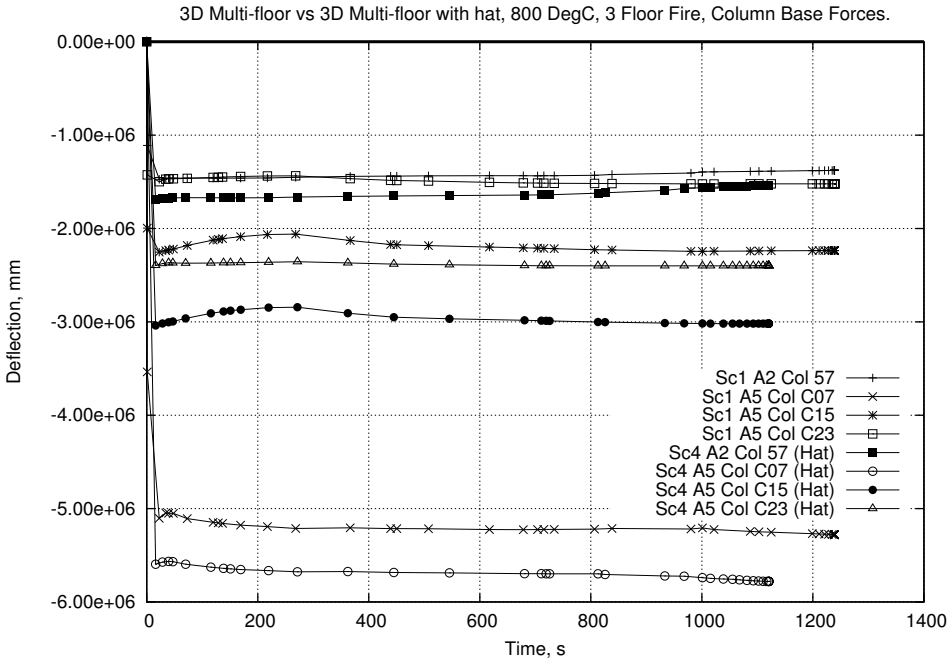

(a)

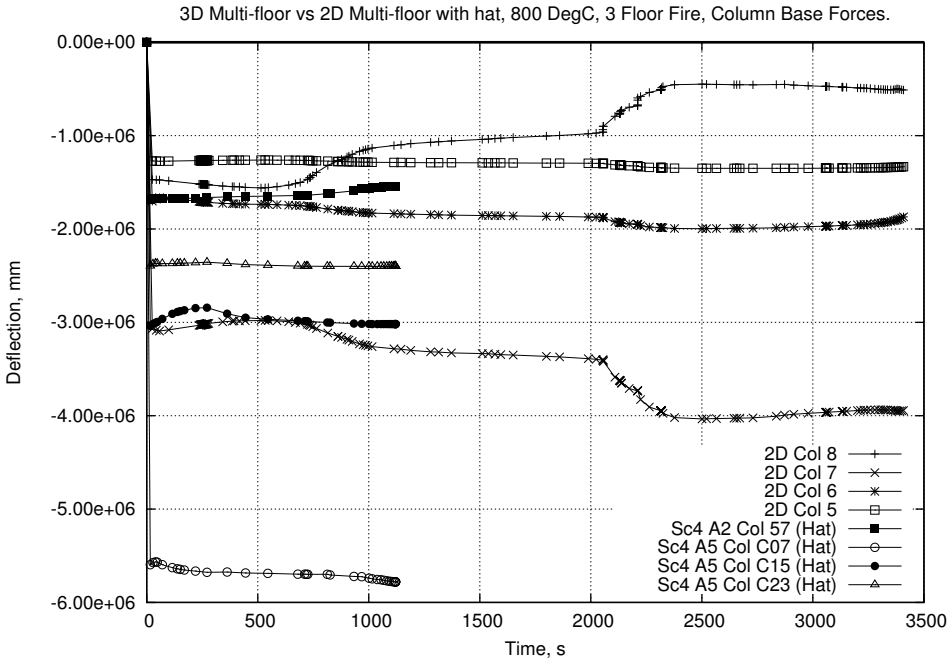

(b)

Note : 2D Col 8 is equivalent to A2 Col 57, 2D Col 7 is equivalent to A5 Col C07, etc.

Figure 7.38: Scenario 4 : Column Base Forces

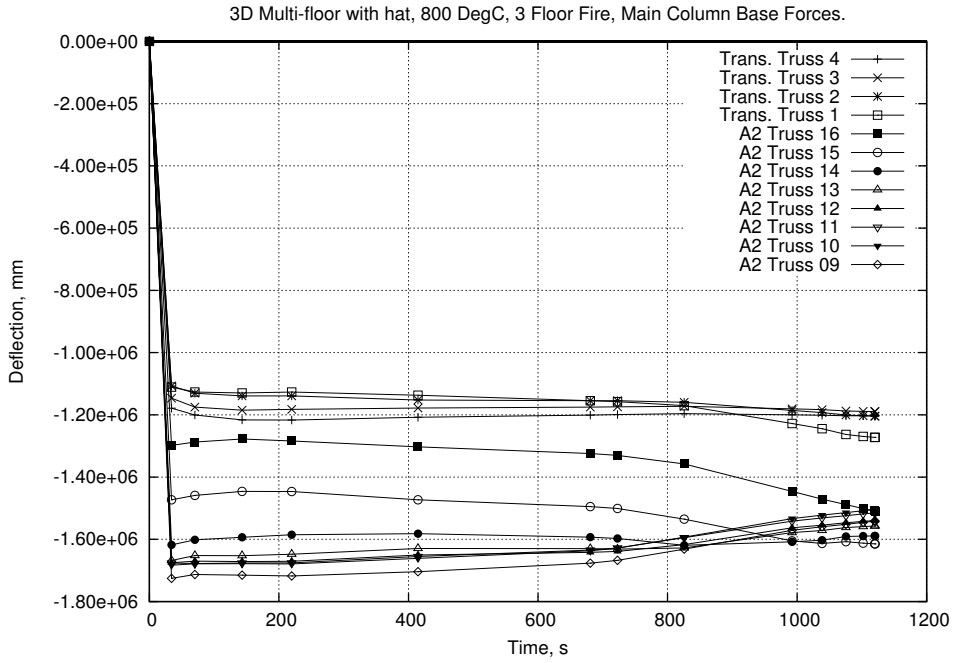

(a)

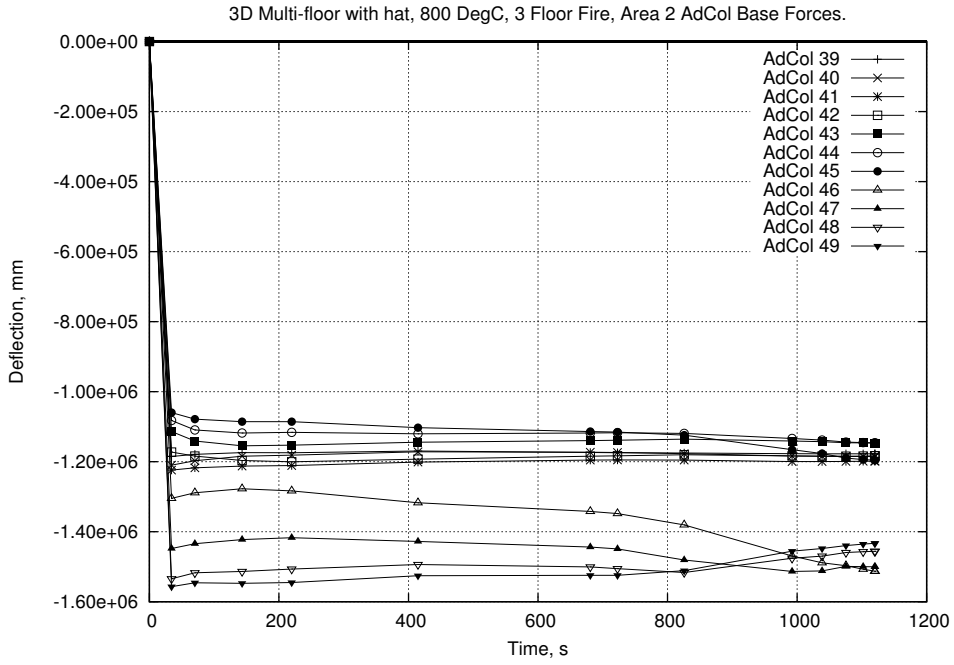

(b)

Figure 7.39: Scenario 4 : Outer Column Base Forces

An examination of the vertical displacement at the top of the columns shows a similar response to Scenario 1. Figure 7.40.a shows the deflection in the main columns in Area 2 for Scenario 4. Cross referencing to Figure 7.16.b it can be seen to be very similar. A direct comparison in Figure 7.40.b between the truss line 12 columns shows just how close the results are. The extra initial deflection in Scenario 4 is due to the extra weight of the hat truss floors. The convergence failure that strikes Scenario 4 may be related to this extremely similar result. It may be that the inclusion of the hat truss floors is stable under normal loading but that the model cannot properly calculate the redistribution of forces as the outer columns begin to fail. It may also be a direct indication that the hat truss cannot in fact redistribute the forces effectively. The slight reduction in time to convergence failure compared to Scenario 1 may be due to the slightly higher loading in the outer columns due to the hat truss floors being added.

In conclusion the effects of the hat truss could not be fully investigated in the 3D models due to problems with convergence. The available results of Scenario 4 agree well with the results from Scenario 1, on which it is closely based. This indicates that the hat truss has little effect on the response of the building in the early stages of the fire because it is not needed. Some of the trends seen in the 2D model, using the same basic scenario, can be seen in Scenario 4 but a full analysis of the later response cannot be presented here. An investigation of the column vertical deflections indicates that the hat truss may be incapable of redistributing the loads effectively in this scenario.

7.2.2.5 Scenario 5 : Quasi-static, 3FF, hat truss, 800°C, heated outer structure

As mentioned in Section 7.1.1 the majority of the 3D models discussed in this chapter did not include heating in the outer structure (i.e. the columns and the spandrel beams). This model is the exception. It was important to test the expansion on a model which included a hat truss as this could alter the column loading more dramatically than if the top of the building was free to expand. The hat truss

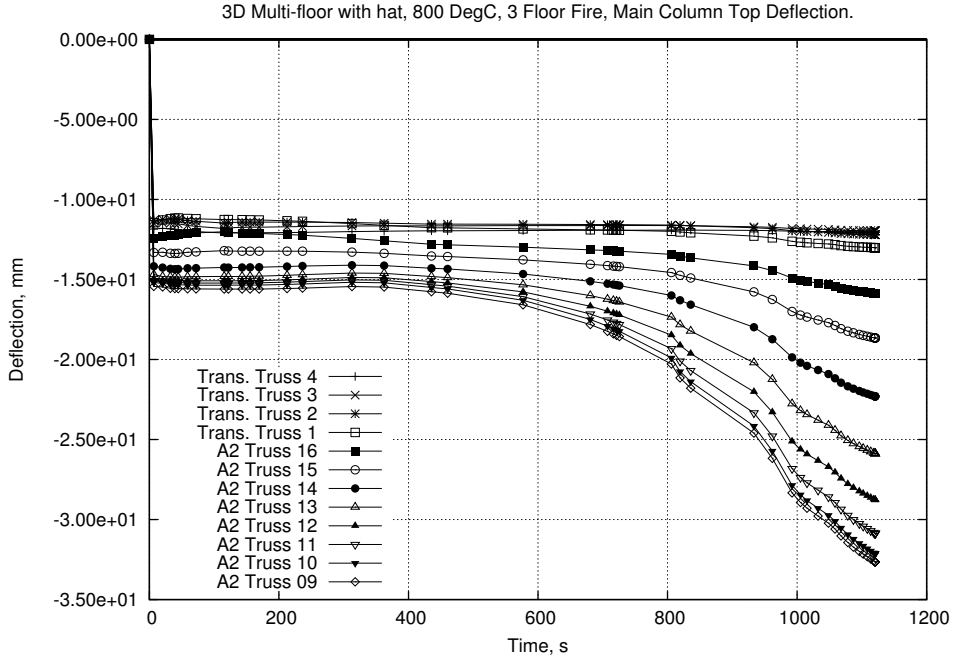

(a)

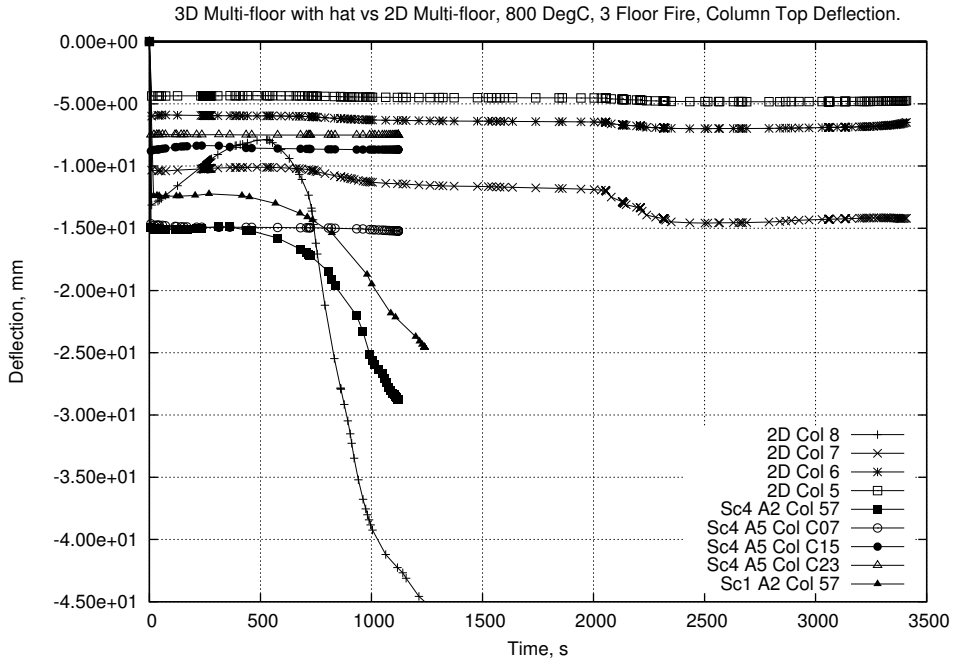

(b)

Figure 7.40: Scenario 4 : Column Vertical Deflection

creates extra restraint for the heated outer columns which, as has been shown in previous work [1, 7], can significantly affect the response of the members.

A brief comparison of the forces to be found in the truss-column connections again shows that this response changes little. Figures 7.41 & 7.42 show Scenario 5 being compared to the 2D version of the scenario and Scenario 4. As with Figures 7.35 & 7.36 the 3D scenarios show a very similar response. In turn the general response trends of the 3D models are closely related to the 2D results.

Investigation of the column base forces shows that the early stages of Scenario 5 proceed in the same manner as Scenario 4. Figure 7.43.a shows a direct comparison between Scenarios 4 and 5 for a selection of columns (marked by the truss they are attached to). The columns chosen are those in which the greatest response is seen. The convergence failure of Scenario 5 appears just before the largest change in response of the columns in Scenario 4. Figure 7.43.b shows a close up of the graph between 600s and 850s and includes all available data points. It is clear by the close spacing of the data points that some highly non-linear effects are occurring at the point that Scenario 5 fails to converge. The extra complexity of the heating in the outer structure appears to be the trigger between failure and success at this point. Scenario 4 manages to resolve the issues and continues for another 500s or so before also failing to converge.

Convergence issues were the overriding factor on Scenario 5 and the results shown here show the maximum analysis time that was reached. No indicators of collapse were present, unlike in Scenarios 1 and 2, and it appears that a local instability occurs at the point the analysis fails to converge. At the point the analysis fails the temperature in the columns is still under 100°C. It is only significantly later in the analysis that the effect of column heating would be seen using this scenario.

7.2.2.6 Scenario 6 : Explicit, 3FF, no hat, 800°C

The issues with convergence were felt throughout this research project. The complexity of the 3D multi-floor models meant that these problems were exacerbated.

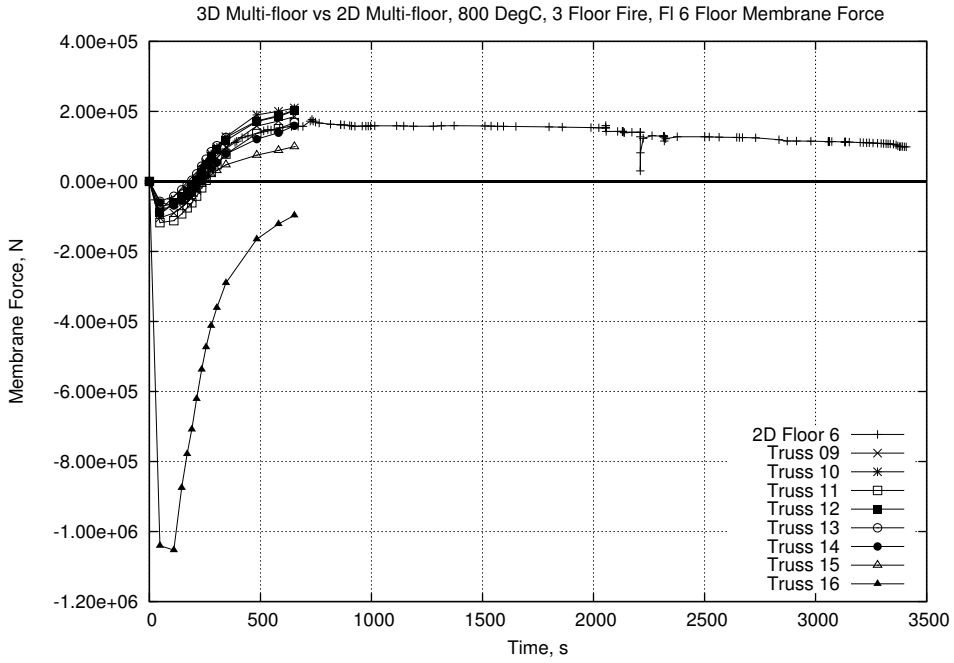

(a)

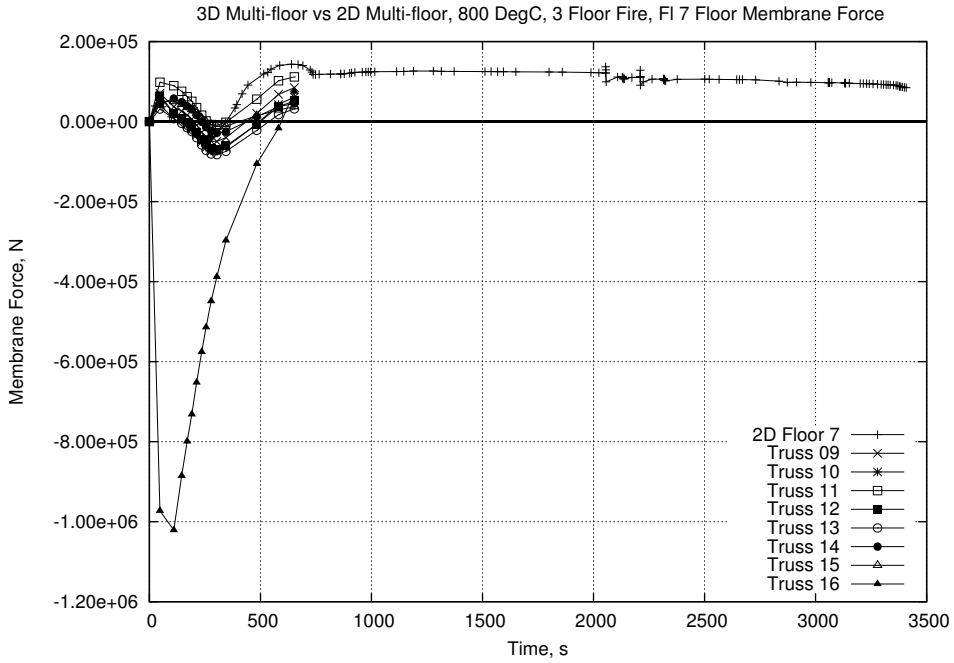

(b)

Figure 7.41: Scenario 5 : Floor Membrane Forces

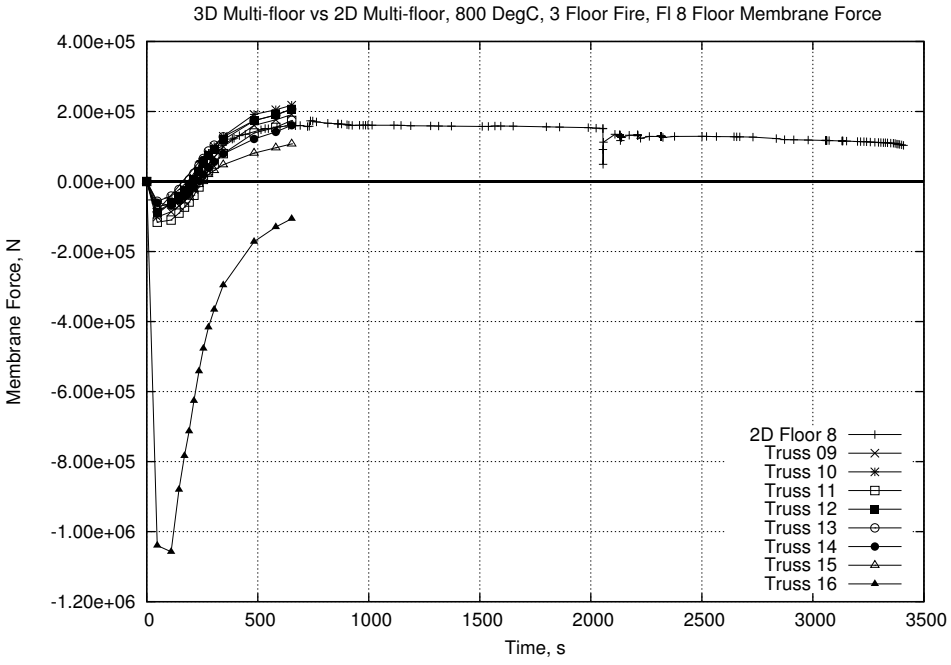

(a)

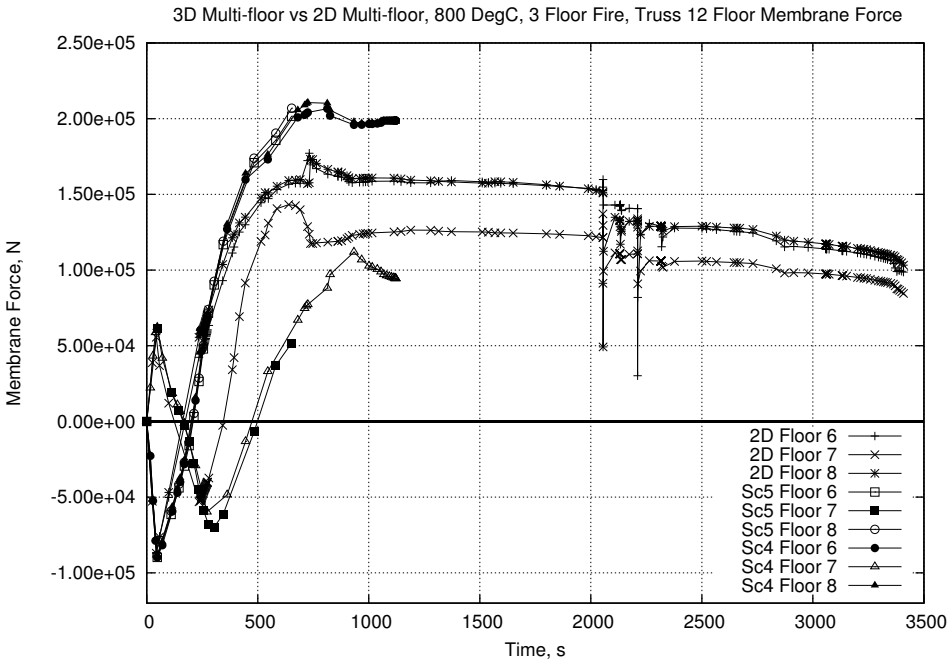

(b)

Figure 7.42: Scenario 5 : Floor Membrane Forces (Cont'd)

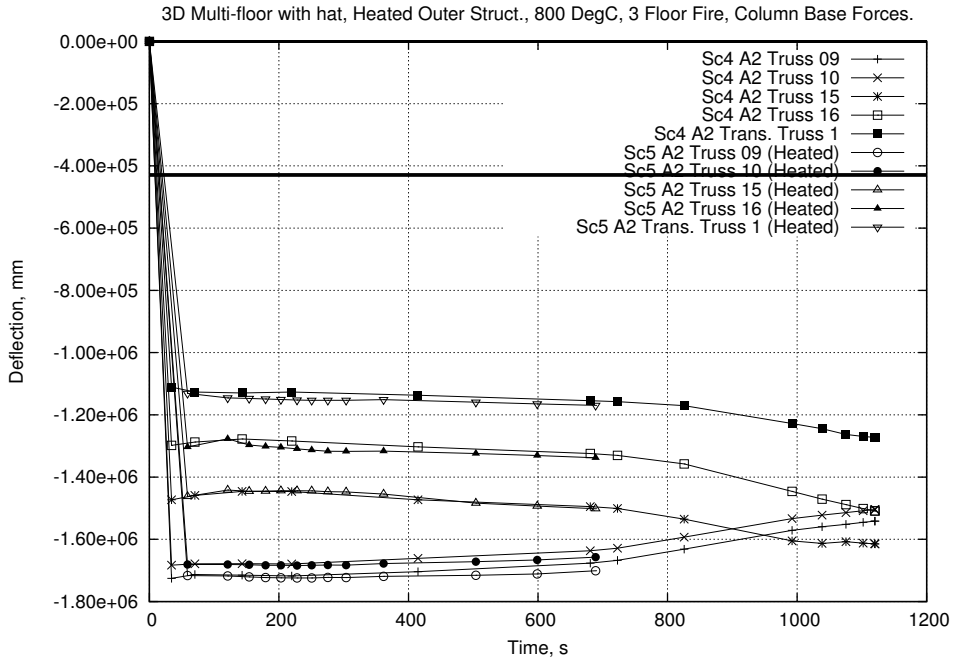

(a)

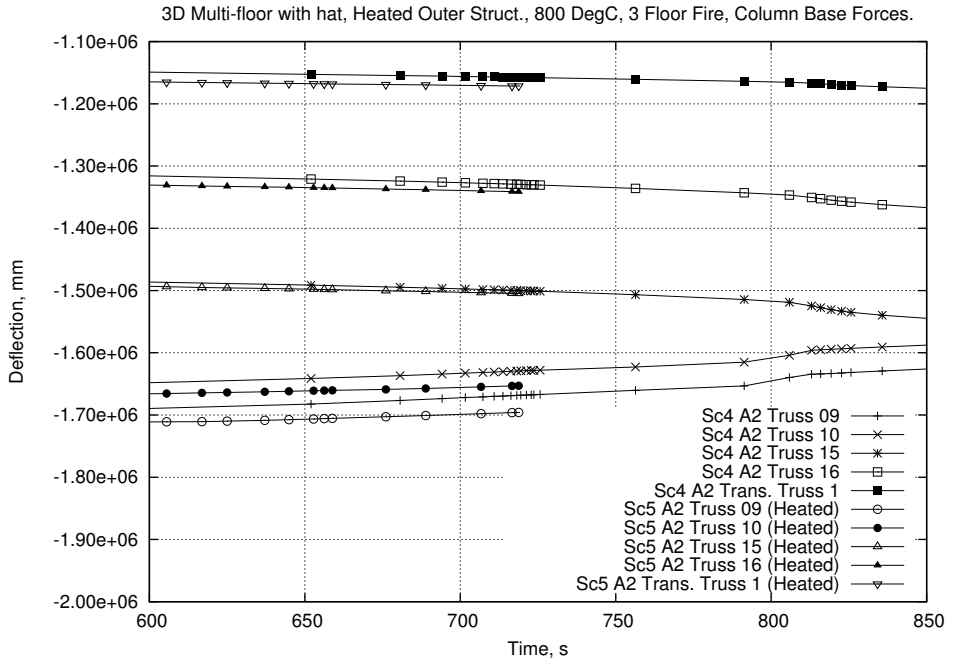

(b)

Figure 7.43: Scenario 5 : Column Base Forces

This is indicated by the fact that none of the 3D Quasi-static models showed direct indications of collapse. To circumvent the issues of convergence two models were run under the Explicit version of ABAQUS.

The main problem with using an Explicit code is that the stable time increment is usually extremely small. For Scenarios 6 and 7 the basic stable time increment was in the order of 10^{-7}s. Considering that the length of time to be investigated was 3600s this size of increment was obviously prohibitively small. When conducting an Explicit analysis there are several options that a user can manipulate to reduce the necessary run time. Some of these are discussed in Appendix A. The main options used here were "time scaling" and "mass scaling". For more details on these methods please refer to Appendix A or to the ABAQUS manuals [73]. Briefly, time scaling involves changing the time the analysis runs for. This can cause issues for convergence in Quasi-static analyses. Mass scaling involves altering the mass matrix of the model in dynamic analyses to increase the time step. This does not alter the mass for loading purposes but instead acts as additional damping in the acceleration terms of the global equilibrium equations. For Scenarios 6 and 7 the analysis was time scaled by a factor of 1000, thereby requiring 3.6s of analysis rather than 3600s. Additionally mass scaling was introduced such that the stable time increment was around $2.6\text{x}10^{-6}$s. This increased the mass of the model as a whole to 250% of its original value for purposes of equilibrium. Mass and time scaling should be used to reach a balance between analysis speed and the validity of results. These methods are discussed in more detail in Appendix A.

The final displaced shape may be seen in Figure 7.44 with vertical displacement contours overlaid. The general response is similar in form to that of the Quasi-static scenarios (cf. Figure 7.5).

The floor membrane forces from Scenario 6 may be seen in Figures 7.45 & 7.46. As with the other scenarios presented in this chapter it compares the values taken from Scenario 6 with those from the appropriate 2D Quasi-static scenario and Scenario 1. The graphs have been constructed such that the peak values from Truss 16 are not shown for clarity in the other responses. As indicated in Chapter 6 the

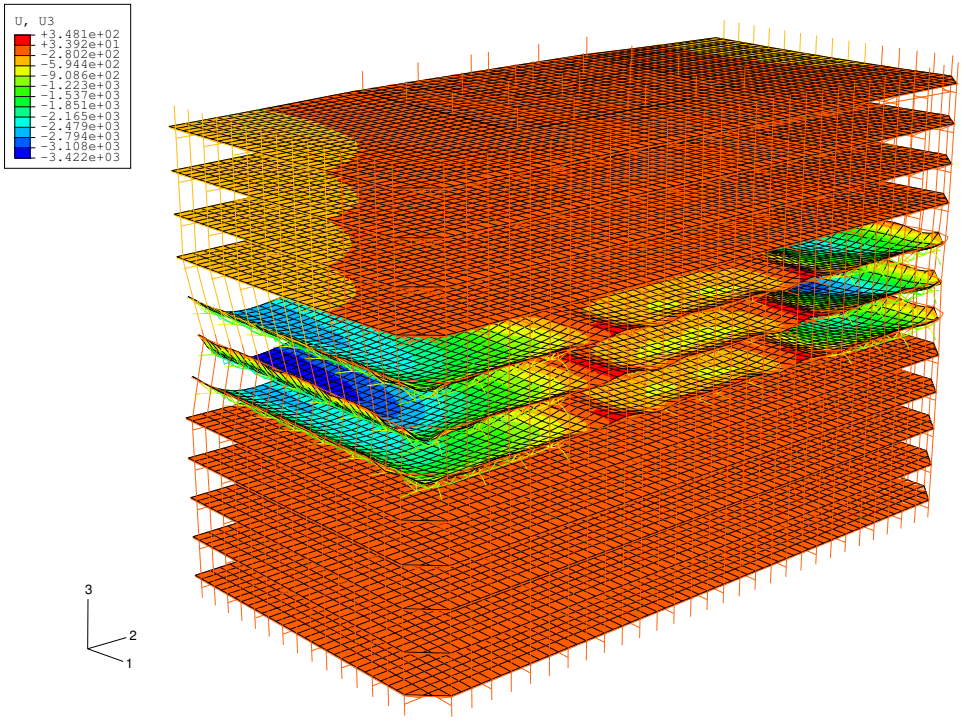

Figure 7.44: Scenario 6 : Final Displaced Shape

response of Truss 16 is heavily influenced by compatibility with the slab and hence produces extreme results.

The extra damping caused by the mass scaling does appear to have degraded the results somewhat. The general trend, when compared to the Quasi-static models, is for the Explicit results to be delayed and, for the force response at least, somewhat amplified. This is consistent with an over-damped model. As the movement of the model is being constrained the thermal expansion is realised as increased forces in the heated members. As this creates a more force-sensitive response based on overcoming the damping, oscillations are seen in the floor membrane forces.

An examination of the column lateral movement, in Figures 7.47 & 7.48, and the midspan truss deflection, in Figure 7.49 & 7.50, helps explain the full response, and how it differs from the Quasi-static models. The extra damping induced by using mass scaling retards the early downward movement of the floor system. Hence the midspan deflections initially show lower values in the Explicit models. The thermal

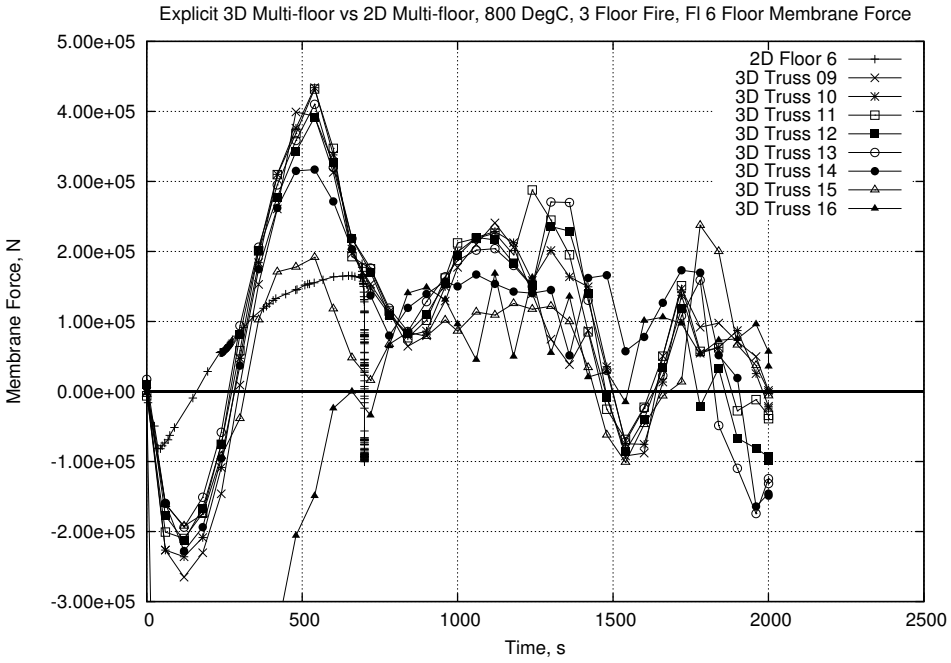

(a)

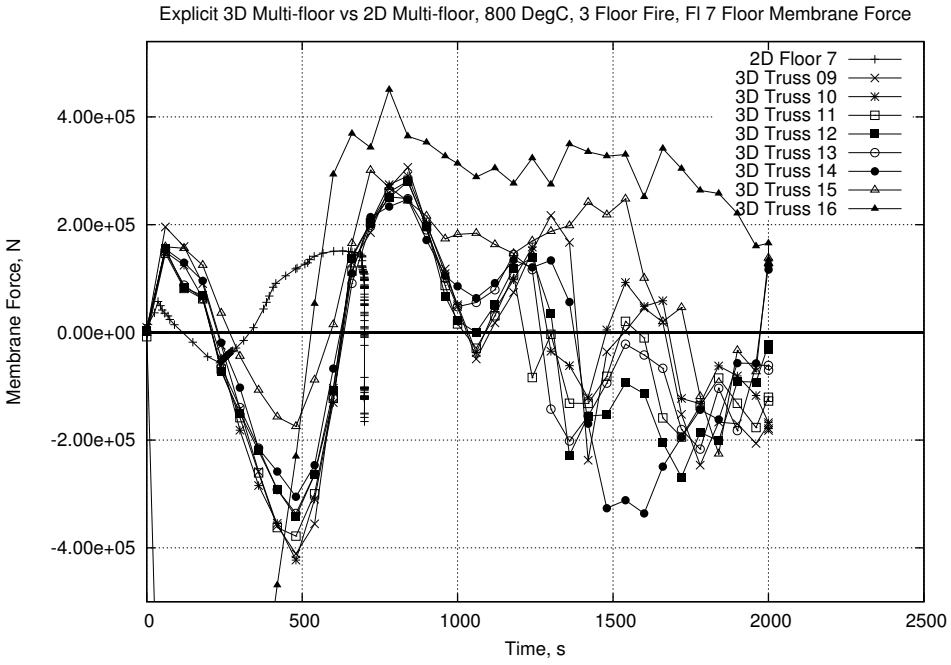

(b)

Figure 7.45: Scenario 6 : Floor Membrane Force Comparison

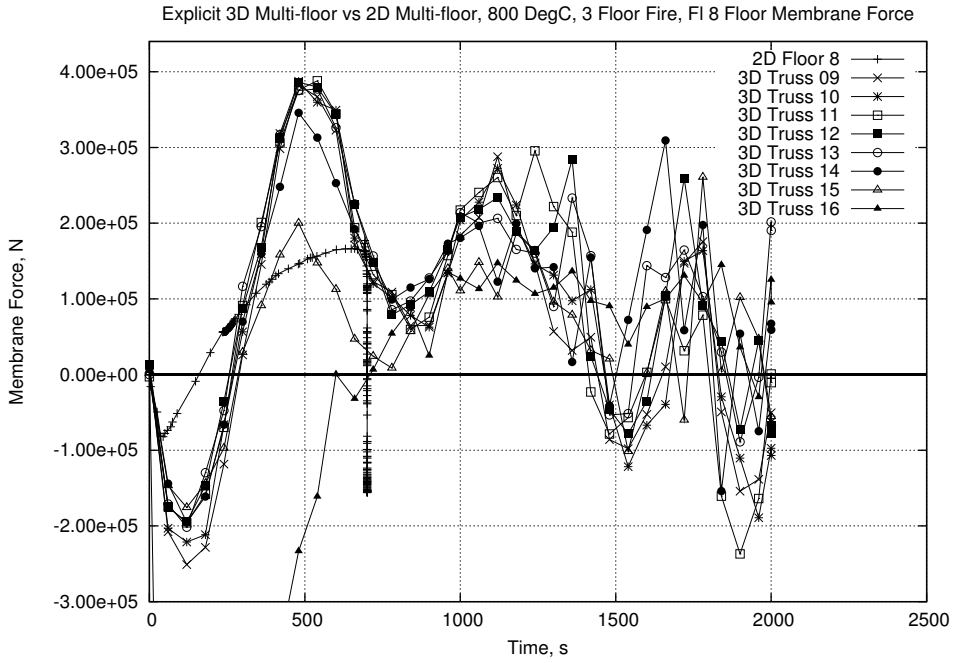

(a)

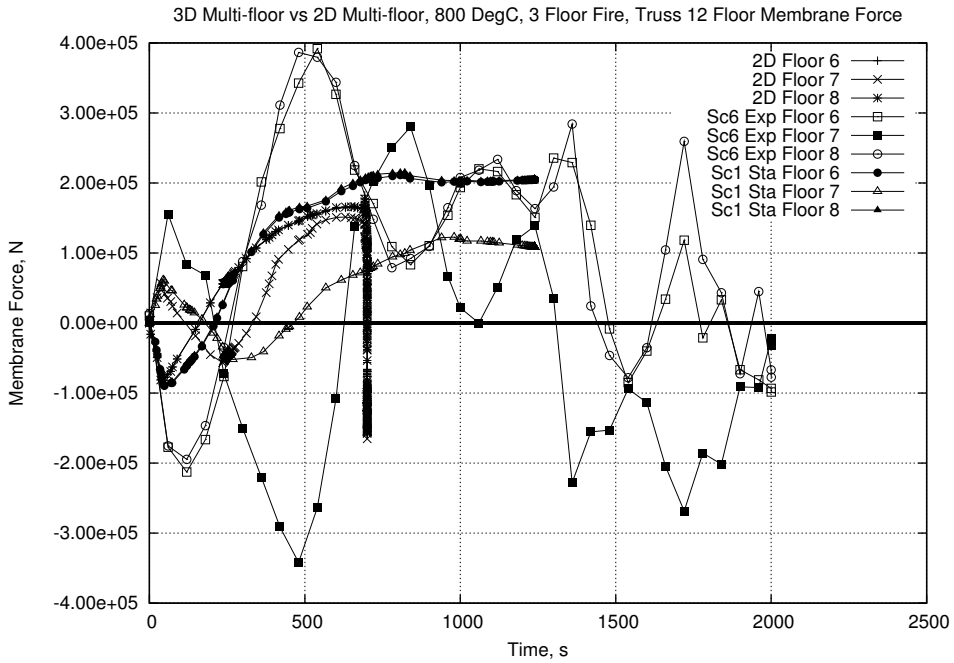

(b)

Figure 7.46: Scenario 6 : Floor Membrane Force Comparison (Cont'd)

expansion cannot be relieved through increased deflections but instead manifests as increased floor membrane force. This in turn leads to increased lateral column movement. At around 500s the increased force in the floor system overcomes the damping and induces higher midspan deflection rates. This is turn induces higher tensile forces and draws the columns inward more. The delay in the displacement and deflection caused by the damping then creates the oscillations seen in the force response.

An examination of the column moments in a similar manner to that shown in Section 4.5.1.2 shows similar evidence. Figure 7.51.a compares the moments in the long span side columns in Scenario 6 to Truss 12 of Scenario 1 for the 5th floor. This is the floor that is effectively a fixed support in the beam theory put forward in Section 4.5.1.2. Although the early responses show rather different results the general trends are similar. The later responses in the Explicit model show good agreement with the Quasi-static model with the moment in the column reaching the predicted yield and becoming reasonably steady. As output was limited from Scenario 6 it was necessary to evaluate the moments in other locations in the columns by other means. Figure 7.51.b shows the moments in the column attached to Truss 12 as evaluated in the same way as the 2D model was in Figure 4.12. The column over the fire floors was assumed to be a beam with point loads provided by the forces in the truss-column connections. As can be seen in Figure 7.51.b the theory results for Ma match well with the actual results taken from ABAQUS. By inference the results for the midspan moment (Mc) will also match well. It is clear that both the "support" and "midspan" moments are reaching the column yield criteria where they stay for around 500s before reducing again. The actual moment result for Ma taken directly from ABAQUS indicate the moment dropping off significantly later but the trends are similar. The drop in column moment from the actual result coincides with the time that the rate of both the column movement and the midspan deflection (as seen in Figures 7.47 through 7.50) begin to increase before the model fails. Thus it may be inferred that global failure of the structure has been initiated but has been delayed somewhat by the level of damping in the

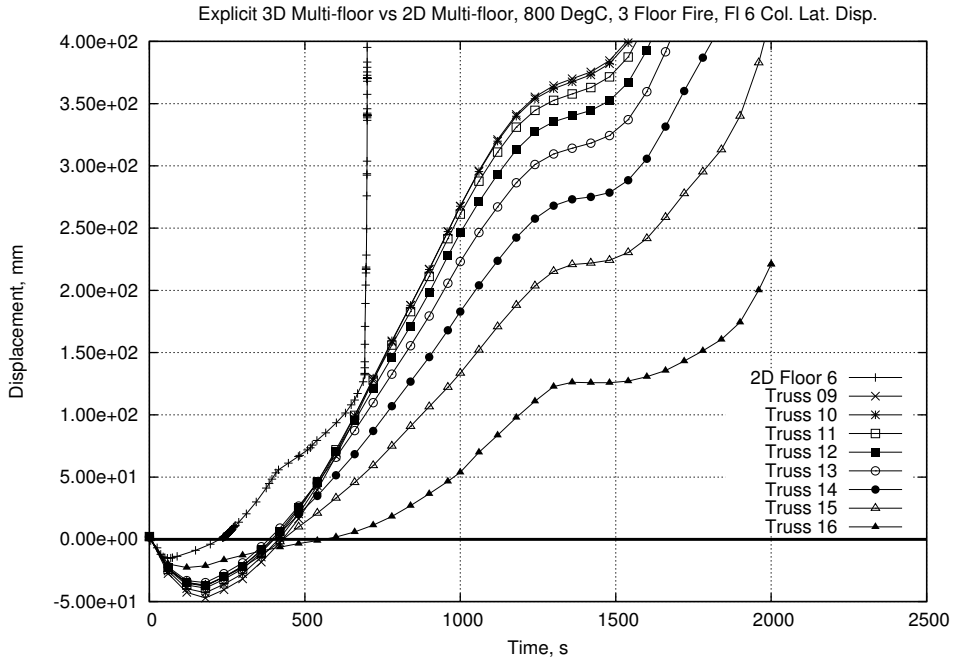

(a)

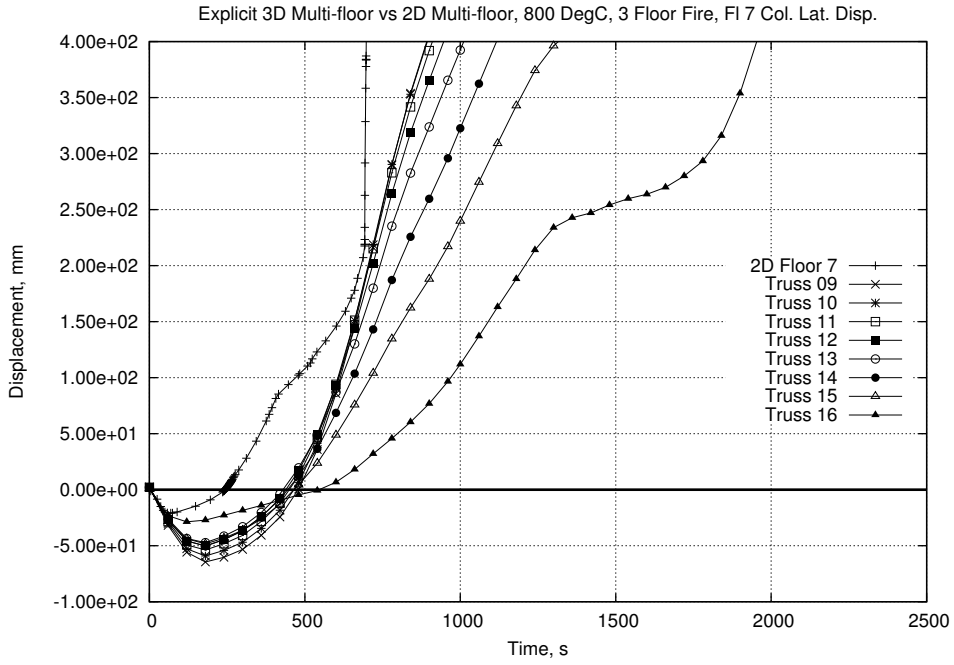

(b)

Figure 7.47: Scenario 6 : Column Lateral Movement Comparison

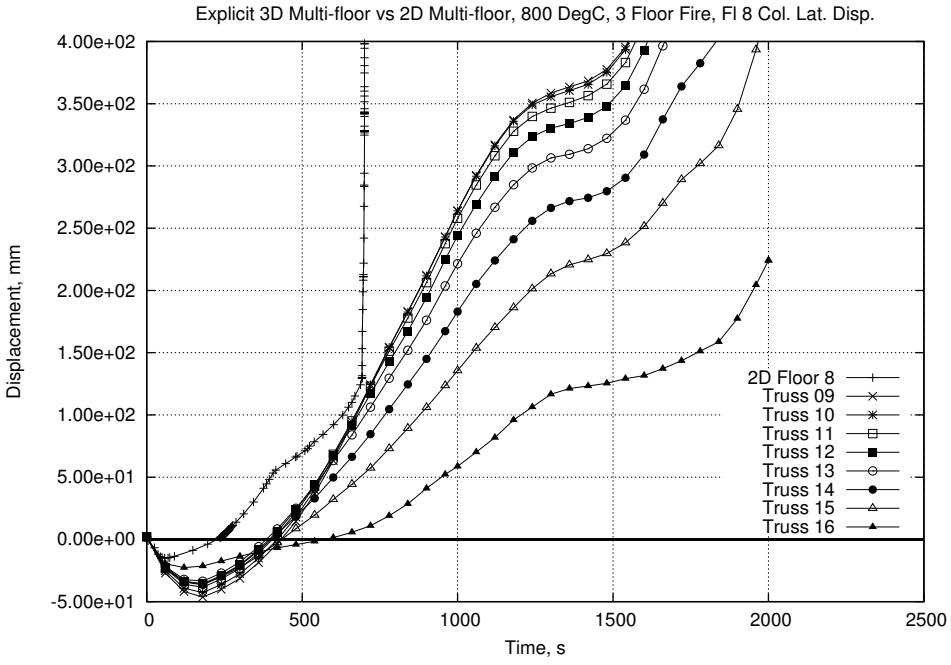

(a)

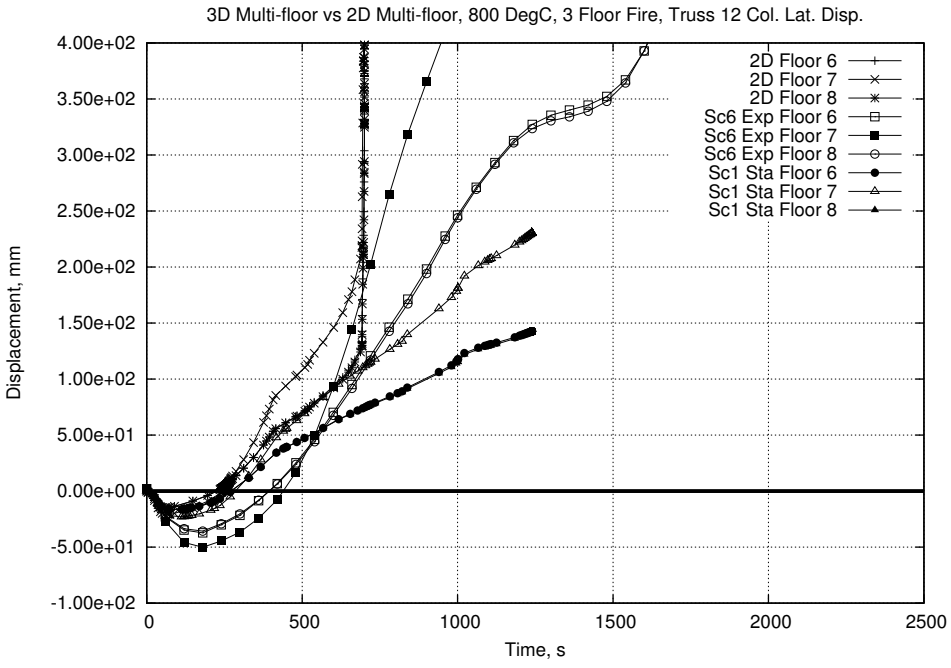

(b)

Figure 7.48: Scenario 6 : Column Lateral Movement Comparison (Cont'd)

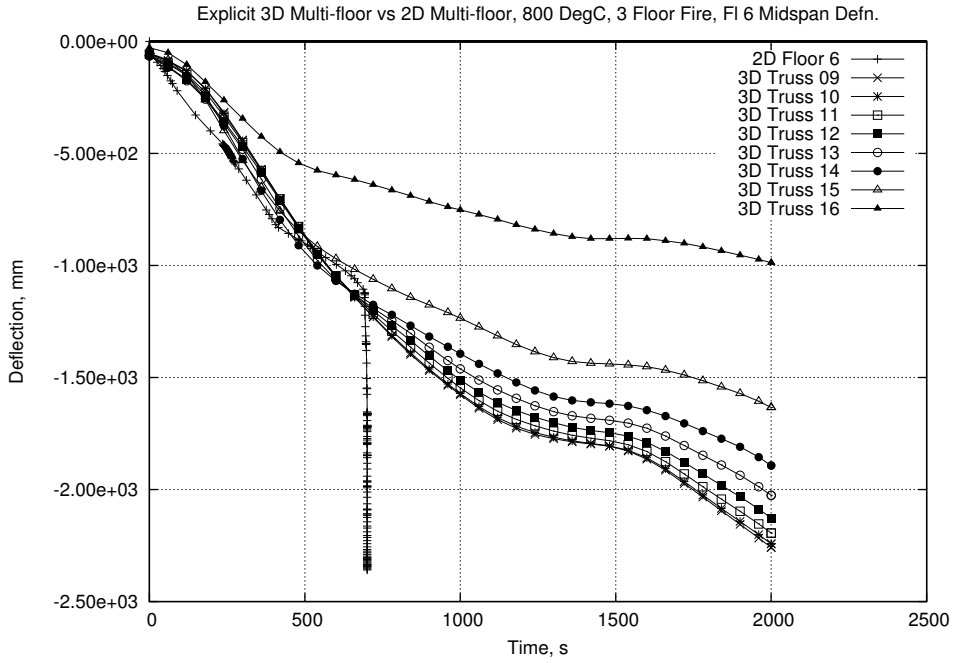

(a)

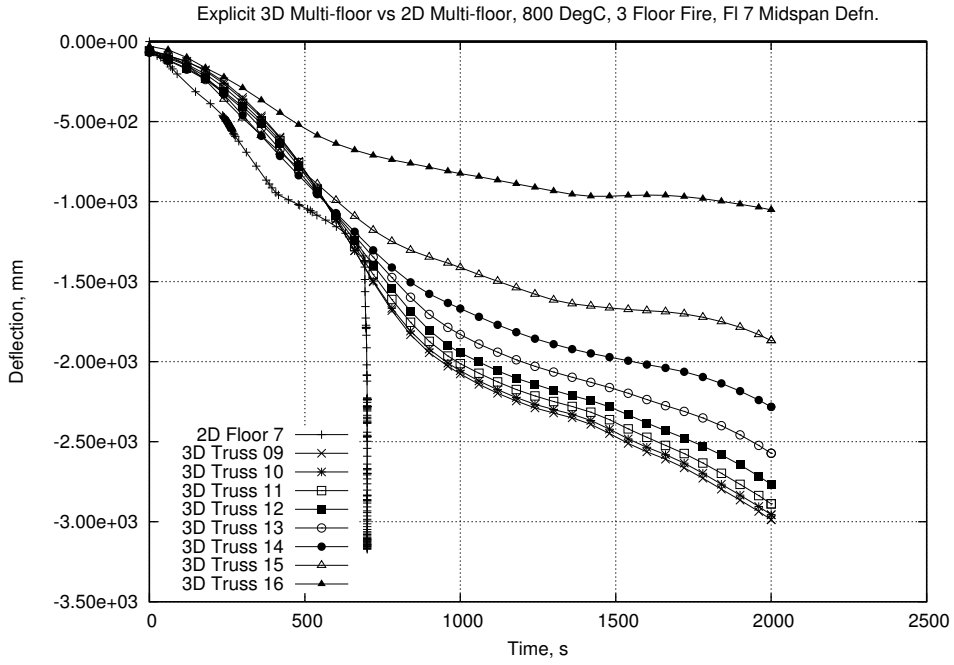

(b)

Figure 7.49: Scenario 6 : Midspan Truss Deflection

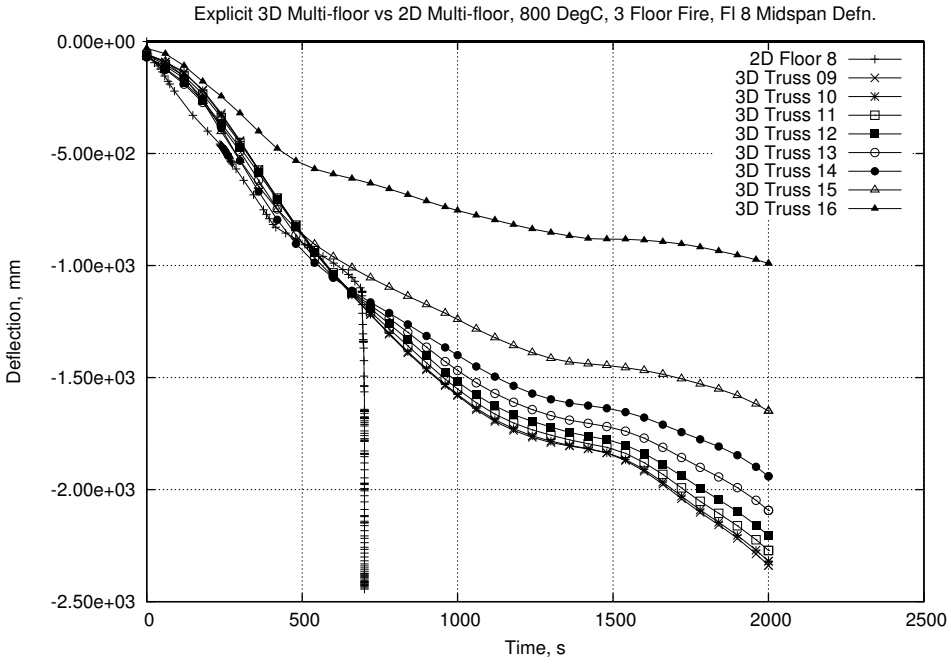

(a)

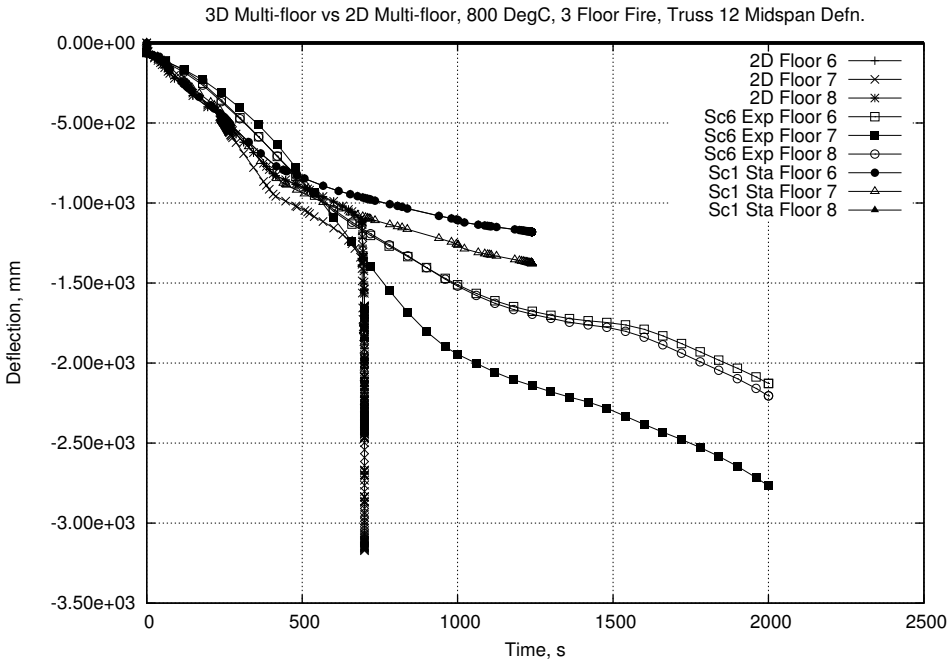

(b)

Figure 7.50: Scenario 6 : Midspan Truss Deflection (Cont'd)

explicit model.

Examination of the columns along the outside of the building yields more evidence that the structure is collapsing. Figure 7.52.a shows the vertical displacement at the top of the long span side columns. The columns in Figure 7.52.a are listed in the order they appear in the structure running from the centre of the long span side to the corner of the building. Both main and intermediate columns are included in the plot. A progressive downward acceleration is seen in these members. The first columns to be affected are those toward the centre of the long span side (A2 Trusses 09 to 11). This agrees with the progression of inward movement of the columns, shown in Figures 7.47 & 7.48, caused by the effects of fire on the floor system.

Figure 7.52.b shows the vertical displacement at the top of the short span side columns. The columns in 7.52.b are listed from the corner of the building toward the centre of the short span side. Again both main and intermediate columns are included. Shortly after 1000s it can be seen that the corner column (A2 Trans. T01) begins to displace downward. This time correlates well with the time when the corner column on the long span side begins to move down (A2 Truss 16). The downwards displacement does not appear to have spread into the columns of Area 4 by the end of the analysis which is an indication of the stiffer structure in this area. A sudden acceleration in the downwards movement of the corner columns in the short span side can be seen at around 1700s. This indicates that the stiff corner assembly is being overcome and that collapse of the structure has been initiated.

The collapse mechanism seen in the 2D models and indicated in the 3D Quasi-static models can clearly be seen in this model, particularly in Figure 7.44. Again the primary collapse mechanism appears to be the yielding of the long span side columns which leads to plastic hinges and a mechanism forming.

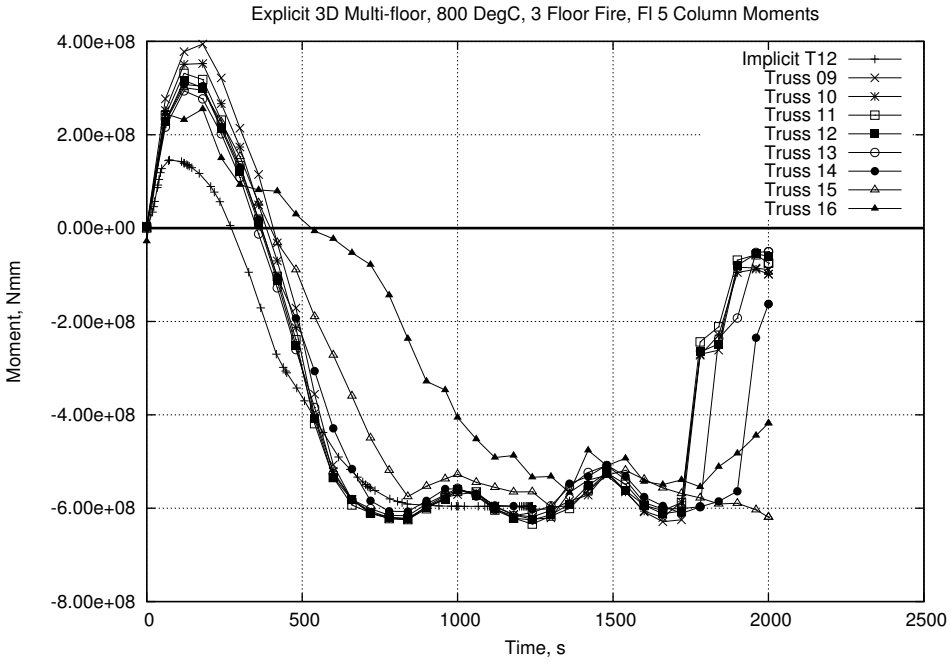

(a)

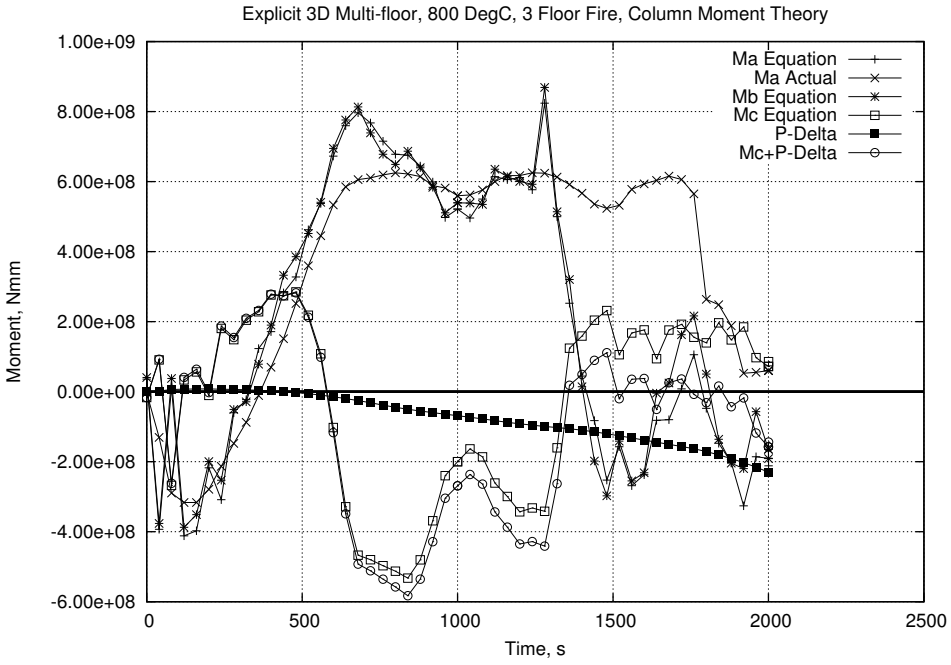

(b)

Figure 7.51: Scenario 6 : Column Moments

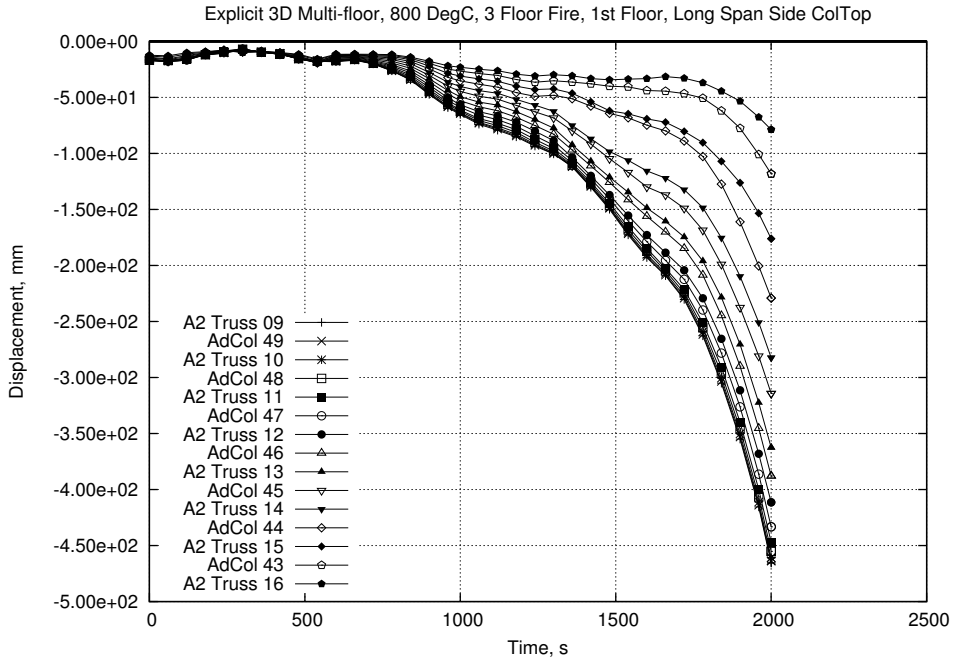

(a)

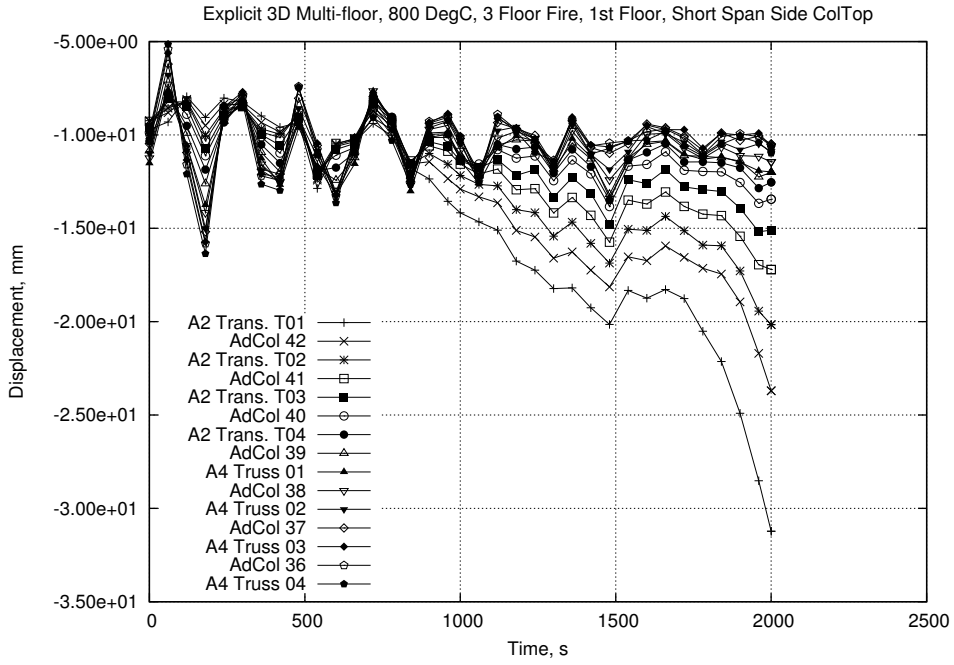

(b)

Figure 7.52: Scenario 6 : Column Top Vertical Displacement

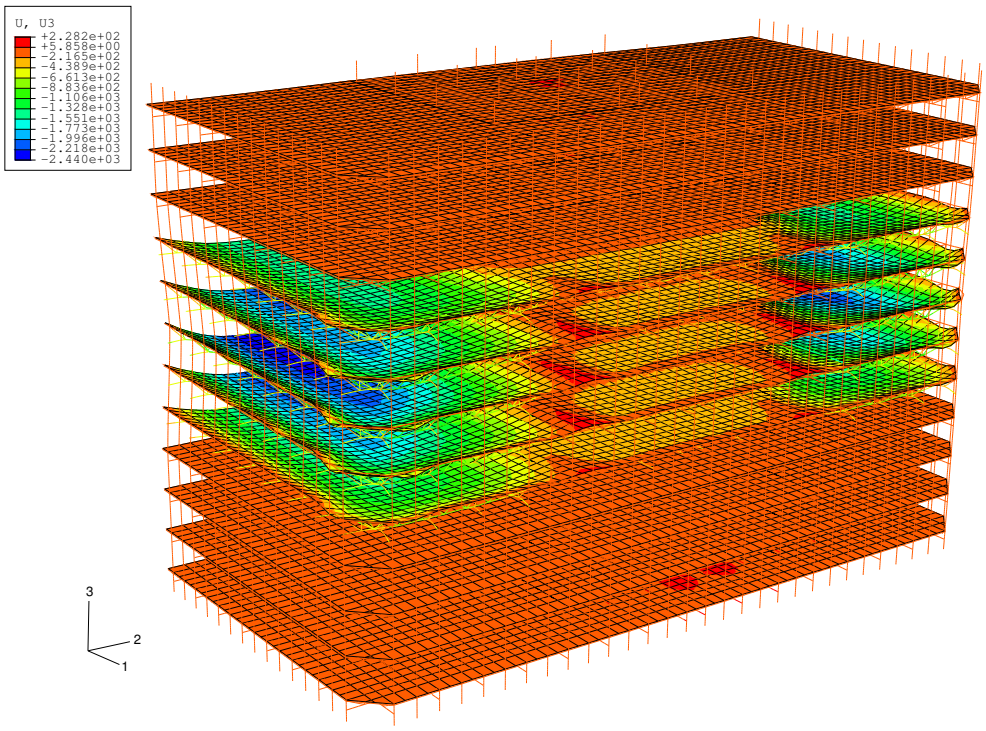

Figure 7.53: Scenario 7 : Final Displaced Shape

7.2.2.7 Scenario 7 : Explicit, 5FF, no hat, 800°C

Scenario 7 was also conducted with a view to create obvious failure mechanisms in the structure. The increased threat to the structure from the 5 floor fire scenario may produce a more obvious failure mechanism than the 3 floor fire version. Reference to Figure 7.53 shows that the final displaced shape agrees well with those seen in other scenarios.

Figures 7.54 & 7.55 show the floor membrane forces in the truss-columns connections. As with Scenario 6 the graphs have been constructed such that the peak forces in Truss 16 are not included to add clarity to the response of the other trusses. The results from floors 6 to 9, from Scenario 7, are compared directly to those taken from the Quasi-static 2D model with a 5 floor fire scenario. The trends seen in the results of Scenario 7 are similar to those seen in the 2D model. As with Scenario 6 the results are exaggerated and delayed but over the entire time of the analysis the general profile of the response is similar.

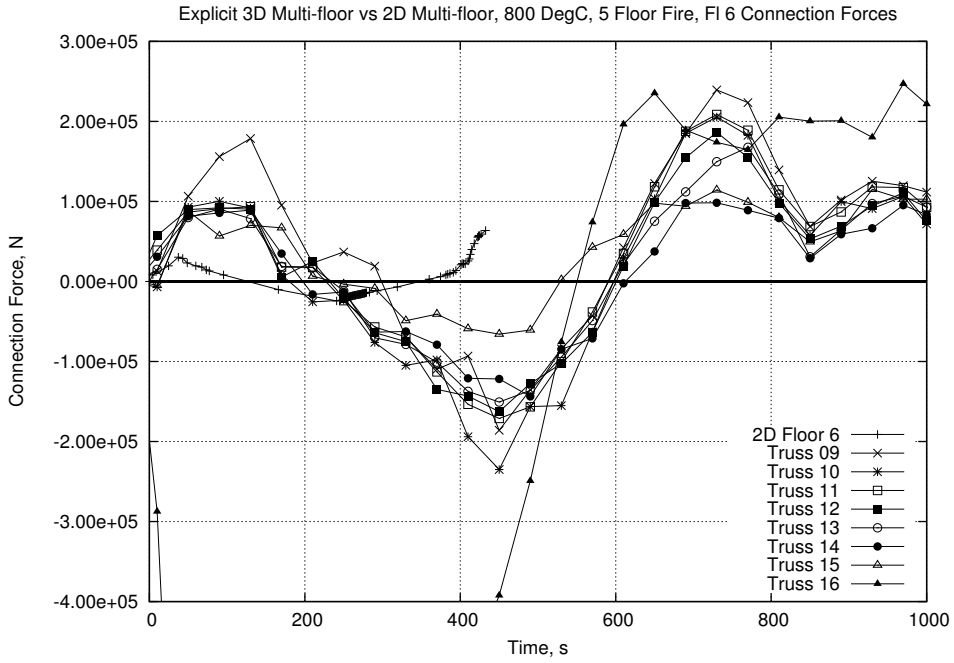

(a)

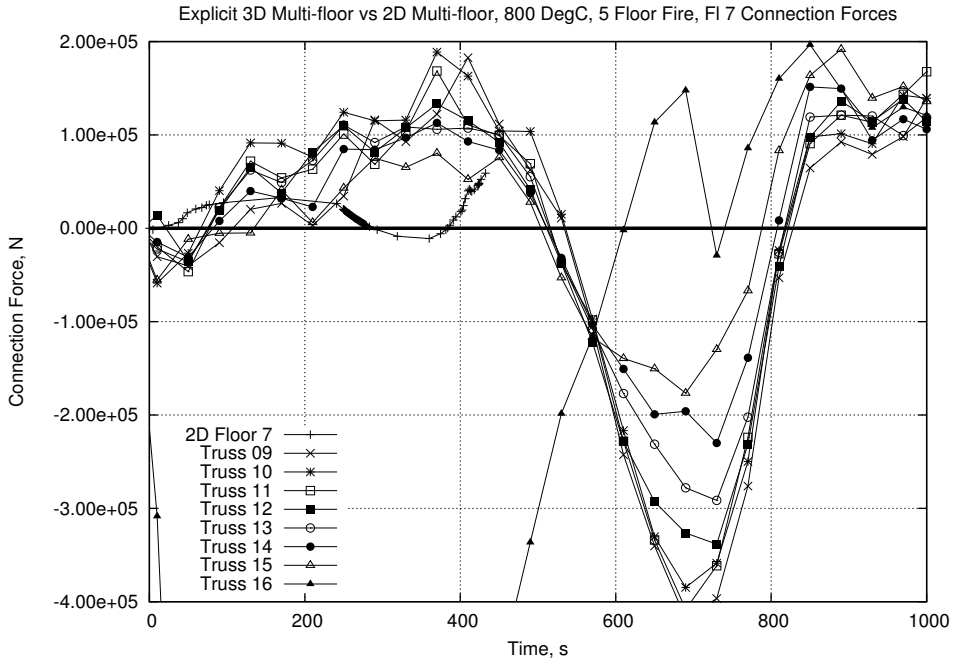

(b)

Figure 7.54: Scenario 7 : Floor Membrane Force Comparison

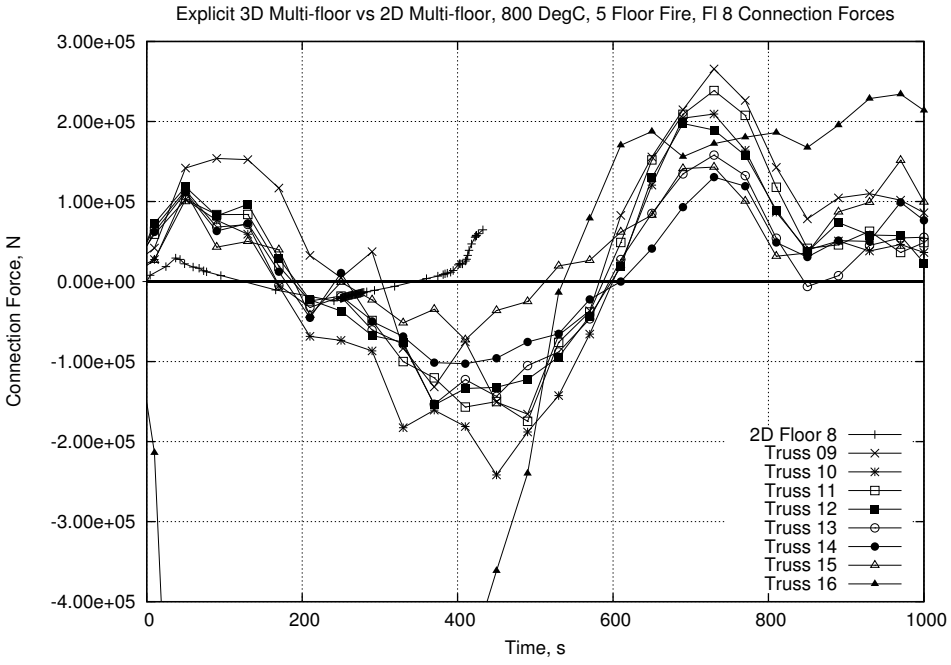

(a)

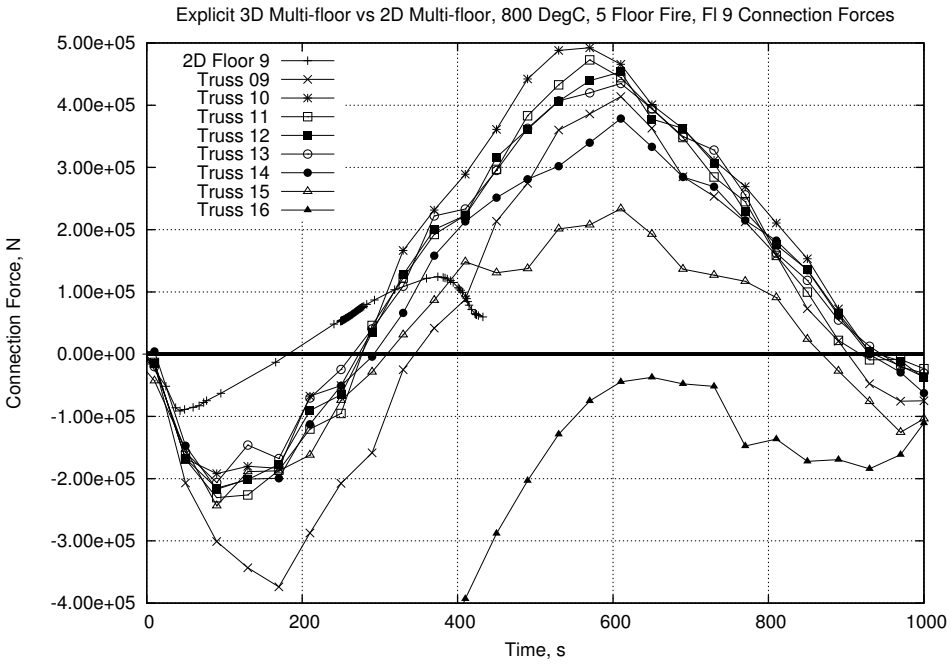

(b)

Figure 7.55: Scenario 7 : Floor Membrane Force Comparison (Cont'd)

Examination of the vertical displacement at the tops of the outer columns shows a similar response to Scenario 6. Figures 7.56.a and 7.56.b show the column top displacement in the long span side and the short span side respectively for Scenario 7. Figure 7.56.a lists the columns in order from the centre of the long span side toward the corner. Figure 7.56.b lists the columns in order from the corner to the middle of the short span side. The progression in downward movement along the long span side is clear. The less restrained columns at the centre of the long span side displace first and this movement works its way along the building face toward the corner. As the corner column on the long span side begins to displace so the corner column on the short span side becomes affected. Shortly before the analysis terminates high deflection rates can be seen in the majority of the columns. As indicated in Chapter 3 at around 800°C the trusses will not be able to restrain the columns from moving. As there is no hat truss present in this scenario there is no way for the structure to support the failing columns hence collapse will initiate.

The results of this scenario are consistent with the Quasi-static scenarios presented in this chapter as well as the 2D models presented in Chapters 4 and 5. The failure of the analysis is seen considerably earlier in this scenario compared to Scenario 6. This is due to Scenario 7 having 5 floors on fire rather than just 3. Strong indications are present that the termination of the analysis is due to collapse of the structure.

7.2.2.8 Scenario 8 : Explicit, 3FF, no hat, 800°C, Ultra high resolution

This scenario was run as a further check that the change from a full resolution system to a half resolution system would not introduce too many errors. This scenario was also run using the Explicit version of ABAQUS due to convergence problems. The structural model was created by other members of the research team [79], is as close to the exact layout of the WTC towers as practicable and uses the same floor model shown in Figure 6.17 (Chapter 6). Mass and time scaling have once again been used to allow the analysis to complete in a reasonable time.

Figure 7.57 shows the final displaced shape of this scenario with vertical (plot .a)

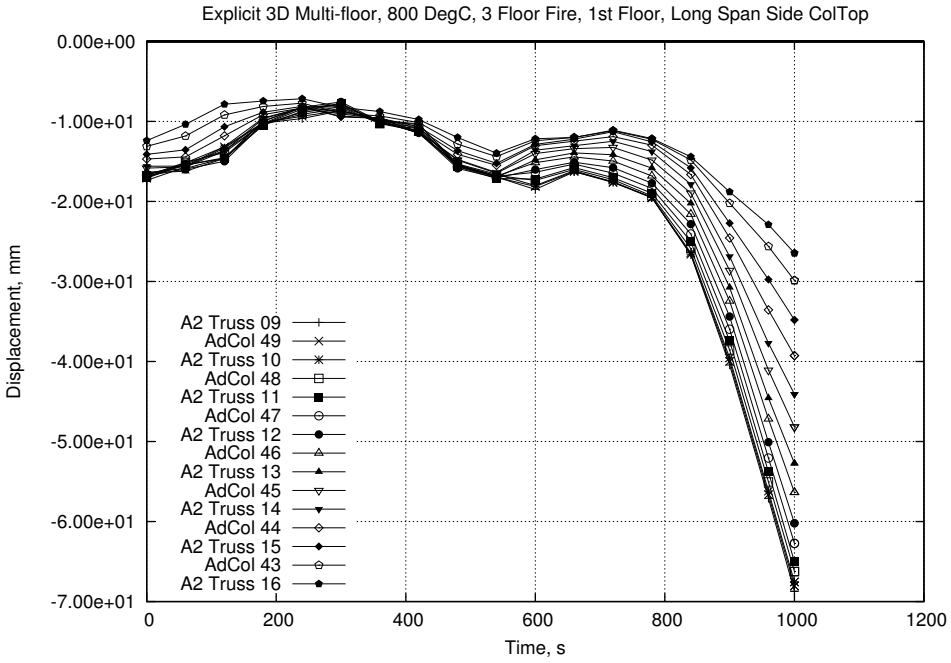

(a)

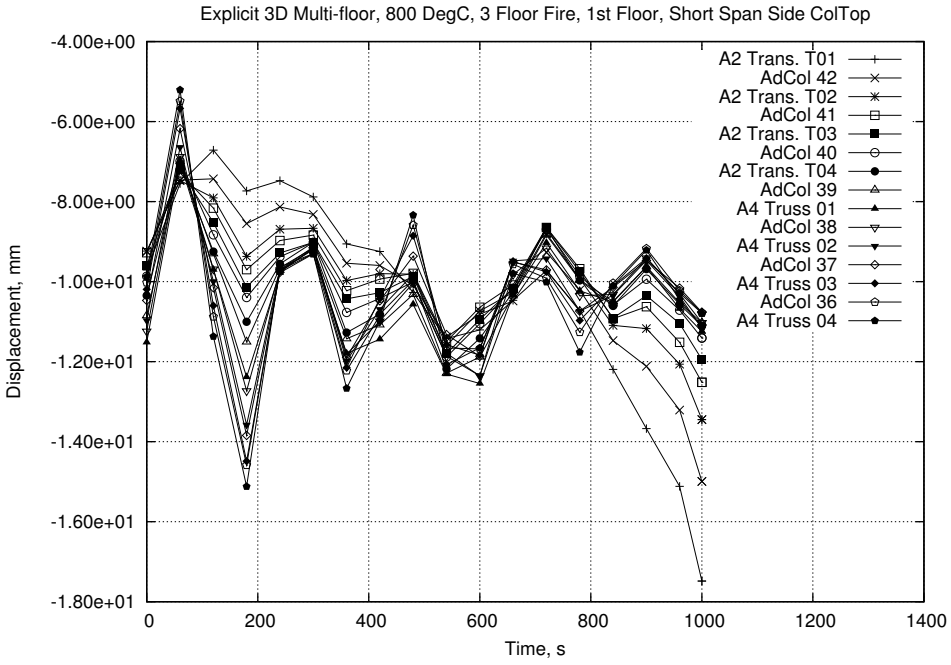

(b)

Figure 7.56: Scenario 7 : Column Top Vertical Displacement

and horizontal (plot .b) deflection contours overlaid. The most obvious mechanisms are the hinges that have formed at the mid-span and ends of the columns over the fire floors. The use of mass scaling appears to again have had an effect on the detailed results. Figure 7.58.a, showing selected lateral column displacements on the 4th floor of Scenario 8, shows very little differential movement in the outer wall. the columns are numbered sequentially from the centre of the long span side toward the corner of the building. This response is in stark contrast with the more gradual response along the outer wall seen in Scenario 1 (Figure 7.8.b for the 7th floor). The lack of differential movement in the columns can also be seen in the plot of column vertical deflections in Figure 7.58.b. As with the other scenarios presented in this chapter runaway is not as sudden or obvious as in the 2D models presented in Chapters 4 & 5.

Figures 7.59 & 7.60 show the moments in a selection of columns in Scenario 8 and compares them to several other models, both Quasi-static and explicit based. The columns chosen in Scenario 8 are again numbered sequentially from the middle of the long span side toward the corner. In this case columns 2, 4 and 6 are main columns (i.e. with a direct connection to the end of a truss) while columns 1, 3 and 5 are intermediate columns.

Figures 7.59.a, 7.59.b and 7.60.a compare the moments in the columns at the bottom, middle and top hinges respectively. As the columns used in this model are unmodified, realistic sections (unlike the columns used in the other models in this thesis) they have half the moment capacity under the appropriate loading. Therefore the plots shown in Figures 7.59 & 7.60 have been normalized against the appropriate moment capacity.

As indicated in the displacement plots in Figure 7.58 there is little differentiation between the columns along the length of the building in Scenario 8. Examination of the moments in the columns in Figures 7.59 & 7.60 do indicate some differentiation, however, between the main columns (2, 4 & 6) and the intermediate columns (1, 3 & 5). In Scenario 8 the moment in the main columns reaches yield significantly before the intermediate columns. Within each column group (i.e. main and intermediate),

however, there is little difference in response and this is seen all along the long span side columns. There is a major change in the reaction between 800 and 1000s when the intermediate columns reach yield at the 3 hinge locations. After this change the moment in the columns at all 3 hinge locations begins to drop. Over the period of time where all the columns reach yield is also when the deflections rates begin to increase rapidly as seen in Figure 7.58. This indicates that collapse is reached at around 1000s but the added damping does not allow the model to represent it immediately. As there is no hat truss there is no way to support the columns after the initiation of a plastic mechanism. Hence the large column displacements, high displacement rate and the fact that the columns have reached yield indicate that a collapse mechanism has formed.

Comparison between the columns in Scenario 8 and the other models shows a close resemblance in the response. As can be seen in Figures 7.59 & 7.60.a the results from Scenario 8 match well with the general response of the 2D and 3D Quasi-static models. The inclusion of the result from Scenario 6 (Exp 3DHR A2 Truss 12) in Figure 7.59.a also indicates the similarities in response between the models. The explicit based models show similarly higher moments initially, which indicates that the effect of the additional damping is having the same effect as described in Section 7.2.2.6. In addition the moment responses in Scenarios 6 and 8 are generally similar throughout the analysis time.

Column 14, the response of which is shown in Figure 7.60.b, is equivalent to Truss 12 from the half resolution models presented in Scenarios 1 to 7 and is therefore compared directly to the 2D results from Scenario 1 in Chapter 4. The comparison again shows similarities in the responses that indicate that the same mechanisms are occurring.

The results of Scenario 8 support 2 main conclusions.

1. That the mechanism found in the 2D models in Chapter 4 can be carried over into large, 3D models of a similar structure.

2. That using a half resolution model gives an adequate representation of the

structural response to fire.

7.3 Conclusions

This chapter has investigated large, 3D multi-storey models of a building. The general response of the building is discussed under Scenario 1 through use of a base case that is similar to previous work done in 2D.

A parametric study has also been conducted using several of the cases investigated in the 2D section of this thesis (Chapter 5). In general the response of the 3D models is similar to the 2D versions. The main differences arise from the greater ability of the 3D structure to redistribute loading.

Full collapse of the structure was not seen in any of the large 3D models with the same kind of clarity indicated in the 2D work. Under close scrutiny, however, strong indications are present in several of the scenarios that collapse is imminent.

Several of the scenarios had particular issues with numerical stability. Appendix A contains a full list of the parameters investigated to overcome such problems. Scenario 3, where the maximum temperature of the steel is limited to 500°C, fails in convergence considerably sooner than the higher temperature Scenario 1. However none of the same failure indicators are present so it may be concluded that local stability issues have become dominant. The lower temperature, hence higher strength, of the steel means that sudden, buckling failure of truss members is more likely. Scenarios 4 and 5, including extra floors with a hat truss, were also dominated by convergence issues. As neither of these models surpassed Scenario 1 (which involved the same basic scenario but lacked a hat truss) it is hard to judge the effect of the hat truss in the later stages of the analysis. It was apparent, however, that the hat truss did not greatly affect the early response of the structure. This was also a finding of the 2D work in Chapters 4 & 5 .

An investigation of the vertical deflections at the top of the column in the various models indicates that Scenarios 1 and 4 (3 floor fire models with and without hat

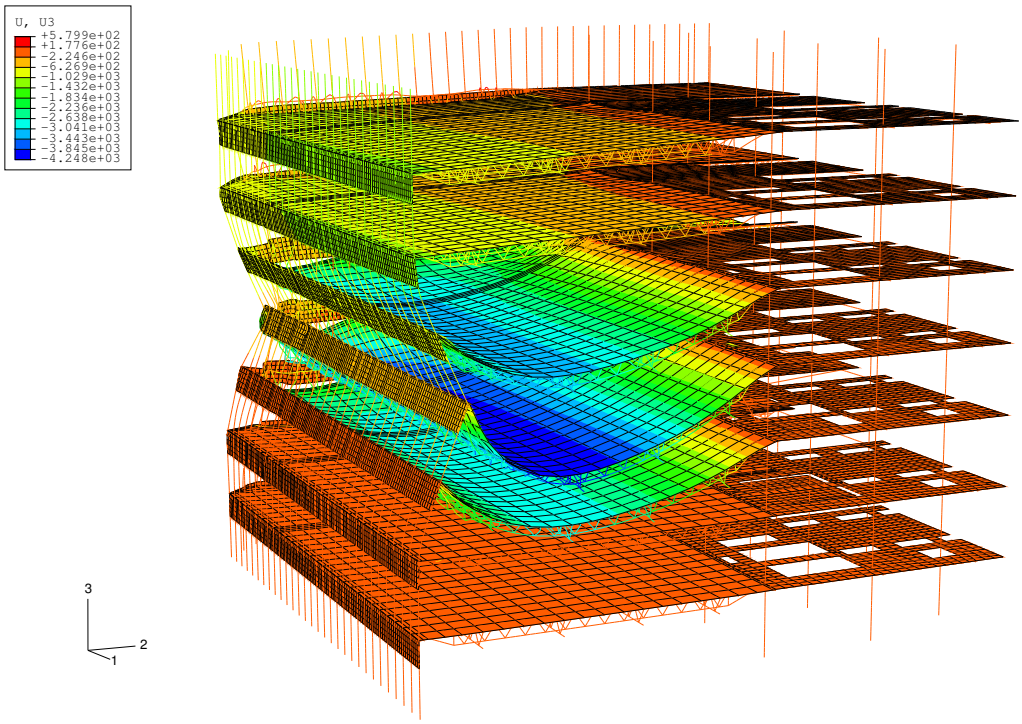

(a)

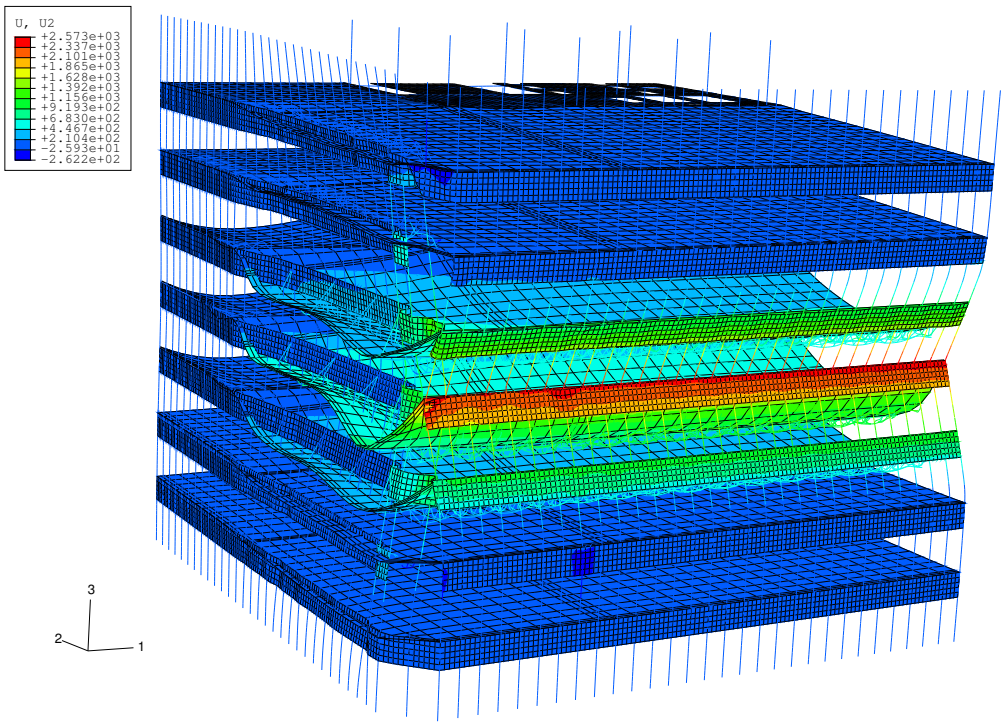

(b)

Figure 7.57: Scenario 8 : Final Displaced Shape

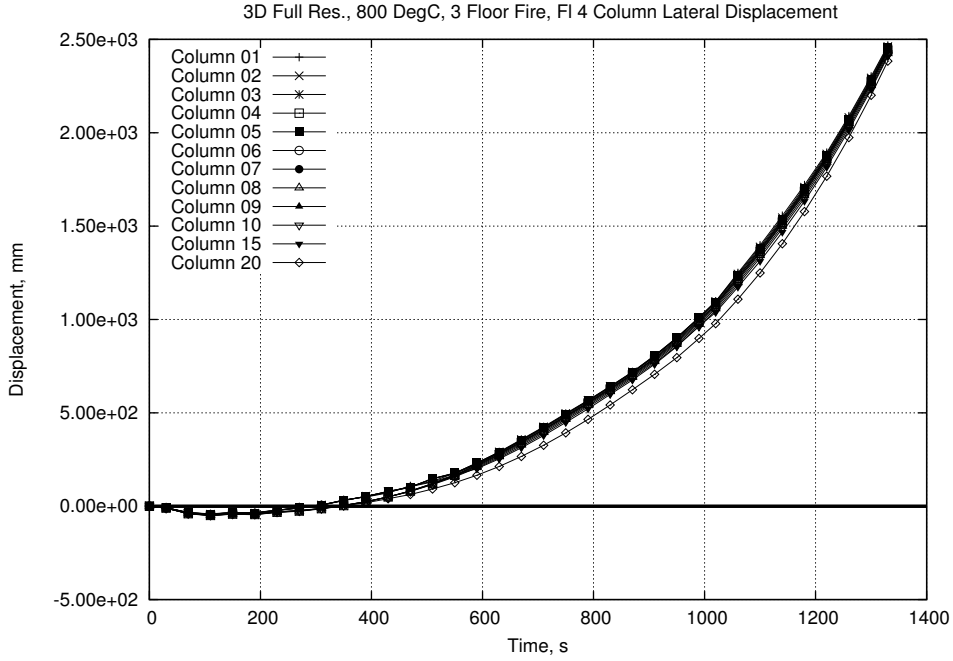

(a)

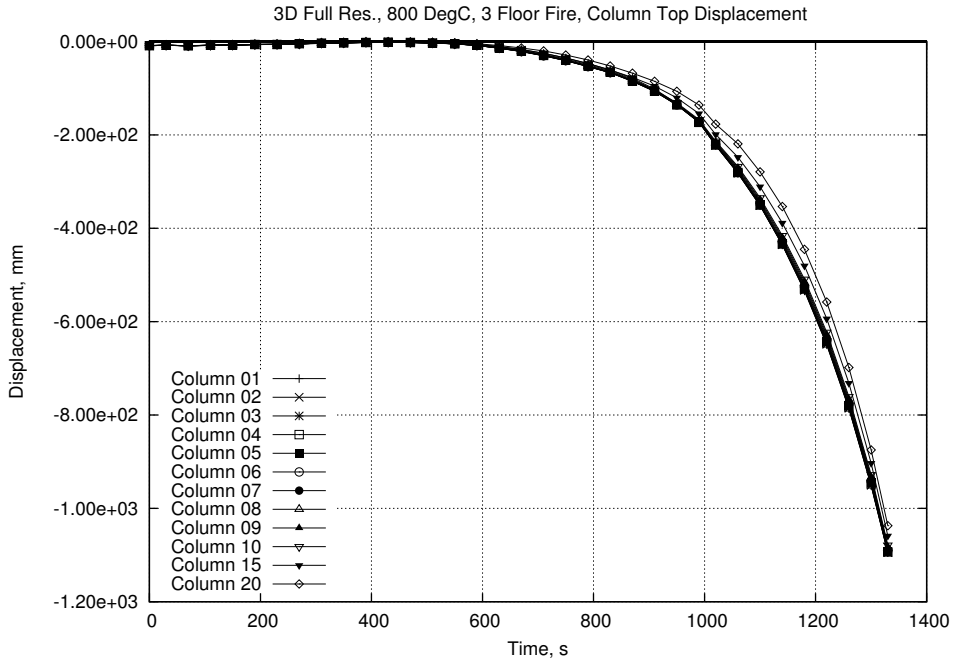

(b)

Figure 7.58: Scenario 8 : Column Displacement

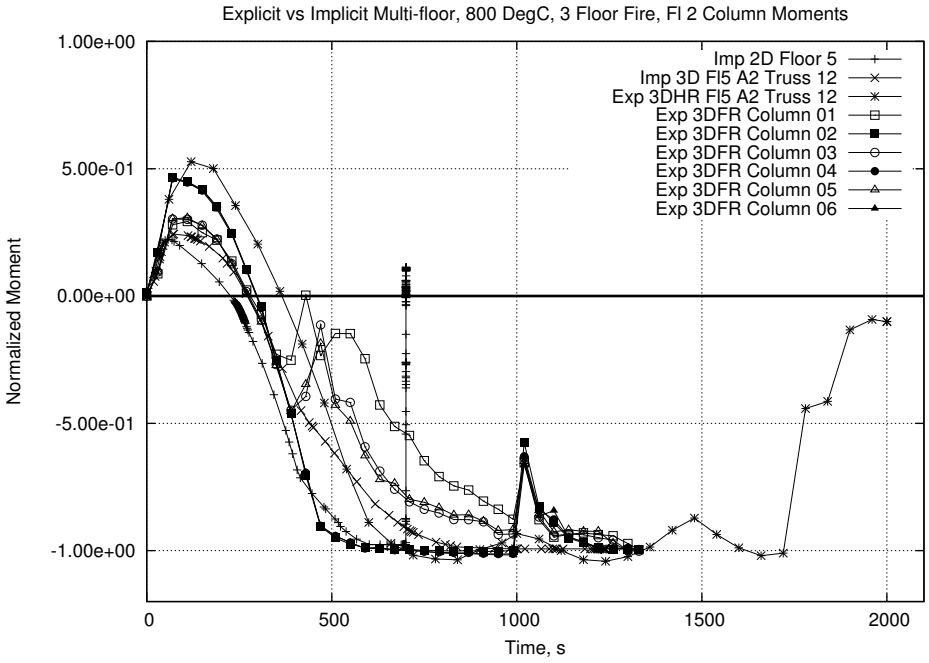

(a)

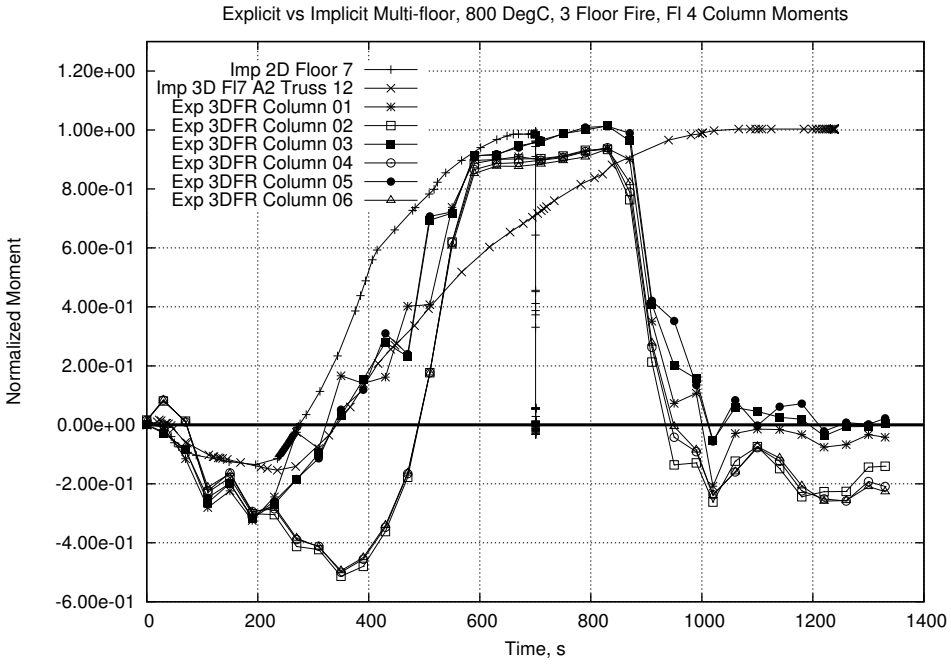

(b)

Figure 7.59: Scenario 8 : Column Moments

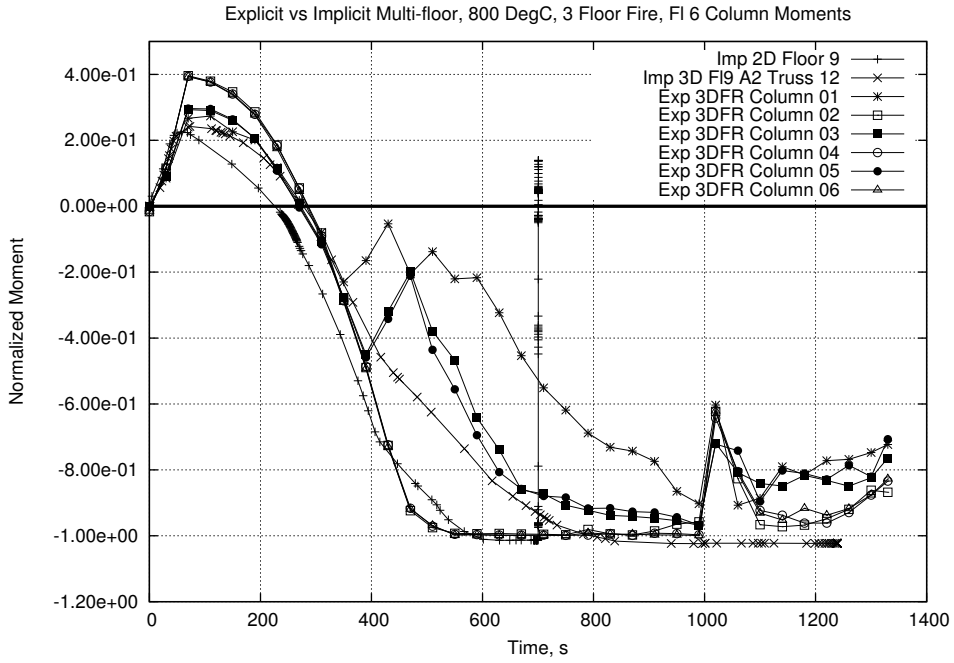

(a)

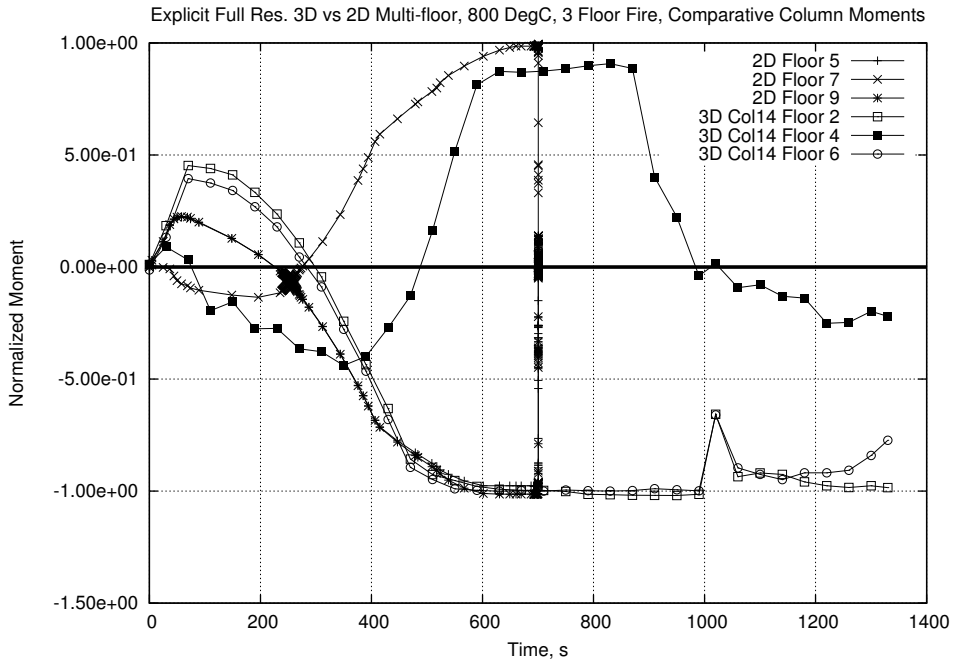

(b)

Figure 7.60: Scenario 8 : Column Moments (Cont'd)

truss respectively) produce very similar results. The convergence failure of Scenario 4 may then be an indication that the hat truss cannot effectively redistribute loading from the outer columns to the core for this scenario. Further investigation is needed on this point, however, before any definite conclusions can be made.

With the obvious stability and convergence issues Scenarios 6 to 8 were conducted using the Explicit version of ABAQUS. In order to allow the Explicit models to run in a useful time frame, time and mass scaling were utilized. The analysis time was reduced to 3.6s rather than 3600s and all time based data was scaled accordingly. Mass scaling was also used to provide additional damping and to allow the stable time increment to be increased. For more details on the effects of these parameters please see Appendix A and the ABAQUS manuals [73]. Such interventions did allow the models to be run relatively quickly but had an impact on the accuracy of the results. The trends seen in the results are extremely similar to the Quasi-static models but the precise details are somewhat different. Excessive damping appears to have been included which leads to the movement in the structure caused by thermal expansion to be slowed significantly. This then leads, initially, to increased forces and then a complex interaction as oscillations are induced in the force response. The final displaced shape is extremely similar to that of the Quasi-static scenarios presented in this chapter and in the 2D analyses of previous chapters. Similarly the failure indicators, i.e. the moments in the columns and the vertical column movement, are showing similar responses indicating failure. Thus it can be concluded that the Explicit models presented in Scenarios 6 and 7 give a reasonable, if not totally accurate, prediction of the response of the structure.

Scenario 8 was a special case based on a different structural model run using the Explicit version of ABAQUS. Scenario 8 involved an full resolution model of a smaller area of the WTC towers which was created by colleagues [79]. The results of this analysis indicate that the collapse mechanism seen in the 2D models in Chapter 4 are valid for large, 3D models of a similar nature. While the level of damping used in the analysis presented here may be too high, qualitatively the

result is the same as those seen in the Quasi-static 2D and 3D models. The results of Scenario 8 also support the view that a half resolution model of the structure will produce an adequate representation of the global response.

Chapter 8

Conclusions and Further Work

The previous chapters have described the work conducted to investigate the effects of heating on long span, truss based, composite floor systems in tall buildings. This final chapter draws together the conclusions made at the different stages and presents some thoughts on where this research could lead.

It should be noted that the results of this research may only be relevant to the simplified types of fires used in the various analyses. Further work should be done to broaden this knowledge base to include the effects of different types of fire and structural form.

8.1 Conclusions

- The design of tall buildings currently does not adequately include the effects of fire on the structure. Treatment of fire design in a similar fashion to ambient live loading for gravity, wind and earthquake and inclusion in the main design stage would lead to more efficient and safer buildings.
- Adherence to current, prescriptive design codes for fire design does not guarantee a quantifiable level of safety.
- Investigations into the results of the Cardington tests have provided a great

deal of information about the effect of real compartment fires on "normal" low-rise composite steel framed office buildings. This information is now being used to increase knowledge about the effects of fire on other structural forms.

- The results of the official NIST investigation into the collapse of the World Trade Center towers are likely to dominate design code progress for a significant length of time. Such recommendations should be implemented intelligently and carefully to allow safe and efficient building design to flourish.

- It is apparent that the response of long span floor systems used in modern tall buildings to fire is not adequately captured by testing partial or scaled sections. Suitable test facilities need to be designed to investigate the full response of such systems beyond the point of failure.

- Failure of truss members is a gradual effect caused by thermal expansion and thermal degradation of material properties.

- Response of truss floor systems is driven by the geometric changes caused by thermal expansion. Restraint to thermal expansion on a global and local scale will affect the response. Similarly differential thermal expansion, both within the slab and between the slab and the steel truss, has a leading role in the full response of this kind of floor system.

- Response of the long span truss investigated in Chapter 3 shows similarities to normal composite beams as described in previous research [1, 7]. Restrained thermal expansion and differential thermal expansion between the steel members and the concrete slab lead to large midspan deflections. These large deflections lead to a transition from the original shear/bending moment load carrying system to a strong secondary system involving catenary/tensile membrane action.

- The initial lateral expansion of the floor system leads to outward movement in the supporting column. The later catenary/tensile membrane action leads

to inward movement of the supporting column. Both of these mechanisms are reliant on the survival of the truss-column connections.

- The floor system retains a significant amount of membrane strength available even after severe heating and deflections have occurred. Hence a significant amount of restraint may still be available to a column connected to this kind of floor system at elevated temperatures.

- Assuming that connections remain intact then failure of the long span truss floor systems investigated here are related more to global failure mechanisms over several floors rather than local effects.

- Local effects in single truss models match well with truss responses in larger models with differences being attributable to restraint effects.

- Full, correct response of a structure may not be accurately represented by a localised model. Global mechanisms may be dominant and therefore models may need several floors for the response to be accurately predicted.

- 2D models with 12 storeys and fires over multiple floors were investigated in Chapters 4 and 5. They exhibit large midspan deflection in the truss floors of the storeys affected by fire.

- Movement of floors can produce a significant effect in the supporting columns. Combination of loss of restraint and increased lateral loading leading to significant inward displacement of columns. This effect is increased as the number of affected floors increases.

- Lateral loading can lead to production of plastic hinges in columns and hence a failure mechanism. An alternative, but related, failure mechanism may appear if the columns have a high stiffness. In this case the transfer of lateral loading from the fire affected floors into the cool interface floors may lead to failure of these floors. This may lead to a "compressive pulse" effect, as described by Usmani [63], and progressive failure of the structure.

- Inclusion of a hat truss in the 2D structure investigated in Chapters 4 and 5 can redistribute loading from the failing outer columns back to the core columns. This delays the onset of global failure until the hat truss is also overcome.

- Increasing the number of floors on fire increases the threat to the structure. As long as temperatures can be kept low then movement in the structure can be kept to a minimum allowing it to transfer loads in a similar manner to that for ambient conditions.

- Under severe fire conditions moving from 3 to 5 floors on fire substantially reduced the time to collapse. This was true for models with and without a hat truss.

- Inclusion of correct thermal expansion effects is required to correctly track the full response of the structure over the analysis time.

- Alteration of the structure to increase numerical efficiency is a valid technique. Care must be taken to retain correct equivalent stiffnesses both in the floor membrane as a whole and in the separate truss and floor slab sections. A major factor in the response of composite floors is the differential thermal expansion between the floor slab and the truss. The altered structure needs to retain the ability to model this adequately.

- Slight imperfections can be introduced to aid convergence in members which exhibit buckling responses without adversely affecting the response of the model. Again care should be taken when using this technique.

- The 3D models investigated in Chapters 6 and 7 included the long span areas investigated previously as well as shorter span areas. Both areas included trusses with the same depth and general geometry. The long span areas displayed larger deflections than shorter span areas. The higher stiffness in the shorter span areas creates lower midspan deflections but higher compression in the floor and thus more outward movement in the column.

- Individual floor models should only be used for single floor fire situations. Multiple individual floor models will not give the same response as a single, multi-storey model, especially if multiple floors are on fire. This is due to the differences in restraint provided by the columns between a single floor model and a multi-storey model with multiple floor fires.

- Responses in 2D and 3D multi-storey models are similar. Primary differences arise from greater redistribution capability of 3D models. This means that the collapse mechanism in the 3D models is a more gradual response. Column failure moves gradually from the less restrained middle of the long span side of the building toward the more highly restrained corners. While definite collapse was not seen, several of the analyses failed in convergence with a large number of columns at yield in combined axial force/bending. This indicates that global stability failure in the structure was imminent.

- The primary collapse mechanism was found to exist in the long span truss areas. The response of the short span area is not the driving factor in the global response. The shorter length of trusses coupled with the same depth and geometry leads to a higher stiffness of the floor in the short span areas. As midspan deflection is limited, compared to the long span areas, the outward movement of the column is increased and the inward movement minimised. It is unclear as to the later response to heating of the short span area due to analysis failure.

- Full collapse of the structure was not as obvious in the 3D models as in the 2D models. Strong indications in the detailed results indicate collapse was imminent at the point of failure of several of the 3D models.

- Implicit and Explicit versions of the multi-storey 3D models give similar final results although the damping included in the Explicit versions appears to be too high for real accuracy. The inclusion of numerical damping is important in such models in order to increase numerical efficiency. However

it is important that the level of damping is tailored correctly for the analysis under investigation.

- Appendix A includes an investigation of various parameters that affect the numerical efficiency and accuracy of results from ABAQUS analyses. These have been included to ensure that a fair balance between accuracy of results and speed of analysis has been maintained.

8.2 Recommendations for Further Work

The results reported in this thesis give an initial indication of the response of long span truss floors, in tall buildings, to the effects of large building fires. A significant amount of further work could be undertaken to further identify such responses.

A brief description of the difference between the responses of the long and short span trusses was given in the chapters describing the 3D models (Chapters 6 and 7). A deeper understanding of trusses under fire conditions would be gained from further research into the effects of length on the response of a building. This applies to both the global and the local responses of such floor systems. As well as trusses other long span floor systems exist, such as castellated and cellular beams. These kinds of section are also regularly being used in buildings while little research into their response to fire has been conducted.

For comparative purposes the materials used in this research were kept constant over all the different models. Although previous research [1, 7] has shown that material properties do not greatly affect a structures response there are some factors that still need to be researched. The NIST report into the collapse of the WTC towers highlighted creep as a major factor under structural analysis of buildings at high temperature. This finding should be verified and investigated further. Further investigation and verification of the ABAQUS concrete Damaged Plasticity model for structures under fire loading would provide a robust material model for use with such models.

The fires used in the analyses presented here were not necessarily realistic. The findings of this research could then be used as a baseline for investigating more realistic temperature-time profiles. Parameters such as the relative rate of heating between the steel and the concrete should be investigated in more detail. The spacial distribution of the fire should also be investigated. In all cases the fires in this research were spatially uniform and did not include any of the core framing of the structure. Other research [52, 62] has used different spacial distributions hence the differences in response between these research projects should be checked. The effects of different heating regimes on the outer structure (i.e. the outer columns and spandrel beams) should be investigated. To what extent will heating the spandrels alter their ability to transfer load between columns.

As well as the effects of different fires there are several structural effects that merit further investigation. The first would be the effects of relative column-floor stiffness on the collapse mechanisms presented in Chapters 4 and 5. Is there an optimum ratio that will limit floor deflections while not endangering column stability or connection integrity? Connection failure in general is an important effect that has also not been investigated here. The effects on the stability of the column may be considerable if connection can fail. While a failed truss-column connection will remove the lateral support of the floor it will also relieve the column of any lateral movement caused by floor displacement. Thermally induced shear in the truss connections should also be investigated. As expansion of the floor plate occurs in 2 directions the connections will undergo shear in both directions in the plane of the column line as well as axial forces.

The models conducted in this thesis used a standard level of loading throughout. This loading was comparable to that used in the official NIST investigation but could be considered relatively light. As this load level induced collapse mechanisms it should be investigated what the effect of higher loading might be.

The effects of supplementary redistribution systems could also be investigated. The hat truss used here had a significant effect on the vulnerability of the 2D models. The WTC tower hat truss was not specifically designed to act under fire conditions

but its presence appears to have made a significant difference to the vulnerability of the structure. Including similar elements at the structural design stage specifically to deal with the effects of fires would again increase the robustness of tall buildings. Due to the problems with convergence seen in the large 3D models presented in this thesis it is not clear how exactly the hat truss contributed. A further study, perhaps using more simple 3D models, might provide useful results.

Bibliography

[1] Susan Lamont (2001), *The behaviour of multi-storey composite steel framed structures in response to compartment fires*, PhD Thesis, University of Edinburgh

[2] Ove Arup (2003), *Strategy for Integrating Structural and Fire Engineering of Steel Structures*, Report for AISC, October 2003

[3] Steel Construction Institute (1991), *Structural fire engineering : investigation of Broadgate Phase 8 fire*, Ascot

[4] British Steel plc. (1998), *The behaviour of multi-storey steel framed buildings in fire,* Technical Report, Swinden Technology Centre

[5] Martin Gillie, Asif Usmani, Michael Rotter & Mark O'Connor (2001), *Modelling of heated composite floor slabs with reference to the Cardington experiments*, Fire Safety Journal 36, pp745-767

[6] B.A. Izzuddin & D.B. Moore (2002), *Lessons from a full scale fire test*, Structures and Buildings 152, pp319-329

[7] Partners in Technology Report (2001), *Behaviour of steel framed structures under fire conditions,* Main Report, University of Edinburgh

[8] Y.Z. Yin & Y.C. Wang (2005), *Analysis of catenary action in steel beams using a simplified hand calculation method, Part 1: Theory and validation for uniform temperature distribution*, Journal of Constructional Steel Research 61, pp183-211

[9] Y.Z. Yin & Y.C. Wang (2005), *Analysis of catenary action in steel beams using a simplified hand calculation method, Part 2: Validation for non-uniform temperature distribution*, Journal of Constructional Steel Research 61, pp213-234

[10] Bailey C.G. (2001), *A Simple new fire design method to predict the structural response of steel frames with composite floors*, NSCC 2001 9th Nordic Steel Construction Conference, Helsinki, Finland, pp 557-564.

[11] Picture (a) courtesy of BRE

[12] Picture (b) copyright L. Borges (2003), www.dec.uc.pt/~lborges/cardington/, accessed October 2005

[13] Neil Cameron (2003), *The Behaviour and Design of Composite Floor Systems in Fire*, PhD Thesis, University of Edinburgh

[14] British Standards Institution (2004), *Eurocode 8 : Design of structures for earthquake resistance. General rules, seismic actions and rules for buildings*, BS EN 1998-1:2004

[15] Lamont S., Lane B., Flint G. and Usmani A.S., *Behaviour of structures in fire and real design - a case study.* Accepted by the Journal of fire protection engineering, April 2005

[16] A.Y Elghazouli & B.A. Izzuddin (2001), *Analytical assessment of the structural performance of composite floors subject to compartment fires,* Fire Safety Journal, Volume 36, Issue 8, November 2001, Pages 769-793

[17] M. Gillie, A.S. Usmani, J.M. Rotter (2001), *A structural analysis of the Cardington British Steel Corner Test*, Journal of Constructional Steel Research Vol.58, pp427-442

[18] R. Becker (2002), *Effect of heat sinks on evolution of longitudinal temperature distributions in steel structures*, Fire Safety Journal 37, pp1-20

[19] Y.Z. Yin & Y.C. Wang (2003), *Numerical simulations of the effects of non-uniform temperature distributions on lateral torsional buckling of steel I-beams*, Journal of Constructional Steel Research 59, pp1009-1033

[20] Faris Ali & David O'Conner (2001), *Structural performance of rotationally restrained steel columns in fire*, Fire Safety Journal 36, pp679-691

[21] Al-Jabri, K.S., Burgess, I.W., Lennon, T. and Plank, R.J., *Spring Stiffness Model for Flexible End-Plate Bare-Steel Joints in Fire*, .J. Construct. Steel Research. 61 (12), (2005) pp 1672-1691.

[22] Block, F.M., Burgess, I.W. and Davison, J.B., *Numerical and Analytical Studies of Joint Component Behaviour in Fire*, Paper S7-4, Third International Workshop on Structures in Fire, Ottawa, Canada, (May 2004) pp 383-395.

[23] Ove Arup, *Madrid Windsor fire: the Arup view*, www.arup.com, accessed November 2005

[24] Bungale S. Taranath (1998), *Steel, concrete and composite design of tall buildings*, Second Edition McGraw Hill

[25] British Standards Institution (2002), *Eurocode 1: Actions on structures. General actions - Densities, self-weight, imposed loads for buildings (AMD Corrigendum 15507)*, BS EN 1991-1.1:2002

[26] British Standards Institution (2004), *Eurocode 2: Design of concrete structures. General rules and rules for buildings*, BS EN 1992-1.1:2004

[27] British Standards Institution (2005), *Eurocode 3: Design of steel structures. General rules and rules for buildings*, BS EN 1993-1.1:2005

[28] British Standards Institution (2004), *Eurocode 4: Design of composite steel and concrete structures. General rules and rules for buildings*, BS EN 1994-1.1:2004

[29] British Standards Institution (2004), *Eurocode 5: Design of timber structures. General - Common rules and rules for buildings*, BS EN 1995-1.1:2004

[30] British Standards Institution (1996), *Eurocode 6: Design of masonry structures. General rules for buildings - rules for reinforced and unreinforced masonry*, DD ENV 1996-1.1:1996

[31] British Standards Institution (2000), *Eurocode 9: Design of aluminium structures. General rules - general rules and rules for buildings*, DD ENV 1999-1-1:2000

[32] H.S. Lew, R.W. Bukowski & N.J. Carino, *Federal Building and Fire Safety Investigation of the World Trade Center Disaster : Design, Construction, and Maintenance of Structural and Life Safety Systems (Draft)*, NIST NCSTAR 1-1 (Draft), June 2005

[33] Pictures copyright John Nve & Ian Lambot, www.pcfandp.com, accessed October 2005

[34] British Standards Institution (2005), *Eurocode 1: Actions on structures. General actions - Wind actions*, BS EN 1991-1.4:2005

[35] F. Sadek, *Federal Building and Fire Safety Investigation of the World Trade Center Disaster : Baseline Structural Performance and Aircraft Impact Damage Analysis of the World Trade Center Towers (Draft)*, NIST NCSTAR 1-2 (Draft), June 2005

[36] British Geological Survey, Kingsley Dunham Centre, Keyworth, Nottingham NG12 5GG, website : http://www.bgs.ac.uk/

[37] USGS National Center 12201 Sunrise Valley Drive Reston, VA 20192, USA, website : http://www.usgs.gov/

[38] Office of the Deputy Prime Minister (UK) (2000), *Building Regulations 2000: Approved Documents B: Fire safety*

[39] British Standards Institution (2003), *Structural use of steelwork in building. Code of practice for fire resistant design*, BS 5950-8:2003

[40] British Standards Institution (1987), *BS 476 Parts 20-23: Fire tests on building materials and structures*, BS 476-20:1987 to BS 476-23:1987

[41] International Organization for Standardization (1999), *ISO 834: Fire-resistance tests – Elements of building construction*, ISO 834-1:1999

[42] ASTM International, *ASTM E119 Standard Test Methods for Fire Tests of Building Construction and Materials*, E119-00a

[43] K. D. Hertz (2003), *Limits of spalling of fire-exposed concrete*, Fire Safety Journal, Volume 38, Issue 2, Pages 103-116

[44] P. Kalifa, F-D. Menneteau and D. Quenard (2000), *Spalling and pore pressure in HPC at high temperatures*, Cement and Concrete Research, Volume 30, Issue 12, Pages 1915-1927

[45] BRE (1985), *The structure of Ronan Point and other Taylor Woodrow-Anglian buildings*, Large panel systems report BR63

[46] Neils C. Lind (1995), *A measure of vulnerability and damage tolerance*, Reliability Engineering and System Safety 48, pp1-6

[47] Jitendra Argawal, David Blockley & Norman Woodman (2003), *Vulnerability of structural systems*, Structural Safety 25, pp263-286

[48] Chi Kin Lu & Siu Lai Chan (2004), *A simulation based large deflection and inelastic analysis of steel frames under fire*, Journal of Constructional Steel Research 60, pp1495-1524

[49] R. Becker (2002), *Structural behavior of simple steel structures with non-uniform longitudinal temperature distributions under fire conditions,* Fire Safety Journal *37, pp495-515*

[50] FEMA (2003), *World Trade Center Building Performance Study : Data Collection, Preliminary Observations and Recommendations*, FEMA Report 403

[51] Partners in Technology Report (2001), *Fundamental Principles of Structural Behaviour under Thermal Effects*, Report TM2, University of Edinburgh

[52] J.L. Gross, T.P. McAllister, *Federal Building and Fire Safety Investigation of the World Trade Center Disaster : Structural Fire Response and Probable Collapse Sequence of the World Trade Center Towers (Draft)*, NIST NCSTAR 1-6 (Draft), June 2005

[53] Matthys Levy & Najib Abboud (2002), *World Trade Center Structural Engineering Investigation*, Weidlinger Associates

[54] ArupFIRE (2002), *World Trade Center Expert Report : Documentation and Analysis of Fire Spread in World Trade Center Events of 9/11*, Ove Arup

[55] NIST, *Federal Building and Fire Safety Investigation of the World Trade Center Disaster : Final report on the collapse of the World Trade Center Towers*, NIST NCSTAR 1, September 2005

[56] J. G. Quintiere, M. di Marzo and R. Becker (2002), *A suggested cause of the fire-induced collapse of the World Trade Towers*, Fire Safety Journal, Volume 37, Issue 7, October 2002, Pages 707-716

[57] R.G. Gann, A. Hamins, K.B. McGrattan, G.W. Mulholland, H.E. Nelson, T.J. Ohlemiller, W.M. Pitts, K.R. Prasad, *Federal Building and Fire Safety Investigation of the World Trade Center Disaster : Reconstruction of the Fires in the World Trade Center Towers (Draft)*, NIST NCSTAR 1-5 (Draft), June 2005

[58] Barbara Lane (2003), *Letter to the Editor regarding "A suggested cause of the fire-induced collapse of the World Trade Towers"*, Fire Safety Journal, Volume 38, Issue 6, October 2003, Pages 589-591

[59] S.K. Choi (2004), *The Structural Behaviour of Composite Truss Systems in Fire*, PhD Thesis, University of Sheffield, Nov 2004

[60] C.G. Bailey, *New Fire design Method for Steel Frames with Composite Floor Slabs*, BRE, 2003

[61] Choi, S.K., Burgess, I.W. and Plank, R.J. (2003), *The Behaviour of Lightweight Composite Floor Trusses in Fire*, ASCE Specialty Conference: Designing Structures for Fire, Baltimore, (Oct 2003) pp 24-32.

[62] A. S. Usmani, Y. C. Chung and J. L. Torero (2003), *How did the WTC towers collapse: a new theory*, Fire Safety Journal, Volume 38, Issue 6, October 2003, Pages 501-533

[63] A.S. Usmani, *Stability of the World Trade Center Twin Towers Structural Frame in Multiple Floor Fires*, ASCE Journal of Engineering Mechanics, June 2005, Pages 654-657

[64] F.W Gayle, R.J Fields, W.E. Luecke, S.W. Banovic, T. Foecke, C.N. McCowan, J.D.McColskey, T.A. Siewart, *Federal Building and Fire Safety Investigation of the World Trade Center Disaster : Mechanical and Metallurgical Analysis of Structural Steel (Draft)*, NIST NCSTAR 1-3 (Draft), June 2005

[65] D.D. Evans, E.D. Kuligowski, W.S. Dols, W.L. Grosshandler, *Federal Building and Fire Safety Investigation of the World Trade Center Disaster : Active Fire Protection Systems (Draft)*, NIST NCSTAR 1-4 (Draft), June 2005

[66] J.D. Averill, D.S. Mileti, R.D. Peacock, E.D. Kuligowski, N Groner, G. Proulx, P.A. Reneke, H.e. Nelson, *Federal Building and Fire Safety Investigation of the World Trade Center Disaster : Occupant Behaviour, Egress and Emergency COmmunications (Draft)*, NIST NCSTAR 1-7 (Draft), June 2005

[67] J.R. Lawson, R.L. Vettori, *Federal Building and Fire Safety Investigation of the World Trade Center Disaster : The Emergency Response (Draft)*, NIST NCSTAR 1-8 (Draft), June 2005

[68] J.L. Gross *et al.*, *Federal Building and Fire Safety Investigation of the World Trade Center Disaster : Component, Connection, and Subsystem Structural Analysis (Draft)*, NIST NCSTAR 1-6C (Draft), June 2005

[69] M.S. Zarghamee, Y. Kitane, O.O. Erbay, T.P. McAllister, J.L. Gross, *Federal Building and Fire Safety Investigation of the World Trade Center Disaster : Global Structural Analysis of the Response of the World Trade Center Towers to Impact Damage and Fire (Draft)*, NIST NCSTAR 1-6D (Draft), June 2005

[70] A.S. Usmani, J.M. Rotter, S. Lamont, A.M. Sanad, M. Gillie (2001), *Fundamental principles of structural behaviour under thermal effects*, Fire Safety Journal Vol.36, pp721-744

[71] G. Flint, A.S. Usmani, S. Lamont, J. Torero, B. Lane, *Effect of Fire on Composite Long Span Truss Floor Systems*, Journal of Constructional Steel Research, accepted 2005

[72] British Standards Institution (2005), *Eurocode 3: Design of steel structures. General rules - Structural fire design*, BS EN 1993-1.2:2005

[73] Hibbett, Karlsson & Sorenson Inc., *ABAQUS v6.4 & v6.5 Manuals,* ABAQUS Manual Set*,* 2003-2004

[74] British Standards Institution (2004), *Eurocode 2: Design of concrete structures. General rules - Structural fire design*, BS EN 1992-1.2:2004

[75] A.S. Usmani, *Internal Communication*

[76] Martin Gillie (2000), *The behaviour of steel-framed composite structures in fire conditions*, PhD Thesis, University of Edinburgh

[77] Burgess, I.W. and Plank, R.J. (1998), *Modelling the fire tests on the Cardington full-scale frame*, Proc. 3rd Cardington conference

[78] G. Flint, A.S. Usmani, S. Lamont, B. Lane, J. Torero, *Structural response of tall buildings to multiple floor fires : Part 1 - General response*, ASCE Journal of Engineering Mechanics, submitted 2005

[79] A.I. Jowsey, G. Payne, *Internal Communication*

[80] J-M. Franssen (2000), *Failure Temperature of a system comprising a restrained column submitted to* fire, Fire Safety Journal, Vol. 34, pages 191-207

[81] Picture courtesy of http://www.shodor.org, accessed November 2005

Appendix A

Modelling Practices

This chapter describes an investigation of various parameters within the ABAQUS FEM software that would affect the convergence rate, and therefore the efficiency, of a model. As the size and complexity of the full 3D multi-floor model precludes it from being used for this kind of testing a half resolution single truss model was constructed. The geometry, loading and fire regime were kept the same throughout the tests. The parameters investigated were those related to analysis type (quasi-static, explicit or implicit) and convergence issues.

This chapter is also designed to be useful for those users of ABAQUS who need to run large scale, complex structural models under the effects of fire.

A.1 Model Description

The portion of structure to be tested was chosen to include as much complexity as possible while still being small enough to run in a reasonable time. To this end it was decided to incorporate one 18.5m long, half resolution truss assembly, a supporting column and the corresponding 4m wide strip of concrete slab (Fig A.1).

The truss was build up in the same way as in the half resolution models in Chapter 6. For increased computing efficiency it was decided to model the towers, and by extension this smaller model, at half resolution. This means that instead of columns

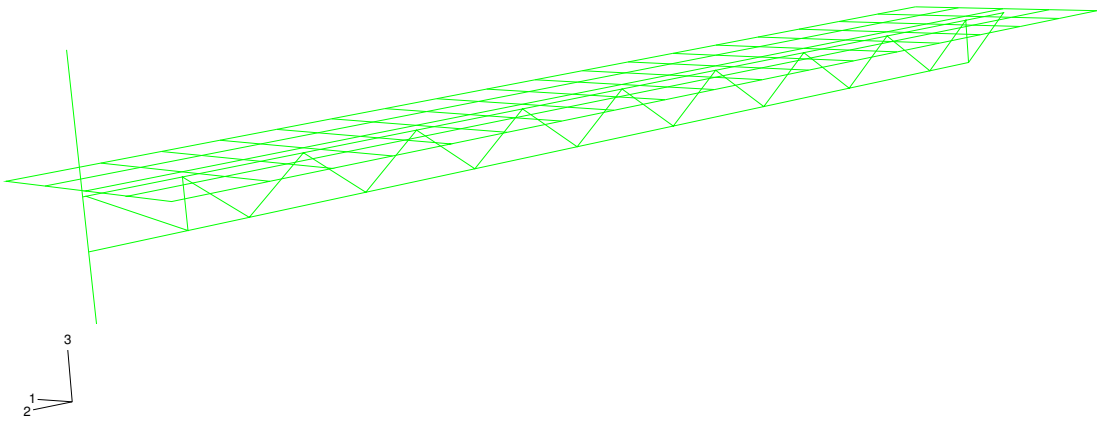

Figure A.1: Structural Mesh

at 1m spacing and truss assemblies at 2m spacing the elements were modelled at 2m and 4m intervals respectively. The member sizes of the trusses, outer columns and the details of the floor slab and its reinforcement have been taken from the FEMA report [50] and preliminary structural reports produced by Weidlinger and Arup [53,54]. The official NIST preliminary report on the WTC towers collapse [32] was then used to verify this information once it was published. These sections were then modified to maintain the buildings structural response at half resolution.

In the model used in this investigation the slab is modelled as a 100mm thick slab of lightweight C30 concrete. Reinforcement has been included as welded wire fabric with 6mm diameter bars at 100mm pitch running in both directions. One layer was provided in both the top and bottom of the slabs and both the core and outer slabs used a cover depth of 30mm. ABAQUS includes rebar as a smeared layer within the shell based on the details given in the input data.

The half resolution system was applied to the layout of the truss systems as well

as the overall member layout. The real truss system is a complex structure involving multiple top and bottom chords and diagonal tie members. These have been lumped together into simple rectangular and circular sections of the appropriate cross sectional areas. The column was dealt with in a similar manner with a box section of equivalent dimensions of two real columns. For more details on the layout of the truss please refer to Chapters 3, 4 & 6.

This model was constructed using the ABAQUS FE code. Within the model all the beam, truss and column members are represented using 2-node, linear beam elements while the slab is made up of 4-node, general purpose shell elements. Geometrical and material non-linearity are explicitly catered for. Steel and concrete properties for elevated temperatures have been extracted from Eurocodes 2 and 3 [26, 27]. The concrete has been modelled using the Concrete Damaged Plasticity material model in the ABAQUS material library.

A.2 Fire Input

The compartment temperatures are based upon a generalized exponential curve given by :

$$T(t) = T_o + (T_{max} - T_o)(1 - e^{(-at)}) \tag{A.1}$$

where T_{max} and T_o are the maximum and ambient compartment temperatures respectively. t represents the time over which the model is analysed. a is an arbitrary 'rate of heating' parameter. For the analyses presented here $a = 0.005$. This creates a compartment fire with a rapid temperature increase coupled with a period of stable temperature. Manipulation of this value and the required maximum compartment temperature can easily create different fire regimes. While such fires are not necessarily completely realistic they can be investigated in a methodical way. For example the 800°C Slow Fire presented in Chapter 3. Such manipulation, combined with using different fire curves for the steel and concrete heat transfer, can create scenarios that include an approximation of the effects of fireproofing.

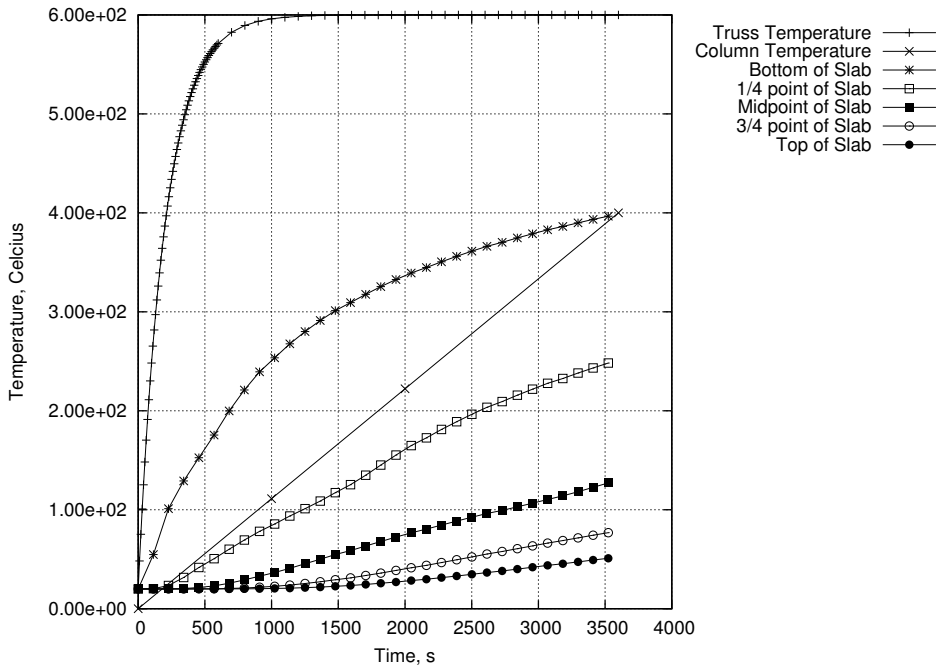

Figure A.2: Temperature Time Distributions

The temperature time distributions for unprotected truss and protected column elements as well as the 100mm thick floor slab may be seen below in Figure A.2. The fire regime used for this Appendix had a maximum compartment temperature of 600^{o}C. Due to the nature of A.1 any alteration to either the a value or the maximum temperature has implications on the rate of heating.

In the analyses presented here the truss is assumed to have no protection and is therefore taken to be equal to the compartment temperature. This simplification again allows the heating regime to be closely controlled and to allow a large difference in the rate of heating between the steel truss and the concrete to be introduced.

The column is assumed to be protected with a fire rated material and therefore undergoes more limited heating. In addition as long as there is only limited external flaming, the external columns' contact with the outside atmosphere would result in a lower temperature. The assumption was then made that the external column would be heated linearly from ambient up to a maximum of 400^{o}C over the course of the analysis. Previous research indicates that this is a reasonable assumption [59]

for protected steel sections.

Failure of the columns is the primary mechanism seen in the work presented in this thesis. However, it is important to note that this failure is brought about by excessive movement in the floors rather than material degradation. At the point in the 2D analyses where the initial failure mechanism becomes apparent (around 700s or so for an 800^{o}C fire over 3 storeys) the column has only risen to around 100^{o}C. In the models without hat truss structure this increase in temperature will not reduce the strength of the materials by any appreciable amount. The heating of the columns becomes more important when a hat truss is added to a structure. Such a device will transfer loads more effectively from the outer columns back into the core. This works both in compression and tension and hence the addition of a hat truss will increase the restraint in the outer columns. Thus the heating of the external columns will introduce restrained thermal expansion which may affect the response of the columns. This effect may be limited, however, by the low temperatures found in the columns at the point of failure (a maximum of around 200^{o}C in the 3D models) and hence the low level of thermal expansion (a maximum of around 0.25%). Previous research by Franssen [80] indicates that effect of restrained thermal expansion in columns may not be a critical factor, especially at low temperatures. Mitigation of restrained thermal expansion in the columns may also occur if they start at a low load ratio and are heated uniformly throughout a structure. This is the situation found in the outer columns in the models described in the main body of this thesis.

In all the models the temperature distribution in the concrete slab is described by applying individual time-temperature curves to 5 different points through the depth of the slab. The points used are the top and bottom surfaces, the quarter points and the mid depth of the slab. The time temperature distributions used in this study were taken from a 1D heat transfer analysis [75]. This method of input into the slab creates a more accurate representation of temperature distribution through the depth of the concrete compared to the mean temperature and gradient method used in previous research [1,7,62]. This is especially true in cases where the compartment

undergoes rapid heating. The underside of the slab may experience extremely high temperatures while the mid-depth of the slab will have barely increased above ambient. A mean temperature and gradient method does not allow the same kind of control over the temperature distribution.

In the case of the 3D model the above fire regime was applied as if the fire existed on the floor below that being modelled. The slab was assumed to be a compartment boundary hence only steel below the slab would be affected by the fire. The slab temperature distributions were created as if it was heated from beneath only.

A.3 Input Parameters Considered

Below is a brief description of which parameters have been investigated in this chapter and their usage. The options presented here are limited to the options investigated and do not represent the total selection available. More detail may be found in the ABAQUS manuals [73]. Where a word or phrase is contained within [ ] this indicates some kind of variable is to be inserted. The results of altering these parameters may be found in Section A.4.

A.3.1 Mesh Imperfections

One of the unrealistic assumptions that is used in computer modelling is that all elements are perfectly straight. In a real structure manufacturing processes and erection tolerances mean that structural elements will never be perfectly straight. While perfectly straight elements helps with positioning nodes it can create problems with convergence if buckling type mechanisms are expected to occur. FEM programs have to calculate the position and forces in all elements in the model at all times. If an element buckling load is approached then the program does not necessarily know in which direction the element will move after buckling. The time step of the analysis will therefore be reduced to extremely small values until the program can determine the buckling response. Therefore adding in a small imper-

fection to the element prescribes to a certain extent the initial direction of buckling failure and can help the analysis converge more efficiently. The slight imperfections that are needed will not necessarily affect the performance of the structure and indeed move the model closer to reality.

The structures to be used in this project were to be made up of a series of trusses. As trusses are made up of a series of slender members buckling responses were expected. A slight sine based imperfection was added to the truss diagonals, and in some cases the bottom chord of the truss. Base models were run using 1mm and 5mm (maximum out of plane) imperfections for members of around 1m in length and in this section this is compared to a model with no imperfections. Validation of this method is presented here in Section A.4 as well as in Chapter 6.

A.3.2 Model Parameters

∗ELEMENT, TYPE=[*variable*]

∗SHELL SECTION

[*shell thickness*, *number of integration points*]

ABAQUS includes a large library of element types that can be used for various types of analysis. It is important that an appropriate element is used. In this project only structural elements have been considered. The models are made up from a combination of beam elements (for the beams and columns) and shell elements (for the concrete slab). The simplest element types were chosen, and hence a check was made to ensure that they were appropriate. 2-noded linear beam elements using Timoshenko theory (B31) and 4 noded general purpose shell elements with reduced integration (S4R) were used. The B31 elements were compared to B33 elements which are 2-noded cubic beam elements using Euler-Bernoulli theory. Euler-Bernoulli beam elements are designed to represent slender beams with no shear deformations. In ABAQUS such beams appear to be limited in the way they can represent large deformations. It is stated in the ABAQUS manual [73] that analyses involving very large rotations (of the order 180°) should use quadratic or

linear beam elements. As significant deformations were expected in the structural steel due to combined gravity and fire loading the B31 elements were deemed to be superior. In the majority of the tests conducted comparing these two elements the B31 element models had fewer problems with convergence than the B33 element models.

For shell sections ABAQUS allows the user to define the number of points through the depth of the shell at which integration points are placed. There are specific rules to follow on this depending on which type of integration is being used (Gaussian or Simpson's). The integration type was kept at the default of Simpson's rule and the number of integration points was altered. The base case used 9 points while the default of 5 was also tested.

A.3.3 Material Parameters

Usage :
*MATERIAL, NAME= [*material name*], RTOL= [*variable*, $default = 0.03$]
*DENSITY
[*material density*]
*ELASTIC
[*elastic material data*]
*[*plasticity model*] (e.g. Plastic, Concrete Damaged Plasticity, etc.)
[*plastic material data*]

Disregarding the last two lines of the set above would input an elastic material into the program. Simple, isotropic elastic material data is input as Young's Modulus of Elasticity and Poisson's Ratio. Various values can be input to make the model sensitive to changes in "field variables" (such as temperature).

The density of the material is most often used for introducing gravity loading (a type of distributed loading) in the model. For Dynamic analyses, either elastic or plastic, a density is required even if gravity loading is not being used. It is important to make sure that the density is input in the same units as the rest

of the loading and dimensional data in the model (i.e. ensure that, say, Newtons and mm are being used throughout). The RTOL value is only needed for Explicit analyses where the material data being provided is not well regularized. More detail about this parameter may be found in Section A.4.2.4 below.

A.3.3.1 Plasticity Models

Steel

Steel is a relatively simple material to model due to its isotropic nature. The full ambient stress strain relationship may be seen in Figure A.3. For simple structural problems the steel stress-strain response is often simplified to the initial bilinear response (Figure A.4). Below the yield stress of the material it acts as a perfectly elastic material with all deformations being recoverable when the load decreases. Above the yield stress the material continues to strain and deform with no increase in load. This is appropriate when small strains are expected and is also conservative for models where moderately large (but less than fracture) strains are expected. The real response for structural steel includes a portion of strain hardening where the strength of the steel increases as the metal is deformed. Eurocode 3 [72] allows for strain hardening to be included in the strength of steel below 400^{o}C as long as it can be shown that sections are of a size such that buckling (local or otherwise) will not occur.

As the temperature of the steel increases material properties change. Eurocode 3 [72] provides equations for determining Elastic Modulus, stress-strain response and coefficient of thermal expansion for temperatures ranging from ambient conditions (20^{o}C) to 1200^{o}C. Figure A.5.a shows the EC3 representation of the change in Elastic Modulus as temperature increases. As the temperature increases the steel softens allowing the steel to deform more easily under load. In addition to this drop in Elastic Modulus the strength of the steel also drops as temperature increases. Figure A.5.b shows the Eurocode 3 plastic properties of steel from ambient to 1100^{o}C. Figure A.5 clearly shows a dramatic reduction in both strength and elastic modulus over temperatures of 500^{o}C. Although major building fires can easily reach

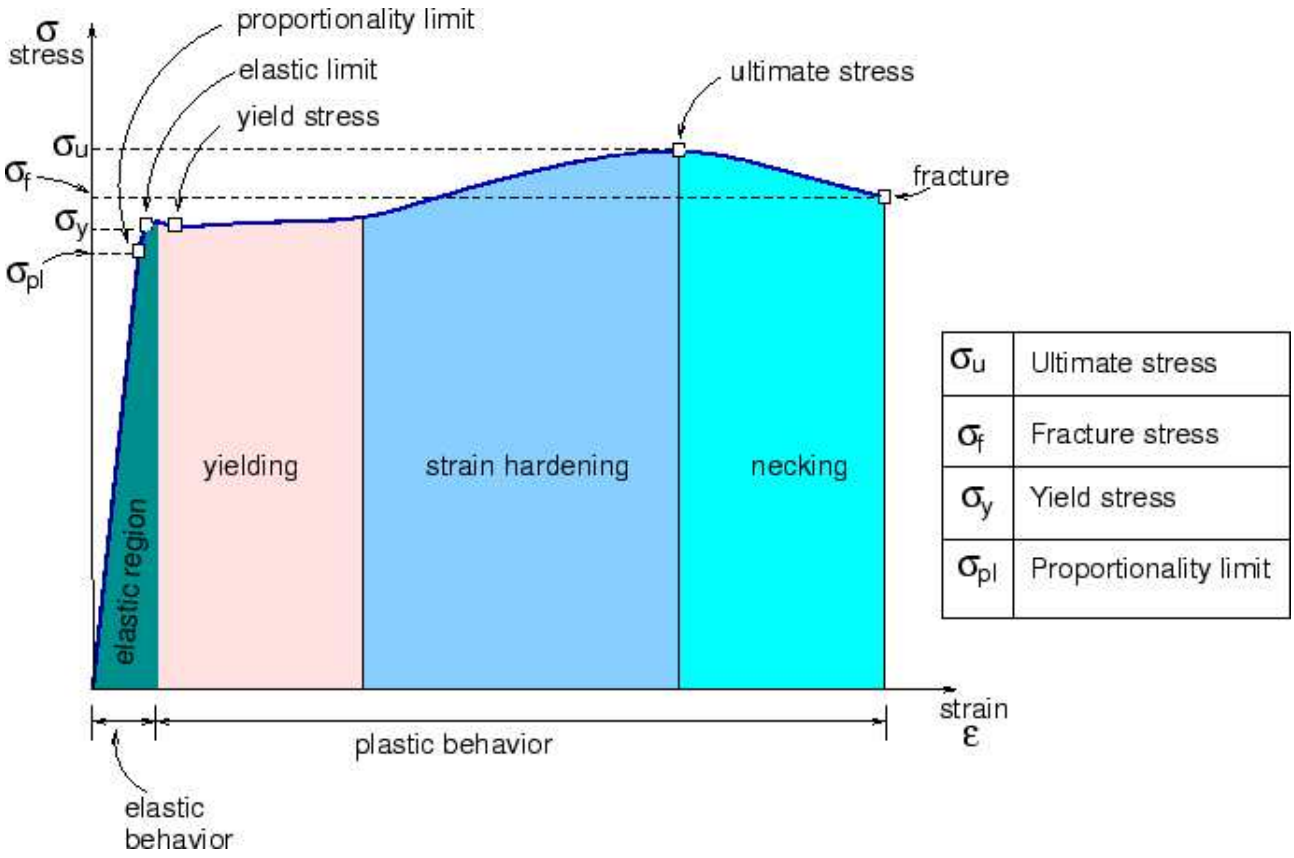

Figure A.3: Ambient Steel Stress-Strain Properties [81]

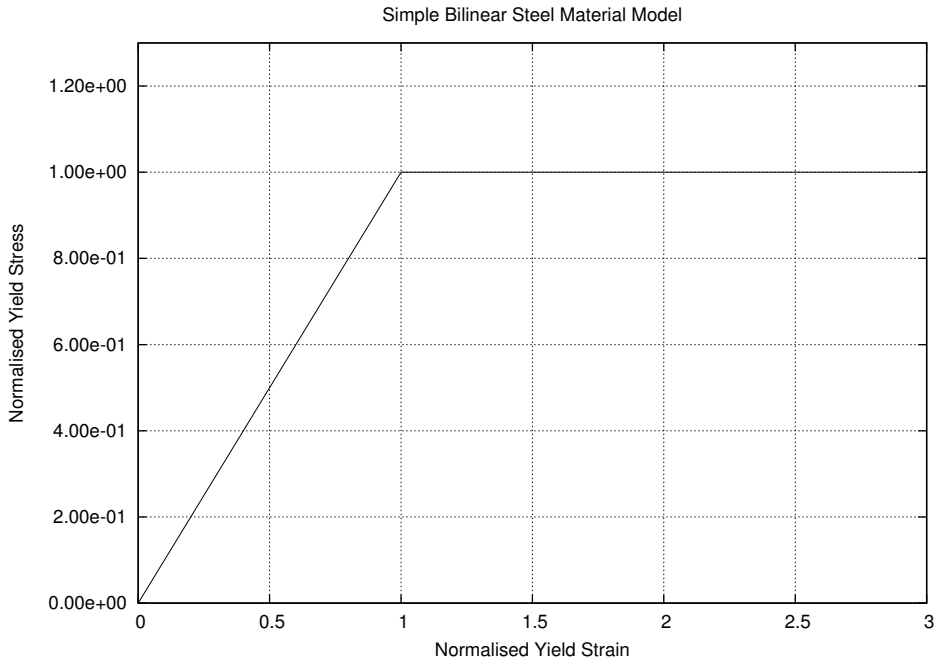

Figure A.4: Bilinear Response

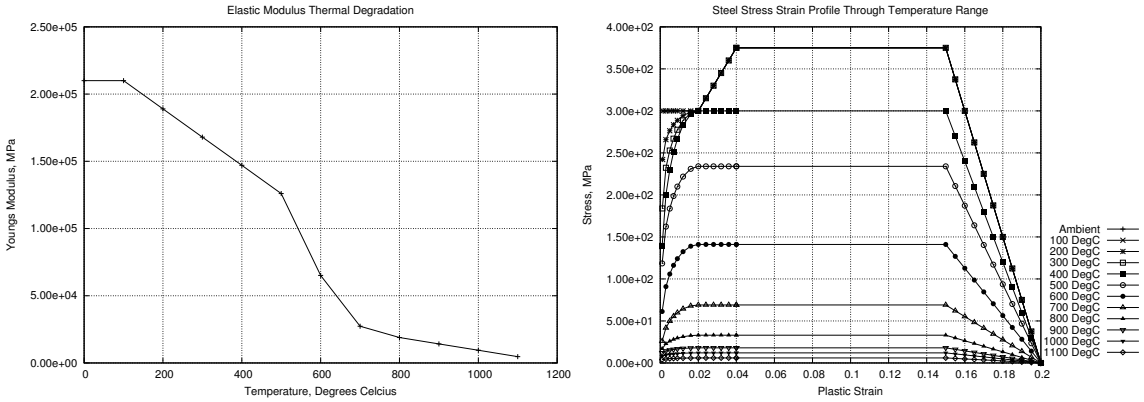

(a) (b)

Figure A.5: Temperature Related Steel Properties

temperatures of over 1000^{o}C it is highly unlikely that the structural steel will reach the melting point of around 1600^{o}C.

The other main response of steel to heating is to expand, indeed it is this expansion effect that drives the full structural response of a building. Eurocode 3 also specifies the values for thermal expansion for elevated temperatures (Figure A.6). The coefficient of expansion increases linearly for most of the temperature range pictured in Figure A.6. Between around 700 and 800^{o}C a phase change occurs in the steel and the material shrinks slightly. This is due to pearlite in the steel changing into austenite. The exact nature of this change is governed by the carbon content of the steel [13] but for design purposes the Eurocode provides a set of equations to predict the coefficient.

The quasi-static nature of numerical modelling being used in this project means that predictions of the state of the structure over the next time/load increment are made. An iterative process then narrows the prediction down until the solution of the equations satisfies some level of accuracy for equilibrium. Any of the input parameters that includes sharp changes or discontinuities can have a severe effect on the rate of convergence and thus the time a model takes to run. For that reason the steel material model used for this investigation is not exactly that shown in Figure

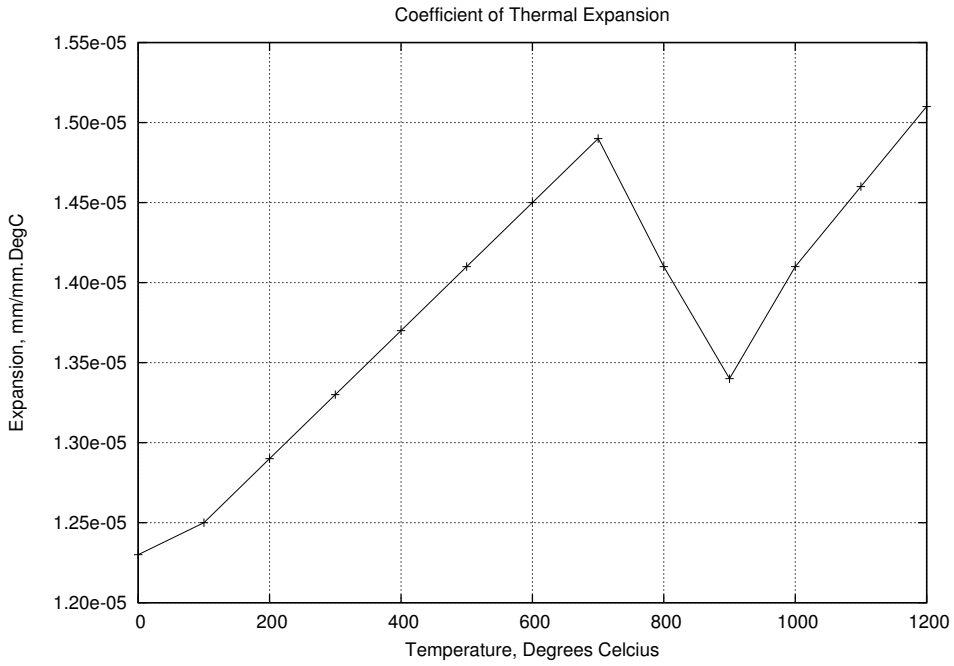

Figure A.6: Coefficient of Thermal Expansion

A.5.b. The sudden changes in the strength profiles that include strain hardening would reduce numerical efficiency. Another part of this conservative assumption, that no strain hardening would be used, is the slender nature of the steel members within the structure. In addition the final reduction in strength would be smoothed out over a larger range of strains than produced by the EC3 calculations. The final stress strain profiles used for the steel can be seen in Figure A.7. No changes were made to the Eurocode values for Elastic Modulus or Coefficient of Thermal Expansion. The values used are those shown in Figures A.5.a and A.7.

In ABAQUS the steel was modelled using a combination of linear isotropic elastic behaviour and isotropic plasticity [73]. This combination allowed the direct input of the profiles shown in Figures A.5.a and A.7. A yield strength of 300MPa was chosen as a reasonable strength for structural grade steel and this strength was used throughout all analyses unless specified otherwise.

Concrete

Concrete is a complicated material to describe and to model. Unlike homoge-

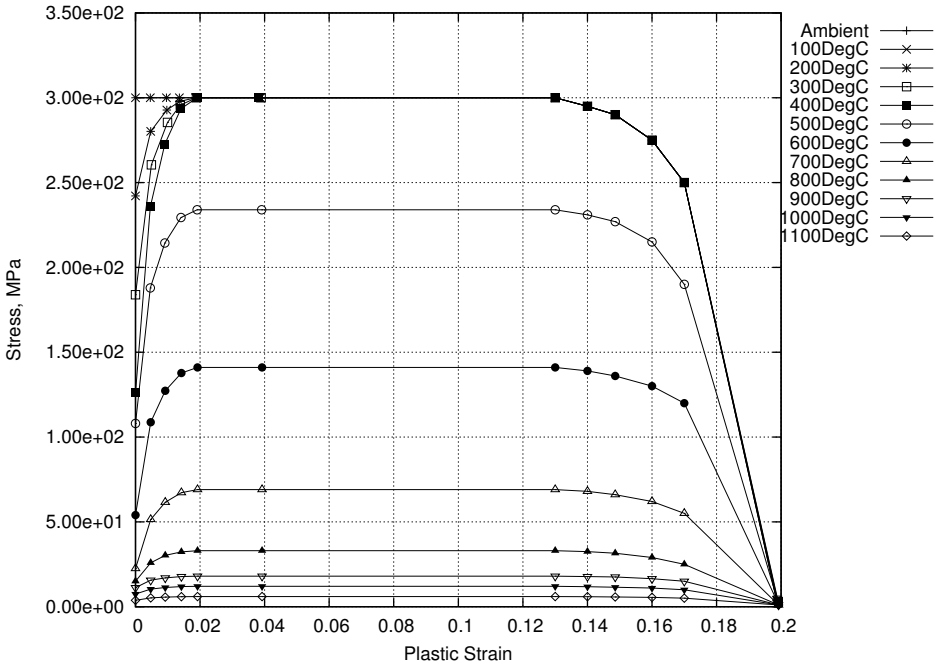

Figure A.7: Final Temperature Related Steel Properties

neous materials like steel and other metals it is made up of a mixture of inert aggregate of different sizes being bound together by a cementicious matrix. Water is also an integral part of the material both as free water held in pores and as water chemically bound within the cement. The interaction between these parts makes concrete good at resisting compressive forces but poor in tension. Modern building design makes efficient use of concrete by attempting to place it in locations where it will only come under compressive loading. Prestressing concrete is also possible to help it withstand tensile forces (the concrete moves into reduced compression rather than actual tension) and to add stiffness.

Other materials, such as steel and, increasingly, carbon fibre, are used to withstand tensile forces. On a local scale steel reinforcing bars are used within concrete beams and slabs. On a larger scale long span floor systems can be constructed that combine steel supporting beams (or trusses) with a concrete floor slab to reduce weight and increase strength. Concrete floor slabs are often cast onto thin, profiled metal decking. The effects of this decking is to ease construction and to provide more efficient placement of concrete. Such decking also works as an extra level of

tension reinforcement when acting compositely with the floor slab.

As with all materials the mechanical properties of concrete change with temperature. On the microscopic scale the heating of concrete induces differential expansion between the aggregate and the binding matrix as well as driving off the water contained within (physically and chemically). This response combined with restrained thermal expansion on the macroscopic scale can produce tensile forces within the material and cause portions of concrete to come loose (sometimes explosively) or "spall" away from the main body of the material. Such spalling can have drastic consequences on the structure. By losing material the cross sectional area of a structural member is reduced, possibly to a level where it is no longer adequate to support the loads it was designed for. Concrete is also an effective insulator thus spalling can also reduce the effectiveness of this insulation. Spalling may expose the reinforcing steel present within reinforced concrete which has the dual effect of increasing the rate of heating of the steel and of reducing the effectiveness with which the steel and concrete act together. This may lead to a reinforced concrete member no longer being able to support the loads it was designed for.

The Eurocode 2 [74] properties for concrete may be found in Figure A.8. A standard, conservative assumption made in concrete design is that the material has zero tensile strength and that all such loading will be withstood by the steel reinforcement. In reality concrete does have some tensile strength. In this project the tensile strength of the concrete has usually been limited to 5% of the maximum compressive strength. Where different properties have been used this fact will be made clear.

The tensile profiles used for different temperatures may be found in Figure A.9. It is recommended that after tensile yield the tensile capacity of concrete be reduced to zero as strain reaches about 10 times yield strain [73] . However for numerical efficiency and to aid convergence the tensile capacity of the concrete was plateaued at the yield level.

Although spalling can produce major effects it is not yet well understood and therefore hard to include in a numerical model. Please see Chapter 2 for more in-

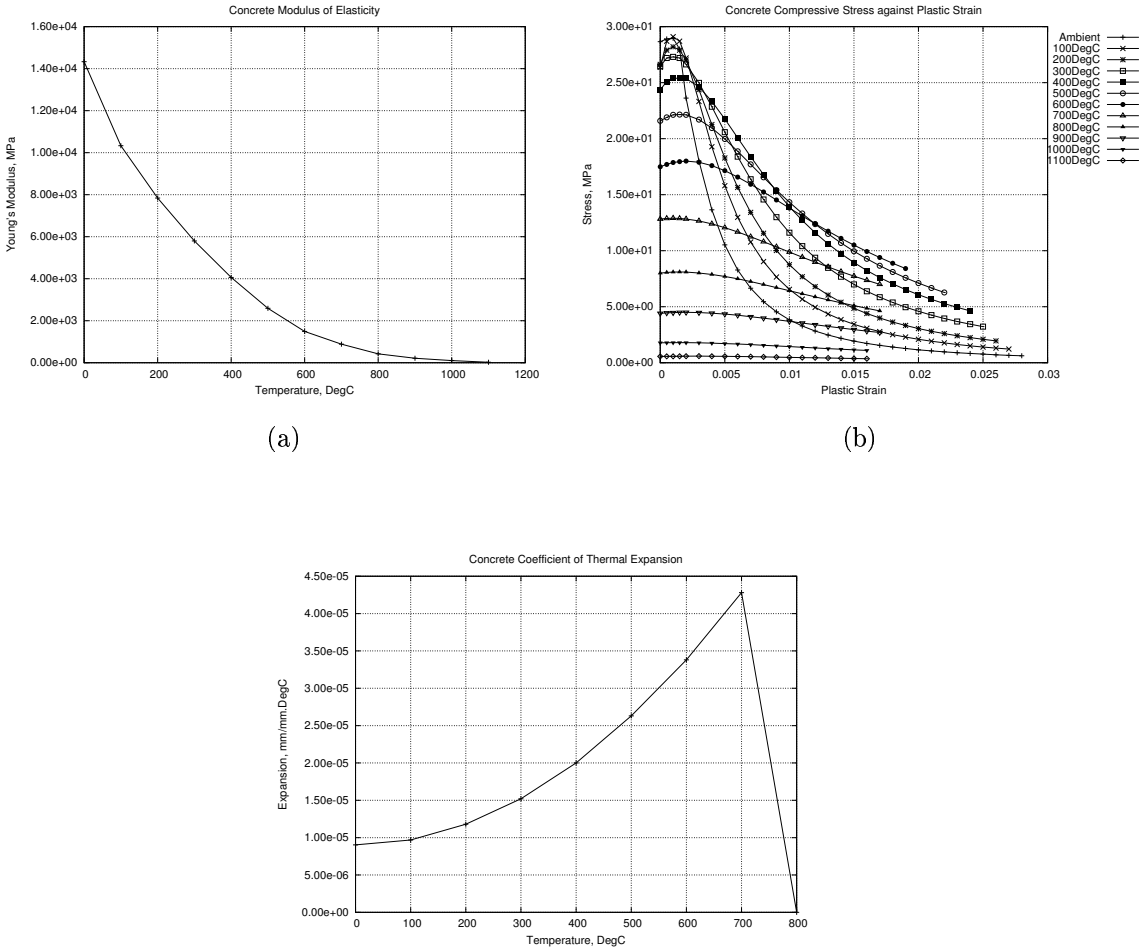

Figure A.8: Concrete Temperature Dependant Material Properties

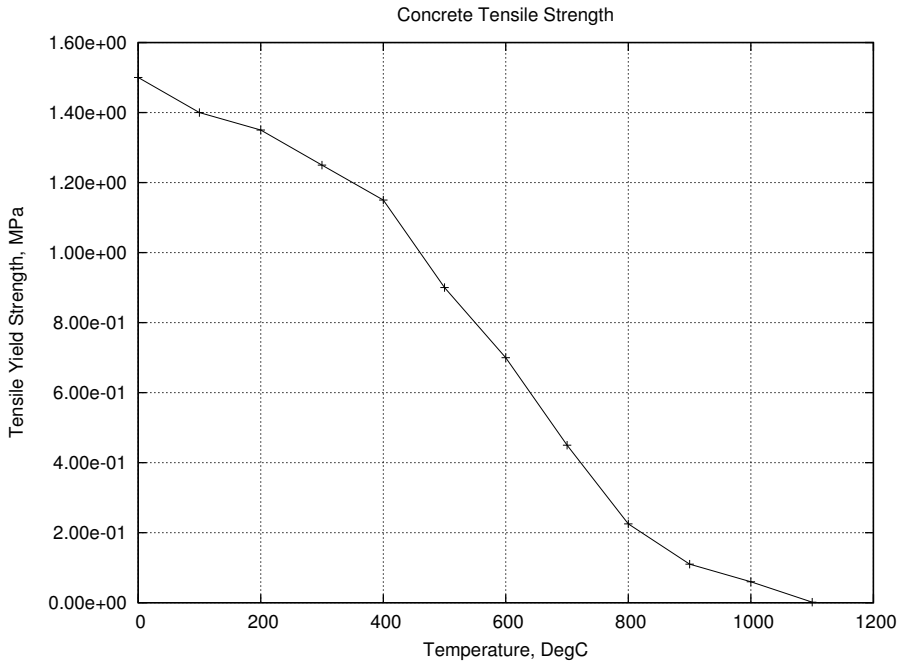

Figure A.9: Concrete Temperature Dependant Tensile Strength

formation on this phenomenon. Previous investigations of the effect of any profiled decking [1, 7, 16] have shown that it has little impact on the overall response of the floor slab. In addition observations of experimental testing and the aftermath of real building fires has shown that such thin metal decks will often debond from the concrete early in a fire due to a combination differential thermal expansion and pressure created by water within the concrete boiling off. As such decks are not routinely insulated they will heat up and therefore lose strength extremely quickly. Thus in all of the structural models investigated for this project the structural effect of any such deck has been ignored. One remaining beneficial effect of the existence of such a deck under fire conditions is that it will stop any spalling material from escaping completely. While there will obviously be a strength loss proportional to the level of spalling the floor slab will not lose the insulating effect of the spalled material.

C30 grade concrete was used throughout this project. This gives a compressive strength of 30MPa.

Concrete Material Models in ABAQUS

There are several material models available in ABAQUS to represent concrete. For this project two in particular were investigated to ascertain which would provide a better representation of the material. These were the ABAQUS Concrete Damaged Plasticity model and the Drucker-Prager model. A short description of both models will be presented here but the full results of the investigation will not.

Drucker Prager : This method uses a group of equations to define a failure surface for the material. Originally used for soils it has been accepted as a reasonable match for other frictional materials such as concrete. This model allow various responses of such materials to be included, such as: pressure dependant yield, isotropic hardening/softening, dilation, creep and sensitivity to strain rate. In the ABAQUS program the user defines either the tensile or the compressive stress-strain relationship for the material. The program then uses various parameters such as Friction Coefficient and Dilation Angle to extrapolate the full failure surface including the tensile or compressive part depending on which was specified. Extra parameters can be added to allow for creep and other factors (see the ABAQUS manual [73] for details). Several previous projects have successfully used this material model for concrete in fire situations [1, 7, 13].

The investigation of the material models showed that the Drucker Prager model was not as versatile as the alternative. Based on the information given in the ABAQUS manual it is intended primarily for monotonic loading and only one behaviour (either tension or compression) may be defined. Extrapolation is used to define the other behaviour. For these reasons the Drucker-Prager was not used for the work presented in this thesis.

It was found that the Drucker-Prager material model gave a less satisfactory response when compared to the Damaged Plasticity model.

ABAQUS Concrete Damaged Plasticity : This material model has only recently been included in the ABAQUS FEM software and as its name suggests

has been specifically designed for concrete. The input parameters are similar to the Drucker Prager model with dilation angle being used to create a failure surface. This model allows the user to define both the compressive and the tensile inelastic response making the final model more accurate in complex situations. Unlike the DP model the ABAQUS concrete model is designed for cyclic and dynamic loading as well as monotonic. This makes it more robust when being used in fire regimes with cooling stages.

The primary advantage this model has over the Drucker-Prager model is the ability to specifically define both the tensile and compressive behaviour of the concrete. This allows greater control over the response of the material. Additionally the Damaged Plasticity model allows the user to introduce degradation of the material stiffness due to cracking and crushing of the concrete. The damaged plasticity model can also model stiffness recovery when moving between tensile and compressive loading. It allows recovery in the material stiffness when the concrete moves into compression after cracking. This recovery is not included if the material subsequently moves back into tension.

The full capabilities of the Concrete Damaged Plasticity material model were not used for this project. This was done in order to reduce the possible convergence problems that damaged plasticity might introduce. The final material models for concrete were created using the Concrete Damaged Plasticity model.

Reinforcement Bars

ABAQUS allows shell sections to include reinforcement as a smeared layer. This method was used to include reinforcement bars in the concrete slab. S460 steel was used for these members and material data was included in the models using isotropic elastic and plastic behaviour in a similar way to the main structural steel. The properties used may be seen in Figure A.10. As the reinforcement was to be embedded in the concrete it would be well insulated from any heating. Therefore a limited range of temperatures was considered for this material. Thermal expansion effects were included using the data from Figure A.6.

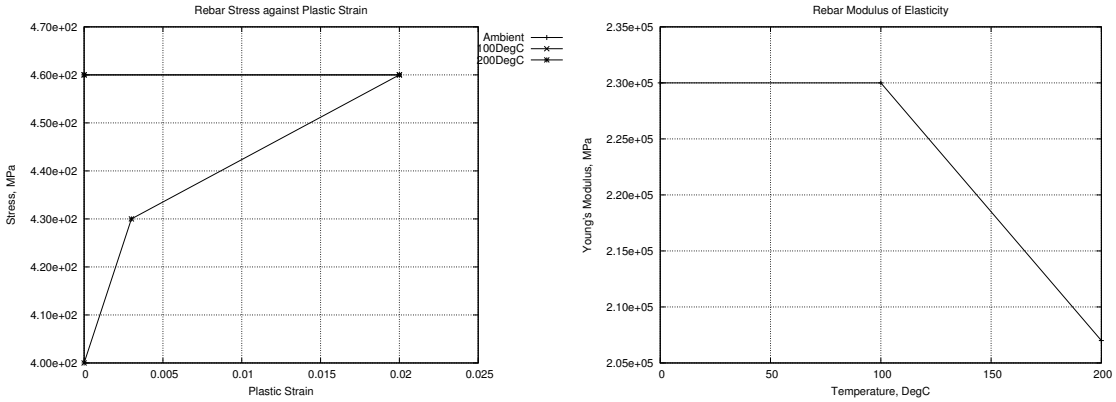

Figure A.10: Reinforcement Steel Properties

A.3.4 Quasi-static Analysis Parameters

Usage :

*STEP, AMPLITUDE=RAMP, INCREMENT= $[variable]$, NLGEOM

*STATIC, STABILIZE=$[variable, default = 2x10^{-4}]$, FACTOR=$[variable]$

$[step\ time\ and\ incrementation\ data]$

*CONTROLS, ANALYSIS=DISCONTINUOUS

The Amplitude term indicates that by default any loading data in the step is to be applied linearly across the step. The alternative is to have all loading applied immediately at the start of the step. The INCREMENT term allows the user to specify a maximum number of increments to be completed. This variable is used to help keep the program from spending too much time on an analysis by quitting out after a designated number of increments. For more information on any of these parameters refer to the ABAQUS Manuals. NLGEOM indicates that non-linear geometry is to be used.

In a Quasi-static analysis it is possible to apply numerical stabilization to the model to assist with convergence. This stabilization adds an artificial viscous force term into the global equilibrium equations. This prohibits the model from moving too quickly and hence eases calculations and increases increment size. Application of such stabilization should be carefully considered as too much can affect the results

of the analysis. There should always be a balance between ease of convergence and the validity of the results being returned by the analysis with the results being the more important aspect.

The two systems used in this investigation use the Stabilize and Factor options. Stabilize allows the user to designate a level of energy that will be removed from the system and automatically calculates a damping factor. The Factor option must be used in conjunction with the Stabilize option but will override any value associated with it. Using Factor the user can directly apply a damping factor to the model.

The last command listed directly affects the convergence criteria. Further modification of all convergence parameters can be undertaken using the Controls command but this should only be attempted with considerable knowledge of the consequences on the results. For this investigation a default control level was used (i.e. Analysis=Discontinuous). This setting allows many more iterations to be completed before increment size is altered during an analysis. Normally if convergence problems occur the increment size will be reduced relatively rapidly and afterward the increment size will be increased gradually. In analyses which involve short term complications, such as buckling of members or concrete cracking, this sudden drop and slow increase can affect the efficiency of the analysis. Including this control overrides the normal incrementation controls and will keep the increment size steady for relatively many more iterations. Note that this control has no effect on the actual increment size necessary for calculation convergence but merely affects the level at which the first iteration of an increment starts.

A.3.5 Explicit Analysis Parameters

Usage :

*STEP,NLGEOM=YES

*DYNAMIC, EXPLICIT

[*step time and incrementation data*]

*[*FIXED or VARIABLE*] MASS SCALING, ELSET= [*target element set*],

DT= [*desired increment size*], NUMBER INTERVAL= [*variable*], TYPE= [*variable*]

The AMPLITUDE and INCREMENT terms may not be used in Explicit. For this reason, depending on load type, RAMP type amplitude curves need to be included manually by using the *AMPLITUDE command. the default for some load types apply all loading will be applied at the start of the step while others default to a Ramp system. Temperature input defaults to a Ramp system but more information on the defaults used should be obtained from the ABAQUS manuals [73] before implementation. While linear systems are easy to create in a few lines of code it is important to make sure that the loading will correctly move from the maximum load from the previous step to the required maximum of the current step. A simple curve defining a linear increase from 0 to 1 over the step will not necessarily produce a Ramp type effect. A Ramp function has to progress linearly from the final load in the step before to the final load in the current step.

Explicit analyses allow the stiffness matrix to be made diagonal and therefore solution of the global equilibrium equations are made significantly more simple. however, this ease of calculation requires the use of very small time steps for the calculations to remain stable. As the matrix inversion and prediction methods used in Implicit formulations are not required it means that Explicit analyses have no problems with convergence. This allows the user to use Time Scaling to speed up an analysis. This technique is described in greater detail below. It is used by including a shorter time value in the step data line and then scaling all time based distributions to match.

The Mass Scaling line makes an analysis run faster by allowing larger increments. Greater detail on this term may be found in the results section below. A more in depth description of the various parameters that may be used with this command may be found in the ABAQUS manual. Mass Scaling works by creating a damping effect though alteration of the model mass matrix. While this can lead to an increased stable time step the increase in inertia in the model can cause inaccuracy.

A.3.6 Implicit Dynamic Analysis Parameters

Usage :
*STEP, AMPLITUDE=RAMP, INCREMENT= [*variable*] , NLGEOM
*DYNAMIC, HAFTOL= [*variable*], ALPHA= [0 *to* -0.333]
[*step time and incrementation data*]

The Amplitude, Increment and NLGEOM terms work in the same manner as described in the Quasi-static section above.

The important parameters for this study were the HAFTOL and ALPHA variables. These variables are described in more detail in the appropriate results section below. Again these parameters are related to convergence and damping within the analysis.

A.4 Results

Tables A.1, A.2 and A.3 below summarize the input data about the tests while there are more detailed descriptions later. The last two columns indicate the effects gained by altering the input data from the base case. Inc. refers to the number or size of increments in the analysis while Acc. indicated how the changes have affected the accuracy of the solution.

Output was taken at the locations shown in Figure A.11. Values at the midspan were used for the section forces in the top and bottom chord of the truss (nodes 1020518 and 1030518 respectively) and for the vertical deflection of the top chord. Section forces and horizontal displacement were taken at the connection between the column and the truss (node 1040100). The results presented here are purely for comparison between cases, for more detail on the effect of heating on long span trusses please refer to Chapter 3.

Sec.	Name	Conc. Str.	Plastic	Element	Shell Int.	Stabilize	Factor	Imperf.	Inc.	Acc.
4.1.1	Base	5%	Yes	B31	9	NA	$1x10^{-6}$	Yes	335	Good
4.1.2	Control	5%	Yes	B31	9	NA	$1x10^{-6}$	Yes	315	Good
4.1.3	DampHi	5%	Yes	B31	9	NA	$1x10^{-4}$	Yes	280	Low
4.1.3	DampLo	5%	Yes	B31	9	NA	$1x10^{-8}$	Yes	378	Good
4.1.4	Elast	5%	No	B31	9	NA	$1x10^{-6}$	Yes	260†	Low
4.1.5	Element	5%	Yes	B33	9	NA	$1x10^{-6}$	Yes	618*	Good
4.1.6	MatProp	5%	Yes	B31	9	NA	$1x10^{-6}$	Yes	336	Good
4.1.7	SinImp	5%	Yes	B31	9	NA	$1x10^{-6}$	No	359	Good
4.1.8	SlabLay	5%	Yes	B31	5	NA	$1x10^{-6}$	Yes	319	Good
4.1.9	StabHi2	5%	Yes	B31	9	$2x10^{2}$	NA	Yes	260†	Low
4.1.9	StabHi	5%	Yes	B31	9	$2x10^{3}$	NA	Yes	260†	Low
4.1.9	StabDef	5%	Yes	B31	9	$2x10^{4}$	NA	Yes	267	Low
4.1.9	StabLo	5%	Yes	B31	9	$2x10^{5}$	NA	Yes	284	Low
4.1.9	StabLo2	5%	Yes	B31	9	$2x10^{6}$	NA	Yes	307	Good

* Note : Analysis failed to complete

†Note : 260 increments is the minimum possible with step data used

Table A.1: Quasi-static Analysis Summary

Sec.	Name	Time	Mass (%)	Conc. Str.	Plastic	Inc. Size	Acc.
4.2.1	Base	3600s	100	Steady	Yes	$8.9x10^{-6}$	Good
4.2.2	Elast	3600s	100	Steady	No	$8.9x10^{-6}$	Low
4.2.3	Mass1	3600s	10,000	Steady	Yes	$3.0x10^{-4}$	Good
4.2.3	Mass2	3600s	450,000	Steady	Yes	$2.0x10^{-3}$	Good
4.2.4	RTOL	3600s	100	Steady	Yes	$8.9x10^{-6}$	Good
4.2.5	Conc	3600s	100	Degrade	Yes	$8.9x10^{-6}$	Good
4.2.6	Time1	360s	100	Steady	Yes	$8.9x10^{-6}$	Good
4.2.6	Time2	36s	100	Steady	Yes	$8.9x10^{-6}$	Good

Table A.2: Explicit Dynamic Analysis Summary

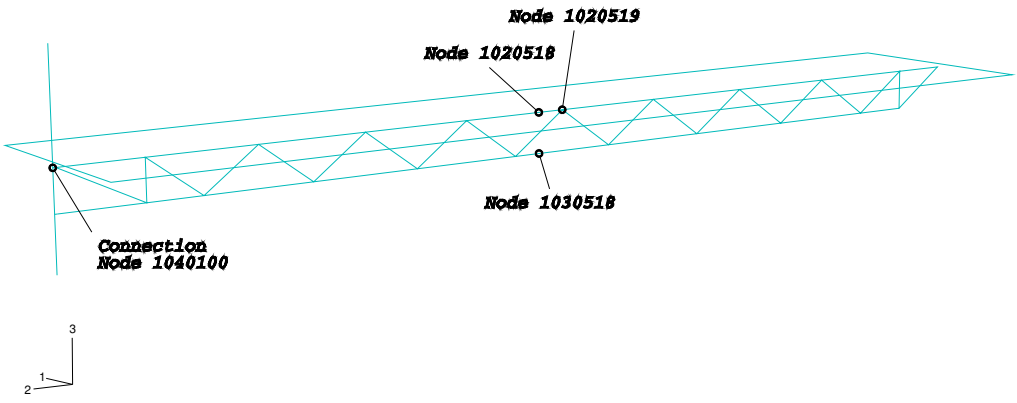

Figure A.11: Output Locations

Sec.	Name	Alpha	Plastic	Slab	HAFTOL	Imperf.	Concrete	Incs to 1000s	Acc.
4.3.1	Base	-0.05	Yes	S4R	$4x10^4$	No	Steady	2382*	Good
4.3.2	DampHalf	-0.15	Yes	S4R	$4x10^4$	No	Steady	1898*	Good
4.3.2	DampFull	-0.333	Yes	S4R	$4x10^4$	No	Steady	1488*	Good
4.3.3	Elastic	-0.05	No	S4R	$4x10^4$	No	Steady	2149	Low
4.3.4	ElType	-0.05	Yes	S4	$4x10^4$	No	Steady	2675*	Good
4.3.5	HAFD10	-0.05	Yes	S4R	$4x10^3$	No	Steady	NA*	Good
4.3.5	HAFX10	-0.05	Yes	S4R	$4x10^5$	No	Steady	474*	Good
4.3.5	HAFX100	-0.05	Yes	S4R	$4x10^6$	No	Steady	384*	Good
4.3.5	HAFX1000	-0.05	Yes	S4R	$4x10^7$	No	Steady	322*	Good
4.3.6	RTOL	-0.05	Yes	S4R	$4x10^4$	No	Steady	2384*	Good
4.3.7	SinImp	-0.05	Yes	S4R	$4x10^4$	Yes	Steady	NA*	Good
4.3.8	Tens	-0.05	Yes	S4R	$4x10^4$	No	Degraded	2755*	Good

* Note : Analysis failed to complete to 3600s

Table A.3: Implicit Dynamic Analysis Summary

A.4.1 Quasi-static Analyses

A.4.1.1 StatBase

The baseline analysis that all other factors were to be compared to had the following parameters :

- Static, Stabilize, Factor=1x10^{-6}
- Concrete tensile strength set to 5% of compressive (1.5MPa)
- B31 beam elements
- 9 integration points in shell sections
- 5mm max. out of plane sine based imperfections in truss diagonals

A.4.1.2 Convergence Controls

This analysis was designed to investigate the effect, if any, of including the ∗Controls, Analysis=Discontinuous command. This command is most useful in analyses that show severely discontinuous behaviour. It increases the number of iterations required before ABAQUS initiates checks for increment size. This allows ABAQUS to keep the increment size relatively large when faced with sudden discontinuities. Use of this command in analyses that do not exhibit this behaviour may reduce the overall efficiency of the analysis. For more details the ABAQUS manual [73] should be referred to.

As can be seen in Figure A.12 the effects of including this command are minimal. As well as the responses overlaying each other for the two models the increments are also spaced identically. This indicates that the analysis is not excessively discontinuous and hence this command is not necessary for a single truss model.

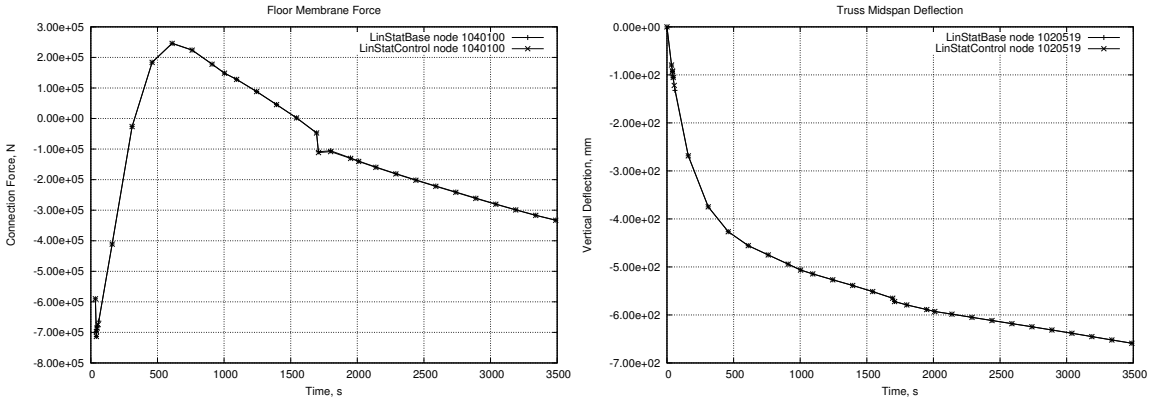

(a) (b)

Figure A.12: Quasi-static : Control Comparison

A.4.1.3 Damping using "Stabilize, Factor="

This comparison gives an indication of the effect of altering the factor assigned to the command $*Static$, $Stabilize$, $Factor$ =. This command adds a viscous damping term to the global equilibrium equations. The base factor of 1x10^{-6} was compared to no damping at all (DampNo) as well as cases with factors 100 times lower and 100 times higher (DampLo and DampHi, respectively). The case in which all damping (DampNo) was removed failed to converge after around 50s. While this case would give the most realistic results the lack of convergence means that it is not a suitable option.

Figure A.13 shows a comparison between the Base case and the DampLo case. The change of stabilization factor has little effect. The close correlation between the results indicates that both are giving valid results and that the Base case damping factor is not too high. Comparison between the Base case and the DampHi case shows that the latter case is too highly stabilized. Significant differences can be seen in all results as shown in Figure A.14. The increased level of damping slows down the movement of the model as a whole. As the midspan deflection of the model is delayed the effects of thermal expansion have to reach equilibrium in some manner and hence the floor membrane force is increased. This will also lead

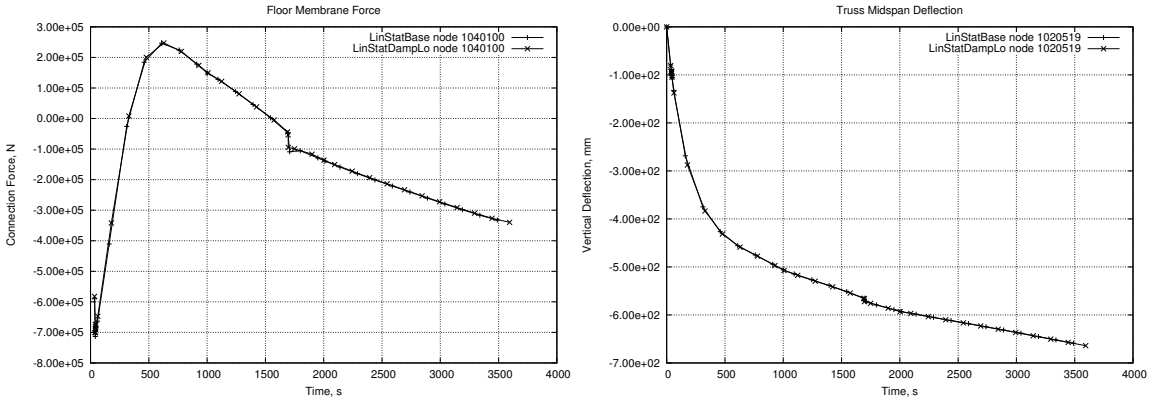

(a) (b)

Figure A.13: Quasi-static : DampLo

to more horizontal displacement at the column.

A.4.1.4 Elastic Only Material Properties

A model was run using the test structure and linear elastic material properties. Such material properties are considerably more easy to implement and hence would increase numerical efficiency. As Figure A.15 indicates this does not give a suitable response when compared to the base case. As the material properties do not allow plastic deformation they are considerably stronger than a more realistic representation of the material. The midspan deflection is therefore resisted by the effectively infinite truss strength which leads to higher connection forces and more column movement. Unlike the Base case the elastic material model case never moves into tensile membrane/catenary action.

A.4.1.5 Element Type (B31 to B33)

A close comparison between the two beam element types shows a mixed result. The force responses from the two analyses (Figure A.16) are somewhat different, although this only appears to lead to a small difference in the midspan deflection shown in Figure A.17.b. The use of B33 elements appears to lead to much more

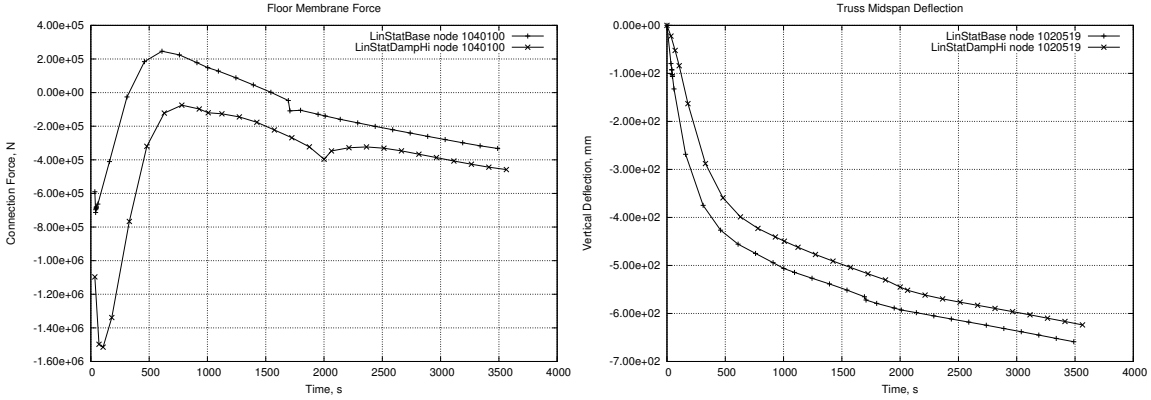

(a) (b)

Figure A.14: Quasi-static : DampHi

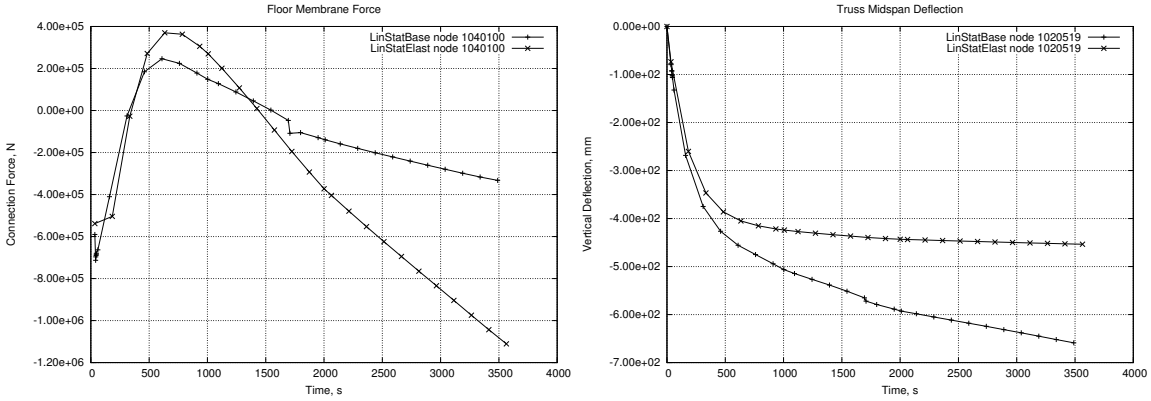

(a) (b)

Figure A.15: Quasi-static : Elastic Material Properties

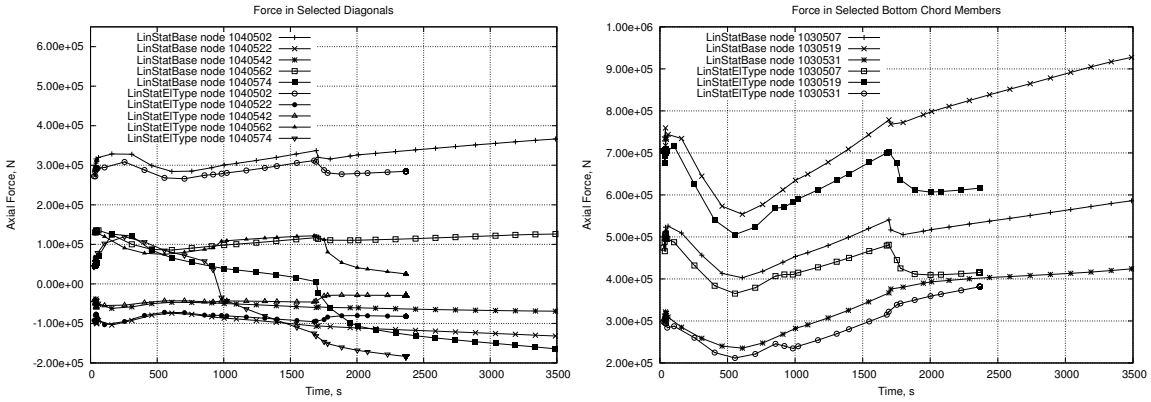

(a) (b)

Figure A.16: Quasi-static : Element Type Truss Forces

extreme buckling responses in the truss diagonals compared to the base case using B31 elements. As the truss diagonals fail more readily this then creates a less stiff floor system. This effect can be seen in Figure A.20.a as the floor remains in tension under the B33 case. In the Base case the floor system gradually pushes the column back outward, indicated by the compressions seen in the truss-column connection. As previously mentioned the local differences in the truss diagonals do not appear to greatly affect the midspan deflection of the floor.

The B33 model encounters considerable convergence difficulty after about 2400s while showing no obvious global failure in the floor system. The differences in local response between the two element types may be worth investigating in more detail. As the B33 model failed to converge, under relatively easy conditions, while the B31 model was stable throughout the analysis time the latter was chosen for use. Later trials on the 3D multi-floor models also indicated that the B31 elements were more stable.

A.4.1.6 Discontinuous Material Properties

This comparison was designed to identify the differences, if any, that would be caused by altering the steel material properties in order to make them less discon-

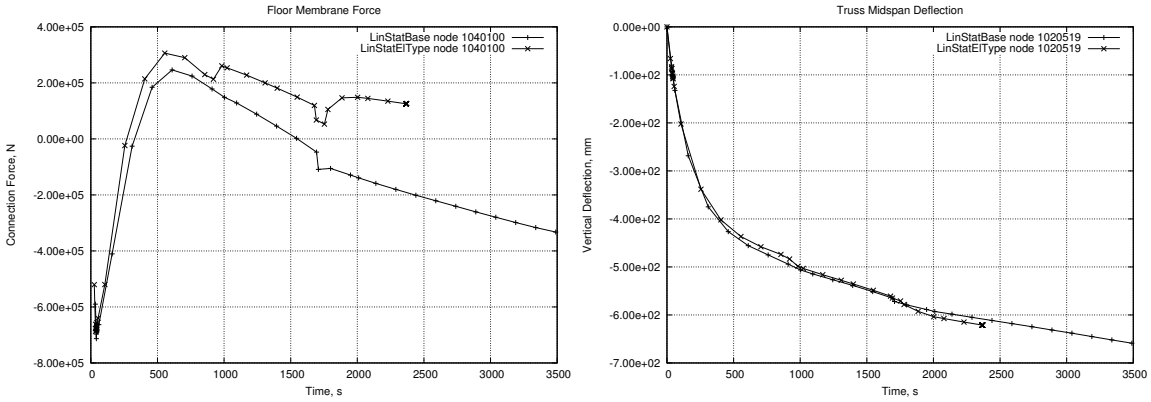

(a) (b)

Figure A.17: Quasi-static : Element Type Global Response

tinuous. The base case used the exact properties as defined by Eurocode 3 [27] as can be seen in Figure A.5. The comparison case used the properties in Figure A.7. These were the final material properties used in the large scale models.

The final properties were designed to be somewhat more computationally efficient as they did not have any major discontinuities. As can be seen in Figure A.18 the results of the two analyses are virtually identical. This gives confidence that the simplification of the material properties in this manner will not affect the results of the larger analyses.

A.4.1.7 Imperfections in Truss Diagonals

As described in Section A.3.1 the truss diagonals in the Base case had sine based imperfections applied to their geometry. This was applied in order to aid convergence as buckling of these members was expected. An analysis was conducted to compare the response with and without these imperfections. The results of the two models compared here are broadly similar as indicated in Figures A.19 and A.20. The biggest difference is the timing of the truss buckling mechanism. The response is seen to happen somewhat earlier in the Base case (with imperfections) while the case without imperfections takes about 500s longer for buckling to appear. The

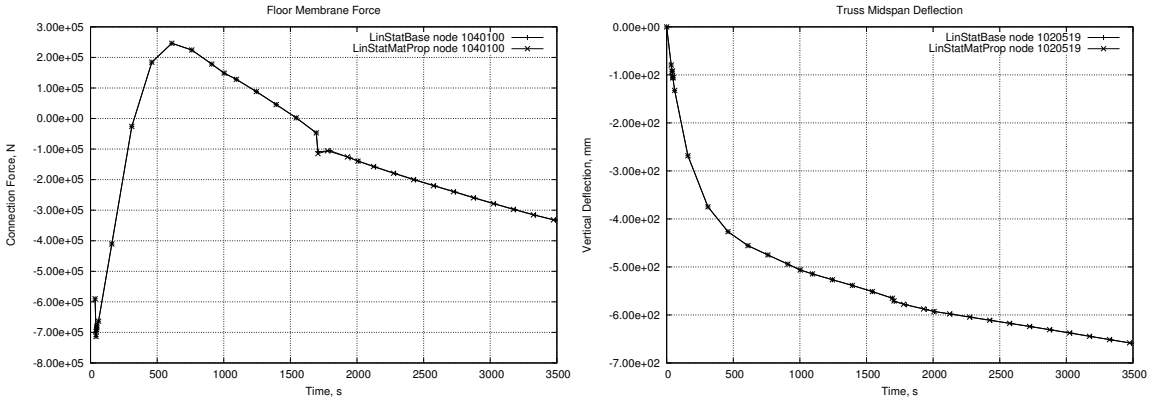

(a) (b)

Figure A.18: Quasi-static : Material Properties Response

response before and after the buckling shows close correlation between the two models and the global response is not greatly altered by the change. This indicates that the timing of the buckling will not greatly affect the response of the model and hence including imperfections appears to be a valid technique. Including the imperfections also has the advantage of creating a smoother response which aids convergence.

A.4.1.8 Slab Calculation Layers

ABAQUS shell sections have the capability to have a variable number of integration points through the depth of the slab. As with other factors in finite element modelling an increased number of integration points will generally give a more accurate answer at the cost of processing time. A test was run to compare the ABAQUS default number (5 layers) of integrations points with a higher number (9 layers). In this comparison the Base case has the higher number of layers and the comparison model (SlabLay) has the default number of layers. As can be seen in Figure A.21 this change makes little difference to the final result. There is a slight change in some of the local details in the truss forces (Figure A.21.a) but this does not lead to any major alteration of the global response that can be seen in Figure

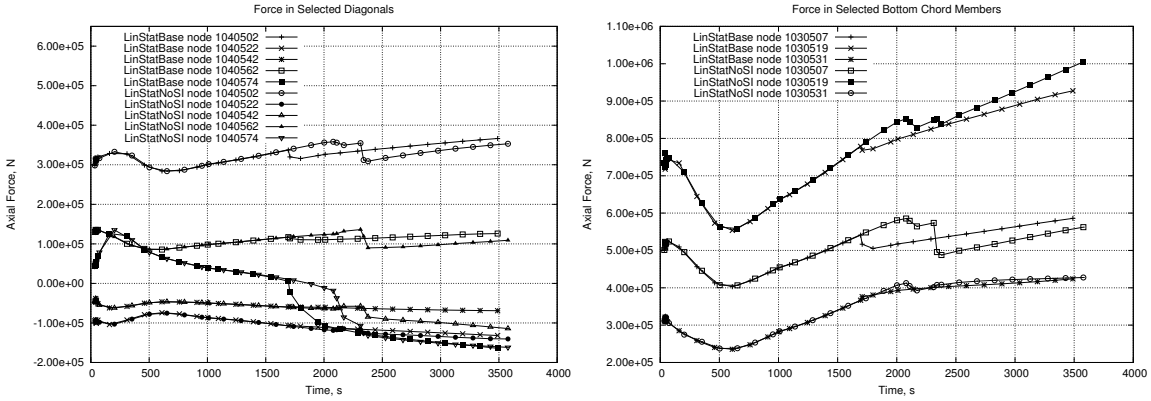

(a) (b)

Figure A.19: Quasi-static : Imperfection Truss Forces

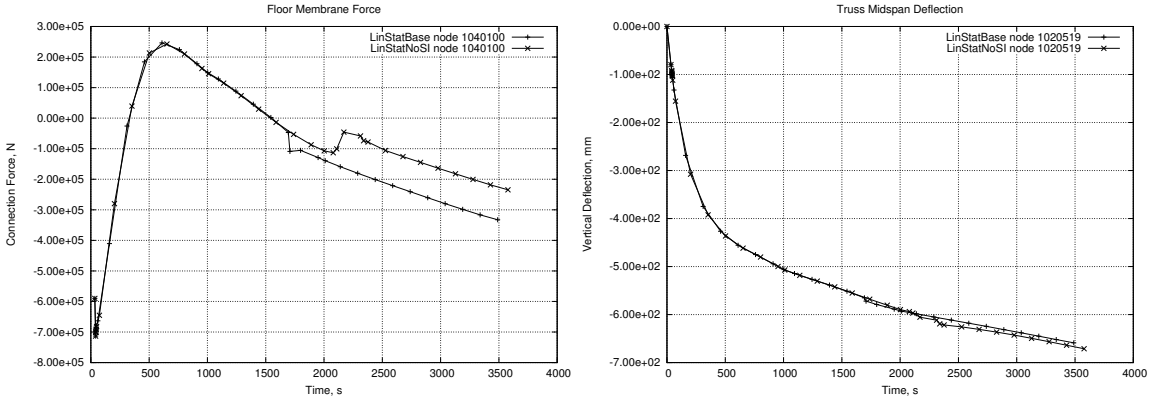

(a) (b)

Figure A.20: Quasi-static : Imperfection Global Response

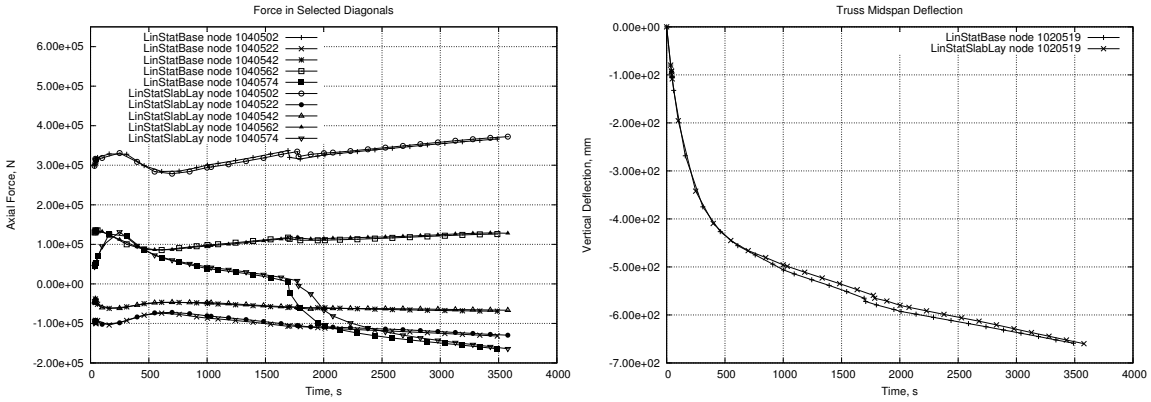

(a) (b)

Figure A.21: Quasi-static : Slab Layers

A.21.b

A.4.1.9 Damping using "Stabilize"

Another way that numerical damping can be introduced to an ABAQUS model is through the use of the *Stabilize* option with its own factor. Again this introduces a viscous damping term in the global equilibrium equations. The primary difference between the two methods reported in this section is that the *Stabilize* method calculates a damping factor automatically while *Stabilize*, $Factor$ = allows the damping factor to be directly entered. To investigate this option several different stabilize values were used. The default dissipated energy fraction is $2x10^{-4}$ with the Hi and Hi2 models having factors 10 and 100 times higher. Similarly the Lo and Lo2 models have factors 10 and 100 times lower.

Figure A.22 shows the comparison of results between the Base case and the case with the default *Stabilize* value. It is obvious that the numerical damping being applied by this factor is far too high. Almost all of the movement in the system is being suppressed which means that the forces in the truss members all increase accordingly.

As the Default level of stabilization is obviously too high any increase in the value

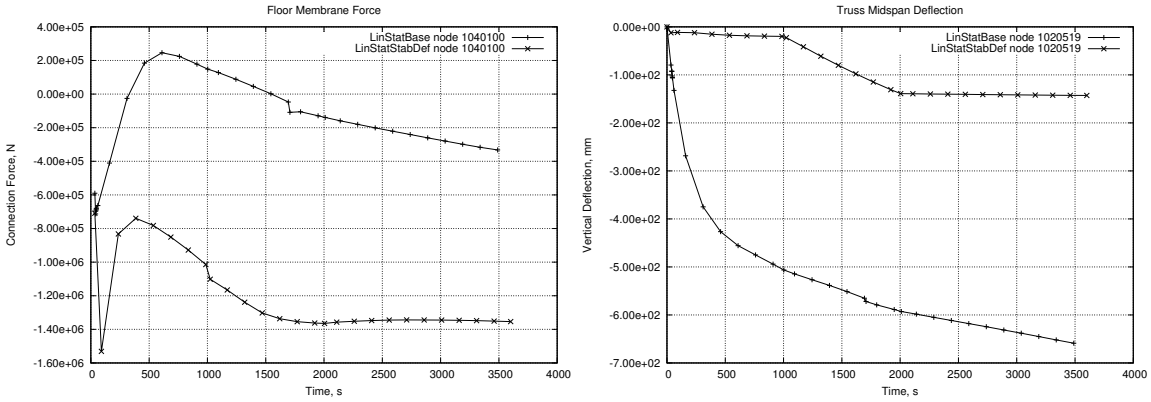

(a) (b)

Figure A.22: Quasi-static : Stabilize Default

further reduces the movement in the system. This can be seen in Figure A.23. As the *Stabilize* value in increased the midspan deflection reduces and the connection forces increase.

Conversely as the stabilize value is reduced the movement in the system increases until it is very close to exactly matching the base case (that is damped using the *Stabilize*, *Factor* option). Figure A.24 shows the comparisons from lower Stabilize values and the base case. As with the use of the *Stabilize*, *Factor* option the actual value of stabilize will have to be tuned specifically for each model under investigation. A parametric study of this option will allow the user to balance and optimize the model between run time and realistic results.

A.4.2 Explicit Dynamic Analyses

The items below include the details of the changes made throughout the parametric study and a comparison of the results to the "base" case for the Explicit analyses. A summary of these models may be found in Table A.2.

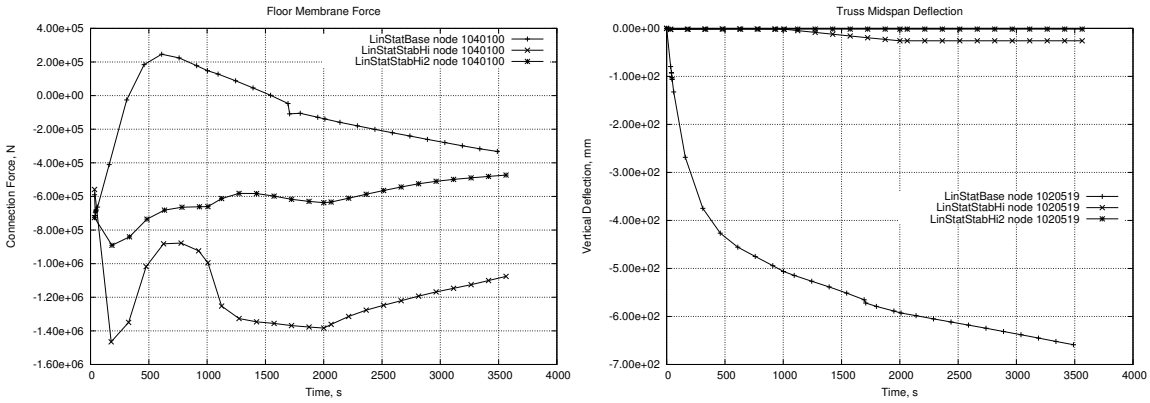

(a) (b)

Figure A.23: Quasi-static : Stabilize Hi & Hi2

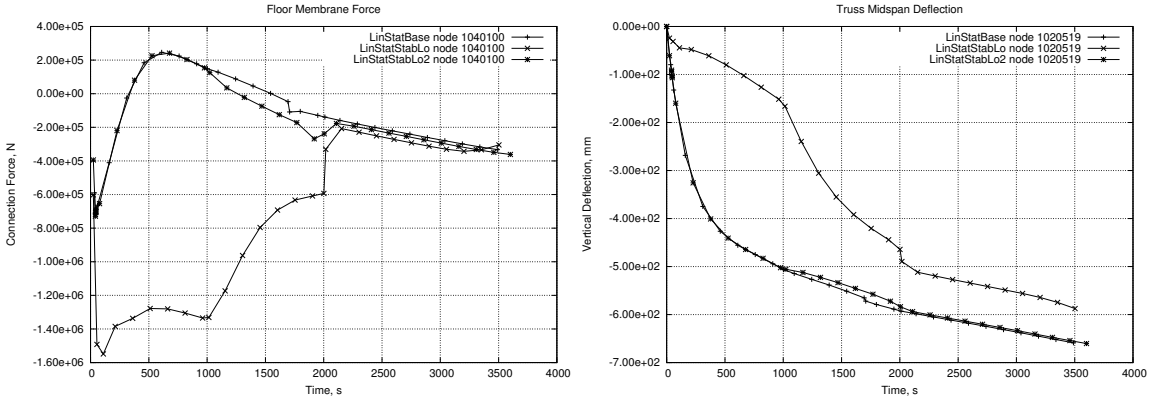

(a) (b)

Figure A.24: Quasi-static : Stabilize Lo & Lo2

A.4.2.1 Explicit Base Case

This analysis was to be used as a basis of comparison for all the Explicit analyses. It includes no time or mass scaling (descriptions of these may be found under the appropriate heading below or in the ABAQUS manuals [73]). The model is set to analyze a 3600 second period with the structure undergoing heating. In the concrete material model the tensile strength was limited to a constant level of 5% of the compressive strength for a particular temperature. Non-linear geometry and material properties were taken into account.

The maximum time reached by the Base case was 250s. This introduces problems when trying to compare against other analyses due to the lack of data about the later stages of the analyses.

A.4.2.2 Elastic Material Properties

This analysis removed all plastic material properties and produced very different results to the base case. It did however only take half the time of the base case to reach the same point. Two examples of the output of this analysis compared to the base case may be found in Figure A.25. Elastic material properties are not a realistic tool when considering the highly non-linear nature of structures under fire loading.

A.4.2.3 Mass Scaling Comparisons 1 & 2

Mass Scaling is a useful option that can be applied to an analysis that is using the Explicit Dynamic solver but is essentially quasi-static in nature, such as thermal effects on a structure. It alters the mass matrix used in the acceleration equations thereby adding extra damping to the model. A similar effect can be introduced by altering the density of the materials used in a model but the method described here allows more control.

Mass scaling allows an increase in the size of stable increment used, speeding up the analysis significantly. In an analysis where it is the dynamic reaction that

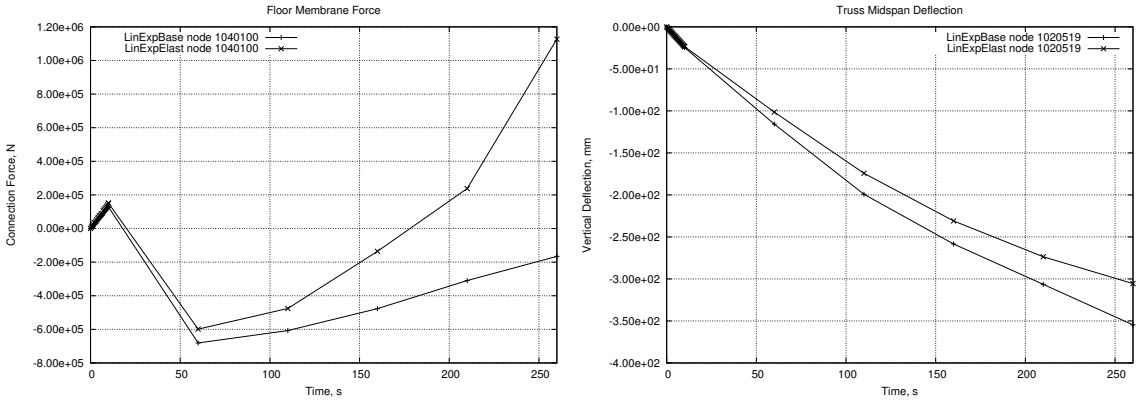

(a) (b)

Figure A.25: Explicit : Elastic Connection Force and Deflection

is sought this can adversely affect the results but as can be seen below a certain amount of mass scaling may be used without affecting the results too much. More information on this technique may be found in the ABAQUS manual [73].

The Mass1 analysis included a small amount of mass scaling increasing the time steps slightly (from 8.9×10^{-6}s to 3.0×10^{-4}s) by increasing the mass matrix to 10,000% of its original value. As can be seen in Figure A.26 this has changed the structural response very little. A major reduction in CPU time can be seen using this option. The base case reaches around 250s in about 24 hours while Mass1 completes in 17 hours and Mass2 competes in 3 hours.

A further increase of increment size to 2×10^{-3}s was instigated in in the Mass 2 model with an increase in mass to 450,000%. The results again matches the base case rather closely, as indicated in Figure A.26. Figure A.26 must, by necessity, concentrate on the early portion because of lack of data from the Base case. Figure A.27 shows a direct comparison between the two mass scaled models for the full analysis time. It is clear that the increase in mass using Mass Scaling produces very little difference between the models.

As with the Quasi-static damping options a parametric study should be conducted if this option is to be used correctly. As each model will be affected differently

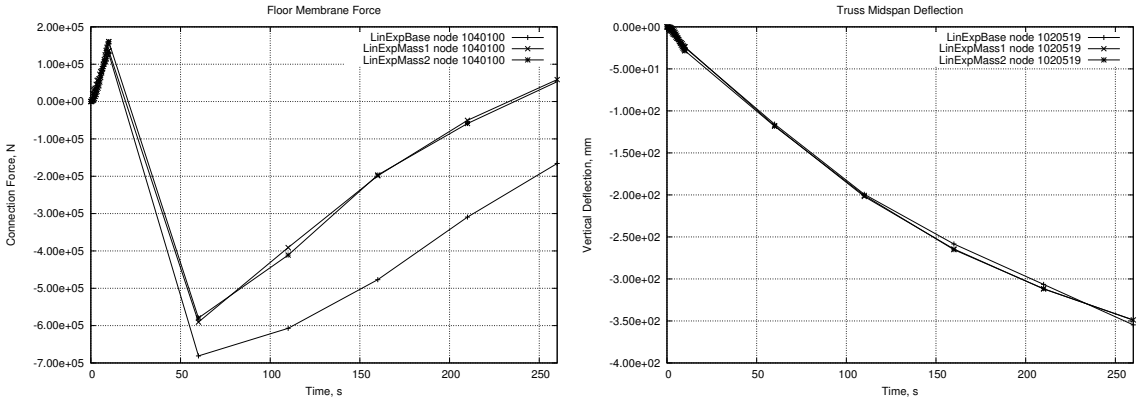

(a) (b)

Figure A.26: Explicit : Mass Scaling Comparison 1

by changes in the mass matrix a balance will have to be struck for each model in terms of time to completion and accuracy of results.

A.4.2.4 Material Property Regularity Tolerance

The RTOL parameter allows the user to bypass, to a certain extent, the internal checking systems that ABAQUS uses on it material model. ABAQUS Explicit requires the material data to be highly organized and as evenly distributed as possible in order to fit a curve to the data. If the data is not organized enough then the analysis fails. The RTOL command alters the tolerance required by ABAQUS when it does the curve fitting process.

This analysis used an older, less organized version of the EC3 material properties and a more relaxed tolerance. As can be seen in Figure A.28 the deflection response (plot .b) is quite close over the extent of the analyses. The force response in Figure A.28.a is slightly changed from the Base case. This analysis also appears to run faster than the base case. This was not what was expected as it was believed that the results would be further from the base case. The faster run time may be caused by the easier curve fitting restrictions. It is possible that as the analysis continued the differences due to the change in material properties would become

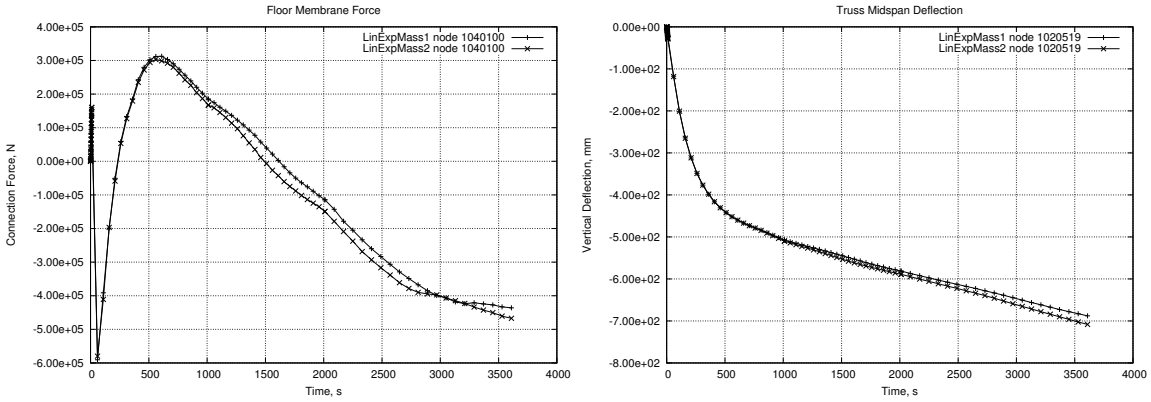

(a) (b)

Figure A.27: Explicit : Mass Scaling Comparison 2

more pronounced.

A.4.2.5 Plastic Tensile Strength Degradation in Concrete

In this case the tensile strength of the concrete was reduced from it's maximum, at 5% of the compressive strength, linearly down to 0 at roughly 10 times yield strain. This analysis produced comparable results to the base case and ran in a comparable time. It may, therefore, be advantageous to run Explicit analysis with fully realistic material properties in such small scale models. The benefits may not scale up to larger analyses and should again be approached on a case-by-case basis. Example plots may be seen in Figure A.29. As the analyses did not run to completion it is impossible to say how different the later response may be, however. It is possible that the reason there is little difference between the analyses is because the concrete is not moving into tensile action in many places at such an early stage.

A.4.2.6 Time Scaling Comparisons 1 & 2

Time Scaling, like mass scaling, may be used to reduce the run time of an Explicit analysis. It works simply by running an analysis for a shorter time and scaling any time based distributions accordingly. More information may be found in the

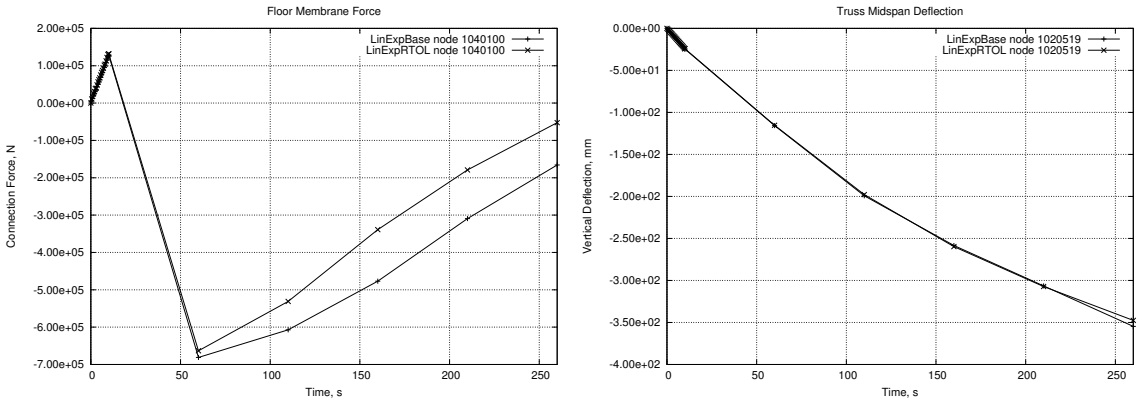

(a) (b)

Figure A.28: Explicit : RTOL Section Forces and Deflections

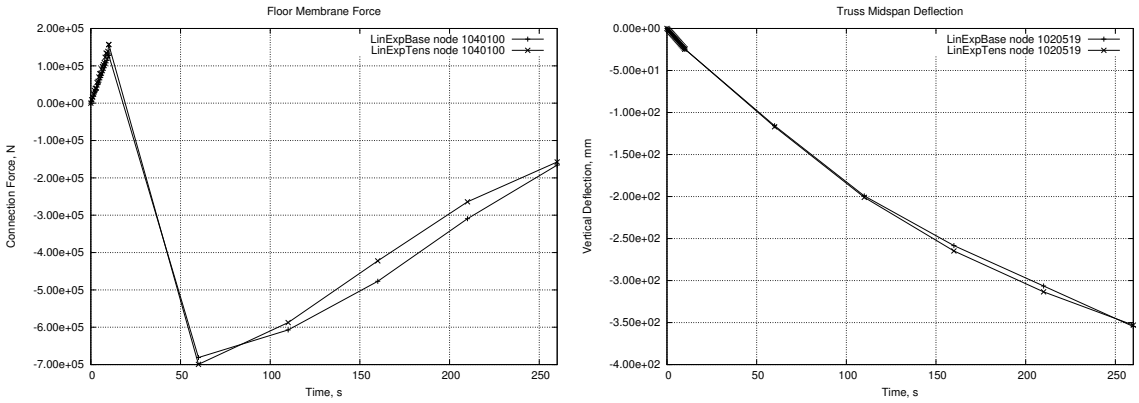

(a) (b)

Figure A.29: Explicit : Tensile Strength Comparison

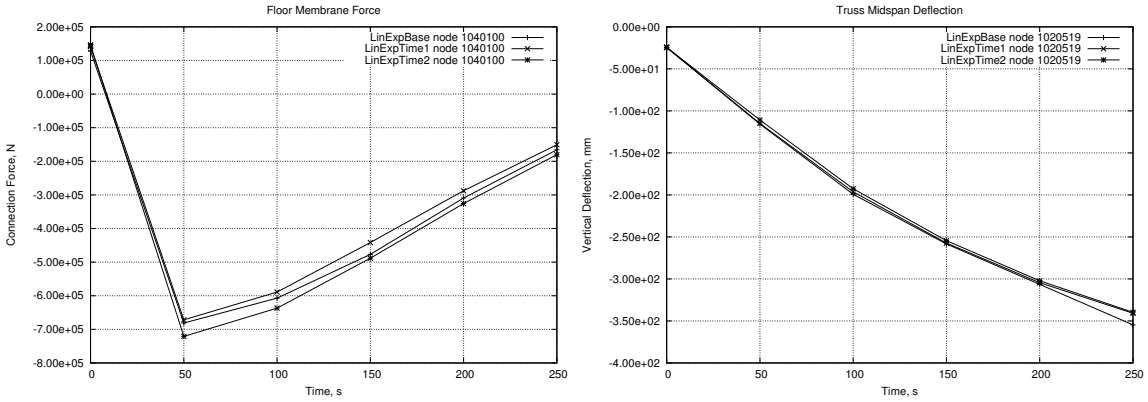

(a) (b)

Figure A.30: Explicit : Time Scaling Comparison 1

ABAQUS manuals [73]. Analyses Time1 and Time2 ran the 3600 base case across 360 seconds and 36 seconds respectively. All time dependant distributions, i.e. the temperature-time distributions, had their time scales altered accordingly. In a similar way to mass scaling this method may not be suitable for an analysis in which the exact dynamic result is the goal. Quasi-static problems may take advantage of this technique.

Figure A.30 shows a direct comparison between the Base case and the two time scaled cases for floor membrane force (plot .a) and midspan deflection (plot .b). The results of the scaled analyses have been expanded up to match the original analysis time. As with the Mass Scaling system presented above the results for the early stages of all the analyses are extremely close.

Figure A.31 shows a direct comparison of the two scaled analyses over a greater length of time. In this case the Time1 analysis terminated on an error at about 2300s (equivalent). The similarities are again apparent and it would seem that for the model under consideration that this level of time scaling does not appreciably alter the results of the analysis. It does, however, considerably decrease the run-time.

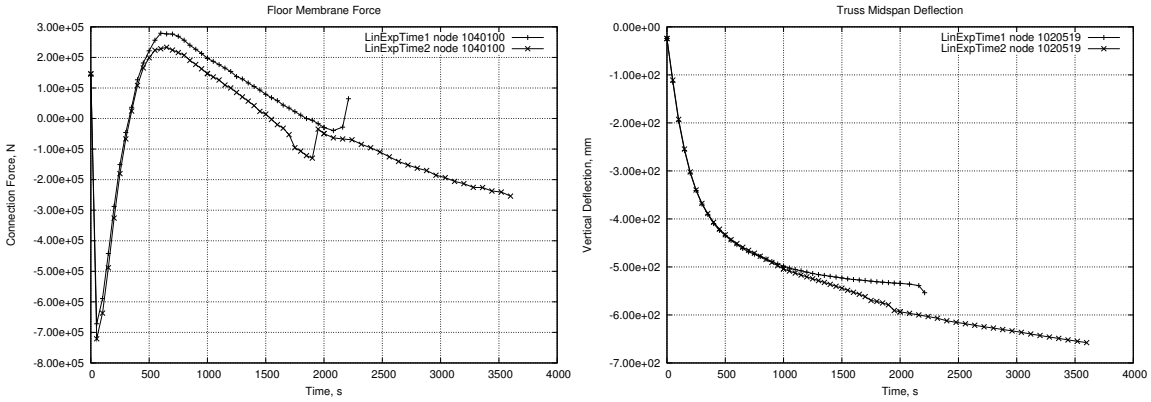

(a) (b)

Figure A.31: Explicit : Time Scaling Comparison 2

A.4.3 Implicit Dynamic Analyses

A.4.3.1 Implicit Base Case

As with the Explicit set of analyses it was necessary to have a basis of comparison to judge the rest of the results with. In this case there were several baseline factors to define. The factors involved will be explained in greater detail later. The baseline values for HAFTOL and numerical damping were 40,000 and -0.05 respectively. Again non-linear geometry and material properties were used. In all the Implicit cases the analysis consists of 4 steps. The first is a quasi-static loading step designed to load the structure. The other 3 steps are the heating steps and these use an Implicit Dynamic analysis. As with the other analyses presented here the models are run over 3600s using the geometry and fire regime described earlier. It was generally found that the model would not run beyond 1000s, unlike the Quasi-static analyses.

A.4.3.2 Alpha Damping

This analysis altered the Alpha factor associated with the implicit steps. the use of this factor adds extra numerical damping to the model. As mentioned above

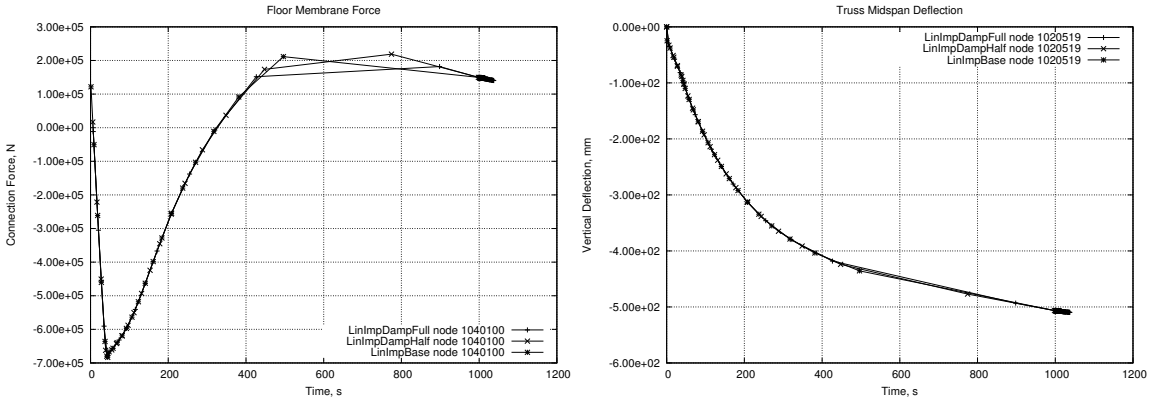

(a) (b)

Figure A.32: Implicit : Alpha Damping Comparisons

the default is -0.05. DampFull was taken at the maximum damping factor allowed at -0.333, DampHalf was taken at -0.15 while DampNo was taken at Alpha = 0 . The analyses at half and full damping matched that of the default case extremely well as may be seen in Figure A.32. The primary differences in the graphs are due to the reduction in data points required to make the traces clear. Increase of the Alpha factor allowed significant savings in CPU time.

The case with no damping was terminated after a significant amount of time had passed with very little advancement. Increments in this analysis were so small that it was deemed pointless to continue. So little of the analysis had been completed that the results are not considered here.

A.4.3.3 Elastic Material Properties

The effects of using non-linear material properties were investigated by conducting one analysis which excluded them. As expected the results are significantly different to the baseline case and are therefore not likely to be as useful. As there are no plastic material effects once the steel stops heating it can take an infinite amount of stress and therefore withstand the slab movement. This will, at the very least, lead to erroneous deflections in the later stages of the analysis. The main advantage to

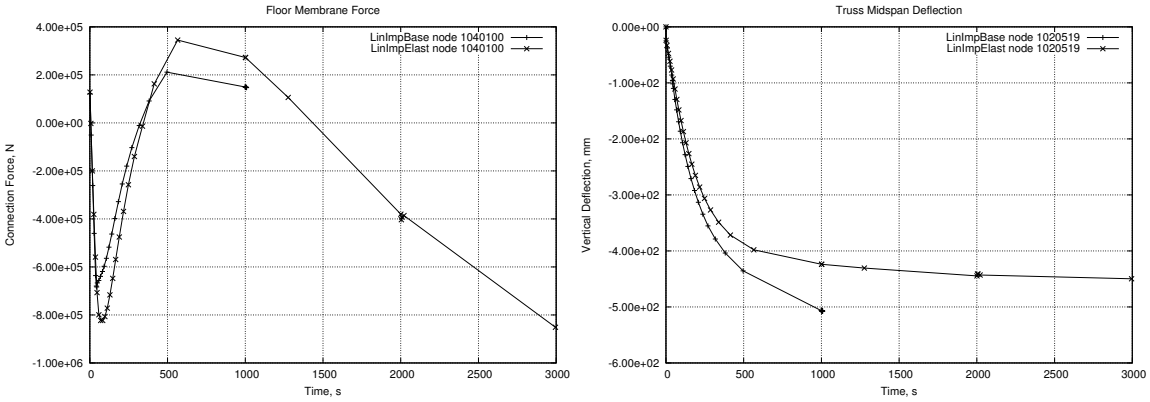

(a) (b)

Figure A.33: Implicit : Elastic Comparisons

this type of analysis is the speed with which it runs. This is not useful though due to the inaccuracy of the results. Comparison graphs for this analysis type may be found in Figure A.33.

A.4.3.4 Element Types

There are a variety of element types that may be used in this type of project. A comparison was undertaken to test the differences and establish the more useful element types. In this case the elements that made up the concrete slab were changed to the standard S4 element rather than the Reduced Integration (S4R) type used in the other analyses. Figure A.34 shows a comparison of results. There are some minor differences in the results between the two but there are no major discrepancies.

A.4.3.5 HAFTOL Analyses

The HAFTOL parameter helps control the accuracy of the solution by limiting the size of increment. It uses the residual forces left from the solution to affect the increment size. The HAFTOL value must, therefore, be linked into particular analysis. If it is too small it keeps the increment size small. If it is of a suitable

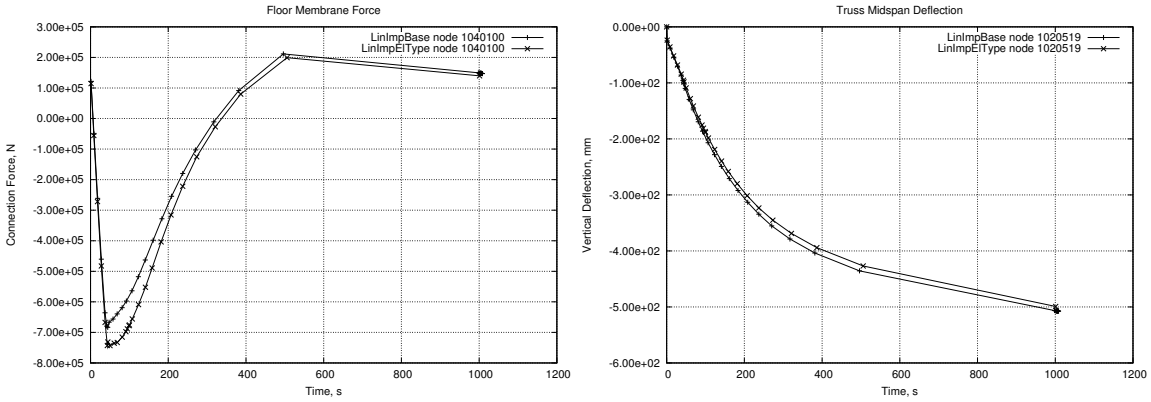

(a) (b)

Figure A.34: Implicit : Element Type Comparisons

size, roughly 10 to 100 times the actual residual forces in the model, then it can allow much faster convergence.

As with some of the parameters discussed in the Explicit portion of this chapter, a large HAFTOL parameter may not produce exact results in a dynamic analysis looking for the exact dynamic response of a structure. In this case however this is not necessary. As can be seen in Figure A.35 altering the HAFTOL value has virtually no impact upon the analysis results. The main effect of altering this value is in the time an analysis takes. In the 10-100 times range there is a significant CPU time saving seen while if the HAFTOL is too large or too small then this may adversely affects the time taken. Again, more information on this parameter may be found in the ABAQUS manual [73].

A.4.3.6 Material Property Regularity

There is no actual RTOL parameter in the Implicit Dynamic type of analysis however it was possible that poorly ordered material could adversely affect the analysis. For this reason a version of the model was run using the same material properties as the RTOL analysis in the Explicit set of models. Reference to Figure A.36 indicates that there is little difference between the two analyses. The only

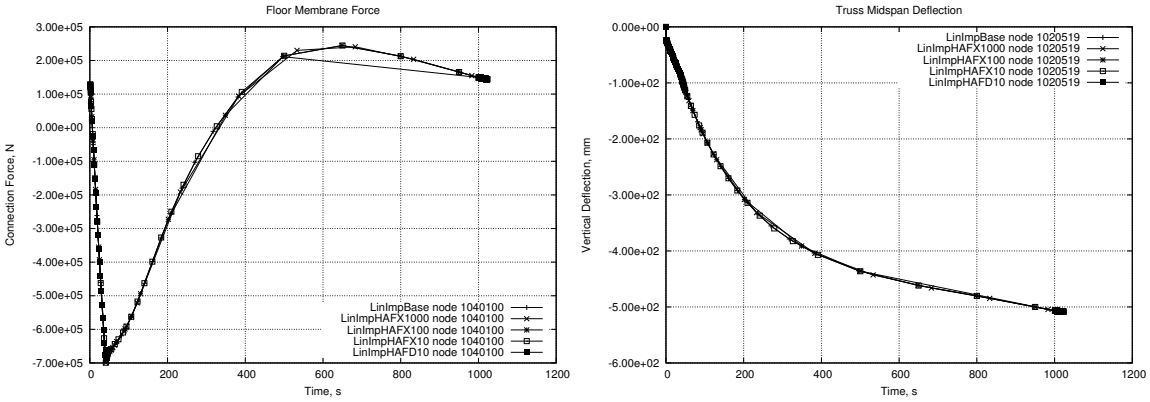

(a) (b)

Figure A.35: Implicit : HAFTOL Comparisons

possible effect that poorly ordered material data may produce is a difference in the analysis speed. This would be caused by the ordering of the material data taking a more significant amount of processor time as well as being a less than optimal solution, therefore incurring convergence penalties.

A.4.3.7 Sine Imperfections in Truss Diagonals

The inclusion of a sine imperfection was seen to ease convergence in the Quasi-static analyses. This comparison was undertaken to investigate the usefulness of such an inclusion in a Dynamic Implicit analysis. The inclusion of such imperfections appears to introduce additional convergence problems in the Dynamic analysis. As such the analysis was terminated after about 100s due to the extremely small time increments.

A comparison of the results gained in the analysis, however, shows that they match the Base case almost exactly when compared in Figure A.37. Extrapolation to later in the analysis is not possible, however, so again a case-by-case basis should be used when utilizing this technique.

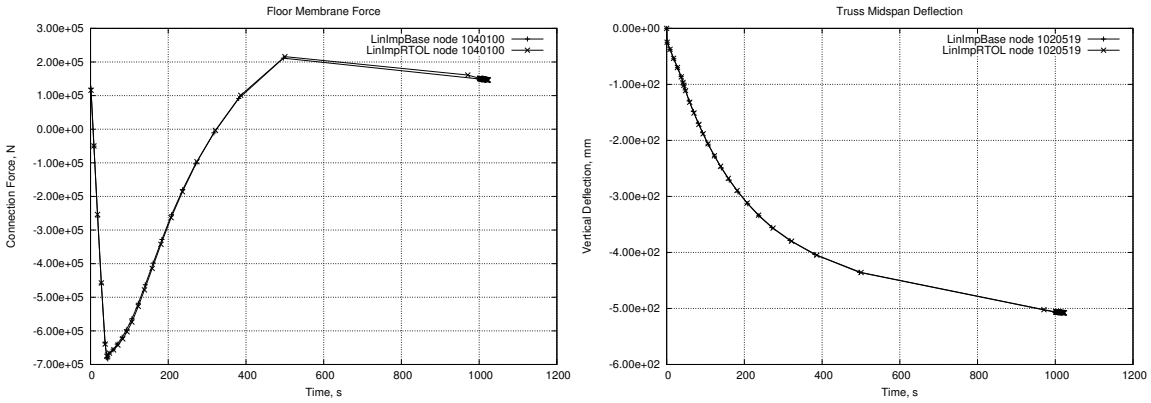

(a) (b)

Figure A.36: Implicit : Material Data Regularity Comparison

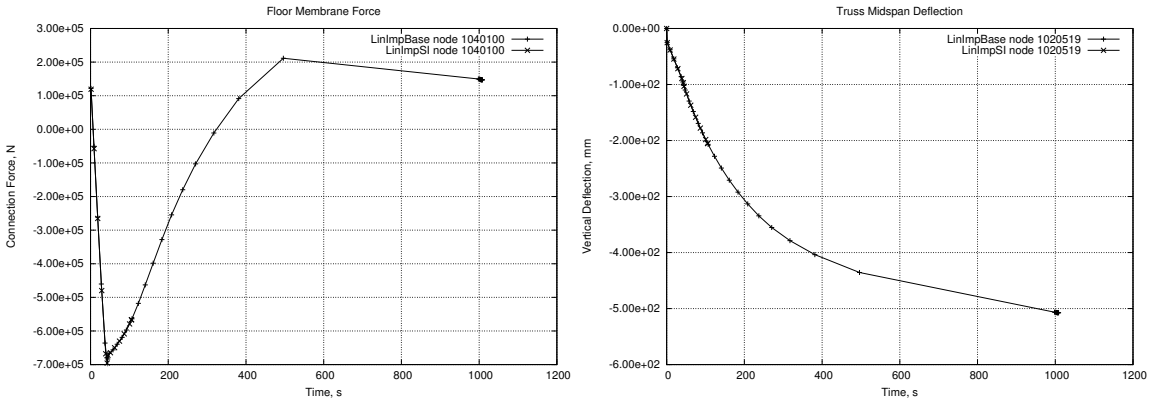

(a) (b)

Figure A.37: Implicit : Sine Imperfection Comparison

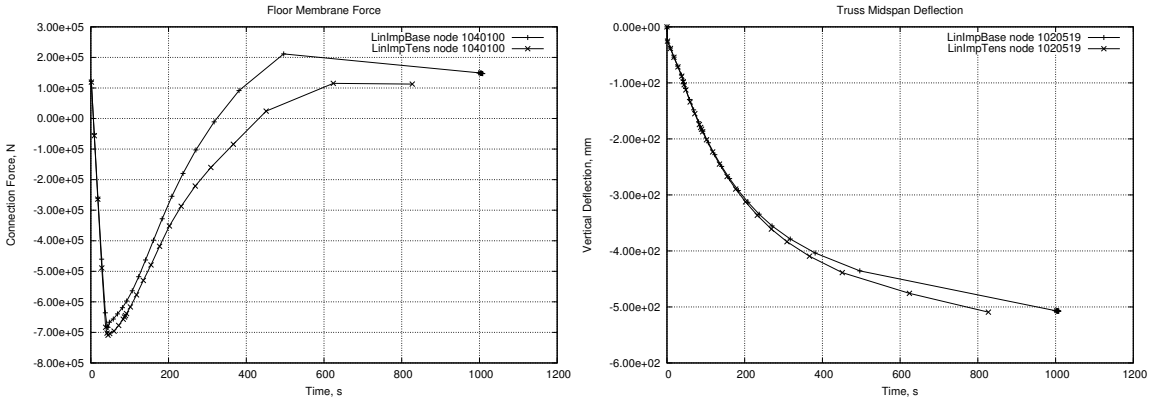

(a) (b)

Figure A.38: Implicit : Concrete Tension Degradation Comparison

A.4.3.8 Plastic Tensile Strength Degradation in Concrete

As with the Explicit set of analyses it was decided to test the effect of reducing the concrete tensile strength after plasticity was reached. The comparisons with the base case may be found in Figure A.38. The response is broadly similar.

A.4.4 Analysis Type Comparisons

A final comparison across the different analysis types (i.e. Quasi-static, etc) can be seen in Figure A.39. Comparison between the Base cases (Figures A.39.a and A.39.b) shows close agreement over the periods of successful convergence. The one difference is the final result in the Explicit base case which may be disregarded as this analysis crashed out with system errors.

Further comparisons made in Figures A.39.c and A.39.d show the Mass and Time Scaled Explicit analyses overlaid with the Base cases. Again over the majority of the analysis time the results are extremely close. Time1 shows a major divergence at around 1000s for unknown reasons. The Time2 analysis, however, matches the Quasi-static base case extremely closely. This then indicates that as long as some kind of parametric check is made on an analysis then Time Scaling appears not to

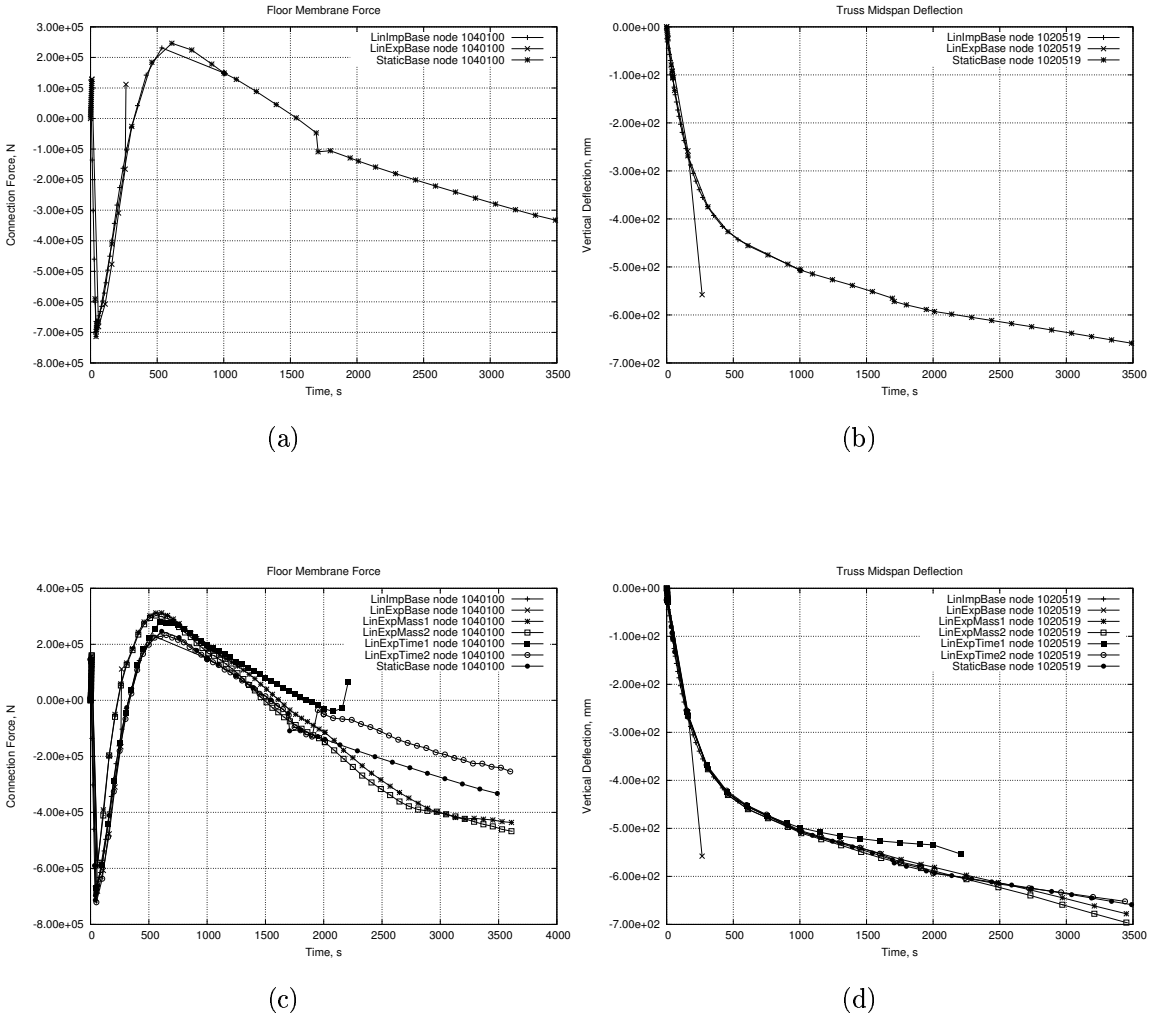

Figure A.39: Analysis Type Comparison

affect the final result greatly. These figures also indicate that Mass Scaling has a greater effect than Time Scaling. For the first half of the analysis the results are extremely close. Toward the end of the analysis it can be seen that the results from Mass1 and Mass2 are beginning to diverge from the Quasi-static and Time2 analyses. Once again if such techniques are to be used it should be with a thorough knowledge of the consequences and, ideally, a reasonable parametric study on the model to be investigated.

A.5 Conclusions

Several different parameters linked to the effectiveness and efficiency of ABAQUS have been investigated and a comparative analysis conducted. For the kind of response expected from a model of the effects of elevated temperatures on a structure it would appear that a Quasi-static analysis provides the most reliable results. The Explicit analyses succeeded in most cases but without the addition of Time and/or Mass Scaling the run times for this type of analysis are prohibitive. The benefits of using an Explicit analysis are not truly realised for the model investigated here due to the small nature of the model and the relative ease with which the Quasi-static analyses converged. The Implicit Dynamic models proved to be the least stable of the set.

Material models were constructed for the steel and concrete in the models. The steel is represented by isotropic elastic and plastic behaviour based on Eurocode 3 data. This data included changes in material properties caused by exposure to elevated temperatures (thermal expansion and degradation).

A parametric study of the options associated with the Concrete Damaged Plasticity and Drucker-Prager material models indicate that the former is the better of the two models to use in this kind of analysis. A set of material data was constructed for the Concrete Damaged Plasticity model based on the equations for concrete strength in Eurocode 2 [26]. This material model was then used for all of the structural models run over the course of this research programme. This model included thermal expansion and degradation effects.

The steel reinforcement for use within the concrete was defined in a similar way to the main structural steel. Isotropic elastic and plastic properties were defined. Thermal expansion and degradation effects were included in the rebar material data but for a more limited range of temperatures due to the insulating properties of the concrete slab.

Within the analysis types various recommendations may be made based upon the results of this study. For the Quasi-static models the primary means of increasing

numerical efficiency was through the use of imperfections in the truss diagonals and through the addition of numerical damping. The effects of these varied depending on the severity of application. The imperfections created a slight change in the timing of responses but did not appear to alter the overall response of the floor system. Damping (by any means) should be implemented carefully as there will always be an optimum position between assisting convergence and affecting the response of the model. Damping should be considered on a case-by-case basis and the final damping value should be based on a parametric study to ensure the validity of results. Options pertaining to the material models should also be investigated to ensure the most realistic model possible.

For Explicit analyses time savings may be made by using an appropriate amount of Time and Mass Scaling. Using an extreme amount of either may provide lower analysis times but may also adversely affect the results. Fully realistic material properties may be used efficiently at this scale as long as the data is included in a suitable format. This may not scale up to larger models but should be tested to allow increased accuracy.

For the Implicit dynamic analyses the main parameters investigated were Damping and the HAFTOL parameter. Including a high damping factor allows for quicker convergence with no apparent effect on result accuracy. Again this may not scale up effectively to larger models and should be carefully checked before implementation. Altering the HAFTOL parameter had negligible effects on the results but did have large implications on the speed of the analysis. HAFTOL values should be tailored for a particular model and indeed for a particular step within an analysis as it may be changed throughout the model run.

The different analysis types appear to give similar results and should be freely interchangeable within the restrictions of the software itself. Care should be taken by the user to fully understand and justify the factors being included in an analysis.

This appendix has indicated several different parameters that can be altered to increase numerical and convergence efficiency. These factors should be investigated on a case-by-case basis before being implemented in a model.

Appendix B

Publications

Title
Permission of co-authors for paper publication
Effect of Fire on Composite Long Span Truss Floor Systems
Structural response of tall buildings to multiple floor fires : Part 1 - General response
Structural response of tall buildings to multiple floor fires : Part 2 - Parametric study

Table B.1: Attached Papers